NANOPARTICLE VACCINES AGAINST INFECTIOUS DISEASES

EDITED BY: Rajko Reljic and África González-Fernández
PUBLISHED IN: Frontiers in Immunology

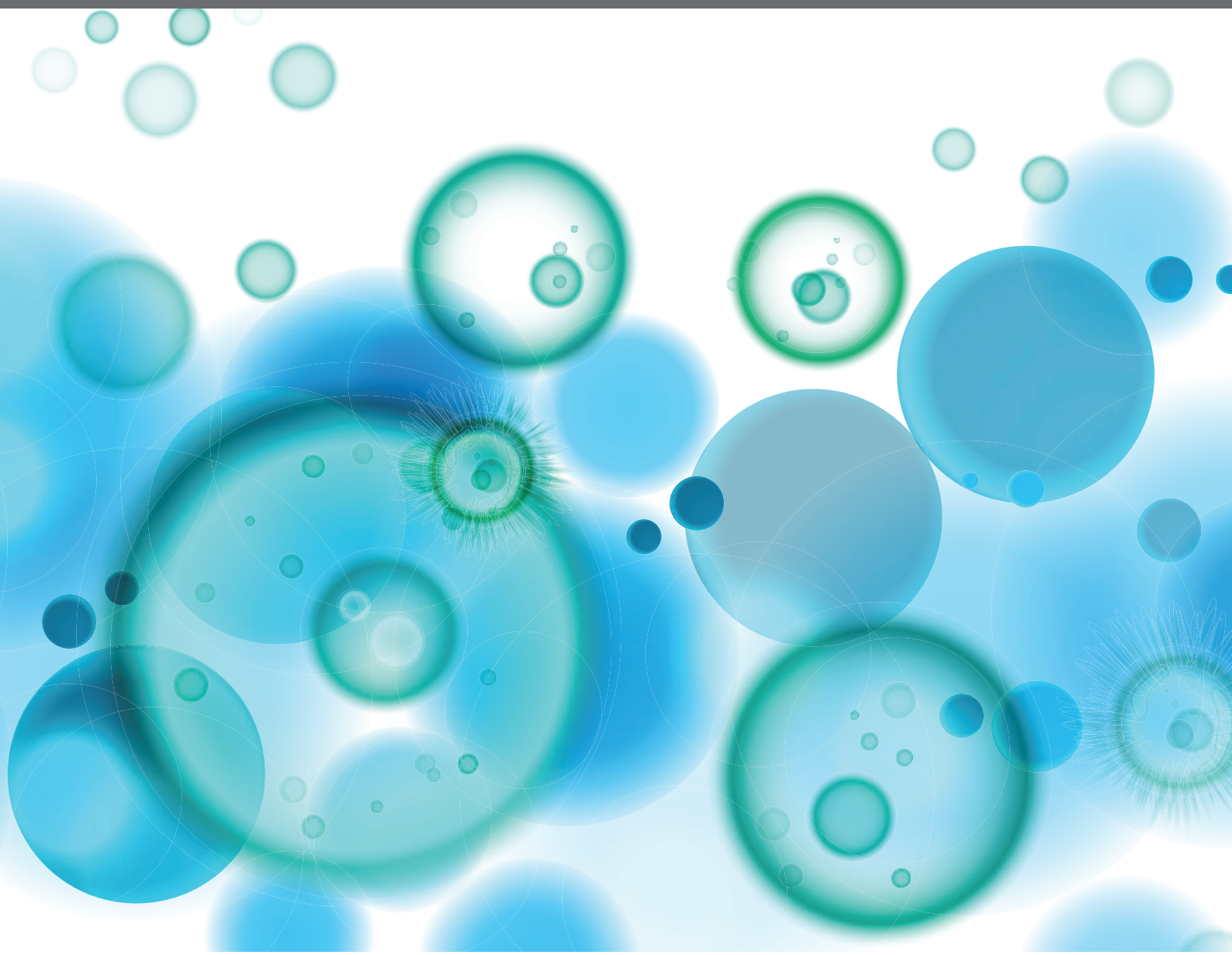

frontiers Research Topics

frontiers

ISSN 1664-8714
ISBN 978-2-88963-327-2
DOI 10.3389/978-2-88963-327-2

About Frontiers

Frontiers is more than just an open-access publisher of scholarly articles: it is a pioneering approach to the world of academia, radically improving the way scholarly research is managed. The grand vision of Frontiers is a world where all people have an equal opportunity to seek, share and generate knowledge. Frontiers provides immediate and permanent online open access to all its publications, but this alone is not enough to realize our grand goals.

Frontiers Journal Series

The Frontiers Journal Series is a multi-tier and interdisciplinary set of open-access, online journals, promising a paradigm shift from the current review, selection and dissemination processes in academic publishing. All Frontiers journals are driven by researchers for researchers; therefore, they constitute a service to the scholarly community. At the same time, the Frontiers Journal Series operates on a revolutionary invention, the tiered publishing system, initially addressing specific communities of scholars, and gradually climbing up to broader public understanding, thus serving the interests of the lay society, too.

Dedication to Quality

Each Frontiers article is a landmark of the highest quality, thanks to genuinely collaborative interactions between authors and review editors, who include some of the world's best academicians. Research must be certified by peers before entering a stream of knowledge that may eventually reach the public - and shape society; therefore, Frontiers only applies the most rigorous and unbiased reviews.
Frontiers revolutionizes research publishing by freely delivering the most outstanding research, evaluated with no bias from both the academic and social point of view. By applying the most advanced information technologies, Frontiers is catapulting scholarly publishing into a new generation.

What are Frontiers Research Topics?

Frontiers Research Topics are very popular trademarks of the Frontiers Journals Series: they are collections of at least ten articles, all centered on a particular subject. With their unique mix of varied contributions from Original Research to Review Articles, Frontiers Research Topics unify the most influential researchers, the latest key findings and historical advances in a hot research area! Find out more on how to host your own Frontiers Research Topic or contribute to one as an author by contacting the Frontiers Editorial Office: researchtopics@frontiersin.org

NANOPARTICLE VACCINES AGAINST INFECTIOUS DISEASES

Topic Editors:
Rajko Reljic, St George's, University of London, United Kingdom
África González-Fernández, Biomedical Research Center (CINBIO), Spain

Citation: Reljic, R., González-Fernández, Á., eds. (2020). Nanoparticle Vaccines Against Infectious Diseases. Lausanne: Frontiers Media SA.
doi: 10.3389/978-2-88963-327-2

Table of Contents

frontiers in Immunology

EDITORIAL
published: 07 November 2019
doi: 10.3389/fimmu.2019.02615

Editorial: Nanoparticle Vaccines Against Infectious Diseases

Rajko Reljic[1]* *and África González-Fernández*[2,3]

[1] Institute for Infection and Immunity, St. George's, University of London, London, United Kingdom, [2] Centro de Investigaciones Biomédicas (CINBIO) (Centro Singular de Investigación de Galicia), Universidad de Vigo, Vigo, Spain, [3] Instituto de Investigación Sanitaria Galicia Sur (IIS-GS), Vigo, Spain

Keywords: nanoparticles, vaccine, liposomes, immunity, infection

Editorial on the Research Topic

Nanoparticle Vaccines Against Infectious Diseases

Vaccines remain the most realistic means of controlling, eliminating, and eventually completely eradicating an infectious disease. Many vaccines have been successfully implemented over the course of recent medical history and some have succeeded in completely (small pox) or near-completely eradicating (polio) their target diseases. However, many human pathogens are still in need of an effective vaccine, including viruses such as human immunodeficiency (HIV), herpes simplex (HSV), respiratory syncytial (RSV), Chikungunya, Dengue, Ebola, and Hepatitis C; bacteria such as *Mycobacterium tuberculosis* or *Salmonella dysenteriae* and parasites such as *Plasmodium* spp., to name a few.

Challenges in developing an effective vaccine against these infectious diseases are multiple, ranging from antigenic variability (HIV), multiple genotypes or serotypes (Norovirus, Dengue, Influenza), complex pathogenesis or life cycle of pathogen (tuberculosis, malaria), lack of correlates of protection (TB) and finally, the paucity of the adjuvants and delivery systems suitable for human application. With regards to the latter, it is true to say that non-live, subunit vaccine development has been historically severely hampered by safety issues associated with the adjuvants and delivery systems.

Nanoparticles (NPs) have emerged as a promising approach for vaccine delivery as both antigen delivery platform and immunomodulators. Their use in vaccine candidates from early preclinical to late stage clinical testing is a testament to their success as a promising, new approach, alongside the more conventional protein plus adjuvant, viral vector, or attenuated whole organism vaccine approaches. There are many different types of NPs, both synthetic and natural, as well as further varieties that are not considered classically as NPs, but are physically and functionally closely related to them, such as liposomes, virus-like particles, bacterial spores, and immunostimulating complexes.

The ability of NPs to interact with immune components and to induce humoral and cellular immune responses make them particularly amenable for vaccine design. Furthermore, they have been successfully applied by different routes (systemic and throughout the mucosa), and have been demonstrated capable of modifying and broadening of the immune profiles. They can increase antigen stability (time, temperature, proteolysis) and confer substantial flexibility to vaccine formulation, allowing the incorporation of diverse antigens and immunostimulants, compared to conventional subunit/adjuvant vaccines.

Many of these advantages are highlighted in this Research Topic but it is also necessary to draw attention to the areas for further improvements, including a better understanding of the mechanisms of NPs vaccine immunogenicity and a more efficient antigen presentation by the molecular histocompatibility complex molecules, especially the so called cross-presentation by class I molecules performed by specialized dendritic cells, following the endocytic/phagocytic uptake of NPs. Also, and very importantly, NPs design and technology may need to be

OPEN ACCESS

Edited and reviewed by:
Denise Doolan,
James Cook University, Australia

***Correspondence:**
Rajko Reljic
rreljic@sgul.ac.uk

Specialty section:
This article was submitted to Vaccines and Molecular Therapeutics, a section of the journal Frontiers in Immunology

Received: *20 September 2019*
Accepted: *21 October 2019*
Published: *07 November 2019*

Citation:
Reljic R and González-Fernández Á (2019) Editorial: Nanoparticle Vaccines Against Infectious Diseases. Front. Immunol. 10:2615. doi: 10.3389/fimmu.2019.02615

further improved to allow for an "off-the-shelf" approach to their application and testing rather than the complex and time/resource demanding process of customized production.

In this Research Topic, we include several articles that focus on NP-based vaccine delivery against infectious diseases and also review articles that summarize and critically assess the progress that has been achieved so far in the specific areas of NP vaccine development. It is hoped that the presented evidence will deepen our understanding of their mode of action and the overall potential of NPs for translation of this vaccine approach to human application.

Thus, Kim et al. reported a novel method of generating bio-designed NPs utilizing a bacterial expression system and the capacity of RNA molecules to act as chaperones. Using Middle East respiratory syndrome-coronavirus (MERS-CoV) as the infection target, they demonstrated that NPs can be assembled in the expression host and that this was entirely dependent on chaperoning capacity of RNA since mutations in the RNA-binding domain abolished formation of NPs. The resulting NPs were immunogenic in mice and induced blocking antibodies against MERS virus. This approach of generating protein-only based NPs could be further optimized (i.e., in terms of yields and homogeneity) and developed as a generic NPs platform against other infectious diseases.

In another article, the utility of mucosally delivered chitosan-based vaccine against swine influenza A virus (SwIAV) was demonstrated by Dhakal et al., who reported that strong cross-reactive mucosal IgA and cellular immune responses in the respiratory tract were induced in young piglets using this vaccination approach. Intranasal delivery of these NPs loaded with SwIAV antigens resulted in a reduced nasal viral shedding and lung virus titres in pigs, suggesting that this vaccination approach could offer a broader coverage than the current attenuated strain-specific SwIAV.

Chitosan was also tested, alongside arginine-rich protamine (PR) and polyarginine (PARG)-based NPs in a more mechanistic in our own studies (Peleteiro et al.), reporting that PR and PARG showed a superior immunomodulating ability, as measured by enhanced reactive oxygen species production, activation of the complement cascade, cytokine production, and mitogen-activated protein (MAP) kinases/nuclear factor κB activation. When complexed with recombinant Hepatitis B glycoprotein, and compared against each other, protamine-based NPs elicited higher IgG levels than PARG NPs.

The utility of NPs as a delivery system for immunododulators and adjuvants rather than antigens was illustrated in the article by Takahashi et al. They showed that the biodegradable carbonate apatite (CA)-based nanoparticles can serve as the delivery system for the CpG oligodeoxynucleotide (CpG ODN) adjuvant and that this combination was more potent in activating dendritic cells and induced more diverse cytokine profiles than CpG ODN alone. When used with a model antigen, the NPs/CpG ODN induced higher level humoral and cellular immune responses in mice, and in particular enhanced CD8+ T cell responses, suggesting that this vaccination approach is particularly suitable for viral infections which require cytotoxic T cells alongside the neutralizing antibodies to control the viremia.

Another example of the benefit of combining NPs with adjuvants was provided also in the study by Malik et al., who showed that an anthrax antigen when combined with trimethyl-chitosan nanoparticles (TMC-PA) and either CpG ODN or polyinosinic: polycytidylic acid (Poly I:C) adjuvant induced higher immune responses in mice than any other combination in that vaccine formulation. In a different approach, Wagner-Muniz et al. reported that laboratory-generated polyanhydride nanoparticles based on 1,8-bis-(p-carboxyphenoxy)-3,6-dioxaoctane (CPTEG), 1,6-bis-(p-carboxyphenoxy)hexane (CPH) and sebacic acid (SA), could be employed as an effective vaccination strategy against *Streptococcus pneumoniae,* with strong immune responses and good-level of protection after the challenge of mice with the bacteria.

Finally, in our own studies (Copland et al.), we demonstrated that mucosal delivery of a mycobacterial poly-antigen coated onto heat-inactivated *Bacillus subtilis* spores ("Spore-FP1") induced systemic and mucosal immune responses in mice, characterized with elevated antigen-specific IgG and IgA titres in the serum and bronchoalveolar lavage, antigen-specific memory T-cell proliferation in both $CD4^+$ and $CD8^+$ compartments, and resident memory T cells accumulation in the lungs. When used to boost the current TB vaccine, BCG, this vaccine candidate provided superior protection in mice challenged with aerosolised *M. tuberculosis*.

In addition, the collection also includes two review articles on lipid-based particles as a highly versatile vaccine delivery system. Thus, Corthesy and Bioley reviewed the potential of liposomes and liposomes derivatives as mucosal vaccine delivery systems, while Nisini et al. performed a critical assessment regarding the application of liposomes in a broader context of infectious diseases. Gao et al. provided an extensive review of the current state of virus-like particles (VLP) as an emerging and highly attractive vaccine delivery system, focusing in particular on the use of VLP in the context of HIV infection. And finally, Pati et al. reviewed the current state of NPs-based vaccines against infectious diseases, highlighting the key challenges and the potential for further progress.

The promising results obtained with several type of NPs highlight the potential of this vaccine approach for the development of new vaccines in the near future. However, further studies are still required to address in greater detail the issues regarding their safety, immunogenicity, stability, cost, scaling-up potential, and the use of appropriate animal models and clinical assays in humans. Even so, the significant body of evidence already generated, as partly illustrated in this Research Topic, underscores the translational potential of NPs in vaccine research and development, not only in the context of infectious diseases but potentially also other conditions such as autoimmune diseases and cancer.

AUTHOR CONTRIBUTIONS

All authors listed have made a substantial, direct and intellectual contribution to the work, and approved it for publication.

FUNDING

This work was financially supported by the EU Horizon2020 Eliciting Mucosal Immunity in Tuberculosis (EMI-TB) project (Grant No. 643558) and the Xunta de Galicia Grupo Referencia Competitiva 2016 (ED431C 2016/041).

Conflict of Interest: The authors declare that the research was conducted in the absence of any commercial or financial relationships that could be construed as a potential conflict of interest.

frontiers in Immunology

ORIGINAL RESEARCH
published: 13 November 2017
doi: 10.3389/fimmu.2017.01539

Induction of Robust B Cell Responses after Influenza mRNA Vaccination Is Accompanied by Circulating Hemagglutinin-Specific ICOS+ PD-1+ CXCR3+ T Follicular Helper Cells

*Gustaf Lindgren[1,2], Sebastian Ols[1,2], Frank Liang[1,2], Elizabeth A. Thompson[1,2], Ang Lin[1,2], Fredrika Hellgren[1,2], Kapil Bahl[3], Shinu John[3], Olga Yuzhakov[3], Kimberly J. Hassett[3], Luis A. Brito[4], Hugh Salter[4,5], Giuseppe Ciaramella[3] and Karin Loré[1,2]**

[1] Department of Medicine Solna, Immunology and Allergy Unit, Karolinska Institutet, Stockholm, Sweden, [2] Center for Molecular Medicine, Karolinska Institutet, Stockholm, Sweden, [3] Valera LLC, Cambridge, MA, United States, [4] Moderna Therapeutics, Cambridge, MA, United States, [5] Department of Clinical Neuroscience, Karolinska Institutet, Stockholm, Sweden

OPEN ACCESS

Edited by:
Rajko Reljic,
St George's, University of London,
United Kingdom

Reviewed by:
Giuseppe Lofano,
Ragon Institute of MGH, MIT and Harvard, United States
Ali Ellebedy,
Washington University in St. Louis, United States

***Correspondence:**
Karin Loré
karin.lore@ki.se

Specialty section:
This article was submitted to Vaccines and Molecular Therapeutics, a section of the journal Frontiers in Immunology

Received: 12 September 2017
Accepted: 27 October 2017
Published: 13 November 2017

Citation:
Lindgren G, Ols S, Liang F, Thompson EA, Lin A, Hellgren F, Bahl K, John S, Yuzhakov O, Hassett KJ, Brito LA, Salter H, Ciaramella G and Loré K (2017) Induction of Robust B Cell Responses after Influenza mRNA Vaccination Is Accompanied by Circulating Hemagglutinin-Specific ICOS+ PD-1+ CXCR3+ T Follicular Helper Cells. Front. Immunol. 8:1539. doi: 10.3389/fimmu.2017.01539

Modified mRNA vaccines have developed into an effective and well-tolerated vaccine platform that offers scalable and precise antigen production. Nevertheless, the immunological events leading to strong antibody responses elicited by mRNA vaccines are largely unknown. In this study, we demonstrate that protective levels of antibodies to hemagglutinin were induced after two immunizations of modified non-replicating mRNA encoding influenza H10 encapsulated in lipid nanoparticles (LNP) in non-human primates. While both intradermal (ID) and intramuscular (IM) administration induced protective titers, ID delivery generated this response more rapidly. Circulating H10-specific memory B cells expanded after each immunization, along with a transient appearance of plasmablasts. The memory B cell pool waned over time but remained detectable throughout the 25-week study. Following prime immunization, H10-specific plasma cells were found in the bone marrow and persisted over time. Germinal centers were formed in vaccine-draining lymph nodes along with an increase in circulating H10-specific ICOS+ PD-1+ CXCR3+ T follicular helper cells, a population shown to correlate with high avidity antibody responses after seasonal influenza vaccination in humans. Collectively, this study demonstrates that mRNA/LNP vaccines potently induce an immunological repertoire associated with the generation of high magnitude and quality antibodies.

Keywords: mRNA vaccine, adaptive immune responses, non-human primates, influenza, T follicular helper cells, germinal centers

Abbreviations: ASCs, antibody-secreting cells; cTfh, circulating T follicular helper; GCs, germinal centers; GLA, glucopyranosyl lipid adjuvant; HA, hemagglutinin; ID, intradermal; IM, intramuscular; LNP, lipid nanoparticle; LN, lymph node; PC, plasma cell; PD-1, programmed death receptor 1; Th, T helper; Tfh, T follicular helper.

INTRODUCTION

Emerging infections such as Ebola, Zika, Chikungunya, and pandemic influenza virus need vaccines that can be rapidly produced with antigen precision. Modified mRNA vaccines have received considerable attention as they are attractive in this aspect and were recently shown to induce sterilizing immunity to Zika virus infection and protection against lethal challenge with influenza virus (1–5). Advances in mRNA synthesis technology have led to increased mRNA stability, optimized translation capacity, and less indiscriminate activation of innate immunity by mRNA vaccines (2, 3, 6). mRNA vaccines do not require device-mediated delivery methods as with DNA vaccines, and there is no concern of pre-existing immunity typically associated with viral vector vaccine platforms (3). mRNA vaccines delivered in lipid nanoparticles (LNP) are well tolerated and highly immunogenic in mice, ferrets, non-human primates, and humans (5, 7). However, the fundamental mechanisms by which mRNA vaccines induce strong antibody responses are largely unknown.

Durable vaccine-induced antibody responses with a high degree of affinity maturation confer protection against most pathogens (8). Antibody-secreting plasma cells (PCs) in the bone marrow determine the magnitude and longevity of vaccine responses (8). PCs are derived from germinal centers (GCs) in secondary lymphoid tissues during the process of establishing humoral immunity after vaccination (9, 10). Within the dark zone of GCs, B cells that encounter cognate antigens undergo multiple rounds of proliferation and somatic hypermutation. This is followed by antibody affinity maturation in the GC-light zone in a T follicular helper (Tfh) cell-dependent manner (11). B cells, expressing high-affinity B cell receptors as a result of the GC reaction, differentiate into either memory B cells or PCs (12). Recently, a subset of CXCR5+ICOS+, programmed death receptor 1+ (PD-1) CD4+ T cells in the blood was termed circulating Tfh (cTfh) cells due to their similarities with Tfh cells in the lymph nodes (LNs) (13–15). As for regular T helper cells, cTfh cells can be subdivided based on cytokine profile and effector function (16). cTfh1 cells (CXCR3+) are proposed to excel at conferring protection against intracellular pathogens whereas cTfh2 cells (CXCR3− CCR6−) and cTfh17 (CXCR3− CCR6+) may be particularly important in the defense against extracellular pathogens and fungi (14). cTfh cells can be detected seven days after influenza vaccination in humans (17–19). CXCR3+ cTfh cells in humans as well as CXCR3+ Tfh cells in LNs of rhesus macaques have been reported to correlate with the generation of high-avidity antibodies following vaccination (17, 18, 20).

Details of the dynamics of B cell responses and the profile of T cell help induced by mRNA vaccines are currently not known. We, therefore, analyzed the development and maintenance of vaccine-specific responses to a non-replicating mRNA construct encoding the hemagglutinin (HA) of a pandemic influenza H10N8 strain (H10). We show that H10-specific CXCR3+ cTfh cells appeared in the blood 1 week after both prime and boost immunization. This was accompanied by robust GC formation in vaccine-draining LNs, a continuous increase in antibody avidity and seeding of H10-specific PCs to the bone marrow, altogether resulting in protective HA inhibition antibody titers sustained over the 25-week study period.

MATERIALS AND METHODS

Production of Modified mRNA and LNP

Modified mRNA encoding the HA of H10N8 influenza A virus (A/Jiangxi-Donghu/346/2013) were generated as previously described (21). The lipid mixture was combined with a 50 mM citrate buffer (pH 4.0) containing mRNA at 3:1 ratio (aqueous:ethanol) using a microfluidic mixer (Precision Nanosystems). For formulations containing glucopyranosyl lipid adjuvant (GLA) (Avanti Lipids), lipids were combined in a molar ratio of 50:9.83:38.5:1.5:0.17 (ionizable lipid:DSPC:cholesterol:PEG-lipid:GLA). All formulations were dialyzed against PBS, concentrated using Amicon ultra centrifugal filters (EMD Millipore) and passed through a 0.22 μm filter. Particles were 80–100 nm in size with >95% RNA encapsulation.

Immunizations and Sample Collection

This animal study was approved by the Local Ethical Committee on Animal Experiments. Chinese rhesus macaques were housed in the Astrid Fagraeus laboratory at Karolinska Institutet according to guidelines of the Association for Assessment and Accreditation of Laboratory Animal Care, and all procedures were performed abiding to the provisions and general guidelines of the Swedish Animal Welfare Agency. Animals were divided into three groups (n = 4/group) receiving H10 mRNA/LNP (50 μg) either by IM or ID delivery or H10 mRNA/LNP co-formulated with GLA adjuvant (5 μg) delivered IM. Prime and boost immunizations were delivered at week 0 and 4, respectively. Animals receiving H10 mRNA/LNP with GLA received an additional boost at week 15. The animals were sedated with ketamine 10–15 mg/kg given IM (Ketaminol 100 mg/ml, Intervet, Sweden) during the immunizations, blood and bone marrow sampling. Bone marrow was sampled before immunization and at 2, 6, and 25 weeks from the humerus as previously described (22).

An axillary LN was collected before vaccination, opposite from the planned vaccination site, and a collateral axillary LN after boost. The animals were anesthetized by IM injection of 10–15 mg/kg of ketamine and 0.05 mg/kg of medetomidine. Carprofen (4 mg/kg) was given IM as analgesia. LNs were removed in an aseptic manner using minimal entry holes with the aim of removing a singular LN in each procedure. The anesthesia was reversed with atipamezole, 0.25 mg/kg IM after suturing.

Blood and Bone Marrow Processing

Peripheral blood was drawn into EDTA tubes and peripheral blood mononuclear cells (PBMCs) were isolated using Ficoll-Paque™ PLUS (GE Healthcare) and washed with PBS. Red blood cells were removed using red blood cell lysis buffer and cells were frozen in 10% DMSO (Sigma-Aldrich) diluted in heat-inactivated FBS. Bone marrow mononuclear cells were isolated and stored in a similar manner as PBMCs.

Lymph Node Processing

Lymph nodes were processed as previously described (23). Briefly, LNs were cleaned of fat and cut into small pieces using surgical scissors before being minced and filtered through 70 μm cell strainers. The cells were frozen as described above.

Hemagglutination Inhibition (HAI) Assay

Hemagglutination inhibition assay was performed using 0.5% turkey red blood cells (Rockland Antibodies and Assays) diluted in PBS to investigate protective antibody titers. Serum was incubated overnight at +37°C with receptor destroying enzymes (Denka Seiken) to prevent non-specific HAI. Serial dilutions (1:2) of serum samples were performed in V-bottom 96-well plates in duplicates, starting from 1:10 dilution. Recombinant HA of H10N8 influenza A virus (4 units), A/Jiangxi-Donghu/346/2013 (Medigen Inc.) were added to diluted serum and incubated for 30 min at room temperature. The reciprocal of the last serum dilution that resulted non-agglutinated red blood cells represented the HAI titer. Titers <10 were assigned as 1.

IgG Avidity ELISA

Clear flat-bottom immune 96-well plates (Thermofisher) were coated for 3 h in 37°C with 100 ng of H10 protein per well. After washing, wells were blocked for 1 h at 37°C in 2% milk powder (blocking buffer) diluted in PBS. Blocking buffer was discarded and plasma samples diluted in blocking buffer were added and incubated for 1 h at 37°C. Plasma was discarded and wells were incubated for 10 min with PBS or sodium thyocyanate (NaSCN) at 1.5–4.5M. After washing, wells were incubated with anti-monkey IgG HRP antibody (Nordic Labs) in washing buffer (0.05% Tween20 in PBS) for 1 h at 37°C. After washing, 100 μl of TMB solution (BioLegend) was added to each well, the reaction was stopped at 5 min with 100 μl of 1M sulfuric acid. Wells were read at 450 nm using an ELISA reader (PerkinElmer).

B Cell ELISpot

The frequency of H10-specific antibody-secreting cells (ASCs) and memory B cells was determined as previously described (24), with some modifications. In brief, MAIPSWU10 96-well plates (Millipore) were coated with 10 μg/ml of anti-human IgG (Fcγ; Jackson ImmunoResearch Laboratories). Cells were transferred in duplicate dilution series and cultured overnight at 37°C. For enumeration of ASCs, cells were plated directly without prior stimulation, whereas for memory B cells, cells were prestimulated for 4 days at 2×10^6 cells/ml with 5 μg/ml CpG-B (ODN 2006; Invivogen), 10 μg/ml Pokeweed mitogen (PWM; Sigma-Aldrich), and 1:10,000 Protein A from Staphylococcus aureus Cowan strain (SAC; Sigma-Aldrich). Plates were washed with PBS containing 0.05% Tween-20 (PBS-T), then incubated with 0.25 μg/ml biotinylated goat anti-human IgG (Fcγ; Jackson ImmunoResearch Laboratories) for total IgG determination, 0.1 μg/ml biotinylated H10 for H10-specific determination, or 0.1 μg/ml biotinylated OVA in PBS-T. The plates were washed and then incubated with streptavidin-conjugated alkaline phosphatase (Mabtech) diluted 1:1,000 in PBS-T. Spots were developed with BCIP/NBT substrate (Mabtech) and counted using an AID ELISpot Reader and version 6 of the accompanying software (Autoimmun Diagnostika). Unspecific spots were subtracted from antigen-specific wells, as defined by spots counted in samples incubated in OVA-probed wells.

Recombinant HA of H10N8 influenza A virus (H10), A/Jiangxi-Donghu/346/2013 (Medigen Inc.), and ovalbumin (OVA; Invivogen) molecules were biotinylated using the EZ-Link Sulfo-NHS-Biotinylation kit (Thermo Fisher) using a 1:1 M ratio and unreacted biotin was removed using the included Zeba Spin Desalting Columns.

Phenotypic Analysis and H10 Recall Assay of Tfh Cells

1.5×10^6 cells from indicated time points were stained with LIVE/DEAD Fixable Blue Dead Cell kit according to manufacturer's protocol (Invitrogen). Samples were surfaced stained with a panel of fluorescently labeled antibodies (Table S1 in Supplementary Material) to identify specific cell subsets. Additionally, 1.5×10^6 PBMCs were rested for 3 h and then stimulated overnight in complete media (10% FCS, 1% penicillin/streptomycin/glutamine in RPMI, all from Gibco, Stockholm, Sweden) in *U*-bottom 96-well plates with H10 peptides (15mers overlapping by 11 amino acids, 2 μg/ml) and Brefeldin A at 10 μg/ml. Cells were stained with surface-specific antibodies (Table S1 in Supplementary Material), fixed, and permeabilized using fixation and permeabilization solution (BD Biosciences) before being stained for intracellular cytokines (Table S1 in Supplementary Material). Samples were resuspended in 1% paraformaldehyde before acquisition using a Fortessa flow cytometer (BD Biosciences). Results were analyzed using FlowJo version 9.7.6. Background cytokine staining was subtracted, as defined by staining in samples incubated without peptide.

Detection of GCs *In Situ*

Extirpated LNs were snap frozen using dry ice in OCT media (Tissue-Tek) and kept in −80°C until use. Tissues were thawed to −20°C and then sectioned (8 μm) and fixed for 15 min in 2% formaldehyde in PBS. Tissues were permeabilized using tris-buffered saline with 0.1% saponin and 1% hepes buffer (permwash with pH 7.4), all future reagents were diluted in permwash. LNs were blocked with 1% FCS and then stained with anti CD3 (Dako), Ki67 (BD), and PD-1 (R&D systems). After this, biotinylated anti-mouse or anti-goat (Dako) or anti-rabbit (Vector Labs) secondary antibodies were added, which were detected by the addition of streptavidin-conjugated Alexa Fluor 405/555/647 (Invitrogen). Image tiles of entire LNs were acquired using a Nikon Eclipse Ti-E confocal microscope. GCs were defined as dense follicular structures including CD3+PD-1+ cells (light zone) and Ki67+ cells (dark zone) (**Figure 3A**). Image analysis was done using CellProfiler software (Broad Institute Inc.) with in-house algorithms. Briefly, GCs were manually identified in the program to enable automatic enumeration of PD-1+ and Ki67+ cells within the individual GCs and the area of the GCs. PD-1+ cells were almost exclusively CD3+ and Ki67+ cells were mostly CD3− (GC B cells).

CXCL13 ELISA

Undiluted plasma stored in −20°C was thawed and analyzed using a Quantikine Human CXCL13/BLC/BCA-1 Elisa (R&D systems) according to manufacturer's instructions.

Detection of Antigen-Specific GC B Cells by Flow Cytometry

2×10^6 cells from LN cell suspensions were stained with LIVE/DEAD Fixable Blue Dead Cell kit according to manufacturer's protocol (Invitrogen). Samples were then incubated with a titrated amount of H10-tetramer probe for 20 min at 4°C. H10-tetramer probes were prepared beforehand by mixing biotinylated H10 protein with streptavidin-BV421 (Biolegend) at a 4:1 M ratio. Samples were washed and stained with a surface antibody cocktail (Table S2 in Supplementary Material). Before intracellular staining (Table S2 in Supplementary Material), samples were fixed and permeabilized using the Transcription Factor Buffer Set (BD Biosciences). Samples were resuspended in 1% paraformaldehyde before acquisition using a Fortessa flow cytometer (BD Biosciences). Results were analyzed using FlowJo version 9.7.6.

Statistical Analysis

Statistical analysis was conducted by Prism Version 6.0 (GraphPad) software. All of the data are presented as the mean ± SEM. Difference between groups was analyzed as described in figure legends. A p-Value <0.05 was considered to be statistically significant.

RESULTS

mRNA Vaccine Encoding H10 Induces Protective Levels of Antibodies

Rhesus macaques were immunized either intramuscularly (IM) or intradermally (ID) with an mRNA vaccine encoding the full-length HA of H10N8 (A/Jiangxi-Donghu/346/2013) (H10) formulated in LNP (**Figure 1A**). A third group received this formulation combined with the TLR4-agonist GLA to evaluate whether an adjuvant could further enhance immune responses. All animals received a homologous prime-boost immunization at 0 and 4 weeks (**Figure 1B**). In addition, the GLA group received a third immunization at 15 weeks.

All animals induced neutralizing antibody titers against HA above the accepted level of protection for seasonal influenza vaccination, as measured by hemagglutination inhibition assay (HAI) (**Figure 1C**) (25). Although some of the animals in the ID group already showed titers at the protective level after the prime immunization, all groups had titers that exceeded this level following boost. The antibody levels persisted above this level for the remainder of the study. The titers were significantly higher in the ID group compared to the IM groups for up to 2 weeks following boost, but were similar thereafter. The GLA group did not show higher HAI titers compared to the other groups, thus indicating that the mRNA/LNP formulation itself was sufficiently immunogenic. The third immunization in the GLA

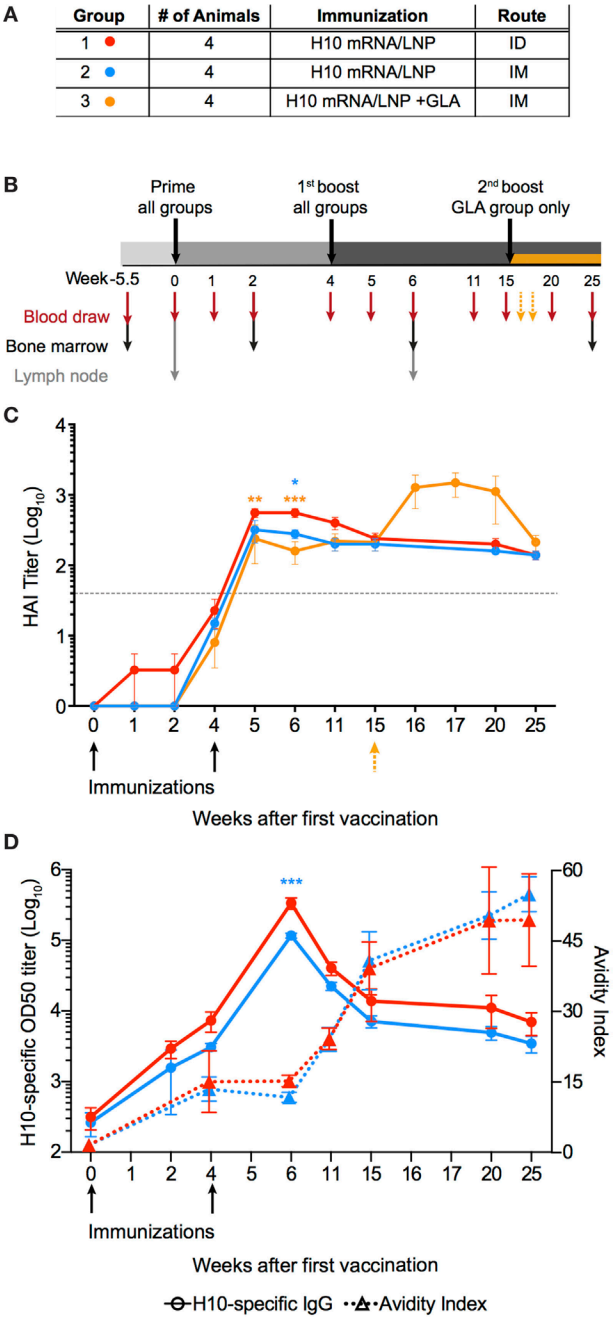

FIGURE 1 | mRNA vaccine encoding influenza H10 elicits high antibody titers by intradermal and intramuscular immunization. Rhesus macaques were vaccinated with mRNA encoding for hemagglutinin of H10N8 influenza encapsulated in LNPs. **(A)** Shows the study groups and **(B)** shows the immunization and sampling schedule. **(C)** Antibody levels over time induced in the different groups as assayed by hemagglutination inhibition assay. Arrows indicate immunizations at week 0 and 4, as well as 15 for the glucopyranosyl lipid adjuvant group only. **(D)** The left y-axis shows antigen-specific plasma IgG titers (circles) and the right y-axis shows avidity index (triangles). Arrows indicate immunizations at week 0, 4. Titers are displayed as mean ± SEM. Dotted line depicts the accepted level of protection for seasonal influenza. Statistics was calculated by two-way ANOVA with Tukey's multiple comparison test: $^*p < 0.05$, $^{**}p < 0.01$, $^{***}p < 0.001$.

group resulted in a transient increase in HAI titers, which returned to similar levels as the other groups 5 weeks later.

Antibody titer, as measured by HAI, is a function of both the quantity and quality of an antibody. However, by combining these two measurements, certain mechanistic insights into antibody development may be lost over time. Therefore, total IgG titers against H10 as well as antibody avidity were measured separately. H10-specific IgG antibody titers were induced in both IM and ID groups after prime immunization. Titers continued to increase at the time of the second immunization and peaked 2 weeks thereafter (**Figure 1D**). The avidity index of H10-specific IgG antibodies as measured by a chaotropic ELISA wash assay, did not increase between 4 and 6 weeks following the second immunization (**Figure 1D**). However, at week 11, there was a clear increase in avidity, which continued to rise until the study end. There were no significant differences in IgG titers or avidity between the ID and IM group, except in the ID group two weeks after boost, which had higher IgG titers ($p < 0.0001$). Collectively, this demonstrates that two immunizations with the H10 mRNA/LNP formulation were sufficient to induce protective and durable antibody titers.

Rapid and Sustained B Cell Responses after mRNA Vaccination

To characterize the kinetics of the B cell responses at the cellular level, the frequency of H10-specific memory B cells was determined by ELISpot (**Figures 2A–C**). Circulating H10-specific memory B cells were readily detectable 2 weeks after the prime immunization (**Figures 2A–C**). Thereafter, the number of H10-specific memory B cells contracted slightly, but expanded following the boost immunization. This was followed by a gradual decline. The GLA group showed an additional increase 2 weeks after the second boost as expected (**Figure 2C**). By study end (25 weeks), the IM and ID groups showed similar levels of circulating H10-specific memory B cells (**Figure 2D**), whereas the GLA group had higher levels due to the second boost.

Similar to the rapid induction of circulating H10-specific memory B cells, we detected H10-specific PCs in the bone marrow 2 weeks after the prime immunization in all groups tested (**Figures 2A–C**). However, in contrast to the memory B cell pool, the number of PCs remained relatively stable throughout the study. This dichotomy in fluctuation between memory B cells and PCs is in line with previous reports on protein vaccine immunizations (24).

The number of H10-specific PCs declined significantly in the IM group compared to the ID group by the end of the study (**Figure 2E**). Next, we analyzed plasmablasts in some of the animals at one week after immunization. The numbers of H10-specific plasmablasts were close to the limit of detection after the prime immunization, but increased to readily detectable levels after the boost immunization (**Figure 2F**).

We had previously shown that the priming of vaccine-specific T cells occurs in the vaccine-draining LNs (23). To investigate whether the priming of B cells also takes place at this site, vaccine-draining LNs were collected 9 days after prime immunization and compared with control LNs that did not drain the vaccine delivery site. H10-specific memory B cells and PCs were detected only in the vaccine-draining LNs (**Figures 2G,H**). This was observed with both ID and IM administration. This demonstrates that the H10 mRNA/LNP vaccine induces robust levels of vaccine-specific memory B cells and PCs following prime immunization and that these levels are sustained.

GC Formation in Vaccine-Draining LNs

Durable levels of H10-specific memory B cells and PCs coupled with a steady increase of IgG antibody avidity induced by the H10 mRNA/LNP vaccine are likely the outcome of a strong GC reaction. Since priming of H10-specific B cells appeared to be restricted to the vaccine-draining LNs, we also analyzed the expansion of GCs at this site. Using immunofluorescence and confocal imaging of cryosections, we quantified the area of GCs, the numbers of PD-1+ Tfh cells, and proliferating Ki67+ cells within individual GCs (26) (**Figure 3A**). Since the HAI titers did not differ between the three study groups, we did not stratify the data by group for this analysis. We evaluated LNs where biopsies from the same animal could be obtained both before immunization and 2 weeks post-boost. All vaccine groups were represented among the seven animals where such set of LNs was available ($n = 1$ from group 1, $n = 4$ from group 2, and $n = 2$ from group 3). We normalized the total GC area and total numbers of GC Tfh cells or GC Ki67+ cells by LN area. In five out of the seven animals, there was an increase in the GC area/LN area ratio post-immunization (**Figure 3B**). There was also an increase in GC Ki67+ cells/LN area ratio and GC Tfh cells/LN area ratio (**Figures 3C,D**). One advantage of analyzing tissue sections over cell suspensions is the option to study individual GCs in intact LN architecture rather than all GC cells combined. The area of individual GCs was significantly increased post-vaccination (**Figure 3E**). This was also observed for Tfh cells and GC Ki67+ cells within individual GCs (**Figures 3F,G**). As expected, the increase in the number of GC Ki67+ cells was greater than the increase in the number of GC Tfh cells, since GC B cells have an enhanced capacity for proliferation (9). To this end, it has been shown that the B cell/Tfh cell ratio is higher in the top neutralizers following HIV Env vaccination (27). We observed a significant increase in the Ki67+ cell/Tfh cell ratio post-vaccination in individual GCs (**Figure 3H**). There was a strong positive correlation between the number of Ki67+ cells and the area within each GC ($p < 0.001$, $R^2 = 0.4613$) (**Figure 3I**). This was also found for the number of GC Tfh cells and the GC area of individual GCs ($p < 0.001$, $R^2 = 0.5869$) (**Figure 3J**). Additionally, Tfh cell numbers correlated with Ki67+ cell numbers within each GC ($p < 0.001$, $R^2 = 0.5617$) (**Figure 3K**).

Increased levels of the chemokine CXCL13 in plasma was recently proposed as a biomarker for GC activity in the LNs (28). There was a modest elevation in CXCL13 levels detected transiently 1 week after prime vaccination, with no noticeable increase observed at 1 or 2 weeks following boost vaccination (**Figure 3L**). GC formation after prime vaccination was also investigated using flow cytometry by enumerating the frequency of BCL6+ Ki67+ GC B cells expressing H10-specific B cell receptors in the vaccine-draining LNs (**Figure 3M**). No H10-specific

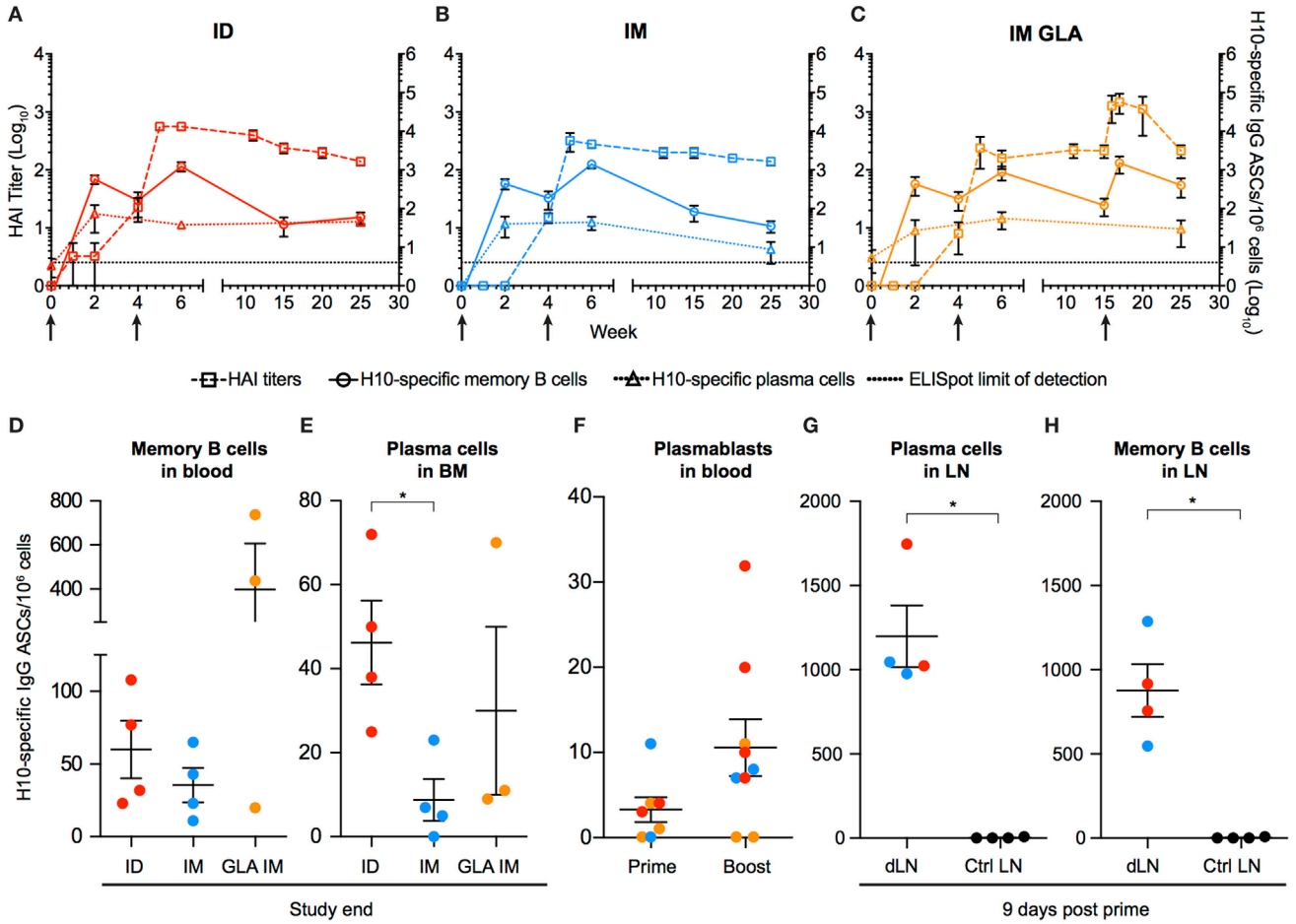

FIGURE 2 | Kinetics of vaccine-induced antibody-secreting cells (ASCs) in bone marrow and blood. **(A–C)** The left *y*-axis shows HAI titers (squares). The right *y*-axis shows H10-specific cultured memory B cells in blood (circles) and H10-specific plasma cells (PCs) in bone marrow (triangles) determined as ASCs per 1×10^6 cells. ASCs were plotted with HAI (squares) for comparison. Dotted line depicts the limit of detection for the ELISpot assay. **(D–E)** Study end values of antigen-specific memory B cells **(D)** and bone marrow PCs **(E)** between the groups. **(F)** Antigen-specific plasmablasts per 1×10^6 cells 7 days after prime and boost. **(G,H)** Naïve animals were immunized and LNs were collected after 9 days. Antigen-specific PCs **(G)** and memory B cells **(H)** in vaccine-draining LNs vs non-draining control LNs. Red colored dots corresponding to intradermal immunization, blue to IM immunization, and orange to IM immunization with glucopyranosyl lipid adjuvant adjuvant. Data show mean ± SEM. Statistics was based on Mann–Whitney *U*-test $^*p < 0.05$.

GC B cells were found in control non-draining LNs, but both unswitched IgM+ and class-switched IgM− BCL6+ Ki67+ GC H10-specific B cells were detected in vaccine-draining LNs 9 days after prime immunization (**Figure 3M**). Taken together, this suggests that the mRNA/LNP vaccine is a potent inducer of GC activity.

Circulating H10-Specific ICOS+ PD-1+ CXCR3+ Tfh Cells Are Induced after Vaccination and Correlate with Antibody Avidity

As mentioned above, cTfh cells can be identified in blood as CXCR5+ICOS+PD-1+ CD4+ T cells. The Th1-polarized CXCR3+ cTfh cell subset specifically has been shown to correlate with high-avidity antibodies 7 days after influenza vaccination in humans (17, 18). Therefore, we investigated cTfh cell subset frequencies pre-vaccination and 7 days following prime and boost. We first concluded that there was no general increase in CXCR3+ or CXCR3− total CD4+ T cells (**Figure 4A**). Next, we analyzed CXCR5+ ICOS+ PD-1+ CXCR3+/− cTfh cells within the central memory (CD28+CD95+) CD4+ T cell population (**Figure 4B**). While there was no increase in CXCR3− cTfh cells (**Figure 4C**), there was a significant increase in the number of CXCR3+ cTfh cells both after prime and boost (**Figure 4D**). No notable differences in overall cTfh cells were found between the ID and IM groups.

We investigated whether the CXCR3+ cTfh cells were expanded in the vaccine-draining LNs before entering the circulation by analyzing the set of LNs collected at nine days post-prime. The frequency of Tfh cells was increased in the vaccine-draining LNs compared to control non-draining LNs (**Figure 4E**). In addition, the majority of the Tfh cells in the vaccine-draining LNs expressed CXCR3 (**Figure 4E**). CXCR3+ Tfh cells in vaccine-draining LNs

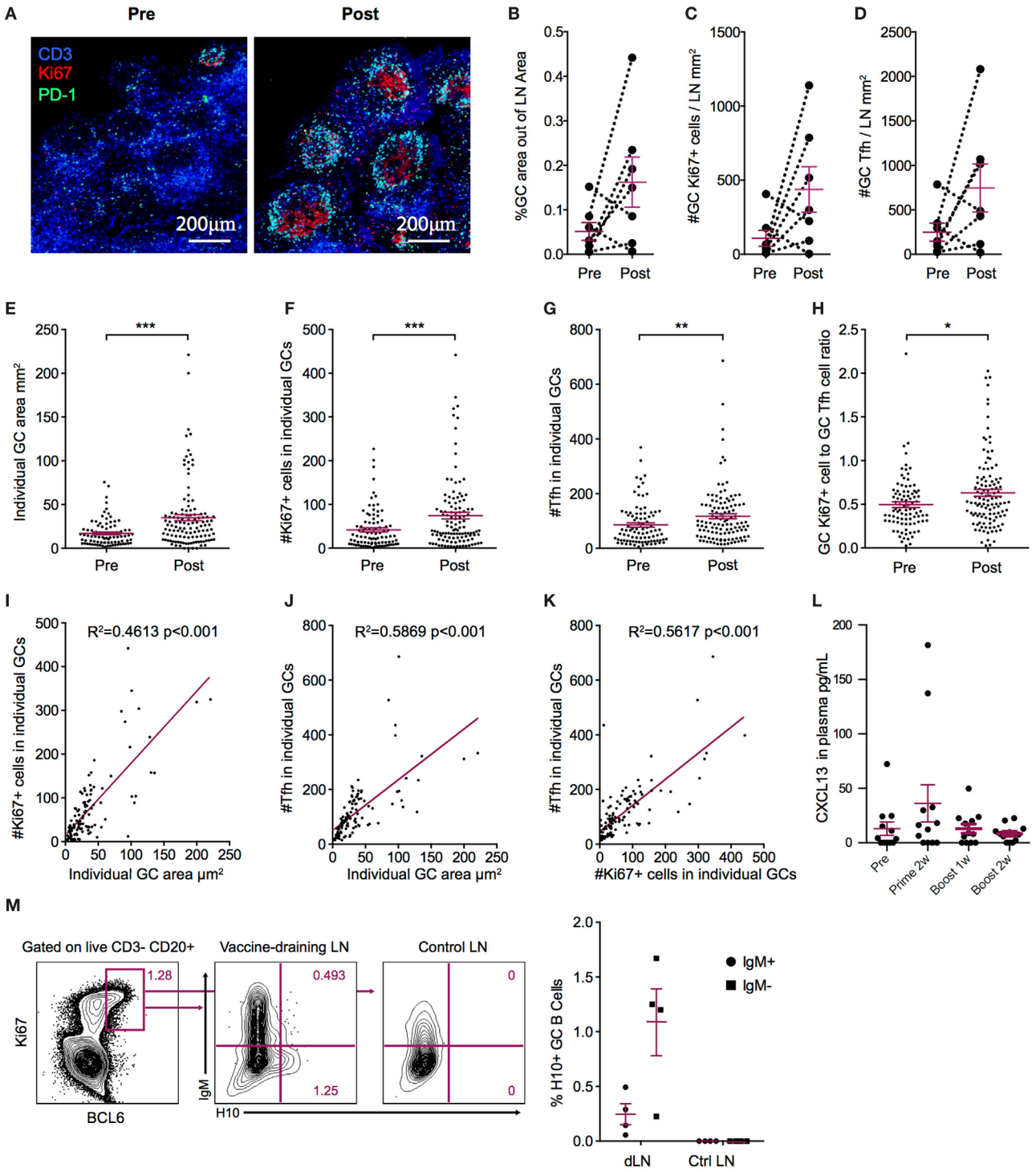

FIGURE 3 | Increased germinal center (GC) activation post influenza mRNA vaccine immunization. Axillary lymph nodes (LNs) were obtained before prime and 2 weeks after boost. A variety of readouts for GC activity were evaluated following the boost immunization. **(A)** LN sections stained for GCs before and after vaccination. Sections were stained with anti-CD3 (blue), PD-1 (green), and Ki67 (red) and follicular structures with CD3+PD-1+ T follicular helper (Tfh) and Ki67+ cells were considered GCs. Images were analyzed with CellProfiler software. **(B–D)** Each LN was analyzed for average GC area and total number of Ki67+ cells and Tfh cells, divided by the LN area for normalization. **(E–H)** Individual GCs represented by dots. **(E)** GC area. **(F)** Number of Tfh cells. **(G)** Number of Ki67+ cells. **(H)** Ki67+ to Tfh cell ratio. **(I–K)** GC architecture homogeneity was investigated by plotting GC area, Tfh, and Ki67+ cell numbers against each other. **(L)** CXCL13 in plasma at indicated time points. **(M)** Antigen-specific GC (CD3− CD20+ BCL6+ Ki67+) B cells in vaccine-draining LNs 9 days after prime vs non-draining control LNs by flow cytometry using an H10 tetramer probe. Data show mean ± SEM. Nonparametric Wilcoxon matched-pairs signed rank test was used for **(B–D)** and Mann–Whitney *U*-test for **(E–H)**. $^{*}p < 0.05$, $^{**}p < 0.01$, $^{***}p < 0.001$.

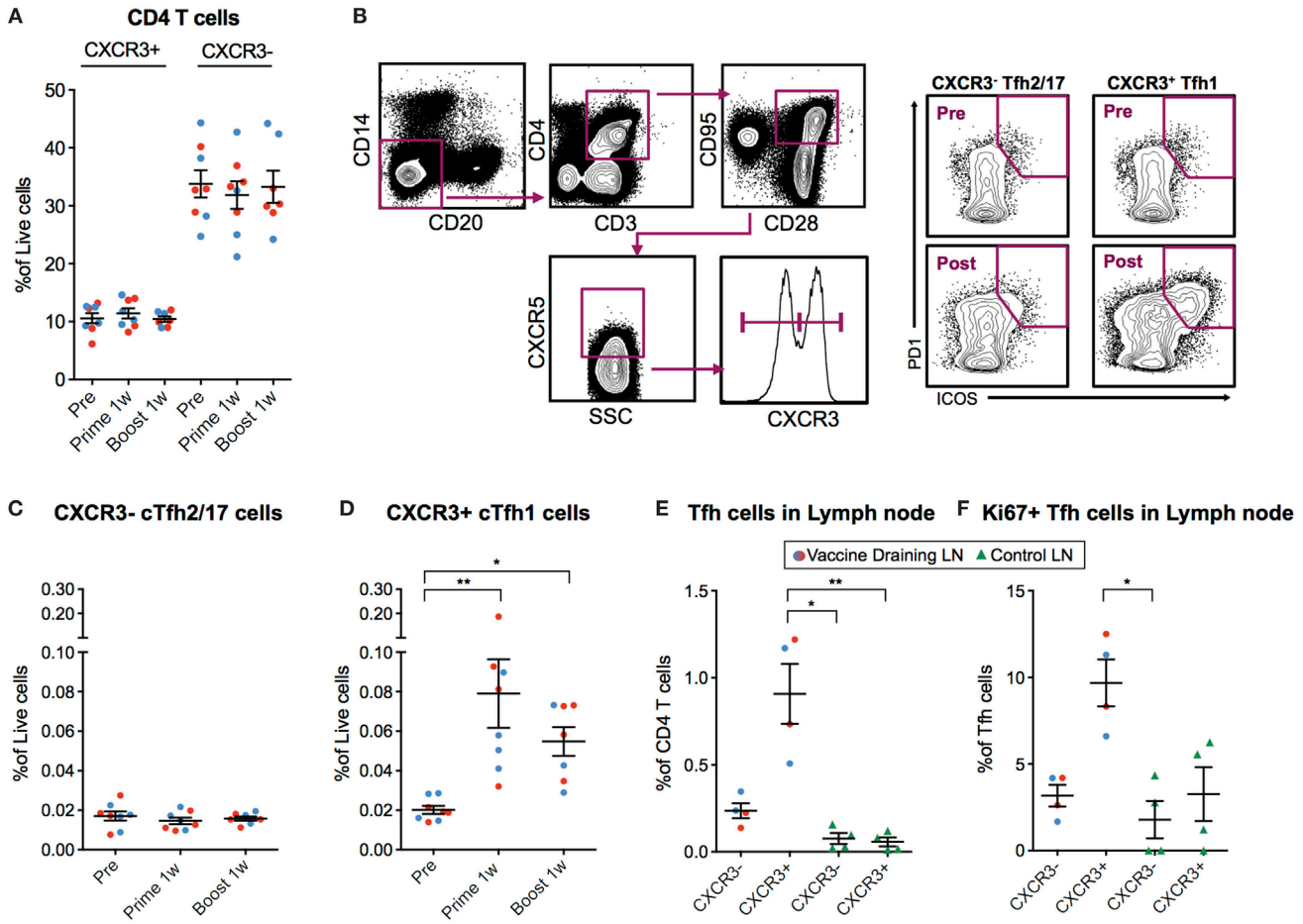

FIGURE 4 | Circulating CXCR3+ T follicular helper (cTfh) cells are detected 7 days postvaccination. **(A)** Peripheral blood mononuclear cells (PBMCs) from before vaccination and 1 week after prime and boost immunization were phenotyped for the frequency of CXCR3 +/− CD4 T cells. cTfh cells from the same time points were enumerated using the gating strategy as indicated in **(B)**. Lymph node cell suspensions after prime immunizations and non-draining LNs were phenotyped for the frequency of Tfh cells and Ki67+ cells using the gating strategy as indicated in **(B)**. **(C,D)** Show the percentage of CXCR3− vs CXCR3+ cTfh cells out of live cells, respectively. **(E)** CXCR3+/− Tfh cells out of CD4+ T Cells in vaccine- and non-draining lymph nodes (LNs). **(F)** Ki67+ cells out of CXCR3+/− Tfh cells in vaccine- and non-draining LNs. Data from the ID and IM group are shown as red and blue, respectively. Data show mean ± SEM. Statistics was based on Wilcoxon matched-pairs signed rank test for **(C,D)** and Kruskal–Wallis test with Dunn's multiple comparison for **(E,F)**, $^{*}p < 0.05$, $^{**}p < 0.01$.

also expressed Ki67 at higher levels than CXCR3− Tfh cells in the same and CXCR3+/− Tfh cells from control LNs (**Figure 4F**). Although difficult to prove, these findings indicate that the cTfh1 polarized cells found in peripheral blood after mRNA vaccine administration may have been generated in the vaccine-draining LNs.

The number of CXCR3+ cTfh cells following boost correlated with antibody avidity at week 6 and 25, with a significant correlation at week 11 ($p = 0.0432$, $R^2 = 0.5916$) (**Figure 5A**). To investigate cTfh cell specificity, PBMCs were stimulated with H10 overlapping peptides and tested for cytokine secretion by a standard intracellular cytokine assay (**Figure 5B**). There were few H10-specific cells as evidenced by IFNγ production within the total CD4+ central memory T cell population 1 week post-prime, but there was a clear increase one week following boost (**Figure 5C**). The peptide stimulation and culture procedure resulted in some loss in the resolution of CXCR5+ICOS+PD-1+CXCR3+ cTfh cellular staining. However, a significant increase in the number of IFNγ+CXCR3+ cTfh cells 1 week after prime and boost was still observed (**Figure 5D**). Collectively, this demonstrates that the H10/LNP vaccine induces H10-specific cTfh cells of the CXCR3+ Th1-polarized profile that correlate with the avidity of H10-specific IgG antibodies.

DISCUSSION

mRNA vaccines can be produced rapidly with high antigen precision, which offers an advantage over the more time-consuming process of producing live-attenuated or subunit protein vaccines (3, 29). Due to antigenic shifts and drifts, the influenza vaccine is renewed yearly to protect against the circulating strains. The mRNA platform would, therefore, be suitable for seasonal

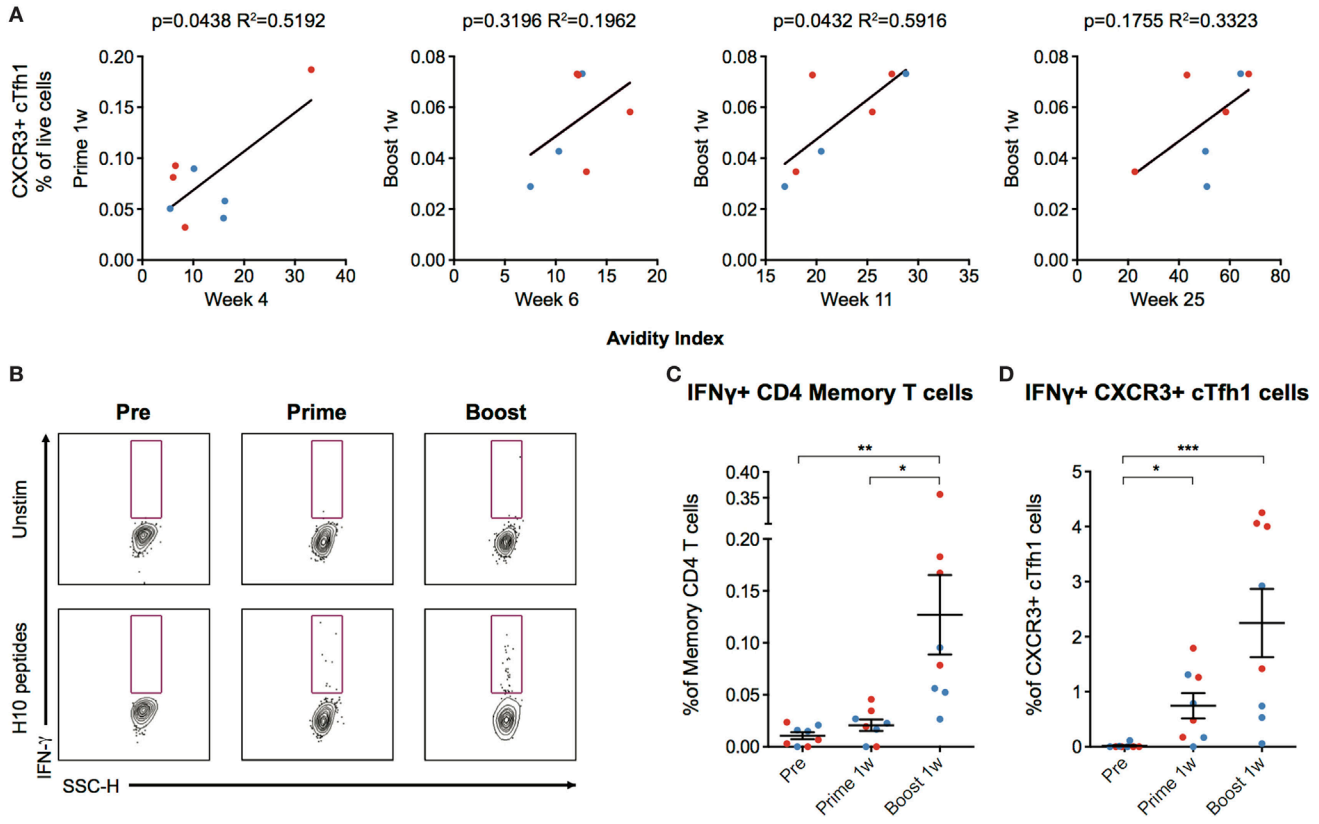

FIGURE 5 | Circulating CXCR3+ T follicular helper (cTfh) cells correlate with antibody avidity and are antigen-specific. **(A)** Correlations between circulating CXCR3+ cTfh cells after prime and boost and avidity index at indicated time points. **(B)** Peripheral blood mononuclear cells were stimulated overnight with an H10 overlapping peptide pool (15mers overlapping by 11 amino acids) to recall H10 specific T follicular helper (Tfh) cells within the memory T cell pool. Representative gates showing IFNγ+ cells within CXCR3+ Tfh cells as gated in **Figure 4B**. **(C)** Percentage of IFNγ+ cells within the overall CD4 T cell memory pool after background subtraction. **(D)** Percentage of IFNγ+ cells within the CXCR3+ cTfh cells after background subtraction. Data from the ID and IM group are shown as red and blue, respectively. Data show mean ± SEM. Statistics were based on Friedman's test with Dunn's multiple comparison $*p < 0.05$, $**p < 0.01$, $***p < 0.001$.

influenza vaccines as well as pandemic influenza strains (4, 5, 29). Although mRNA vaccines have already advanced to clinical trials, little is known of the adaptive immune profile induced by such vaccines. Therefore, this study focused on key immunological events resulting in antibody responses to an mRNA/LNP vaccine, using rhesus macaques whose immune system closely resembles that of humans. Influenza HA was chosen as the antigen due to the clinical relevance for the mRNA platform and that the levels of antibodies required for protection against seasonal influenza are well-characterized and could be benchmarked against (25). However, important to note is that all the animals in our study were naïve to influenza before immunization, which is in contrast to a clinical setting where most humans will have some degree of pre-existing immunity due to vaccination or prior infection. Therefore, the presence of cross-reactive HA-specific memory B cells and T cells may result in a stronger priming response than recorded in the rhesus macaques, although pre-existing immunity to HA of the pandemic influenza strain H10N8 used in this study is relatively rare in humans.

Seasonal influenza vaccines have been shown to induce protection in 60–90% of recipients (30, 31). In our study, we found that two animals in the ID group reached the accepted level of protection as measured by HAI titers after prime immunization. Animals across the groups reached this level after boost immunization and remained above this level for the entire 25-week study. It is plausible that all animals would have reached protective levels after the prime immunization if more time had been allowed since both the HAI and IgG titers were gradually increasing prior to the boost.

The memory B cell pool expanded quickly after prime immunization, suggesting that the mRNA platform is efficient at priming naïve B cells. H10-specific IgG titers were readily detectable 2 weeks after prime, but neutralization capacity, as measured by HAI titers, was found in a single animal at this time point. This could be explained by the initial low affinity of the memory B cell population, which would lead to insufficient neutralization.

The seeding of PCs into the bone marrow was also detected at 2 weeks post-prime immunization in all groups. The frequency of vaccine-specific PCs that were generated with the mRNA vaccine is comparable to that reported with recombinant HA protein co-administered with a strong adjuvant in the same animal model (24). Also, additional boosts did not increase the PC compartment in the bone marrow with either of the vaccine platforms (24).

Regulation of the PC pool in the bone marrow is not well known. We found that the PC levels remained relatively constant once established after the prime, despite HAI titers and H10-specific IgG titers increasing significantly post-boost. H10-specific IgG titers waned more rapidly than HAI titers. This may be explained by the observed increase in antibody avidity, which suggests increased survival of high affinity PCs and/or ongoing affinity maturation in GCs long after immunization. Supportive of the latter hypothesis is that GC B cells have been found to persist for several weeks following immunization (27). High affinity B cell clones are selected to become long-lived PCs that migrate to the bone marrow (32). Vaccine platforms that are powerful at generating antibody responses have shown superior GC formation capacities (23, 33, 34). With the clear GC activation found at 2 weeks following boost immunization, additional affinity maturation and subsequent differentiation of long-lived PCs likely continued for some time thereafter. Since affinity maturation occurs before the differentiation of PCs, it is possible that the PCs seeded early into the bone marrow were replaced by higher affinity PCs derived from the GC reaction induced by the boost immunization. This would explain the increase in antibody avidity found here.

To improve the efficacy of vaccines, there has been much focus on identifying immunological events, including biomarkers, which lead to the production of high titer protective antibodies. Tfh cells and their circulating counterparts have emerged as key players for dictating the antibody responses (35). As mentioned previously, studies have shown that CXCR3+ cTfh cells correlate with high-avidity antibodies against influenza after vaccination in humans (17, 18). It has also been shown that cTfh cell levels can predict the seroconversion in humans to influenza vaccination (36). In rhesus macaques, CXCR3+ Tfh levels in LNs were shown to correlate with avidity, longevity, and neutralization capacity of HIV vaccine-induced antibodies (20). In line with these observations, we found that the mRNA/LNP vaccine platform specifically induced an increase in CXCR3+ cTfh cells, which correlated with increased IgG avidity. This could indicate that CXCR3+ cTfh cells are important for selecting and expanding B cells of high affinity. Whether inducing cTfh cells toward the CXCR3+ phenotype is caused by the vaccine platform or the HA antigen remains to be elucidated. To this end, a type I IFN-mediated Th1-polarization after mRNA vaccine administration has been described and shown to at least partly be caused by TLR7/8 ligation (37, 38).

In vitro studies have proposed that CXCR3+ cTfh cells preferentially provide help to memory B cells compared to naïve B cells (14). However, CXCR3+ and CXCR3− Tfh cells sorted from rhesus LNs showed that there was no difference in their B cell help capacity (20). Since the vaccinated animals in our study showed a rapid induction of memory B cells, plasmablasts, and PCs, there was clearly an efficient priming of naïve B cells despite being naïve to influenza.

Furthermore, it has been proposed that the main function of CXCR3+ cTfh cells is to select memory B cells of high affinity, leading to rapid expansion of this population upon new antigen encounter (17). With regards to influenza, where the circulating strain changes every year, the ability to select for high-affinity B cell clones against the circulating strain is critical. Recent studies have shown that the cTfh cells that increase in blood after influenza vaccination represent memory Tfh cells that have been reactivated upon antigen re-exposure (19). cTfh cells can home to the LNs and differentiate into GC Tfh cells to facilitate the GC response (39, 40). Induction of vaccine-specific cTfh cells is, therefore, a central mechanism in vaccine-mediated protection, since these cells facilitate quick re-stimulation of memory B cells in the GC reaction. We found H10-specific cells within the CXCR3+ cTfh cell population. As a considerable proportion of ICOS and PD-1 expression was lost during the overnight stimulation, the number of H10-specific CXCR3+ cTfh cells may be underestimated.

Since CXCR3+ Tfh1 cells have been shown to be inferior to CXCR3− Tfh2/17 cells at providing help to naïve B cells, it was suggested that an influenza vaccine inducing Tfh2/17 cells rather than Tfh1 cells would be preferable (14, 41). However, passive transfer of antibody clones against HA in mice showed that only Th1-polarized IgG2a, and not Th2-polarized IgG1, conferred protection against lethal challenge, despite that the antibodies had the same ability to bind the antigen (35, 42, 43). This was proposed to be due to the different Fc regions of the antibodies and indicates that antibodies generated by help from cTfh cells of the Th1 subtype may be critical for the induction of protection against influenza.

In summary, we show here that an influenza mRNA/LNP vaccine induces robust GC and B cell responses, including PCs seeding into the bone marrow. Antibody avidity increases over time and is accompanied by cTfh cells of the CXCR3+ subtype. Collectively, this gives insights into the adaptive immune profile generated by mRNA/LNP vaccines and may indicate that this platform is particularly powerful for infections such as influenza that require a Th1-profile.

ETHICS STATEMENT

Chinese rhesus macaques were housed in the Astrid Fagraeus laboratory at Karolinska Institutet according to guidelines of the Association for Assessment and Accreditation of Laboratory Animal Care, and all procedures were performed abiding to the provisions and general guidelines of the Swedish Animal Welfare Agency. This animal study was approved by the Local Ethical Committee on Animal Experiments.

AUTHOR CONTRIBUTIONS

GL, FL, KB, SJ, KH, LB, HS, GC, and KL designed research. GL, SO, FL, ET, AL, FH, KB, SJ, KH, LB, HS, GC, and KL performed experiments and contributed with vaccines. GL, SO, FL, ET, FH, GC, and KL analyzed data. GL, SO, FL, ET, KB, and KL wrote the paper. All authors reviewed the paper.

ACKNOWLEDGMENTS

We wish to thank Drs. Mats Spångberg and Bengt Eriksson and their personnel at the Astrid Fagraeus laboratory at Karolinska

Institutet for expert assistance and care of the animals. We also thank Dr. Gunilla Karlsson Hedestam for advice and Tyler Sandberg and Joel Holmberg should be thanked for technical assistance. This study was partly supported by a grant to KL supported by Vetenskapsrådet. GL, SO, ET, and AL are recipients of faculty salary grants from Karolinska Institutet. AL is also supported by a grant from the China Scholarship Council.

REFERENCES

1. Pardi N, Hogan MJ, Pelc RS, Muramatsu H, Andersen H, DeMaso CR, et al. Zika virus protection by a single low-dose nucleoside-modified mRNA vaccination. *Nature* (2017) 543:248–51. doi:10.1038/nature21428
2. Richner JM, Himansu S, Dowd KA, Butler SL, Salazar V, Fox JM, et al. Modified mRNA vaccines protect against Zika virus infection. *Cell* (2017) 168:1114–25. e10. doi:10.1016/j.cell.2017.02.017
3. Ulmer JB, Geall AJ. Recent innovations in mRNA vaccines. *Curr Opin Immunol* (2016) 41:18–22. doi:10.1016/j.coi.2016.05.008
4. Petsch B, Schnee M, Vogel AB, Lange E, Hoffmann B, Voss D, et al. Protective efficacy of in vitro synthesized, specific mRNA vaccines against influenza A virus infection. *Nat Biotechnol* (2012) 30:1210–6. doi:10.1038/nbt.2436
5. Bahl K, Senn JJ, Yuzhakov O, Bulychev A, Brito LA, Hassett KJ, et al. Preclinical and clinical demonstration of immunogenicity by mRNA vaccines against H10N8 and H7N9 influenza viruses. *Mol Ther* (2017) 25:1316–27. doi:10.1016/j.ymthe.2017.03.035
6. Sahin U, Kariko K, Tureci O. mRNA-based therapeutics – developing a new class of drugs. *Nat Rev Drug Discov* (2014) 13:759–80. doi:10.1038/nrd4278
7. Coelho T, Adams D, Silva A, Lozeron P, Hawkins PN, Mant T, et al. Safety and efficacy of RNAi therapy for transthyretin amyloidosis. *N Engl J Med* (2013) 369:819–29. doi:10.1056/NEJMoa1208760
8. Plotkin SA. Correlates of protection induced by vaccination. *Clin Vaccine Immunol* (2010) 17:1055–65. doi:10.1128/CVI.00131-10
9. Victora GD, Nussenzweig MC. Germinal centers. *Annu Rev Immunol* (2012) 30:429–57. doi:10.1146/annurev-immunol-020711-075032
10. Nutt SL, Hodgkin PD, Tarlinton DM, Corcoran LM. The generation of antibody-secreting plasma cells. *Nat Rev Immunol* (2015) 15:160–71. doi:10.1038/nri3795
11. Crotty S. Follicular helper CD4 T cells (TFH). *Annu Rev Immunol* (2011) 29:621–63. doi:10.1146/annurev-immunol-031210-101400
12. Suan D, Sundling C, Brink R. Plasma cell and memory B cell differentiation from the germinal center. *Curr Opin Immunol* (2017) 45:97–102. doi:10.1016/j.coi.2017.03.006
13. Morita R, Schmitt N, Bentebibel SE, Ranganathan R, Bourdery L, Zurawski G, et al. Human blood CXCR5(+)CD4(+) T cells are counterparts of T follicular cells and contain specific subsets that differentially support antibody secretion. *Immunity* (2011) 34:108–21. doi:10.1016/j.immuni.2010.12.012
14. Schmitt N, Bentebibel SE, Ueno H. Phenotype and functions of memory Tfh cells in human blood. *Trends Immunol* (2014) 35:436–42. doi:10.1016/j.it.2014.06.002
15. Heit A, Schmitz F, Gerdts S, Flach B, Moore MS, Perkins JA, et al. Vaccination establishes clonal relatives of germinal center T cells in the blood of humans. *J Exp Med* (2017) 214(7):2139–52. doi:10.1084/jem.20161794
16. Geginat J, Paroni M, Maglie S, Alfen JS, Kastirr I, Gruarin P, et al. Plasticity of human CD4 T cell subsets. *Front Immunol* (2014) 5:630. doi:10.3389/fimmu.2014.00630
17. Bentebibel SE, Khurana S, Schmitt N, Kurup P, Mueller C, Obermoser G, et al. ICOS(+)PD-1(+)CXCR3(+) T follicular helper cells contribute to the generation of high-avidity antibodies following influenza vaccination. *Sci Rep* (2016) 6:26494. doi:10.1038/srep26494
18. Bentebibel SE, Lopez S, Obermoser G, Schmitt N, Mueller C, Harrod C, et al. Induction of ICOS+CXCR3+CXCR5+ TH cells correlates with antibody responses to influenza vaccination. *Sci Transl Med* (2013) 5:176ra132. doi:10.1126/scitranslmed.3005191
19. Herati RS, Muselman A, Vella L, Bengsch B, Parkhouse K, Del Alcazar D, et al. Successive annual influenza vaccination induces a recurrent oligoclonotypic memory response in circulating T follicular helper cells. *Sci Immunol* (2017) 2: eaag2152. doi:10.1126/sciimmunol.aag2152
20. Iyer SS, Gangadhara S, Victor B, Gomez R, Basu R, Hong JJ, et al. Codelivery of envelope protein in alum with MVA vaccine induces CXCR3-biased CXCR5+ and CXCR5- CD4 T cell responses in rhesus macaques. *J Immunol* (2015) 195:994–1005. doi:10.4049/jimmunol.1500083
21. Richner JM, Himansu S, Dowd KA, Butler SL, Salazar V, Fox JM, et al. Modified mRNA vaccines protect against Zika virus infection. *Cell* (2017) 169(1):176. doi:10.1016/j.cell.2017.03.016
22. Spangberg M, Martinez P, Fredlund H, Karlsson Hedestam GB, Sundling C. A simple and safe technique for longitudinal bone marrow aspiration in cynomolgus and rhesus macaques. *J Immunol Methods* (2014) 408:137–41. doi:10.1016/j.jim.2014.05.004
23. Liang F, Lindgren G, Sandgren KJ, Thompson EA, Francica JR, Seubert A, et al. Vaccine priming is restricted to draining lymph nodes and controlled by adjuvant-mediated antigen uptake. *Sci Trans Med* (2017) 9:eaal2094. doi:10.1126/scitranslmed.aal2094
24. Sundling C, Martinez P, Soldemo M, Spångberg M, Bengtsson KL, Stertman L, et al. Immunization of macaques with soluble HIV type 1 and influenza virus envelope glycoproteins results in a similarly rapid contraction of peripheral B-cell responses after boosting. *J Infect Dis* (2013) 207:426–31. doi:10.1093/infdis/jis696
25. Trombetta CM, Perini D, Mather S, Temperton N, Montomoli E. Overview of serological techniques for influenza vaccine evaluation: past, present and future. *Vaccines (Basel)* (2014) 2:707–34. doi:10.3390/vaccines2040707
26. Lamprecht M, Sabatini D, Carpenter A. CellProfiler™: free, versatile software for automated biological image analysis. *Biotechniques* (2007) 42:71–5. doi:10.2144/000112257
27. Havenar-Daughton C, Carnathan DG, Torrents de la Peña A, Pauthner M, Briney B, Reiss SM, et al. Direct probing of germinal center responses reveals immunological features and bottlenecks for neutralizing antibody responses to HIV Env Trimer. *Cell Rep* (2016) 17:2195–209. doi:10.1016/j.celrep.2016.10.085
28. Havenar-Daughton C, Lindqvist M, Heit A, Wu JE, Reiss SM, Kendric K, et al. CXCL13 is a plasma biomarker of germinal center activity. *Proc Natl Acad Sci U S A* (2016) 113:2702–7. doi:10.1073/pnas.1520112113
29. Hekele A, Bertholet S, Archer J, Gibson DG, Palladino G, Brito LA, et al. Rapidly produced SAM((R)) vaccine against H7N9 influenza is immunogenic in mice. *Emerg Microbes Infect* (2013) 2:e52. doi:10.1038/emi.2013.54
30. Osterholm MT, Kelley NS, Sommer A, Belongia EA. Efficacy and effectiveness of influenza vaccines: a systematic review and meta-analysis. *Lancet Infect Dis* (2012) 12:36–44. doi:10.1016/S1473-3099(11)70295-X
31. Michiels B, Govaerts F, Remmen R, Vermeire E, Coenen S. A systematic review of the evidence on the effectiveness and risks of inactivated influenza vaccines in different target groups. *Vaccine* (2011) 29:9159–70. doi:10.1016/j.vaccine.2011.08.008
32. Weisel FJ, Zuccarino-Catania GV, Chikina M, Shlomchik MJ. A temporal switch in the germinal center determines differential output of memory B and plasma cells. *Immunity* (2016) 44:116–30. doi:10.1016/j.immuni.2015.12.004
33. Ma Y, Ross AC. Toll-like receptor 3 ligand and retinoic acid enhance germinal center formation and increase the tetanus toxoid vaccine response. *Clin Vaccine Immunol* (2009) 16:1476–84. doi:10.1128/CVI.00282-09
34. Martinez-Murillo P, Tran K, Guenaga J, Lindgren G, Àdori M, Feng Y, et al. Particulate array of well-ordered HIV clade C Env trimers elicits neutralizing antibodies that display a unique V2 cap approach. *Immunity* (2017) 46(804–817):e807. doi:10.1016/j.immuni.2017.04.021
35. Michelle DLH, Linterman A. Can follicular helper T cells be targeted to improve vaccine efficacy? *F1000Res* (2016). doi:10.12688/f1000research.7388.1

SUPPLEMENTARY MATERIAL

The Supplementary Material for this article can be found online at http://www.frontiersin.org/article/10.3389/fimmu.2017.01539/full#supplementary-material.

TABLE S1 | List of antibodies used for flow cytometry.

TABLE S2 | List of antibodies used for flow cytometry.

36. Pilkinton MA, Nicholas KJ, Warren CM, Smith RM, Yoder SM, Talbot HK, et al. Greater activation of peripheral T follicular helper cells following high dose influenza vaccine in older adults forecasts seroconversion. *Vaccine* (2017) 35:329–36. doi:10.1016/j.vaccine.2016.11.059
37. Kranz LM, Diken M, Haas H, Kreiter S, Loquai C, Reuter KC, et al. Systemic RNA delivery to dendritic cells exploits antiviral defence for cancer immunotherapy. *Nature* (2016) 534:396–401. doi:10.1038/nature18300
38. Zhang X, Casartelli N, Lemoine S, Mozeleski B, Azria E, Le Ray C, et al. Plasmacytoid dendritic cells engagement by influenza vaccine as a surrogate strategy for driving T-helper type 1 responses in human neonatal settings. *J Infect Dis* (2014) 210:424–34. doi:10.1093/infdis/jiu103
39. He J, Tsai LM, Leong YA, Hu X, Ma CS, Chevalier N, et al. Circulating precursor CCR7(lo)PD-1(hi) CXCR5(+) CD4(+) T cells indicate Tfh cell activity and promote antibody responses upon antigen reexposure. *Immunity* (2013) 39:770–81. doi:10.1016/j.immuni.2013.09.007
40. Sage PT, Alvarez D, Godec J, von Andrian UH, Sharpe AH. Circulating T follicular regulatory and helper cells have memory-like properties. *J Clin Invest* (2014) 124:5191–204. doi:10.1172/JCI76861
41. Locci M, Havenar-Daughton C, Landais E, Wu J, Kroenke MA, Arlehamn CL, et al. Human circulating PD-1+CXCR3-CXCR5+ memory Tfh cells are highly functional and correlate with broadly neutralizing HIV antibody responses. *Immunity* (2013) 39:758–69. doi:10.1016/j.immuni.2013.08.031
42. DiLillo DJ, Tan GS, Palese P, Ravetch JV. Broadly neutralizing hemagglutinin stalk-specific antibodies require FcgammaR interactions for protection against influenza virus in vivo. *Nat Med* (2014) 20:143–51. doi:10.1038/nm.3443
43. Snapper CM, Paul WE. Interferon-gamma and B cell stimulatory factor-1 reciprocally regulate Ig isotype production. *Science* (1987) 236:944–7. doi:10.1126/science.3107127

Conflict of Interest Statement: The authors declare that no conflict of interest exists. The authors KB, HS, KH, LB, HS, and GC are employees of Moderna Therapeutics.

frontiers in Immunology

CORRECTION
published: 02 April 2019
doi: 10.3389/fimmu.2019.00614

Corrigendum: Induction of Robust B Cell Responses After Influenza mRNA Vaccination Is Accompanied by Circulating Hemagglutinin-Specific ICOS+ PD-1+ CXCR3+ T Follicular Helper Cells

*Gustaf Lindgren[1,2], Sebastian Ols[1,2], Frank Liang[1,2], Elizabeth A. Thompson[1,2], Ang Lin[1,2], Fredrika Hellgren[1,2], Kapil Bahl[3], Shinu John[3], Olga Yuzhakov[3], Kimberly J. Hassett[3], Luis A. Brito[4], Hugh Salter[4,5], Giuseppe Ciaramella[3] and Karin Loré[1,2]**

[1] Department of Medicine Solna, Immunology and Allergy Unit, Karolinska Institutet, Stockholm, Sweden, [2] Center for Molecular Medicine, Karolinska Institutet, Stockholm, Sweden, [3] Valera LLC, Cambridge, MA, United States, [4] Moderna Therapeutics, Cambridge, MA, United States, [5] Department of Clinical Neuroscience, Karolinska Institutet, Stockholm, Sweden

OPEN ACCESS

Approved by:
Frontiers in Immunology
Editorial Office,
Frontiers Media SA, Switzerland

***Correspondence:**
Karin Loré
karin.lore@ki.se

Specialty section:
This article was submitted to Vaccines and Molecular Therapeutics, a section of the journal Frontiers in Immunology

Received: 21 February 2019
Accepted: 07 March 2019
Published: 02 April 2019

Citation:
Lindgren G, Ols S, Liang F, Thompson EA, Lin A, Hellgren F, Bahl K, John S, Yuzhakov O, Hassett KJ, Brito LA, Salter H, Ciaramella G and Loré K (2019) Corrigendum: Induction of Robust B Cell Responses After Influenza mRNA Vaccination Is Accompanied by Circulating Hemagglutinin-Specific ICOS+ PD-1+ CXCR3+ T Follicular Helper Cells. Front. Immunol. 10:614. doi: 10.3389/fimmu.2019.00614

Keywords: mRNA vaccine, adaptive immune responses, non-human primates, influenza, T follicular helper cells, germinal centers

A Corrigendum on

Induction of Robust B Cell Responses after Influenza mRNA Vaccination Is Accompanied by Circulating Hemagglutinin-Specific ICOS+ PD-1+ CXCR3+ T Follicular Helper Cells
by Lindgren, G., Ols, S., Liang, F., Thompson, E. A., Lin, A., Hellgren, F., et al. (2017). Front. Immunol. 8:1539. doi: 10.3389/fimmu.2017.01539

In the original article, Liang et al. (44) was not cited in the article. The citation has now been inserted in the **Results, mRNA vaccine encoding H10 induces protective levels of antibodies**, paragraph two and should read:

"All animals induced neutralizing antibody titers against HA above the accepted level of protection for seasonal influenza vaccination, as measured by hemagglutination inhibition assay (HAI) (Figure 1C) as we have reported earlier (25, 44). Although some of the animals in the ID group already showed titers at the protective level after the prime immunization, all groups had titers that exceeded this level following boost. The antibody levels persisted above this level for the remainder of the study. The titers were significantly higher in the ID group compared to the IM groups for up to 2 weeks following boost, but were similar thereafter. The GLA group did not show higher HAI titers compared to the other groups, thus indicating that the mRNA/LNP formulation itself was sufficiently immunogenic.

The third immunization in the GLA group resulted in a transient increase in HAI titers, which returned to similar levels as the other groups 5 weeks later."

The authors apologize for this error and state that this does not change the scientific conclusions of the article in any way.

REFERENCES

25. Trombetta CM, Perini D, Mather S, Temperton N, Montomoli E. Overview of serological techniques for influenza vaccine evaluation: past, present and future. Vaccines (Basel) (2014) 2:707–34. doi: 10.3390/vaccines20 40707

44. Liang F, Lindgren G, Lin A, Thompson EA, Ols S, et al. Efficient targeting and activation of antigen presenting cells *in vivo* after modified mRNA vaccine administration in rhesus macaques. *Mol Ther.* (2017) 25:2635–47. doi: 10.1016/j.ymthe.2017.08.006

frontiers in Immunology

ORIGINAL RESEARCH
published: 27 November 2017
doi: 10.3389/fimmu.2017.01649

Single Dose of Consensus Hemagglutinin-Based Virus-Like Particles Vaccine Protects Chickens against Divergent H5 Subtype Influenza Viruses

Peipei Wu[1,2,3†], Jihu Lu[1,2,3†], Xuehua Zhang[1,2,3†], Mei Mei[1,2,3], Lei Feng[1,2,3], Daxin Peng[3,4], Jibo Hou[1,2,3], Sang-Moo Kang[5], Xiufan Liu[3,4] and Yinghua Tang[1,2,3]**

[1] Institute of Veterinary Immunology & Engineering, Jiangsu Academy of Agricultural Sciences, Nanjing, China, [2] National Research Center of Engineering and Technology for Veterinary Biologicals, Jiangsu Academy of Agricultural Sciences, Nanjing, China, [3] Jiangsu Co-Innovation Center for the Prevention and Control of Important Animal Infectious Disease and Zoonosis, Yangzhou, China, [4] Animal Infectious Disease Laboratory, College of Veterinary Medicine, Yangzhou University, Yangzhou, China, [5] Center for Inflammation, Immunity & Infection, Institute for Biomedical Sciences, Georgia State University, Atlanta, GA, United States

OPEN ACCESS

Edited by:
África González-Fernández, Centro de Investigaciones Biomédicas (CINBIO), Spain

Reviewed by:
Michael Schotsaert, Icahn School of Medicine at Mount Sinai, United States
Mathew Paul, St George's, University of London, United Kingdom

***Correspondence:**
Xiufan Liu
xfliu@yzu.edu.cn;
Yinghua Tang
tyinghua@yahoo.com

[†]These authors have contributed equally to this work.

Specialty section:
This article was submitted to Vaccines and Molecular Therapeutics, a section of the journal Frontiers in Immunology

Received: 03 June 2017
Accepted: 10 November 2017
Published: 27 November 2017

Citation:
Wu P, Lu J, Zhang X, Mei M, Feng L, Peng D, Hou J, Kang S-M, Liu X and Tang Y (2017) Single Dose of Consensus Hemagglutinin-Based Virus-Like Particles Vaccine Protects Chickens against Divergent H5 Subtype Influenza Viruses. Front. Immunol. 8:1649. doi: 10.3389/fimmu.2017.01649

The H5 subtype highly pathogenic avian influenza (HPAI) virus is one of the greatest threats to global poultry industry. To develop broadly protective H5 subunit vaccine, a recombinant consensus HA sequence (rHA) was constructed and expressed in virus-like particles (rHA VLPs) in the baculovirus-insect cell system. The efficacy of the rHA VLPs vaccine with or without immunopotentiator (CVCVA5) was assessed in chickens. Compared to the commercial Re6 or Re6-CVCVA5 vaccines, single dose immunization of chickens with rHA VLPs or rHA-CVCVA5 vaccines induced higher levels of serum hemagglutinin inhibition titers and neutralization titers, mucosal antibodies, IFN-γ and IL-4 cytokines in sera, and cytotoxic T lymphocyte responses. The rHA VLPs vaccine was superior to the commercial Re6 vaccine in conferring cross-protection against different clades of H5 subtype viruses. This study reports that H5 subtype consensus HA VLP single dose vaccination provides broad protection against HPAI virus in chickens.

Keywords: H5 subtype influenza virus, vaccine, consensus, virus-like particles, broad protection

INTRODUCTION

The H5 subtype highly pathogenic avian influenza (HPAI) viruses not only affect millions of domestic poultry, including chickens, ducks, and geese, as well as thousands of migratory wild birds, but also risk to the public health. Since the H5 subtype HPAI viruses emerged in Southeast Asia in 1990s and have evolved into 10 phylogenetic clades (0–9) and more than 30 subclades based on their hemagglutinin (HA) genes (1, 2). Recently, H5 HPAI viruses of subclade 2.3.4 revealed a novel propensity to reassort with neuraminidase (NA) subtypes other than N1, including H5N2, H5N5, H5N6, and H5N8 (3–5).

A strategy of culling in combination with vaccination is a major current measure to prevent and control the spread of H5 HPAI viruses in several countries and regions (6–8). In China, a series of recombinant commercial vaccines, Re1, Re3–Re8, Re10, D7, and D8, have been developed and updated since 2004 to ensure an antigenic match between the vaccines and the circulating strains (8). However, H5 subtype HPAI viruses are still the pathogen with leading potential threat for poultry industry in China. It has been an everlasting difficult situation that the existing vaccine does not

provide optimal protection against the emergence of new variants. The rapid mutation of the H5 viruses continues to bypass the time-consuming procedures of screening vaccine candidates during development of traditional inactivated whole-virus vaccine. Besides, propagation of influenza virus in the embryonated chicken eggs during preparation of inactivated virus vaccine produces biohazardous waste materials and leads potential threat to animal and human public health.

In this regard, there is an urgent need for developing an effective, broadly cross-protective, and safe H5 vaccine for use in poultry farms. Consensus sequences contain the most common residue at each position after aligning with a population of sequences. Previous studies reported that the consensus HA-based influenza vaccine candidates have elicited cross-reactive immune responses (9–12). There are commercial trivalent HA protein vaccines consisting of three insect-cell-derived full-length HAs similar to the seasonal trivalent inactivated vaccine, which represents an alternative to chicken-egg derived vaccines. In this study, we developed an insect-cell-derived consensus H5 subtype HA gene based virus-like particles (rHA VLPs) vaccine. Single dose immunization of chickens with rHA VLPs vaccines elicited serum and mucosal antibodies and cell-mediated immune responses at high levels, and induced cross-protection against subclade 2.3.4.6 and clade 7 of H5 HPAI viruses.

MATERIALS AND METHODS

Cell Lines, Viruses

Spodoptera frugiperda Sf9 insect cells (CRL-1711; ATCC, Manassas, VA, USA) were maintained in serum-free SF900II medium (Invitrogen, Carlsbad, CA, USA) at 27°C and used for production of recombinant baculoviruses (rBVs) and VLPs. Two HPAI strains (ZJ and DT) used as challenge virus were originated from clade 2.3.4.6 (A/Chicken/Zhejiang/2011, ZJ, H5N2) and clade 7 (A/Chicken/Huadong/4/2008, DT, H5N1). In this study, the recombinant Re6 commercial vaccines, and chicken sera against monovalent Re5, Re6, Re7, and Re8 antigens were purchased from Weike Biotechnology Co., Ltd., Harbin, China. Four commercial recombinant vaccines of Re5, Re6, Re7, and Re8 were inactivated whole-virus-based mineral oil emulsion vaccines (Weike). The six inner genes of four recombinant vaccine strains are derived from A/Puerto Rico/8/1934 virus (PR8, H1N1). The HA and NA genes of Re5–Re8 are derived from different subclades of H5 wild-type viruses, Re5 from strain of A/duck/Anhui/1/2006 (clade 2.3.4) (8), Re6 from virus of A/duck/Guangdong/S1322/2006 (clade 2.3.2) (8), Re7 from strain of A/Chicken/Liaoning/S4092/2011 (clade 7.2) (13), and Re8 from A/chicken/Guizhou/4/13 (clade 2.3.4.4) (14).

Preparation of Consensus HA Gene-Based Recombinant Proteins

It is known that nucleotide changes are more often because of non-sense mutations. Thus, the frequency of mutations at the nucleotide level is higher than that of the amino acid changes. Other researchers have also reported the consensus sequence derived from the nucleotide level (15). The complete open reading frame (ORF) of consensus HA was derived from the consensus nucleotide sequences of the H5 subtype HA after mega-aligning available complete H5 subtype HA sequences which isolated from 2004 to 2012 in China and originated from avian species in GenBank with Clustal V program (Lasergene, v.11; DNAStar, Madison, WI, USA). A total number of 304 HA sequences were analyzed in this study and the highest frequency of nucleotides in each position was selected to generate the consensus HA. The additional leucine zipper GCN-pII sequence was fused to the C-terminal end of the selected HA gene to form trimers as described (16). This engineered recombinant HA was named as rHA. In the results of the complete HA ORF consensus sequence after mega-aligning, the most adaption region is the HA1 head domain (61–161 aa), compared to the relatively conserved HA2 domain during evolution. The codon of the rHA ORF was optimized according to the codon usage frequency of *S. frugiperda* cell by Gene Script Co. Ltd (Nanjing, Jiangsu, China).

The optimized rHA ORF genes were cloned into the pFastBac vector plasmid to make recombinant Bacmid baculovirus DNAs using DH10Bac competent cells (rAcNPV, Invitrogen, Carlsbad, CA, USA). A recombinant baculoviruses (rBVs) expressing influenza rHA protein was generated by transfection of *Sf*9 insect cells according to the manufacturer's instruction. *Sf*9 cells were infected (1.0 multiplicity of infection, MOI) with rBVs expressing HA. After 4 days, the cell culture supernatants were harvested for preparation of vaccines.

Analysis of the Recombinant HA Proteins with Western Blot

The indirect immunofluorescence assay (IFA) was carried out to test the expression of HA in infected *Sf*9 cells after 72 h. The primary antibody was chicken anti-sera against Re6 antigen at a dilution of 1:800, and the secondary antibody was FITC labeled goat anti-chicken IgY (1:500) (Southern Biotech, Birmingham, AL, USA).

The infected insect cells were harvested after inoculation of a single rHA rBVs for 96 h, and disrupted by ultrasonic for 30 min to prepare cell lysates under the condition of maintaining the temperature at 0–4°C. The sonicated cell lysates were cleared by low-speed centrifugation (10,000 × *g* for 20 min at 4°C) to remove cell debris. The rHA VLPs in the supernatants were pelleted by ultracentrifugation (100,000 × *g* for 60 min). The sedimented particles were resuspended in phosphate-buffered saline (PBS) at 4°C overnight and further purified through a 20–30–60% discontinuous sucrose gradient at 100,000 × *g* for 2 h at 4°C (17).

For Western blot analysis to determine the expression of rHA, infected cells were dissolved in sodium dodecyl sulfate (SDS)-polyacrylamide gel electrophoresis (PAGE) sample buffer (50 mM Tris, 3% β-mercaptoethanol, 2% SDS, 10% glycerol), separated by SDS-PAGE, and then transferred to nitrocellulose membranes, subsequently probed with sera (1: 1,000) derived from Re5 and Re6 vaccine-immunized chickens, respectively. The secondary antibodies were HPR-labeled goat anti-chicken IgY (1:2,000) (SoutherBiotech, Birmingham, AL, USA).

The functionality of rHA protein incorporated into VLPs was quantified by hemagglutination assay (HA assay) using

1% (v:v) chicken red blood cells. The concentration of protein was measured by Pierce BCA Protein Assay Kit (Thermo Fisher Scientific).

Electron Microscopy

For negative staining of VLPs, sucrose gradient-purified VLPs were applied to a carbon-coated Formvar grid for 30 s. Excess VLPs suspension was removed by blotting with filter paper, and the grid was immediately stained with 1% phosphotungstic acid for 90 s. Excess stain was removed by filter paper, and the samples were examined using a transmission electron microscope.

Vaccine and Immunopotentiators

The purified recombinant HA proteins were recovered to same volume before ultracentrifugation treatment. The diluent is phosphate buffer solution (pH 7.2, PBS). The rHA (ca. 12 μg/dose) were prepared as water-in-oil emulsion with or without immunopotentiator CVCVA5, named as rHA or rHA-CVCVA5, respectively. The rHA antigen stock solutions were normalized so that the vaccine preparations had the same reciprocal of hemagglutination titers equal to or higher than 256 as measured with 1% chicken red blood cells. This range of titers is a prerequisite for the monovalent Re6 vaccine preparations with mineral oil-in-water emulsion adjuvant in the manufacture company. The preparation of rHA-CVCVA5 was followed as described in our previous reports (18–20). Briefly, the components of CVCVA5 are composed of an aqueous phase that contains L–D isoform muramyl dipeptide (MDP) (InvivoGen), poly I:C (InvivoGen), levamisole hydrochloride (Sigma) added to rHA antigen solution as well as an oil phase of resiquimod (InvivoGen) and imiquimod (InvivoGen) added to Marcol 52 mineral oil (ESSO). One volume aqueous phase was mixed with three volumes of an oil phase. The rHA vaccine preparation in water-in oil emulsion did not contain the adjuvant ingredients of CVCVA5. Preparation of the emulsion form of CVCVA5 was similar to that of the rHA-CVCVA5, having PBS substituted with the rHA antigen solutions and 10-fold concentration of the ingredients of the CVCVA5 as those in the rHA-CVCVA5. The H5-CVCVA5 vaccines were prepared by mixing the commercial H5 (Re6, Weike) subtype vaccine (v/v, 1:9) with an emulsion form of CVCVA5.

Immunization and Challenge

Groups ($n = 25$ in each group) of 3-week-old age specific pathogen-free (SPF) chickens (Leghorn breed, *Gallus gallus domesticus*) or 15- to 18-day-old age Hy Line Brown breed commercial chickens (*Gallus gallus domesticus*) were used to determine the immunogenicity and efficacy of the recombinant rHA VLPs. The vaccine test groups included the rHA with or without of CVCVA5. The commercial H5 subtype vaccines (Re6) were set as comparison control with or without CVCVA5, and a group of unvaccinated chickens as a naïve control. Serum samples from all birds were collected at 2 and 3 weeks postvaccination (PV).

Chickens from each test group were randomly selected and intranasal challenged with 100 LD_{50} (0.1 ml) H5 wild-type influenza viruses (ZJ and DT) at 3 weeks PV. These challenge viruses were derived from the clade of 2.3.4.6 (A/Chicken/Zhejiang/201, ZJ, H5N2, $n = 10$ in each challenge group) and clade 7 (A/Chicken/Huadong/4/2008, DT, H5N1, $n = 10$ in each challenge group) (19). Chickens were monitored and recorded clinical signs and body weights for 14 days post challenge (PC). All survival chickens were killed humanely at the end of monitoring experiments. Oropharyngeal and cloacal swab samples were collected at 3, 5, and 7 days PC, or collected from the dead chickens during the observation period. Virus isolation from the swab samples was performed as previously described (21).

Antibody and Cytokine Tests

Serum antibody levels were titrated by hemagglutinin inhibition (HI) assay or serum-neutralization (SN) assay in DF-1 cell (ATCC, CRL-12203) (19, 22). The SN assay was performed as following described. Briefly, all serum samples from chickens were heat-inactivated (56°C, 30 min). The twofold serial dilutions of serum samples were mixed with equal volumes of 200 mean tissue culture infective dose ($TCID_{50}$) of H5 subtype variant viruses (ZJ, DT). After 1 h incubation at 37°C, the mixtures were inoculated into the 96-well plates with a monolayer of DF-1 cells, a chicken embryo fibroblasts cell line, and then incubated to observe cytopathic effects (CPE) daily for up to 5 days. The cell death or CPE were used to determine the end-point titers that were calculated as the highest reciprocal dilution of sera at which virus infection is blocked in DF-1 cells according to the method of Reed and Muench (23).

The chicken cytokine levels of IFN-γ (Invitrogen, CA, USA) and IL-4 (USCN, Wuhan, China) in sera at 2 and 3 weeks PV were measured by commercially available ELISA kits following the manufacturer's instructions as described in our previous reports (19, 20). The mucosal antibodies from bronchoalveolar lavage fluids (BAL) were determined by an HI assay.

Cytotoxic T Lymphocytes (CTL) Assay

Cytotoxic T lymphocytes activity was measured by the lactate dehydrogenase (LDH) cytotoxicity assay kit (Takara, Kyoto, Japan), which is a non-radioactive method to detect the stable cytosolic enzyme LDH released from lysed cells. The assay was performed with the manufacturer's instruction and our previous study (19, 20). Briefly, the target cells that derived from the inbred SPF chickens (B12/B12) embryo fibroblast cells were infected for 8 h with ZJ or DT virus with MOI of 0.1. The target cells (10^4 cells in 100 μl/well) infected or uninfected were also seeded to each well. The effector cells derived from peripheral blood mononuclear cells isolated from the inbred SPF chickens at 21 days PV, which previously immunized with H5 rHA vaccine or the commercial H5 subtype vaccine (Re6) with or without CVCVA5 adjuvants, respectively. Various amounts of effector T cells were added to each well. Each cell sample was plated in triplicates. Microtiter plates were centrifuged at 250 × *g* for 5 min and incubated in a humidified chamber at 37°C, 5% CO_2. After 4-h incubation, the supernatants were harvested, followed by the addition of the substrate tetrazolium salt. The OD values were read at 490 nm in an enzyme-linked immunosorbent assay reader. The specific LDH activity release was calculated by using the following formula: (experimental release − spontaneous release)/(maximum release − spontaneous release) × 100.

Statistics

Experimental data are presented as mean ± SD of the mean. Prism 7 (GraphPad Software, Inc., San Diego, CA, USA) was used for data analysis. The statistical significance was analyzed with Student's *t*-test or a one-way analysis of variance. Comparisons used to generate *P* values are indicated by horizontal lines (*$P < 0.05$; **$P < 0.01$; ***$P < 0.001$).

Ethics Statement

All animal studies were carried out in accordance with the recommendations in the National Guide for the Care and Use of Laboratory Animals. The protocol (VMRI-AP150306) was approved by the Review Board of National Research Center of Engineering and Technology for Veterinary Biologicals, Jiangsu Academy of Agricultural Sciences and Yangzhou University. The surgery and euthanasia were performed under anesthesia with sodium pentobarbital solution (100 mg/kg body weight) *via* an intravenous route to minimize suffering. All experiments involved in the live H5 subtype viruses were performed in the biosafety level 3 laboratory facilities. At the end of experiments, the discarded live viruses, wastes, and infected animal carcasses were autoclaved and incinerated to eliminate biohazards.

RESULTS

Production and Analysis of rHA-Based Influenza VLPs

The recombinant HA proteins were produced in insect cells, which were infected with rBVs expressing the H5 subtype AIVs consensus HA gene with poly-basic residues at the cleavage site. The expression of rHA proteins was observed with indirect IFA in *Sf*9 insect cells 72 h after infection with rHA rBVs (**Figure 1**),

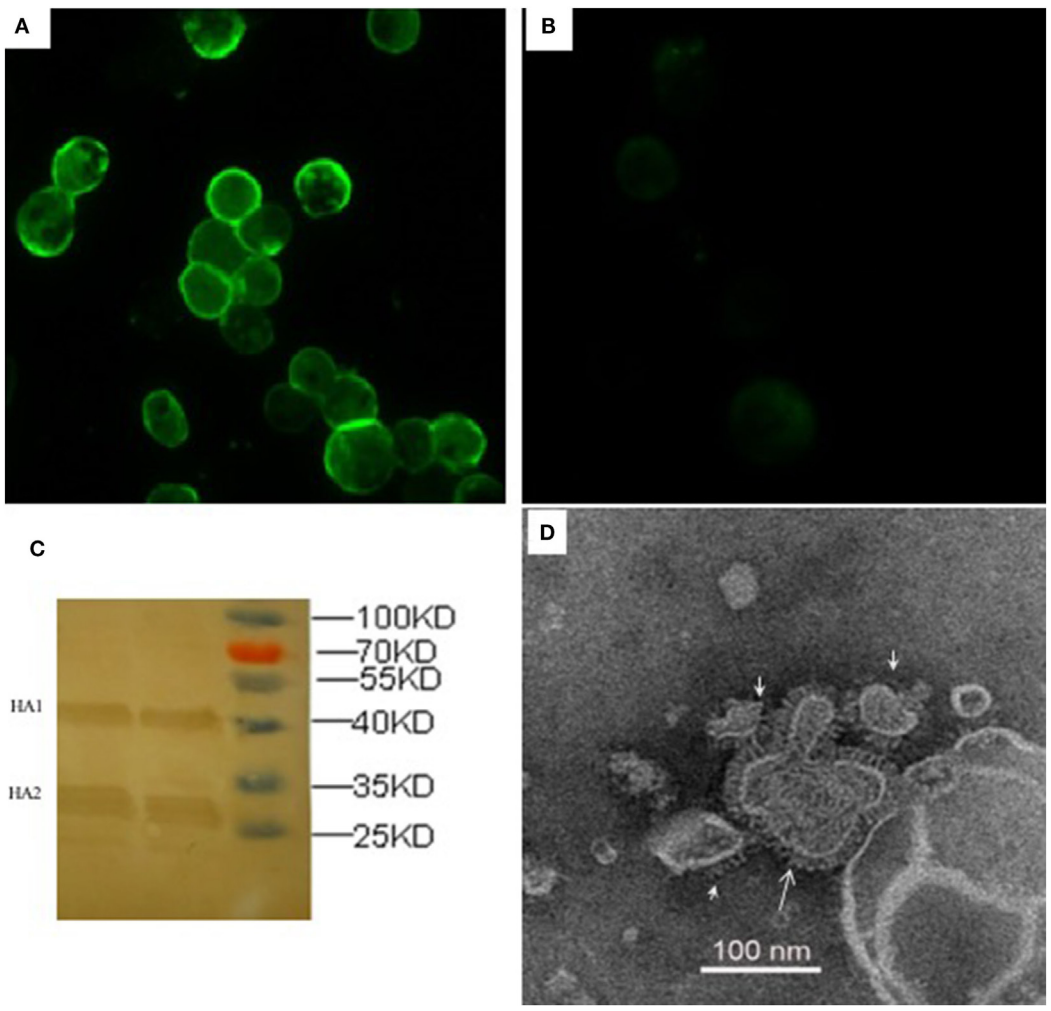

FIGURE 1 | Characterization of recombinant consensus HA (rHA) proteins by indirect immunofluorescence assay (IFA), western blotting, and electron microscopy. IFA was analyzed in *Sf*9 cells infected with recombinant baculoviruses (rBVs) of HA **(A)** or only empty baculoviruses **(B)** after 72 h. The antibodies used in the test include chicken sera of anti-H5 (Re6 vaccine) for the primary reaction and goat anti-chicken IgY for the secondary antibody detection. **(C)** Western blotting analysis of the expression of recombinant HA proteins. **(D)** Negative staining electron microscopy of rHA-based influenza VLPs produced from the *Sf*9 cells infected with rBVs expressing a single consensus recombinant HA gene.

whereas there was no specific fluorescence in control baculovirus infected cells (**Figure 1**). As for further evidence, two major visible bands, HA1 and HA2 fragments, were presented in the Western blot analysis which is consistent with a previous study (24). The functionality of rHA incorporated into VLPs (rHA VLPs) was assessed by the hemagglutination assay with 1% cRBC. No activity of hemagglutination was observed when the VLPs were denatured by heat treatment at 100°C for 10 min (data not shown). The reciprocal hemagglutinin titers of the rHA rBV-infected *Sf*9 cell culture supernatants reached to 64 before treating with ultrasonic, and increased to 2,048 after ultrasonic treatment. The increment in HA titers was speculated due to the release of rHA VLPs from the cellular membranes after the ultrasonic treatment of cell lysis. The total protein concentration of culture supernatants was 120 μg/mL measured by the BCA kit.

The size and morphology of rHA VLPs were examined by electron microscopy (**Figure 1**). The morphology of VLPs resembles that of influenza virus particles, and the spikes were observed on their surfaces which is characteristic of influenza virus HA proteins on virions.

H5 rHA Displays Cross-Reactivity to Immune Sera Induced by H5 Vaccines

The antigenicity of H5 rHA vaccine was determined *via* HI tests in cross reactions with sera raised by antigenically different H5 vaccines, and compared to those reactions with the viral antigens of Re5, Re6, Re7, and Re8. Except the HI titers from the homologous pairs of serum and antigen, the HI titers against the rHA antigen were higher than those that of the viral antigens, the Re5, Re6, Re7, and Re8, cross reacted with sera induced by Re5, Re6, Re7, and Re8 vaccines, respectively. Compared to the sera derived from Re5, Re6, and Re8 vaccines, the serum derived from Re7 vaccine was poorly reactive to rHA and other viral antigens (**Figure 2**).

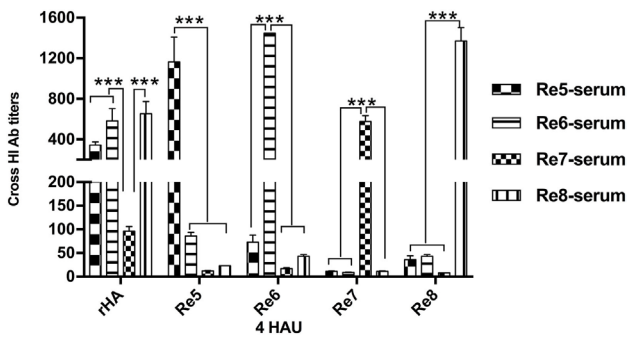

FIGURE 2 | Hemagglutinin inhibition (HI) cross-reactivity of H5 rHA protein to sera raised by different vaccines. The HI tests were carried out with the recombinant protein of consensus H5 HA (rHA), viral antigens of Re5, Re6, Re7, and Re8 as 4 hemagglutinin units (HAU)/25 μl in three replicates. The six inner genes of Re5, Re6, Re7, and Re8 vaccine strains are derived from A/Puerto Rico/8/1934 virus (PR8, H1N1), the HA and neuraminidase genes of Re5 from strain of A/duck/Anhui/1/2006 (clade 2.3.4), of Re6 from virus of A/duck/Guangdong/S1322/2006 (clade 2.3.2), of Re7 from A/Chicken/Liaoning/S4092/2011 (clade 7.2), and of Re8 from A/chicken/Guizhou/4/13 (clade 2.3.4.4). The statistical significance was analyzed with Student's *t*-test. ***$P < 0.001$.

H5 rHA VLPs Vaccines Elicit Immune Responses in Chickens

To determine whether influenza H5 rHA VLPs induce immune responses specific to influenza virus HA protein, groups of 3-week-old SPF chickens were subcutaneously vaccinated one time with influenza rHA vaccine (12 μg/dose) with or without immunopotentiator (rHA, rHA-CVCVA5), and Re6 vaccine in the presence or absence of immunopotentiator as controls (Re6, Re6-CVCVA5). The levels of serum antibody against different antigens were measured by HI assay at 2 and 3 weeks after a single dose vaccination. Using 4 HA units (HAU) of Re6 as a testing antigen, the HI titers of chickens shot with the Re6 vaccine were higher than those that induced by the rHA vaccine, similarly, HI titers induced by Re6-CVCVA5 vaccine were higher than those by the rHA-CVCVA5 vaccine at 2- or 3-week PV (**Figure 3A**). However, the HI titers raised by vaccination with rHA-containing vaccines were higher than those induced by Re6-containing vaccines when measured with the 4 HAU of Re7, Re8, or rHA testing antigens, respectively (**Figures 3B–D**).

The efficacy of rHA vaccines was also assessed in 15- to 18-day-old commercial chickens. Consistent with the results of SPF chickens, lower HI levels were observed in the rHA-containing vaccine groups compared to those in the Re6-containing vaccines groups, as measured by using 4 HAU of the Re6 as a testing antigen. In contrast, the HI antibody titers in rHA-containing vaccine groups were higher than those of the Re6-containing vaccine groups when determined with the rHA and Re7 antigens, respectively. Similar levels of HI antibodies against the Re8 antigen were observed in chickens which received Re6- or rHA-containing vaccines (**Figures 3E–H**).

H5 rHA VLPs Vaccination Induces Enhanced Levels of Serum Virus Neutralization Titers and Mucosal Antibodies in SPF Chickens

Serum-neutralization activity against the variants of ZJ or DT virus strains was carried out. Serum samples from the chickens that were immunized with rHA VLPs vaccine in the presence or absence of CVCVA5 and Re6 plus CVCVA5 vaccines showed significantly higher neutralization titers than those of the chickens that were immunized with Re6 vaccine without immnopotentiators at 2 and 3 weeks PV (**Figures 4A,B**).

The mucosal antibody titers in the BAL fluids at 3 weeks PV were also measured by HI assay with Re6, Re7, Re8, and rHA VLPs as 4 HAU antigens. Higher HI titers in BAL fluids from the rHA-CVCVA5 or Re6-CVCVA5 vaccine groups were observed compared to those groups that received rHA or Re6 vaccine without immunopotentiators (**Figure 4C**).

H5 rHA VLPs Vaccination Induces Increased Levels of Serum Cytokines and CTL Responses in SPF Chickens

To investigate the induction of cytokines after vaccination, we measured the levels of IFN-γ and IL-4 in serum at 2 and

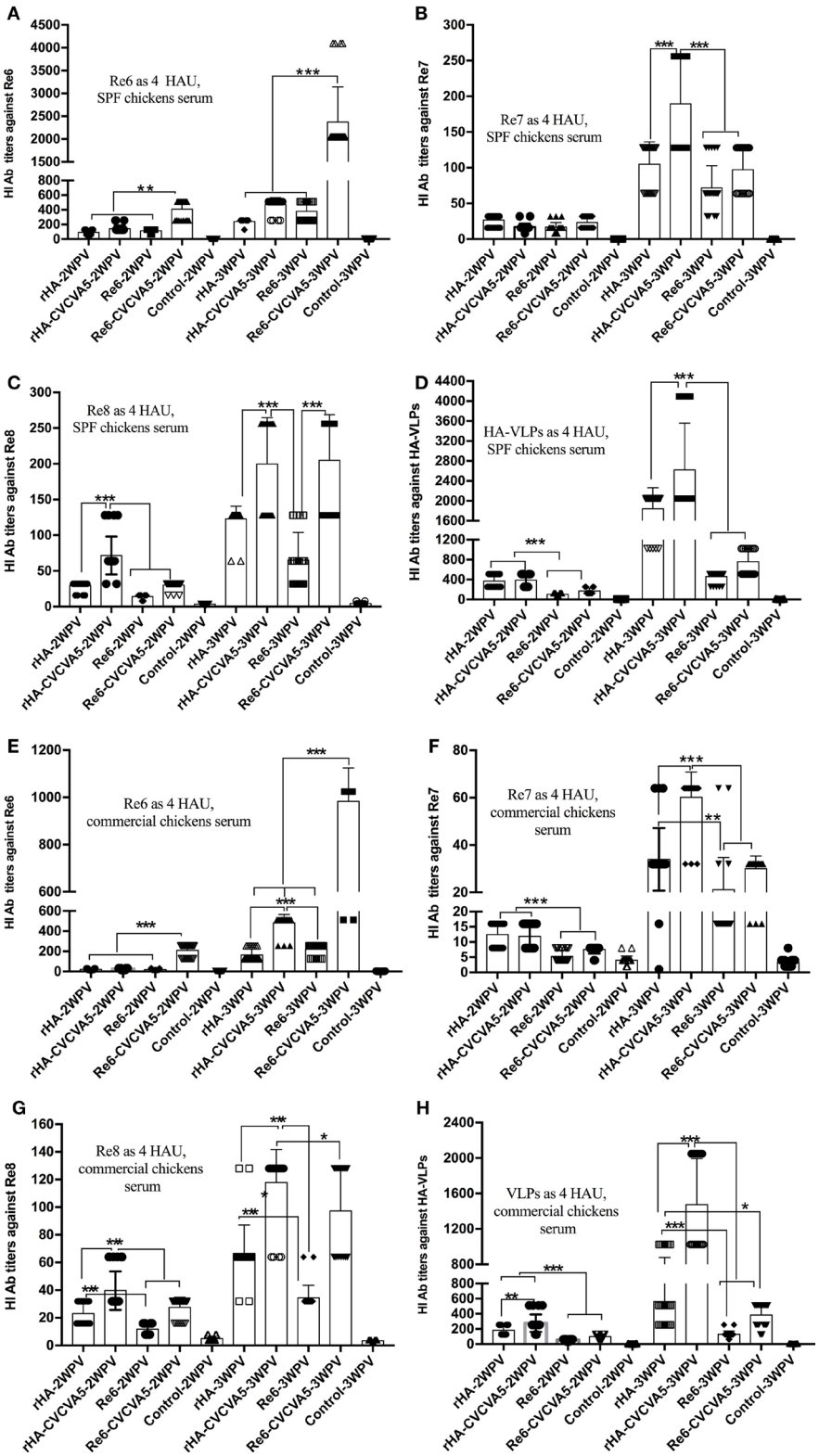

FIGURE 3 | Hemagglutinin inhibition (HI) titers of immune sera from vaccinated specific pathogen-free (SPF) and commercial chickens. The SPF **(A–D)** or commercial **(E–H)** chickens were subcutaneously immunized with rHA VLPs vaccine with (rHA-CVCVA5) or without immunopotentiator (rHA), or Re6 vaccine with (Re6-CVCVA5) or without immunopotentiator (Re6). The serum samples were collected at 2- and 3-week postvaccination. The HI titers of SPF chickens sera were measured with 4 HAU testing antigens of Re6 **(A)**, Re7 **(B)**, Re8 **(C)**, and rHA **(D)**, and commercial chickens sera with 4 HAU antigens of Re6 **(E)**, Re7 **(F)**, Re8 **(G)**, and rHA **(H)**. The statistical significance was analyzed with Student's *t*-test or a one-way analysis of variance. $^{**}P < 0.01$, $^{***}P < 0.001$.

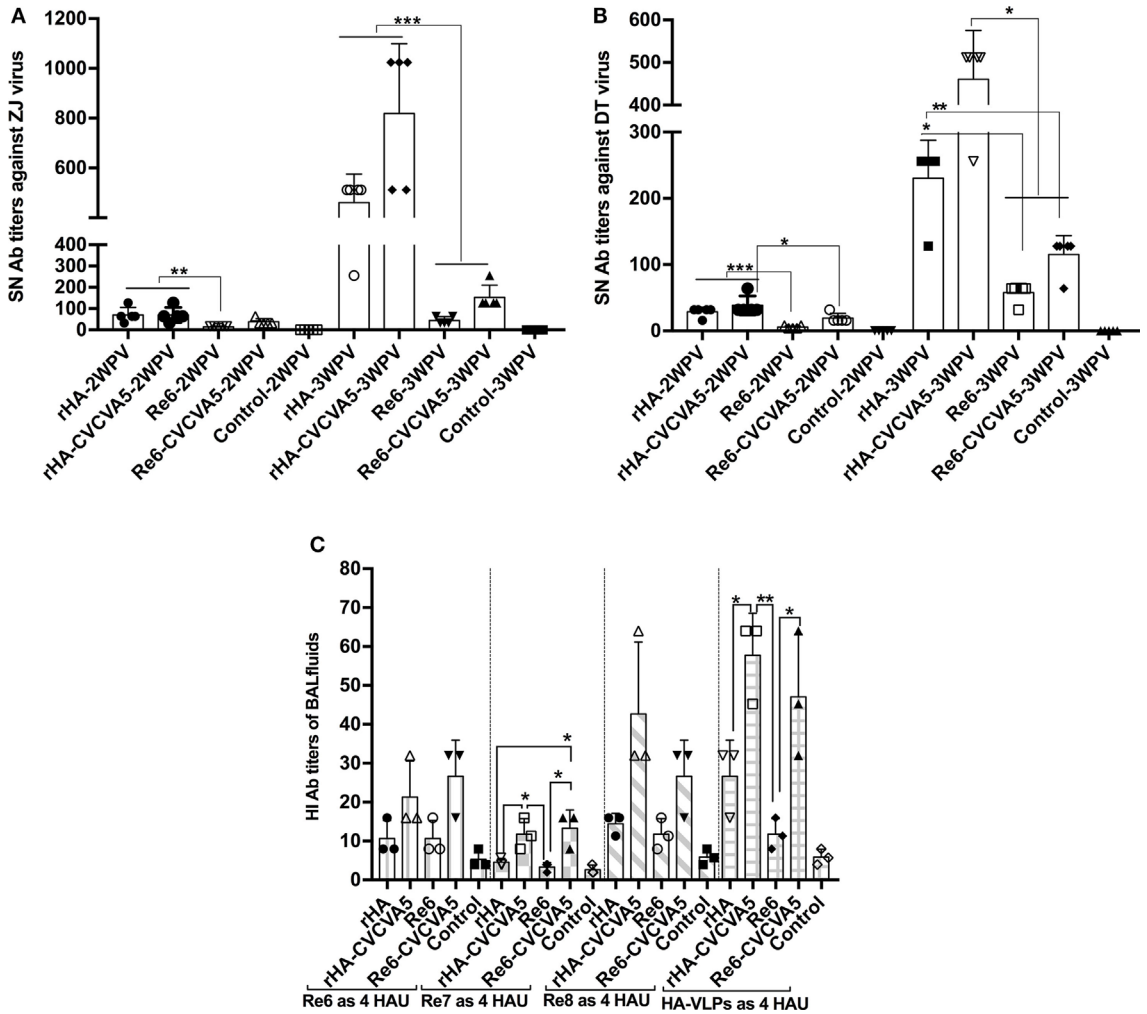

FIGURE 4 | Serum-neutralization (SN) titers and hemagglutinin inhibition (HI) antibody titers in bronchoalveolar lavage (BAL) fluids. SN assays were performed in DF-1 cells. A fixed viral solution (200 $TCID_{50}$, ZJ, or DT viruses) was reacted with the same volume of twofold serial diluted serum solutions. The pooled (five pooled in one) sera samples ($n = 5$) were derived from each group of the specific pathogen-free chickens vaccinated with rHA or Re6 vaccine with or without adjuvant. Both DT (clade 7) and ZJ (subclade 2.3.4.6) viruses were isolated from chickens **(A,B)**. The mucosal antibodies derived from BAL fluids ($n = 3$) were measured by HI assay with 4 HAU of Re6, Re7, Re8, and rHA at 3-week postvaccination **(C)**. The statistical significance was analyzed with Student's *t*-test or a one-way analysis of variance. $^{**}P < 0.01$, $^{***}P < 0.001$.

3 weeks PV. Both levels of IFN-γ and IL-4 were significantly increased in the chickens received rHA-CVCVA5 or Re6-CVCVA5 vaccine, and slightly increased in the rHA vaccine group (**Figures 5A,B**). The increased magnitude of IFN-γ was higher than that of the IL-4.

Cytotoxic T lymphocytes play an important role in the control of virus infections. The adjuvanted rHA and Re6 vaccines elicited a robust CTL response compared to those of the non-adjuvanted rHA and Re6 vaccines. Further analysis demonstrated that vaccination of chickens with the adjuvanted rHA vaccine induced slightly higher levels of the CTL responses than those by vaccination with Re6 vaccines in the presence or absence of adjuvants. The CTL immune responses from the Re6 vaccine groups were low which was similar to that of the control groups (**Figures 5C,D**).

H5 rHA VLPs Vaccine Confers Cross-Protection against Heterogeneous Strains

To investigate whether rHA vaccine could confer cross-protection against a lethal challenge with heterogeneous virus, the rHA-vaccinated chickens were challenged with ZJ (clade 2.3.4.6) and DT (clade 7) viruses, respectively (**Figure 6**). After a lethal ZJ virus challenge, all birds survived in vaccine groups of rHA, rHA-CVCVA5, and Re6-CVCVA5 (**Figure 6A**). In contrast, only 30% (3/10) chickens survived in the Re6 vaccine group, and all chickens died of infection in the control group. In the challenge test with DT virus, all chickens survived the infection in the rHA and the rHA plus CVCVA5 vaccine groups. Two out of ten chickens were dead in the groups of Re6-CVCVA5. Only two out of ten chickens survived in the Re6 (clade 2.3.2) vaccine group and no chicken survived in the control group (**Figure 6B**).

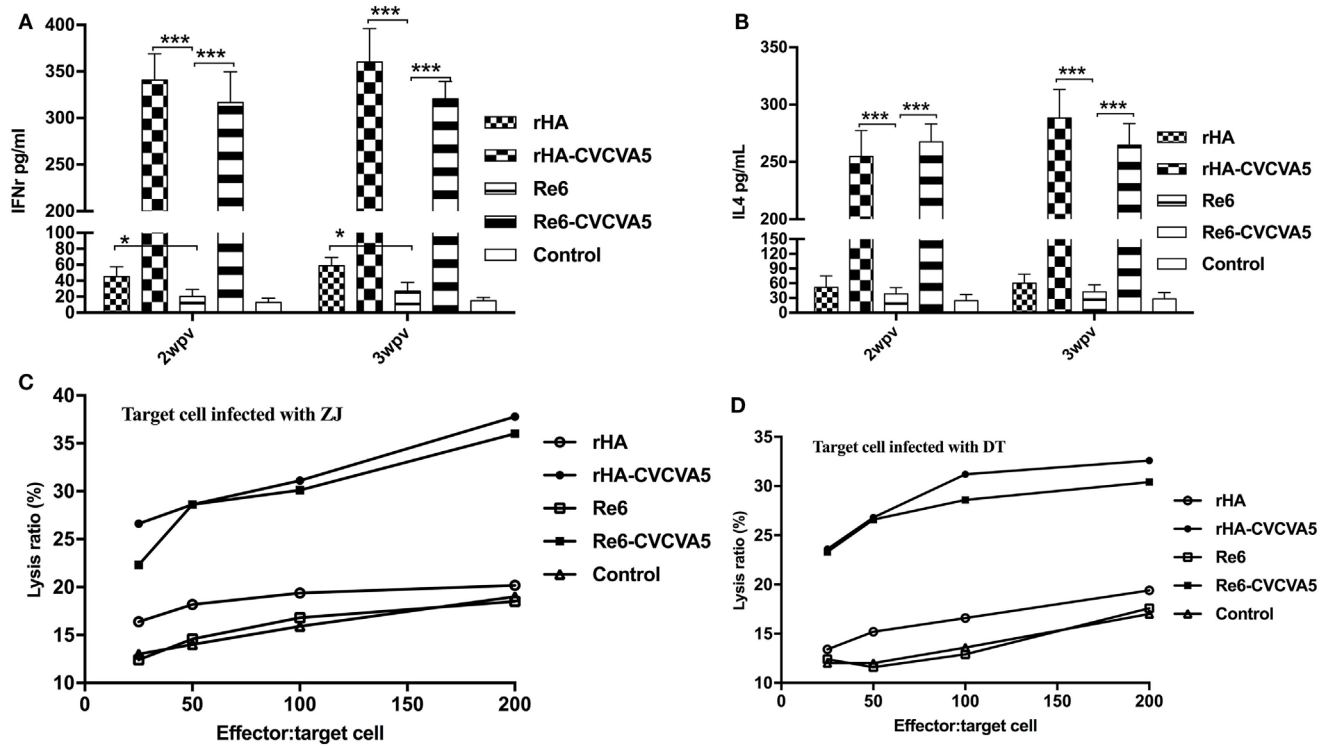

FIGURE 5 | Levels of cytokines in sera and cytotoxic T lymphocytes activity in peripheral blood mononuclear cells after vaccination. The cytokines levels of IFN-γ **(A)** and IL-4 **(B)** in specific pathogen-free (SPF) chickens sera were determined by ELISA Kits at 2- and 3-week postvaccination from each group ($n = 3$). Cytotoxic T cells were derived from vaccinated inbred chickens. Inbred chicken embryo fibroblasts infected with DT or ZJ H5 subtype AI viruses were used as target cells. PBMCs derived from the SPF chickens vaccinated with rHA or Re6 vaccine with or without adjuvants, or from control group, were used as effector cells **(C,D)**. $^{*}P < 0.05$, $^{***}P < 0.001$.

After challenge with ZJ virus, the body weight still slightly increased in chickens received with the rHA and the rHA-CVCVA5 vaccines. The birds in the rHA-CVCVA5 vaccine group gained the most weight among all challenge groups. The body weights of the chickens were nearly unchanged in the Re6-CVCVA5 vaccine group during 14 days of the monitoring period. In contrast, the chickens significantly lost weight in the Re6 vaccine and the control groups after challenge with ZJ virus (**Figure 6C**). However, only the rHA-CVCVA5 vaccine group showed a weight gain after challenge with DT virus. The birds in the rHA VLPs and Re6-CVCVA5 groups slightly lost weight at day 8–11, and then quickly recovered to initial weight during the 14-day of observation period. Similar to the challenge with ZJ virus, the chickens also exhibited rapid weight loss in the groups of the Re6 vaccine and control after challenge with DT virus (**Figure 6D**).

The excreted viruses *via* oropharynx and cloaca were analyzed to determine the virus replication at 3, 5, and 7 days PC with ZJ and DT viruses (**Table 1**). After ZJ virus challenge, virus shedding was not detected in chickens from the rHA-CVCVA5 vaccine group, and one bird was positive of virus isolation in both the rHA and the Re6-CVCVA5 groups. All birds were shedding viruses in the Re6 vaccine and control groups. A similar pattern of virus shedding was observed after DT virus challenge (**Table 1**). Chickens in the rHA-CVCVA5 group were free from virus detection. Three chickens in the rHA group and four chickens in the Re6-CVCVA5 group recovered viruses from swab samples. All birds in the Re6 vaccine and control groups excreted viruses PC.

DISCUSSION

In this study, we investigated immune responses induced by consensus HA sequence-based VLPs vaccine (rHA) in chickens, including serological and mucosal HI antibodies, cytokines, and induction of cross-protection against two heterologous subclades of H5 subtype AI virus challenge.

Development of vaccine based on the consensus HA sequences is one of the potential strategies to induce broadly protective immune responses against influenza viruses with high mutation rates and antigenic diversities. Consensus sequences encode the most common residues found at each position for the selected population, which are compatible with the site mutation residues in different clade viruses. We have compared the consensus HA sequence from the amino acid residues with that from the nucleotide level, and there were slightly differences mainly located at 310–340 amino acid residues (data not shown). It is expected

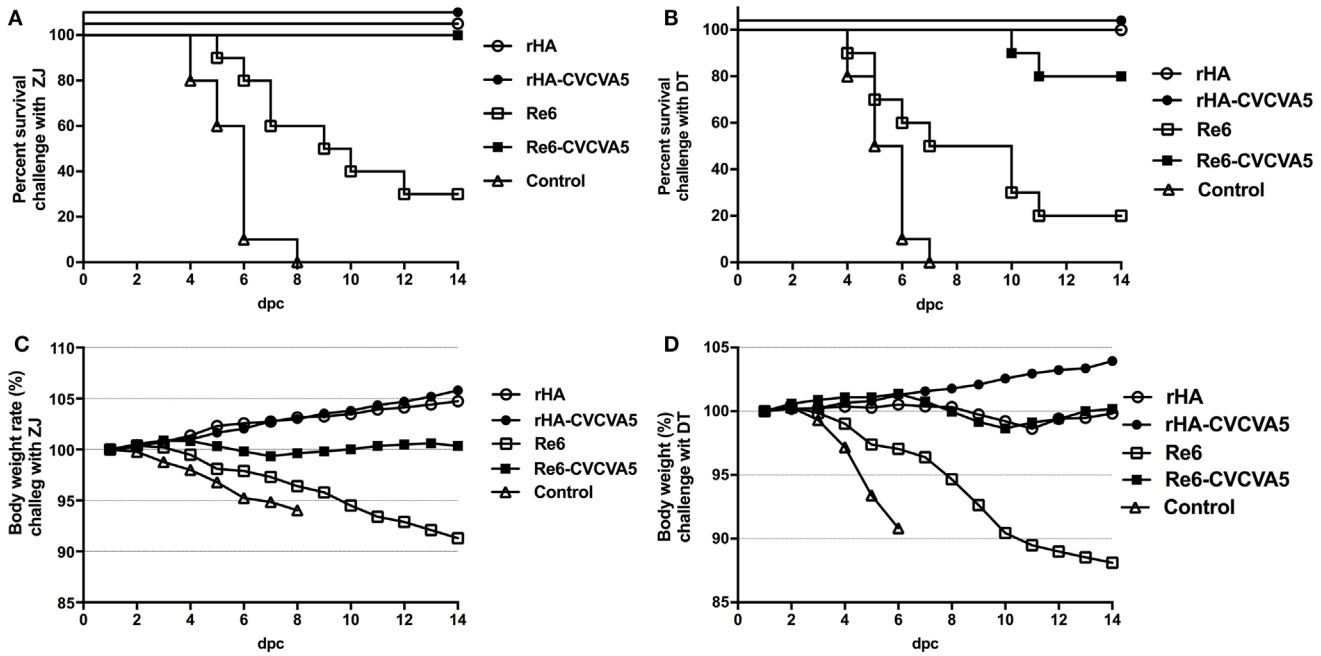

FIGURE 6 | Survival rates and body weight changes of the specific pathogen-free (SPF) chickens after heterologous virus challenge. At 3 weeks postvaccination, groups of SPF chickens (n = 10) were intranasally challenged with 100 LD_{50} viruses of ZJ (A/Chicken/Zhejiang/2011, H5N2, subclade of 2.3.4.6) **(A)**, or DT (A/Chicken/Huadong/4/2008, H5N, clade 7) **(B)**, and the clinical symptoms or death, and body weight changes were daily monitored and recorded for 14 days post challenge **(C,D)**.

TABLE 1 | Virus shedding and clinical symptoms after challenge of chickens.

Group	Challenge virus	Oropharyngeal swab (virus shedding number/total number)			Cloacal swab (virus shedding number/total number)			Total virus shedding number/total number	No. clinical symptoms
		3 dpc	5 dpc	7 dpc	3 dpc	5 dpc	7 dpc		
rHA	ZJ	0/10	1/10	1/10	0/10	1/10	1/10	1/10	0
rHA-CVCVA5	ZJ	0/10	0/10	0/10	0/10	0/10	0/10	0/10	0
Re6	ZJ	3/10	3/10	6/10	3/10	6/10	10/10	10/10	9
Re6-CVCVA5	ZJ	0/10	1/10	0/10	0/10	1/10	1/10	1/10	0
Control	ZJ	10/10	10/10	10/10	10/10	10/10	10/10	10/10	10
rHA	DT	2/10	2/10	3/10	2/10	3/10	3/10	3/10	0
rHA-CVCVA5	DT	0/10	0/10	0/10	0/10	0/10	0/10	0/10	0
Re6	DT	5/10	6/10	7/10	4/10	7/10	10/10	10/10	9
Re6-CVCVA5	DT	1/10	2/10	3/10	2/10	3/10	4/10	4/10	4
Control	DT	10/10	10/10	10/10	10/10	10/10	10/10	10/10	10

ZJ virus is the abbreviation virus strain name of A/Chicken/Zhejiang/2011 (H5N2), attributed to the subclade of 2.3.4.6, and DT is virus of A/Chicken/Huadong/4/2008 (H5N1), clade 7. The oropharyngeal and cloacal swab samples were collected at 3, 5, and 7 days post challenge. Virus positivity or shedding was determined by inoculating each swab solution into 3 eggs of 10-day-old specific pathogen-free chicken embryos. The virus isolation positive swab means one or more of the inoculated egg allantoic fluids with reciprocal of hemagglutination titers higher than 4. rHA, H5 rHA VLPs vaccine. Re6, a commercial vaccine strain with HA and neuraminidase from A/duck/Guangdong/S1322/2006 (H5N1, clade 2.3.2) and six inner genes from PR8 (H1N1).

that consensus sequences at nucleotide levels would be stable in mRNA translation. Besides, we have developed a wild-type Re6 HA-based vaccine which was poorly immunogenic and conferred partial protection against challenge with ZJ and DT viruses (data not published). In contrast to the single virus strain sequence-based subunit vaccine providing strain-restricted immunity, the consensus-based vaccines have been previously investigated as a strategy for eliciting broadly reactive immune responses for different pathogens, including chikungunya virus (25), hepatitis B virus (26), hepatitis C virus (27), Middle East respiratory virus (28), HIV-1 (29), and influenza (10, 30, 31).

The consensus rHA VLPs based vaccines elicited protective immune responses similar to those of the inactivated whole-virus vaccine, and could be applied to the assessment criteria

of commercial inactivated virus vaccine, the index including serum HI titers and protective efficacy PC. We have also tested the efficacy of a single copy of the M2 ectodomain (M2e) as a broad-spectrum influenza vaccine candidate in chickens (22). Nevertheless, its further application was restricted by the lack of an appropriate method to evaluate the immune response elicited by the M2e antigens in chickens.

The rHA vaccine in the absence of CVCVA5 elicited higher levels of serological and mucosal antibody responses than those of the Re6 vaccine without CVCVA5 in terms of the HI antibody titers against the Re7 and Re8 antigens in both of the SPF and commercial chickens, and of the SN titers in DF-1 cells. However, higher levels of HI titers after Re6 vaccination were observed when using Re6 as a test antigen in both the SPF and commercial chickens because of an Re6 antigen exactly matching with the Re6 vaccine. In contrast to the HI titers, the neutralizing titers more closely reflect the capability of antibodies inhibiting the replication and propagation of virus. The results of humoral immune responses indicated that the rHA-based vaccine can elicit broad-spectrum antibodies reactive to different antigens, which is consistent with other influenza vaccines based on consensus HA sequences (10).

The VLPs vaccines were superior to the inactivated whole-virus vaccine in eliciting cell-mediated immune responses in animal models as reported in previous studies (17, 32, 33). The residual recombinant baculoviruses in the rHA vaccine preparations can activate Toll-like receptors, which correlated with cellular immune response. In this study, we have also monitored slightly higher levels of IFN-γ and CTL responses induced by the rHA VLPs vaccine in the absence of CVCVA5 compared to those of the Re6 vaccine without CVCVA5.

The challenge studies were carried out with two heterogeneous H5 subtype virus strains (ZJ and DT). The results from this study provide evidence that the rHA VLPs vaccines could be applicable to the field where there exist different subclades of H5 subtype viruses. In contrast to the Re6 vaccine in the absence of immunopotentiator, the rHA vaccine without immunopotentiator broadly protected the vaccinated chickens free from weight loss and death after infection with heterogeneous viruses. The multi-immune components including humoral antibodies, cytokine responses, and CTL activities elicited by the rHA vaccines with CVCVA5 adjuvants could contribute to broad protection against H5 subtype variants infection.

Besides construction of the broad-spectrum antigen, the adjuvant is another option to improve the efficacy of vaccines. The adjuvant, CVCVA5, was shown to be effective on improving the efficacy of the commercial inactivated monovalent or polyvalent vaccines in our previous studies (18, 19). Compared to the rHA and Re6 vaccines in the absence of adjuvant, CVCVA5 adjuvanted vaccine formulations moderately increased the serum antibody levels, significantly improved antibody levels in BAL, and also significantly enhanced the levels of CTL immune responses and cytokines such as IFN-γ and IL-4 in both adjuvanted rHA and Re6 vaccines. There is no significant difference in the protection rates among the groups of rHA vaccine with or without immunopotentiator, suggesting major roles of humoral antibodies in conferring cross-protection by consensus rHA vaccination. In contrast to the rHA vaccine, the increased cellular immune responses in the commercial Re6-CVCVA5 vaccine appear to play pivotal roles in providing effective protection against heterologous virus challenge when antibodies alone are insufficient for effective protection.

In this study, we have reported HA consensus sequence-based H5 rHA VLPs vaccines, which elicited a broad-spectrum serum and mucosal antibody response, and protected chickens experimentally challenged with different subclades of H5 subtype viruses. The results from this study support that development of subunit VLP vaccines based on consensus HA sequences conferring a broad-spectrum protection can provide a potential application in poultry farm with continuing antigenic drift variants.

ETHICS STATEMENT

All animal studies were carried out in accordance with the recommendations in the National Guide for the Care and Use of Laboratory Animals. The protocol (VMRI-AP150306) was approved by the Review Board of National Research Center of Engineering and Technology for Veterinary Biologicals, Jiangsu Academy of Agricultural Sciences and Yangzhou University. The surgery and euthanasia were performed under anesthesia with sodium pentobarbital solution (100 mg/kg body weight) *via* intravenous route to minimize suffering. All experiments involved in the live H5 subtype viruses were performed in the biosafety level 3 laboratory facilities. At the end of experiments, the discarded live viruses, wastes, and infected animal carcasses were autoclaved and incinerated to eliminate biohazards.

AUTHOR CONTRIBUTIONS

Conceived and designed the experiments: YT, PW, JL, XZ, and XL. Performed the experiments: YT, PW, JL, XZ, MM, and LF. Analyzed the data: YT, PW, JL, XZ, XL, and DP. Contributed reagents/materials/analysis tools: YT, PW, JL, XZ, MM, LF, JH, and DP. Wrote and edited the paper: YT, PW, S-MK, DP, and XL. All authors read and approved the final manuscript.

FUNDING

This work was partially supported by the National Key R&D Program of China (2017YFD0500706) (YT), Central Finance Funds for Agrotechnical Popularization grants (TG(15)067) (YT), Jiangsu Agriculture Science and Technology Innovation Fund (CX(15)1063) (YT), the Special Fund for Agroscientific Research in the Public Interest (201303046) (YT), and NIH AI105170 (S-MK), AI093772 (S-MK), AI119366 (S-MK). The funders had no role in study design, data collection and analysis, decision to publish, or preparation of the manuscript.

REFERENCES

1. Writing Committee of the Second World Health Organization Consultation on Clinical Aspects of Human Infection with Avian Influenza AV, Abdel-Ghafar AN, Chotpitayasunondh T, Gao Z, Hayden FG, Nguyen DH, et al. Update on avian influenza A (H5N1) virus infection in humans. *N Engl J Med* (2008) 358(3):261–73. doi:10.1056/NEJMra0707279
2. Smith GJ, Donis RO; World Health Organization/World Organisation for Animal HF, Agriculture Organization HEWG. Nomenclature updates resulting from the evolution of avian influenza A(H5) virus clades 2.1.3.2a, 2.2.1, and 2.3.4 during 2013-2014. *Influenza Other Respir Viruses* (2015) 9(5):271–6. doi:10.1111/irv.12324
3. de Vries E, Guo H, Dai M, Rottier PJ, van Kuppeveld FJ, de Haan CA. Rapid emergence of highly pathogenic avian influenza subtypes from a subtype H5N1 hemagglutinin variant. *Emerg Infect Dis* (2015) 21(5):842–6. doi:10.3201/eid2105.141927
4. Claes F, Morzaria SP, Donis RO. Emergence and dissemination of clade 2.3.4.4 H5Nx influenza viruses-how is the Asian HPAI H5 lineage maintained. *Curr Opin Virol* (2016) 16:158–63. doi:10.1016/j.coviro.2016.02.005
5. Sun H, Pu J, Hu J, Liu L, Xu G, Gao GF, et al. Characterization of clade 2.3.4.4 highly pathogenic H5 avian influenza viruses in ducks and chickens. *Vet Microbiol* (2016) 182:116–22. doi:10.1016/j.vetmic.2015.11.001
6. Swayne DE, Pavade G, Hamilton K, Vallat B, Miyagishima K. Assessment of national strategies for control of high-pathogenicity avian influenza and low-pathogenicity notifiable avian influenza in poultry, with emphasis on vaccines and vaccination. *Rev Sci Tech* (2011) 30(3):839–70. doi:10.20506/rst.30.3.2081
7. Swayne DE. Impact of vaccines and vaccination on global control of avian influenza. *Avian Dis* (2012) 56(4 Suppl):818–28. doi:10.1637/10183-041012-Review.1
8. Li C, Bu Z, Chen H. Avian influenza vaccines against H5N1 'bird flu'. *Trends Biotechnol* (2014) 32(3):147–56. doi:10.1016/j.tibtech.2014.01.001
9. Chen MW, Cheng TJ, Huang Y, Jan JT, Ma SH, Yu AL, et al. A consensus-hemagglutinin-based DNA vaccine that protects mice against divergent H5N1 influenza viruses. *Proc Natl Acad Sci U S A* (2008) 105(36):13538–43. doi:10.1073/pnas.0806901105
10. Giles BM, Ross TM. A computationally optimized broadly reactive antigen (COBRA) based H5N1 VLP vaccine elicits broadly reactive antibodies in mice and ferrets. *Vaccine* (2011) 29(16):3043–54. doi:10.1016/j.vaccine.2011.01.100
11. Wang G, Yin R, Zhou P, Ding Z. Combination of the immunization with the sequence close to the consensus sequence and two DNA prime plus one VLP boost generate H5 hemagglutinin specific broad neutralizing antibodies. *PLoS One* (2017) 12(5):e0176854. doi:10.1371/journal.pone.0176854
12. Zhou H, Huang Y, Yuan S, Li Y, Wu S, Xu J, et al. Sequential immunization with consensus influenza hemagglutinins raises cross-reactive neutralizing antibodies against various heterologous HA strains. *Vaccine* (2017) 35(2):305–12. doi:10.1016/j.vaccine.2016.11.051
13. Liu L, Zeng X, Chen P, Deng G, Li Y, Shi J, et al. Characterization of clade 7.2 H5 avian influenza viruses that continue to circulate in chickens in China. *J Virol* (2016) 90(21):9797–805. doi:10.1128/JVI.00855-16
14. Zeng X, Chen P, Liu L, Deng G, Li Y, Shi J, et al. Protective efficacy of an H5N1 inactivated vaccine against challenge with lethal H5N1, H5N2, H5N6, and H5N8 influenza viruses in chickens. *Avian Dis* (2016) 60(1 Suppl):253–5. doi:10.1637/11179-052015-ResNoteR
15. Novitsky V, Smith UR, Gilbert P, McLane MF, Chigwedere P, Williamson C, et al. Human immunodeficiency virus type 1 subtype c molecular phylogeny: consensus sequence for an aids vaccine design? *J Virol* (2002) 76(11):5435–51. doi:10.1128/jvi.76.11.5435-5451.2002
16. Lin SC, Huang MH, Tsou PC, Huang LM, Chong P, Wu SC. Recombinant trimeric HA protein immunogenicity of H5N1 avian influenza viruses and their combined use with inactivated or adenovirus vaccines. *PLoS One* (2011) 6(5):e20052. doi:10.1371/journal.pone.0020052
17. Quan FS, Huang C, Compans RW, Kang SM. Virus-like particle vaccine induces protective immunity against homologous and heterologous strains of influenza virus. *J Virol* (2007) 81(7):3514–24. doi:10.1128/JVI.02052-06
18. Tang Y, Lu J, Wu P, Liu Z, Tian Z, Zha G, et al. Inactivated vaccine with adjuvants consisting of pattern recognition receptor agonists confers protection against avian influenza viruses in chickens. *Vet Microbiol* (2014) 172(1–2):120–8. doi:10.1016/j.vetmic.2014.05.007
19. Lu J, Wu P, Zhang X, Feng L, Dong B, Chu X, et al. Immunopotentiators improve the efficacy of oil-emulsion-inactivated avian influenza vaccine in chickens, ducks and geese. *PLoS One* (2016) 11(5):e0156573. doi:10.1371/journal.pone.0156573
20. Wu P, Lu J, Feng L, Wu H, Zhang X, Mei M, et al. Antigen-sparing and enhanced efficacy of multivalent vaccines adjuvanted with immunopotentiators in chickens. *Front Microbiol* (2017) 8:927. doi:10.3389/fmicb.2017.00927
21. Tang Y, Wu P, Peng D, Wang X, Wan H, Zhang P, et al. Characterization of duck H5N1 influenza viruses with differing pathogenicity in mallard (*Anas platyrhynchos*) ducks. *Avian Pathol* (2009) 38(6):457–67. doi:10.1080/03079450903349147917119981xs
22. Tang Y, Gong Y, Wang Y, Wu P, Liu Y, Lu J, et al. Chimaeric VP2 proteins from infectious bursal disease virus containing the N-terminal M2e of H9 subtype avian influenza virus induce neutralizing antibody responses to both viruses. *Avian Pathol* (2013) 42(3):260–7. doi:10.1080/03079457.2013.782096
23. Reed LJ, Muench A. A simple method of estimating fifty per cent endpoints. *Am J Epidemiol* (1938) 27(3):493–7. doi:10.1093/oxfordjournals.aje.a118408
24. Suguitan AL Jr, Cheng X, Wang W, Wang S, Jin H, Lu S. Influenza H5 hemagglutinin DNA primes the antibody response elicited by the live attenuated influenza A/Vietnam/1203/2004 vaccine in ferrets. *PLoS One* (2011) 6(7):e21942. doi:10.1371/journal.pone.0021942
25. Muthumani K, Lankaraman KM, Laddy DJ, Sundaram SG, Chung CW, Sako E, et al. Immunogenicity of novel consensus-based DNA vaccines against Chikungunya virus. *Vaccine* (2008) 26(40):5128–34. doi:10.1016/j.vaccine.2008.03.060
26. Obeng-Adjei N, Yan J, Choo D, Weiner D. Immunogenicity of novel consensus-based DNA vaccines against hepatitis B core antigen. (106.1). *J Immunol* (2011) 186(1 Suppl):101–6.
27. Latimer B, Toporovski R, Yan J, Pankhong P, Khan A, Sardesai N, et al. A polyantigenic genotype 1a/1b consensus hepatitis C virus DNA vaccine induces broadly reactive HCV-specific cellular immune responses in both mice and non-human primates (VAC7P.985). *J Immunol* (2014) 192(1 Suppl):130–41.
28. Muthumani K, Falzarano D, Reuschel EL, Tingey C, Flingai S, Villarreal DO, et al. A synthetic consensus anti-spike protein DNA vaccine induces protective immunity against Middle East respiratory syndrome coronavirus in nonhuman primates. *Sci Transl Med* (2015) 7(301):301ra132. doi:10.1126/scitranslmed.aac7462
29. Yan J, Corbitt N, Pankhong P, Shin T, Khan A, Sardesai NY, et al. Immunogenicity of a novel engineered HIV-1 clade C synthetic consensus-based envelope DNA vaccine. *Vaccine* (2011) 29(41):7173–81. doi:10.1016/j.vaccine.2011.05.076
30. Laddy DJ, Yan J, Corbitt N, Kobasa D, Kobinger GP, Weiner DB. Immunogenicity of novel consensus-based DNA vaccines against avian influenza. *Vaccine* (2007) 25(16):2984–9. doi:10.1016/j.vaccine.2007.01.063
31. Carter DM, Darby CA, Lefoley BC, Crevar CJ, Alefantis T, Oomen R, et al. Design and characterization of a computationally optimized broadly reactive hemagglutinin vaccine for H1N1 influenza viruses. *J Virol* (2016) 90(9):4720–34. doi:10.1128/JVI.03152-15
32. Pinto LA, Edwards J, Castle PE, Harro CD, Lowy DR, Schiller JT, et al. Cellular immune responses to human papillomavirus (HPV)-16 L1 in healthy volunteers immunized with recombinant HPV-16 L1 virus-like particles. *J Infect Dis* (2003) 188(2):327–38. doi:10.1086/376505
33. Pillay S, Shephard EG, Meyers AE, Williamson AL, Rybicki EP. HIV-1 subtype C chimaeric VLPs boost cellular immune responses in mice. *J Immune Based Ther Vaccines* (2010) 8:7. doi:10.1186/1476-8518-8-7

Conflict of Interest Statement: The authors declare that the research was conducted in the absence of any commercial or financial relationships that could be construed as a potential conflict of interest. YT, PW, JL, XZ, MM, LF, and JH are authors on a pending China patent application describing the culture and produce of rHA in bioreactor system (Title: Preparation method of the H5 subtype HA-based subunit vaccine. Reference number: 201710140542.2).

frontiers in Immunology

ORIGINAL RESEARCH
published: 04 January 2018
doi: 10.3389/fimmu.2017.01885

Efficacy of a Virus-Like Nanoparticle As Treatment for a Chronic Viral Infection Is Hindered by IRAK1 Regulation and Antibody Interference

*Karine Chartrand[1], Marie-Ève Lebel[1], Esther Tarrab[1], Pierre Savard[2], Denis Leclerc[2] and Alain Lamarre[1]**

[1]*Immunovirology Laboratory, Institut national de la recherche scientifique (INRS), INRS-Institut Armand-Frappier, Laval, Quebec, Canada,* [2]*Infectious Disease Research Center, Department of Microbiology, Infectiology and Immunology, Laval University, Quebec City, Quebec, Canada*

Although vaccination has been an effective way of preventing infections ever since the eighteenth century, the generation of therapeutic vaccines and immunotherapies is still a work in progress. A number of challenges impede the development of these therapeutic approaches such as safety issues related to the administration of whole pathogens whether attenuated or inactivated. One safe alternative to classical vaccination methods gaining recognition is the use of nanoparticles, whether synthetic or naturally derived. We have recently demonstrated that the papaya mosaic virus (PapMV)-like nanoparticle can be used as a prophylactic vaccine against various viral and bacterial infections through the induction of protective humoral and cellular immune responses. Moreover, PapMV is also very efficient when used as an immune adjuvant in an immunotherapeutic setting at slowing down the growth of aggressive mouse melanoma tumors in a type I interferon (IFN-I)-dependent manner. In the present study, we were interested in exploiting the capacity of PapMV of inducing robust IFN-I production as treatment for the chronic viral infection model lymphocytic choriomeningitis virus (LCMV) clone 13 (Cl13). Treatment of LCMV Cl13-infected mice with two systemic administrations of PapMV was ineffective, as shown by the lack of changes in viral titers and immune response to LCMV following treatment. Moreover, IFN-α production following PapMV administration was almost completely abolished in LCMV-infected mice. To better isolate the mechanisms at play, we determined the influence of a pretreatment with PapMV on secondary PapMV administration, therefore eliminating potential variables emanating from the infection. Pretreatment with PapMV led to the same outcome as an LCMV infection in that IFN-α production following secondary PapMV immunization was abrogated for up to 50 days while immune activation was also dramatically impaired. We showed that two distinct and overlapping mechanisms were responsible for this outcome. While short-term inhibition was partially the result of interleukin-1 receptor-associated kinase 1 degradation, a crucial component of the toll-like receptor 7 signaling pathway, long-term inhibition was mainly due to interference by PapMV-specific antibodies. Thus, we identified a possible pitfall in the use of virus-like particles for the systemic treatment of chronic viral infections and discuss mitigating alternatives to circumvent these potential problems.

Keywords: plasmacytoid dendritic cells, PapMV, interferon-α, IRAK1, Sca-1, antibodies, lymphocytic choriomeningitis virus clone 13

OPEN ACCESS

Edited by:
Rajko Reljic, St George's, University of London, United Kingdom

Reviewed by:
Pablo Penaloza, Northwestern University, United States
Owen Kavanagh, York St John University, United Kingdom

****Correspondence:***
Alain Lamarre
alain.lamarre@iaf.inrs.ca

Specialty section:
This article was submitted to Vaccines and Molecular Therapeutics, a section of the journal Frontiers in Immunology

Received: *18 September 2017*
Accepted: *11 December 2017*
Published: *04 January 2018*

Citation:
Chartrand K, Lebel M-È, Tarrab E, Savard P, Leclerc D and Lamarre A (2018) Efficacy of a Virus-Like Nanoparticle As Treatment for a Chronic Viral Infection Is Hindered by IRAK1 Regulation and Antibody Interference. Front. Immunol. 8:1885. doi: 10.3389/fimmu.2017.01885

INTRODUCTION

Type I interferons (IFN-I), mainly IFN-α and IFN-β, are a family of cytokines with potent antiviral and immunomodulatory properties. The effects of these cytokines on their milieu are complex and affect multiple cells of the immune system by: (i) inducing activation of dendritic cells (DCs) (1, 2); (ii) sustaining activation of $CD8^+$ T cells (3, 4); and (iii) inducing differentiation of B cells into antibody secreting cells (5, 6). Thus early IFN-I production is essential for the control of most viral infections such as mouse hepatitis virus (MHV) (7), lymphocytic choriomeningitis virus (LCMV) (8, 9), or simian immunodeficiency virus (SIV) (10). However, whereas early and transient expression of IFN-I controls the infection, prolonged exposure bears detrimental effects to the host's immune response (10–12). The balancing act between the positive and negative effects of the IFN-I response is observed in the clinical setting as displayed by the well-documented adverse effects of IFN therapy (13, 14). Thus, despite being the standard-of-care against various diseases, emerging therapies now focus on IFN-free alternatives.

Upon viral infection, plasmacytoid DCs (pDCs) are characterized as the main producers of IFN-I [reviewed in Ref. (15, 16)]. This major characteristic is mainly due to their Toll-like receptor (TLR) expression profile. While other innate immune cells express a wide array of TLRs, pDCs mainly express the endosomal TLR7 and TLR9 (16), which bind genetic material typically associated with viral pathogens, such as ssRNA and unmethylated DNA, respectively. These receptors are also capable of recognizing analogs of their natural ligands such as imidazoquinoline and CpG for TLR7 and TLR9, respectively (17). Through their production of IFN-I, pDCs also serve as a bridge between innate and adaptive immune responses as illustrated by their ability to activate natural killer cells (18), other DCs (19, 20) as well as T cells (18, 21). Consequently, upon pDC depletion, mice become highly susceptible to viral infection with MHV (7), herpes simplex virus (22, 23), LCMV (24), vesicular stomatitis virus (18), or the murine cytomegalovirus (18) among others.

By harnessing the central role of pDCs, we have demonstrated the potential for the use of a plant virus-like nanoparticle as a vaccine candidate as well as an adjuvant in various infectious models (25–34). Our platform is based on the papaya mosaic virus (PapMV) nanoparticle that contains a non-replicative synthetic ssRNA rendering it safe for future human use. The synthetic ssRNA found inside the capsid is recognized by the TLR7 of pDCs (31), leading to the production of IFN-α (26, 31, 35), IL-6 (30, 31) along with other cytokines and chemokines. PapMV resultantly activates DCs, macrophages, T cells as well as B cells (26, 28, 31, 35), making this platform versatile in activating the immune system. Furthermore, we have shown that PapMV induces protective immune responses against pathogens when used as a vaccine platform or an adjuvant (26–34, 36) and slows melanoma development when used in an immunotherapeutic setting (37).

Considering that PapMV induces strong IFN-I responses, we sought to evaluate its potential as an immune adjuvant for the treatment for chronic viral infections with the objective of replacing exogenous IFN-α administration with endogenous IFN-α secretion following systemic PapMV delivery. This approach would provide a universally applicable immune stimulatory molecule that could be used against all viral infections without requiring expression of defined viral antigens. We observed that treatment of mice chronically infected with the persistent strain of LCMV (LCMV-Cl13) with PapMV was unable to clear the infection. Moreover, multiple administrations of PapMV induced an immune tolerance as shown by the almost complete abrogation of IFN-α production following secondary PapMV administration. We show that this tolerization is the result of a combination of factors including interleukin-1 receptor-associated kinase 1 (IRAKI) degradation and interference by PapMV-specific antibodies. This information will be crucial for further clinical development of the PapMV platform.

Abbreviations: BFA, Brefeldin A; BMpDCs, bone marrow-derived plasmacytoid dendritic cells; dpi, days postinfection; FBS, fetal bovine serum; HBV, hepatitis B virus; HCV, hepatitis C virus; IFN, interferon; IRAK1, interleukin-1 receptor-associated kinase 1; LCMV Cl13, lymphocytic choriomeningitis virus clone 13; LPS, lipopolysaccharide; MFI, mean fluorescence intensity; MHC-I, class I major histocompatibility complex; PapMV, papaya mosaic virus nanoparticle; pDCs, plasmacytoid dendritic cells; Poly I:C, polyinosinic:polycyticylic acid; TLR, toll-like receptor; WT, wild type.

MATERIALS AND METHODS

Ethics Statement

This study was performed in accordance with the Canadian Council on Animal Care guidelines. All *in vivo* experiments were reviewed and approved by the Institut national de la recherche scientifique animal care committee.

Mice

Female 6- to 10-week-old C57BL/6 mice were purchased from Charles River Laboratories. J_HT mice were kindly provided by Dr. Rolf Zinkernagel (Zurich University, Switzerland).

Cells and Virus

Lymphocytic choriomeningitis virus Cl13 was kindly provided by Dr. Rolf Zinkernagel (Zurich University, Switzerland). MC57G fibroblast were cultured in minimal essential medium with Earle's salt (Wisent, St-Bruno, QC, Canada) containing 5% heat inactivated fetal bovine serum (FBS) (PAA Laboratories, Mississauga, ON, Canada).

PapMV Nanoparticles

PapMV nanoparticles were provided by Folia Biotech (Quebec, QC, Canada) and were produced as described before (30). Briefly, coat proteins are self assembled *in vitro* around a non-coding ssRNA. Lipopolysaccharide (LPS) contamination was always <50 endotoxin units/mg protein and considered as negligible.

LCMV Cl13 Infection and Treatment

Mice were infected with 2×10^6 pfu of LCMV Cl13 i.v. and treated with 400 µg of PapMV i.v. on days 3 and 5. Serum was collected 6 h following each treatment to assess IFN-α production. Blood was

collected 8 days postinfection (dpi) and mononuclear cells were isolated by density gradient over Ficoll-Paque (GE Healthcare Life Sciences, Mississauga, ON, Canada) and centrifuged at 1,200 rpm for 20 min at room temperature. Cells were collected and washed with PBS then stained for 30 min at 37°C with $GP_{33–41}$ PE tetramers, which were synthesized as previously described (38), to label $CD8^+$ T cells specific for the MHC-I gp33 epitope of LCMV. Extracellular staining was performed on unwashed cells for 20 min at 4°C. Following a wash, cells were fixed with fixation buffer (Biolegend, San Diego, CA, USA) for 20 min at room temperature then analyzed by flow cytometry on a BDLSR Fortessa (BD Biosciences, Mississauga, ON, Canada). Spleens collected 30 dpi were disrupted between frosted microscope slides and cells were stained to assess $CD8^+$ T cells $GP_{33–41}{}^+$ cells as described above. Cells were also incubated with Brefeldin A (BFA) (Sigma, Oakville, ON, Canada) for 5 h at 37°C to inhibit vesicular transport. Spleen cells were then stained for intracellular cytokine production (see below). Blood, spleen, kidney, liver, and brain were also collected 30 dpi to assess viral burden. Organs were mechanically disrupted and supernatants were tittered on MC57G cells by focus forming assay to assess viral burden as previously described (39).

Immunizations

Mice were injected with 100 or 400 μg of PapMV i.v., 50 μg of imiquimod (R837) (InvivoGen, San Diego, CA, USA), 25 μg of LPS (Sigma), 50 μg of Poly I:C (InvivoGen), or control.

Organ Processing

Spleen and bones from hind legs were collected at various time points following immunization. Spleens were subjected to digestion with 1 mg/mL of collagenase D (Roche, Mississauga, ON, Canada) for 15 min at 37°C. Femurs, tibias, and iliac crests were flushed and single cell suspensions from both spleen and bone marrow were subjected to red blood cell lysis followed by flow cytometry staining.

Bone Marrow-Derived Plasmacytoid Dendritic Cells (BMpDCs)

Bone marrow-derived pDCs were prepared by flushing the bone marrow of femurs, tibias and iliac crests, and subjected to red blood cell lysis. Cells were seeded at 2×10^6 cells/mL in RPMI 1640 (Wisent) containing 10% FBS, 100 IU penicillin, 100 μg/ml streptomycin (Wisent), 55 μM β-mercaptoethanol, 1 mM sodium pyruvate, 1× MEM non-essential amino acids, and 10 mM HEPES (Gibco) supplemented with 200 ng/ml of FLT3-L (BioXcell, Lebanon, PA, USA). On days 7–9, cells were stimulated with 100 μg/ml of PapMV, 25 μg/ml of imiquimod (R837) (InvivoGen), 12.5 μg/ml of polyinosinic:polycyticylic acid (Poly I:C) (InvivoGen) or control. On days 8–10, supernatants were frozen at −20°C for IFN-α detection and cells stained for flow cytometry analysis or cell sorting.

Serum Transfer

Mice were immunized with 100 μg PapMV i.v. on day 0. On day 5 or 25, mice were euthanized and blood was collected by cardiac puncture. Blood was allowed to clot for 30 min at room temperature. Tubes were then centrifuged at 1,500 *g* for 10 min at room temperature. Sera were pooled and injected i.p. to mice whereby the serum from two mice was used to inject one mouse. After 24 h, mice were immunized with 100 μg of PapMV or control i.v. Serum was collected 6 h later to quantify IFN-α and PapMV-specific antibodies and activation of pDCs was assessed in spleen 24 h postimmunization.

Flow Cytometry

Analysis of surface antigens were performed with the following antibodies and markers: CD3 (145-2C11), CD4 (RM4-5), CD8 (53-6.7), CD44 (IM7), CD62L (MEL-14), PD-1 (29F1A12), Zombie Aqua, CD11b (M1/70), CD11c (N418), CD45R/B220 (RA3-6B2), CD317 (927), CD86 (GL-1), CD69 (H1.2F3), Sca-1 (E13-161.7) (Biolegend). Fc receptors were blocked using a purified anti CD16/32 antibody (2.4G2) (BioXcell). Identification of pDCs was based on their viability (Zombie $Aqua^-$) and their surface antigen expression ($CD11c^{int}$, $CD11b^{lo}$, $B220^+$, and $CD317^+$). For intracellular staining, IFN-γ (XMG1.2), TNF-α (MP6-XT22), IL-2 (JES6-5H4) (Biolegend), IFN-α (RMMA-1) (PBL Assay Science, Piscataway, NJ, USA), IRAK1 (D51G7) as well as isotype control antibodies were used (Cell Signaling Technologies, Beverly, MA, USA) after permeabilization using the Intracellular Staining Permeabilization Wash Buffer 10× and Fixation Buffer following instructions of manufacturer (Biolegend). Data were acquired using BDLSR Fortessa Flow Cytometer (BD Biosciences) and analyzed using the FlowJo software (FlowJo, LLC).

IFN-α Intracellular Staining

Mice were immunized with 400 μg of PapMV i.v. as described above. Spleens and bone marrows were collected 4 h postimmunization and processed as described above. Cells were then incubated with BFA for 4 h at 37°C followed by IFN-α intracellular staining as described above.

Cell Sorting

Bone marrow-derived pDCs were stimulated for 24 or 48 h and stained for sorting. Fc receptors were blocked as previously described and pDCs were identified as $CD11c^+B220^+PDCA1^+$. Cells were collected in FBS then washed twice with cold PBS followed by protein extraction (see below). Sort was performed using a BD FACSJazz (BD Biosciences).

Immunoblotting

For immunoblotting, cells were harvested and lysed in Triton X-100 lysis buffer [20 mM Tris-HCl pH 8.0, 1% Triton X-100, 10% Glycerol, 150 mM NaCl, protease inhibitor cocktail (Roche)]. Lysates were then loaded on a 10% SDS-PAGE followed by transfer on a polyvinylidene difluoride membranes (BioRad, Mississauga, ON, Canada). Membranes were blocked in 5% dry milk TBS-T (TBS, 0.1% Tween-20) for 2 h at room temperature. Primary antibodies against mouse IRAK1 and β-actin (Cell Signaling Technologies) were diluted in TBS-T and incubated with the membranes o/n at 4°C. Antirabbit IgG HRP (Jackson ImmunoResearch, West Grove, PA, USA) were used as secondary antibodies whereby they were diluted in TBS-T and incubated

with the membranes for 1 h at room temperature. Detection was performed with ECL chemiluminescence kit (BioRad).

ELISA and Multiplex

Interferon-α levels in mice serum or cell culture supernatants were quantified by ELISA according to the manufacturer's directions (Affymetrix eBiosciences). TNF-α, IL-6, IL-10, IL12p40, IL12p70, IL-9, IL-15, KC, G-CSF, M-CSF, RANTES, MIP-1α, MIP-1β, MIP-2, IP-10, and MCP-1 levels in mice serum were quantified using Milliplex Map Mouse Cytokine/Chemokine Premixed 32 Plex (Millipore, Etobicoke, Canada) according to manufacturer's directions. Measurement of median fluorescence intensity (MFI) was performed using Bio-plex (Biorad). PapMV-specific antibody titers were determined as described previously (25). Detection of PapMV-specific IgM was performed with peroxidase-conjugated goat antimouse IgM (Jackson Immunoresearch Laboratories).

Statistical Analysis

Statistical analysis was performed with GraphPad Prism Software (GraphPad Software). Error bars represent SEM. Two-tailed Student's *t*-test was used and Welch's correction was applied when needed.

RESULTS

Treatment of Chronic LCMV Cl13 Infection with PapMV Does Not Improve Viral Clearance

The impact of IFN-α on viral infections in mice was shown to vary according to the kinetics and strength of production during the ongoing infection. Early IFN-α was shown to be essential to the control of the infection (7, 9, 10, 40) while long-term IFN-α was detrimental to the host and favored viral persistence (10–12). In one such study, treatment of LCMV Cl13-infected mice with exogenous IFN-α on days 3 and 5 postinfection resulted in the increase of $GP_{33–41}$-specific $CD8^+$ T cells as well as a decrease in viral load 32 dpi (8). This led us to hypothesize that the treatment of a chronic infection such as LCMV Cl13 with PapMV could result in a similar clearance of the virus given the capacity of PapMV to induce potent IFN-α production following immunization (26, 31, 35). We therefore infected mice with LCMV Cl13 and treated them 3 and 5 dpi with 400 μg of PapMV i.v. Blood was collected at various time points to assess viral load, which was not affected by the treatments with PapMV (**Figure 1A**). To assess the efficiency of the PapMV treatment, serum was collected 6 h following the treatment on days 3 and 5 and IFN-α was quantified by ELISA. Although the administration of 400 μg of PapMV induced strong IFN-α production in naive mice, LCMV Cl13-infected mice barely produced IFN-α at all (**Figure 1B**) whether assessed after the first treatment on day 3 or the second treatment on day 5. These results indicate that the infection with LCMV Cl13 hinders IFN-α production following PapMV administration. Of note, PapMV not only induces IFN-α in immunized mice but also other cytokines and chemokines such as IL-6, IP-10, and MCP-1 (31, 35), which rely on different sets of signaling pathways than

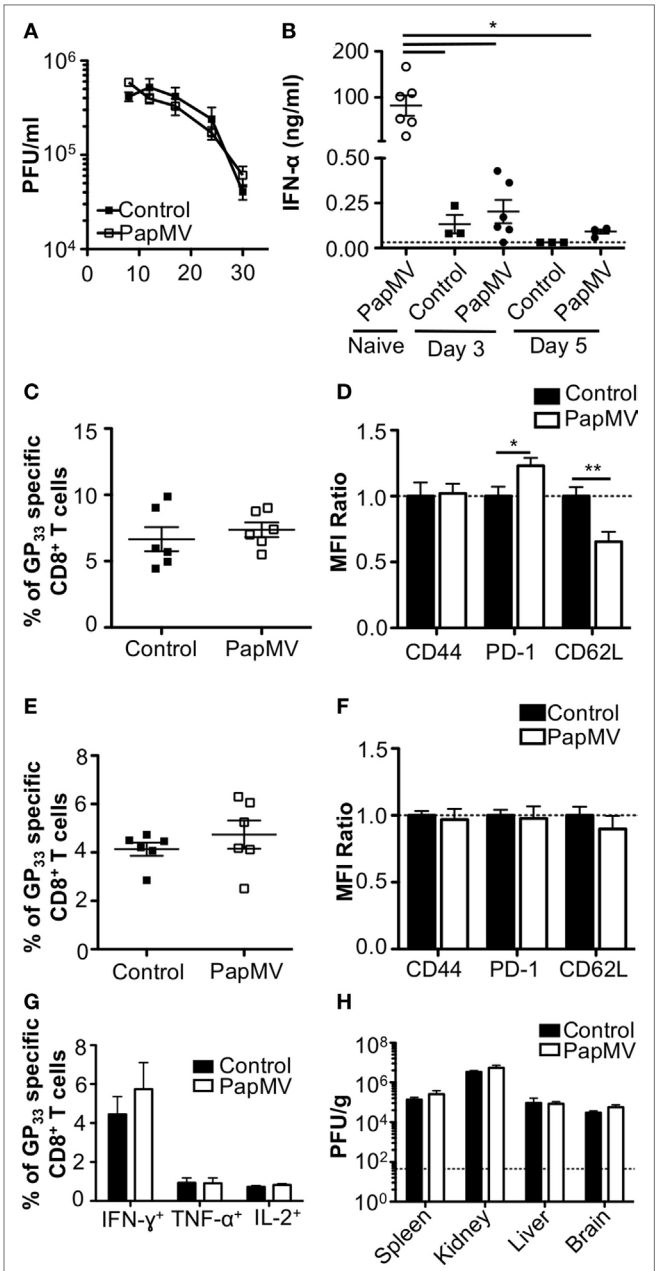

FIGURE 1 | Treatment of an established lymphocytic choriomeningitis virus clone 13 (LCMV Cl13) infection with PapMV does not improve viral clearance. Mice were infected with LCMV Cl13 followed by treatments with PapMV on days 3 and 5 **(A)** Kinetics of viral burden expressed as LCMV Cl13 PFU/ml of blood **(B)** ELISA quantification of interferon (IFN)-α in serum of mice 6 h following treatment with control or PapMV. **(C)** Percentages of GP_{33}-specific $CD8^+$ T cells in the blood 8 dpi. **(D)** CD44, PD-1, and CD62L expression on $CD8^+$ T cells in blood 8 dpi. **(E)** Percentages of GP_{33}-specific $CD8^+$ T cells in the spleen 30 dpi. **(F)** CD44, PD-1, and CD62L expression on $CD8^+$ T cells in the spleen 30 dpi. **(G)** Percentages of $CD8^+$ T cells producing IFN-γ, TNF-α, or IL-2 in response to a stimulation with the $GP_{33–41}$ peptide for 5 h. **(H)** Viral loads of LCMV Cl13 in spleen, kidney, liver, and brain 30 dpi. Results are expressed as PFU/g of each organ. For **(D,F)**, results are expressed as a ratio of the sample's mean fluorescence intensity (MFI) over the average MFI of control samples (*$p < 0.05$; **$p < 0.01$; ***$p < 0.001$) ($n = 2$, three mice per group).

IFN-α for their production. It is therefore possible that immune cells were activated through these auxiliary cytokines following treatment with PapMV despite the absence of detectable IFN-α in the serum. To test this, we assessed activation of $CD8^+$ T cells as well as the proportion of $GP_{33–41}$-specific $CD8^+$ T cells. The proportion of $GP_{33–41}$-specific $CD8^+$ T cells in blood on day 8 postinfection was similar in groups treated with the control or PapMV (**Figure 1C**) and a similar trend was noticed for the expression of CD44 on $CD8^+$ T cells (**Figure 1D**). We also assessed exhaustion of $CD8^+$ T cells by means of PD-1 expression, which was increased in mice treated with PapMV compared to mice treated with control (**Figure 1D**). Expression of CD62L on $CD8^+$ T cells was reduced in PapMV compared to mice treated with control (**Figure 1D**). Together, these data indicate that the treatment of LCMV Cl13-infected mice with PapMV on days 3 and 5 does not increase the activation of $CD8^+$ T cells. However, these treatments seem to increase the exhaustion of $CD8^+$ T cells as indicated by the increased expression of the inhibitory receptor PD-1 (41). PapMV treatment did not lead to homing of $CD8^+$ T cells in lymphoid organs, as shown by their decrease in CD62L expression, an adhesion molecule involved in the homing of lymphocytes to secondary lymphoid organs. The percentage of $GP_{33–41}$-specific $CD8^+$ T cells was not different on day 30 postinfection between control and PapMV-treated group (**Figure 1E**). As well, the expression of PD-1, CD44, and CD62L was not significantly different between these two groups (**Figure 1F**). Furthermore, our results revealed that the functionality of $GP_{33–41}$-specific $CD8^+$ T cells was not affected by the treatment of LCMV Cl13 infection with PapMV, as shown by the similar percentage of IFN-γ, TNF-α, or IL-2 positive $CD8^+$ T cells in the spleen (**Figure 1G**) between control and PapMV-treated groups. To further confirm that the PapMV treatments had no effect on the clearance of LCMV Cl13, we collected lymphoid and non-lymphoid organs at 30 dpi and assessed the viral load of LCMV Cl13. In the spleen, kidney, liver and brain, both groups displayed similarly elevated LCMV Cl13 titers (**Figure 1H**), which, along with previous data, indicated that treatment with PapMV was ineffective in clearing an LCMV Cl13 infection. Notably, it has been shown that cells previously infected with chronic viruses such as hepatitis B virus (HBV) (42, 43) or hepatitis C virus (HCV) (44, 45) were unresponsive to further TLR ligand stimulation. Based on our findings, we surmise that a possible TLR tolerance mechanism might be at play after an LCMV Cl13 infection, therefore hindering further activation of immune cells by a subsequent TLR ligand stimulation such as PapMV.

Pretreatment with PapMV Inhibits Further Effects of Secondary PapMV Administration

Lymphocytic choriomeningitis virus clone 13 activates immune cells through the TLR7/MyD88 endosomal pathway (46) as well as the RIG-I/Mda5 cytosolic pathway (47). In order to exclude activation and cytokine production caused by engagement of the RIG-I/Mda5 pathway, we decided to move to a PapMV-only based model in which only TLR7 is stimulated. We therefore pretreated mice with PapMV at different time intervals ranging from 1 to 50 days prior to a second immunization with PapMV. Sera were collected 6 h following the second immunization to assess IFN-α production by ELISA. A single administration of PapMV induced strong IFN-α production, as detected in the serum 6 h postimmunization (**Figure 2A**). When mice were pretreated with 100 µg of PapMV, the production of IFN-α was abolished following a secondary immunization for up to 50 days following pretreatment (**Figure 2A**). A similar hindrance was observed in the production of TNF-α, IL-6, IL-12p40, IL-12p70, and IL-15, whereas production of IL-10 and IL-9 was enhanced and unaffected, respectively (Figure S1 in Supplementary Material). Similarly, production of various chemokines and growth factors was also suppressed following a second immunization as observed with the production of M-CSF, RANTES, MIP-1α, MIP-1β, IP-10, and MCP-1 whereas production of KC, G-CSF, and MIP-2 was enhanced or unaffected (Figure S1 in Supplementary Material). While there are other cytokines and chemokines that are differentially regulated upon PapMV administration, we focused on IFN-α production based on its wide-ranging use in therapeutic settings (14).

Since pDCs are major producers of IFN-α upon stimulation with a TLR7 ligand, we sought to determine whether the absence of IFN-α was due to a lack of activation of pDCs. Spleens of mice pretreated with 100 µg of PapMV were collected 24 h following the second immunization and activation of pDCs was assessed by

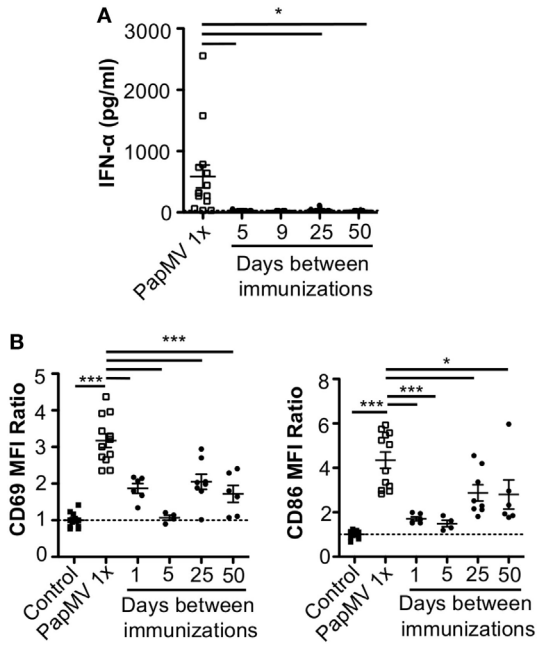

FIGURE 2 | Pretreatment with PapMV prevents plasmacytoid dendritic cells (pDCs) from responding to a subsequent PapMV administration. **(A)** ELISA quantification of interferon (IFN)-α in serum 6 h following immunization with PapMV once (PapMV 1×) or preceded by pretreatment with PapMV at various time intervals. **(B)** CD69 (left) and CD86 (right) expression on splenic pDCs 24 h following immunization with PapMV once (PapMV 1×) or preceded by pretreatment with PapMV at various time intervals. Results are expressed as a ratio of the sample's mean fluorescence intensity (MFI) over the average MFI of control samples (*$p < 0.05$; **$p < 0.01$; ***$p < 0.001$) ($n = 2–8$, two to four mice per group).

flow cytometry. As seen with IFN-α production, a single immunization with PapMV induced upregulation of CD69 and CD86 (**Figure 2B**) on pDCs. Conversely, when mice were pretreated with PapMV 1–5 days prior to a second immunization, pDCs were unable to respond to the second immunization, as observed by the absence of CD69 or CD86 upregulation (**Figure 2B**). Here, we found that the expression of activation markers on pDCs on day 1 after the pretreatment was due to remnants of the initial immunization rather than the activation of pDCs following the second immunization (Figure S2 in Supplementary Material). With a 25-day or more lag between the pretreatment and the second immunization, pDCs were activated by the second immunization although to a lesser intensity than mice treated only once with PapMV (**Figure 2B**). Altogether, these results demonstrate that the administration of PapMV induces a refractory state in pDCs rendering them unable to respond to further PapMV immunizations. In short intervals, this effect is completely inhibitory while for longer intervals the inhibition is only partial, indicating that distinct mechanisms are possibly concomitantly interfering with the response.

Refractory State Induced by PapMV Pretreatment Affects the Response to Other TLR7 and TLR4 Ligands but Not TLR3

To assess whether the refractory state induced by a pretreatment with PapMV affected only further administrations of PapMV, we pretreated mice with PapMV and then challenged them 5 days later with LPS, R837, or Poly I:C, which are ligands for TLR4, TLR7, and TLR3, respectively. We then assessed the expression of CD69 on pDCs (**Figure 3A**). As expected, mice treated with LPS, R837, or Poly I:C alone showed an upregulation of CD69 on pDCs, indicating activation. When mice were pretreated with PapMV, subsequent immunizations with LPS or R837 were not as efficient in inducing the activation of pDCs as immunizations in naive animals but still showed some degree of CD69 upregulation. These results indicate that the inhibition induced by pretreatment with PapMV not only impacts subsequent immunizations with PapMV but also other TLR7 ligands as well at other TLR pathways, such as TLR4, although the inhibition

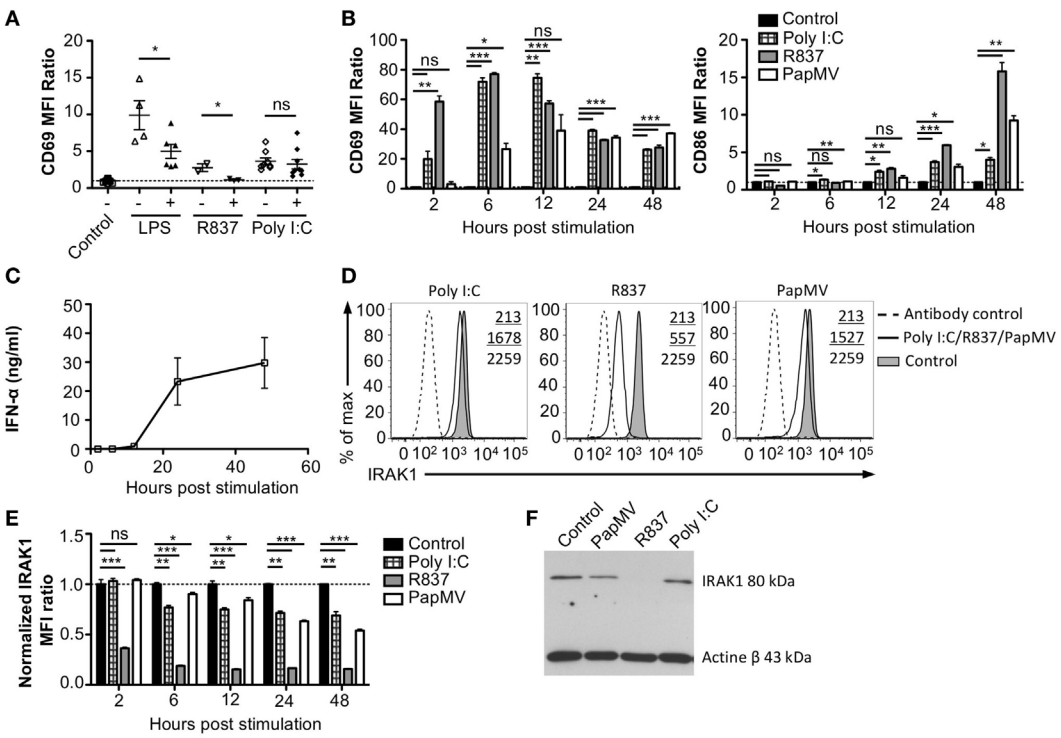

FIGURE 3 | Interleukin-1 receptor-associated kinase 1 (IRAK1) is degraded by PapMV in bone marrow-derived plasmacytoid dendritic cells. **(A)** CD69 expression on splenic plasmacytoid dendritic cells (pDCs) 6 h following the last immunization with the control and R837 and 24 h following immunization with the control, lipopolysaccharide (LPS), or polyinosinic:polycyticylic acid (Poly I:C) once (–) or preceded with a pretreatment with PapMV (+) 5 days prior (n = 2–3, two to three mice per group, one representative experiment is shown for R837 samples). **(B)** CD69 (left) and CD86 (right) expression on bone marrow-derived BMpDCs 2–48 h poststimulation with control (black bars), Poly I:C (checkered bars), R837 (gray bars), or PapMV (white bars). **(C)** ELISA quantification of IFN-α in culture supernatant from BMpDCs stimulated 2–48 h with PapMV. **(D)** Representative overlay histograms of IRAK1 expression in BMpDCs following a stimulation of 24 h with control (filled graph), Poly I:C, R837, or PapMV (full line), or secondary antibody staining control (dashed line). **(E)** IRAK1 expression in BMpDCs 2–48 h following stimulation with the control (black bars), Poly I:C (checkered bars), R837 (gray bars), or PapMV (white bars). **(F)** Immunoblot of IRAK1 (top) and actin-β (bottom) of BMpDCs 24 h following stimulation with control, PapMV, R837, or Poly I:C. BMpDCs were sorted to isolate pDCs prior to protein extraction and immunoblotting. **(A,B,E)** Results are expressed as a ratio of the MFI of the sample on the average MFI of control samples. **(A)** (n = 2, two to three mice per group) **(B,D,E)** (representative experiment of two to ten experiments, two to three replicates per group) **(C)** (n = 2, 2 replicates per time point) (*p < 0.05; **p < 0.01; ***p < 0.001).

is less pronounced. Strikingly, unlike the inhibition observed with LPS and R837, administration of PapMV prior to Poly I:C resulted in the expression of CD69, indicative of pDC activation, which was similar in the control and treated groups (**Figure 3A**). Altogether, these results point toward an inhibitory mechanism induced by PapMV pretreatment that affects TLR7 and TLR4 pathways while the TLR3 pathway remains unaffected.

Stimulation with PapMV Induces Degradation of IRAK1 in pDCs

Toll-like receptor pathways are not specific to each receptor. Indeed, most of the complexes implicated in the signaling cascades are shared across pathways [reviewed in Ref. (48, 49)]. If PapMV were to affect the TLR7 signaling pathway, other TLR signaling pathways would also be affected, resulting in the cross-inhibition observed when cells are pretreated with PapMV. Indeed, such cross-inhibition was observed in response to stimulations with various TLR ligands such as TLR4 ligands (50–52) TLR7 ligands (52, 53) and TLR9 ligands (51, 53), establishing the presence of homo and hetero tolerance in the TLR signaling pathways. In these studies, one common mechanism reported to be involved in the observed cross tolerance was through the degradation of IRAK1 (52, 54, 55), a kinase implicated in all MyD88-dependant TLR signaling pathways, therefore excluding TLR3, which signals through a MyD88-independent pathway (56). Therefore, we assessed IRAK1 expression in pDCs by flow cytometry and immunoblotting to analyze the regulation of IRAK1 following PapMV stimulation. Given that pDCs account for only 0.2% of all splenocytes, we evaluated the response of pDCs to PapMV *in vitro* using BMpDCs. After differentiation of bone marrow cells with Flt3L for 8 days, cells were stimulated with PapMV. Similar to our observations from *in vivo* splenic pDCs, BMpDCs were readily activated by various TLR ligands including PapMV as shown by the upregulation of CD69, CD86 (**Figure 3B**) and the accumulation of IFN-α in culture supernatants following stimulation (**Figure 3C**). Since PapMV activates BMpDCs, we investigated the regulation of IRAK1 following stimulation with various TLR ligands. We first assessed IRAK1 expression by flow cytometry following various incubation periods of BMpDCs with TLR7 ligands, PapMV and R837, or TLR3 ligand, Poly I:C. As expected, R837 induced a strong downregulation of IRAK1 after 24 h in BMpDCs *in vitro* (**Figures 3D,E**). Surprisingly, stimulation of BMpDCs with Poly I:C induced a small downregulation of IRAK1 starting at 6 h poststimulation. Stimulation of BMpDCs with PapMV induced the degradation of IRAK1 albeit to a lesser extent than R837 and with slower kinetics (**Figures 3D,E**). To confirm the modulation of IRAK1 expression, we sorted pDCs 24 h poststimulation with PapMV, R837 and Poly I:C and extracted total cellular proteins to evaluate the expression of IRAK1 by immunoblotting. We found that 24 h post-R837-stimulation, the expression of IRAK1 was undetectable (**Figure 3F**) while stimulation with Poly I:C did not induce any degradation of IRAK1 (**Figure 3F**). IRAK1 was also degraded following stimulation of BMpDCs with PapMV although the extent of degradation was lower in comparison to that observed with R837 (**Figure 3F**). When comparing IRAK1 expression ratios obtained by western blot and flow cytometry (**Table 1**; **Figures 3E,F**), we noticed similar ratios between the two assays for R837 and PapMV stimulated BMpDCs while the ratios vary for Poly I:C stimulated BMpDCs. Taken together, these results indicate that PapMV induces the degradation of IRAK1 in pDCs, which could in part explain the tolerance observed when mice are pretreated with PapMV.

PapMV Induces the Upregulation of Sca-1 on pDCs Despite Its Expression Not Being Associated with IFN-α Production

Heterogeneity in the pDC population has been described (57–60) although the biological significance of this phenomenon is still largely unknown. Various reports have, however, indicated that two subsets of pDCs expressing different sets of markers were differentially associated with IFN-α production following TLR stimulation (57–59, 61). Among these studies, it has been suggested that expression of Sca-1 could discriminate between IFN-α producing pDCs and those that do not: Sca-1$^+$ pDCs were weak producers of IFN-α while Sca-1$^-$ pDCs were strong producers (61). Thus, by evaluating the expression of Sca-1 in pDCs, we sought to determine whether it could explain the inhibition in IFN-α production observed with longer periods between PapMV treatments. As previously described (61), pDCs from the spleen are mostly Sca-1$^+$ (88.45% **Figure 4A**; Spleen; Naive) while pDCs from the bone marrow, although still in majority Sca-1$^+$ (69.90% **Figure 4A**; Bone marrow; Naive), display of a larger population of Sca-1$^-$ than in the spleen. After an immunization with PapMV, the proportion of pDCs expressing Sca-1 increased to close to 100% in both the spleen and the bone marrow (**Figure 4A**) and remained elevated for at least 5 days in both organs. The distribution of Sca-1 expression among pDCs returned to naive and control levels by 25 days post-PapMV immunization. To determine which of the Sca-1 expression profile was associated with IFN-α production, we performed IFN-α intracellular staining on pDCs from spleen and bone marrow of mice immunized with 400 μg of PapMV 4 h prior. In the spleen, most IFN-α$^+$ pDCs were Sca-1$^+$ (**Figure 4B**). However, in the bone marrow, both Sca-1$^-$ and Sca-1$^+$ pDCs were expressing IFN-α after a PapMV immunization (**Figure 4B**). No significant difference was denoted between the two groups in the bone marrow. Niederquell et al. (61) proposed that Sca-1$^-$ pDCs could be precursors of Sca-1$^+$ pDCs. In this regard, it is possible that the proportion of Sca-1$^+$ IFN-α$^+$ pDCs are in fact Sca-1$^-$ cells that are upregulating Sca-1 in response to stimulation. When intracellular staining for IFN-α was performed 2 and 6 h postimmunization to assess the progression of

TABLE 1 | Comparison of IRAK1 regulation ratios by flow cytometry and Western blot.

Sample	Flow cytometry ratio	Immunoblot band intensity ratio
Control	1.000	1.000
PapMV	0.631	0.587
R837	0.166	0.026
Polyinosinic:polycyticylic acid	0.716	1.011

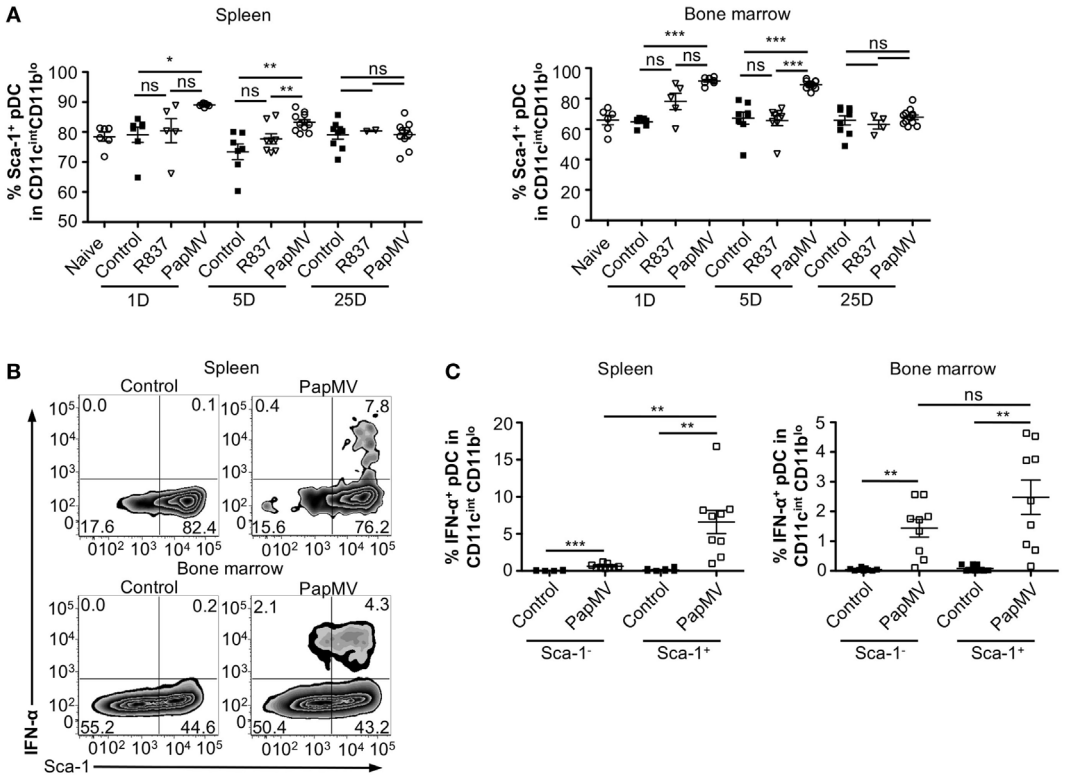

FIGURE 4 | PapMV induces Sca-1 on splenic and bone marrow-derived plasmacytoid dendritic cell (pDCs), despite its expression not being associated with interferon (IFN)-α production. **(A)** Percentages of pDCs from spleen (left) and bone marrow (right) positive for Sca-1 expression 1, 5, and 25 days following an immunization with control (black squares), R837 (open inverted triangles), and PapMV (open circles) (n = 2–4, 1–3 mice per group). **(B)** Representative flow cytometry plots of IFN-α production by pDCs according to their Sca-1 expression profile 4 h postimmunization followed by a 4-h incubation with Brefeldin A (BFA). Spleen (top) and bone marrow (bottom) samples are represented. **(C)** Percentages of intracellular IFN-α$^+$ pDCs found in the spleen (left) and the bone marrow (right) 4 h following an immunization with control or PapMV followed by 4-h incubation with BFA before intracellular staining (*p < 0.05; **p < 0.01; ***p < 0.001).

the IFN-α$^+$ population with respect to Sca-1 expression in both spleen and bone marrow, no difference was observed between the three time points (data not shown). Altogether, these results indicate that although PapMV induces expression of Sca-1, IFN-α production does not seem to be associated with Sca-1 expression in this experimental setting.

Antibodies Are Responsible for Long-term Attenuation of the Response of pDCs to PapMV Immunization

Our results suggest that inhibition of the response to multiple administrations of PapMV is induced through shared mechanisms between TLR-associated pathways for short periods (**Figure 3A**) and PapMV-specific components that affect IFN-α production (**Figure 2A**) as well as pDC activation (**Figure 2B**) for longer periods. We were therefore interested in assessing the role played by antibodies in the refractory state induced by PapMV pretreatment knowing that they were shown to affect responses to prime-boost vaccine regimens in other systems (62, 63). We determined the antibody-mediated impact of PapMV pretreatment on further PapMV immunizations using J_HT mice, which lack functional B cells and consequently also lack antibodies (64). As observed in C57Bl/6 mice (**Figure 2A**), a single immunization with PapMV in J_HT mice induced the production of IFN-α (**Figure 5A**) although in a slightly more pronounced fashion. When a PapMV pretreatment was administered 5, 9, or 25 days prior to secondary PapMV immunizations, the production of IFN-α following the second immunization was equivalent to the response of naive animals, which differed significantly from results obtained in C57Bl/6 mice (**Figure 5A**). Since IFN-α production was not affected by the pretreatment, we examined the expression of CD69 and CD86 on pDCs after multitreatments with PapMV. Similarly to what was observed with IFN-α production, CD69 and CD86 (**Figure 5B**) expression on pDCs was not significantly different between naive mice and PapMV pretreated mice receiving a PapMV immunization. To confirm that the IFN-α production and pDC activation in J_HT mice was due to the absence of antibodies and not of B cells, we performed transfer experiments with immune serum. Since two different profiles are observed at day 5 and day 25 in wild-type (WT) mice with respect to the inhibition generated by a PapMV pretreatment, we assessed the kinetics of IgM and IgG production in the serum of mice after a PapMV immunization (**Figure 5C**). As expected, both IgM and IgG specific for PapMV were found in the serum of WT mice 5 days postimmunization while 25 days postimmunization, only a high IgG titer was

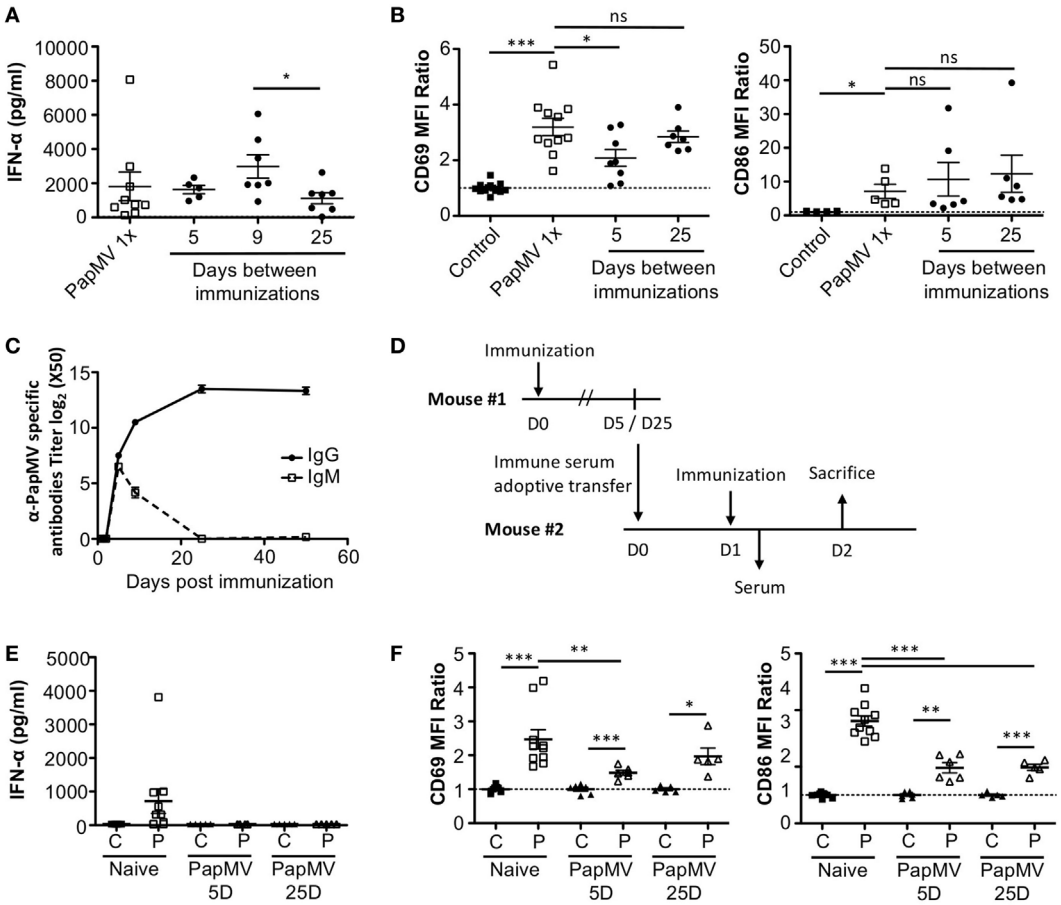

FIGURE 5 | PapMV-specific antibodies are responsible for the long-term attenuation of plasmacytoid dendritic cell (pDC) activation in response to a secondary immunization with PapMV. **(A)** ELISA quantification of interferon (IFN)-α in serum of J_HT mice 6 h following immunization with PapMV once (PapMV 1×) or preceded by a PapMV pretreatment at various intervals (n = 2–5, two to four mice per group). **(B)** CD69 (left) and CD86 (right) expression on splenic pDCs of J_HT mice 24 h following immunization with control, PapMV once (PapMV 1×) or preceded with a pretreatment with PapMV at various time intervals. **(C)** Kinetics of PapMV-specific IgG and IgM development in C57Bl/6 mouse serum after immunization with PapMV as determined by ELISA. **(D)** Schematic representation of the serum transfer experiments. **(E)** ELISA quantification of IFN-α in serum of C57Bl/6 mice transferred with immune serum 6 h following an immunization with control (C) or PapMV (P). **(F)** CD69 (left) and CD86 (right) expression on splenic pDCs of serum transferred C57Bl/6 mice immunized with control (C) or PapMV (P). **(B,E)** Results are expressed as a ratio of the MFI of the sample of the average MFI of controls (n = 3–6, one to three mice per group) (*$p < 0.05$; **$p < 0.01$; *** $p < 0.001$).

detected. Transfers were carried out with serum collected either 5 or 25 days after PapMV administration pooled from matched groups. The serum from the equivalent of two mice was injected into one recipient mouse, which was immunized with PapMV 24 h later (**Figure 5D**). IFN-α production was assessed in the serum 6 h postimmunization while pDC activation was assessed 24 h postimmunization. Injection of naive serum did not affect the production of IFN-α (**Figure 5E** compared to **Figure 2A**) nor did it affect the activation of pDCs as shown by the expression of CD69 and CD86 (**Figure 5F** compared to **Figure 2B**). However, when PapMV-immune serum taken at 5 or 25 days was administered to mice, the following immunization with PapMV showed no production of IFN-α (**Figure 5E**) and a significant decrease in the expression of CD69 and CD86 on pDCs (**Figure 5F**) although not as much as observed in WT mice. Altogether, these results indicate that PapMV-specific antibodies play a significant role in the long-term inhibition and attenuation of the immune response following a pretreatment with PapMV.

DISCUSSION

Interferon-α has long been a treatment of choice for chronic viral infections, whether used alone or in combination with other treatments such as ribavirin in the treatment of HCV. Due to its toxicity, the medical community is moving away from IFN-α-based treatments toward alternatives bearing better adverse event profiles. One alternative toward this end would be to induce endogenous IFN-α production by the host instead of administering high doses of exogenous IFN-α. It is with this aim that we used PapMV nanoparticles, which contain a non-coding ssRNA molecule rendering it non-replicative. PapMV induces the production of IFN-α by pDCs without causing any adverse effects

when administered systemically and could therefore potentially accelerate the clearance of a persistent LCMV Cl13 infection. This approach would also be potentially applicable to other viral infections, as it would not require expression of virus-specific antigens. We observed that sequential application of PapMV treatment has limitations attributed to regulation of the TLR7 pathway as well as the presence of PapMV-specific antibodies upon the first immunization.

The treatment of an LCMV Cl13 infection with PapMV proved to be inefficient as no changes in viral loads or in LCMV-specific immune responses were observed following treatment (**Figure 1**). Like PapMV, LCMV Cl13 is also a TLR7 ligand [reviewed in Ref. (15, 16)]. It is therefore possible that the stimulation of TLR7 by LCMV Cl13 induces TLR tolerance similar to that observed when other TLR ligands are used as stimulators (50–53). Further stimulation of the TLR pathways would therefore be inefficient in LCMV-infected mice. Similarly, previous research has shown that stimulation of HBV-infected (42, 43) or HCV-infected (44, 45, 65) human cells with TLR ligands was unable to induce the production of cytokines and activate infected DCs.

Whereas we were unable to clear an LCMV Cl13 infection using PapMV administration, treatment of viral infections with exogenous IFN-α early in the course of the infection has been shown to be efficient in the control of LCMV (8), SIV (10), or RSV (40). Of note, in the successful treatment of an LCMV Cl13 infection with IFN-α, Wang et al. administered the IFN-α5 subtype. However, the IFN-α subtype profile elicited by PapMV has yet to be determined. Thus, the discrepancy observed could be due to a difference in the IFN-α subtype given the disparity in the immunomodulatory effects and antiviral capacities borne by different subtypes (66–68). Furthermore, contrary to direct IFN-α injection, treatment with PapMV requires uptake of the nanoparticle, release and degradation of the ssRNA inside the endosome before IFN-α can be produced following activation of the TLR7 signaling cascade (26, 28, 31). Although this sequence of events ensures specificity and safety, it is likely more susceptible to various regulatory mechanisms.

Lymphocytic choriomeningitis virus Cl13 stimulates immune cells not only through the TLR7/MyD88 pathway (15, 16) but also through the RIG-I/Mda5 pathway (47). In order to further study the mechanisms at play in this setting and isolate the TLR7 pathway from other variables of the LCMV infection, we pretreated mice with PapMV followed by a second immunization at various time points. This approach recapitulated the results observed in LCMV-infected mice with almost complete abrogation of IFN-α production and pDC activation following the secondary PapMV immunization for short time intervals between immunizations and significant impairment for longer intervals (**Figure 2**). A similar outcome was observed for the production of various cytokines and chemokines such as TNF-α, IL-6, IL-12p40, IL-12p70, IL-15, M-CSF, RANTES, and IP-10 while others were either not affected or enhanced by the secondary immunization (Figure S1 in Supplementary Material). This suggests that PapMV stimulates other pathways in addition to TLR7 leading to a broad activation of the immune system and that these pathways might be differently affected by multiple PapMV administrations. Nonetheless, the main outcome of multiple systemic administrations of PapMV, at least for the TLR7 pathway, is the suppression of the secondary response. This outcome was also observed in previous studies and is indicative of TLR tolerance (discussed below) (50, 52–54). We posit that the inability of subsequent PapMV immunizations to drive a robust response may also be dependent on the route of administration. This conclusion comes from our previous findings showing that sequential intranasal instillations could potentiate PapMV treatments (30). In the previous study, immunizations were separated by seven days and the last immunization led to a higher production of various cytokines in bronchoalveolar lavages. In an intratumoral injection model, we also observed that multiple administrations of PapMV led to decreased tumor growth when administered alone or in combination with other immunotherapies and sustained IFN-α following multiple administrations (37). Pretreatment with PapMV is therefore able to potentiate further PapMV administrations when delivered locally. Limitations are however observed when PapMV is administered systemically, as shown in this study. The development of immunization regimens alternating between various administration routes could therefore be an interesting alternative to mitigate the pitfall of sequential systemic treatments.

With regard to the tolerization of TLRs, we found that degradation of IRAK1 played a central role. This is in agreement with other studies illustrating that this kinase, which is shared across most of the TLR pathways (56), is degraded following TLR2, TLR4, TLR7 and TLR9 stimulation (52, 55, 69, 70). Although this degradation has been shown to last at least 48 h poststimulation (54, 55) both *in vivo* and *in vitro,* the length of this refractory period has yet to be determined. Here, we show that the stimulation of BMpDCs with PapMV induces a partial degradation of IRAK1, which was observed by flow cytometry and later confirmed by immunoblotting (**Figure 3**). Of note, we observed a stronger IRAK1 degradation with R837 than with PapMV, which might be due to the different nature of both TLR7 agonists. Indeed, R837 is a small synthetic molecule that does not require uptake to reach the endosome of cells. It is therefore easier and faster for this molecule to reach more cells and induce the degradation of IRAK1 in a more robust fashion. On the other hand, PapMV is a particulate molecule that has to be taken up by immune cells to reach the endosome thus elongating the interval between the stimulation and the apparent degradation of IRAK1 (71). It would also be of particular interest to verify the regulation of IRAK1 in pDCs *in vivo*. However, due to the low proportion of pDCs in the spleen, we were limited to conducting our analyses *in vitro* to determine the regulation of IRAK1 in BMpDCs. It is important to note that our results revealed only a partial role played by IRAK1 in the tolerance observed following multiple administrations of PapMV. Indeed, stimulation of BMpDCs with PapMV did not induce complete degradation of IRAK1, suggesting that there could be residual proteins left in the cells capable of proceeding through the signaling cascade when further encountering PapMV. This led us to investigate other potential inhibitory mechanisms.

Niederquell et al. suggested that expression of Sca-1 could discriminate between subsets of pDCs able or not to produce IFN-α in response to TLR stimulation (53). We therefore hypothesized

that sequential PapMV administrations could preferentially stimulate or expand pDC subsets unable to produce IFN-α, which might explain the abrogation of IFN-α production upon secondary immunizations. However, in our system, Sca-1 expression on pDCs was not associated with the capacity to produce IFN-α in response to PapMV. While we used a particulate molecule, Niederquell et al. used CpG ODN as a TLR9 ligand. Given that TLR7 and TLR9 are not stimulated by the same ligands (RNA vs. DNA) and similar to R837, CpG ODN is a small synthetic molecule, the kinetics of activation are therefore different in both models. In this regard, other markers such as Ly49Q (57), CD123 (72), and CD9 (59) that have also been associated with IFN-α production might be more informative.

Administration of plant virus-like particles in mice leads to the rapid production of specific antibodies [reviewed in Ref. (73)]. Since antibodies are generated following PapMV injection, we were interested in assessing their impact on multiple administration regimens. We showed by immunizing J_HT mice, which are devoid of B cells and antibodies, as well as performing serum transfer, that PapMV-specific antibodies generated after the first administration were largely responsible for the tolerance to a second PapMV injection. In the short-term immunization regimen (5 days), there was retained inhibition of pDC activation in J_HT mice as shown by the slightly diminished expression of CD69 following a second immunization relative to the naive group (**Figure 5B**). When transferring PapMV immune serum from day 5 postimmunization into naive C57Bl/6 mice followed by PapMV immunization, we observed lower expression levels of CD69 and CD86 compared to mice receiving a single PapMV administration (**Figure 5F** compared to **Figure 2B**). This is either due to an underlying mechanism independent of antibodies or due to the titer of antibody transferred. Although the titer of PapMV specific antibodies found in mice receiving serum transfers is lower than what is found in PapMV immunized mice (Figure S3 in Supplementary Material), this was enough to interfere with the subsequent PapMV immunization by inhibiting the production of IFN-α on both days 5 and 25. To overcome this limitation, one could administer immunogenically distinct plant virus-like particles to circumvent the effect of antibodies. It would also be interesting to explore the use of different injection routes and whether or not antibodies can also interfere with the response to subsequent injections.

Other directions are currently being assessed to potentiate systemically administered PapMV. We have previously shown that our platform could be modified in order to display various epitopes on the surface of the nanoparticle (25, 27, 28, 33, 74–76). These engineered particles showed immunostimulatory properties similar and sometimes better than the original platform following immunization (25, 27, 28, 33, 74, 76). A new strategy that we are currently investigating is the use of a sortase-mediated antigen coupling technique, which permits the fusion of epitopes directly on the surface of PapMV without the need to genetically modify the sequence of the coat protein (36). Immunizations with such PapMV-fused platforms lead to the development of protective humoral responses (36). Different immunization regimen as well as different chronic viral infection models could here be tested to evaluate the potential of PapMV in treating other diseases. The results obtained during this study open the way to study other potential uses for PapMV such as in the treatment of autoimmune diseases. It was previously shown that in the absence of IFN-α, whether in IFNAR-deficient mice or through the use of IFNAR antibody blockade, autoimmune symptoms of lupus prone mice were improved (77, 78). Multiple systemic administrations of PapMV induced an inhibition of IFN-α production providing a potential therapeutic approach for such an application.

In this study, we showed that treatment of a chronic virus infection with PapMV has limitations and still needs to be improved. Although a single administration of PapMV induces strong immune responses, recall systemic immunizations are much less potent partly due to IRAK1 degradation but mainly to interference by PapMV-specific antibodies. Our results also demonstrate that the PapMV platform is able to induce an immune response following a pretreatment although not yet to a degree that would be able to clear an ongoing viral infection. Although this outcome is not favorable in the context of chronic viral infections, it could be of interest for other diseases such as autoimmunity. Further improvements will therefore be needed for this promising therapeutic approach to be used in the treatment of chronic viral infections or other IFN-dependent chronic diseases.

ETHICS STATEMENT

This study was carried out in accordance with the recommendations of the Canadian Council on Animal Care guidelines. The protocol was approved by the Institut national de la recherche scientifique Animal Care Committee.

AUTHOR CONTRIBUTIONS

KC, M-ÈL, and AL conceived and designed the experiments; KC, M-ÈL, and ET performed the experiments; PS developed the PapMV manufacturing process; KC, AL, and DL cowrote the article.

ACKNOWLEDGMENTS

We thank Dr. Armstrong Murira and Dr. Albert Parisien for critically reviewing the manuscript.

FUNDING

This work was financially supported by Canadian Institutes of Health Research Grant MOP-89833 and the Jeanne and J.-Louis Lévesque Chair in Immunovirology from the J.-Louis Lévesque Foundation. KC and M-ÈL acknowledge studentship support from the Fonds de Recherche du Québec – Santé.

SUPPLEMENTARY MATERIAL

The Supplementary Material for this article can be found online at http://www.frontiersin.org/articles/10.3389/fimmu.2017.01885/full#supplementary-material.

FIGURE S1 | Multiplex quantification of cytokines and chemokines in serum 6 h following the last immunization with PapMV. Immunizations were performed 7 or 14 days following a first immunization with PapMV (n = 1, five mice per group).

FIGURE S2 | CD69 expression kinetics on plasmacytoid dendritic cells after PapMV immunization. Results are presented as a ratio of the MFI of the sample over the average mean fluorescence intensity of controls (n = 1–7, one to three mice per group).

FIGURE S3 | ELISA quantification of PapMV-specific IgG in serum of mice transferred with immune sera 6 h following an immunization with control or PapMV. Immune sera were collected 5 and 25 days following PapMV immunization (n = 2, two to three mice per group).

REFERENCES

1. Santini SM, Lapenta C, Logozzi M, Parlato S, Spada M, Di Pucchio T, et al. Type I interferon as a powerful adjuvant for monocyte-derived dendritic cell development and activity in vitro and in Hu-PBL-SCID mice. *J Exp Med* (2000) 191(10):1777–88. doi:10.1084/jem.191.10.1777
2. Montoya M, Schiavoni G, Mattei F, Gresser I, Belardelli F, Borrow P, et al. Type I interferons produced by dendritic cells promote their phenotypic and functional activation. *Blood* (2002) 99(9):3263–71. doi:10.1182/blood.V99.9.3263
3. Marrack P, Kappler J, Mitchell T. Type I interferons keep activated T cells alive. *J Exp Med* (1999) 189(3):521–30. doi:10.1084/jem.189.3.521
4. Kolumam GA, Thomas S, Thompson LJ, Sprent J, Murali-Krishna K. Type I interferons act directly on CD8 T cells to allow clonal expansion and memory formation in response to viral infection. *J Exp Med* (2005) 202(5):637–50. doi:10.1084/jem.20050821
5. Le Bon A, Schiavoni G, D'Agostino G, Gresser I, Belardelli F, Tough DF. Type i interferons potently enhance humoral immunity and can promote isotype switching by stimulating dendritic cells in vivo. *Immunity* (2001) 14(4):461–70. doi:10.1016/S1074-7613(01)00126-1
6. Jego G, Palucka AK, Blanck JP, Chalouni C, Pascual V, Banchereau J. Plasmacytoid dendritic cells induce plasma cell differentiation through type I interferon and interleukin 6. *Immunity* (2003) 19(2):225–34. doi:10.1016/S1074-7613(03)00208-5
7. Cervantes-Barragan L, Zust R, Weber F, Spiegel M, Lang KS, Akira S, et al. Control of coronavirus infection through plasmacytoid dendritic-cell-derived type I interferon. *Blood* (2007) 109(3):1131–7. doi:10.1182/blood-2006-05-023770
8. Wang Y, Swiecki M, Cella M, Alber G, Schreiber RD, Gilfillan S, et al. Timing and magnitude of type I interferon responses by distinct sensors impact CD8 T cell exhaustion and chronic viral infection. *Cell Host Microbe* (2012) 11(6):631–42. doi:10.1016/j.chom.2012.05.003
9. Sullivan BM, Teijaro JR, de la Torre JC, Oldstone MB. Early virus-host interactions dictate the course of a persistent infection. *PLoS Pathog* (2015) 11(1):e1004588. doi:10.1371/journal.ppat.1004588
10. Sandler NG, Bosinger SE, Estes JD, Zhu RT, Tharp GK, Boritz E, et al. Type I interferon responses in rhesus macaques prevent SIV infection and slow disease progression. *Nature* (2014) 511(7511):601–5. doi:10.1038/nature13554
11. Teijaro JR, Ng C, Lee AM, Sullivan BM, Sheehan KC, Welch M, et al. Persistent LCMV infection is controlled by blockade of type I interferon signaling. *Science* (2013) 340(6129):207–11. doi:10.1126/science.1235214
12. Wilson EB, Yamada DH, Elsaesser H, Herskovitz J, Deng J, Cheng G, et al. Blockade of chronic type I interferon signaling to control persistent LCMV infection. *Science* (2013) 340(6129):202–7. doi:10.1126/science.1235208
13. Aul C, Gattermann N, Germing U, Heyll A. Adverse effects of interferon treatment. In: Aul C, Schneider W, editors. *Interferons: Biological Activities and Clinical Efficacy*. Berlin, Heidelberg: Springer (1997). p. 250–66.
14. Sleijfer S, Bannink M, Van Gool AR, Kruit WH, Stoter G. Side effects of interferon-alpha therapy. *Pharm World Sci* (2005) 27(6):423–31. doi:10.1007/s11096-005-1319-7
15. Gilliet M, Cao W, Liu YJ. Plasmacytoid dendritic cells: sensing nucleic acids in viral infection and autoimmune diseases. *Nat Rev Immunol* (2008) 8(8):594–606. doi:10.1038/nri2358
16. Swiecki M, Colonna M. The multifaceted biology of plasmacytoid dendritic cells. *Nat Rev Immunol* (2015) 15(8):471–85. doi:10.1038/nri3865
17. Lee J, Chuang TH, Redecke V, She L, Pitha PM, Carson DA, et al. Molecular basis for the immunostimulatory activity of guanine nucleoside analogs: activation of toll-like receptor 7. *Proc Natl Acad Sci U S A* (2003) 100(11):6646–51. doi:10.1073/pnas.0631696100
18. Swiecki M, Gilfillan S, Vermi W, Wang Y, Colonna M. Plasmacytoid dendritic cell ablation impacts early interferon responses and antiviral NK and CD8(+) T cell accrual. *Immunity* (2010) 33(6):955–66. doi:10.1016/j.immuni.2010.11.020
19. Fonteneau JF, Larsson M, Beignon AS, McKenna K, Dasilva I, Amara A, et al. Human immunodeficiency virus type 1 activates plasmacytoid dendritic cells and concomitantly induces the bystander maturation of myeloid dendritic cells. *J Virol* (2004) 78(10):5223–32. doi:10.1128/JVI.78.10.5223-5232.2004
20. Yoneyama H, Matsuno K, Toda E, Nishiwaki T, Matsuo N, Nakano A, et al. Plasmacytoid DCs help lymph node DCs to induce anti-HSV CTLs. *J Exp Med* (2005) 202(3):425–35. doi:10.1084/jem.20041961
21. Fonteneau JF, Gilliet M, Larsson M, Dasilva I, Munz C, Liu YJ, et al. Activation of influenza virus-specific CD4+ and CD8+ T cells: a new role for plasmacytoid dendritic cells in adaptive immunity. *Blood* (2003) 101(9):3520–6. doi:10.1182/blood-2002-10-3063
22. Lund JM, Linehan MM, Iijima N, Iwasaki A. Cutting edge: plasmacytoid dendritic cells provide innate immune protection against mucosal viral infection in situ. *J Immunol* (2006) 177(11):7510–4. doi:10.4049/jimmunol.177.11.7510
23. Swiecki M, Wang Y, Gilfillan S, Colonna M. Plasmacytoid dendritic cells contribute to systemic but not local antiviral responses to HSV infections. *PLoS Pathog* (2013) 9(10):e1003728. doi:10.1371/journal.ppat.1003728
24. Cervantes-Barragan L, Lewis KL, Firner S, Thiel V, Hugues S, Reith W, et al. Plasmacytoid dendritic cells control T-cell response to chronic viral infection. *Proc Natl Acad Sci U S A* (2012) 109(8):3012–7. doi:10.1073/pnas.1117359109
25. Denis J, Majeau N, Acosta-Ramirez E, Savard C, Bedard MC, Simard S, et al. Immunogenicity of papaya mosaic virus-like particles fused to a hepatitis C virus epitope: evidence for the critical function of multimerization. *Virology* (2007) 363(1):59–68. doi:10.1016/j.virol.2007.01.011
26. Acosta-Ramirez E, Perez-Flores R, Majeau N, Pastelin-Palacios R, Gil-Cruz C, Ramirez-Saldana M, et al. Translating innate response into long-lasting antibody response by the intrinsic antigen-adjuvant properties of papaya mosaic virus. *Immunology* (2008) 124(2):186–97. doi:10.1111/j.1365-2567.2007.02753.x
27. Denis J, Acosta-Ramirez E, Zhao Y, Hamelin ME, Koukavica I, Baz M, et al. Development of a universal influenza A vaccine based on the M2e peptide fused to the papaya mosaic virus (PapMV) vaccine platform. *Vaccine* (2008) 26(27–28):3395–403. doi:10.1016/j.vaccine.2008.04.052
28. Lacasse P, Denis J, Lapointe R, Leclerc D, Lamarre A. Novel plant virus-based vaccine induces protective cytotoxic T-lymphocyte-mediated antiviral immunity through dendritic cell maturation. *J Virol* (2008) 82(2):785–94. doi:10.1128/JVI.01811-07
29. Savard C, Guerin A, Drouin K, Bolduc M, Laliberte-Gagne ME, Dumas MC, et al. Improvement of the trivalent inactivated flu vaccine using PapMV nanoparticles. *PLoS One* (2011) 6(6):e21522. doi:10.1371/journal.pone.0021522
30. Mathieu C, Rioux G, Dumas MC, Leclerc D. Induction of innate immunity in lungs with virus-like nanoparticles leads to protection against influenza and *Streptococcus pneumoniae* challenge. *Nanomedicine* (2013) 9(7):839–48. doi:10.1016/j.nano.2013.02.009
31. Lebel ME, Daudelin JF, Chartrand K, Tarrab E, Kalinke U, Savard P, et al. Nanoparticle adjuvant sensing by TLR7 enhances CD8+ T cell-mediated protection from *Listeria monocytogenes* infection. *J Immunol* (2014) 192(3):1071–8. doi:10.4049/jimmunol.1302030
32. Rioux G, Mathieu C, Russell A, Bolduc M, Laliberte-Gagne ME, Savard P, et al. PapMV nanoparticles improve mucosal immune responses to the trivalent inactivated flu vaccine. *J Nanobiotechnology* (2014) 12:19. doi:10.1186/1477-3155-12-19
33. Carignan D, Therien A, Rioux G, Paquet G, Gagne ML, Bolduc M, et al. Engineering of the PapMV vaccine platform with a shortened M2e

peptide leads to an effective one dose influenza vaccine. *Vaccine* (2015) 33(51): 7245–53. doi:10.1016/j.vaccine.2015.10.123
34. Rioux G, Carignan D, Russell A, Bolduc M, Gagne ME, Savard P, et al. Influence of PapMV nanoparticles on the kinetics of the antibody response to flu vaccine. *J Nanobiotechnology* (2016) 14(1):43. doi:10.1186/s12951-016-0200-2
35. Lebel ME, Langlois MP, Daudelin JF, Tarrab E, Savard P, Leclerc D, et al. Complement component 3 regulates IFN-alpha production by plasmacytoid dendritic cells following TLR7 activation by a plant virus-like nanoparticle. *J Immunol* (2016) 199. doi:10.4049/jimmunol.1601271
36. Therien A, Bedard M, Carignan D, Rioux G, Gauthier-Landry L, Laliberte-Gagne ME, et al. A versatile papaya mosaic virus (PapMV) vaccine platform based on sortase-mediated antigen coupling. *J Nanobiotechnology* (2017) 15(1):54. doi:10.1186/s12951-017-0289-y
37. Lebel ME, Chartrand K, Tarrab E, Savard P, Leclerc D, Lamarre A. Potentiating cancer immunotherapy using papaya mosaic virus-derived nanoparticles. *Nano Lett* (2016) 16(3):1826–32. doi:10.1021/acs.nanolett.5b04877
38. Altman JD, Moss PA, Goulder PJ, Barouch DH, McHeyzer-Williams MG, Bell JI, et al. Phenotypic analysis of antigen-specific T lymphocytes. *Science* (1996) 274(5284):94–6. doi:10.1126/science.274.5284.94
39. Battegay M, Cooper S, Althage A, Banziger J, Hengartner H, Zinkernagel RM. Quantification of lymphocytic choriomeningitis virus with an immunological focus assay in 24- or 96-well plates. *J Virol Methods* (1991) 33(1–2):191–8. doi:10.1016/0166-0934(91)90018-U
40. Smit JJ, Rudd BD, Lukacs NW. Plasmacytoid dendritic cells inhibit pulmonary immunopathology and promote clearance of respiratory syncytial virus. *J Exp Med* (2006) 203(5):1153–9. doi:10.1084/jem.20052359
41. Wherry EJ, Ha SJ, Kaech SM, Haining WN, Sarkar S, Kalia V, et al. Molecular signature of CD8+ T cell exhaustion during chronic viral infection. *Immunity* (2007) 27(4):670–84. doi:10.1016/j.immuni.2007.09.006
42. Xie Q, Shen HC, Jia NN, Wang H, Lin LY, An BY, et al. Patients with chronic hepatitis B infection display deficiency of plasmacytoid dendritic cells with reduced expression of TLR9. *Microbes Infect* (2009) 11(4):515–23. doi:10.1016/j.micinf.2009.02.008
43. Xu N, Yao HP, Lv GC, Chen Z. Downregulation of TLR7/9 leads to deficient production of IFN-alpha from plasmacytoid dendritic cells in chronic hepatitis B. *Inflamm Res* (2012) 61(9):997–1004. doi:10.1007/s00011-012-0493-z
44. Rodrigue-Gervais IG, Jouan L, Beaule G, Sauve D, Bruneau J, Willems B, et al. Poly(I:C) and lipopolysaccharide innate sensing functions of circulating human myeloid dendritic cells are affected in vivo in hepatitis C virus-infected patients. *J Virol* (2007) 81(11):5537–46. doi:10.1128/JVI.01741-06
45. Yonkers NL, Rodriguez B, Milkovich KA, Asaad R, Lederman MM, Heeger PS, et al. TLR ligand-dependent activation of naive CD4 T cells by plasmacytoid dendritic cells is impaired in hepatitis C virus infection. *J Immunol* (2007) 178(7):4436–44. doi:10.4049/jimmunol.178.7.4436
46. Borrow P, Martinez-Sobrido L, de la Torre JC. Inhibition of the type I interferon antiviral response during arenavirus infection. *Viruses* (2010) 2(11):2443–80. doi:10.3390/v2112443
47. Zhou S, Cerny AM, Zacharia A, Fitzgerald KA, Kurt-Jones EA, Finberg RW. Induction and inhibition of type I interferon responses by distinct components of lymphocytic choriomeningitis virus. *J Virol* (2010) 84(18):9452–62. doi:10.1128/JVI.00155-10
48. Blasius AL, Beutler B. Intracellular toll-like receptors. *Immunity* (2010) 32(3):305–15. doi:10.1016/j.immuni.2010.03.012
49. Lester SN, Li K. Toll-like receptors in antiviral innate immunity. *J Mol Biol* (2014) 426(6):1246–64. doi:10.1016/j.jmb.2013.11.024
50. Lehner MD, Morath S, Michelsen KS, Schumann RR, Hartung T. Induction of cross-tolerance by lipopolysaccharide and highly purified lipoteichoic acid via different toll-like receptors independent of paracrine mediators. *J Immunol* (2001) 166(8):5161–7. doi:10.4049/jimmunol.166.8.5161
51. Dalpke AH, Lehner MD, Hartung T, Heeg K. Differential effects of CpG-DNA in toll-like receptor-2/-4/-9 tolerance and cross-tolerance. *Immunology* (2005) 116(2):203–12. doi:10.1111/j.1365-2567.2005.02211.x
52. Nahid MA, Benso LM, Shin JD, Mehmet H, Hicks A, Ramadas RA. TLR4, TLR7/8 agonist-induced miR-146a promotes macrophage tolerance to MyD88-dependent TLR agonists. *J Leukoc Biol* (2016) 100(2):339–49. doi:10.1189/jlb.2A0515-197R
53. Hayashi T, Gray CS, Chan M, Tawatao RI, Ronacher L, McGargill MA, et al. Prevention of autoimmune disease by induction of tolerance to toll-like receptor 7. *Proc Natl Acad Sci U S A* (2009) 106(8):2764–9. doi:10.1073/pnas.0813037106
54. Siedlar M, Frankenberger M, Benkhart E, Espevik T, Quirling M, Brand K, et al. Tolerance induced by the lipopeptide Pam3Cys is due to ablation of IL-1R-associated kinase-1. *J Immunol* (2004) 173(4):2736–45. doi:10.4049/jimmunol.173.4.2736
55. Bourquin C, Hotz C, Noerenberg D, Voelkl A, Heidegger S, Roetzer LC, et al. Systemic cancer therapy with a small molecule agonist of toll-like receptor 7 can be improved by circumventing TLR tolerance. *Cancer Res* (2011) 71(15):5123–33. doi:10.1158/0008-5472.CAN-10-3903
56. Kawai T, Akira S. The role of pattern-recognition receptors in innate immunity: update on toll-like receptors. *Nat Immunol* (2010) 11(5):373–84. doi:10.1038/ni.1863
57. Omatsu Y, Iyoda T, Kimura Y, Maki A, Ishimori M, Toyama-Sorimachi N, et al. Development of murine plasmacytoid dendritic cells defined by increased expression of an inhibitory NK receptor, Ly49Q. *J Immunol* (2005) 174(11):6657–62. doi:10.4049/jimmunol.174.11.6657
58. Pelayo R, Hirose J, Huang J, Garrett KP, Delogu A, Busslinger M, et al. Derivation of 2 categories of plasmacytoid dendritic cells in murine bone marrow. *Blood* (2005) 105(11):4407–15. doi:10.1182/blood-2004-07-2529
59. Bjorck P, Leong HX, Engleman EG. Plasmacytoid dendritic cell dichotomy: identification of IFN-alpha producing cells as a phenotypically and functionally distinct subset. *J Immunol* (2011) 186(3):1477–85. doi:10.4049/jimmunol.1000454
60. Zhang H, Gregorio JD, Iwahori T, Zhang X, Choi O, Tolentino LL, et al. A distinct subset of plasmacytoid dendritic cells induces activation and differentiation of B and T lymphocytes. *Proc Natl Acad Sci U S A* (2017) 114(8):1988–93. doi:10.1073/pnas.1610630114
61. Niederquell M, Kurig S, Fischer JA, Tomiuk S, Swiecki M, Colonna M, et al. Sca-1 expression defines developmental stages of mouse pDCs that show functional heterogeneity in the endosomal but not lysosomal TLR9 response. *Eur J Immunol* (2013) 43(11):2993–3005. doi:10.1002/eji.201343498
62. Barouch DH, Pau MG, Custers JH, Koudstaal W, Kostense S, Havenga MJ, et al. Immunogenicity of recombinant adenovirus serotype 35 vaccine in the presence of pre-existing anti-Ad5 immunity. *J Immunol* (2004) 172(10):6290–7. doi:10.4049/jimmunol.172.10.6290
63. Sumida SM, Truitt DM, Kishko MG, Arthur JC, Jackson SS, Gorgone DA, et al. Neutralizing antibodies and CD8+ T lymphocytes both contribute to immunity to adenovirus serotype 5 vaccine vectors. *J Virol* (2004) 78(6):2666–73. doi:10.1128/JVI.78.6.2666-2673.2004
64. Chen J, Trounstine M, Alt FW, Young F, Kurahara C, Loring JF, et al. Immunoglobulin gene rearrangement in B cell deficient mice generated by targeted deletion of the JH locus. *Int Immunol* (1993) 5(6):647–56. doi:10.1093/intimm/5.6.647
65. Villacres MC, Literat O, DeGiacomo M, Du W, Frederick T, Kovacs A. Defective response to toll-like receptor 3 and 4 ligands by activated monocytes in chronic hepatitis C virus infection. *J Viral Hepat* (2008) 15(2):137–44. doi:10.1111/j.1365-2893.2007.00904.x
66. Yeow WS, Lawson CM, Beilharz MW. Antiviral activities of individual murine IFN-alpha subtypes in vivo: intramuscular injection of IFN expression constructs reduces cytomegalovirus replication. *J Immunol* (1998) 160(6):2932–9.
67. van Pesch V, Lanaya H, Renauld JC, Michiels T. Characterization of the murine alpha interferon gene family. *J Virol* (2004) 78(15):8219–28. doi:10.1128/JVI.78.15.8219-8228.2004
68. Gerlach N, Gibbert K, Alter C, Nair S, Zelinskyy G, James CM, et al. Anti-retroviral effects of type I IFN subtypes in vivo. *Eur J Immunol* (2009) 39(1):136–46. doi:10.1002/eji.200838311
69. Albrecht V, Hofer TP, Foxwell B, Frankenberger M, Ziegler-Heitbrock L. Tolerance induced via TLR2 and TLR4 in human dendritic cells: role of IRAK-1. *BMC Immunol* (2008) 9:69. doi:10.1186/1471-2172-9-69
70. Liu YC, Simmons DP, Li X, Abbott DW, Boom WH, Harding CV. TLR2 signaling depletes IRAK1 and inhibits induction of type I IFN by TLR7/9. *J Immunol* (2012) 188(3):1019–26. doi:10.4049/jimmunol.1102181
71. Smith DM, Simon JK, Baker JR Jr. Applications of nanotechnology for immunology. *Nat Rev Immunol* (2013) 13(8):592–605. doi:10.1038/nri3488
72. Schwab N, Zozulya AL, Kieseier BC, Toyka KV, Wiendl H. An imbalance of two functionally and phenotypically different subsets of plasmacytoid dendritic cells characterizes the dysfunctional immune regulation in multiple sclerosis. *J Immunol* (2010) 184(9):5368–74. doi:10.4049/jimmunol.0903662

73. Lebel ME, Chartrand K, Leclerc D, Lamarre A. Plant viruses as nanoparticle-based vaccines and adjuvants. *Vaccines (Basel)* (2015) 3(3):620–37. doi:10.3390/vaccines3030620
74. Leclerc D, Beauseigle D, Denis J, Morin H, Pare C, Lamarre A, et al. Proteasome-independent major histocompatibility complex class I cross-presentation mediated by papaya mosaic virus-like particles leads to expansion of specific human T cells. *J Virol* (2007) 81(3):1319–26. doi:10.1128/JVI.01720-06
75. Rioux G, Majeau N, Leclerc D. Mapping the surface-exposed regions of papaya mosaic virus nanoparticles. *FEBS J* (2012) 279(11):2004–11. doi:10.1111/j.1742-4658.2012.08583.x
76. Babin C, Majeau N, Leclerc D. Engineering of papaya mosaic virus (PapMV) nanoparticles with a CTL epitope derived from influenza NP. *J Nanobiotechnology* (2013) 11:10. doi:10.1186/1477-3155-11-10
77. Santiago-Raber ML, Baccala R, Haraldsson KM, Choubey D, Stewart TA, Kono DH, et al. Type-I interferon receptor deficiency reduces lupus-like disease in NZB mice. *J Exp Med* (2003) 197(6):777–88. doi:10.1084/jem.20021996
78. Baccala R, Gonzalez-Quintial R, Schreiber RD, Lawson BR, Kono DH, Theofilopoulos AN. Anti-IFN-alpha/beta receptor antibody treatment ameliorates disease in lupus-predisposed mice. *J Immunol* (2012) 189(12):5976–84. doi:10.4049/jimmunol.1201477

Conflict of Interest Statement: DL is the founder and a shareholder of Folia Biotech. Inc., a Canadian Biotechnology Company with the mandate to commercialize the PapMV Technology. The other authors have no financial conflicts of interest.

frontiers in Immunology

REVIEW
published: 05 February 2018
doi: 10.3389/fimmu.2018.00155

The Multirole of Liposomes in Therapy and Prevention of Infectious Diseases

*Roberto Nisini[1], Noemi Poerio[2], Sabrina Mariotti[1], Federica De Santis[2] and Maurizio Fraziano[2]**

[1] Dipartimento di Malattie Infettive, Istituto Superiore di Sanità, Rome, Italy, [2] Dipartimento di Biologia, Università degli Studi di Roma "Tor Vergata", Rome, Italy

Liposomes are closed bilayer structures spontaneously formed by hydrated phospholipids that are widely used as efficient delivery systems for drugs or antigens, due to their capability to encapsulate bioactive hydrophilic, amphipathic, and lipophilic molecules into inner water phase or within lipid leaflets. The efficacy of liposomes as drug or antigen carriers has been improved in the last years to ameliorate pharmacokinetics and capacity to release their cargo in selected target organs or cells. Moreover, different formulations and variations in liposome composition have been often proposed to include immunostimulatory molecules, ligands for specific receptors, or stimuli responsive compounds. Intriguingly, independent research has unveiled the capacity of several phospholipids to play critical roles as intracellular messengers in modulating both innate and adaptive immune responses through various mechanisms, including (i) activation of different antimicrobial enzymatic pathways, (ii) driving the fusion–fission events between endosomes with direct consequences to phagosome maturation and/or to antigen presentation pathway, and (iii) modulation of the inflammatory response. These features can be exploited by including selected bioactive phospholipids in the bilayer scaffold of liposomes. This would represent an important step forward since drug or antigen carrying liposomes could be engineered to simultaneously activate different signal transduction pathways and target specific cells or tissues to induce antigen-specific T and/or B cell response. This lipid-based host-directed strategy can provide a focused antimicrobial innate and adaptive immune response against specific pathogens and offer a novel prophylactic or therapeutic option against chronic, recurrent, or drug-resistant infections.

Keywords: liposome, infectious disease, therapy, immunotherapy, drug, vaccine, adjuvant, immunomodulation

OPEN ACCESS

Edited by:
Rajko Reljic, St George's, University of London, United Kingdom

Reviewed by:
Arun Kumar, Linköping University, Sweden
Giampiero Pietrocola, University of Pavia, Italy

****Correspondence:***
Maurizio Fraziano
fraziano@bio.uniroma2.it

Specialty section:
This article was submitted to Vaccines and Molecular Therapeutics, a section of the journal Frontiers in Immunology

Received: *28 November 2017*
Accepted: *17 January 2018*
Published: *05 February 2018*

Citation:
Nisini R, Poerio N, Mariotti S, De Santis F and Fraziano M (2018) The Multirole of Liposomes in Therapy and Prevention of Infectious Diseases. Front. Immunol. 9:155. doi: 10.3389/fimmu.2018.00155

INTRODUCTION

Liposomes are small artificial spherical vesicles constituted by one or more phospholipid bilayers with the polar groups of phospholipids oriented to the inner and outer aqueous phase. Such a structure explains the high propensity of liposomes to be encapsulated with hydrophilic, hydrophobic, and amphiphilic drugs within the inner aqueous compartment, the lipid bilayers, and at their interfaces, respectively (1). Liposomes can be classified as unilamellar (ULV) or multilamellar (MLV) vesicles (2), depending on the structure of the bilayer (**Figure 1**). ULV are characterized by the presence of a

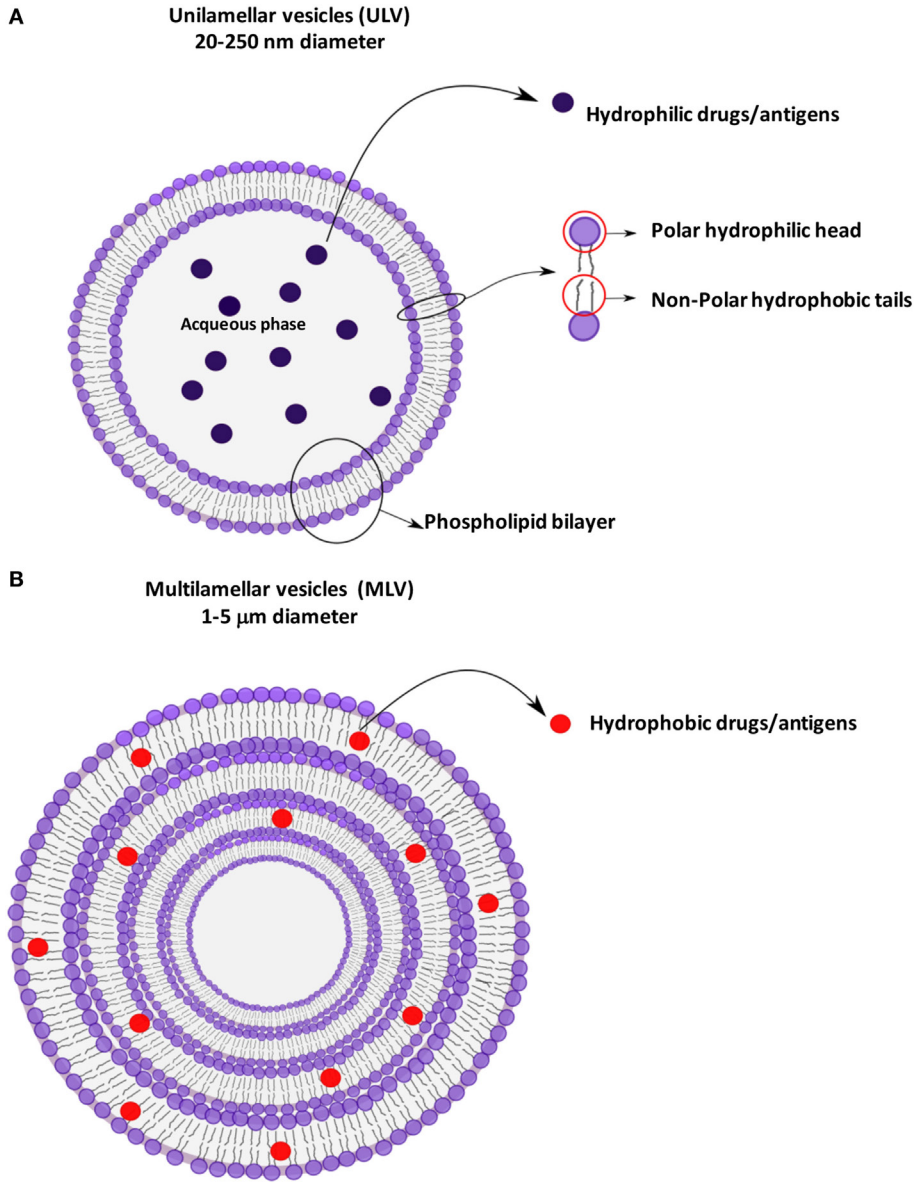

FIGURE 1 | Schematic representation of liposomes showing the different antigen encapsulation propensity: unilamellar **(A)** and multilamellar **(B)** vesicles.

single-lipid bilayer of 20–250 nm diameter, which enclose a large aqueous core and are ideally suited for the encapsulation of hydrophilic drugs/antigens (2). Conversely, MLV are characterized by the presence of two or more concentric lipid bilayers of 1–5 μm diameter that preferentially entrap lipid soluble molecules (2). Liposomes are extensively used as carriers for active molecules in cosmetic and pharmaceutical industries as well as in food and farm industries, where liposomes encapsulation has also been studied to entrap unstable substances such as antioxidants, flavors, and antimicrobials. The phospholipid protective shield forms a barrier, which is normally resistant to the action of enzymes, pH, and free radicals within the body, thus protecting the cargo from degradation until the release occurs at the target cell, organ, or system. Because of the high biocompatibility, biodegradability, low toxicity, and capability to encapsulate hydrophilic and hydrophobic compounds (2), liposomes represent the most successful drug carrier system known to date. Many liposome formulations for the treatment of cancer, fungal, and viral infection as well as pain management are available in clinical use, and many other formulations are being tested in different phases of clinical trials (3). From their first description in 1960s, many liposomes have been produced with distinctive characteristics, which strictly depend on the nature of lipid components, on their possible chemical modifications, and on their surface charge. In particular, early conventional liposomes were mainly constituted by natural phospholipids such as phosphatidylcholine (PC), sphyngomielin, and monosyaloganglioside (4). However, this formulation was subjected to several critical issues, such as the instability in

plasma and short blood circulation half-life, due to their interaction with high- and low-density lipoproteins that resulted in the rapid release of the encapsulated drug into the plasma, and the efficient liposome uptake and removal from circulation by the macrophage system. Moreover, in most cases, negatively charged liposomes have a shorter half-life in the blood than neutral liposomes, and positively charged liposomes are toxic and quickly removed from circulation (5). The addition of cholesterol (Chol) in liposome formulation reduced the permeability of lipid bilayer, increased the liposome stability, and reduced the rapid release of encapsulated bioactive compound (6). The size was also shown to be a crucial determinant for circulation half-life of liposomes, as their elimination by phagocytes is directly correlated to the liposome diameter: MLV with diameters ranging from 500 to 5,000 nm are quickly removed by phagocytes, whereas ULV with diameters between 20 and 50 nm show the less propensity to be internalized by macrophages (5), but are characterized by a low volume available for drug entrapment.

Improvement of liposome technology involved the generation of stealth liposome, targeted liposomes, immunoliposomes, and stimuli responsive liposomes (**Figure 2**). The stealth strategy is based on the possibility to coat the external liposome surface with biocompatible hydrophilic polymer conjugates, such as polyethylene glycol (PEG), chitosan, and others, which reduces immunogenicity and macrophage uptake. Stealth liposome technology makes liposome capable to escape phagocytosis, to reduce toxicity due to the presence of charged lipids, and to increase blood circulation half-life. However, an important limitation of stealth liposomes is their large biodistribution in tissues, as encapsulated bioactive molecules cannot be selectively delivered to target cells (7). Targeted liposomes where therefore designed to counterbalance the large body distribution of stealth liposomes. Targeted liposomes are characterized by the presence of membranes functionalized with glycoproteins, polysaccharides, or ligands for specific receptors that determine the preferential accumulation of liposomes in selected tissues, so that the liposome drug/antigen cargo can be preferentially released in predetermined target cells or organs (7). A further strategy to deliver entrapped drug/antigen in the desired tissue/cell is represented by immunoliposomes, which are functionalized by antibodies or antibody fragments (8), and stimuli responsive liposomes. Examples of stimuli responsive liposomes are the pH-sensitive liposomes (9), which undergo conformational and chemical changes in response to acid pH, and temperature sensitive liposomes (10), which keep their cargo encapsulated at body temperature, but discharge it upon local heating.

In addition to the delivery of drugs, liposomes may also be used for many other purposes through the modification of their composition and cargo. In vaccinology, for example, liposomes can be formulated with the inclusion of antigens (lipids, nucleic acids, proteins, and peptides), and/or with pathogen-associated molecular patterns (PAMPs), which confer adjuvant properties aimed at modulating the inflammatory microenvironment where T lymphocyte priming occurs (11, 12). At the moment, a number of liposome formulations are in clinical trials as adjuvant for prophylactic as well as therapeutic vaccines against malaria, influenza, tuberculosis (TB), human immunodeficiency virus (HIV), and dengue fever (13), whereas Cervarix®, Inflexal®, and Epaxal® are commercially available liposome vaccines against infection by human papilloma virus (HPV), influenza virus, and hepatitis A virus, respectively. Finally, lipids are important second messengers in the regulation of molecular pathways associated with phagosome maturation and activation of antimicrobial responses (14). Thus, the possibility exists to deliver selected lipid second messengers into infected cells through targeted liposomes to activate antimicrobial molecular pathways against specific bacterial pathogens (15).

This review summarizes the recent developments in liposome technology aimed at the generation of novel prophylactic as well as therapeutic tools to control infectious diseases.

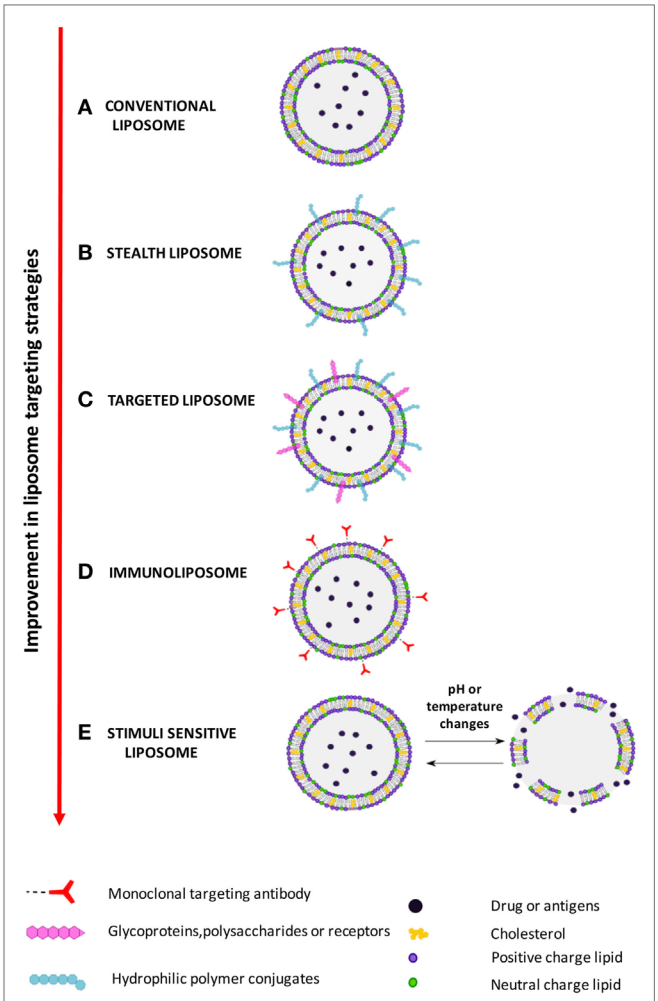

FIGURE 2 | Improvement in liposome targeting strategies. **(A)** Conventional liposomes; **(B)** long circulating stealth liposomes with membrane functionalized with hydrophilic polymeric conjugates, such as polyethylene glycol (PEG), to avoid elimination by reticuloendothelial system; **(C)** targeted liposomes with membranes functionalized with glycoproteins, polysaccharides, or ligands of cell/tissue-specific receptors; **(D)** immunoliposomes, a specific form of targeted liposomes, with membrane functionalized with antibodies or antibody fragments; **(E)** stimuli responsive (pH or temperature) liposomes, which release the encapsulate drug following exposure to acid pH or heating.

LIPOSOMES AS CARRIER FOR DRUGS

The fate of drugs administered to a living organism varies according to several variables, including distribution, metabolism, and excretion. After a drug enters the systemic circulation, it is not distributed uniformly to the body's tissues due to differences in organ blood perfusion, tissue affinity, local pH, and permeability of cell membrane. Thus, a significant amount of a given drug does not reach the target cell or organ. The consequence of the uneven distribution is a reduced concentration of drug reaching the target cells and the interaction of the drug with bystander targets. Increasing the dose of the drug helps reaching the therapeutic concentration at the target level and also increases the effects of the drug on other cells, concurring to amplify side or adverse events of drug administration. The ratio between the blood concentration at which the drug is effective and the concentration at which the drug becomes toxic is defined therapeutic index (TI): the larger is the TI, the safer is the drug. It has to be further stressed that the ultimate target of drugs is generally an intracellular reaction site and the interaction of drugs with the cellular/bacterial lipid membrane is expected to occur at some point, affecting, sometimes severely, drug bioavailability, and efficacy (16). In the absence of specific mechanisms of intracellular transportation, the chemical nature of the drug dictates the level of entrance into cells. An interesting example is given by the different intracellular accumulation rates observed for four structurally similar quinolones: ciprofloxacin, levofloxacin, garenoxacin, and moxifloxacin (17). Quinolones were shown to exert a condensing effect on the membrane bilayer and the condensing effect differed among the quinolones: even small differences in their chemical structure were shown to influence their lipophilicity, the consequent capacity to cross cell membranes and to accumulate intracellularly, and the eventual antimicrobial effect (18). Thus, the search of innovative approaches to increase drug transport across the cell membrane or to improve the permeability of small molecule, peptide, and/or protein–drugs to access the cytoplasm is a hot field in pharmacology (19).

Within a few years after the first description of "swollen phospholipid systems" by Bangham and colleagues (20), various enclosed phospholipid structures consisting of single bilayers, initially termed "banghaosomes" and then "liposomes" (21), were described (22). The observation that liposomes can entrap drugs made these nanoparticles an interesting tool exploitable as new drug delivery systems (23, 24). The observation that the anticancer drug cytosine arabinoside was successfully delivered by liposomes to tumor cells with a significant increase in the survival times of mice affected by L1210 leukemia (25) was one of the first demonstrations of the suitability of liposomes as drug delivery system. Murine L1210 leukemia became "model system" for testing the therapeutic outcomes of anticancer drugs delivered by a large variety of liposome with different characteristics (26). Another advantage that became evident using liposome-entrapped drugs was the reduction of drug toxicity: drugs entrapped in liposomes are not bioavailable until they are released in target organs. Amphotericin B (AmB) and doxorubicin entrapped in liposomes (26) were extensively studied and the pioneering *in vitro* and *in vivo* studies ultimately led to the first clinical trials of liposomal drugs (27). However, the first tested "large ULV" for drug delivery showed their limits and many efforts have been made to design liposomes able to target specific cells and favor drug release for an optimized release rate of entrapped drug from the liposomes. For the optimal therapeutic activity, drugs must be released from liposomes to the disease site, where they should become bioavailable at a concentration within their therapeutic window for a sufficient time (26). One of the first obstacles that appeared clear when using large ULV was the rapid clearance of liposomes operated by the phagocyte system in the liver and spleen. Several approaches were tested, ranging from variation in liposome dimension to treatment of liposomes with serum albumin or variation in bilayer composition and Chol content (26). A significant step forward in the field of drug delivered by liposomes was made thanks to the observation that attaching PEG to proteins causes an increase of their circulation half-life (28). When the procedure was applied to the liposome system, it was evident that grafting of PEG to the liposome surface resulted in diminished clearance of liposomes by macrophages (29) and, the PEG-liposomes (stealth liposomes), unlike previously tested ULV, were shown to have dose-independent pharmacokinetics (30). The improvements in the therapeutic outcomes of stealth liposomes in comparison with conventional ULV for a variety of therapeutics was demonstrated in different animal models of disease (26), and then in the humans, where the long circulation half-life of a doxorubicin entrapped in PEG–liposomes was confirmed. Shortly thereafter, doxorubicin entrapped in stealth liposomes was used in the first clinical trial for the treatment of Kaposi's sarcoma in HIV patients (31). The persistence of stealth liposomes in the circulation facilitated their accumulation in highly vascularized sites, such as tumors or inflammatory sites. However, it appeared clear that both the efficacy and the TI would increase if drug-bearing liposomes could be selectively addressed to target cells.

Active targeting could be accomplished by coupling targeting ligands to the surface of liposomes, such as proteins, peptides, carbohydrates, or monoclonal antibodies or their fragments (fragment antigen-binding and single-chain variable fragment) (32). Thus, targeted liposomes can be selectively taken up by cells that overexpress the receptor for the moiety, so improving therapeutic outcomes by increasing efficacy and reducing off-target toxicity (32). Among the different moieties that can be covalently or non-covalently attached to the liposome surface, antibodies and antibody fragments are the most widely employed, producing immunoliposomes (33). Spragg and coworkers demonstrated that E-selectin-targeted immunoliposomes for doxorubicin delivery mediated marked cytotoxicity when incubated with activated human umbilical vein endothelial cells (HUVECs) that express E-selectin, but not when incubated with non-activated HUVECs (34). Following these promising results, methods for antibody coupling to liposomes have been developed (33) and different antibodies or fragments have been attached to liposomes, particularly through reactions with maleimide. Examples include immunoliposomes targeted to soluble *Leishmania* antigens, EFGR for glioma, endoglin (CD105), fibroblast activation protein, and HER2 for breast cancer, among others (35–38).

In addition to the possible systemic use, i.e., intravenous administration (39), liposomes have been designed for aerosol administration (40) or intradermal administration due to their lipophilic properties suitable for skin penetration (41). The functionalization of liposomes makes it possible to design drug delivery systems suitable for the treatment of different diseases according to their pathogenesis and localization. Among other diseases, liposomes have been primarily and deeply studied for cancer treatment. The narrow TI of antitumor drugs, i.e., the narrow window between their effective doses and those at which they produce adverse toxic effects, makes liposomes as ideal carriers for this type of drugs (42). Indeed, the majority of liposome-delivered drugs available for clinical use (**Table 1**) and in advanced phase III studies to date belongs to this category (3).

The property of encapsulation of drugs in liposomes to enhance the TI of various agents was the reason for the first use of anti-infectious drugs in severely ill patients with renal failure. To date, the only drug delivered by liposomes approved for clinical use in the field of infectious disease is AmB, but many studies are ongoing aimed at taking advantage of this versatile platform to treat patients with a variety of different infectious diseases. Three formulations of AmB for parenteral use were made available differing for liposome formulation and indications. Abelcet® was developed in 1995 for the treatment of invasive fungal infections refractory to conventional AmB desoxycholate therapy or when renal impairment or unacceptable toxicity precludes the use of conventional AmB (3). Abelcet® has a 1:1 drug:lipid molar ratio with a drug concentration ranging from 25 to about 50% molar (49). Ambisome® was approved in 1997 for the treatment of severe fungal infections including leishmaniasis, aspergillosis, blastomycosis, coccidioidomycosis in febrile, neutropenic patients, and a severe form of meningitis in individuals infected with HIV (3). Ambisome® is also indicated for the treatment of invasive systemic infections caused by *Aspergillus* sp., *Candida* sp., or *Cryptococcus* sp. in renal impaired patients or in patients who cannot tolerate therapy with free AmB (50). Amphotec® is a freeze-dried lipid-based formulation of AmB. The sodium salt of cholesteryl sulfate forms a thermodynamically stable colloidal complex with AmB at a 1:1 drug-to-lipid molar ratio (3).

In the field of parasitic infections, several studies were performed to test the efficacy of liposome-encapsulated drugs. In the treatment of leishmaniosis, an interesting approach is based on the use of dinitroanilines, because of their specific binding to parasite but not human tubulins. However, their low water solubility and instability have blocked their development as antiparasitic agents (51). Encapsulation of drug by dimyristoyl PC- and dimyristoyl phosphatidylglycerol-based liposomes overcome those limitations and allowed to efficiently deliver the drugs, reaching a therapeutic advantage as demonstrated in animal models (51). Another drug under test for liposome delivery is buparvaquone, an extensively studied drug for the treatment of visceral leishmaniosis. da Costa-Silva et al. reported that buparvaquone, which has an immunomodulatory effect in host cells, when entrapped in phosphatidylserine (PS) exposing-liposomes, as a delivery approach to macrophage, is highly effective at low doses at eliminating *Leishmania infantum* parasites in a hamster model (52).

In the fight against malaria, the majority of drugs under development are lipophilic and characterized by poor plasma solubility and large biodistribution volumes with low accumulation in red blood cells (RBC). As a consequence, these drugs have shown limited therapeutic activity against intra-erythrocyte *plasmodia* (53). Rajendran et al. developed lipid formulations of soy-PC Chol containing either stearylamine (SA) or phosphatidic acid (PA) and different densities of distearoyl phosphatidylethanolamine-methoxy-PEG 2000 as a delivery system to test the antimalarial activity of monensin. Monensin entrapped in such liposome formulations was tested both in *in vitro* systems of *Plasmodium falciparum* cultures and in *in vivo* murine models of *Plasmodium berghei* infection and found to be more effective than free monensin given at comparable doses (54). The trans platinum–chloroquine diphosphate dichloride was recently successfully tested after its encapsulation into PEGylated neutral and cationic liposomes to fight parasites resistant to traditional drugs and proposed as a new therapeutic tool against malaria (55). Preliminary assays conducted in 1987 using passively loaded chloroquine into RBC-targeted immunoliposomes resulted in significant *P. berghei* growth inhibition in mice, when compared with administration of the free compound (56). More recently, the immunoliposome strategy against malaria was tested taking advantage of a monoclonal antibody specific for a 52-kDa RBC surface antigen characteristic of the murine erythroid lineage

TABLE 1 | Liposome-delivered drugs in clinical use for the treatment of tumor.

Commercial name	Drug	Liposome composition	Indications
Doxil®	Doxorubicin	PEGylated liposome	Advanced ovarian cancer, multiple myeloma and human immunodeficiency virus (HIV)-associated Kaposi's sarcoma
Myocet®	Doxorubicin	Nonpegylated liposome	Breast cancer (43)
DaunoXome®	Daunorubicin	Small size liposome	HIV-associated Kaposi's sarcoma (44)
Depocyt®	Cytarabine/Ara-C	Multivesicular particles with a granular structure: DepoFoam™	Neoplastic meningitis (45)
Mepact®	Mifamurtide: immunostimulant muramyltripeptide	Multilamellar vesicles	High-grade, resectable, non-metastatic bone tumors combined with postoperative combination chemotherapy in children (46)
Marqibo®	Vincristine	Optisomes: sphingomyelin/cholesterol liposome	Adult patients with Philadelphia chromosome-negative acute lymphoblastic leukemia (47)
Onivyde™	Irinotecan	Multilamellar vesicles	Metastatic adenocarcinoma of the pancreas (48)

and specifically expressed from the early proerythroblast to mature RBC stages. These immunoliposomes loaded with two novel antimalarial lipophilic drug candidates in the mouse model of *Plasmodium yoelii* increased the TI and efficacy of the used drug (53). Liposomes exposing PS-specific peptide may represent a further strategy to target *plasmodia* infected RBC in apoptosis (eryptosis:erythrocyte apoptosis) that have been tested in malaria treatment, with promising results (57). Experimental malaria may also represent a model to study the combined effect of anti-infective drugs and anti-inflammatory compounds aimed to limit immunopathogenic reactions in critical anatomic sites, such as the brain. Guo et al. tested liposome-encapsulated β-methasone hemisuccinate in a murine model of experimental cerebral malaria and found that this anti-inflammatory liposome-delivered drug prolonged the survival time of infected animals, permitting the administration of anti-malarial drug before the development of severe anemia (58). In addition to malaria, liposomes, as part of nanopharmaceuticals, are promising tools under investigation for the treatment of several other parasitic diseases including schistosomiasis (59, 60) and acanthamoebiasis (61), which are grouped under the term of neglected diseases (62).

In 2016, it was estimated that there were nine million new TB cases in the world and around half a million of them were caused by multidrug-resistant (MDR) *Mycobacterium tuberculosis* (Mtb) strains (Global tuberculosis Report 2017. http://www.who.int/tb/publications/global_report/en/ Health Organization, Geneva, Switzerland). The research is focused in developing new antimicrobials, but the need to reach a sufficiently high drug concentration inside the lung macrophages and the appearance of MDR and extensively drug-resistant (XDR) Mtb strains represent two major obstacles to reach this goal (63, 64). A possible strategy to the development of new anti-TB therapeutics is based on the administration of drugs contained in specific nanodevices (62), which, preferentially targeting macrophages, allows the use of lower drug dosage and the reduction of undesirable side effects as well as the limitation of Mtb resistance mechanisms. In this line, an interesting contribution to the development of innovative anti-TB therapeutic strategies is the inhalation therapy with liposomes carrying anti-TB drugs. The inhaled drug is expected to be rather effective in the overt presence of bacteria as in smear-positive cases of TB in which the bronchial tree may be directly connected with the cavitary lesions, where Mtb rapidly multiplies. Liposomes delivering anti-TB drugs may offer several advantages over dry powder inhalable formulations of anti-TB drug (65, 66) or other aerosol administrable nanoparticles (67), such as the increase of drug half-life and the possibility to target the intracellular pathogen (68). However, difficulties may arise to efficiently entrap some of the drugs required for TB treatment into liposomes. Justo and Moraes showed that passive encapsulation of isoniazid and pyrazinamide in liposomes during dry lipid film hydration at initial drug-to-lipid molar ratios of 13.3 can be achieved with efficiencies of 2.5 and of 2.2%, respectively, equivalent to final drug-to-lipid molar ratios of 0.33 and 0.29 (69). Moreover, they were also able to incorporate ethionamide during the dry lipid film production step with a 42% trapping efficiency, equivalent to a low final drug-to-lipid molar ratio of 0.04 (69). Justo and Moraes were unable to efficiently incorporate rifampicin and streptomycin in the vesicles under the conditions tested. In contrast, Zaru et al. succeeded in entrap rifampicin in liposomes made of phospholipon 90®, soy lecithin, and Chol using the film hydration method followed by procedures of freeze dry (70). A deeper deposition of rifampicin entrapped in these liposomes in comparison with rifampicin suspension was found in lung airways of rats after nebulization of a nose-only exposure chamber, encouraging the use of liposomes in aerosol therapy of TB (71). An additional aspect to be faced is the stability of liposome-entrapped drugs. Stability may be enhanced by the use of pro-liposomes, i.e., free flowing granular products composed of drug and phospholipid precursors, which on hydration lead to liposomes (72, 73) that have a higher stability upon reconstitution. A new single-step and fast spray drying technique for pro-liposome powder preparation was developed (74, 75) using a systematic method known as "Quality by Design" (71): a systematic approach to develop drug products that includes evaluation of formulation parameters to achieve defined final product quality (76). The method was used to prepare rifapentine-loaded pro-liposomes, which resulted in an average size of 578 nm and an efficiency of encapsulation around 70% (71). The pro-liposome with a drug/hydrogenated soy-PC ratio of 1:2 and SA as a charge-inducing agent (74, 75) are promising formulations and represent possible new tools to approach therapy of infectious diseases based on the optimization of the delivery of old drugs. However, liposomes may be also considered for the delivery of new developed drugs to reduce or delay the appearance of drug resistance.

Liposome-entrapped drugs or immunomodulating agents are being developed for the treatment of many other diseases (see some examples in **Table 2**). However, clinical trials based on innovative liposome strategies should take into account also possible side effects that these drug formulations may have, particularly when given intravenously, and the fulfillment of several regulatory landscape. Both FDA and EMA have developed specific guidelines to be fulfilled in clinical trials with reference to future novel liposomal products (77, 78).

TABLE 2 | Possible applications of liposome-encapsulated drug.

Disease/field	Drug	Reference
Glaucoma	Dorzolamide	(79)
Uveoretinitis	Imiximab	(80)
Age-related macular degeneration	Verteporfina	(3)
Pulmonary hypertension	Phosphodiesterase 5 inhibitors	(81)
Post ischemia	Streptokinasis	(82)
Pain management	Diacylglycerol lipase-beta inhibitors	(83)
Anesthesia	Bupivacaine	(84, 85)
Skin disorders	Various drug	(41, 86, 87)
Autoimmune diseases	Infliximab, other immunosuppressants	(80, 88, 89)
Others	Nucleic acid	(87)
	siRNA	(90)

LIPOSOMES AS "DIRECT" ENHANCERS OF INNATE ANTIMICROBIAL IMMUNE RESPONSE

For long time, the function of lipids was believed to be limited to their role as structural components of membranes or principal form of energy storage in cells. However, during the past 30 years, their important role in cell physiology has been disclosed and lipids have been identified as fundamental players in many cellular functions, including, among others, the regulation of signaling, organization of membranes, intracellular vesicle trafficking, and phagocytosis. Particularly interesting is the role of lipids in the physiology and pathology of phagocytosis, which represents a critical step in the effector function of innate immunity. In fact, the phagosome formation and maturation are functions involving coordinated signaling, targeting, and trafficking events largely regulated by lipid moieties (91, 92). In this process, several lipid species accumulate in membrane microdomains, where they associate in signaling transduction platforms (93). In addition, several lipids can (i) promote positive (convex) or negative (concave) membrane curvature, (ii) recruit signal proteins by binding to specific lipid-binding domains (**Table 3**), and (iii) confer an electrostatic potential on membrane to attract opposite charged key signaling and effector proteins (91–93). Thus, intracellular vesicle trafficking is finely regulated by a topologically and temporally controlled lipid expression whose main role, in the case of phagocytosis, is to promote the fusion/fission events, which starting from phagosomes leads to the generation of a bactericidal phagolysosome (PL) (14). Phagocytosis starts with particle recognition by phagocytic receptors and proceeds with phagocytic cup formation, phagosome sealing (PSL), and internalization (**Figure 3A**). In particular, one of the first events occurring during phagocytic receptor signaling is a local rapid accumulation of phosphatidylinositol (PI) 4,5-bis phosphate [$PI(4,5)P_2$] (94), mediated by PI 4-phosphate 5-kinases (PIP5Ks), whose activity both regulates phospholipase D (PLD) and is regulated by PA, the product of PLD (95). Few minutes after accumulation, $PI(4,5)P_2$ is rapidly degraded by phospholipase Cγ (PLCγ) or phosphorylated, by type I phosphoinositide 3-kinase (PI3K), to $PI(3,4,5)P_3$ (96), whose formation is required for pseudopod extension and phagosome formation (97). The rise of $PI(3,4,5)P_3$ at sites of phagocytic receptor engagement promotes the recruitment of PLCγ through its pleckstrin homology (PH) domain (98), with the consequent hydrolysis of $PI(4,5)P_2$ to diacylglycerol (DAG), which in turn can be converted in PA by DAG kinases (99). PA, $PI(4,5)P_2$, and $PI(3,4,5)P_3$ represent the most important lipid second messengers involved in the early phases of phagocytosis. These lipids contribute to the lateral spreading of phagocyte receptor signaling, which is important to integrate the signals elicited by sparsely phagocytic receptors and to cytoskeletal remodeling. Remodeling culminates with the formation of pseudopods, which surrounding the phagocytic target and sealing at their distal tips, form the phagosome (96). Phosphoinositides are key molecules in modulating cytoskeletal reorganization starting from the early phases of phagocytosis: $PI(3,4,5)P_3$ contributes by recruiting WAVE and myosin X to forming phagosomes, while $PI(4,5)P_2$ can promote actin polimerization by (i) inducing WASP dependent Arp2/3 activation, (ii) removing capping proteins like profilin from the ends of actin filaments, and (iii) stimulating gelsolin-mediated severing of actin filaments and hence allowing fast growth of barbed ends (91). PI 3-kinase (Vps34) is expressed in early phagosomes (EPs) and causes enrichment in PI 3-phosphate (PI(3)P), which is crucial for EP maturation since it recruits multiple effectors through highly specific interactions with FYVE and phox-homology (PX) domains on target proteins, such as early endosome antigen-1, endosomal sorting complex required for transport (ESCRT)-0, sorting nexins, and p40phox of NADPH oxidase (100, 101). In EPs, also PA has an important role because it contributes to the assembly and activation of NADPH oxidase by interacting directly with p47phox and by recruiting and activating a number of protein and lipid kinases, including Fgr, the type I PIP5KI, and type 1 sphingosine kinase (14, 102). During the transition from early to late phagosome (LP) stage, PI(3)P is then lost as a consequence of hydrolysis catalyzed by a phosphoinositide lipid 3-phosphatases and PI 4-phosphate [PI(4)P] is rapidly acquired as a result of the enrichment in PI(4)P kinase 2A and such acquisition is associated with fusion of autophagosomes

TABLE 3 | Lipid-binding domains and protein interaction of the most representative bioactive lipids involved in phagocytosis process.

Lipid	Binding domains	Reference
PI(3)P	FYVE	(106)
	PX	(107)
PI(4)P	ENTH	(108)
	PH	(109)
PI(5)P	PHD	(110)
$PI(4,5)P_2$	ENTH	(111)
	ANTH	(112)
	PH	(113)
	C2	(114)
	FERM	(115)
	PTB	(116)
$PI(3,5)P_2$	ENTH	(117)
	GRAM	(118)
$PI(3,4)P_2$	PX	(119)
	PH	(107)
$PI(3,4,5)P_3$	PX	(119)
	PH	(120)
	PTB	(121)
PA	PH	(122)
	PX	(123)
	C2	(124)
Protein interactions		
LBPA	Alix binding	(125)
S1P	SCaMPER	(126)
AA	NOX-2 activation	(127)

PI, phosphatidylinositol; PI(3)P, PI 3-phosphate; PI(4)P, PI 4-phosphate; PI(5)P, PI 5-phosphate; $PI(4,5)P_2$, PI 4,5-bisphosphate; $PI(3,5)P_2$, PI 3,5-bisphosphate; $PI(3,4)P_2$, PI 3,4-bisphosphate; $PI(3,4,5)P_3$, PI 3,4,5-trisphosphate; PA, phosphatidic acid; LBPA, lysobisphosphatidic acid; S1P, sphingosine 1-phosphate; AA, arachidonic acid; PH, pleckstrin homology; PX, phox-homology.

with lysosomes (LYs) (103). LP stage is also characterized by the presence of PI 5-phosphate [PI(5)P] and PI 3,5-bisphosphate [PI(3,5)P_2]. In particular, PI(3,5)P_2 can be generated by the enzymatic activity of both PI3K and phosphoinositide 5 kinase (PI5K), starting from PI(3)P and PI(5)P, respectively, and takes part in endolysosome morphology, acidification, and trafficking (104). PI(5)P can be directly produced from PI by the means of the PI5K or by dephosphorylation of PI(3,5)P_2 by myotubularin 3-phosphatases and seems to be involved in actin remodeling and in protein sorting in endosomal compartment (105).

Phospholipids may also contribute to the membrane surface charge. Changes in the content of anionic phospholipids are accompanied by marked alterations in the surface charge of the membrane of nascent phagosome, where proteins that associate with the membrane by electrostatic interactions may relocate (128). For example, the dislocation of phosphoinositides [prevalently PI(4,5)P_2 and PI(3,4,5)P_3] causes the modification of surface charge observed after PSL, and the different charge facilitates the dissociation of target proteins causing the termination of signaling and cytoskeleton assembly (92). Similarly, during phagosome maturation, the cytosolic leaflet of phagosomes remains negatively charged and this is prevalently due to accumulation of PS (129). Such a negative charge serves to target proteins with polycationic clusters or polybasic domains and seems to be an important determinant in the distribution of both synaptotagmins, which control membrane fusion events (130), and small GTPases of the Rab and Rho superfamilies, which are critical for both phagosome formation and maturation (131). Thus, the level of anionic phospholipids, including PS and phosphoinositide species, may provide an electrostatic switch to control protein recruitment and vesicle trafficking.

In addition to activation of different signaling pathways, phospholipids can promote phagosome maturation process by inducing positive or negative membrane curvatures. For example, PA is a cone-shaped (type II) lipid that induces negative (concave) curvature of membranes (132), whereas lysobisphosphatidic acid, an inverted cone-shaped fusogenic lipid, forces positive (convex) membrane curvature (125). The resulting changes in membrane curvature activate specific curvature sensors, which are protein motifs or domains, such as amphipathic lipid-packing sensor motifs and BAR domains, which act as geometry sensing tools (133). These sensors play important roles in membrane

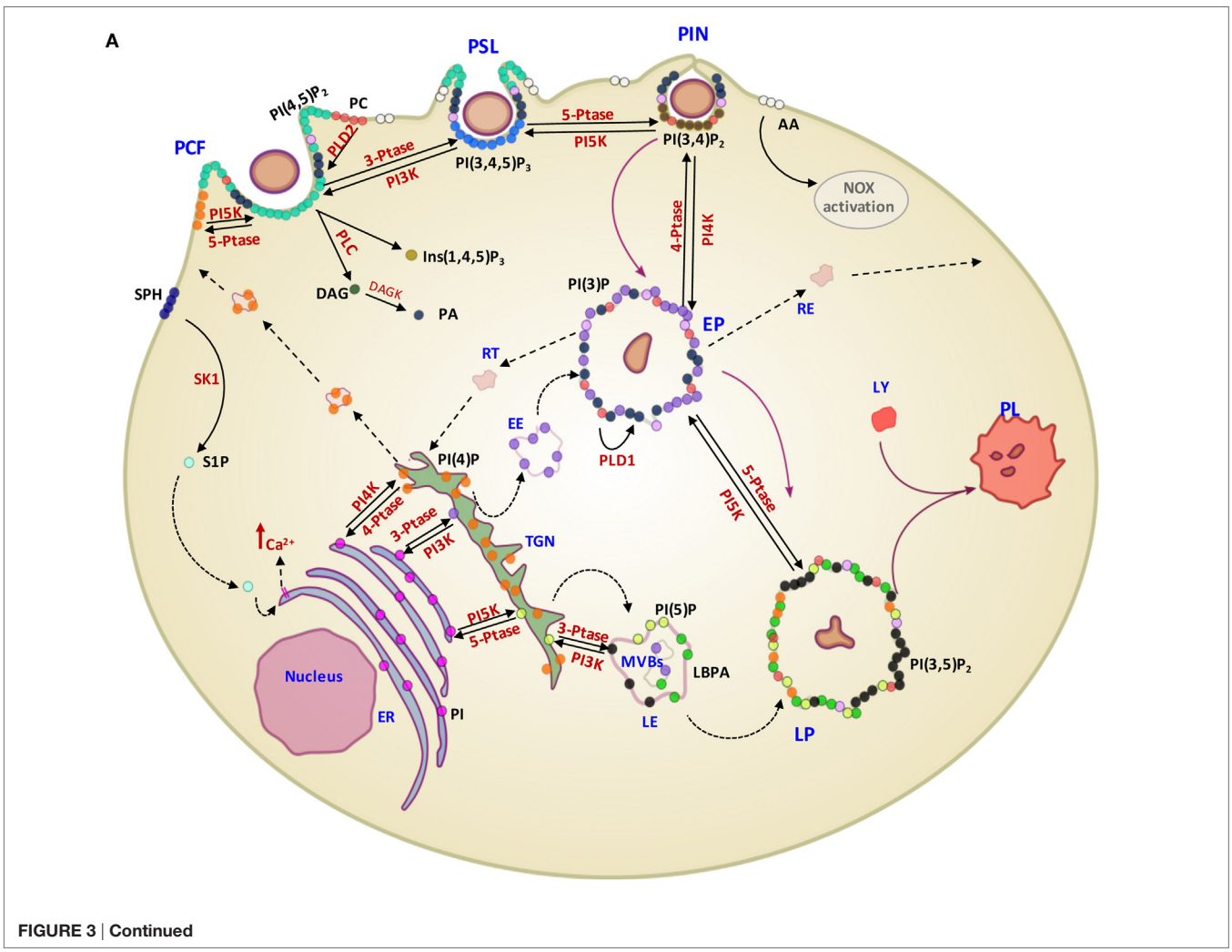

FIGURE 3 | **Continued**

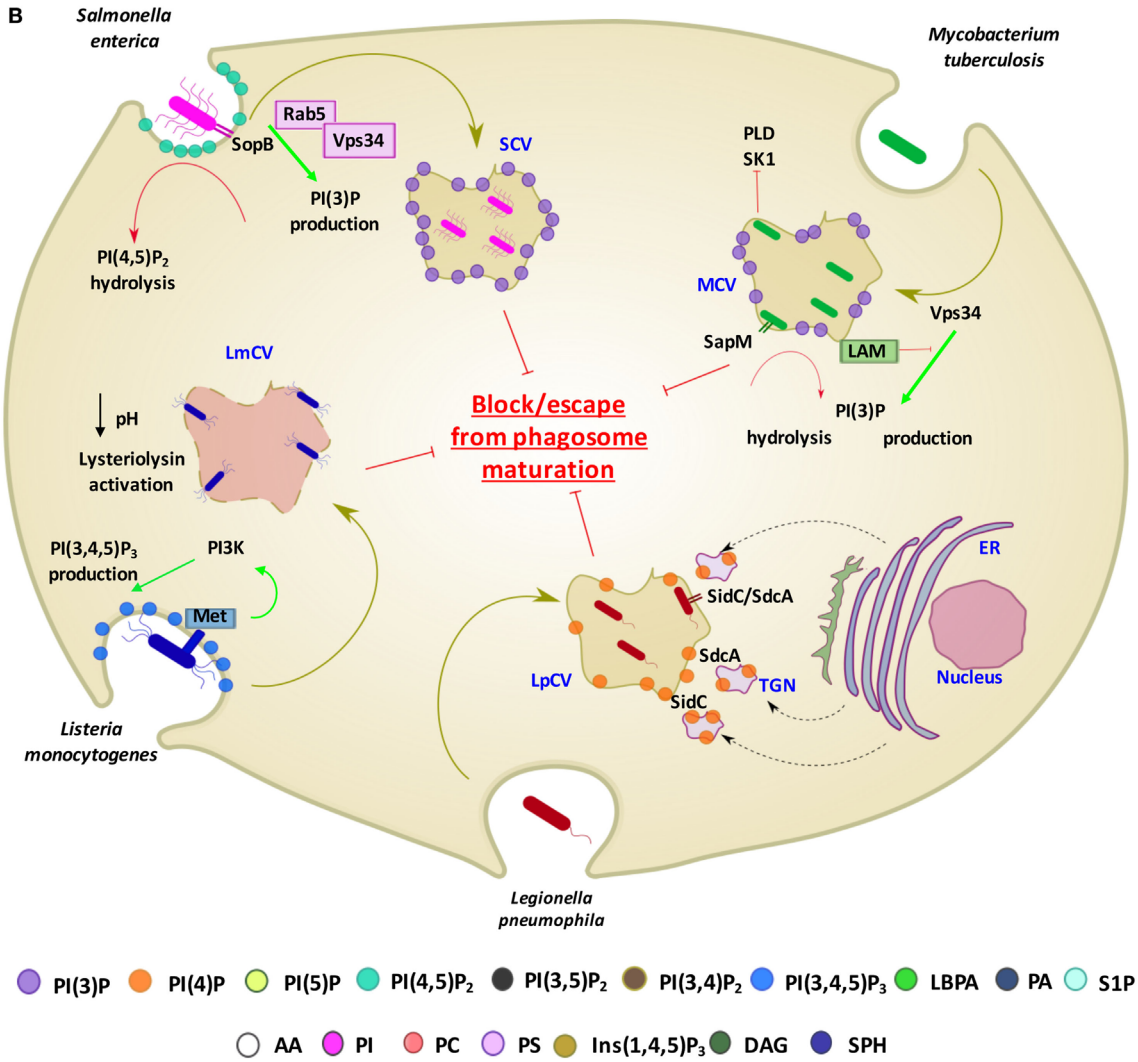

FIGURE 3 | Contribution of different lipid second messengers to phagocytosis from phagosome formation to PL maturation and examples of interference by pathogens. **(A)** The first event which occur during particulate engulfment is the PCF and the rapid accumulation of PI(4,5)P_2 levels, mediated by PI5K and made possible thanks to the translocation of PI(4)P from Golgi to the membrane. PI(4,5)P_2 can also be converted in Ins(1,4,5)P_3 and DAG by the means of PLC and, furthermore, DAG can be metabolized to PA through the DAGK activity. PA is also early generated by the activation of PLD2, which hydrolyzes PC to PA and choline. Moreover, in this stage, there is a rapid generation of S1P, produced by the phosphorylation of sphingosine by the means of SK1, which in turn may activate sphingolipid Ca^{2++}-release-mediating protein of endoplasmic reticulum (SCaMPER). Following, at the stage of PSL, PI(4,5)P_2 is phosphorylated to PI(3,4,5)P_3 by PI3K, which is converted to PI(3,4)P_2 by 5-PTase during PIN. EP is characterized by the presence of PI(3)P, resulting by both its translocation from Golgi and the dephosphorylation of PI(3,4)P_2, mediated by 4-PTase. Although PA is present in the early stage of phagocytosis process, at this stage its conversion starting to PC is mediated by the action of PLD1. LP is characterized by the presence of PI(3,5)P_2, PI(5)P, and LBPA. In particular, PI(3,5)P_2 can be generated by the enzymatic activity of both PI5K and PI3K, starting from PI(3)P and PI(5)P, respectively. PI is the precursor of PI(3)P, PI(4)P, and PI(5)P and their phosphorylation is mediated by PIK3, PI4K, and PI5K, respectively, in ER. **(B)** Examples of pathogen interference with host lipid metabolism associated with phagosome maturation. *Salmonella enterica* secretes the PI phosphatases SopB, which has a direct effect on the PI(4,5)P_2 hydrolysis and an indirect effect on PI(3)P production through the recruitment of Rab5 and its associated enzyme PI3K (Vps34). *Mycobacterium tuberculosis* (Mtb) produces a secretory acid phosphatase (SapM) and LAM, which hydrolyzes PI(3)P and inhibites the generation of PI(3)P, respectively. Moreover, Mtb is able to inhibit SK1 and PLD action. *Lysteria monocytogenes* invades cells by binding to the host cell Met receptor, which leads to activation of PI3Ks and PI(3,4,5)P_3 production and promotes a partial phagosome maturation resulting in a pH decrease and lysteriolysin activation. *Legionella pneumophila*, sequesters endosomes, enriched in PI(4)P, from TGN through SidC and SdcA bacterial proteins, and hence creating replicating vacuoles for itself. *Abbreviations for lipids*: PI(3)P, PI 3-phosphate; PI(4)P, PI 4-phosphate; PI(5)P, PI 5-phosphate; PI(4,5)P_2, PI 4,5-bisphosphate; PI(3,4)P_2, PI 3,4-bisphosphate; PI(3,4,5)P_3, PI 3,4,5-trisphosphate; LBPA, lysobisphosphatidic acid; PA, phosphatidic acid; AA, arachidonic acid; PI, phosphatidylinositol; PC, phosphatidylcholine; PS, phosphatidylserine; Ins (1,4,5)P_3, inositol 3,4,5 trisphosphate; DAG, diacylglycerol; SPH, sphingosine; S1P, sphingosine 1-phosphate; LAM, lipoarabinomannan. *Abbreviations for enzymes*: PLD-1, phospholipase D-1; PLD-2, phospholipase D-2; PLC, phospholipase C; DAGK, diacylglycerol kinase; SK1, sphingosine kinase 1; PI3K, phosphoinositide 3-kinase; PI4K, PI 4-kinase; PI5K, phosphoinositide 5 kinase; 3-PTase, PI 3-phosphatase; 4-PTase, PI 4-phosphatase; 5-PTase, PI 5-phosphatase; *Other abbreviations*: PCF, phagocytic cup formation; PSL, phagosome sealing; PIN, phagosome internalization; EP, early phagosome; LP, late phagosome; PL, phagolysosome; LY, lysosome; EE, early endosome; LE, late endosome; MVBs, multivesicular bodies; RE, recycling endosome; RT, retrograde traffic; TGN, trans Golgi network; ER, endoplasmic reticulum; SCV, *Salmonella* containing vacuole; MCV, *Mycobacterium* containing vacuole; LmCV, *Listeria* containing vacuole; LpCV, *Legionella* containing vacuole.

trafficking and remodeling, by regulating membrane protein concentration, enzyme activation, lipid composition, and vesicle fusion events (134).

The translocation of PS on the outer leaflet of plasma membrane represents one of the early events of apoptosis, occurring in both infected and uninfected apoptotic cells, and represents an "eat-me" signal for macrophages (135–138). The functional consequence of a PS-dependent recognition and phagocytosis of apoptotic bodies (efferocytosis) by macrophages is the release of TGF-β, IL-10, and the inhibition of the production of pro-inflammatory cytokines, such as TNF-α and IL-1β (139). These features have been previously reported as a possible therapeutic strategy to reduce immunopathologic responses (136, 140). However, if phagocytosis involves apoptotic bodies derived from cells expressing PAMPs, as in the case of apoptosis mediated by an infectious agent, phagocytosis causes activation of antigen-presenting cells (APCs) and release of IL-6, TGF-β, and IL-23, leading to a preferential activation of pro-inflammatory Th17 cells (141). Moreover, apoptotic bodies from macrophages infected by *Mycobacterium bovis* bacille Calmette–Guerin (BCG) have been reported to promote antigen cross-presentation and $CD8^+$ T cell activation as well as an *in vivo* increased protection against experimental TB in mice (142). Coherently, emulsified PS has been described as a simple and efficient carrier to deliver antigenic peptide epitopes to professional APCs to induce both helper and cytotoxic T cell response *in vivo* (143).

Considering the crucial role of lipids in the activation of antimicrobial response, many intracellular bacterial pathogens evolved strategies aimed at interfering, at different levels, with lipid metabolism to generate specific pathogen-containing-vacuoles permitting their intracellular survival (14) (**Figure 3B**). *Salmonella enterica* exploits type III secretion system to secrete the PI phosphatases SopB, a phosphoinositide phosphatases able to dephosphorylate $PI(4,5)P_2$. Decreased levels of $PI(4,5)P_2$ reduce the surface charge of the *Salmonella* containing vacuole (SCV) and promote membrane fission by reorganizing the actin cytoskeleton during bacterial internalization (144). SopB also recruits the RAB GTPase RAB5 protein and the RAB5 effector Vps34, a PI3K that accumulates PI(3)P on the SCV surface and interferes with the maturation to next LP stage (144). *Listeria monocytogenes* invades host cells by recognition of Met receptor by bacterial internalin B (InlB), which leads to the PI3K activation and consequent enhancement of $PI(3,4,5)P_3$ levels. Such increase in $PI(3,4,5)P_3$ promotes the fusion of early endosomes with the bacterial vacuole, allowing partial maturation of phagosome before lysis of the phagosome and escape into cytoplasm due to the pH-dependent activation of listeriolysin (145). *Legionella pneumophila*, through SidC and SdcA proteins, anchors to PI(4)P expressing endosomes from trans Golgi network to form a replicative niche for the pathogen (146). Mtb, as well as BCG, interferes with PL maturation (15, 136, 147) by depleting the phagosome of PI(3)P and hence arresting the vacuole in an immature form (148). The mycobacterial secretory acid phosphatase (SapM) acts in concert with the mycobacterial lipoarabinomannan (LAM), a phosphatydilinositol analog, to avoid the formation of PI(3)P by hydrolysis of the phosphate group (149) and by inhibiting the activity of type III PI3K Vps34 (150), respectively. Finally, an inhibition in host PLD activation was observed during early phases of interaction between Mtb and macrophage (151). This inhibition was not due to differences in protein expression, suggesting a metabolic control of the enzyme. Interestingly, an upstream inhibition of sphingosine-kinase exerted by Mtb was also reported which may be responsible of the reduced calcium mobilization (152) and the consequent inhibition of Ca^{++}-dependent PLD activation (153) observed during *in vitro* Mtb infection.

Given the well-defined role of certain lipids in the physiology of phagocytosis, the possibility to modulate the phagosome maturation process by the use of bioactive lipids has been suggested as a strategy to increase the efficacy of innate bactericidal mechanisms. In this context, Anes et al. showed that selected bioactive lipids, such as arachidonic acid, ceramide, sphingosine, sphingomyelin, and sphingosine 1-phosphate (S1P), activate phagosome actin assembly and maturation resulting in killing of pathogenic mycobacteria in murine macrophages (154). Moreover, S1P and its analog lysophosphatidic acid (LPA) were both described to activate PLD-mediated and PL maturation-dependent mycobactericidal response in human macrophages (155, 156) and in type II alveolar epithelial cells (157) in *in vitro* models of Mtb infection, highlighting the role of PA in the activation of antimycobacterial response. Interestingly, and of high translational value, both lysophospholipids promoted antimicrobial response, resulting in a significant intracellular killing of endogenous mycobacteria, in bronchoalveolar lavage (BAL) cells from pulmonary TB patients (155, 158). Finally, the intranasal administration of S1P or LPA in murine models of primary Mtb infection significantly reduced pulmonary mycobacterial burden and histophatology (156, 159, 160). On these grounds, the targeted delivery of several bioactive lipids into macrophages to increase their innate anti-bacterial mechanisms could be useful for the treatment of Mtb infection. However, such a delivery is challenging, due to lipid pharmacokinetic properties and to the difficulties to target specific cells. The possibility to incorporate lipid second messengers in Janus-faced liposomes may represent a strategy to overcome these limitations (15, 136). The main feature of these liposomes is the asymmetric distribution of phospholipids within the liposome membrane, with inner leaflet expressing bioactive lipids involved in phagosome maturation, and the outer surface expressing PS, representing an "eat-me" signal for macrophages. PA delivered by this strategy allowed to enhance PL maturation-dependent (myco)bactericidal response of macrophages and BAL cells from TB patients as well as from patients affected by MDR bacterial pneumonia (15, 136). Notably, both PA and PI(5)P delivered by Janus-faced liposomes were able to enhance antimicrobial response against *Pseudomonas aeruginosa* in an *in vitro* cellular model of cystic fibrosis by using macrophages expressing a pharmacologically inhibited or a naturally mutated cystic fibrosis transmembrane conductance regulator (15), which are characterized by impaired phagosome maturation (161). These experimental evidences suggest the possibility to use liposomes to deliver bioactive lipids to enhance phagosome maturation-dependent antimicrobial response and to restore the PL maturation pathway, which can be corrupted by specific pathogens (15).

LIPOSOMES AS "INDIRECT" ENHANCERS OF ADAPTIVE ANTIMICROBIAL RESPONSE

Vaccines represent a great contribution of medical sciences to the reduction of the deaths caused by infectious diseases. The majority of currently available vaccines induce neutralizing or opsonizing pathogen-specific antibody responses to protect against infectious diseases. However, a number of diseases are caused by pathogens that are not controlled by humoral responses and novel vaccine formulations aimed at generating protective pathogen-specific immune responses are under testing or development. According to the pathogen virulence factors or mechanisms of pathogenesis, novel vaccines are being designed to enhance either cellular immune responses, with prevalence of cytotoxic T cells, or polarization of specific T cell subpopulations, or aimed at increasing the response at mucosal or systemic sites. One of the strategies currently under development is based on the use of recombinant antigens (subunit vaccines) in association with adjuvants able to modulate/polarize the developing immune response. Recombinant antigens show a higher safety profile and lower reactogenicity, but are characterized by a reduced immunogenicity in comparison with inactivated or attenuated whole cell vaccines. As a consequence, adjuvants are generally included to vaccine formulations to provide the necessary inflammatory microenvronment required for the activation of innate immunity cells and the following priming and expansion of naïve T cells for the development of appropriate adaptive immune response. Thus, adjuvants are generally defined as substances that (i) facilitate a depot effect and deliver the antigen in proximity of APC, (ii) generate an inflammatory microenvironment necessary for the activation of APC, and (iii) induce the secretion of specific cytokine patterns by APC for the differentiation of naïve T cells into different $CD4^+$ and/or $CD8^+$ T cell subpopulations.

In addition to their suitability as drug carriers, liposomes represent an extraordinary tool for the devise of innovative vaccines, as they can be designed for the antigen delivery (see chapter 5) and/or for their possible adjuvancy function (162). In fact, several liposome adjuvants have been licensed for human use and others are being evaluated in clinical trials (**Table 4**). However, many other formulations are possible and have been or could be tested for efficacy and safety. In this regard, different liposome adjuvant formulations can be produced with different properties according to the (i) lipid composition, (ii) liposome size, (iii) liposome charge, and (iv) inclusion of function modifiers such as PAMPs.

Lipid Composition

The choice of liposomal lipid composition (in terms of hydrocarbon length, unsaturation, charge, and headgroup species of the lipids) influences the physico-chemical features of the liposomes, such as the lipid bilayer fluidity, which can in turn influence immune response. For instance, the degree of saturation or the length of fatty acids may affect the strength of the van der Waals forces among neighboring chains. Thus, phospholipids with longer saturated hydrocarbon chains show higher tendencies to interact each other and to form rigidly ordered bilayer structures than shorter and/or unsaturated hydrocarbon chains, which form liposomes with fluid and disordered bilayers (163). Membrane liposome fluidity in turn affects antigen presentation as it has been previously shown that fluid disordered phase liposomes promoted MHC class I presentation pathway to a higher degree than the solid ordered liposomes (164). Furthermore, in *in vivo* studies, solid ordered liposomes prepared using dimethyldioleoylammonium (DDA) induced 100-fold higher Th1 response than the fluid liposome counterpart prepared using the unsaturated analog DDA bromide (165). Inclusion of Chol is also known to influence bilayer fluidity and is commonly incorporated within liposomes as it can enhance liposome stability. The impact of Chol on adjuvancy is actually controversial, with some studies showing improvements and others reduction of immune response (166). Cationic adjuvant formulation (CAF)01 is actually a commercially available liposome adjuvant formulation that is composed of DDA stabilized with trehalose 6,6-dibehenate (TDB), a glycolipid synthetic variant of mycobacterial cord factor. TDB activates macrophages and dendritic cells (DCs) *via* Syk–Card9–Bcl10–Malt1 signaling pathway and when administrated

TABLE 4 | Examples of liposome adjuvants vaccines against infectious disease in market or tested in clinical trials.

Target	Immuno modulators	Lipid formulation	Antigen	Phase	Clinical trials.gov identifier
HAV	HA + NA	DOPC:DOPE	Inactivated HAV	Licensed (Epaxal®)	
Human papilloma virus	MPLA + aluminum hydroxide (AS04)	n.d.	L1	Licensed (Cervarix®)	
Influenza virus	–	DOPC:DOPE	HA	Licensed (Inflexal®)	
Influenza virus	–	CCS/C ("VaxiSome")	HA	II	NCT00915187
Mycobacterium tuberculosis	TDB (CAF01)	DDA	Ag85b + ESAT6	I	NCT00922363
Plasmodium Falciparum	MPLA + QS21 (AS01)	n.d.	RTS,S	III	NCT00872963
P. falciparum	MPLA + QS21 (AS01)	n.d.	FMP012	I	NCT02174978
P. falciparum	MPLA + QS21 (AS01)	n.d.	RH5.1	I/IIa	NCT02927145
P. falciparum	EPA/AS01	n.d.	Pfs25M + Pfs230D1	I	NCT02942277

This compilation was generated with data from ClinicalTrials.gov.

DOPC, dioleoylPC; DOPE, dioleoly-sn-glycero-phophoethanolamine; DDA, dimethyldioleoylammonium; HA, hemaglutinin; NA, neuroaminidase; TDB, trehalose6,6-dibehenate; MPLA, monophosphoryl lipid A; QS21, triterpene glucoside compound derived from the Quillaja saponaria tree; CCS, N-palmityol-derythro-sphingosyl-Carbamoyl-Spermine; CCS/C, N-palmityol-derythro-sphingosyl-Carbamoyl-Spermine/Cholesterol; EPA, ExoProtein A (a detoxified form of exotoxin A from Pseudomonas aeruginosa); n.d., not determined; CFA, cationic adjuvant formulation; HAV, hepatitis A virus.

in combination with a Mtb subunit vaccine induced a robust and combined antigen-specific Th1 and Th17 responses and partial protection against Mtb challenge (165, 167).

Liposome Size

The dimension of liposomes can impact adjuvant efficacy and several studies have shown that Th1 or Th2 response can be evoked by using particles with different diameter (168). In this context, a significantly higher Th1 response, as measured in terms of IL-12-dependent IFN-γ secretion and serum IgG2a production, has been reported following vaccination with large vesicles (≥225 nm diameter), whereas the same antigen encapsulated in small liposomes (≤155 nm diameter) induced a prevalent Th2 response as determined in terms of IgG1 and increased lymph node (LN) IL-5 production (169). Such a different outcome can reflect differences in particle trafficking to LNs: small particles (20–200 nm) freely traffics to the draining LNs where they are taken up by LN resident DCs, whereas larger vesicles (500–2,000 nm) are internalized by tissue-resident DC (170). Different antigen presentation pathway has also been observed following internalization by phagocytes: antigen encapsulated in large (560 nm) vesicles localized in early immature phagosomes, where class II antigen-processing pathway could be intercepted for recognition by $CD4^+$ T cells, while antigen encapsulated in small (155 nm) vesicles were rapidly transferred to late endosomes/lysosomes, with a consequent reduced class II-restricted Ag-presenting efficiency (171).

Liposome Charge

Liposome charge may have critical effects on the adjuvant properties of liposomes. Cationic liposomes may interact with the negatively charged mucosal surfaces and exibit increased mucoadesion, leading to reduced clearance rate, prolonged exposure time of the antigen at the mucosal surface (depot effect), enhanced endocytosis of liposomes by APC (13, 172–175), and increased cell-mediated immune response (173) when compared with neutral liposomes, which tended to induce antibody immune response (176). However, anionic liposomes may also modulate immune response in the context of novel formulations of liposomal adjuvants. As above described, PS is expressed on the outer membrane leaflet of apoptotic bodies and represents an "eat-me" signal for macrophages and DC, which express specific PS receptors. Phagocytes that internalize apoptotic bodies through PS became polarized toward a tolerogenic response (177). However, when the recognition occurs in the presence of selected PAMPs a Th17-differentiating cytokine profile is produced (170) and a similarly efficient class II- and class I-restricted antigen presentation is induced (143).

Function Modifiers

The procedures of liposome preparations make possible to include within the liposome structure different function modifiers molecules, such as PAMPs. The addition of function modifiers molecules may permit to design APC-targeted liposomes able to modulate the effector function of APC, including the profile of secreted cytokine that, in turn, can induce the differentiation of diverse T helper cell subpopulations (178). For example, the immunization of mice with liposomes containing ovalbumin (OVA) and oligodeoxynucleotide (ODN) with CpG motifs (ligand for TLR-9) induced a Th1-type immune response, with enhanced production of IFN-γ and of IgG2a, whereas the same antigen encapsulated with Pam3CSK4 (a TLR-2 ligand consisting of tri-palmitoyl-*S*-glyceryl cysteine lipopeptide with a pentapeptide SKKKK) induced increased levels of IgG1, suggesting a Th2-oriented immune response (179, 180). Another example is given by the lipophilic muramyldipeptide (MDP) analogs MDP phosphatidylethanolamine as well as the MDP glyceroldipalmitate that induced higher antibody titers, Th1 response, and IFN-γ levels if added to liposomal formulations containing hepatitis B surface antigen (HBsAg) (181). Thus, the use of different PAMPs can modulate the immune response against the same antigen, in dependence on the targeted TLR.

Monophosphoryl lipid A (MPLA) is a safe and potent liposome adjuvant used with many candidate antigens for new vaccines in the fight against several types of cancer and anti-infective vaccines such as malaria and HIV-1 (182). For example, RTS,S (a particulate antigen consisting of hepatitis B particles coexpressing epitopes derived from *P. falciparum* circumsporozoite protein) induced an *in vivo* cytotoxic T-lymphocyte response and a dose-dependent enhancement of the specific IgG levels when entrapped in liposomes containing MPLA and not when encapsulated in liposomes missing MPLA (183). Moreover, a recent paper demonstrated that the *P. falciparum* Protein-013 can induce a potent and sterilizing immune response when formulated with small ULV containing a synthetic MPLA derivative (3D-PHAD®) and the QS-21 (184). Similarly, Nagill and Kaur encapsulated the 78-kDa antigen of *Leishmania donovani* with MPLA, resulting in decreased parasite burden after challenge in immunized mice (185).

Korsholm et al. described a novel $CD8^+$ T-cell-inducing adjuvant, CAF09, consisting of DDA-liposomes stabilized with monomycoloyl glycerol-1 (a synthetic analog of a mycobacterial cell wall lipid and a potent stimulator of human DCs) and combined with the TLR3 ligand Poly(I:C) (186). CAF09 was used to test immunogenicity of the model antigen OVA as well as several antigens of Mtb (TB10.3, H56), HIV (Gag p24), HPV (E7) in mice and resulted in a high frequency of antigen-specific $CD8^+$ T cells (186). In the mouse model of subcutaneous HPV-16 E7-expressing TC-1 skin tumor, immunization with the E7 antigen and CAF09 as adjuvant significantly reduced the growth of the tumor (186). Another widely studied liposome carrier is the cationic liposome–DNA complex (CLDC) that is prepared by mixing liposomes and ODN with CpG motifs, which activate TLR9. Bernstein and colleagues demonstrated that CLDC increased the immune response against simian immunodeficiency virus induced by vaccines. The immunization of rhesus macaques with CLDC induced a potent virus-specific B- and T-cell response in comparison to control animals (12, 187). Moreover, in mice expressing hepatitis B virus, the CLDC was tested as adjuvant for HBsAg. Whereas HBsAg induces only a B-cell immune response, the viral antigen formulated together with CLDC elicited both T- and B-cell responses (12, 188).

LIPOSOMES AS ANTIGEN CARRIER IN INNOVATIVE VACCINE PREPARATIONS

Allison and Gregoriadis were the first to describe the capacity of liposomes to elicit immune responses against associated or incorporated antigens (12, 189). Water-soluble compounds (peptides, proteins, carbohydrates, nucleic acids, and haptens), depending on the chemical properties, can be linked to the surface of liposomes, by stable chemical bond or by adsorption, or can be trapped inside the aqueous inner space, whereas lipophilic compounds (antigens, lipopeptides, linker molecules, and adjuvants) can be inserted into the lipid bilayer (12, 190). Surface-exposed antigens are available for and can stimulate B-cell for antibody production, while both surface-exposed and encapsulated antigens, which require intracellular liposome disruption to be accessible, may induce T-cell responses. Liposome-encapsulated protein antigens have been frequently used and several studies well documented the MHC class-I presentation and induction of cytotoxic T lymphocytes (CTLs) by antigens formulated inside liposomes. H-2 antigens entrapped in egg lecithin plus Chol (30% w/w) liposomes induced a potent anti-H-2 CTL allo-response (191). Human LS174T colon tumor cell membranes encapsulated into liposomes (PC/Chol/PA 7:2:1) elicit *in vitro* specific primary and secondary xenogeneic immune responses in murine splenocytes (192). Induction of antiviral immunity by liposome-encapsulated peptides was tested by Ludewig and colleagues that showed the high immunogenicity of peptides derived from the glycoprotein of the lymphocytic choriomeningitis virus when administered intradermally in mice (193). In addition, these authors used the liposome to prime a strong MHC class I-restricted T-cell response specific for 10 diverse epitopes of hepatitis C virus (HCV) (12, 194). In the fight against Ebola Zaire (EBO-Z) virus, the protective efficacy of liposome-encapsulated [L(EV)] irradiated EBO-Z, containing all of the native EBO-Z proteins was evaluated (195). Mice immunized intravenously with L(EV) and challenged with a uniformly lethal mouse-adapted variant of EBO-Z were totally protected from illness and death compared with mice vaccinated intravenously with the irradiated virus non-encapsulated that presented a 55% of survival (195). Liposomes were also formulated with the pH-sensitive 3-methyl-glutarylated hyperbranched poly(glycidol) (MGlu-HPG) and used to entrap OVA. Such MGlu-HPG formulations elicited a strong T cell activation that was inhibited using blocking antibodies against MHC class-I/MHC class-II molecules, suggesting the involvement of MHC class I- and II-restricted antigen presentation (12, 196). Ding and colleagues developed the so-called RAFTsomes, a liposome incorporating membrane microdomains of APCs with enriched epitope/MHC complexes. OVA epitope loaded RAFTsome immunization gave high anti-OVA IgG1 levels and the immunized mice were protected from OVA-expressing EG.7 tumor cell inoculation challenge (197).

Mucosal surfaces are the main entry site for most environmental antigens and the mucosal immunity plays a critical role in preventing the initial infection of many pathogens. Several studies are focused on figuring out the ability of liposomes to act as efficient mucosal antigen delivery system. A potential mucosal carrier formulation has been developed by Gupta and Vyas that encapsulated HBsAg in liposomes coupled with *Ulex europaeus* agglutinin 1, a lectin isolated from *U. europaeus* seeds. After oral immunization, lectinized liposomes were predominantly targeted to M cells on intestinal Peyer's patches, inducing a strong anti-HBsAg IgG response in serum, anti-HBsAg IgA in various mucosal fluids, and cytokine levels in the spleen homogenates (198). Figueiredo and colleagues described another mucosal formulation composed of *Streptococcus equi* antigens encapsulated inside PC/Chol/SA liposomes or inside chitosan nanoparticles. Mice immunized intranasally with both delivery systems developed mucosal, humoral, and cellular immune responses, but higher secretory IgA levels in the lung were observed following vaccination with chitosan nanoparticles, due to their enhanced mucoadhesive properties (12, 199). Wang and colleagues encapsulated the OVA in a galactosylated liposome carrier in which a galactosyl lipid (galactose conjugated covalently with 1,2-didodecanoyl-sn-glycero-3-phosphoethanolamine) was incorporated into a liposomal bilayer. OVA-encapsulated targeted galactosylated liposome elicited in the nasal and lung wash fluid a significantly higher OVA-specific secretory IgA titers and serum IgG antibody levels than control mice (200). Traditional phosphodiester liposomes are not stable and could be easily degraded in the gastrointestinal tract. Zhang and colleagues described the archaeosomes, a novel oral delivery system based on the polar lipid fraction E isolated from *Sulfolobus acidocaldarius*. The archaeosomes had significant higher stability in simulated gastric and intestinal fluids after oral administration and induced a strong serum IgG as well as mucosal IgA immune response. Moreover, such delivery system elicited antigen-specific MHC class I-restricted T cell proliferation (201).

Liposomes are versatile tool to encapsulate and deliver a wide range of molecules, not only proteins but also glycolipid antigens. Kallert et al. demonstrated that purified mycobacterial LAM can be efficiently delivered into $CD1^+$ APC *via* liposomes and this delivery system induces robust LAM-specific Th1-biased CD1-restricted T-cell responses in primary human cells (202). The authors used liposomes consisted of egg-PC, Chol, and stearylated octaarginine and proved that octaarginine, a cell-penetrating peptide consisting of eight positively charged arginines, increases the glycolipid antigen accumulation into lipid-APCs. The efficacy of octaarginine-containing liposomes was also tested in *in vivo* models of immunization using both BCG primed guinea pigs (203), where these liposomes induced a delayed type hypersensitivity reaction in the skin and in rhesus macaques, using glucose monomycolate (GMM) as antigen, where a CD1-restricted Th1-skewed immune response was observed (202, 204). In a recent study, GMM-containing liposomes were decorated with a high-affinity glycan ligand of the sialic acid-binding Ig-like lectin-7, a siglec receptor expressed on DC that mediates rapid endocytosis and transport of its cargo to LYs (205). This elegant targeting platform leads to a robust GMM-specific CD1-restricted activation of T cells. One way to ensure rapid and specific liposome uptake by leukocyte subsets is decoration of liposomes with antibodies against a cell subset-specific antigen. Klauber et al. reported a liposomal drug delivery system for robust and specific targeting of monocytes and DCs consisting of sterically stabilized liposomes with surface-conjugated antibodies against

C-type lectin "Dendritic Cell Immunoreceptor" (206). Using this method, they were able to activate the targeted cells and improve the ability of the agonist to induce secretion of key anticancer cytokines (IL-12p70, IFN-γ, and IFN-α).

Typically, exogenous antigens residing in proteolytic PLs are directed to MHC class II-expressing compartments (MIIC) where peptides resulting from antigen proteolysis are loaded on the neoformed class II molecules to be expressed on cell membrane. Thus, bioactive lipids like PI(3)P, promoting (auto) PL biogenesis, can in turn promote class II antigen presentation pathway (207). Harding and colleagues (208) used liposomes composed of dioleoyl PC/dioleoyl PS (DOPC/DOPS) or dioleoyl phosphatidylethanolamine/palmitoyl homocysteine (DOPE/PHC) at 4:1 molar ratios with four different encapsulated protein antigens (OVA, murine hemoglobin, bovine ribonuclease, or hen egg lysozyme) and proved that macrophages efficiently processed the encapsulated Ag. These liposomes were able to sequester their contents from potential endosomal processing events and release them only after delivery to LYs for efficient MHC class II presentation (208).

The antigen presentation pathway leading to the loading of exogenous antigens on MHC class I molecules is called cross-presentation. Cross-presentation can occur *via* a vacuolar and a cytosolic pathway. The vacuolar pathway bypasses the cytosolic steps and TAP- or proteasome-sensitivity, is dependent on lysosomal proteases, and invokes a peptide exchange step for reloading of endocytosed MHC-I complexes, which are then rerouted directly back to the plasma membrane in a Brefeldin A-insensitive manner (209). The cytosolic route, considered to be the most important, is TAP and proteasome dependent and allows the export of the antigen into the cytosol through the acquisition of the traslocon SEC61 on antigen-containing endosomes from the endoplasmic reticulum (ER)-associated degradation pathway (210). Although no specific lipid second messengers promoting cross-presentation pathway have been identified so far, the involvement of specific membrane contact sites between ER and phagosomes (211) suggests that specific signal lipids can be involved. The permanence of the antigen in a non-proteolytic compartment represents a condition promoting cross-presentation and explains why DC, whose phagosomes show reduced acidity and limited proteolysis, have better cross-presentation capability than macrophages. In this context, cationic liposomes, but not anionic liposomes, that increase the lysosomal pH in DCs and reduce antigen degradation, promote antigen cross-presentation and $CD8^+$ T-cell cross-priming (212, 213). As an alternative strategy to promote antigen delivery to cytoplasm and make it available for class I antigen presentation, Miura et al. developed liposomes carrying OVA modified with KALA peptide, an α-elical cationic peptide derived from the sequence of the N-terminal segment of the hemagglutinin (HA)-2 subunit of the influenza virus HA, which is involved in the fusion of the viral envelope with the cell membrane (214), and show membrane destabilizing properties (215). MHC class I presentation pathway can also be favored using pH-sensitive liposomes. For example, Reddy et al. have shown that OVA entrapped in pH-sensitive liposomes (DOPE/1,2-dioleoyl-sn-glycero-3-succinate 1:1 and DOPC/PS/Chol 5:2:3) allowed MHC class I presentation of OVA peptides by mouse thymoma cells, which were lysed by OVA-specific $CD8^+$ T lymphocytes (216).

Liposomes can be designed to carry antigens within the acqueous phase, encapsulated inside the lipid bilayer, or exposed onto the liposome surface and this can result in different outcomes of the immune response. Investigation of HA adsorption versus encapsulation and coencapsulation of ODN with CpG motifs in 3β-[*N*-(*N*′,*N*′-dimethylaminoethane)-carbamoyl] Chol (DC-chol) liposomes demonstrated that encapsulated HA was less immunogenic than adsorbed HA (217). Moreover, Takagi and colleagues immunized human-HLA-transgenic mice with liposomes exposing several epitope-peptides derived from HCV in their external layer and observed that 1 mouse- and 3 human MHC-restricted peptides protected and conferred long-term memory to vaccinated animals (218). Immunization of HLA-A*0201-transgenic mice with liposomes conjugated with peptides designed according to the sequence of highly conserved antigens of influenza viruses and HLA-A*0201 binder, induced antigen-specific $CD8^+$ T-cells, and mediated protection of mice challenged intranasally with the influenza viruses H1N1 or H3N2 (219). Similarly, when the peptide nucleoprotein (NP)366–374, designed according to the sequence of the NP of influenza H3N2 virus, was coupled with liposomes and used to immunize mice induced peptide-specific $CD8^+$ T-cells and the replication of influenza H3N2 virus was successfully suppressed in the lung of challenged mice (220). Naito and colleagues reported that OVA chemically coupled with the surface of liposome *via* amino groups using glutaraldehyde induced Ag-specific IgG but not IgE Ab production (221), showing that liposomes can be exploited to develop vaccines devoid of allergenic potential. Moreover, liposomes showed different capacities to induce class I or class II presentation of the delivered antigen depending on the mobility of their membranes. Taneichi et al. reported that OVA coupled with liposome constituted by unsaturated fatty acid was presented to both $CD4^+$ and $CD8^+$ T lymphocytes, while OVA conjugated to liposomes constituted by saturated fatty acid were not presented to $CD8^+$ T lymphocytes (222). The *in vivo* induction of CTL and the eradication of E.G7 tumor in mice confirmed the capacity to induce cross-presentation by Ag-conjugated liposomes prepared including unsaturated fatty acid in the bilayer (222). Masek and colleagues used small Ni-chelating liposomes exposing on their surface the *Candida albicans* His-tagged antigen hsp (hsp90-CA) with the MDP derivative C18-*O*-6-norAbuMDP as adjuvant. These liposomes were phagocytosed by human DCs *in vitro* and *in vivo* in mice, where induced antigen-specific Th1 and Th2 responses without side effects (223). At least in theory, the covalent attachment of protein antigens to nanocarriers could modify protein structure and mask epitopes, altering the antibody response. Watson and colleagues tested this hypothesis using metal chelation *via* nitrilotriacetic acid (NTA) to attach antigens to liposomes instead of covalent linkage. OVA and a peptide derived from the membrane-proximal region of HIV-1 gp41 (N-MPR) were attached *via* NTA or covalent linkage. Covalently attached N-MPR or OVA elicited stronger antibody responses than NTA-anchored antigens excluding the possible masking effect of covalent binding (224). Finally, antigen modification may

also impact the response against haptens as reported by a study by Matyas et al., where the authors conjugated haptenic compounds to protein carriers and embed them in the outer surface of MPLA-containing liposomes. Four synthetic opiate haptens were conjugated to carrier proteins and induced high levels of specific antibodies to synthetic heroin haptens following *in vivo* immunization that might be useful as a candidate vaccine to heroin and similar opiates (225).

Self-amplifying messenger RNA (mRNA) technology has been developed for *in situ* expression of antigens and represents a new platform for innovative vaccine applications (226) with the advantage that unlike DNA, mRNA-based vaccines do not integrate into chromosomes avoiding the risks of oncogenesis and insertional mutagenesis (227). Liposomes were identified as the more suitable delivery system for non-amplifying or self-amplifying mRNA vaccine, and it was rapidly evident that mRNA encapsulated inside liposomes can activate innate immunity through toll-like and RIG-I-like receptors (228, 229).

Richner and colleagues tested the efficacy of this novel technology in a vaccine against Zika virus using a modified mRNA-encoding prM-E gene that produced virus-like particles with a reduced cross-reactivity with the related dengue virus (230). Two immunizations induced a strong protective humoral response against Zika infection in mouse model and reduced the cross-reactive response against the related virus dengue. For this experiment, liposomes were obtained taking advantage of a method developed by Chen and colleague, consisting of ionizable lipid, DSPC, CHOL, and PEG-lipid (dissolved in ethanol at the molar ratios 50:10:38.5:1.5) combined with a citrate buffer containing mRNA (3:1 = aqueous:ethanol, pH 4.0) using a microfluidizer. The dialyzed and concentrated liposome preparations resulted in 80–100 nm in size and more than 90% encapsulation (231).

The mRNA-based liposomes were also tested to induce humoral responses against influenza A virus in a mouse model. Lipid nanoparticles were engineered to deliver a synthetic, self-amplifying mRNA encoding seasonal influenza HA and tested their immunogenicity in mouse model. This mRNA-based vaccine elicited an immune response comparable to that obtained with the licensed influenza subunit vaccine and all the immunized animals showed HA inhibition and neutralizing antibody titers against the virus 14 days after the second immunization (232). In another study, the immunogenicity of lipid nanoparticles encapsulating a modified non-replicating mRNA encoding influenza H10 HA was tested in *rhesus macaques*. This study showed that anti-HA protective antibody titers and MHC class II-restricted H10-specific T cell response were elicited after two intradermal or intramuscular immunizations. Moreover, this study provided evidences on cells and mechanisms responsible for the efficacy of mRNA vaccinations: following the administration of mRNA–liposomes, DCs, monocytes, and neutrophils were recruited to the site of immunization and draining LNs, but only DCs and monocytes internalized liposomes, produced virus antigens, translating the mRNA, and upregulated costimulatory molecules. This *in vivo* antigen production and activation of APCs lead to the priming of a potent H10-specific MHC class II-restricted T cell response (233). The superiority of liposome encapsulation versus other delivery systems of mRNA was stressed by the group of Bogers and colleagues, who proved the immunogenicity and the safety of cationic liposomes formulated with the mRNA encoding for a clade C envelope glycoprotein of HIV in *rhesus macaques*. This formulation elicited a cellular immune response and a neutralizing antibody response stronger than those elicited by self-amplifying mRNA encapsulated in a viral replicon particle or by a recombinant HIV envelope protein formulated with MF59 adjuvant (234).

ENGINEERING MULTIROLE LIPOSOMES ABLE TO DELIVER DRUGS, ANTIGENS, ADJUVANTS, AND/OR LIPID SECOND MESSENGERS AS AN ADDITIONAL TOOL TO CONTRAST INFECTIOUS DISEASES

Infectious diseases are the leading causes of morbidity and mortality worldwide and the increasing incidence of treatment-resistant infections has become a major global concern for their epidemic potential (235). In 2016, WHO reported 6×10^5 new cases of TB with resistance to rifampicin, the most effective first-line anti-TB drug, of which 4.9×10^5 had MDR TB and about 9.5% of MDR-TB cases have additional drug resistance and were defined XDR-TB.[1] Moreover, 2.3×10^4 in US[2] and 2.5×10^4 deaths in Europe[3] are attributable each year to infections caused by Gram-positive (*Streptococcus penumoniae, Staphylococcus aureus*), and Gram-negative (*Pseudomonas* spp., *Acinetobacter* spp., and *Enterobacteriaceae*) bacteria with multidrug- or pan-antibiotic resistance. As a consequence, the development of novel antimicrobial agents and/or other immunotherapeutic options represents a global health priority (236). To this regard, several therapeutic strategies, targeting the host rather than the pathogen, have been proposed and are under development as adjunctive treatments, in particular for MDR TB (235). Examples of host-directed therapies are the reinfusion of *in vitro* expanded pathogen-specific autologous T cells, the administration of micronutrients, antimicrobial peptides, or immune modulators and therapeutic vaccines (235).

Liposomes may offer several advantages in the design of novel pathogen- or host-directed therapies and vaccines, since these nanoparticles can be engineered as delivery system as well as immune modulators. In clinical applications, liposomal drugs have been proven their ability to "passively" accumulate at sites of increased vasculature permeability and for their ability to reduce the side effects of the encapsulated drugs in comparison to free drugs (237). This has resulted in an overall increase in TI, so that liposomal drug delivery has become an established technology platform in some circumstances and has gained considerable clinical acceptance (26). A new frontier in liposome-based approaches against infectious diseases may be envisaged if liposomes are designed as carrier of antigens or drugs in addition to molecules with immunomodulatory functions (**Figure 4**). For example, antigen-loaded liposome carrying different PAMPs inside or exposed on their outer surface leaflet, would target plasma membrane-associated or intracellular pattern-recognition

[1] http://www.who.int/tb/publications/global_report/en/.
[2] https://www.cdc.gov/drugresistance/threat-report-2013/index.html.
[3] http://www.ema.europa.eu/ema/index.jsp?curl=pages/news_and_events/news/2009/11/news_detail_000044.jsp&mid=WC0b01ac058004d5c1.

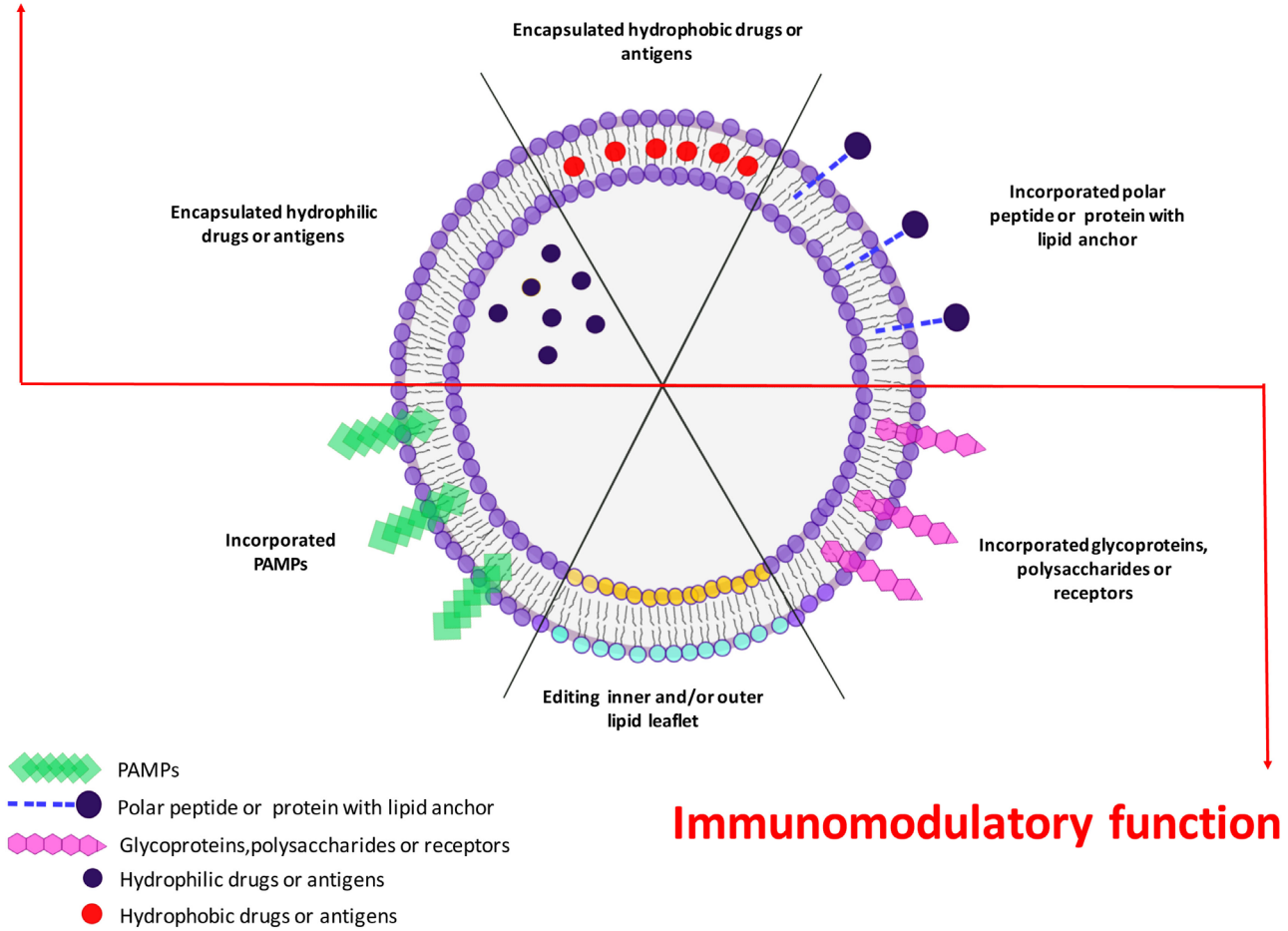

FIGURE 4 | Plasticity of liposome technology. Liposome technology allows combining the selective delivery of drugs or antigens (upper side) with immunomodulatory functions played by incorporated pathogen-associated molecular patterns (PAMPs) or selected bioactive phospholipids (lower side). The simultaneous delivery of antigen/drugs and immunomodulatory molecules makes liposomes a versatile platform to design different therapeutic or prophylactic tools to face pathogen-specific strategies.

receptors, respectively, and consequently activate APC to secrete different cytokines, which in turn may drive diverse polarizations of the antigen-specific adaptive immune response (11). It is also possible to engineer asymmetric liposomes that express different lipids at the outer and inner membrane leaflet (15, 136, 238). In this regard, PS may be included in the constitutive lipids of the outer liposome leaflet to target specific cells, like macrophages, whereas lipid second messengers, such as PA or PI(3)P, can be incorporated in the inner leaflet to be delivered to the cell microvesicular system to modulate intracellular endosome trafficking (15, 136, 238). Pathogens may target host lipid metabolism and PL maturation as an intracellular survival strategy and mechanism of immunoevasion (14, 144–146, 148–152, 238–241). The growing evidences for a crucial role played by lipid second messengers in PL biogenesis (91–94, 129) opens new therapeutic possibilities for the reactivation/enhancement of antimicrobial innate immune response with the specific intracellular delivery of lipid second messengers taking advantage of the liposome technology. Since scaling up, stability and regulatory issues are commonly successfully addressed, the clinical availability of novel liposome formulations can be foreseen in the near future. The possibility to enhance/correct specific molecular pathways by lipid second messengers, used for liposome scaffold, may represent a further added value to the plethora of different possibilities offered by liposomes technology and a possible novel host-directed therapy to face the global emergence of antimicrobial resistance.

AUTHOR CONTRIBUTIONS

All authors made substantial contributions to the conception or design of the work. NP, SM, and FS contributed to the acquisition, analysis, interpretation of data for the work. NP and FS drew the figures. RN and MF wrote the work. All authors revised critically the work for important intellectual content, gave final approval of the version to be published, and agreed to be accountable for all aspects of the work in ensuring that questions related to the accuracy or integrity of any part of the work are appropriately investigated and resolved.

ACKNOWLEDGMENTS

Authors would like to thank Raffaela Teloni for technical assistance.

FUNDING

Research supported by (i) the Horizon 2020 Programme of European Commission, grant "EMI-TB"; Eliciting Mucosal Immunity against Tuberculosis—grant # 643558; and "TBVAC2020; Advancing novel and promising TB vaccine candidates from discovery to preclinical and early clinical development"—grant# 643381; (ii) Italian Foundation for Cystic Fibrosis, "Preclinical study of a host-directed therapy based on Metformin and bioactive liposomes for the control of multidrug-resistant *P. aeruginosa* infection"—grant #14/2017; (iii) Italian Foundation for multiple sclerosis, grant #2016/R/22; and (iv) Ministero della Salute Italiana, Ricerca Finalizzata grant: "Nanotechnology for the multiplex diagnosis of infectious diseases"—grant# PE-2011-02346849.

REFERENCES

1. Abu Lila AS, Ishida T. Liposomal delivery systems: design optimization and current applications. *Biol Pharm Bull* (2017) 40(1):1–10. doi:10.1248/bpb.b16-00624
2. Bozzuto G, Molinari A. Liposomes as nanomedical devices. *Int J Nanomedicine* (2015) 10:975–99. doi:10.2147/IJN.S68861
3. Bulbake U, Doppalapudi S, Kommineni N, Khan W. Liposomal formulations in clinical use: an updated review. *Pharmaceutics* (2017) 9(2):1–33. doi:10.3390/pharmaceutics9020012
4. Mufamadi MS, Pillay V, Choonara YE, Du Toit LC, Modi G, Naidoo D, et al. A review on composite liposomal technologies for specialized drug delivery. *J Drug Deliv* (2011) 2011:939851. doi:10.1155/2011/939851
5. Immordino ML, Dosio F, Cattel L. Stealth liposomes: review of the basic science, rationale, and clinical applications, existing and potential. *Int J Nanomedicine* (2006) 1(3):297–315.
6. Damen J, Regts J, Scherphof G. Transfer and exchange of phospholipid between small unilamellar liposomes and rat plasma high density lipoproteins. Dependence on cholesterol content and phospholipid composition. *Biochim Biophys Acta* (1981) 665(3):538–45. doi:10.1016/0005-2760(81)90268-X
7. Torchilin VP. Recent advances with liposomes as pharmaceutical carriers. *Nat Rev Drug Discov* (2005) 4(2):145–60. doi:10.1038/nrd1632
8. Manjappa AS, Chaudhari KR, Venkataraju MP, Dantuluri P, Nanda B, Sidda C, et al. Antibody derivatization and conjugation strategies: application in preparation of stealth immunoliposome to target chemotherapeutics to tumor. *J Control Release* (2011) 150(1):2–22. doi:10.1016/j.jconrel.2010.11.002
9. Lu Y, Sun W, Gu Z. Stimuli-responsive nanomaterials for therapeutic protein delivery. *J Control Release* (2014) 194:1–19. doi:10.1016/j.jconrel.2014.08.015
10. Li L, ten Hagen TL, Schipper D, Wijnberg TM, van Rhoon GC, Eggermont AM, et al. Triggered content release from optimized stealth thermosensitive liposomes using mild hyperthermia. *J Control Release* (2010) 143(2):274–9. doi:10.1016/j.jconrel.2010.01.006
11. Perrie Y, Crofts F, Devitt A, Griffiths HR, Kastner E, Nadella V. Designing liposomal adjuvants for the next generation of vaccines. *Adv Drug Deliv Rev* (2016) 99(Pt A):85–96. doi:10.1016/j.addr.2015.11.005
12. Schwendener RA. Liposomes as vaccine delivery systems: a review of the recent advances. *Ther Adv Vaccines* (2014) 2(6):159–82. doi:10.1177/2051013614541440
13. Bernasconi V, Norling K, Bally M, Hook F, Lycke NY. Mucosal vaccine development based on liposome technology. *J Immunol Res* (2016) 2016:5482087. doi:10.1155/2016/5482087
14. Steinberg BE, Grinstein S. Pathogen destruction versus intracellular survival: the role of lipids as phagosomal fate determinants. *J Clin Invest* (2008) 118(6):2002–11. doi:10.1172/JCI35433
15. Poerio N, Bugli F, Taus F, Santucci MB, Rodolfo C, Cecconi F, et al. Liposomes loaded with bioactive lipids enhance antibacterial innate immunity irrespective of drug resistance. *Sci Rep* (2017) 7:45120. doi:10.1038/srep45120
16. Peetla C, Stine A, Labhasetwar V. Biophysical interactions with model lipid membranes: applications in drug discovery and drug delivery. *Mol Pharm* (2009) 6(5):1264–76. doi:10.1021/mp9000662
17. Michot JM, Seral C, Van Bambeke F, Mingeot-Leclercq MP, Tulkens PM. Influence of efflux transporters on the accumulation and efflux of four quinolones (ciprofloxacin, levofloxacin, garenoxacin, and moxifloxacin) in J774 macrophages. *Antimicrob Agents Chemother* (2005) 49(6):2429–37. doi:10.1128/AAC.49.6.2429-2437.2005
18. Bensikaddour H, Snoussi K, Lins L, Van Bambeke F, Tulkens PM, Brasseur R, et al. Interactions of ciprofloxacin with DPPC and DPPG: fluorescence anisotropy, ATR-FTIR and 31P NMR spectroscopies and conformational analysis. *Biochim Biophys Acta* (2008) 1778(11):2535–43. doi:10.1016/j.bbamem.2008.08.015
19. Yang NJ, Hinner MJ. Getting across the cell membrane: an overview for small molecules, peptides, and proteins. *Methods Mol Biol* (2015) 1266:29–53. doi:10.1007/978-1-4939-2272-7_3
20. Bangham AD, Standish MM, Watkins JC. Diffusion of univalent ions across the lamellae of swollen phospholipids. *J Mol Biol* (1965) 13(1):238–52. doi:10.1016/S0022-2836(65)80093-6
21. Deamer DW. From "banghasomes" to liposomes: a memoir of Alec Bangham, 1921-2010. *FASEB J* (2010) 24(5):1308–10. doi:10.1096/fj.10-0503
22. Batzri S, Korn ED. Single bilayer liposomes prepared without sonication. *Biochim Biophys Acta* (1973) 298(4):1015–9. doi:10.1016/0005-2736(73)90408-2
23. Gregoriadis G. The carrier potential of liposomes in biology and medicine (second of two parts). *N Engl J Med* (1976) 295(14):765–70. doi:10.1056/NEJM197609302951406
24. Gregoriadis G. The carrier potential of liposomes in biology and medicine (first of two parts). *N Engl J Med* (1976) 295(13):704–10. doi:10.1056/NEJM197609232951305
25. Kobayashi T, Tsukagoshi S, Sakurai Y. Enhancement of the cancer chemotherapeutic effect of cytosine arabinoside entrapped in liposomes on mouse leukemia L-1210. *Gann* (1975) 66(6):719–20.
26. Allen TM, Cullis PR. Liposomal drug delivery systems: from concept to clinical applications. *Adv Drug Deliv Rev* (2013) 65(1):36–48. doi:10.1016/j.addr.2012.09.037
27. Uziely B, Jeffers S, Isacson R, Kutsch K, Wei-Tsao D, Yehoshua Z, et al. Liposomal doxorubicin: antitumor activity and unique toxicities during two complementary phase I studies. *J Clin Oncol* (1995) 13(7):1777–85. doi:10.1200/JCO.1995.13.7.1777
28. Abuchowski A, McCoy JR, Palczuk NC, van Es T, Davis FF. Effect of covalent attachment of polyethylene glycol on immunogenicity and circulating life of bovine liver catalase. *J Biol Chem* (1977) 252(11):3582–6.
29. Papahadjopoulos D, Allen TM, Gabizon A, Mayhew E, Matthay K, Huang SK, et al. Sterically stabilized liposomes: improvements in pharmacokinetics and antitumor therapeutic efficacy. *Proc Natl Acad Sci U S A* (1991) 88(24):11460–4. doi:10.1073/pnas.88.24.11460
30. Allen TM, Hansen C. Pharmacokinetics of stealth versus conventional liposomes: effect of dose. *Biochim Biophys Acta* (1991) 1068(2):133–41. doi:10.1016/0005-2736(91)90201-I
31. James ND, Coker RJ, Tomlinson D, Harris JR, Gompels M, Pinching AJ, et al. Liposomal doxorubicin (Doxil): an effective new treatment for Kaposi's sarcoma in AIDS. *Clin Oncol (R Coll Radiol)* (1994) 6(5):294–6. doi:10.1016/S0936-6555(05)80269-9
32. Eloy JO, Petrilli R, Trevizan LNF, Chorilli M. Immunoliposomes: a review on functionalization strategies and targets for drug delivery. *Colloids Surf B Biointerfaces* (2017) 159:454–67. doi:10.1016/j.colsurfb.2017.07.085
33. Petrilli R, Eloy JO, Lee RJ, Lopez RFV. Preparation of immunoliposomes by direct coupling of antibodies based on a thioether bond. *Methods Mol Biol* (2018) 1674:229–37. doi:10.1007/978-1-4939-7312-5_19
34. Spragg DD, Alford DR, Greferath R, Larsen CE, Lee KD, Gurtner GC, et al. Immunotargeting of liposomes to activated vascular endothelial cells: a strategy for site-selective delivery in the cardiovascular system. *Proc Natl Acad Sci U S A* (1997) 94(16):8795–800. doi:10.1073/pnas.94.16.8795

35. Yang T, Choi MK, Cui FD, Kim JS, Chung SJ, Shim CK, et al. Preparation and evaluation of paclitaxel-loaded PEGylated immunoliposome. *J Control Release* (2007) 120(3):169–77. doi:10.1016/j.jconrel.2007.05.011
36. Pan X, Wu G, Yang W, Barth RF, Tjarks W, Lee RJ. Synthesis of cetuximab-immunoliposomes via a cholesterol-based membrane anchor for targeting of EGFR. *Bioconjug Chem* (2007) 18(1):101–8. doi:10.1021/bc060174r
37. Eskandari F, Talesh GA, Parooie M, Jaafari MR, Khamesipour A, Saberi Z, et al. Immunoliposomes containing soluble Leishmania antigens (SLA) as a novel antigen delivery system in murine model of leishmaniasis. *Exp Parasitol* (2014) 146:78–86. doi:10.1016/j.exppara.2014.08.016
38. Rabenhold M, Steiniger F, Fahr A, Kontermann RE, Ruger R. Bispecific single-chain diabody-immunoliposomes targeting endoglin (CD105) and fibroblast activation protein (FAP) simultaneously. *J Control Release* (2015) 201:56–67. doi:10.1016/j.jconrel.2015.01.022
39. Lopez-Berestein G, Fainstein V, Hopfer R, Mehta K, Sullivan MP, Keating M, et al. Liposomal Amphotericin B for the treatment of systemic fungal infections in patients with cancer: a preliminary study. *J Infect Dis* (1985) 151(4):704–10. doi:10.1093/infdis/151.4.704
40. Lee WH, Loo CY, Traini D, Young PM. Nano- and micro-based inhaled drug delivery systems for targeting alveolar macrophages. *Expert Opin Drug Deliv* (2015) 12(6):1009–26. doi:10.1517/17425247.2015.1039509
41. Ternullo S, de Weerd L, Mari Holsaeter A, Eide Flaten G, Skalko-Basnet N. Going skin deep: a direct comparison of penetration potential of lipid-based nanovesicles on the isolated perfused human skin flap model. *Eur J Pharm Biopharm* (2017) 121:14–23. doi:10.1016/j.ejpb.2017.09.006
42. Malam Y, Loizidou M, Seifalian AM. Liposomes and nanoparticles: nanosized vehicles for drug delivery in cancer. *Trends Pharmacol Sci* (2009) 30(11):592–9. doi:10.1016/j.tips.2009.08.004
43. Balazsovits JA, Mayer LD, Bally MB, Cullis PR, McDonell M, Ginsberg RS, et al. Analysis of the effect of liposome encapsulation on the vesicant properties, acute and cardiac toxicities, and antitumor efficacy of doxorubicin. *Cancer Chemother Pharmacol* (1989) 23(2):81–6. doi:10.1007/BF00273522
44. Forssen EA, Coulter DM, Proffitt RT. Selective in vivo localization of daunorubicin small unilamellar vesicles in solid tumors. *Cancer Res* (1992) 52(12):3255–61.
45. Kim S, Chatelut E, Kim JC, Howell SB, Cates C, Kormanik PA, et al. Extended CSF cytarabine exposure following intrathecal administration of DTC 101. *J Clin Oncol* (1993) 11(11):2186–93. doi:10.1200/JCO.1993.11.11.2186
46. Meyers PA, Schwartz CL, Krailo MD, Healey JH, Bernstein ML, Betcher D, et al. Osteosarcoma: the addition of muramyl tripeptide to chemotherapy improves overall survival – a report from the Children's Oncology Group. *J Clin Oncol* (2008) 26(4):633–8. doi:10.1200/JCO.2008.14.0095
47. Krishna R, Webb MS, St Onge G, Mayer LD. Liposomal and nonliposomal drug pharmacokinetics after administration of liposome-encapsulated vincristine and their contribution to drug tissue distribution properties. *J Pharmacol Exp Ther* (2001) 298(3):1206–12.
48. Wang-Gillam A, Li CP, Bodoky G, Dean A, Shan YS, Jameson G, et al. Nanoliposomal irinotecan with fluorouracil and folinic acid in metastatic pancreatic cancer after previous gemcitabine-based therapy (NAPOLI-1): a global, randomised, open-label, phase 3 trial. *Lancet* (2016) 387(10018):545–57. doi:10.1016/S0140-6736(15)00986-1
49. Lister J. Amphotericin B lipid complex (Abelcet) in the treatment of invasive mycoses: the North American experience. *Eur J Haematol Suppl* (1996) 57:18–23.
50. Adler-Moore J, Proffitt RT. AmBisome: liposomal formulation, structure, mechanism of action and pre-clinical experience. *J Antimicrob Chemother* (2002) 49(Suppl 1):21–30. doi:10.1093/jac/49.suppl_1.21
51. Carvalheiro M, Esteves MA, Santos-Mateus D, Lopes RM, Rodrigues MA, Eleuterio CV, et al. Hemisynthetic trifluralin analogues incorporated in liposomes for the treatment of leishmanial infections. *Eur J Pharm Biopharm* (2015) 93:346–52. doi:10.1016/j.ejpb.2015.04.018
52. da Costa-Silva TA, Galisteo AJ Jr, Lindoso JA, Barbosa LR, Tempone AG. Nanoliposomal buparvaquone immunomodulates leishmania infantum-infected macrophages and is highly effective in a murine model. *Antimicrob Agents Chemother* (2017) 61(4):e02297-16. doi:10.1128/AAC.02297-16
53. Moles E, Galiano S, Gomes A, Quiliano M, Teixeira C, Aldana I, et al. ImmunoPEGliposomes for the targeted delivery of novel lipophilic drugs to red blood cells in a falciparum malaria murine model. *Biomaterials* (2017) 145:178–91. doi:10.1016/j.biomaterials.2017.08.020
54. Rajendran V, Rohra S, Raza M, Hasan GM, Dutt S, Ghosh PC. Stearylamine liposomal delivery of monensin in combination with free artemisinin eliminates blood stages of *Plasmodium falciparum* in culture and *P. berghei* infection in murine malaria. *Antimicrob Agents Chemother* (2015) 60(3):1304–18. doi:10.1128/AAC.01796-15
55. Ibrahim S, Tagami T, Ozeki T. Effective-loading of platinum-chloroquine into PEGylated neutral and cationic liposomes as a drug delivery system for resistant malaria parasites. *Biol Pharm Bull* (2017) 40(6):815–23. doi:10.1248/bpb.b16-00914
56. Agrawal AK, Singhal A, Gupta CM. Functional drug targeting to erythrocytes in vivo using antibody bearing liposomes as drug vehicles. *Biochem Biophys Res Commun* (1987) 148(1):357–61. doi:10.1016/0006-291X(87)91118-1
57. Tagami T, Yanai H, Terada Y, Ozeki T. Evaluation of phosphatidylserine-specific peptide-conjugated liposomes using a model system of malaria-infected erythrocytes. *Biol Pharm Bull* (2015) 38(10):1649–51. doi:10.1248/bpb.b15-00310
58. Guo J, Waknine-Grinberg JH, Mitchell AJ, Barenholz Y, Golenser J. Reduction of experimental cerebral malaria and its related proinflammatory responses by the novel liposome-based beta-methasone nanodrug. *Biomed Res Int* (2014) 2014:292471. doi:10.1155/2014/292471
59. Tomiotto-Pellissier F, Miranda-Sapla MM, Machado LF, Bortoleti B, Sahd CS, Chagas AF, et al. Nanotechnology as a potential therapeutic alternative for schistosomiasis. *Acta Trop* (2017) 174:64–71. doi:10.1016/j.actatropica.2017.06.025
60. Frezza TF, de Souza AL, Prado CC, de Oliveira CN, Gremiao MP, Giorgio S, et al. Effectiveness of hyperbaric oxygen for experimental treatment of schistosomiasis mansoni using praziquantel-free and encapsulated into liposomes: assay in adult worms and oviposition. *Acta Trop* (2015) 150:182–9. doi:10.1016/j.actatropica.2015.07.022
61. Faber K, Zorzi GK, Brazil NT, Rott MB, Teixeira HF. siRNA-loaded liposomes: inhibition of encystment of *Acanthamoeba* and toxicity on the eye surface. *Chem Biol Drug Des* (2017) 90(3):406–16. doi:10.1111/cbdd.12958
62. Islan GA, Duran M, Cacicedo ML, Nakazato G, Kobayashi RKT, Martinez DST, et al. Nanopharmaceuticals as a solution to neglected diseases: is it possible? *Acta Trop* (2017) 170:16–42. doi:10.1016/j.actatropica.2017.02.019
63. Pandey R, Khuller GK. Solid lipid particle-based inhalable sustained drug delivery system against experimental tuberculosis. *Tuberculosis (Edinb)* (2005) 85(4):227–34. doi:10.1016/j.tube.2004.11.003
64. Pandey R, Khuller GK. Antitubercular inhaled therapy: opportunities, progress and challenges. *J Antimicrob Chemother* (2005) 55(4):430–5. doi:10.1093/jac/dki027
65. Parumasivam T, Chang RY, Abdelghany S, Ye TT, Britton WJ, Chan HK. Dry powder inhalable formulations for anti-tubercular therapy. *Adv Drug Deliv Rev* (2016) 102:83–101. doi:10.1016/j.addr.2016.05.011
66. Rawal T, Parmar R, Tyagi RK, Butani S. Rifampicin loaded chitosan nanoparticle dry powder presents an improved therapeutic approach for alveolar tuberculosis. *Colloids Surf B Biointerfaces* (2017) 154:321–30. doi:10.1016/j.colsurfb.2017.03.044
67. Parumasivam T, Leung SS, Quan DH, Triccas JA, Britton WJ, Chan HK. Rifapentine-loaded PLGA microparticles for tuberculosis inhaled therapy: preparation and in vitro aerosol characterization. *Eur J Pharm Sci* (2016) 88:1–11. doi:10.1016/j.ejps.2016.03.024
68. Pham DD, Fattal E, Tsapis N. Pulmonary drug delivery systems for tuberculosis treatment. *Int J Pharm* (2015) 478(2):517–29. doi:10.1016/j.ijpharm.2014.12.009
69. Justo OR, Moraes AM. Incorporation of antibiotics in liposomes designed for tuberculosis therapy by inhalation. *Drug Deliv* (2003) 10(3):201–7. doi:10.1080/713840401
70. Zaru M, Sinico C, De Logu A, Caddeo C, Lai F, Manca ML, et al. Rifampicin-loaded liposomes for the passive targeting to alveolar macrophages: in vitro and in vivo evaluation. *J Liposome Res* (2009) 19(1):68–76. doi:10.1080/08982100802610835
71. Mehanna MM, Mohyeldin SM, Elgindy NA. Respirable nanocarriers as a promising strategy for antitubercular drug delivery. *J Control Release* (2014) 187:183–97. doi:10.1016/j.jconrel.2014.05.038
72. Rojanarat W, Nakpheng T, Thawithong E, Yanyium N, Srichana T. Inhaled pyrazinamide proliposome for targeting alveolar macrophages. *Drug Deliv* (2012) 19(7):334–45. doi:10.3109/10717544.2012.721144

73. Rojanarat W, Changsan N, Tawithong E, Pinsuwan S, Chan HK, Srichana T. Isoniazid proliposome powders for inhalation-preparation, characterization and cell culture studies. *Int J Mol Sci* (2011) 12(7):4414–34. doi:10.3390/ijms12074414
74. Patil-Gadhe AA, Kyadarkunte AY, Pereira M, Jejurikar G, Patole MS, Risbud A, et al. Rifapentine-proliposomes for inhalation: in vitro and in vivo toxicity. *Toxicol Int* (2014) 21(3):275–82. doi:10.4103/0971-6580.155361
75. Patil-Gadhe A, Pokharkar V. Single step spray drying method to develop proliposomes for inhalation: a systematic study based on quality by design approach. *Pulm Pharmacol Ther* (2014) 27(2):197–207. doi:10.1016/j.pupt.2013.07.006
76. Pramod K, Tahir MA, Charoo NA, Ansari SH, Ali J. Pharmaceutical product development: a quality by design approach. *Int J Pharm Investig* (2016) 6(3):129–38. doi:10.4103/2230-973X.187350
77. EMA. *Reflection Paper on the Data Requirements for Intravenous Liposomal Products Developed with Reference to an Innovator Liposomal Product*. EMA/CHMP/806058/2009/Rev 02. London, UK: European Medicines Agency (2013).
78. FDA. *Liposome Drug Products Chemistry, Manufacturing, and Controls; Human Pharmacokinetics and Bioavailability; and Labeling Documentation Guidance for Industry*. Pharmaceutical Quality/CMC (Revision I). Silver Spring, MD: Food and Drug Administration (2015).
79. Kouchak M, Malekahmadi M, Bavarsad N, Saki Malehi A, Andishmand L. Dorzolamide nanoliposome as a long action ophthalmic delivery system in open angle glaucoma and ocular hypertension patients. *Drug Dev Ind Pharm* (2017) (9):1–16. doi:10.1080/03639045.2017.1386196
80. Zhang R, Qian J, Li X, Yuan Y. Treatment of experimental autoimmune uveoretinitis with intravitreal injection of infliximab encapsulated in liposomes. *Br J Ophthalmol* (2017) 101(12):1731–8. doi:10.1136/bjophthalmol-2016-310044
81. Bowles EA, Feys D, Ercal N, Sprague RS. Liposomal-delivery of phosphodiesterase 5 inhibitors augments UT-15C-stimulated ATP release from human erythrocytes. *Biochem Biophys Rep* (2017) 12:114–9. doi:10.1016/j.bbrep.2017.09.002
82. Kumar L, Verma S, Vaidya B. Liposomes for the delivery of streptokinase. *Ther Deliv* (2017) 8(10):855–66. doi:10.4155/tde-2017-0026
83. Shin M, Snyder HW, Donvito G, Schurman LD, Fox TE, Lichtman AH, et al. Liposomal delivery of diacylglycerol lipase-beta inhibitors to macrophages dramatically enhances selectivity and efficacy in vivo. *Mol Pharm* (2017). doi:10.1021/acs.molpharmaceut.7b00657
84. Malik O, Kaye AD, Kaye A, Belani K, Urman RD. Emerging roles of liposomal bupivacaine in anesthesia practice. *J Anaesthesiol Clin Pharmacol* (2017) 33(2):151–6. doi:10.4103/joacp.JOACP_375_15
85. Beiranvand S, Moradkhani MR. Bupivacaine versus liposomal bupivacaine for pain control. *Drug Res (Stuttg)* (2017). doi:10.1055/s-0043-121142
86. Abdel-Mottaleb MM, Moulari B, Beduneau A, Pellequer Y, Lamprecht A. Nanoparticles enhance therapeutic outcome in inflamed skin therapy. *Eur J Pharm Biopharm* (2012) 82(1):151–7. doi:10.1016/j.ejpb.2012.06.006
87. Zakrewsky M, Kumar S, Mitragotri S. Nucleic acid delivery into skin for the treatment of skin disease: proofs-of-concept, potential impact, and remaining challenges. *J Control Release* (2015) 219:445–56. doi:10.1016/j.jconrel.2015.09.017
88. Pujol-Autonell I, Mansilla MJ, Rodriguez-Fernandez S, Cano-Sarabia M, Navarro-Barriuso J, Ampudia RM, et al. Liposome-based immunotherapy against autoimmune diseases: therapeutic effect on multiple sclerosis. *Nanomedicine (Lond)* (2017) 12(11):1231–42. doi:10.2217/nnm-2016-0410
89. Pang L, Macauley MS, Arlian BM, Nycholat CM, Paulson JC. Encapsulating an immunosuppressant enhances tolerance induction by Siglec-engaging tolerogenic liposomes. *Chembiochem* (2017) 18(13):1226–33. doi:10.1002/cbic.201600702
90. Perri V, Pellegrino M, Ceccacci F, Scipioni A, Petrini S, Gianchecchi E, et al. Use of short interfering RNA delivered by cationic liposomes to enable efficient down-regulation of PTPN22 gene in human T lymphocytes. *PLoS One* (2017) 12(4):e0175784. doi:10.1371/journal.pone.0175784
91. Yeung T, Ozdamar B, Paroutis P, Grinstein S. Lipid metabolism and dynamics during phagocytosis. *Curr Opin Cell Biol* (2006) 18(4):429–37. doi:10.1016/j.ceb.2006.06.006
92. Yeung T, Grinstein S. Lipid signaling and the modulation of surface charge during phagocytosis. *Immunol Rev* (2007) 219:17–36. doi:10.1111/j.1600-065X.2007.00546.x
93. Bohdanowicz M, Grinstein S. Role of phospholipids in endocytosis, phagocytosis, and macropinocytosis. *Physiol Rev* (2013) 93(1):69–106. doi:10.1152/physrev.00002.2012
94. Levin R, Grinstein S, Schlam D. Phosphoinositides in phagocytosis and macropinocytosis. *Biochim Biophys Acta* (2015) 1851(6):805–23. doi:10.1016/j.bbalip.2014.09.005
95. Jenkins GH, Fisette PL, Anderson RA. Type I phosphatidylinositol 4-phosphate 5-kinase isoforms are specifically stimulated by phosphatidic acid. *J Biol Chem* (1994) 269(15):11547–54.
96. Levin R, Grinstein S, Canton J. The life cycle of phagosomes: formation, maturation, and resolution. *Immunol Rev* (2016) 273(1):156–79. doi:10.1111/imr.12439
97. Cox D, Tseng CC, Bjekic G, Greenberg S. A requirement for phosphatidylinositol 3-kinase in pseudopod extension. *J Biol Chem* (1999) 274(3):1240–7. doi:10.1074/jbc.274.3.1240
98. Falasca M, Logan SK, Lehto VP, Baccante G, Lemmon MA, Schlessinger J. Activation of phospholipase C gamma by PI 3-kinase-induced PH domain-mediated membrane targeting. *EMBO J* (1998) 17(2):414–22. doi:10.1093/emboj/17.2.414
99. Bohdanowicz M, Schlam D, Hermansson M, Rizzuti D, Fairn GD, Ueyama T, et al. Phosphatidic acid is required for the constitutive ruffling and macropinocytosis of phagocytes. *Mol Biol Cell* (2013) 24(11):1700–12, S1–7. doi:10.1091/mbc.E12-11-0789
100. Flannagan RS, Cosio G, Grinstein S. Antimicrobial mechanisms of phagocytes and bacterial evasion strategies. *Nat Rev Microbiol* (2009) 7(5):355–66. doi:10.1038/nrmicro2128
101. Lemmon MA. Phosphoinositide recognition domains. *Traffic* (2003) 4(4):201–13. doi:10.1034/j.1600-0854.2004.00071.x
102. Ktistakis NT, Delon C, Manifava M, Wood E, Ganley I, Sugars JM. Phospholipase D1 and potential targets of its hydrolysis product, phosphatidic acid. *Biochem Soc Trans* (2003) 31(Pt 1):94–7. doi:10.1042/bst0310094
103. Albanesi J, Wang H, Sun HQ, Levine B, Yin H. GABARAP-mediated targeting of PI4K2A/PI4KIIalpha to autophagosomes regulates PtdIns4P-dependent autophagosome-lysosome fusion. *Autophagy* (2015) 11(11):2127–9. doi:10.1080/15548627.2015.1093718
104. Dove SK, Dong K, Kobayashi T, Williams FK, Michell RH. Phosphatidylinositol 3,5-bisphosphate and Fab1p/PIKfyve underPPIn endo-lysosome function. *Biochem J* (2009) 419(1):1–13. doi:10.1042/BJ20081950
105. Boal F, Mansour R, Gayral M, Saland E, Chicanne G, Xuereb JM, et al. TOM1 is a PI5P effector involved in the regulation of endosomal maturation. *J Cell Sci* (2015) 128(4):815–27. doi:10.1242/jcs.166314
106. Gaullier JM, Simonsen A, D'Arrigo A, Bremnes B, Stenmark H, Aasland R. FYVE fingers bind PtdIns(3)P. *Nature* (1998) 394(6692):432–3. doi:10.1038/28767
107. Kanai F, Liu H, Field SJ, Akbary H, Matsuo T, Brown GE, et al. The PX domains of p47phox and p40phox bind to lipid products of PI(3)K. *Nat Cell Biol* (2001) 3(7):675–8. doi:10.1038/35083070
108. Hirst J, Motley A, Harasaki K, Peak Chew SY, Robinson MS. EpsinR: an ENTH domain-containing protein that interacts with AP-1. *Mol Biol Cell* (2003) 14(2):625–41. doi:10.1091/mbc.E02-09-0552
109. Levine TP, Munro S. Targeting of Golgi-specific pleckstrin homology domains involves both PtdIns 4-kinase-dependent and -independent components. *Curr Biol* (2002) 12(9):695–704. doi:10.1016/S0960-9822(02)00779-0
110. Gozani O, Karuman P, Jones DR, Ivanov D, Cha J, Lugovskoy AA, et al. The PHD finger of the chromatin-associated protein ING2 functions as a nuclear phosphoinositide receptor. *Cell* (2003) 114(1):99–111. doi:10.1016/S0092-8674(03)00480-X
111. Itoh T, Koshiba S, Kigawa T, Kikuchi A, Yokoyama S, Takenawa T. Role of the ENTH domain in phosphatidylinositol-4,5-bisphosphate binding and endocytosis. *Science* (2001) 291(5506):1047–51. doi:10.1126/science.291.5506.1047
112. Ford MG, Pearse BM, Higgins MK, Vallis Y, Owen DJ, Gibson A, et al. Simultaneous binding of PtdIns(4,5)P2 and clathrin by AP180 in the nucleation of clathrin lattices on membranes. *Science* (2001) 291(5506):1051–5. doi:10.1126/science.291.5506.1051

113. Lemmon MA, Ferguson KM, O'Brien R, Sigler PB, Schlessinger J. Specific and high-affinity binding of inositol phosphates to an isolated pleckstrin homology domain. *Proc Natl Acad Sci U S A* (1995) 92(23):10472–6. doi:10.1073/pnas.92.23.10472
114. Corbalan-Garcia S, Garcia-Garcia J, Rodriguez-Alfaro JA, Gomez-Fernandez JC. A new phosphatidylinositol 4,5-bisphosphate-binding site located in the C2 domain of protein kinase Calpha. *J Biol Chem* (2003) 278(7):4972–80. doi:10.1074/jbc.M209385200
115. Hamada K, Shimizu T, Matsui T, Tsukita S, Hakoshima T. Structural basis of the membrane-targeting and unmasking mechanisms of the radixin FERM domain. *EMBO J* (2000) 19(17):4449–62. doi:10.1093/emboj/19.17.4449
116. Stolt PC, Jeon H, Song HK, Herz J, Eck MJ, Blacklow SC. Origins of peptide selectivity and phosphoinositide binding revealed by structures of disabled-1 PTB domain complexes. *Structure* (2003) 11(5):569–79. doi:10.1016/S0969-2126(03)00068-6
117. Eugster A, Pecheur EI, Michel F, Winsor B, Letourneur F, Friant S. Ent5p is required with Ent3p and Vps27p for ubiquitin-dependent protein sorting into the multivesicular body. *Mol Biol Cell* (2004) 15(7):3031–41. doi:10.1091/mbc.E03-11-0793
118. Tsujita K, Itoh T, Ijuin T, Yamamoto A, Shisheva A, Laporte J, et al. Myotubularin regulates the function of the late endosome through the gram domain-phosphatidylinositol 3,5-bisphosphate interaction. *J Biol Chem* (2004) 279(14):13817–24. doi:10.1074/jbc.M312294200
119. Manna D, Albanese A, Park WS, Cho W. Mechanistic basis of differential cellular responses of phosphatidylinositol 3,4-bisphosphate- and phosphatidylinositol 3,4,5-trisphosphate-binding pleckstrin homology domains. *J Biol Chem* (2007) 282(44):32093–105. doi:10.1074/jbc.M703517200
120. Lee JS, Kim JH, Jang IH, Kim HS, Han JM, Kazlauskas A, et al. Phosphatidylinositol (3,4,5)-trisphosphate specifically interacts with the phox homology domain of phospholipase D1 and stimulates its activity. *J Cell Sci* (2005) 118(Pt 19):4405–13. doi:10.1242/jcs.02564
121. Di Paolo G, De Camilli P. Phosphoinositides in cell regulation and membrane dynamics. *Nature* (2006) 443(7112):651–7. doi:10.1038/nature05185
122. Zhao DM, Thornton AM, DiPaolo RJ, Shevach EM. Activated CD4+CD25+ T cells selectively kill B lymphocytes. *Blood* (2006) 107(10):3925–32. doi:10.1182/blood-2005-11-4502
123. Karathanassis D, Stahelin RV, Bravo J, Perisic O, Pacold CM, Cho W, et al. Binding of the PX domain of p47(phox) to phosphatidylinositol 3,4-bisphosphate and phosphatidic acid is masked by an intramolecular interaction. *EMBO J* (2002) 21(19):5057–68. doi:10.1093/emboj/cdf519
124. Jose Lopez-Andreo M, Gomez-Fernandez JC, Corbalan-Garcia S. The simultaneous production of phosphatidic acid and diacylglycerol is essential for the translocation of protein kinase Cepsilon to the plasma membrane in RBL-2H3 cells. *Mol Biol Cell* (2003) 14(12):4885–95. doi:10.1091/mbc.E03-05-0295
125. Matsuo H, Chevallier J, Mayran N, Le Blanc I, Ferguson C, Faure J, et al. Role of LBPA and Alix in multivesicular liposome formation and endosome organization. *Science* (2004) 303(5657):531–4. doi:10.1126/science.1092425
126. Wojcik-Piotrowicz K, Kaszuba-Zwoinska J, Rokita E, Thor P. Cell viability modulation through changes of Ca(2+)-dependent signalling pathways. *Prog Biophys Mol Biol* (2016) 121(1):45–53. doi:10.1016/j.pbiomolbio.2016.01.004
127. Shiose A, Sumimoto H. Arachidonic acid and phosphorylation synergistically induce a conformational change of p47phox to activate the phagocyte NADPH oxidase. *J Biol Chem* (2000) 275(18):13793–801. doi:10.1074/jbc.275.18.13793
128. Grinstein S. Imaging signal transduction during phagocytosis: phospholipids, surface charge, and electrostatic interactions. *Am J Physiol Cell Physiol* (2010) 299(5):C876–81. doi:10.1152/ajpcell.00342.2010
129. Yeung T, Heit B, Dubuisson JF, Fairn GD, Chiu B, Inman R, et al. Contribution of phosphatidylserine to membrane surface charge and protein targeting during phagosome maturation. *J Cell Biol* (2009) 185(5):917–28. doi:10.1083/jcb.200903020
130. Honigmann A, van den Bogaart G, Iraheta E, Risselada HJ, Milovanovic D, Mueller V, et al. Phosphatidylinositol 4,5-bisphosphate clusters act as molecular beacons for vesicle recruitment. *Nat Struct Mol Biol* (2013) 20(6):679–86. doi:10.1038/nsmb.2570
131. Heo WD, Inoue T, Park WS, Kim ML, Park BO, Wandless TJ, et al. PI(3,4,5)P3 and PI(4,5)P2 lipids target proteins with polybasic clusters to the plasma membrane. *Science* (2006) 314(5804):1458–61. doi:10.1126/science.1134389
132. Kooijman EE, Chupin V, de Kruijff B, Burger KN. Modulation of membrane curvature by phosphatidic acid and lysophosphatidic acid. *Traffic* (2003) 4(3):162–74. doi:10.1034/j.1600-0854.2003.00086.x
133. Antonny B. Mechanisms of membrane curvature sensing. *Annu Rev Biochem* (2011) 80:101–23. doi:10.1146/annurev-biochem-052809-155121
134. McMahon HT, Gallop JL. Membrane curvature and mechanisms of dynamic cell membrane remodelling. *Nature* (2005) 438(7068):590–6. doi:10.1038/nature04396
135. Ciaramella A, Cavone A, Santucci MB, Garg SK, Sanarico N, Bocchino M, et al. Induction of apoptosis and release of interleukin-1 beta by cell wall-associated 19-kDa lipoprotein during the course of mycobacterial infection. *J Infect Dis* (2004) 190(6):1167–76. doi:10.1086/423850
136. Greco E, Quintiliani G, Santucci MB, Serafino A, Ciccaglione AR, Marcantonio C, et al. Janus-faced liposomes enhance antimicrobial innate immune response in *Mycobacterium tuberculosis* infection. *Proc Natl Acad Sci U S A* (2012) 109(21):E1360–8. doi:10.1073/pnas.1200484109
137. Mariotti S, Pardini M, Teloni R, Gagliardi MC, Fraziano M, Nisini R. A method permissive to fixation and permeabilization for the multiparametric analysis of apoptotic and necrotic cell phenotype by flow cytometry. *Cytometry A* (2017) 91(11):1115–24. doi:10.1002/cyto.a.23268
138. Santucci MB, Amicosante M, Cicconi R, Montesano C, Casarini M, Giosue S, et al. *Mycobacterium tuberculosis*-induced apoptosis in monocytes/macrophages: early membrane modifications and intracellular mycobacterial viability. *J Infect Dis* (2000) 181(4):1506–9. doi:10.1086/315371
139. Birge RB, Ucker DS. Innate apoptotic immunity: the calming touch of death. *Cell Death Differ* (2008) 15(7):1096–102. doi:10.1038/cdd.2008.58
140. Erwig LP, Henson PM. Immunological consequences of apoptotic cell phagocytosis. *Am J Pathol* (2007) 171(1):2–8. doi:10.2353/ajpath.2007.070135
141. Torchinsky MB, Garaude J, Blander JM. Infection and apoptosis as a combined inflammatory trigger. *Curr Opin Immunol* (2010) 22(1):55–62. doi:10.1016/j.coi.2010.01.003
142. Winau F, Weber S, Sad S, de Diego J, Hoops SL, Breiden B, et al. Apoptotic vesicles crossprime CD8 T cells and protect against tuberculosis. *Immunity* (2006) 24(1):105–17. doi:10.1016/j.immuni.2005.12.001
143. Ichihashi T, Satoh T, Sugimoto C, Kajino K. Emulsified phosphatidylserine, simple and effective peptide carrier for induction of potent epitope-specific T cell responses. *PLoS One* (2013) 8(3):e60068. doi:10.1371/journal.pone.0060068
144. Ham H, Sreelatha A, Orth K. Manipulation of host membranes by bacterial effectors. *Nat Rev Microbiol* (2011) 9(9):635–46. doi:10.1038/nrmicro2602
145. Pizarro-Cerda J, Charbit A, Enninga J, Lafont F, Cossart P. Manipulation of host membranes by the bacterial pathogens *Listeria*, *Francisella*, *Shigella* and *Yersinia*. *Semin Cell Dev Biol* (2016) 60:155–67. doi:10.1016/j.semcdb.2016.07.019
146. Weber SS, Ragaz C, Reus K, Nyfeler Y, Hilbi H. *Legionella pneumophila* exploits PI(4)P to anchor secreted effector proteins to the replicative vacuole. *PLoS Pathog* (2006) 2(5):e46. doi:10.1371/journal.ppat.0020046
147. Taus F, Santucci MB, Greco E, Morandi M, Palucci I, Mariotti S, et al. Monosodium urate crystals promote innate anti-mycobacterial immunity and improve BCG efficacy as a vaccine against tuberculosis. *PLoS One* (2015) 10(5):e0127279. doi:10.1371/journal.pone.0127279
148. Chua J, Deretic V. *Mycobacterium tuberculosis* reprograms waves of phosphatidylinositol 3-phosphate on phagosomal organelles. *J Biol Chem* (2004) 279(35):36982–92. doi:10.1074/jbc.M405082200
149. Wong D, Chao JD, Av-Gay Y. *Mycobacterium tuberculosis*-secreted phosphatases: from pathogenesis to targets for TB drug development. *Trends Microbiol* (2013) 21(2):100–9. doi:10.1016/j.tim.2012.09.002
150. Vergne I, Chua J, Deretic V. Tuberculosis toxin blocking phagosome maturation inhibits a novel Ca2+/calmodulin-PI3K hVPS34 cascade. *J Exp Med* (2003) 198(4):653–9. doi:10.1084/jem.20030527
151. Auricchio G, Garg SK, Martino A, Volpe E, Ciaramella A, De Vito P, et al. Role of macrophage phospholipase D in natural and CpG-induced antimycobacterial activity. *Cell Microbiol* (2003) 5(12):913–20. doi:10.1046/j.1462-5822.2003.00330.x
152. Malik ZA, Thompson CR, Hashimi S, Porter B, Iyer SS, Kusner DJ. Cutting edge: *Mycobacterium tuberculosis* blocks Ca2+ signaling and

phagosome maturation in human macrophages via specific inhibition of sphingosine kinase. *J Immunol* (2003) 170(6):2811–5. doi:10.4049/jimmunol.170.6.2811
153. Greco E, De Spirito M, Papi M, Fossati M, Auricchio G, Fraziano M. CpG oligodeoxynucleotides induce Ca2+-dependent phospholipase D activity leading to phagolysosome maturation and intracellular mycobacterial growth inhibition in monocytes. *Biochem Biophys Res Commun* (2006) 347(4):963–9. doi:10.1016/j.bbrc.2006.06.186
154. Anes E, Kuhnel MP, Bos E, Moniz-Pereira J, Habermann A, Griffiths G. Selected lipids activate phagosome actin assembly and maturation resulting in killing of pathogenic mycobacteria. *Nat Cell Biol* (2003) 5(9):793–802. doi:10.1038/ncb1036
155. Garg SK, Valente E, Greco E, Santucci MB, De Spirito M, Papi M, et al. Lysophosphatidic acid enhances antimycobacterial activity both in vitro and ex vivo. *Clin Immunol* (2006) 121(1):23–8. doi:10.1016/j.clim.2006.06.003
156. Garg SK, Volpe E, Palmieri G, Mattei M, Galati D, Martino A, et al. Sphingosine 1-phosphate induces antimicrobial activity both in vitro and in vivo. *J Infect Dis* (2004) 189(11):2129–38. doi:10.1086/386286
157. Greco E, Santucci MB, Sali M, De Angelis FR, Papi M, De Spirito M, et al. Natural lysophospholipids reduce *Mycobacterium tuberculosis*-induced cytotoxicity and induce anti-mycobacterial activity by a phagolysosome maturation-dependent mechanism in A549 type II alveolar epithelial cells. *Immunology* (2010) 129(1):125–32. doi:10.1111/j.1365-2567.2009.03145.x
158. Garg SK, Santucci MB, Panitti M, Pucillo L, Bocchino M, Okajima F, et al. Does sphingosine 1-phosphate play a protective role in the course of pulmonary tuberculosis? *Clin Immunol* (2006) 121(3):260–4. doi:10.1016/j.clim.2006.09.002
159. Delogu G, Sali M, Rocca S, Quintiliani G, Santucci MB, Greco E, et al. Lysophosphatidic acid enhances antimycobacterial response during in vivo primary *Mycobacterium tuberculosis* infection. *Cell Immunol* (2011) 271(1):1–4. doi:10.1016/j.cellimm.2011.05.014
160. Sali M, Delogu G, Greco E, Rocca S, Colizzi V, Fadda G, et al. Exploiting immunotherapy in *Mycobacterium tuberculosis*-infected mice: sphingosine 1-phosphate treatment results in a protective or detrimental effect depending on the stage of infection. *Int J Immunopathol Pharmacol* (2009) 22(1):175–81. doi:10.1177/039463200902200120
161. Di A, Brown ME, Deriy LV, Li C, Szeto FL, Chen Y, et al. CFTR regulates phagosome acidification in macrophages and alters bactericidal activity. *Nat Cell Biol* (2006) 8(9):933–44. doi:10.1038/ncb1456
162. Tandrup Schmidt S, Foged C, Korsholm KS, Rades T, Christensen D. Liposome-based adjuvants for subunit vaccines: formulation strategies for subunit antigens and immunostimulators. *Pharmaceutics* (2016) 8(1):1–22. doi:10.3390/pharmaceutics8010007
163. Rawicz W, Olbrich KC, McIntosh T, Needham D, Evans E. Effect of chain length and unsaturation on elasticity of lipid bilayers. *Biophys J* (2000) 79(1):328–39. doi:10.1016/S0006-3495(00)76295-3
164. Tanaka Y, Taneichi M, Kasai M, Kakiuchi T, Uchida T. Liposome-coupled antigens are internalized by antigen-presenting cells via pinocytosis and cross-presented to CD8 T cells. *PLoS One* (2010) 5(12):e15225. doi:10.1371/journal.pone.0015225
165. Christensen D, Henriksen-Lacey M, Kamath AT, Lindenstrom T, Korsholm KS, Christensen JP, et al. A cationic vaccine adjuvant based on a saturated quaternary ammonium lipid have different in vivo distribution kinetics and display a distinct CD4 T cell-inducing capacity compared to its unsaturated analog. *J Control Release* (2012) 160(3):468–76. doi:10.1016/j.jconrel.2012.03.016
166. van Houte AJ, Snippe H, Schmitz MG, Willers JM. Characterization of immunogenic properties of haptenated liposomal model membranes in mice. V. Effect of membrane composition on humoral and cellular immunogenicity. *Immunology* (1981) 44(3):561–8.
167. Werninghaus K, Babiak A, Gross O, Holscher C, Dietrich H, Agger EM, et al. Adjuvanticity of a synthetic cord factor analogue for subunit *Mycobacterium tuberculosis* vaccination requires FcRgamma-Syk-Card9-dependent innate immune activation. *J Exp Med* (2009) 206(1):89–97. doi:10.1084/jem.20081445
168. Mann JF, Shakir E, Carter KC, Mullen AB, Alexander J, Ferro VA. Lipid vesicle size of an oral influenza vaccine delivery vehicle influences the Th1/Th2 bias in the immune response and protection against infection. *Vaccine* (2009) 27(27):3643–9. doi:10.1016/j.vaccine.2009.03.040
169. Brewer JM, Tetley L, Richmond J, Liew FY, Alexander J. Lipid vesicle size determines the Th1 or Th2 response to entrapped antigen. *J Immunol* (1998) 161(8):4000–7.
170. Manolova V, Flace A, Bauer M, Schwarz K, Saudan P, Bachmann MF. Nanoparticles target distinct dendritic cell populations according to their size. *Eur J Immunol* (2008) 38(5):1404–13. doi:10.1002/eji.200737984
171. Brewer JM, Pollock KG, Tetley L, Russell DG. Vesicle size influences the trafficking, processing, and presentation of antigens in lipid vesicles. *J Immunol* (2004) 173(10):6143–50. doi:10.4049/jimmunol.173.10.6143
172. Foged C, Arigita C, Sundblad A, Jiskoot W, Storm G, Frokjaer S. Interaction of dendritic cells with antigen-containing liposomes: effect of bilayer composition. *Vaccine* (2004) 22(15–16):1903–13. doi:10.1016/j.vaccine.2003.11.008
173. Henriksen-Lacey M, Christensen D, Bramwell VW, Lindenstrom T, Agger EM, Andersen P, et al. Liposomal cationic charge and antigen adsorption are important properties for the efficient deposition of antigen at the injection site and ability of the vaccine to induce a CMI response. *J Control Release* (2010) 145(2):102–8. doi:10.1016/j.jconrel.2010.03.027
174. Miller CR, Bondurant B, McLean SD, McGovern KA, O'Brien DF. Liposome-cell interactions in vitro: effect of liposome surface charge on the binding and endocytosis of conventional and sterically stabilized liposomes. *Biochemistry* (1998) 37(37):12875–83. doi:10.1021/bi980096y
175. Nakanishi T, Kunisawa J, Hayashi A, Tsutsumi Y, Kubo K, Nakagawa S, et al. Positively charged liposome functions as an efficient immunoadjuvant in inducing immune responses to soluble proteins. *Biochem Biophys Res Commun* (1997) 240(3):793–7. doi:10.1006/bbrc.1997.7749
176. Hussain MJ, Wilkinson A, Bramwell VW, Christensen D, Perrie Y. Th1 immune responses can be modulated by varying dimethyldioctadecylammonium and distearoyl-sn-glycero-3-phosphocholine content in liposomal adjuvants. *J Pharm Pharmacol* (2014) 66(3):358–66. doi:10.1111/jphp.12173
177. Hoffmann PR, Kench JA, Vondracek A, Kruk E, Daleke DL, Jordan M, et al. Interaction between phosphatidylserine and the phosphatidylserine receptor inhibits immune responses in vivo. *J Immunol* (2005) 174(3):1393–404. doi:10.4049/jimmunol.174.3.1393
178. Agrawal S, Agrawal A, Doughty B, Gerwitz A, Blenis J, Van Dyke T, et al. Cutting edge: different toll-like receptor agonists instruct dendritic cells to induce distinct Th responses via differential modulation of extracellular signal-regulated kinase-mitogen-activated protein kinase and c-Fos. *J Immunol* (2003) 171(10):4984–9. doi:10.4049/jimmunol.171.10.4984
179. Bal SM, Hortensius S, Ding Z, Jiskoot W, Bouwstra JA. Co-encapsulation of antigen and toll-like receptor ligand in cationic liposomes affects the quality of the immune response in mice after intradermal vaccination. *Vaccine* (2011) 29(5):1045–52. doi:10.1016/j.vaccine.2010.11.061
180. Giddam AK, Zaman M, Skwarczynski M, Toth I. Liposome-based delivery system for vaccine candidates: constructing an effective formulation. *Nanomedicine (Lond)* (2012) 7(12):1877–93. doi:10.2217/nnm.12.157
181. Jain V, Vyas SP, Kohli DV. Well-defined and potent liposomal hepatitis B vaccines adjuvanted with lipophilic MDP derivatives. *Nanomedicine* (2009) 5(3):334–44. doi:10.1016/j.nano.2008.12.004
182. Alving CR, Rao M, Steers NJ, Matyas GR, Mayorov AV. Liposomes containing lipid A: an effective, safe, generic adjuvant system for synthetic vaccines. *Expert Rev Vaccines* (2012) 11(6):733–44. doi:10.1586/erv.12.35
183. Richards RL, Rao M, Wassef NM, Glenn GM, Rothwell SW, Alving CR. Liposomes containing lipid A serve as an adjuvant for induction of antibody and cytotoxic T-cell responses against RTS,S malaria antigen. *Infect Immun* (1998) 66(6):2859–65.
184. Genito CJ, Beck Z, Phares TW, Kalle F, Limbach KJ, Stefaniak ME, et al. Liposomes containing monophosphoryl lipid A and QS-21 serve as an effective adjuvant for soluble circumsporozoite protein malaria vaccine FMP013. *Vaccine* (2017) 35(31):3865–74. doi:10.1016/j.vaccine.2017.05.070
185. Nagill R, Kaur S. Enhanced efficacy and immunogenicity of 78kDa antigen formulated in various adjuvants against murine visceral leishmaniasis. *Vaccine* (2010) 28(23):4002–12. doi:10.1016/j.vaccine.2010.01.015
186. Korsholm KS, Hansen J, Karlsen K, Filskov J, Mikkelsen M, Lindenstrom T, et al. Induction of CD8+ T-cell responses against subunit antigens by the novel cationic liposomal CAF09 adjuvant. *Vaccine* (2014) 32(31):3927–35. doi:10.1016/j.vaccine.2014.05.050

187. Bernstein DI, Farley N, Bravo FJ, Earwood J, McNeal M, Fairman J, et al. The adjuvant CLDC increases protection of a herpes simplex type 2 glycoprotein D vaccine in guinea pigs. *Vaccine* (2010) 28(21):3748–53. doi:10.1016/j.vaccine.2009.10.025
188. Morrey JD, Motter NE, Chang S, Fairman J. Breaking B and T cell tolerance using cationic lipid–DNA complexes (CLDC) as a vaccine adjuvant with hepatitis B virus (HBV) surface antigen in transgenic mice expressing HBV. *Antiviral Res* (2011) 90(3):227–30. doi:10.1016/j.antiviral.2011.04.006
189. Allison AG, Gregoriadis G. Liposomes as immunological adjuvants. *Nature* (1974) 252(5480):252. doi:10.1038/252252a0
190. Watson DS, Endsley AN, Huang L. Design considerations for liposomal vaccines: influence of formulation parameters on antibody and cell-mediated immune responses to liposome associated antigens. *Vaccine* (2012) 30(13):2256–72. doi:10.1016/j.vaccine.2012.01.070
191. Hale AH. H-2 antigens incorporated into phospholipid vesicles elicit specific allogeneic cytotoxic T lymphocytes. *Cell Immunol* (1980) 55(2):328–41. doi:10.1016/0008-8749(80)90165-3
192. Raphael L, Tom BH. In vitro induction of primary and secondary xenoimmune responses by liposomes containing human colon tumor cell antigens. *Cell Immunol* (1982) 71(2):224–40. doi:10.1016/0008-8749(82)90258-1
193. Ludewig B, Barchiesi F, Pericin M, Zinkernagel RM, Hengartner H, Schwendener RA. In vivo antigen loading and activation of dendritic cells via a liposomal peptide vaccine mediates protective antiviral and anti-tumour immunity. *Vaccine* (2000) 19(1):23–32. doi:10.1016/S0264-410X(00)00163-8
194. Engler OB, Schwendener RA, Dai WJ, Wolk B, Pichler W, Moradpour D, et al. A liposomal peptide vaccine inducing CD8+ T cells in HLA-A2.1 transgenic mice, which recognise human cells encoding hepatitis C virus (HCV) proteins. *Vaccine* (2004) 23(1):58–68. doi:10.1016/j.vaccine.2004. 05.009
195. Rao M, Bray M, Alving CR, Jahrling P, Matyas GR. Induction of immune responses in mice and monkeys to Ebola virus after immunization with liposome-encapsulated irradiated Ebola virus: protection in mice requires CD4(+) T cells. *J Virol* (2002) 76(18):9176–85. doi:10.1128/JVI.76.18.9176-9185.2002
196. Hebishima T, Yuba E, Kono K, Takeshima SN, Ito Y, Aida Y. The pH-sensitive fusogenic 3-methyl-glutarylated hyperbranched poly(glycidol)-conjugated liposome induces antigen-specific cellular and humoral immunity. *Clin Vaccine Immunol* (2012) 19(9):1492–8. doi:10.1128/CVI.00273-12
197. Ding Q, Chen J, Wei X, Sun W, Mai J, Yang Y, et al. RAFTsomes containing epitope-MHC-II complexes mediated CD4+ T cell activation and antigen-specific immune responses. *Pharm Res* (2013) 30(1):60–9. doi:10.1007/s11095-012-0849-7
198. Gupta PN, Vyas SP. Investigation of lectinized liposomes as M-cell targeted carrier-adjuvant for mucosal immunization. *Colloids Surf B Biointerfaces* (2011) 82(1):118–25. doi:10.1016/j.colsurfb.2010.08.027
199. Figueiredo L, Cadete A, Goncalves LM, Corvo ML, Almeida AJ. Intranasal immunisation of mice against *Streptococcus equi* using positively charged nanoparticulate carrier systems. *Vaccine* (2012) 30(46):6551–8. doi:10.1016/j.vaccine.2012.08.050
200. Wang HW, Jiang PL, Lin SF, Lin HJ, Ou KL, Deng WP, et al. Application of galactose-modified liposomes as a potent antigen presenting cell targeted carrier for intranasal immunization. *Acta Biomater* (2013) 9(3):5681–8. doi:10.1016/j.actbio.2012.11.007
201. Li Z, Zhang L, Sun W, Ding Q, Hou Y, Xu Y. Archaeosomes with encapsulated antigens for oral vaccine delivery. *Vaccine* (2011) 29(32):5260–6. doi:10.1016/j.vaccine.2011.05.015
202. Kallert S, Zenk SF, Walther P, Grieshober M, Weil T, Stenger S. Liposomal delivery of lipoarabinomannan triggers *Mycobacterium tuberculosis* specific T-cells. *Tuberculosis (Edinb)* (2015) 95(4):452–62. doi:10.1016/j.tube.2015.04.001
203. Komori T, Nakamura T, Matsunaga I, Morita D, Hattori Y, Kuwata H, et al. A microbial glycolipid functions as a new class of target antigen for delayed-type hypersensitivity. *J Biol Chem* (2011) 286(19):16800–6. doi:10.1074/jbc.M110.217224
204. Morita D, Miyamoto A, Hattori Y, Komori T, Nakamura T, Igarashi T, et al. Th1-skewed tissue responses to a mycolyl glycolipid in mycobacteria-infected rhesus macaques. *Biochem Biophys Res Commun* (2013) 441(1):108–13. doi:10.1016/j.bbrc.2013.10.021
205. Kawasaki N, Rillahan CD, Cheng TY, Van Rhijn I, Macauley MS, Moody DB, et al. Targeted delivery of mycobacterial antigens to human dendritic cells via Siglec-7 induces robust T cell activation. *J Immunol* (2014) 193(4):1560–6. doi:10.4049/jimmunol.1303278
206. Klauber TCB, Laursen JM, Zucker D, Brix S, Jensen SS, Andresen TL. Delivery of TLR7 agonist to monocytes and dendritic cells by DCIR targeted liposomes induces robust production of anti-cancer cytokines. *Acta Biomater* (2017) 53:367–77. doi:10.1016/j.actbio.2017.01.072
207. Schmid D, Pypaert M, Munz C. Antigen-loading compartments for major histocompatibility complex class II molecules continuously receive input from autophagosomes. *Immunity* (2007) 26(1):79–92. doi:10.1016/j.immuni.2006.10.018
208. Harding CV, Collins DS, Kanagawa O, Unanue ER. Liposome-encapsulated antigens engender lysosomal processing for class II MHC presentation and cytosolic processing for class I presentation. *J Immunol* (1991) 147(9):2860–3.
209. Joffre OP, Segura E, Savina A, Amigorena S. Cross-presentation by dendritic cells. *Nat Rev Immunol* (2012) 12(8):557–69. doi:10.1038/nri3254
210. Zehner M, Marschall AL, Bos E, Schloetel JG, Kreer C, Fehrenschild D, et al. The translocon protein Sec61 mediates antigen transport from endosomes in the cytosol for cross-presentation to CD8(+) T cells. *Immunity* (2015) 42(5):850–63. doi:10.1016/j.immuni.2015.04.008
211. Nunes-Hasler P, Demaurex N. The ER phagosome connection in the era of membrane contact sites. *Biochim Biophys Acta* (2017) 1864(9):1513–24. doi:10.1016/j.bbamcr.2017.04.007
212. Gao J, Ochyl LJ, Yang E, Moon JJ. Cationic liposomes promote antigen cross-presentation in dendritic cells by alkalizing the lysosomal pH and limiting the degradation of antigens. *Int J Nanomedicine* (2017) 12:1251–64. doi:10.2147/IJN.S125866
213. Liu L, Ma P, Wang H, Zhang C, Sun H, Wang C, et al. Immune responses to vaccines delivered by encapsulation into and/or adsorption onto cationic lipid-PLGA hybrid nanoparticles. *J Control Release* (2016) 225:230–9. doi:10.1016/j.jconrel.2016.01.050
214. Moore NM, Sheppard CL, Barbour TR, Sakiyama-Elbert SE. The effect of endosomal escape peptides on in vitro gene delivery of polyethylene glycol-based vehicles. *J Gene Med* (2008) 10(10):1134–49. doi:10.1002/jgm.1234
215. Miura N, Akita H, Tateshita N, Nakamura T, Harashima H. Modifying antigen-encapsulating liposomes with KALA facilitates MHC class I antigen presentation and enhances anti-tumor effects. *Mol Ther* (2017) 25(4):1003–13. doi:10.1016/j.ymthe.2017.01.020
216. Reddy R, Zhou F, Huang L, Carbone F, Bevan M, Rouse BT. pH sensitive liposomes provide an efficient means of sensitizing target cells to class I restricted CTL recognition of a soluble protein. *J Immunol Methods* (1991) 141(2):157–63. doi:10.1016/0022-1759(91)90142-3
217. Barnier-Quer C, Elsharkawy A, Romeijn S, Kros A, Jiskoot W. Adjuvant effect of cationic liposomes for subunit influenza vaccine: influence of antigen loading method, cholesterol and immune modulators. *Pharmaceutics* (2013) 5(3):392–410. doi:10.3390/pharmaceutics5030392
218. Takagi A, Kobayashi N, Taneichi M, Uchida T, Akatsuka T. Coupling to the surface of liposomes alters the immunogenicity of hepatitis C virus-derived peptides and confers sterile immunity. *Biochem Biophys Res Commun* (2013) 430(1):183–9. doi:10.1016/j.bbrc.2012.11.028
219. Matsui M, Kohyama S, Suda T, Yokoyama S, Mori M, Kobayashi A, et al. A CTL-based liposomal vaccine capable of inducing protection against heterosubtypic influenza viruses in HLA-A*0201 transgenic mice. *Biochem Biophys Res Commun* (2010) 391(3):1494–9. doi:10.1016/j.bbrc.2009.12.100
220. Nagata T, Toyota T, Ishigaki H, Ichihashi T, Kajino K, Kashima Y, et al. Peptides coupled to the surface of a kind of liposome protect infection of influenza viruses. *Vaccine* (2007) 25(26):4914–21. doi:10.1016/j.vaccine.2007.04.010
221. Naito S, Horino A, Nakayama M, Nakano Y, Nagai T, Mizuguchi J, et al. Ovalbumin-liposome conjugate induces IgG but not IgE antibody production. *Int Arch Allergy Immunol* (1996) 109(3):223–8. doi:10.1159/000237241
222. Taneichi M, Ishida H, Kajino K, Ogasawara K, Tanaka Y, Kasai M, et al. Antigen chemically coupled to the surface of liposomes are cross-presented to CD8+ T cells and induce potent antitumor immunity. *J Immunol* (2006) 177(4):2324–30. doi:10.4049/jimmunol.177.4.2324
223. Masek J, Bartheldyova E, Turanek-Knotigova P, Skrabalova M, Korvasova Z, Plockova J, et al. Metallochelating liposomes with associated lipophilised norAbuMDP as biocompatible platform for construction of vaccines with recombinant His-tagged antigens: preparation, structural study and

immune response towards rHsp90. *J Control Release* (2011) 151(2):193–201. doi:10.1016/j.jconrel.2011.01.016
224. Watson DS, Platt VM, Cao L, Venditto VJ, Szoka FC Jr. Antibody response to polyhistidine-tagged peptide and protein antigens attached to liposomes via lipid-linked nitrilotriacetic acid in mice. *Clin Vaccine Immunol* (2011) 18(2):289–97. doi:10.1128/CVI.00425-10
225. Matyas GR, Mayorov AV, Rice KC, Jacobson AE, Cheng K, Iyer MR, et al. Liposomes containing monophosphoryl lipid A: a potent adjuvant system for inducing antibodies to heroin hapten analogs. *Vaccine* (2013) 31(26):2804–10. doi:10.1016/j.vaccine.2013.04.027
226. Brito LA, Kommareddy S, Maione D, Uematsu Y, Giovani C, Berlanda Scorza F, et al. Self-amplifying mRNA vaccines. *Adv Genet* (2015) 89:179–233. doi:10.1016/bs.adgen.2014.10.005
227. Pardi N, Weissman D. Nucleoside modified mRNA vaccines for infectious diseases. *Methods Mol Biol* (2017) 1499:109–21. doi:10.1007/978-1-4939-6481-9_6
228. Desmet CJ, Ishii KJ. Nucleic acid sensing at the interface between innate and adaptive immunity in vaccination. *Nat Rev Immunol* (2012) 12(7):479–91. doi:10.1038/nri3247
229. Kariko K, Ni H, Capodici J, Lamphier M, Weissman D. mRNA is an endogenous ligand for toll-like receptor 3. *J Biol Chem* (2004) 279(13):12542–50. doi:10.1074/jbc.M310175200
230. Richner JM, Himansu S, Dowd KA, Butler SL, Salazar V, Fox JM, et al. Modified mRNA vaccines protect against Zika virus infection. *Cell* (2017) 168(6):1114–25.e10. doi:10.1016/j.cell.2017.02.017
231. Chen S, Tam YYC, Lin PJC, Sung MMH, Tam YK, Cullis PR. Influence of particle size on the in vivo potency of lipid nanoparticle formulations of siRNA. *J Control Release* (2016) 235:236–44. doi:10.1016/j.jconrel.2016.05.059
232. Hekele A, Bertholet S, Archer J, Gibson DG, Palladino G, Brito LA, et al. Rapidly produced SAM((R)) vaccine against H7N9 influenza is immunogenic in mice. *Emerg Microbes Infect* (2013) 2(8):e52. doi:10.1038/emi.2013.54
233. Liang F, Lindgren G, Lin A, Thompson EA, Ols S, Rohss J, et al. Efficient targeting and activation of antigen-presenting cells in vivo after modified mRNA vaccine administration in rhesus macaques. *Mol Ther* (2017) 25(12):2635–47. doi:10.1016/j.ymthe.2017.08.006
234. Bogers WM, Oostermeijer H, Mooij P, Koopman G, Verschoor EJ, Davis D, et al. Potent immune responses in rhesus macaques induced by nonviral delivery of a self-amplifying RNA vaccine expressing HIV type 1 envelope with a cationic nanoemulsion. *J Infect Dis* (2015) 211(6):947–55. doi:10.1093/infdis/jiu522
235. Zumla A, Rao M, Wallis RS, Kaufmann SH, Rustomjee R, Mwaba P, et al. Host-directed therapies for infectious diseases: current status, recent progress, and future prospects. *Lancet Infect Dis* (2016) 16(4):e47–63. doi:10.1016/S1473-3099(16)00078-5
236. Zumla A, Memish ZA, Maeurer M, Bates M, Mwaba P, Al-Tawfiq JA, et al. Emerging novel and antimicrobial-resistant respiratory tract infections: new drug development and therapeutic options. *Lancet Infect Dis* (2014) 14(11):1136–49. doi:10.1016/S1473-3099(14)70828-X
237. Douer D. Efficacy and safety of vincristine sulfate liposome injection in the treatment of adult acute lymphocytic leukemia. *Oncologist* (2016) 21(7):840–7. doi:10.1634/theoncologist.2015-0391
238. Sarantis H, Grinstein S. Subversion of phagocytosis for pathogen survival. *Cell Host Microbe* (2012) 12(4):419–31. doi:10.1016/j.chom.2012.09.001
239. Mariotti S, Pardini M, Gagliardi MC, Teloni R, Giannoni F, Fraziano M, et al. Dormant *Mycobacterium tuberculosis* fails to block phagosome maturation and shows unexpected capacity to stimulate specific human T lymphocytes. *J Immunol* (2013) 191(1):274–82. doi:10.4049/jimmunol.1202900
240. Goldberg MF, Saini NK, Porcelli SA. Evasion of innate and adaptive immunity by *Mycobacterium tuberculosis*. *Microbiol Spectr* (2014) 2(5):1–24. doi:10.1128/microbiolspec.MGM2-0005-2013
241. Liu CH, Liu H, Ge B. Innate immunity in tuberculosis: host defense vs pathogen evasion. *Cell Mol Immunol* (2017) 14(12):963–75. doi:10.1038/cmi.2017.88

Conflict of Interest Statement: All the authors declare no business relationship that might lead to a conflict of interest.

frontiers in Immunology

REVIEW
published: 28 February 2018
doi: 10.3389/fimmu.2018.00345

Virus-Like Particle, Liposome, and Polymeric Particle-Based Vaccines against HIV-1

*Yong Gao, Chanuka Wijewardhana and Jamie F. S. Mann**

Department of Microbiology and Immunology, University of Western Ontario, London, ON, Canada

It is acknowledged that vaccines remain the best hope for eliminating the HIV-1 epidemic. However, the failure to produce effective vaccine immunogens and the inability of conventional delivery strategies to elicit the desired immune responses remains a central theme and has ultimately led to a significant roadblock in HIV vaccine development. Consequently, significant efforts have been applied to generate novel vaccine antigens and delivery agents, which mimic viral structures for optimal immune induction. Here, we review the latest developments that have occurred in the nanoparticle vaccine field, with special emphasis on strategies that are being utilized to attain highly immunogenic, systemic, and mucosal anti-HIV humoral and cellular immune responses. This includes the design of novel immunogens, the central role of antigen-presenting cells, delivery routes, and biodistribution of nanoparticles to lymph nodes. In particular, we will focus on virus-like-particle formulations and their preclinical uses within the HIV prophylactic vaccine setting.

Keywords: HIV-1, vaccine, virus-like particles, nanoparticles, immunogenicity

OPEN ACCESS

Edited by:
Rajko Reljic,
St George's, University of London, United Kingdom

Reviewed by:
Thorsten Demberg,
Immatics Biotechnologies, Germany
Evelina Angov,
Walter Reed Army Institute of Research, United States

****Correspondence:***
Jamie F. S. Mann
jmann62@uwo.ca

Specialty section:
This article was submitted to Vaccines and Molecular Therapeutics, a section of the journal Frontiers in Immunology

Received: *29 November 2017*
Accepted: *07 February 2018*
Published: *28 February 2018*

Citation:
Gao Y, Wijewardhana C and Mann JFS (2018) Virus-Like Particle, Liposome, and Polymeric Particle-Based Vaccines against HIV-1. Front. Immunol. 9:345. doi: 10.3389/fimmu.2018.00345

INTRODUCTION

Human immunodeficiency virus-1 (HIV-1) and HIV-2 have emerged as the result of zoonotic lentiviral transmissions of simian immunodeficiency viruses (SIV), from chimpanzees/gorillas and sooty mangabeys, respectively, into the human population. First identified as the etiological agent behind acquired immunodeficiency syndrome (AIDS) in humans in the early 1980s, HIV has continued to spread into a global pandemic and major public health concern. At the end of 2015 alone, there were 36.7 million people infected with HIV with an additional 2.1 million new infections that same year. Excluding parenteral infections, HIV acquisition is almost entirely transmitted through sexual intercourse. Worldwide, approximately 80% of the 30 million people infected with HIV acquired the virus through heterosexual transmission, with receptive vaginal and anal intercourse accounting for 60–70 and 5–10%, respectively, of the global total.

Human immunodeficiency virus infection is characterized by the catastrophic depletion of CD4 T cells—the very cells that orchestrate host immune responses against invading pathogens. The combination of viral cytopathic effects, cell suicide by caspase-1 mediated pyroptosis, and caspase-3-mediated apoptosis are the major mechanisms behind the depletion of CD4 T cells (1). Over time, the continued depletion of CD4 T cells causes an AIDS-defining illness where people become susceptible to a plethora of opportunistic infections.

During heterosexual transmission, HIV-1 enters the body through the genital mucosa, while in male to male transmission, HIV-1 enters through the rectal or upper gastrointestinal mucosa. Numerous factors contribute to HIV-1 transmission rates across genital and gut mucosal surfaces, including the viral load in the donor during sexual contact, presence of pre-existing mucosal infections, trauma, inflammation, frequency of sexual contacts, male circumcision, receptive anal intercourse, and whether individuals used barrier contraceptives such as condoms. The current paradigm suggests HIV enters anatomical sites with micro-abrasions, likely occurring as a direct result of sexual activity, thus providing more direct access to target cells residing in submucosal tissues. It is important to note that mucosal frontline surfaces, such as the endocervix, transformation zone, and gastrointestinal mucosa, have only a single layer of columnar epithelium to separate the external environment from the sterile inner sanctum of the body. Thus, these surfaces are more susceptible to microtraumas and likely serve as entry points for HIV. After the initial seeding of an infecting founder population, the virus spreads to regional lymph nodes and then disseminates systemically. The narrow timeframe from breaching the mucosal frontline through to primary foci development and immediately prior to lymph node distribution is often referred to as the "window of opportunity" (2). This represents the instance where a potential vaccine candidate might be maximally effective at aborting an infection event. During this window of opportunity, HIV may also be at its most vulnerable state during infection considering only one or few HIV-1 clones were transmitted from a highly diverse HIV population in the recipient.

Due to the advent of antiretroviral therapies (ART), HIV is no longer a death sentence. From 1995–2010, approximately 5.1 million AIDS-related deaths were averted in low- and middle-income countries due to greater accessibility of ART (3). Current combination antiretroviral therapies (cART) inhibits various points of the viral replication cycle and, is most effective as a triple therapy regiment to prevent the induction of escape mutants. Although cART can decrease viral load in the blood to undetectable levels, it remains a non-curative strategy against HIV due to the presence of the latent reservoir (4). This is because cART can only target actively replicating virus and, therefore, cannot impact the latent reservoir.

EARLY ATTEMPTS AT HIV VACCINES

Initial HIV vaccine candidates to enter human clinical trials were subunit vaccines based on the surface Env glycoprotein. These were mainly soluble monomeric gp120 or gp160 constructs (5–7). These early attempts at vaccines provided the necessary evidence for protection against homologous SIV-HIV (SHIV) chimeric virus challenge in non-human primates (NHPs) (8). Unfortunately, these vaccines were not protective against a heterologous virus challenge despite inducing strong immune responses and the animals remained susceptible to infections with heterologous SHIV viruses (9). Despite this, numerous gp120 subunit vaccines have been designed and evaluated in human clinical trials to provide proof of principle for vaccine-mediated protection against infection. An example of an early monomeric gp120 vaccine trial conducted in human volunteers was the Phase III efficacy trial (VAX003). This study was conducted within an injection drug using cohort in Thailand. The vaccine (AIDSVAX B/E) consisted of a combination of recombinant clade B and E gp120 antigens adjuvanted with alum. The vaccine ultimately provided no significant levels of protection against infection among the participants, with 8.4% in the vaccine arm and 8.3% in the placebo arm becoming infected (10, 11). Another notable human vaccine trial was the VAX004, which employed the AIDSVAX B/B vaccine and showed near identical results in North America and in the Netherlands. This vaccine was given to men who have sex with men (MSM) and women at high risk for sexually transmitted HIV infection cohorts (12, 13). Despite eliciting high homologous neutralizing antibody titers against the applied vaccine strains, only weak neutralizing antibody responses were detected within recipients. Overall, both VAX003 and VAX004 vaccine trials failed to show protection from HIV infection, despite being immunogenic. Such studies helped initiate the search for new and improved immunogens and the development of oligomeric Env structures to better mimic the HIV-1 functional spike. In theory, trimeric Envs may be advantageous to predecessor monomeric vaccine candidates as it is thought they might be able to induce conformationally dependent antibodies. Most of the trimeric Env immunogens, the so-called gp140 immunogens consisting of gp120 and the ectodomain of gp41 (14–16), elicit significantly higher titers of neutralizing antibodies compared to the monomeric Env forms (17–21), however, the breath of neutralization is still limited. Attempts to enhance the immunogenicity of Env antigens, i.e., increase the neutralizing antibody levels, involved modifying Env molecules by deleting the highly glycosylated V2 domain. Unfortunately, this had minimal impact in eliciting broadly neutralizing antibodies. Trimeric gp140 with new disulfide bonds to stabilize gp120–gp41 interactions were tested for immunogenicity within novel prime-boost immunization protocols (22). When rabbits were primed with DNA encoding a membrane bound form of gp140 by electroporation followed by disulfide-stabilized trimeric gp140 booster immunizations *via* the intramuscular (IM), intradermal (I.D.), or subcutaneous (S.C.) routes, high titers of neutralizing antibodies against homologous viruses could be elicited.

Since these early failed attempts at vaccination, numerous DNA, and viral vector platforms have been created and evaluated as anti-HIV vaccine candidates. While DNA/RNA and viral vectors do not fall under the mandate of this review, it is worth mentioning the only clinical trial to date to have demonstrated any efficacy against HIV acquisition was RV144—the phase III "Thai Trial." In 2009, the results from the RV144 trial were released, demonstrating the effectiveness of an ALVAC vaccine prime followed by an AIDSVAX boost. The ALVAC prophylactic vaccine component was a canarypox vector encoding HIV-1 Gag, Pol, and gp120 Env while the AIDSVAX boost consisted of gp120 B/E adsorbed to alum. A modest benefit of 31.2% vaccine efficacy was demonstrated in the vaccine arm using this regimen (23). Interestingly, in a *post hoc* analysis of the protection data, it was observed that should the study have stopped after the first year of implementation, vaccine efficacy would have been as high as 60%, indicating a non-sustained protection from acquisition was

achieved. In terms of the immune correlates of protection a weak neutralizing antibody response was again observed; however, non-neutralizing plasma IgG binding antibodies to the top of the Env V1/V2 variable loop were associated with protection (24).

NANOPHARMACEUTICAL-BASED VACCINES

Soluble gp120 monomers and more advanced trimeric forms of Env failed to elicit the protective responses necessary to prevent HIV acquisition. Thus, a critical goal in HIV vaccine design has been to try and understand why this has been the case. Collectively, the knowledge that (1) infused neutralizing antibody protects against viral challenge in non-human primates (NHP) studies, (2) a percentage of individuals will generate neutralizing antibody responses against the autologous infecting virus, and that (3) highly potent neutralizing antibody can be generated in some individuals, solidifies the notion that an anti-HIV B cell response can be protective. As neutralizing antibodies are directed against the surface glycoprotein, presentation of natural Env structures, mimicking the native viral Env is deemed imperative to eliciting a neutralizing immune response. Resolving this scientific challenge has led to re-engineering of the Env itself to achieve a native conformation. As a result, numerous antigenic structures have been developed, including germline revertants targeting the N332 supersite and near native trimers candidates such as BG505 SOSIP.664 (25–27). These new immunogens, designed to harness anti-HIV neutralizing antibody responses can elicit autologous neutralizing antibody responses and depending on how they have been utilized, can elicit heterologous Tier 2 neutralizing antibody. However, these and other such candidate vaccine antigens do require mutations in their amino acid sequences to increase stability and this can come at the expense of losing antigenic conformation. For reviews more focused on HIV-1 Env-based vaccines, several recent articles have been published which may be of interest to readers (28, 29).

Virus-Like Particles (VLPs)

To overcome these afore-mentioned issues in antigen design, Env trimers have been expressed in lipid membranes. This enables their conformations to more accurately resemble native and functional Env spikes found on infectious virus. Taking this into consideration, nanoparticle platforms such as VLPs provide the ideal technology to express HIV Env immunogens. VLPs are non-infectious and genomeless multiprotein structures that mimic the conformation of viral proteins in their natural environment. These self-assembling molecules can generate ordered arrays of polypeptides that come together to form the VLP. The resulting repetitive geometry offers maximal VLP–host interactions due to increased avidity (30). As a result, VLPs can present viral antigens in their authentic conformation and maximally stimulate resulting immune responses (31).

The use of VLPs as potential vaccine candidates offers numerous advantages over traditional strategies. VLPs have the unique ability to present viral Env spikes in their natural conformation and, therefore, the potential to elicit neutralizing antibody responses against HIV. This feature is often lost when antigens are purified from pathogens or when pathogens are rendered inert through chemical or heat inactivation. VLP vaccines are also cheaper than subunit vaccines since less of the vaccine can be administered without impairing the resulting immune response. Another attractive property of VLP vaccines are their particulate structure, which allows them to be efficiently taken up by antigen-presenting cells (APCs) and stimulate strong humoral and cellular immune responses (32, 33) since they can be presented on both MHC class I and class II molecules (34, 35). In addition, their polyvalency allows for efficient B cell receptor (BCR) crosslinking and activation.

Although several commercially available VLP vaccine formulations are available to protect against Hepatitis B, Hepatitis E, and human papillomavirus (HPV), none exist for HIV (**Table 1**). One of the prominent prophylactic VLP vaccine formulations against the Hepatitis B virus is RECOMBIVAX®. It mainly consists of Hepatitis B surface antigen that spontaneously assembles into ~20 nm lipid-containing particles (36). The major prophylactic vaccine against the hepatitis E virus is the Hecolin® vaccine, whose major constituent is a small portion of the Hepatitis E capsid protein that self assembles into 20–30 nm particles (36). Gardasil® is a major prophylactic VLP vaccine formulation against HPV. It is synthesized by expressing HPV L1 capsid protein, which spontaneously assembles into immunogenic non-infectious VLPs that can induce the same neutralizing antibody responses as the native virions (37).

There are five main platforms that are currently utilized to produce VLP vaccines: bacteria, yeast, insect cells, mammalian

TABLE 1 | Pharmaceutical virus-like particle-based vaccines.

Name	Major antigen constituent	Approval status	Protection against	Approximate size	Route of immunization	Adjuvant used
Recombivax™	Hepatitis B surface antigen with Hepatitis B-derived lipids	First approved in USA, 1983	Hepatitis B	20 nm	IM	Alum
Hecolin®	Hepatitis E capsid protein	First approved in China, 2011	Hepatitis E	20–30 nm	IM	Aluminum hydroxide
Gardasil™	Human Papillomavirus (HPV) L1 capsid protein	First approved in USA, 2006	HPV 6, 11, 16, 18	55 nm	IM	Alum
Cervarix®	HPV L1 capsid protein	First approved in USA, 2009	HPV 16, 18	55 nm	IM	AS04

IM, intramuscular.

cells, and plants. Although leveraging bacteria to produce VLPs is the most scalable and cost-effective approach, they are unable to perform the essential post-translational modifications for optimal immunogenicity in human (31). In addition, the use of bacteria may introduce contaminating endotoxins into vaccine formulations. Yeast are also scalable and cost-effective approaches to producing VLPs; however, unlike bacteria, they can perform eukaryotic post-translational modifications such as glycosylation. Insect cells can be induced to produce VLPs through baculovirus expression systems. This system can produce large quantities of VLPs in their natural conformation but must be purified from baculovirus contaminants. In fact, these components may obscure the immune response against the epitopes of the VLP (38). VLP production through mammalian cells cannot be scaled up as efficiently as bacteria, yeast, or insect expression systems. In addition, the use of mammalian cell systems runs the risk of human viral pathogen contamination (39); however, they have the most accurate and complex post-translational modifications (40). Therefore, this system is particularly advantageous for constructing complex VLPs. Plants can be induced to produce VLPs through *Agrobacterium tumefaciens*, a Gram-negative soil-based bacteria used to transform plant cells (41). Although plant-based expression systems are easy to scale up and contain no human-derived viral contamination, these VLPs cannot undergo the same post-translational modifications that are done in mammalian cells, thus reducing immunogenicity.

The HIV-1 Env trimer is synthesized as a 160 kDa precursor and is processed by protease to yield a surface and transmembrane subunit during its passage through the secretory pathway. The resulting surface bound oligomer comprises three non-covalently associated gp120 and gp41 subunits. The surface gp120 is responsible for binding host cell target receptors (CD4) and co-receptors (CCR5) whereas the gp41 anchors Env in the membrane. Taking the well-characterized influenza virus as a model system shows that the virus may require only 2–3 trimers to engage with its cellular receptors to create a pre-fusion structure. However, it is believed that 6–8 trimers may be necessary to build the stable fusion pore (42). This question has been hard to address in the context of HIV-1 for a number of reasons including the fact that (1) a large percentage of HIV virions (>99%) are replication defective, (2) the sparsity of intact Env trimers on the viral surface (7–14 spikes/virion), (3) spontaneous shedding of gp120 from Env complexes, and (4) heterogeneity among the HIV-1 Env complexes (42). This has resulted in a number of conflicting studies suggesting a single trimer is necessary (42) or perhaps between five and eight trimers may be necessary for infection (43, 44). More recently, work done by the Trkola group has suggested divergent HIV strains differ in their stoichiometry for entry, requiring ~1–7 trimers, with the majority of HIV strains requiring 2–3 trimers for infection (45). In the context of eliciting humoral immune responses within the host, the surface Env density is important for efficient BCR crosslinking, leading to B cell clonal expansion and antibody affinity maturation. Unfortunately, HIV's low density of Env spikes (7–14 spikes/virus) is substantially lower than that seen for other viruses, such as influenza (400–500 spikes/virus), vesicular stomatitis virus (VSV, 1,200 spikes/virion), Rous sarcoma virus (RSV, ~118 spikes/virion), and even compared to the related SIV (~70 spikes/virion) (46). Therefore, attempts to increase surface HIV Env density on VLPs may facilitate more protective immune responses. Using fluorescence activated cell (FACS) sorting to isolate producer cells that are recognized by trimer cross reactive broadly neutralizing antibody, Stano et al., sought to isolate and propagate producer cells displaying higher levels of antigenically correct Env (46). Following multiple rounds of FACS sorting, monodisperse VLP formulations were generated that had a 10-fold higher Env density per particle (~127 spikes/particle) than control viral particles. When the Env was sequenced, a truncation in the C-terminal tail of Env was seen. Although the high-density Env particles displayed a greater infectivity compared to normal pseudoviruses, they exhibited similar levels of neutralization sensitivity (46). However, the high Env density VLPs were superior activators of broadly neutralizing VRC01 B cells as determined by upregulation in CD69, IL-6, and TNF-a production and BCR downregulation. This collectively indicates superior BCR clustering and activation (46).

One of the major roadblocks to an effective HIV-1 vaccine is the sheer diversity of the viral swarm. A preventative vaccine must be protective against HIV strains/subtypes circulating in multiple geographic regions. Polyvalent Env vaccines are one such approach to overcome the viral diversity and involve the use of heterogeneous Env mixtures to expose developing immune responses to a multitude of Env conformations (47). This is thought to help promote immuno-focusing of B cell responses onto more conserved regions of vulnerability such as the Env CD4-binding site and MPER while also promoting antibody breadth. To address this issue, Pankrac et al. developed a chimeric HIV-1 VLP formulation capable of accommodating near full length (NFL) genomes of HIV-1 that captures the viral diversity within infected individuals (47). To do this, the authors took the plasma of five pre-cART HIV positive volunteers and engineered the isolated virus into a mixed VLP formulation. By inserting mutations into integrase and a series of substitutions into the RNA packaging element, the resulting VLPs had dramatically reduced genomic RNA and lost the functional ability of viral integrase. They also deleted the 5′LTR so that the probability of reverse transcription was eliminated. Collectively, these "dead" viral particles were shown to have similar morphology to wild-type virus, contained p24 and p17, as well as expressed functional Env, Tat and Rev (47, 48). Upon exposure of HIV-1 infected CD4 T cells to dendritic cells (DCs) pulsed with the heterologous VLPs, a strong IFN-g response was detected, indicating the ability to generate antigen-specific CD4 T cell recall responses. In addition, when the VLPs were used to pulse PBMC cultures, the authors demonstrated Granzyme B production, a biological marker for cytotoxicity (47). Finally, the VLPs were also shown to be able to prime and boost a CD4 adaptive immune response *in vitro* using healthy donor CD4 T cell-DC co-cultures (47). This polyvalent VLP vaccine formulation is called ACT-VEC and is now being evaluated in non-human primates (NHPs) for its immunogenicity.

Trying to understand the host and viral factors that influence HIV infection and how the virus crosses the mucosal barrier might lead to more efficacious HIV vaccines. This has led to the characterization of the phenotypic properties of transmitted/founder (T/F) viruses to see if transmission is through stochastic

events or whether the genetic bottle neck selects for viruses with certain properties. Features associated with transmitted viruses include CCR5 tropism, short variable loops and less N-linked glycan residues. With such distinguishing features in mind, McClure et al. tested the antigenicity and immunogenicity of DNA and modified vaccinia Ankara expressed VLPs, displaying native forms of T/F clade C Envs (49). The hypothesis being that the VLPs expressed Envs with or without administered gp120 might elicit a broadly neutralizing antibody response. This interesting study proceeded investigations into the clade C infection occurring within an infected individual that eventually developed a broadly neutralizing antibody response against the CH103 CD4-binding site (50). Significantly, the VLP expressing vectored immunogens boosted with gp120 were immunogenic in NHPs and despite a complex regimen elicited a neutralizing antibody response in 50% of the macaques tested, with antibody directed toward the CD4-binding site. Thus, demonstrating that a VLP prime plus gp120 boost using a T/F Env to be capable of inducing autologous Tier 2 neutralizing antibody to the CD4-binding site (49).

Liposomes

Antigen delivery by liposomal vesicles was demonstrated over 30 years ago when unilamellar vesicles were generated that were composed of phosphatidylserine. These liposomes contained poliovirus and purified poliovirus RNA. They were found to be infectious and could be potentially utilized as a delivery agent for biological macromolecules (51). Liposomes can either be microparticles or colloidal carriers (52), with a diameter ranging from 20 nm to more than 10 μm (53). There are many types of liposomes (e.g., multilamellar vesicles and large or small unilamellar vesicles), with the conventional ones composed of biodegradable and non-toxic zwitterionic phospholipids, such as phosphatidylcholine, phosphatidylserine, and cholesterol (52–54). The formation of liposomes is a spontaneous occurrence when lipids are subjected to hydration (52), enabling the formation of lipid bilayers surrounding an aqueous core. The first efforts at using liposomal technologies for delivery of candidate HIV vaccine antigens occurred nearly 25 years ago by Bui et al. (55). In this first attempt, the authors utilized a non-glycosylated, denatured gp120 called HIV Env-2-3-SF2 as the vaccine immunogen, and co-formulated the antigen with either alum or liposome. The HIV Env-2-3-SF2 alum and HIV Env-2-3-SF2 liposome immune responses were then potentiated using liposomal IL-7. The result was the demonstration that liposomal HIV Env antigens elicited stronger antibody titers than the alum formulations and that the responses could be enhanced using liposomal IL-7. Notably, cytotoxic T lymphocyte (CTL) responses were greater in the liposomal arm than the alum treatment regimen (55).

Interbilayer-cross-linked multilamellar vesicles (ICMV) with His-tagged gp140 trimers anchored onto the surface of the delivery agent using Ni-NTA functionalized lipids were recently explored (56). The aim being to deliver a high quality, B cell triggering-gp140 trimer immunogen, previously demonstrated to elicit high titers of potent cross clad neutralizing antibody responses (57). The ICMV-gp140 nanoparticles were adjuvanted with TLR4 agonist MPLA and used to assess humoral immune response induction in mice and compared to gp140 adjuvanted with SAS (oil in water adjuvant containing MPLA trehalose-6,6′-dimycolate). The trimer-loaded ICMV particles were superior inducers of humoral immune responses compared to gp140 alone or adjuvanted with SAS, with the breadth of the anti-HIV antibody response increased in response to ICVM surface anchoring—including against the conserved MPER sequence of gp41. Unfortunately, due to the use of the murine model, the authors did not test neutralizing antibody production (56).

In a separate study, Ingale et al., utilized single bilayer liposomes, displaying well-ordered, high-density trimers, such as JRFL-SOSIP, and JRFL-NFL, for better B cell activation (58). The trimers were conjugated to the surface of the liposomes, by electrostatic interaction using the cholesterol substitute, DGS-NTA(Ni), and c-terminal His-tagged HIV-1 trimers. As a result, the liposomal formulation containing the surface trimers more efficiently stimulated B cell germinal center formation compared to soluble trimers demonstrating the necessity for membrane display. Furthermore, there appeared to be a suggestion that the liposomal trimers promoted stronger antibody titers to the native trimers and to generate low level tier 2 homologous neutralizing antibody (58). As antigens coupled to the surface of liposomes are exposed to interstitial lymphatic fluid as they transit into the draining lymph nodes, the Bale et al.'s study suggested that it might be possible for surface displayed antigen that are non-covalently bound to be susceptible to dissociation from the liposome prior to B cell contact (59). Therefore, the authors created a second-generation liposomal formulation where HIV-1 Env trimers were coupled to synthetic single layer liposomes by alternative means. Here, the authors found that maleimide-thiol covalent coupling of trimers to liposomes elicited higher anti-HIV Env IgG antibody responses than soluble trimers or trimers coupled to liposomes *via* non-covalent metal chelation. Furthermore, the liposomes-coupled antigens were better activators of B cells as determined through Ca^{2+} flux measurements. Finally, murine immunogenicity studies demonstrate that the covalent coupling of antigens enabled the expansion of B cell germinal center reactions, over and above what was seen with soluble antigens, and that they also blocked the access of B cells and antibody to the c-terminal end of the exposed Env spike, suggesting that the trimers were intact at the point of immune recognition and adaptive immune activation (59). Taken together, this suggest that the particulate display of high-density antigen arrays on the surface of liposomes elicits improved B cell responses over previous soluble versions of the same trimers.

A promising vaccine candidate has been the membrane proximal region (MPER) of Env. This gp41 region is the target for several neutralizing antibodies and is attractive as a vaccine candidate due to its conserved and linear nature. A significant drawback to MPER immunogens is its inherent lack of immunogenicity. Recently Hanson et al. utilized 150 nm liposomes as membrane display vehicles to promote a more native vaccine antigen conformation (60). In this example, the authors evaluated the strength and durability of humoral immune responses elicited by MPER peptides anchored to the surface of liposomes *via* palmitoyl tails. The liposomal anchored peptides were compared to alum and complete Freund's oil-based emulsion adjuvant.

Liposomal anchored peptides successfully elicited MPER-specific IgG antibody while alum and Freund's adjuvants did not. Critically, anti-MPER antibody responses could be augmented through the inclusion of adjuvants, such as TLR4 agonist (MPLA), TLR9, or STING Interestingly, intrastructural help through helper epitopes promoted IgG responses to MPER without increasing B cell responses against the help sequence (60).

Polymeric Nanoparticles

Polymeric nanoparticles are very promising candidate delivery systems and adjuvants for a range of vaccine antigens. Their favorability stems from their ease of synthesis, biocompatibility, their biodegradable nature, the fact they are non-immunogenic, non-toxic and fairly inexpensive. Numerous different polymeric nanoparticle exist but the most frequently encountered types include chitosan, poly(lactic-co-glycolic acid) (PLGA) and poly(lactic acid) (PLA) (**Table 2**).

Chitosan (Poly(D-Glucosamine))

This cationic polysaccharide, polymeric nanoparticle is derived from the deacetylation of chitin, a naturally occurring polymer found in the cuticles of insect species and crustaceans, such as crabs and shrimp. Due to its strong immune-stimulatory properties and low immunogenicity, chitosan has frequently been utilized as an antigen delivery system. A significant advantage of chitosan to conventional adjuvants such as alum is its ability to promote T_H1 immune responses and to also act as both delivery system and adjuvant when applied to mucosal surfaces.

In 2016, Cosgrove et al., published the first comparative Phase 1 clinical trial investigating the safety and immunogenicity of three HIV-1 clade C gp140 vaccinations delivered by either the IM, intranasal (IN), and intravaginal routes in women (62). The vaccine antigens were co-formulated with either glucopyranosyl lipid adjuvant (GLA), chitosan nanoparticles or an aqueous

TABLE 2 | (A) Liposome and polymeric particle vaccines; (B) liposome and polymeric particle vaccines against human immunodeficiency virus (HIV)/simian immunodeficiency virus (SIV).

Particle type	Antigen arrangement	Resulting immune response	Adjuvant used	Animal model	Publication
(A) Liposome and polymeric particle vaccines					
Liposome	ICMV with His-tagged gp140 trimers anchored onto Ni-NTA functionalized liposome particles	Humoral immune response induced. Breadth of anti-HIV responses increased in response to ICVM surface anchoring	MPLA	Mouse	(56)
Liposome	Single bilayer liposomes displaying high-density His-tagged JRFL-SOSIP and JRFL-NFL Env trimers. Conjugation to liposomal surfaces through DGS-NTA(Ni) non-covalent linkage	B cell germinal center formation and induction of low-level tier two homologous antibodies	ISCO-MATRIX	Mouse	(58)
Liposome	CLDCs are particles loaded with antigen and DNA containing CpG ODN motifs. The cationic component of CLDCs ensure entry into endosomal compartments, whereas the CpG ODNs trigger endosomal TLR9	Animals immunized with CLDC adjuvanted SIV-derived antigens developed more robust SIV-specific T and B cell responses compared to animals that were not immunized with CLDC. In addition, CLDC-treated animals developed better memory response as evident following immunization with whole AT-2 inactivated SIVmac239	CLDC	Rhesus macaque	(61)
Liposome	Single bilayer liposomes displaying high-density His-tagged Env trimers conjugated to liposomal surfaces through maleimide-thiol covalent linkage	Anti-HIV Env IgG responses elicted. Increased activation of B cells and germinal center formation	ISCO-MATRIX	Mouse	(59)
Liposome	MPER peptides anchored to liposomes surface through palmitoyl tails to form 150 nm particles	Induction of anti-MPER antibody responses that is maximized by adjuvanting with MPLA, or TLR9, or STING agonists	Alum, Freund's adjuvant, MPLA, TLR9, and STING agonists	Mouse	(60)
(B) Liposome and polymeric particle vaccines against HIV/SIV					
Chitosan	HIV-1 clade C gp140 co-formulated with chitosan and delivered intranasally	Induction of CD4 T cell responses. Serum antibody responses were generated following IM boost	Chitosan	Human	(62)
Chitosan	Trimeric CN54gp140 co-formulated with chitosan	Increase in systemic IgA and IgG anti-gp140 antibodies following intranasal and sublingual delivery	Chitosan	Mouse	(63)
PLGA	HIV-1 p24-Nef peptide chemically conjugated to TLR5 agonist, FLiC and co-formulated with PLGA nanoparticles	Increased IgG1 and IgG2a titers, cytotoxic T lymphocyte (CTL) killing activity, and lymphocyte proliferative response following ID immunization	FLiC	Mouse	(64)
PLGA	PLGA encapsulated TLR9 agonist, CpG, and MPLA with HIV CTL epitopes	Strong immune response against multiple splenocyte CTL epitopes as measured by IFN-g release	MPLA and CpG	C57BL/6 mouse	(65)

ICMV, interbilayer-cross-linked multilamellar vesicles; Ni-NTA, nickel-nitrotriacetic acid; MPLA, 3-O-deacyl-4′-monophosphoryl lipid A; SAS, Sigma Adjuvant System; PLGA, poly(D,L-lactic-co-glycolic acid); CLDC, cationic liposome-DNA complex.

gel, respectively. Within this study, chitosan was ineffectual at promoting humoral immune responses despite the evidence from previous clinical studies, suggesting that chitosan increased potent antibody responses to vaccine immunogens. Interestingly, the authors noted that gp140 co-formulated with chitosan and intranasally delivered resulted in induction of CD4 T cell responses and upon IM boosting, all individuals generated a detectable serum antibody response. This suggests, that the chitosan-gp140 mucosal vaccination primed for an anamnestic serological response. However, it is unclear as to why the priming was restricted to CD4 T cells or if it had indeed primed B cells, but the responses were too low to measure (62). How nanoparticulate chitosan acts as adjuvant is currently unknown; however, recent evidence suggests that it promotes DC maturation through type 1 interferons and increases antigen-specific T cell responses in a type 1 IFN receptor-dependent manner (66). The latter requiring cytoplasmic sensors cGAS and STING, as well as both mitochondrial reactive oxygen intermediates and cytoplasmic DNA (66).

Chitosan has also served as a formulation adjuvant by promoting penetration enhancement of formulations, enabling their uptake and increasing the bioavailability of vaccine antigens when applied topically to mucosal surfaces. This was clearly demonstrated by Klein et al., who compared various polymeric penetration enhancers to promote trans-mucosal delivery of trimeric CN54gp140 protein (63). In this study, chitosan increased the systemic antibody levels of both IgG and IgA anti-gp140 antibodies following IN and sublingual delivery and increased antigen-specific antibody responses in the vagina of intranasally vaccinated mice. It is clear in this study that various polymeric formulations had differing abilities to augment immune responses and that the route of delivery was also a significant factor (63).

PLGA (Poly(D,L-Lactic-co-Glycolic Acid)) Nanoparticles

The use of PLGA as a nanoparticle vaccine delivery system has been studied comprehensively over the last two decades, resulting in numerous publications. However, it is the ability of PLGA nanoparticles to entrap bacterial toxoids/antigen or surface display antigens and induce long-lasting immune responses in small animal models which makes them an attractive delivery system (67–71). Early attempts at using PLGA formulations for delivery of recombinant HIV gp120 were centered on the ability of PLGA to release antigens over an extended period, promoting continuous antigenic exposure and immune education (72). These PLGA vaccines were designed to be single shot vaccines, which provide a pulsatile release of contained antigen and QS-21 adjuvant at intervals of 6 months. The resulting antibody response caused neutralization against the matched strain of HIV-1 and providing evidence for PLGA to be a slow release system (72). Since these early attempts, sophisticated attempts at using PLGA formulations as an HIV vaccine have been made (**Table 2**). For instance, the HIV-1 p24-Nef peptide was chemically conjugated to TLR5 agonist FLiC and co-formulated with PLGA nanoparticles (64). Upon intradermal vaccination in mice, the combination of TLR agonist and nanoparticle was shown to increase vaccine immunogenicity by increasing lymphocyte proliferative responses reducing the immunogenic dose required (64). In another example, Rubsamen et al. utilized PLGA encapsulated TLR9 agonist, CpG, and TLR4 agonist Monophosphoryl lipid A (MPLA) in the injection solution to augment immune responses to the delivered HIV CTL epitopes (65). The formulations resulted in immune responses against multiple splenocyte CTL epitopes as measured by IFN-g release (65).

NANO-VACCINE TRAFFICKING AND INTERACTIONS WITH HOST IMMUNE CELLS

The immune response to nanoparticle formulations such as liposomes, poly(D,L-lactide-co-glycolide) (PLGA), and VLPs are known to elicit both arms of the immune response. Understanding the cellular events involved in such vaccines are critical for their development as vaccine strategies and advancing test formulations to human clinical trials. Specifically, the molecular and cellular interactions occurring between nanoparticles and the vaccinated host immune system (i.e., effects on DCs, T and B lymphocytes, and lymphoid tissues) will be essential. Although many alternative vaccination routes have been explored in animal models and in humans, most vaccine studies employ IM vaccination. Intradermal (ID) vaccination demonstrates strong immune reactions to vaccinating antigens in a dose sparing manner compared to IM vaccination; however, ID vaccination is associated with a higher frequency of undesired side effects. Thus, we will concentrate on nanoparticle vaccines administered *via* the IM route.

The skeletal muscle system is one of the largest cellular compartments within the human body. Muscles are composed of large multinucleated syncytial muscle fibers which generate the necessary mechanical forces for locomotion. Following an injury to the muscle fibers, the surrounding satellite cells become activated and proliferate. The resulting myeloblasts fuse to become multinucleated myotubes, which will then go on to differentiate into mature muscle fibers. Under non-inflamed conditions, only a very few resident immune cells have been described to be present in the muscle (73). These include APCs such as macrophages and DCs; however, during pathological conditions, other immune cells such as monocytes, neutrophils, and lymphocytes can infiltrate the tissue (74). The introduction of vaccine antigens such as nanoparticles with adjuvants into the muscle environment induce transient inflammatory reactions at the delivery site, resulting in immune cell infiltration (74). Muscle cells can respond to the inflammatory mediators that are secreted by neighboring myocytes as well as resident and infiltrating immune cells. Myocytes express a range of receptors for cytokines, such as IL-1, IL-6, and IFN-g. Furthermore, they express chemokine receptors, such as CCR2, CCR4, and CCR10, which enable them to participate in surveying the local environment (75). The introduction of nanoparticles into the musculature enables their uptake by APCs such as DC and macrophages that are in the epimysium and perimysium interstitial spaces surrounding the entire muscle and muscle fascicles (76). The APCs produce pro-inflammatory mediators and chemokines that activate the myocytes and attract circulating immune cells and migrating APCs into the tissue. In support of this

pro-inflammatory role of myocytes within the vaccinated muscle was the research published by Mosca et al. They used microarray and immunofluorescence analysis of the murine muscle after oil-in-water emulsion MF59 adjuvant, CpG, or alum injection (77). While CpG and alum induced time-dependent changes in 387 and 312 genes, respectively, MF59 induced changes in 891 genes, with recruitment of MHC II and CD11b cells within the injection site. Interestingly, the early response proteins penetraxin 3 and JunB were induced upon MF59 delivery, indicating that MF59 directly activated muscle fibers (77). Furthermore, IM injection was shown to be associated with release of ATP from local muscle fibers, which was important in the recruitment of immune cells to site of vaccination and the magnitude of the resulting immune response (78).

Neutrophils and monocytes have been found to be the first cells to infiltrate vaccinated muscle. This infiltration is normally detected within 3–6 h post-delivery. DCs are essential to adaptive immune response, and it is, therefore, not surprising that their recruitment is also rapid. These APCs take up exogenous nanoparticles, become activated, and in the case of DCs, migrate toward the draining lymph nodes. During this transit, the DCs upregulate co-stimulatory molecules, such as MHC II, CD80/86, and CD40. They also secrete cytokines and lose the ability to phagocytose antigens in preference for increased presenting capabilities. Once in the draining lymph nodes, the DCs initiate the adaptive immune response through activation of T and B cells. Remarkably, it is now becoming apparent that upon vaccination, intact nanoparticles such as VLPs can enter the draining lymph node without the requirement for DC-mediated transport (79). Using a mouse model, Cubas et al., demonstrated that IM vaccination with SHIV VLPs efficiently trafficked to the draining lymph nodes, although some speculation arose regarding VLP nanoparticle uptake by blood capillaries in the muscle and trafficking to the spleen (79). Nevertheless, once the VLPs were in the lymph node, the intact SHIV VLPs were detected in the subcapsular sinus (79). Once antigens enter the lymph node, they have been shown to reside there for extended periods of time. In the case of HIV-1, follicular DCs have been shown to retain non-degraded, viral particles in the form of immune complexes on their dendrites for months (80), thereby promoting germinal center reactions; however, it is unclear how long the SHIV VLPs were detectable in this instance.

Many factors, including, size, shape, charge, and receptor–ligand binding potential of nanoparticles dictate their distribution and cellular uptake upon vaccination, and therefore impact prevailing immune responses. VLPs are typically 20–150 nm in diameter, and excluding charge and receptor tropism, the size of the nanoparticle plays an important role in uptake and immunity. Generally, speaking nanoparticles and VLPs between 25 and 40 nm can effectively penetrate tissues upon delivery (81) and must exceed 10 nm to escape renal filtration. Nanoparticle vaccines exceeding 500 nm are likely taken up by APC at the injection site while nanoparticles and VLPs below 200 nm are mainly internalized by DCs, and in the free, intact, form will more likely accumulate in the liver and secondary lymphoid structures (82).

Over the years, numerous nano-vaccine delivery technologies have been investigated for optimal immune priming by examining the size of the nano-formulation (83–85). Using a combination of electron microscopy and dynamic light scattering, Mann et al., revealed that orally delivered, low diameter lipid-based vesicles (10–100 nm), containing influenza vaccine antigen, elicited a T_H2 biased immune response in mice. This contrasted with similar vesicle compositions with an average diameter of 980 nm, which had a significantly greater T_H1 bias (86). This work was supported by other previous research using lipid-based nanoparticle formulations delivered parenterally, where small lipid-based nano-vaccines (<155 nm) promoted T_H2 responses while larger vesicles (>225 nm) elicited T_H1 biased responses (87). It has been suggested that the T_H1/T_H2 polarizing effects related to nano-vaccine size might be due to efficiency of antigen presentation by the phagocytosed nano-vaccines by the APCs. An interesting manuscript by Brewer et al. provided evidence for altered trafficking of internalized antigens dependent on delivery systems size. Using murine macrophages, the authors described the trafficking of antigen loaded, large particles (560 nm), into early endosome-like phagosomes, whereas the smaller particles (155 nm) and soluble antigen were rapidly localized to endo-lysosomes (88). In this case, MHC II was detected in both compartments regardless of the T_H1/T_H2 bias. The internalization of large vesicles was also found to be mediated by actin-dependent phagocytosis, while the smaller vesicles were taken up in an actin-independent manner (88). These findings taken together suggest that nanoparticle size could significantly influence not only vaccine antigen uptake by APCs, but also influence their intracellular trafficking potential, dissemination around the body, and the ultimate immune outcome.

STRATEGIES TO INCREASE IMMUNOGENICITY OF NANO-VACCINES

One of the basic tenants of immunology states that antigens can induce immune responses, if it is perceived as being "foreign" by the host. However, non-self-antigens do not always trigger immune responses. Even if they do, they can be poorly immunogenic. For the immune system to become sufficiently mobilized, it must identify some sort of "danger." This can occur in a number of ways including, (1) the recognition of exogenous signals by innate immune cells through pathogen-associated molecular patterns (PAMPS) and (2) being activated in response to recognition of danger-associated molecular patterns, which are endogenous molecules released by damaged or perturbed tissues/cells (89). Such immune stimulatory signals are often applied to vaccines in the form of adjuvants (90–92). Adjuvants are defined as agents which act to enhance the quantity and quality of immune responses to co-formulated immunogens. Mechanistically, adjuvants work by either simply arranging, aggregating, transporting, shielding antigens, or by stimulating pro-inflammatory signaling pathways conducive to enhancing immunogenicity. In other words, adjuvants increase the strength and effectiveness of vaccines. As an example, live attenuated vaccines do not necessarily require any additional help in generating immune responses as they exhibit low level infections. In contrast, highly purified subunit and inactivated vaccines are often poorly immunogenic and may not

sufficiently activate innate immunity and generate the necessary pro-inflammatory environment that is conducive to the production of protective responses. Nanoparticle formulations such as VLPs may also display poor immunogenicity, compared to live attenuated vaccines and are therefore often delivered with an adjuvant to maximize an efficient immune response. Over the years, numerous adjuvant technologies have been applied to nanoparticle formulations. In an attempt to attain more and more protective responses and to also overcome potential side effects associated with highly immune-stimulatory adjuvants, mixed adjuvant regimens have gained in popularity. Recently, a number of excellent reviews have been published concerning adjuvants for HIV-1 vaccines (93, 94), so we will discuss only a few of the more common adjuvants below, some of which are detailed in **Table 3**.

Alum

Alum is one of the first adjuvants to be developed for augmenting vaccine elicited immune responses having first been demonstrated to act as an adjuvant by Glenny et al., in 1926. Since then, aluminum adjuvants have become the most widely utilized adjuvant and have been used in diphtheria, tetanus, pertussis and poliomyelitis vaccines in many countries for more than 70 years. Alum salts, form polydisperse crystalline particles (~2–10 μm in diameter) capable of adsorbing subunit vaccines onto their surface, thereby increasing BCR crosslinking, presentation to APCs, and can act to form an antigen depot at the vaccination site (95). Critically, alum adjuvants have been described to be potent inducers of IL-1 secretion *in vitro* within APC population, such as DCs and macrophages via NLRP3 inflammasome activation (96). While Alum has been used as an adjuvant in licensed HPV, HBV, and HEV VLP vaccines, how it functions as an adjuvant in the context of VLP vaccines is not clearly understood. Certainly, VLPs are readily phagocytosed by APCs due to their particulate nature. Furthermore, they are decorated with vaccine antigens on their surface, which enables BCR crosslinking. Thus, the adjuvant effects of alum, in the context of these VLP vaccines, may be due to antigenic depot effects and activation of the inflammasome.

The use of alum to augment antiviral immunity has been evaluated in the context of therapeutic HIV vaccines. Although therapeutic vaccinations are now aimed at a sterilizing or functional cure, initial attempts in the 1990s and early 2000s were made to therapeutically "modulate" immune responses to curb CD4 T cell decline and lower the rate of AIDS progression (48, 104). As decreasing anti-p24 responses had been correlated with clinical progression to AIDS, a p24-based vaccination was developed as a potential method to elevate p24 immune responses in HIV-infected individuals. In a randomized placebo-controlled trial that enrolled 304 HIV-infected individuals (CD4 counts <350 cells/μl), individuals were administered monthly IM injections of either (1) alum, (2) p24 VLP (500 μg) + alum, or (3) p24 VLP (1,000 μg) + alum (105). The volunteers maintained ART during the study which consisted of Zidovudine (ZDU) with or without didanosine or zalcitabine. CD4 T cells counts were monitored for the 6 months of treatment and then for an additional 6 months of follow-up. The study failed to demonstrate any benefit of immunization with p24 VLP despite adjuvanting with alum. Interestingly, no statistically significant antibody responses were detected against p24 or p17 but instead were detected against the carrier protein, Ty. Furthermore, a decline in CD4 T cells was recorded over time with no statistically significant difference between treatment regimens (105). In a similar follow-up

TABLE 3 | Adjuvants used in HIV vaccine strategies.

Name	Structure	Proposed mechanism of action
Alum	Polydisperse crystalline particles that are 2–10 μm in diameter	Antigen depot effect at vaccination site (95) in addition to potent IL-1 secretion and NLRP3 inflammasome activation (96)
MPLA	LPS-derived MPL molecules lacking: O-antigen, a fatty acid chain, and a phosphate group	Promotes T_H1 immune responses without the safety concerns that are associated with LPS
GLA	Synthetic lipid A-like molecule administered in AF or SE formulations	TLR4 agonist that promotes T-bet-dependent T_H1 immune response in addition to enhancing protection against a range of intracellular pathogens (97). GLA adjuvant effects are MyD88- and TRIF dependent
Flagellin	Major protein constituent of Gram-negative flagella. Usually incorporated into VLP vaccines	TLR5 agonist that is dependent on MyD88. It activates NF-κB in epithelial cells and APC populations (98)
AS04	Combination adjuvant that consists of alum and MPLA	Combining alum and MPLA causes a synergistic effect and results in the induction of higher quality antibody and neutralizing antibody titers (99)
MF59	Squalene-based	Induces production of antigen-specific CD4 T cell responses in addition to robust memory T and B cell responses
ISCOMATRIX	A matrix of saponin, cholesterol, phospholipid, and hydrophobic antigens which form molecular cages that are 40–50 nm in diameter (100)	Potent inducer of T_H1 and T_H2 responses which results in high frequency antigen-specific CD8 T cell responses (100)
Hiltonol	Poly-IC derivative: synthetic dsRNA that is stabilized using poly-lysine	TLR3 agonist that promotes the production of DC1 (101)
Resiquimod	Low molecular weight tricyclic molecule	TLR7/8 agonist that is dependent on MyD88
CpG DNA	Single-stranded DNA molecule containing multiple CpG motifs	TLR9 agonist that promotes the induction of a T_H1 response

This list is not exhaustive; it covers the more commonly used adjuvants. AS01 [used in HIV vaccines (102)], AS02, AS03, and CAF01 [used in HIV vaccines (16, 103)] among others are not on the list.

LPS, lipopolysaccharide; GLA, glucopyranosyl lipid adjuvant; AF, aqueous nanosuspension; SE, squalene-based oil-in-water nanoemulsion; Poly-IC, polyinosinic–polycytidylic acid; DC1, type 1-polarized dendritic cells.

study, 61 individuals were recruited and split into three treatment arms and received either (1) ZDU + IM alum, (2) ZDU + IM p24 VLP (500 μg) + alum, or (3) placebo capsules + IM p24 VLP (500 μg) + alum (106). This was conducted to evaluate the therapeutic effect of p24 VLP vaccination with ZDU on p24 antibody production and CD4 T cell counts, as well as any impact on viral loads. Despite the treatment being well tolerated, no significant differences between the treatment arms were recorded in any of the antibody and cellular immune responses measured (106).

Alum has also been used as an adjuvant for VLPs used for prophylactic vaccine strategies for prevention of HIV acquisition. Insect cell expression systems have been used to generate chimeric VLPs that express the V3 domain and a linear section of the discontinuous CD4-binding domain of gp120 within gag (107). Subsequent vaccination of rabbits with the various chimeric VLP constructs without adjuvant generated antibody responses to the Pr55 gag carrier component. Interestingly, most of the antibody response was specific to the gag insertion site. Despite generating weak neutralizing antibody responses, vaccination of mice with the different non-adjuvanted chimeric VLPs could generate strong MHC class I CTL responses. However, when the recombinant antigen was adsorbed with alum, its potential for CTL induction was drastically reduced or inhibited (107). Further studies in NHPs using two differing HIV-1 virus-like Pr55 gag VLP vaccine constructs without adjuvant revealed that IM vaccination with both types of VLP induced elevated titers of anti-gag antibody responses, but it was Pr55 gag/env VLPs expressing the full gp120 at the outer surface of the particle, which generated substantial anti-Env antibody titers with a neutralizing phenotype (108). Furthermore, both Gag and Env cytotoxic T lymphocyte (CTL) responses were induced (108).

Collectively, the literature presented suggests that despite Alum's positive influence in some preclinical experiments and in some clinically approved VLP formulations, its inappropriate use can diminish the effects of test vaccines, resulting in ineffectual immune responses. Thus, inclusion of alum as a VLP adjuvant in any preclinical or clinical trial must be scrutinized.

Pattern Recognition Receptor (PRR) Agonists

The most highly characterized PAMP sensors are the innate immune system PRRs for which several families have been classified. The C-type lectin toll-like receptors (TLR) are the best-defined families of PRRs. They are expressed by a plethora of mammalian cells as either endosomal or plasma membrane bound receptors. Cell surface TLRs (4, 1/2, 2/6, 5) detect conserved microbial patterns present on the cell surface such as LPS and flagellin, while endosomal TLRs (3, 7, 8, 9) detect microbial genomic material such as double-stranded RNA and DNA and single-stranded RNA (109). Detection of bacteria or viral particles by the various TLRs expressed by APCs, such as DCs, macrophages, and B cells, is normally followed by endocytosis/phagocytosis and subsequent processing and presentation to T cells *via* MHC. The MHC presentation to T cells occurs in the context of several signals, including, co-stimulatory molecules, cytokines, and by TLR ligation. Collectively, this stimulates T cells to surpass the minimal activation thresholds for naïve T cells to partake in immune responses. Due to their abilities to activate innate signaling pathways, PRR ligands are an expanding field of study for HIV vaccine design. This includes the use of TLR4 (MPL) and 7/8 (R848) agonists encapsulated in PLGA particles admixed with VLPs expressing SIV gp160 and Gag (110), the incorporation of TLR7/8 (Resiquimod) and 9 (CpG) into oil-in-water emulsions for responses against HIV-1 Env gp140 (111) and the use of TLR3 (Poly IC:LC, Hiltonol), TLR4 (MPL derivative, E6020) and TLR 7 (a proprietary benzonaphthyridine from Novartis) agonists to characterize vaccine-mediated evolution of Env-specific B cell ontogenies (112). Normally, the microbial antigen and TLR ligand are physically associated (i.e., contained within the same pathogenic organism), and therefore are co-delivered to the same phagosomal/endosomal compartment within the APC. During vaccinations, PAMPs are generally admixed with antigens and, therefore, may not be associated as having a common derivation, unless the PAMP and antigen enter the same endosome. The latter requiring large excesses of PAMPs over what is required for APC and T cell activation (113). Therefore, formulating TLR ligands onto the surface or within nano-vaccines serves as a promising way to optimally stimulate APCs. The TLR7 agonist Imiquimod has been approved for topical delivery in humans for genital warts as a 5% cream (Aldara™) (114). However, its systemic application has been limited because of toxicity. Due to its hydrophobic nature, entrapment within polymeric nanoparticles offers an alternative strategy for imiquimod delivery, greatly reducing its toxicity. A study by Jimenez-Sanchez et al., reported on polylactide (PLA)-based micelles with entrapped TLR7 and HIV-1 gag p24 decorating the surface of the nanosystem. As would be expected, encapsulated imiquimod induced stronger DC stimulation than free imiquimod with encapsulated ligand triggering NF-κB and MAPK pathways (114). In another study, Francica et al. immunized NHPs with HIV gp140 Env with several adjuvants. When the authors co-formulated gp140 with TLR4/7 agonists and alum, they revealed that anti-Env antibody titers were boosted 3- to 10-fold higher than antibody titers induced with alum and gp140 alone. Interestingly, while TLR4 and alum enhanced a set of inflammatory genes, TLR7 suppressed alum-specific inflammatory genes in preference for interferon-responsive genes (115). This suggests that different TLR ligands can have different transcriptional effects against co-formulated adjuvants.

MPL and GLA

The detoxified TLR-4 ligand, 3-*O*-deacyl-4′-monophosphoryl lipid A (MPLA), is a lipopolysaccharide (LPS)-derived, heterogeneous blend of varying length MPL molecules from *Salmonella minnesota R595*. The MPLA extraction and treatment procedure resulted in three distinct modifications compared to the parent molecule: (1) the removal of the core polysaccharide containing the O-antigen, (2) the removal of one phosphate group, and (3) one fatty acid chain (116, 117). MPLA has been shown to promote T_H1 immune responses and to have a favorable safety profile when compared to LPS (118–120). Since the identification of MPLA as an adjuvant, newer generations of TLR-4 agonists have been

developed, such as a synthetic lipid A-like molecule called GLA. GLA adjuvant is either administered in aqueous nanosuspension (AF) or more often, co-formulated with a squalene-based oil-in-water nanoemulsion (SE). GLA-SE is now a clinical stage vaccine adjuvant that also promotes T-bet-dependent T_H1 immune responses and enhances protection against a range of intracellular pathogens (97). In fact, it is unsurprising since most TLRs use MyD88 except TLR3, that GLA-SE has been shown to signal through TRIF and MyD88 and that both are necessary for GLA-SE adjuvant activity (121). $CD4^+$ T cells are the central orchestrators of adaptive immune responses and provide the critical instructions for directing antibody production by B cells and CD8 T cell memory development (122, 123). Therefore, it is notable that, in terms of T cell responses, GLA-SE has been shown to promote polyfunctional CD4 T cell reactions characterized by CD154, IFN-g, TNF-a, GM-CSF, and IL-2 expression and the potential for GLA-SE induced IFN-a to trap immune cells in draining lymph nodes *via* CD69 expression (97). Immunization with *Mycobacterium tuberculosis* antigen and GLA-SE has resulted in elevated antigen specific B cell responses, elevated antibody concentrations, and increased follicular T helper and T_H1 biased CD4 T cell numbers compared with adjuvants alum, GLA without SE, or SE alone (124). Furthermore, there is evidence to suggest that GLA-SE augments early innate IFN-g production by CD8 T and NK cells (97).

More recently, it has become clear that TLR4 agonists and TLR7 agonists may be highly synergistic in amplifying immune responses. This can be seen by increased cytokine secretion, heightened germinal center formation, and both antibody class switching and diversity (125, 126). Hence, the development of a nanoliposome formulation that co-localizes TLR4 and TLR7 agonists to the same APCs, which synergistically enhances immune responses have been developed. These TLR4/7 lipid nanoparticle adjuvants have been co-formulated with VLP containing SIVmac239 Env and Gag with the aim of comparing the immunogenicity of soluble gp140 Env and a protein immunogen to Env expressed on the surface of VLPs (127). Interestingly the nanoparticle adjuvant used in combination with soluble gp140 vaccine antigen performed better than the nanoparticle adjuvant co-formulated with VLPs. Specifically, the anti-Env antibody responses and Env-specific plasmablast numbers were greater in magnitude in serum for the soluble gp140 compared to VLP vaccine groups (127). To test the efficacy of TLR4/7-adjuvanted VLPs compared to soluble gp140, vaccinated macaques were challenged weekly with an SIVsmE660 swarm, and although there was a delay in infection with the adjuvanted VLP treatment group compared to the adjuvanted soluble gp140 treatment group, it was not statistically significant. The inclusion of the adjuvant did, however, enhance protection for both soluble gp140 and VLPs compared to the non-adjuvanted controls (127).

Adjuvant System 04 (AS04)

Adjuvant System 04 is a new combination adjuvant developed by GlasxoSmithKline Biologicals and consists of Aluminum salts and MPLA. The AS04 adjuvant is utilized in two licensed vaccines, Cervarix® and Fendrix®. Cervarix® contains VLPs of the L1 capsid protein from oncogenic HPV strains 16 and 18 expressed through an insect cell expression system. Fendrix® works against hepatitis B virus (128–130). It should be pointed out that a second HPV vaccine based on recombinant expression of major capsid antigen L1 in yeast is marketed by Merck &Co. under the brand name Gardasil®(131). In terms of Cervarix®, AS04 was selected as the adjuvant of choice because of its safety performance in mice and NHP studies and because it demonstrated induction of higher quality antibody and neutralizing anti-HPV titers response compared to alum alone (99). In the HPV16/18 clinical study, the VLP formulation adjuvanted with AS04 was proven effective against cervical intraepithelial neoplasia lesions and protective against strains phylogenetically related to HPV16/18 such as HPV31, HPV33, and HPV45 (132, 133). Comparing the AS04-adjuvanted HPV16/18 vaccine to alum adjuvanted HPV6/11/16/18 in women aged 18–45 revealed the former to elicit higher levels of neutralizing antibodies and higher frequencies of memory B cells and CD4 T cells (134).

MF59

The adjuvant MF59 was first approved in Italy in 1997 after Novartis conducted clinical trials in 1992 (135). MF59 is a squalene-based oil-in-water emulsion stabilized by Tween 80 and Span 85 surfactants (136). Due to its extensive safety profile and efficacy in preclinical and human clinical trials, it is now FDA approved and a component in licensed influenza vaccines such as FLUAD®, Aflunov®, Focetria®, and Celtura® (137). In addition, it is also being evaluated as an adjuvant in candidate HIV vaccine formulations. Although a complete understanding behind the mechanism of action of MF59's is still being defined, the widely held theory is that MF59 activates injection site tissue-resident APCs such as macrophages along with the transient release of ATP from the injected muscle (78). Upon activation, these tissue-resident cells secrete various chemokines and cytokines, which causes a localized inflammatory reaction, resulting in recruitment of more immune cells into the injection site. Vaccine antigen–APC interaction is, therefore, increased, augmenting transport of antigen into local draining lymph nodes and T cell priming. In terms of humoral immune responses, MF59 has been shown to increase antibody affinity maturation to vaccine antigens as well as the diversity of epitopes recognized (138). How this occurs may be due to findings that MF59 enhances antigen-specific IgG antibody responses to vaccine antigens by promoting T follicular helper cell (T_{FH}) responses (139). While few studies have evaluated ways to augment the development of T_{FH} cell responses through vaccination, these highly specialized cells are critical for humoral immunity through provision of help by means of both contact-dependent and independent mechanisms with T_{FH} cell responses directly controlling the magnitude of germinal center B cell responses (140). Therefore, MF59 represents a very promising adjuvant for future vaccine development. Recently, Vargas-Inchaustegui, et al. demonstrated that an SIV vaccine-prime consisting of an Adenovirus 5 host range (Ad5hr) mutant, encoding SIV Gag, Nef, Rev, and Env followed by IM boosts with SIV monomeric gp120 or oligomeric gp140 protein adjuvanted with MF59 can induce long-lived germinal center, Env-specific IL-21^+T_{FH} cells

in rhesus macaque lymph nodes (140). However, while MF59 has been reported to promote germinal center formation and T_{FH} cell induction in previous studies (139, 141), within this study the corresponding effects of the boost to one of the components of the vaccine (SIVmac239 Env) were not as pronounced as that seen in Ad5hr vaccine-prime (140). Whether this lack of increased T_{FH} cell induction by MF59 adjuvanted boost is due to nature of the vaccine antigen being used or its exposure time in the body compared to the viral vector remains to be determined (140).

Previously, Guillon et al. quantitatively and qualitatively tested the antibody response in rabbits induced by PLA nanoparticles and MF59 adjuvant. Using three different antigens, HIV-1 p24, WT HIV-1 Tat, and a detoxified Tat, both adjuvant platforms induced similar levels and kinetics of serum IgG (142). Strikingly, the authors noted differences in the antigenic domains that elicited the antibody response. Serum from p24 vaccinated rabbits showed MF59 induced antibodies that recognized peptides all along the p24 protein sequence while the PLA nanoparticles directed the antibody response toward an immunodominant domain of p24 (190–224). Potentially indicating that adsorption of antigens onto the surface of particles might unmask, or alter the conformation of antigens, revealing alternative immunodominant epitopes not revealed by soluble antigens (142).

ISCOMATRIX

This adjuvant was designed as an improvement over its predecessor, the ISCOM (immunostimulating complex) adjuvant. The original formula was a mix of saponin, cholesterol, phospholipid, and other hydrophobic compounds (143). The major drawback to the original formulation was that the vaccine antigen had to be integrated into the hydrophobic structure of the adjuvant, greatly limiting the types of antigen that could be administered with ISCOM (100). To address these issues, Pearse & Drane developed ISCOMATRIX, which did not require the incorporation of antigen. This newer formulation was similar; however, was produced using purified fractions of *Quillaja Saponaria*, cholesterol, and phospholipids. When formulated together, the lipid and QS21 components assemble into 40–50 nm cage-like structures that entrap the vaccine antigen. Unlike other adjuvant systems, the ISCOMATRIX–antigen preparation infiltrates the draining lymph node and interacts with lymph node-resident DCs and other APCs within the first 2 h of immunization. Interestingly, there are two waves of antigen presentation when ISCOMATRIX is used. The first round of antigen presentation occurs when ISCOMATRIX–antigen complexes infiltrate the draining lymph node, whereas the second round of antigen presentation occurs 24–48 h post-inoculation. This is due to tissue-resident DCs that take up ISCOMATRIX–antigen complexes and traffic to draining lymph nodes.

Morelli et al. describe ISCOMATRIX as an integrated adjuvant system because it combines the innate and adaptive arms of the immune system in a TLR-independent but MyD88-dependent manner. In particular, when DCs take up ISCOMATRIX into endosomes or phagolysosomes, these cellular compartments undergo acidification and releases the ISCOMATRIX–antigen complexes into the cytoplasm of the cell. This enables presentation through MHC class I pathway for cross-presentation to CD8 T cells. As expected, antigen is also presented on MHC class II for presentation to CD4 T cells and induction of B cell responses. In terms of T cell responses toward ISCOMATRIX–antigen complexes, it activates both T_H1 and T_H2 responses as noted by rapid IL-5 and IFN-g production following immunization (144).

As mentioned previously, Ingale et al. evaluated the *in vivo* delivery of soluble JRFL SOSIP trimers in ISCOMATRIX and JRFL SOSIP trimer-conjugated liposomes in ISCOMATRIX. Isolation of lymph node cells indicated increased percentages of GL7+ germinal center B cells from mice administered the liposome-conjugated vaccine (58). Within this study, the delivery and evaluation of well-ordered, high-density Env trimers was the main goal of the research, as such there was no evaluation of the SOSIP Env trimers in the absence of ISCOMATRIX, making it difficult to understand the precise effect of the adjuvant. In a separate study, evaluating germinal center formation and neutralizing antibody responses to HIV Env trimers, Havenar-Daughton et al., using a modified BG505 SOSIP (BG505 SOSIP. v5.2), compared two different adjuvants (PLGA/R848 + MPL vs ISCOMATRIX) for generation of autologous tier 2 neutralizing antibody production in NHPs. In this example, approximately 75% of the vaccinated NHPs generated a detectable neutralizing antibody response but neither adjuvant significantly outperformed the other in terms of elicited Env antibody titer, V3 peptide antibody binding titer or neutralizing antibody titer (145). Interestingly, three NHPs from the PLGA group and 1 NHP from the ISCOMATRIX group were identified as top tier 2 autologous neutralizing antibody producers (titers >1:200). Although it should be noted that both groups had different numbers of animals, with the PLGA treatment group having the most. While these results were promising, no viral challenge was performed (145). Collectively, this suggests that ISCOMATRIX is a promising vaccine adjuvant with the potential to significantly augment B cell immune responses.

Surface Functionalized Nano-Vaccines

The co-delivery of vaccine antigens with adjuvants has long been known to augment both B and T cell immune responses. As previously mentioned, current scientific dogma suggests for optimal adjuvant activity, the vaccine antigen and the adjuvant should be targeted to the same APC. Co-delivery of vaccine antigens and adjuvants can normally be achieved using covalent linkages between the two components, ensuring that the antigen and adjuvant will end up in the same endo-lysosomal compartments for maximal PRR engagement and proteolytic degradation. However, due to the increased costliness and in some cases, difficulty of conjugating certain complex antigens or heavily glycosylated antigens to the adjuvant makes this process unfavorable. Therefore, newer ways to formulate antigens and adjuvants are necessary. Interestingly, the use of nano-vaccines offers an alternative mechanism by which antigens and adjuvants can be co-delivered for optimal immune responses. Through cell surface expression, a range of recombinant vaccine adjuvants can be incorporated into budding VLP nano-vaccines, ensuring that surface expressed immunogens are presented alongside

the adjuvant. In a study by Franco et al., immuno-stimulatory murine CD40L was expressed on the surface of HIV VLPs, with the aim of targeting HIV-1 gag proteins to DCs and activating the CD40 receptor (146). Through fusion to the CD40L ectodomain with baculovirus gp64, the authors significantly enhanced CD40L expression by the VLPs and demonstrated that the CD40L/gp160 VLPs enhanced IL-12 production from DCs. Further *in vivo* testing of the CD40L/gp160 VLPs in mice demonstrated the vaccine construct to induce strong CD4 and CD8 cell-mediated immune responses compared to CD40L-VLP constructs expressing either full length murine CD40L or murine CD40L fused to gp41(146).

Numerous studies have shown that cytokines serve to be promising adjuvants for vaccines. For instance, an SIV239-based heterologous prime-boost vaccine, co-expressing GM-CSF, was shown to convey 71% protective efficacy against intrarectal $SIV_{SM}E660$ challenge when compared to 25% in the non-GM-CSF adjuvanted group (147). In this case, the GM-CSF adjuvant was shown to enhance the avidity of the anti-Env IgG antibody response, augment the neutralizing activity of the sera, and enhance ADCC activity (147). More recently, a gain of function fusokine (GM-CSF + IL-4, aka GIFT4) membrane bound construct was utilized as a VLP bearing, B cell adjuvant (148). Anchoring of the fusokine into the Env-enriched VLP membrane was achieved by fusing CD59 glycolipid, glycophosphatidyl-inositol (GPI) sequence to GIFT4. The chimeric VLP constructs were administered as an IM-prime, IN-boost in Guinea pigs resulting in high levels of systemic antibody responses. In addition to this, the elicited antibodies exhibited higher avidity, improved neutralization breadth, and were detected in both serum and mucosal secretions (148).

Flagellin, in the monomeric form, is a TLR5, MyD88-dependent signal agonist derived from Gram-negative bacteria flagella. Flagellin is the major protein of the flagellum filament, which extends from the outer membrane of many locomotive Gram-negative bacteria and is responsible for the organism's locomotive ability. Flagellin is highly pro-inflammatory, activating NF-kB in a variety of cells, such as epithelia and APC populations such as monocytes and DCs (98). As the TLR5 receptor is found to be expressed in APCs, it has been suggested that flagellin-containing VLPs may be phagocytosed after TLR5 binding and enhance antigen presentation due to innate signaling within the same cell. In an interesting study by Wang et al., a membrane-anchored form of flagellin was incorporated into a chimeric influenza VLP (149). The results clearly demonstrated that flagellin-containing VLPs could elicit significantly higher antibody responses than unadjuvanted VLPs and that the adjuvant activity was not restricted to humoral immunity. In the latter case, MHC class I and II peptide stimulated splenocyte cultures were shown to have increased cellular immune responses and the mice vaccinated with adjuvanted VLP to be more resistant to heterologous influenza challenge infection than non-adjuvanted controls (149). The membrane-anchored flagellin was also combined into HIV VLPs as a molecular adjuvant using the guinea pig model (150). Both systemic (IM) and mucosal (IN) routes of vaccination elicited serological and mucosal antibody responses, with IgG sera levels correlating with neutralization. Of note, the neutralizing antibody response was broadened against the five tested strains from clades B and C (150).

Surface functionalizing of nanoparticles can also increase the bioavailability of vaccine antigen cargos through enhanced vaccine penetration in tissues. For instance, through decorating the surface of nano-vaccines with mucosal M cell targeting moieties, the bioavailability of mucosally applied vaccine formulations can be increased and antigen-specific immune responses significantly augmented. For instance, through surface functionalizing of PEGylated PLGA nano-vaccines with integrin binding RGD tripeptide (Arg-Gly-Asp), Garinot et al. were able to significantly increase the transport of particles using an *in vitro* model of follicle associated epithelium (Caco-2 cells and Raji B cells) and also monocultures of Caco-2 cells. Oral application of the RGD-nanoparticles was also shown to be immunogenic in some mice, with some animals having elevated anti-OVA IgG antibody responses and splenic IFN-γ T cell responses (151). Additional M cell targeting moieties, such as fucose binding lectin *Ulex euopaeus* agglutinin1 and reovirus sigma protein-1 have also previously been studied as virus, nanoparticle and microparticle targeting strategies for drugs and vaccines (152–156). Alternatively, cell penetrating peptides such as HIV-1 Tat, or CD71 receptor targeting protein such as transferrin have been bio-coupled to vaccine antigens and nano-vaccines for delivery to various cell types and organs (157). Therefore, the functionalization of the surface of nano-vaccines represents an exciting area of active investigation with the potential to significantly tailor vaccines to specific cells, tissues, and organs for optimal immune protection.

SUMMARY AND CONCLUSION

The last three decades has seen tremendous advancements in our understanding of HIV acquisition, treatment, and prevention. During this time, several vaccine efficacy trials have been completed and all have failed to prevent HIV infections apart from the modestly effective RV144. A major impediment to a successful vaccine has been antigen design and delivery. Crucial to overcoming this roadblock has been the development of nanoparticles to stabilize and orientate candidate vaccine immunogens for optimal immune triggering. Within this review we have covered the basis for vaccine development and the promising nanoparticle-based approaches to answer some of the very complicated issues surrounding HIV vaccine progress. Nanoparticle-based vaccines have demonstrated themselves to be versatile, and depending on which antigen, adjuvant and delivery route used, can have significant impacts on prevailing immune responses. While nanoparticle vaccines hold great promise, a significant number of unknowns still exist, and when answered could greatly advance our understanding on how to maximally deliver promising vaccine immunogens. These include a better understanding of the effects of charge, size, structure, and potential toxic side effects with various nanoparticle platforms.

While the major focus of this nanoparticle review has been on the development of neutralizing antibody, nanoparticle formulations targeting the V1/V2 region of Env by non-neutralizing

antibody is a significant area of interest and needs to be explored further. Justification for this is drawn from the correlates of protection from the RV144 study, which is being further evaluated and validated by on-going clinical trials in Thailand and Africa. In addition, although most vaccines are delivered systemically, HIV is predominantly transmitted through mucosal surfaces and as such, it is imperative that vaccine candidates be developed that can either augment mucosal immunity or be designed to draw protective systemic responses into the mucosal environment. The latter point would enable the provision of protective frontline responses within tissues at risk of infection. The only caveat being that mucosal tissue activation and vaccine-induced inflammation be carefully managed, to not increase the likelihood of transmission by growing the number of potential target cells.

Finally, the use of nanoparticle technology will also undoubtedly have a significant role to play in therapeutic HIV vaccines. The thought of an HIV-1 cure was once regarded a dream. Now, growing evidence suggests that a cure could be a reality and the generation of vaccine induced antiviral immunity will take center stage. There are numerous cure technologies that currently being evaluated, however it is the "Shock and Kill" tactic that has garnered significant attention. Several latency reversal agents have been devised to reactivate (shock) latent virus into transcriptional activity; however, vaccines that can prime for protective antibody and cytotoxic T and NK cell responses will be essential for subsequent viral eradication (kill).

We are clearly entering an exciting time for HIV vaccine development and nanoparticle formulations will have a lot to offer. As long as there is continued support for the nanoparticle vaccine effort, prophylactic and therapeutic HIV/AIDS interventions will continue to advance until such time as a vaccine becomes a reality.

AUTHORS CONTRIBUTIONS

YG, CW, and JM wrote sections of the manuscript and YG, CW, and JM edited the manuscript.

ACKNOWLEDGMENTS

The authors would like to thank Dr. Katja Klein for helping design and edit this manuscript.

FUNDING

JM is funded through a research award from the Canadian Institute of Health Research (grant number: PJT 149075).

REFERENCES

1. Doitsh G, Galloway NL, Geng X, Yang Z, Monroe KM, Zepeda O, et al. Cell death by pyroptosis drives CD4 T-cell depletion in HIV-1 infection. *Nature* (2014) 505:509–14. doi:10.1038/nature12940
2. McMichael AJ, Borrow P, Tomaras GD, Goonetilleke N, Haynes BF. The immune response during acute HIV-1 infection: clues for vaccine development. *Nat Rev Immunol* (2010) 10:11–23. doi:10.1038/nri2674
3. Fettig J, Swaminathan M, Murrill CS, Kaplan JE. Global epidemiology of HIV. *Infect Dis Clin North Am* (2014) 28:323–37. doi:10.1016/j.idc.2014.05.001
4. Rasmussen TA, Tolstrup M, Winckelmann A, Ostergaard L, Sogaard OS. Eliminating the latent HIV reservoir by reactivation strategies: advancing to clinical trials. *Hum Vaccin Immunother* (2013) 9:790–9. doi:10.4161/hv.23202
5. Belshe RB, Clements ML, Dolin R, Graham BS, McElrath J, Gorse GJ, et al. Safety and immunogenicity of a fully glycosylated recombinant gp160 human immunodeficiency virus type 1 vaccine in subjects at low risk of infection. National institute of allergy and infectious diseases AIDS vaccine evaluation group network. *J Infect Dis* (1993) 168:1387–95. doi:10.1093/infdis/168.6.1387
6. Keefer MC, Graham BS, Belshe RB, Schwartz D, Corey L, Bolognesi DP, et al. Studies of high doses of a human immunodeficiency virus type 1 recombinant glycoprotein 160 candidate vaccine in HIV type 1-seronegative humans. The AIDS vaccine clinical trials network. *AIDS Res Hum Retroviruses* (1994) 10:1713–23. doi:10.1089/aid.1994.10.1713
7. Gorse GJ, Rogers JH, Perry JE, Newman FK, Frey SE, Patel GB, et al. HIV-1 recombinant gp160 vaccine induced antibodies in serum and saliva. The NIAID AIDS vaccine clinical trials network. *Vaccine* (1995) 13:209–14. doi:10.1016/0264-410X(95)93138-Y
8. Mooij P, van der Kolk M, Bogers WM, ten Haaft PJ, Van Der Meide P, Almond N, et al. A clinically relevant HIV-1 subunit vaccine protects rhesus macaques from in vivo passaged simian-human immunodeficiency virus infection. *AIDS* (1998) 12:F15–22. doi:10.1097/00002030-199805000-00002
9. Stott EJ, Almond N, Kent K, Walker B, Hull R, Rose J, et al. Evaluation of a candidate human immunodeficiency virus type 1 (HIV-1) vaccine in macaques: effect of vaccination with HIV-1 gp120 on subsequent challenge with heterologous simian immunodeficiency virus-HIV-1 chimeric virus. *J Gen Virol* (1998) 79(Pt 3):423–32. doi:10.1099/0022-1317-79-3-423
10. Perez-Losada M, Jobes DV, Sinangil F, Crandall KA, Arenas M, Posada D, et al. Phylodynamics of HIV-1 from a phase III AIDS vaccine trial in Bangkok, Thailand. *PLoS One* (2011) 6:e16902. doi:10.1371/journal.pone.0016902
11. Pitisuttithum P, Gilbert P, Gurwith M, Heyward W, Martin M, van Griensven F, et al. Randomized, double-blind, placebo-controlled efficacy trial of a bivalent recombinant glycoprotein 120 HIV-1 vaccine among injection drug users in Bangkok, Thailand. *J Infect Dis* (2006) 194:1661–71. doi:10.1086/508748
12. Flynn NM, Forthal DN, Harro CD, Judson FN, Mayer KH, Para MF, et al. Placebo-controlled phase 3 trial of a recombinant glycoprotein 120 vaccine to prevent HIV-1 infection. *J Infect Dis* (2005) 191:654–65. doi:10.1086/428404
13. Perez-Losada M, Jobes DV, Sinangil F, Crandall KA, Posada D, Berman PW. Phylodynamics of HIV-1 from a phase-III AIDS vaccine trial in North America. *Mol Biol Evol* (2009) 27:417–25. doi:10.1093/molbev/msp254
14. Pancera M, Lebowitz J, Schon A, Zhu P, Freire E, Kwong PD, et al. Soluble mimetics of human immunodeficiency virus type 1 viral spikes produced by replacement of the native trimerization domain with a heterologous trimerization motif: characterization and ligand binding analysis. *J Virol* (2005) 79:9954–69. doi:10.1128/JVI.79.15.9954-9969.2005
15. Dey B, Pancera M, Svehla K, Shu Y, Xiang SH, Vainshtein J, et al. Characterization of human immunodeficiency virus type 1 monomeric and trimeric gp120 glycoproteins stabilized in the CD4-bound state: antigenicity, biophysics, and immunogenicity. *J Virol* (2007) 81:5579–93. doi:10.1128/JVI.02500-06
16. Forsell MN, Schief WR, Wyatt RT. Immunogenicity of HIV-1 envelope glycoprotein oligomers. *Curr Opin HIV AIDS* (2009) 4:380–7. doi:10.1097/COH.0b013e32832edc19
17. Bomsel M, Tudor D, Drillet AS, Alfsen A, Ganor Y, Roger MG, et al. Immunization with HIV-1 gp41 subunit virosomes induces mucosal antibodies protecting nonhuman primates against vaginal SHIV challenges. *Immunity* (2011) 34:269–80. doi:10.1016/j.immuni.2011.01.015
18. Barnett SW, Lu S, Srivastava I, Cherpelis S, Gettie A, Blanchard J, et al. The ability of an oligomeric human immunodeficiency virus type 1 (HIV-1) envelope antigen to elicit neutralizing antibodies against primary HIV-1 isolates is improved following partial deletion of the second hypervariable region. *J Virol* (2001) 75:5526–40. doi:10.1128/JVI.75.12.5526-5540.2001
19. Grundner C, Li Y, Louder M, Mascola J, Yang X, Sodroski J, et al. Analysis of the neutralizing antibody response elicited in rabbits by repeated inoculation

with trimeric HIV-1 envelope glycoproteins. *Virology* (2005) 331:33–46. doi:10.1016/j.virol.2004.09.022
20. Kim M, Qiao ZS, Montefiori DC, Haynes BF, Reinherz EL, Liao HX. Comparison of HIV Type 1 ADA gp120 monomers versus gp140 trimers as immunogens for the induction of neutralizing antibodies. *AIDS Res Hum Retroviruses* (2005) 21:58–67. doi:10.1089/aid.2005.21.58
21. Wang S, Pal R, Mascola JR, Chou TH, Mboudjeka I, Shen S, et al. Polyvalent HIV-1 env vaccine formulations delivered by the DNA priming plus protein boosting approach are effective in generating neutralizing antibodies against primary human immunodeficiency virus type 1 isolates from subtypes A, B, C, D and E. *Virology* (2006) 350:34–47. doi:10.1016/j.virol.2006.02.032
22. Beddows S, Schulke N, Kirschner M, Barnes K, Franti M, Michael E, et al. Evaluating the immunogenicity of a disulfide-stabilized, cleaved, trimeric form of the envelope glycoprotein complex of human immunodeficiency virus type 1. *J Virol* (2005) 79:8812–27. doi:10.1128/JVI.79.14.8812-8827.2005
23. Rerks-Ngarm S, Pitisuttithum P, Nitayaphan S, Kaewkungwal J, Chiu J, Paris R, et al. Vaccination with ALVAC and AIDSVAX to prevent HIV-1 infection in Thailand. *N Engl J Med* (2009) 361:2209–20. doi:10.1056/NEJMoa0908492
24. Montefiori DC, Karnasuta C, Huang Y, Ahmed H, Gilbert P, de Souza MS, et al. Magnitude and breadth of the neutralizing antibody response in the RV144 and Vax003 HIV-1 vaccine efficacy trials. *J Infect Dis* (2012) 206:431–41. doi:10.1093/infdis/jis367
25. Pugach P, Ozorowski G, Cupo A, Ringe R, Yasmeen A, de Val N, et al. A native-like SOSIP.664 trimer based on an HIV-1 subtype B env gene. *J Virol* (2015) 89:3380–95. doi:10.1128/JVI.03473-14
26. Escolano A, Steichen JM, Dosenovic P, Kulp DW, Golijanin J, Sok D, et al. Sequential immunization elicits broadly neutralizing anti-HIV-1 antibodies in Ig knockin mice. *Cell* (2016) 166:1445–58.e1412. doi:10.1016/j.cell.2016.07.030
27. Steichen JM, Kulp DW, Tokatlian T, Escolano A, Dosenovic P, Stanfield RL, et al. HIV vaccine design to target germline precursors of glycan-dependent broadly neutralizing antibodies. *Immunity* (2016) 45:483–96. doi:10.1016/j.immuni.2016.08.016
28. Asbach B, Wagner R. Particle-based delivery of the HIV envelope protein. *Curr Opin HIV AIDS* (2017) 12:265–71. doi:10.1097/COH.0000000000000366
29. Temchura V, Uberla K. Intrastructural help: improving the HIV-1 envelope antibody response induced by virus-like particle vaccines. *Curr Opin HIV AIDS* (2017) 12:272–7. doi:10.1097/COH.0000000000000358
30. Lopez-Sagaseta J, Malito E, Rappuoli R, Bottomley MJ. Self-assembling protein nanoparticles in the design of vaccines. *Comput Struct Biotechnol J* (2016) 14:58–68. doi:10.1016/j.csbj.2015.11.001
31. Roldão A, Mellado MCM, Castilho LR, Carrondo MJT, Alves PM. Virus-like particles in vaccine development. *Expert Rev Vaccines* (2010) 9:1149–76. doi:10.1586/erv.10.115
32. Gamvrellis A, Leong D, Hanley JC, Xiang SD, Mottram P, Plebanski M. Vaccines that facilitate antigen entry into dendritic cells. *Immunol Cell Biol* (2004) 82:506–16. doi:10.1111/j.0818-9641.2004.01271.x
33. Slutter B, Jiskoot W. Sizing the optimal dimensions of a vaccine delivery system: a particulate matter. *Expert Opin Drug Deliv* (2016) 13:167–70. doi:10.1517/17425247.2016.1121989
34. Bachmann MF, Lutz MB, Layton GT, Harris SJ, Fehr T, Rescigno M, et al. Dendritic cells process exogenous viral proteins and virus-like particles for class I presentation to CD8+ cytotoxic T lymphocytes. *Eur J Immunol* (1996) 26:2595–600. doi:10.1002/eji.1830261109
35. Ruedl C, Storni T, Lechner F, Bachi T, Bachmann MF. Cross-presentation of virus-like particles by skin-derived CD8(-) dendritic cells: a dispensable role for TAP. *Eur J Immunol* (2002) 32:818–25. doi:10.1002/1521-4141(200203)32:3<818::AID-IMMU818>3.0.CO;2-U
36. Zhao Q, Li S, Yu H, Xia N, Modis Y. Virus-like particle-based human vaccines: quality assessment based on structural and functional properties. *Trends Biotechnol* (2013) 31:654–63. doi:10.1016/j.tibtech.2013.09.002
37. McNeil C. Who invented the VLP cervical cancer vaccines? *J Natl Cancer Inst* (2006) 98:433. doi:10.1093/jnci/djj144
38. Liu FX, Wu XD, Li L, Liu ZS, Wang ZL. Use of baculovirus expression system for generation of virus-like particles: successes and challenges. *Protein Expr Purif* (2013) 90:104–16. doi:10.1016/j.pep.2013.05.009
39. Jayapal KP, Wlaschin KF, Hu WS, Yap MGS. Recombinant protein therapeutics from CHO cells–20 years and counting. *Chem Eng Prog* (2007) 103:40–7.
40. Zhu JW. Mammalian cell protein expression for biopharmaceutical production. *Biotechnol Adv* (2012) 30:1158–70. doi:10.1016/j.biotechadv.2011.08.022
41. Ma JKC, Drake PMW, Christou P. The production of recombinant pharmaceutical proteins in plants. *Nat Rev Genet* (2003) 4:794–805. doi:10.1038/nrg1177
42. Yang X, Kurteva S, Ren X, Lee S, Sodroski J. Stoichiometry of envelope glycoprotein trimers in the entry of human immunodeficiency virus type 1. *J Virol* (2005) 79:12132–47. doi:10.1128/JVI.79.11.7279.2005
43. Klasse PJ. Modeling how many envelope glycoprotein trimers per virion participate in human immunodeficiency virus infectivity and its neutralization by antibody. *Virology* (2007) 369:245–62. doi:10.1016/j.virol.2007.06.044
44. Magnus C, Rusert P, Bonhoeffer S, Trkola A, Regoes RR. Estimating the stoichiometry of human immunodeficiency virus entry. *J Virol* (2009) 83:1523–31. doi:10.1128/JVI.01764-08
45. Brandenberg OF, Magnus C, Rusert P, Regoes RR, Trkola A. Different infectivity of HIV-1 strains is linked to number of envelope trimers required for entry. *PLoS Pathog* (2015) 11:e1004595. doi:10.1371/journal.ppat.1004595
46. Stano A, Leaman DP, Kim AS, Zhang L, Autin L, Ingale J, et al. Dense array of spikes on HIV-1 virion particles. *J Virol* (2017) 91:e415–7. doi:10.1128/JVI.00415-17
47. Pankrac J, Klein K, McKay PF, King DFL, Bain K, Knapp J, et al. A heterogeneous human immunodeficiency virus-like particle (VLP) formulation produced by a novel vector system. *NPJ Vaccines* (2018) 3:2. doi:10.1038/s41541-017-0040-6
48. Pankrac J, Klein K, Mann JFS. Eradication of HIV-1 latent reservoirs through therapeutic vaccination. *AIDS Res Ther* (2017) 14:45. doi:10.1186/s12981-017-0177-4
49. McCurley NP, Domi A, Basu R, Saunders KO, LaBranche CC, Montefiori DC, et al. HIV transmitted/founder vaccines elicit autologous tier 2 neutralizing antibodies for the CD4 binding site. *PLoS One* (2017) 12:e0177863. doi:10.1371/journal.pone.0177863
50. Liao HX, Lynch R, Zhou T, Gao F, Alam SM, Boyd SD, et al. Co-evolution of a broadly neutralizing HIV-1 antibody and founder virus. *Nature* (2013) 496:469–76. doi:10.1038/nature12053
51. Paphadjopoulos D, Wilson T, Taber R. Liposomes as vehicles for cellular incorporation of biologically active macromolecules. *In Vitro* (1980) 16:49–54. doi:10.1007/BF02618199
52. Sharma A, Sharma US. Liposomes in drug delivery: progress and limitations. *Intern J Pharm* (1997) 154:123–40. doi:10.1016/S0378-5173(97)00135-X
53. Kersten GF, Crommelin DJ. Liposomes and ISCOMS as vaccine formulations. *Biochim Biophys Acta* (1995) 1241:117–38. doi:10.1016/0304-4157(95)00002-9
54. Storm G, Crommelin DJ. Liposomes: quo vadis? *Pharm sci technol* (1998) 1:19–31. doi:10.1016/S1461-5347(98)00007-8
55. Bui T, Dykers T, Hu SL, Faltynek CR, Ho RJ. Effect of MTP-PE liposomes and interleukin-7 on induction of antibody and cell-mediated immune responses to a recombinant HIV-envelope protein. *J Acquir Immune Defic Syndr* (1994) 7:799–806.
56. Pejawar-Gaddy S, Kovacs JM, Barouch DH, Chen B, Irvine DJ. Design of lipid nanocapsule delivery vehicles for multivalent display of recombinant Env trimers in HIV vaccination. *Bioconjug Chem* (2014) 25:1470–8. doi:10.1021/bc5002246
57. Kovacs JM, Nkolola JP, Peng H, Cheung A, Perry J, Miller CA, et al. HIV-1 envelope trimer elicits more potent neutralizing antibody responses than monomeric gp120. *Proc Natl Acad Sci U S A* (2012) 109:12111–6. doi:10.1073/pnas.1204533109
58. Ingale J, Stano A, Guenaga J, Sharma SK, Nemazee D, Zwick MB, et al. High-density array of well-ordered HIV-1 spikes on synthetic liposomal nanoparticles efficiently activate B cells. *Cell Rep* (2016) 15:1986–99. doi:10.1016/j.celrep.2016.04.078
59. Bale S, Goebrecht G, Stano A, Wilson R, Ota T, Tran K, et al. Covalent linkage of HIV-1 trimers to synthetic liposomes elicits improved b cell and antibody responses. *J Virol* (2017) 91(16):e443–417. doi:10.1128/JVI.00443-17
60. Hanson MC, Abraham W, Crespo MP, Chen SH, Liu H, Szeto GL, et al. Liposomal vaccines incorporating molecular adjuvants and intrastructural

T-cell help promote the immunogenicity of HIV membrane-proximal external region peptides. *Vaccine* (2015) 33:861–8. doi:10.1016/j.vaccine.2014.12.045
61. Fairman J, Moore J, Lemieux M, Van Rompay K, Geng Y, Warner J, et al. Enhanced in vivo immunogenicity of SIV vaccine candidates with cationic liposome-DNA complexes in a rhesus macaque pilot study. *Hum Vaccin* (2009) 5:141–50. doi:10.4161/hv.5.3.6589
62. Cosgrove CA, Lacey CJ, Cope AV, Bartolf A, Morris G, Yan C, et al. Comparative immunogenicity of HIV-1 gp140 vaccine delivered by parenteral, and mucosal routes in female volunteers; MUCOVAC2, a randomized two centre study. *PLoS One* (2016) 11:e0152038. doi:10.1371/journal.pone.0152038
63. Klein K, Mann JF, Rogers P, Shattock RJ. Polymeric penetration enhancers promote humoral immune responses to mucosal vaccines. *J Control Release* (2014) 183:43–50. doi:10.1016/j.jconrel.2014.03.018
64. Rostami H, Ebtekar M, Ardestani MS, Yazdi MH, Mahdavi M. Co-utilization of a TLR5 agonist and nano-formulation of HIV-1 vaccine candidate leads to increased vaccine immunogenicity and decreased immunogenic dose: a preliminary study. *Immunol Lett* (2017) 187:19–26. doi:10.1016/j.imlet.2017.05.002
65. Rubsamen RM, Herst CV, Lloyd PM, Heckerman DE. Eliciting cytotoxic T-lymphocyte responses from synthetic vectors containing one or two epitopes in a C57BL/6 mouse model using peptide-containing biodegradable microspheres and adjuvants. *Vaccine* (2014) 32:4111–6. doi:10.1016/j.vaccine.2014.05.071
66. Carroll EC, Jin L, Mori A, Munoz-Wolf N, Oleszycka E, Moran HBT, et al. The vaccine adjuvant chitosan promotes cellular immunity via DNA sensor cGAS-STING-dependent induction of type I interferons. *Immunity* (2016) 44:597–608. doi:10.1016/j.immuni.2016.02.004
67. Jones DH, McBride BW, Jeffery H, O'Hagan DT, Robinson A, Farrar GH. Protection of mice from *Bordetella pertussis* respiratory infection using microencapsulated pertussis fimbriae. *Vaccine* (1995) 13:675–81. doi:10.1016/0264-410X(95)99876-J
68. Gupta RK, Alroy J, Alonso MJ, Langer R, Siber GR. Chronic local tissue reactions, long-term immunogenicity and immunologic priming of mice and guinea pigs to tetanus toxoid encapsulated in biodegradable polymer microspheres composed of poly lactide-co-glycolide polymers. *Vaccine* (1997) 15:1716–23. doi:10.1016/S0264-410X(97)00116-3
69. Singh M, Li XM, Wang H, McGee JP, Zamb T, Koff W, et al. Controlled release microparticles as a single dose diphtheria toxoid vaccine: immunogenicity in small animal models. *Vaccine* (1998) 16:346–52. doi:10.1016/S0264-410X(97)80912-7
70. Johansen P, Moon L, Tamber H, Merkle HP, Gander B, Sesardic D. Immunogenicity of single-dose diphtheria vaccines based on PLA/PLGA microspheres in guinea pigs. *Vaccine* (1999) 18:209–15. doi:10.1016/S0264-410X(99)00191-7
71. Venkataprasad N, Coombes AG, Singh M, Rohde M, Wilkinson K, Hudecz F, et al. Induction of cellular immunity to a mycobacterial antigen adsorbed on lamellar particles of lactide polymers. *Vaccine* (1999) 17:1814–9. doi:10.1016/S0264-410X(98)00372-7
72. Cleland JL, Powell MF, Lim A, Barron L, Berman PW, Eastman DJ, et al. Development of a single-shot subunit vaccine for HIV-1. *AIDS Res Hum Retroviruses* (1994) 10(Suppl 2):S21–6.
73. Liang F, Ploquin A, Hernandez JD, Fausther-Bovendo H, Lindgren G, Stanley D, et al. Dissociation of skeletal muscle for flow cytometric characterization of immune cells in macaques. *J Immunol Methods* (2015) 425:69–78. doi:10.1016/j.jim.2015.06.011
74. Pillon NJ, Bilan PJ, Fink LN, Klip A. Cross-talk between skeletal muscle and immune cells: muscle-derived mediators and metabolic implications. *Am J Physiol Endocrinol Metab* (2013) 304:E453–65. doi:10.1152/ajpendo.00553.2012
75. Sell H, Kaiser U, Eckel J. Expression of chemokine receptors in insulin-resistant human skeletal muscle cells. *Horm Metab Res* (2007) 39:244–9. doi:10.1055/s-2007-972577
76. Chazaud B, Brigitte M, Yacoub-Youssef H, Arnold L, Gherardi R, Sonnet C, et al. Dual and beneficial roles of macrophages during skeletal muscle regeneration. *Exerc Sport Sci Rev* (2009) 37:18–22. doi:10.1097/JES.0b013e318190ebdb
77. Mosca F, Tritto E, Muzzi A, Monaci E, Bagnoli F, Iavarone C, et al. Molecular and cellular signatures of human vaccine adjuvants. *Proc Natl Acad Sci U S A* (2008) 105:10501–6. doi:10.1073/pnas.0804699105
78. Vono M, Taccone M, Caccin P, Gallotta M, Donvito G, Falzoni S, et al. The adjuvant MF59 induces ATP release from muscle that potentiates response to vaccination. *Proc Natl Acad Sci U S A* (2013) 110:21095–100. doi:10.1073/pnas.1319784110
79. Cubas R, Zhang S, Kwon S, Sevick-Muraca EM, Li M, Chen C, et al. Virus-like particle (VLP) lymphatic trafficking and immune response generation after immunization by different routes. *J Immunother* (2009) 32:118–28. doi:10.1097/CJI.0b013e31818f13c4
80. Keele BF, Tazi L, Gartner S, Liu Y, Burgon TB, Estes JD, et al. Characterization of the follicular dendritic cell reservoir of human immunodeficiency virus type 1. *J Virol* (2008) 82:5548–61. doi:10.1128/JVI.00124-08
81. Smith DM, Simon JK, Baker JR Jr. Applications of nanotechnology for immunology. *Nat Rev Immunol* (2013) 13:592–605. doi:10.1038/nri3488
82. Hoshyar N, Gray S, Han H, Bao G. The effect of nanoparticle size on in vivo pharmacokinetics and cellular interaction. *Nanomedicine (Lond)* (2016) 11:673–92. doi:10.2217/nnm.16.5
83. Gutierro I, Hernandez RM, Igartua M, Gascon AR, Pedraz JL. Size dependent immune response after subcutaneous, oral and intranasal administration of BSA loaded nanospheres. *Vaccine* (2002) 21:67–77. doi:10.1016/S0264-410X(02)00435-8
84. Gutierro I, Hernandez RM, Igartua M, Gascon AR, Pedraz JL. Influence of dose and immunization route on the serum Ig G antibody response to BSA loaded PLGA microspheres. *Vaccine* (2002) 20:2181–90. doi:10.1016/S0264-410X(02)00146-9
85. Benson RA, MacLeod MK, Hale BG, Patakas A, Garside P, Brewer JM. Antigen presentation kinetics control T cell/dendritic cell interactions and follicular helper T cell generation in vivo. *Elife* (2015) 4:e06994. doi:10.7554/eLife.06994
86. Mann JF, Shakir E, Carter KC, Mullen AB, Alexander J, Ferro VA. Lipid vesicle size of an oral influenza vaccine delivery vehicle influences the Th1/Th2 bias in the immune response and protection against infection. *Vaccine* (2009) 27:3643–9. doi:10.1016/j.vaccine.2009.03.040
87. Brewer JM, Tetley L, Richmond J, Liew FY, Alexander J. Lipid vesicle size determines the Th1 or Th2 response to entrapped antigen. *J Immunol* (1998) 161:4000–7.
88. Brewer JM, Pollock KG, Tetley L, Russell DG. Vesicle size influences the trafficking, processing, and presentation of antigens in lipid vesicles. *J Immunol* (2004) 173:6143–50. doi:10.4049/jimmunol.173.10.6143
89. De Nardo D. Toll-like receptors: activation, signalling and transcriptional modulation. *Cytokine* (2015) 74:181–9. doi:10.1016/j.cyto.2015.02.025
90. Buffa V, Klein K, Fischetti L, Shattock RJ. Evaluation of TLR agonists as potential mucosal adjuvants for HIV gp140 and tetanus toxoid in mice. *PLoS One* (2012) 7:e50529. doi:10.1371/journal.pone.0050529
91. McKay PF, Cope AV, Mann JF, Joseph S, Esteban M, Tatoud R, et al. Glucopyranosyl lipid A adjuvant significantly enhances HIV specific T and B cell responses elicited by a DNA-MVA-protein vaccine regimen. *PLoS One* (2014) 9:e84707. doi:10.1371/journal.pone.0084707
92. McKay PF, King DF, Mann JF, Barinaga G, Carter D, Shattock RJ. TLR4 and TLR7/8 adjuvant combinations generate different vaccine antigen-specific immune outcomes in minipigs when administered via the ID or IN routes. *PLoS One* (2016) 11:e0148984. doi:10.1371/journal.pone.0148984
93. Moody MA. Modulation of HIV-1 immunity by adjuvants. *Curr Opin HIV AIDS* (2014) 9:242–9. doi:10.1097/COH.0000000000000052
94. McElrath MJ. Adjuvants: tailoring humoral immune responses. *Curr Opin HIV AIDS* (2017) 12:278–84. doi:10.1097/COH.0000000000000365
95. Lindblad EB. Aluminium compounds for use in vaccines. *Immunol Cell Biol* (2004) 82:497–505. doi:10.1111/j.0818-9641.2004.01286.x
96. Oleszycka E, Moran HB, Tynan GA, Hearnden CH, Coutts G, Campbell M, et al. IL-1alpha and inflammasome-independent IL-1beta promote neutrophil infiltration following alum vaccination. *FEBS J* (2016) 283:9–24. doi:10.1111/febs.13546
97. Dubois Cauwelaert N, Desbien AL, Hudson TE, Pine SO, Reed SG, Coler RN, et al. The TLR4 agonist vaccine adjuvant, GLA-SE, requires canonical and atypical mechanisms of action for TH1 induction. *PLoS One* (2016) 11:e0146372. doi:10.1371/journal.pone.0146372

98. Yoon SI, Kurnasov O, Natarajan V, Hong M, Gudkov AV, Osterman AL, et al. Structural basis of TLR5-flagellin recognition and signaling. *Science* (2012) 335:859–64. doi:10.1126/science.1215584
99. Giannini SL, Hanon E, Moris P, Van Mechelen M, Morel S, Dessy F, et al. Enhanced humoral and memory B cellular immunity using HPV16/18 L1 VLP vaccine formulated with the MPL/aluminium salt combination (AS04) compared to aluminium salt only. *Vaccine* (2006) 24:5937–49. doi:10.1016/j.vaccine.2006.06.005
100. Morelli AB, Becher D, Koernig S, Silva A, Drane D, Maraskovsky E. ISCOMATRIX: a novel adjuvant for use in prophylactic and therapeutic vaccines against infectious diseases. *J Med Microbiol* (2012) 61:935–43. doi:10.1099/jmm.0.040857-0
101. Zhu X, Nishimura F, Sasaki K, Fujita M, Dusak JE, Eguchi J, et al. Toll like receptor-3 ligand poly-ICLC promotes the efficacy of peripheral vaccinations with tumor antigen-derived peptide epitopes in murine CNS tumor models. *J Transl Med* (2007) 5:10. doi:10.1186/1479-5876-5-10
102. Dinges W, Girard PM, Podzamczer D, Brockmeyer NH, Garcia F, Harrer T, et al. The F4/AS01B HIV-1 vaccine candidate is safe and immunogenic, but does not show viral efficacy in antiretroviral therapy-naive, HIV-1-infected adults: a randomized controlled trial. *Medicine (Baltimore)* (2016) 95:e2673. doi:10.1097/MD.0000000000002673
103. Gram GJ, Karlsson I, Agger EM, Andersen P, Fomsgaard A. A novel liposome-based adjuvant CAF01 for induction of CD8(+) cytotoxic T-lymphocytes (CTL) to HIV-1 minimal CTL peptides in HLA-A*0201 transgenic mice. *PLoS One* (2009) 4:e6950. doi:10.1371/journal.pone.0006950
104. Barouch DH, Deeks SG. Immunologic strategies for HIV-1 remission and eradication. *Science* (2014) 345:169–74. doi:10.1126/science.1255512
105. Smith D, Gow I, Colebunders R, Weller I, Tchamouroff S, Weber J, et al. Therapeutic vaccination (p24-VLP) of patients with advanced HIV-1 infection in the pre-HAART era does not alter CD4 cell decline. *HIV Med* (2001) 2:272–5. doi:10.1046/j.1468-1293.2001.00080.x
106. Kelleher AD, Roggensack M, Jaramillo AB, Smith DE, Walker A, Gow I, et al. Safety and immunogenicity of a candidate therapeutic vaccine, p24 virus-like particle, combined with zidovudine, in asymptomatic subjects. Community HIV research network investigators. *AIDS* (1998) 12:175–82. doi:10.1097/00002030-199802000-00007
107. Wagner R, Deml L, Schirmbeck R, Niedrig M, Reimann J, Wolf H. Construction, expression, and immunogenicity of chimeric HIV-1 virus-like particles. *Virology* (1996) 220:128–40. doi:10.1006/viro.1996.0293
108. Wagner R, Teeuwsen VJ, Deml L, Notka F, Haaksma AG, Jhagjhoorsingh SS, et al. Cytotoxic T cells and neutralizing antibodies induced in rhesus monkeys by virus-like particle HIV vaccines in the absence of protection from SHIV infection. *Virology* (1998) 245:65–74. doi:10.1006/viro.1998.9104
109. Pandey S, Kawai T, Akira S. Microbial sensing by toll-like receptors and intracellular nucleic acid sensors. *Cold Spring Harb Perspect Biol* (2014) 7:a016246. doi:10.1101/cshperspect.a016246
110. Iyer SS, Gangadhara S, Victor B, Shen X, Chen X, Nabi R, et al. Virus-like particles displaying trimeric simian immunodeficiency virus (SIV) envelope gp160 enhance the breadth of DNA/modified vaccinia virus ankara SIV vaccine-induced antibody responses in rhesus macaques. *J Virol* (2016) 90:8842–54. doi:10.1128/JVI.01163-16
111. Moody MA, Santra S, Vandergrift NA, Sutherland LL, Gurley TC, Drinker MS, et al. Toll-like receptor 7/8 (TLR7/8) and TLR9 agonists cooperate to enhance HIV-1 envelope antibody responses in rhesus macaques. *J Virol* (2014) 88:3329–39. doi:10.1128/JVI.03309-13
112. Francica JR, Sheng Z, Zhang Z, Nishimura Y, Shingai M, Ramesh A, et al. Analysis of immunoglobulin transcripts and hypermutation following SHIV(AD8) infection and protein-plus-adjuvant immunization. *Nat Commun* (2015) 6:6565. doi:10.1038/ncomms7565
113. Iwasaki A, Medzhitov R. Regulation of adaptive immunity by the innate immune system. *Science* (2010) 327:291–5. doi:10.1126/science.1183021
114. Jimenez-Sanchez G, Pavot V, Chane-Haong C, Handke N, Terrat C, Gigmes D, et al. Preparation and in vitro evaluation of imiquimod loaded polylactide-based micelles as potential vaccine adjuvants. *Pharm Res* (2015) 32:311–20. doi:10.1007/s11095-014-1465-5
115. Francica JR, Zak DE, Linde C, Siena E, Johnson C, Juraska M, et al. Innate transcriptional effects by adjuvants on the magnitude, quality, and durability of HIV envelope responses in NHPs. *Blood Adv* (2017) 1:2329–42. doi:10.1182/bloodadvances.2017011411
116. Ulrich JT, Myers KR. Monophosphoryl lipid A as an adjuvant. Past experiences and new directions. *Pharm Biotechnol* (1995) 6:495–524. doi:10.1007/978-1-4615-1823-5_21
117. Schulke S, Vogel L, Junker AC, Hanschmann KM, Flaczyk A, Vieths S, et al. A fusion protein consisting of the vaccine adjuvant monophosphoryl lipid A and the allergen ovalbumin boosts allergen-specific Th1, Th2, and Th17 responses in vitro. *J Immunol Res* (2016) 2016:4156456. doi:10.1155/2016/4156456
118. Wheeler AW, Marshall JS, Ulrich JT. A Th1-inducing adjuvant, MPL, enhances antibody profiles in experimental animals suggesting it has the potential to improve the efficacy of allergy vaccines. *Int Arch Allergy Immunol* (2001) 126:135–9. doi:10.1159/000049504
119. Baldrick P, Richardson D, Elliott G, Wheeler AW. Safety evaluation of monophosphoryl lipid A (MPL): an immunostimulatory adjuvant. *Regul Toxicol Pharmacol* (2002) 35:398–413. doi:10.1006/rtph.2002.1541
120. Arias MA, Van Roey GA, Tregoning JS, Moutaftsi M, Coler RN, Windish HP, et al. Glucopyranosyl lipid adjuvant (GLA), a synthetic TLR4 agonist, promotes potent systemic and mucosal responses to intranasal immunization with HIVgp140. *PLoS One* (2012) 7:e41144. doi:10.1371/journal.pone.0041144
121. Orr MT, Duthie MS, Windish HP, Lucas EA, Guderian JA, Hudson TE, et al. MyD88 and TRIF synergistic interaction is required for TH1-cell polarization with a synthetic TLR4 agonist adjuvant. *Eur J Immunol* (2013) 43:2398–408. doi:10.1002/eji.201243124
122. Owens T, Zeine R. The cell biology of T-dependent B cell activation. *Biochem Cell Biol* (1989) 67:481–9. doi:10.1139/o89-078
123. Bourgeois C, Tanchot C. Mini-review CD4 T cells are required for CD8 T cell memory generation. *Eur J Immunol* (2003) 33:3225–31. doi:10.1002/eji.200324576
124. Desbien AL, Dubois Cauwelaert N, Reed SJ, Bailor HR, Liang H, Carter D, et al. IL-18 and subcapsular lymph node macrophages are essential for enhanced B cell responses with TLR4 agonist adjuvants. *J Immunol* (2016) 197:4351–9. doi:10.4049/jimmunol.1600993
125. Kasturi SP, Skountzou I, Albrecht RA, Koutsonanos D, Hua T, Nakaya HI, et al. Programming the magnitude and persistence of antibody responses with innate immunity. *Nature* (2011) 470:543–7. doi:10.1038/nature09737
126. Wiley SR, Raman VS, Desbien A, Bailor HR, Bhardwaj R, Shakri AR, et al. Targeting TLRs expands the antibody repertoire in response to a malaria vaccine. *Sci Transl Med* (2011) 3:93ra69. doi:10.1126/scitranslmed.3002135
127. Kasturi SP, Kozlowski PA, Nakaya HI, Burger MC, Russo P, Pham M, et al. Adjuvanting a simian immunodeficiency virus vaccine with toll-like receptor ligands encapsulated in nanoparticles induces persistent antibody responses and enhanced protection in TRIM5alpha restrictive macaques. *J Virol* (2017) 91:e01844. doi:10.1128/JVI.01844-16
128. Harper DM, Franco EL, Wheeler C, Ferris DG, Jenkins D, Schuind A, et al. Efficacy of a bivalent L1 virus-like particle vaccine in prevention of infection with human papillomavirus types 16 and 18 in young women: a randomised controlled trial. *Lancet* (2004) 364:1757–65. doi:10.1016/S0140-6736(04)17398-4
129. Harper DM, Franco EL, Wheeler CM, Moscicki AB, Romanowski B, Roteli-Martins CM, et al. Sustained efficacy up to 4.5 years of a bivalent L1 virus-like particle vaccine against human papillomavirus types 16 and 18: follow-up from a randomised control trial. *Lancet* (2006) 367:1247–55. doi:10.1016/S0140-6736(06)68439-0
130. Paavonen J, Jenkins D, Bosch FX, Naud P, Salmeron J, Wheeler CM, et al. Efficacy of a prophylactic adjuvanted bivalent L1 virus-like-particle vaccine against infection with human papillomavirus types 16 and 18 in young women: an interim analysis of a phase III double-blind, randomised controlled trial. *Lancet* (2007) 369:2161–70. doi:10.1016/S0140-6736(07)60946-5
131. Wang JW, Roden RB. Virus-like particles for the prevention of human papillomavirus-associated malignancies. *Expert Rev Vaccines* (2013) 12:129–41. doi:10.1586/erv.12.151
132. Paavonen J, Naud P, Salmeron J, Wheeler CM, Chow SN, Apter D, et al. Efficacy of human papillomavirus (HPV)-16/18 AS04-adjuvanted vaccine against cervical infection and precancer caused by oncogenic HPV types (PATRICIA): final analysis of a double-blind, randomised study in young women. *Lancet* (2009) 374:301–14. doi:10.1016/S0140-6736(09)61248-4
133. Kavanagh K, Pollock KG, Potts A, Love J, Cuschieri K, Cubie H, et al. Introduction and sustained high coverage of the HPV bivalent vaccine leads

to a reduction in prevalence of HPV 16/18 and closely related HPV types. *Br J Cancer* (2014) 110:2804–11. doi:10.1038/bjc.2014.198
134. Einstein MH, Baron M, Levin MJ, Chatterjee A, Edwards RP, Zepp F, et al. Comparison of the immunogenicity and safety of cervarix and gardasil human papillomavirus (HPV) cervical cancer vaccines in healthy women aged 18-45 years. *Hum Vaccin* (2009) 5:705–19. doi:10.4161/hv.5.10.9518
135. O'Hagan DT, Ott GS, Nest GV, Rappuoli R, Giudice GD. The history of MF59((R)) adjuvant: a phoenix that arose from the ashes. *Expert Rev Vaccines* (2013) 12:13–30. doi:10.1586/erv.12.140
136. O'Hagan DT, Ott GS, De Gregorio E, Seubert A. The mechanism of action of MF59 – an innately attractive adjuvant formulation. *Vaccine* (2012) 30:4341–8. doi:10.1016/j.vaccine.2011.09.061
137. Pellegrini M, Nicolay U, Lindert K, Groth N, Della Cioppa G. MF59-adjuvanted versus non-adjuvanted influenza vaccines: integrated analysis from a large safety database. *Vaccine* (2009) 27:6959–65. doi:10.1016/j.vaccine.2009.08.101
138. Khurana S, Verma N, Yewdell JW, Hilbert AK, Castellino F, Lattanzi M, et al. MF59 adjuvant enhances diversity and affinity of antibody-mediated immune response to pandemic influenza vaccines. *Sci Transl Med* (2011) 3:85ra48. doi:10.1126/scitranslmed.3002336
139. Mastelic Gavillet B, Eberhardt CS, Auderset F, Castellino F, Seubert A, Tregoning JS, et al. MF59 mediates its B cell adjuvanticity by promoting T follicular helper cells and thus germinal center responses in adult and early life. *J Immunol* (2015) 194:4836–45. doi:10.4049/jimmunol.1402071
140. Vargas-Inchaustegui DA, Demers A, Shaw JM, Kang G, Ball D, Tuero I, et al. Vaccine induction of lymph node-resident simian immunodeficiency virus env-specific t follicular helper cells in rhesus macaques. *J Immunol* (2016) 196:1700–10. doi:10.4049/jimmunol.1502137
141. Lofano G, Mancini F, Salvatore G, Cantisani R, Monaci E, Carrisi C, et al. Oil-in-water emulsion MF59 increases germinal center B cell differentiation and persistence in response to vaccination. *J Immunol* (2015) 195:1617–27. doi:10.4049/jimmunol.1402604
142. Guillon C, Mayol K, Terrat C, Compagnon C, Primard C, Charles MH, et al. Formulation of HIV-1 Tat and p24 antigens by PLA nanoparticles or MF59 impacts the breadth, but not the magnitude, of serum and faecal antibody responses in rabbits. *Vaccine* (2007) 25:7491–501. doi:10.1016/j.vaccine.2007.08.060
143. Morein B, Sundquist B, Hoglund S, Dalsgaard K, Osterhaus A. Iscom, a novel structure for antigenic presentation of membrane proteins from enveloped viruses. *Nature* (1984) 308:457–60. doi:10.1038/308457a0
144. Wilson NS, Yang B, Morelli AB, Koernig S, Yang A, Loeser S, et al. ISCOMATRIX vaccines mediate CD8+ T-cell cross-priming by a MyD88-dependent signaling pathway. *Immunol Cell Biol* (2012) 90:540–52. doi:10.1038/icb.2011.71
145. Havenar-Daughton C, Carnathan DG, Torrents de la Pena A, Pauthner M, Briney B, Reiss SM, et al. Direct probing of germinal center responses reveals immunological features and bottlenecks for neutralizing antibody responses to HIV env trimer. *Cell Rep* (2016) 17:2195–209. doi:10.1016/j.celrep.2016.10.085
146. Franco D, Liu W, Gardiner DF, Hahn BH, Ho DD. CD40L-containing virus-like particle as a candidate HIV-1 vaccine targeting dendritic cells. *J Acquir Immune Defic Syndr* (2011) 56:393–400. doi:10.1097/QAI.0b013e31820b844e
147. Lai L, Kwa S, Kozlowski PA, Montefiori DC, Ferrari G, Johnson WE, et al. Prevention of infection by a granulocyte-macrophage colony-stimulating factor co-expressing DNA/modified vaccinia ankara simian immunodeficiency virus vaccine. *J Infect Dis* (2011) 204:164–73. doi:10.1093/infdis/jir199
148. Feng H, Zhang H, Deng J, Wang L, He Y, Wang S, et al. Incorporation of a GPI-anchored engineered cytokine as a molecular adjuvant enhances the immunogenicity of HIV VLPs. *Sci Rep* (2015) 5:11856. doi:10.1038/srep11856
149. Wang BZ, Quan FS, Kang SM, Bozja J, Skountzou I, Compans RW. Incorporation of membrane-anchored flagellin into influenza virus-like particles enhances the breadth of immune responses. *J Virol* (2008) 82:11813–23. doi:10.1128/JVI.01076-08
150. Vassilieva EV, Wang BZ, Vzorov AN, Wang L, Wang YC, Bozja J, et al. Enhanced mucosal immune responses to HIV virus-like particles containing a membrane-anchored adjuvant. *MBio* (2011) 2:e328–310. doi:10.1128/mBio.00328-10
151. Garinot M, Fievez V, Pourcelle V, Stoffelbach F, des Rieux A, Plapied L, et al. PEGylated PLGA-based nanoparticles targeting M cells for oral vaccination. *J Control Release* (2007) 120:195–204. doi:10.1016/j.jconrel.2007.04.021
152. Foster N, Clark MA, Jepson MA, Hirst BH. *Ulex europaeus* 1 lectin targets microspheres to mouse Peyer's patch M-cells in vivo. *Vaccine* (1998) 16:536–41. doi:10.1016/S0264-410X(97)00222-3
153. Wu Y, Wang X, Csencsits KL, Haddad A, Walters N, Pascual DW. M cell-targeted DNA vaccination. *Proc Natl Acad Sci U S A* (2001) 98:9318–23. doi:10.1073/pnas.161204098
154. Manocha M, Pal PC, Chitralekha KT, Thomas BE, Tripathi V, Gupta SD, et al. Enhanced mucosal and systemic immune response with intranasal immunization of mice with HIV peptides entrapped in PLG microparticles in combination with *Ulex europaeus*-I lectin as M cell target. *Vaccine* (2005) 23:5599–617. doi:10.1016/j.vaccine.2005.06.031
155. Gupta PN, Khatri K, Goyal AK, Mishra N, Vyas SP. M-cell targeted biodegradable PLGA nanoparticles for oral immunization against hepatitis B. *J Drug Target* (2007) 15:701–13. doi:10.1080/10611860701637982
156. Ma T, Wang L, Yang T, Ma G, Wang S. M-cell targeted polymeric lipid nanoparticles containing a toll-like receptor agonist to boost oral immunity. *Int J Pharm* (2014) 473:296–303. doi:10.1016/j.ijpharm.2014.06.052
157. Sharma G, Lakkadwala S, Modgil A, Singh J. The role of cell-penetrating peptide and transferrin on enhanced delivery of drug to brain. *Int J Mol Sci* (2016) 17:E806. doi:10.3390/ijms17060806

Conflict of Interest Statement: The authors declare that the research was conducted in the absence of any commercial or financial relationships that could be construed as a potential conflict of interest.

frontiers in Immunology

ORIGINAL RESEARCH
published: 02 March 2018
doi: 10.3389/fimmu.2018.00325

Room Temperature Stable PspA-Based Nanovaccine Induces Protective Immunity

*Danielle A. Wagner-Muñiz[1], Shannon L. Haughney[2], Sean M. Kelly[2], Michael J. Wannemuehler[1,3] and Balaji Narasimhan[2,3]**

[1] Department of Veterinary Microbiology and Preventive Medicine, Iowa State University, Ames, IA, United States, [2] Department of Chemical and Biological Engineering, Iowa State University, Ames, IA, United States, [3] Nanovaccine Institute, Iowa State University, Ames, IA, United States

Streptococcus pneumoniae is a major causative agent of pneumonia, a debilitating disease particularly in young and elderly populations, and is the leading worldwide cause of death in children under the age of five. While there are existing vaccines against *S. pneumoniae*, none are protective across all serotypes. Pneumococcal surface protein A (PspA), a key virulence factor of *S. pneumoniae*, is an antigen that may be incorporated into future vaccines to address the immunological challenges presented by the diversity of capsular antigens. PspA has been shown to be immunogenic and capable of initiating a humoral immune response that is reactive across approximately 94% of pneumococcal strains. Biodegradable polyanhydrides have been studied as a nanoparticle-based vaccine (i.e., nanovaccine) platform to stabilize labile proteins, to provide adjuvanticity, and enhance patient compliance by providing protective immunity in a single dose. In this study, we designed a room temperature stable PspA-based polyanhydride nanovaccine that eliminated the need for a free protein component (i.e., 100% encapsulated within the nanoparticles). Mice were immunized once with the lead nanovaccine and upon challenge, presented significantly higher survival rates than animals immunized with soluble protein alone, even with a 25-fold reduction in protein dose. This lead nanovaccine formulation performed similarly to protein adjuvanted with Alum, however, with much less tissue reactogenicity at the site of immunization. By eliminating the free PspA from the nanovaccine formulation, the lead nanovaccine was efficacious after being stored dry for 60 days at room temperature, breaking the need for maintaining the cold chain. Altogether, this study demonstrated that a single dose PspA-based nanovaccine against *S. pneumoniae* induced protective immunity and provided thermal stability when stored at room temperature for at least 60 days.

Keywords: pneumococcal infections, pneumococcal surface protein A, polyanhydride, nanovaccine, room temperature stability

OPEN ACCESS

Edited by:
Rajko Reljic, St George's, University of London, United Kingdom

Reviewed by:
Giampiero Pietrocola, University of Pavia, Italy
Anita S. Iyer, Harvard Medical School, United States

***Correspondence:**
Balaji Narasimhan
nbalaji@iastate.edu

Specialty section:
This article was submitted to Vaccines and Molecular Therapeutics, a section of the journal Frontiers in Immunology

Received: *07 December 2017*
Accepted: *06 February 2018*
Published: *02 March 2018*

Citation:
Wagner-Muñiz DA, Haughney SL, Kelly SM, Wannemuehler MJ and Narasimhan B (2018) Room Temperature Stable PspA-Based Nanovaccine Induces Protective Immunity. Front. Immunol. 9:325. doi: 10.3389/fimmu.2018.00325

INTRODUCTION

Community-acquired pneumonia is a debilitating disease and is globally responsible for 16% of deaths in children under the age of five annually (1). *Streptococcus pneumoniae*, a causative agent of bacterial pneumonia, is a Gram-positive bacterial pathogen of humans, which colonizes the upper respiratory tract and leads to the development of potentially life-threatening diseases, such as otitis

media, sinusitis, and pneumonia, with pneumonia being the most serious of these conditions (2, 3). While otitis media and sinusitis are not as severe, they still account for seven million cases in the United States annually (2). *S. pneumoniae* is asymptomatically carried in approximately 25% of healthy individuals and is spread between individuals through respiratory droplets, with children serving as the primary transmission source to adults (4–7). Pneumococcal infections are most prevalent in infants, young children, and the elderly, accounting for over $3 billion spent annually in direct healthcare spending; in addition, 60–87% of all pneumococcal bacteremia cases are associated with pneumonia in adults (2). While control of *S. pneumoniae* by antibiotics has been beneficial, up to 50% of all strains are resistant to erythromycin, with 97% of those also being resistant to azithromycin, making intervention strategies such as vaccination a necessary component of health care management (8). To date, the single most effective advance in the field of pneumonia prevention has been through immunization, though existing vaccines are still not completely effective (9, 10).

Current preventive strategies involve the use of pneumococcal polysaccharide vaccines (PPVs) and pneumococcal conjugate vaccines (PCVs). PPVs (T-independent antigens) comprise capsular polysaccharides, which are poorly immunogenic in very young and elderly individuals, while PCVs (T-dependent antigens) are more effective in these at-risk populations because of the adjoined protein component. While the introduction of PPV23, PCV7, and PCV13 have had significant contributions in reducing the overall global burden of pneumococcal pneumonia, there is still room for improvement (11). As it currently stands, infection with strains not covered by vaccine serotype infections account for approximately 50% of all deaths in individuals over 55 years of age (12). In addition, it has been observed that introduction of new vaccine strategies against *S. pneumoniae*, such as the introduction of PCV10 immunization program for children in the Netherlands or use of PCV7 in Spain, may be directly correlated to an increased emergence of disease caused by non-vaccine serotype strains cases (13–15). It was demonstrated that PCV7 immunization, which contains the 19F serotype antigen, actually caused an increase in pneumococcal infections by the closely related 19A serotype (16). Globally, this is of particular concern when considering the development of a universal vaccine, as it is now clear that the prevalence of certain serotypes differs greatly between age, geographic region, and ethnicity (3, 17, 18). PPV23 encompasses the most pneumococcal serotypes of the commercially available vaccines. However, it is not recommended for use in children under the age of 18 months because of their poor antibody response to T-independent polysaccharide antigens, explaining why PCV13 is recommended for this age group. While the use of PCV and PPV vaccine formulations have effectively reduced the incidence of pneumococcal pneumonia, there is a need for newer vaccines to protect against the emergence of non-vaccine strains of *S. pneumoniae* (19). Coupled with the phase variation in expression of capsular and surface protein antigens, broadly protective vaccines against colonization and invasive pneumococcal disease are likely to require the inclusion of more conserved antigens that will also facilitate the induction of antigen-specific $CD4^+$ T cells (20, 21).

S. pneumoniae has several key virulence factors that play a critical role in colonization, transmission, and tissue damage, including pneumolysin, two neuraminidases, and pneumococcal surface protein A (PspA). PspA is a choline binding protein, one of the most abundant proteins located on the pneumococcal cell surface, and has been shown to be of particular importance in facilitating nasopharangyl colonization through inhibiting host complement responses (22). In the design of new vaccines against *S. pneumoniae*, it is important to consider a target immunogen that will be capable of inducing a broad, serotype-independent, protective immune response. PspA has been of recent interest as a potential vaccine candidate due to its location on the cell surface of all 95 strains of *S. pneumoniae* currently known and its critical role in pneumococcal pathogenesis (3, 23, 24). Anti-PspA antibodies to clades 1 and 2 of PspA have been shown to be cross-protective against *S. pneumoniae* strains encompassing all six clades of PspA, and provide protection when passively transferred to naïve mice as a therapeutic intervention following septic *S. pneumoniae* challenge (17, 25–27). The ability to provide protection across many serotypes of *S. pneumoniae* using only two clades of PspA allows for the design of a broadly cross-protective vaccine when compared to vaccines containing numerous capsular polysaccharides.

Polyanhydride nanoparticle-based vaccines (i.e., nanovaccines) represent next-generation vaccine platforms against pathogens such as *S. pneumoniae*. These nanovaccines are formulated using random copolymers based on 1,8-bis-(p-carboxyphenoxy)-3,6-dioxaoctane (CPTEG), 1,6-bis-(p-carboxyphenoxy)hexane (CPH), and sebacic acid (SA) and have been extensively studied as a nanovaccine platform against infectious pathogens, such as influenza virus, *Yersinia pestis*, and *Bacillus anthracis* (28–31).

Polyanhydrides provide vaccine delivery benefits and adjuvant properties that make them well suited as a vaccine delivery platform. These materials exhibit high biocompatibility with minimal injection site reactivity (32–34) (i.e., tenderness, swelling, and pain) in comparison to traditional adjuvants, such as Alum, which has been associated with immunization site tenderness and pain, and are currently FDA-approved for use to treat malignant gliomas in the brain (35, 36). In addition, polyanhydrides are hydrophobic and exhibit surface erosion characteristics, which helps stabilize labile proteins, protects protein denaturation from enzymatic cleavage and acidic degradation products, and allows for the prolonged release of antigen (28, 37–41). The sustained release of antigen allows for enhanced bioavailability of antigen to drive adaptive immune responses and allows for single dose administration and dose-sparing capabilities (30, 42–44). Previous work has shown that mice immunized with a single dose of nanovaccine encapsulating *Y. pestis* fusion protein F1-V were completely protected against *Y. pestis* lethal challenge after at least 280 days post-immunization (DPI) (31). Varying polyanhydride copolymer composition has shown to modulate internalization and persistence within APCs *in vitro*, as well as induction of both cellular and humoral immune responses *in vivo* indicating the ability to tailor polymer chemistry in order to rationally design nanovaccines that optimally inducing antigen-specific protective immunity (31, 42, 45–54).

Previous work from our laboratories has demonstrated that PspA encapsulated into nanoparticles maintained its stability, conformational structure, as well as biological activity upon release, which was measured using an apolactoferrin binding assay (37). In this same work, mice immunized with a single dose of the nanovaccine generated robust antibody titer and avidity to PspA, equivalent to that of antigen adjuvanted with MPLA. However, the protective efficacy of a PspA-based nanovaccine against lethal challenge has not been demonstrated. In this study, the ability of various polyanhydride nanovaccine chemistries as vaccine candidates was evaluated and it was demonstrated that a lead PspA-based nanovaccine protected animals against lethal challenge with a 25-fold reduction in overall PspA dose. Furthermore, this lead formulation was shown to be capable of storage at room temperature for at least 2 months without any loss of efficacy.

MATERIALS AND METHODS

Materials

Chemicals used for monomer and polymer synthesis included sodium hydroxide, hydrobenzoic acid, dibromohexane, 1-methyl-2-pyrrolidinone, SA monomer, and triethylene glycol purchased from Sigma Aldrich (St. Louis, MO, USA). Acetic anhydride, ethyl ether, petroleum ether, chloroform, methylene chloride, hexane, acetone, sulfuric acid, potassium carbonate, dimethyl formamide, toluene, acetonitrile, N,N-dimethylacetamide, and acetic acid were purchased from Fisher Scientific (Fairlawn, NJ, USA); 4-p-fluorobenzonitrile was purchased from Apollo Scientific (Cheshire, UK). For ^{1}H NMR analysis of the copolymers, deuterated chloroform and dimethyl sulfoxide were purchased from Cambridge Isotope Laboratories (Andover, MA, USA). The N-terminal region of a recombinant PspA (UAB055, PspA/Rx1 AA1 to 303, clade 2 PspA of the PspA family 1) was produced by Dr. David McPherson (University of Alabama at Birmingham) as described previously (55). Prior to immunization, endotoxin was removed from the protein using endotoxin removal beads (Miltenyi Biotec, Bergisch Gladbach, Germany) according to the manufacturer's instructions followed by dialysis and lyophilization. The final endotoxin content of the protein was determined to be less than 1.9 EU/mg as determined by a limulus amebocyte lysate chromogenic endotoxin quantification kit (Thermo Fisher Scientific).

Copolymer and Nanoparticle Synthesis

Monomers of CPH and CPTEG were synthesized as previously described (28, 49). A 50:50 molar composition copolymer of CPH and CPTEG and a 20:80 molar composition copolymer of CPH and SA was synthesized using melt condensation as described by Torres et al. (28). PspA protein, 1% (w/w), was encapsulated into polyanhydride nanoparticles using solid/oil/oil nanoprecipitation, as previously described (37). Excess buffer was removed from PspA protein solution using a 5 kDa MWCO dialysis microcentrifuge tube and the resulting protein solution was lyophilized overnight at −40°C under vacuum. The lyophilized protein and the respective copolymer was then dissolved in methylene chloride at a concentration of 20 mg/mL of solvent. The solution was sonicated using the VibraCell ultrasonic probe (Sonics & Materials, Inc., Newtown, CT, USA) to ensure complete dissolution and homogenization of the protein and the copolymer. The resulting solution was then added to pentane at a 1–200 (v/v) ratio of methylene chloride to pentane at 20°C for the 20:80 CPH:SA nanoparticle formulation or at a 1–250 (v/v) ratio of methylene chloride to pentane at −40°C and for the 50:50 CPTEG:CPH nanoparticle formulation. Nanoparticles were collected using vacuum filtration. Surface charge of representative 20:80 CPH:SA and 50:50 CPTEG:CPH nanoparticle formulations were measured using quasi-elastic light scattering (Zetasizer Nano, Malvern Instruments Ltd., Worcester, UK).

Animals

CBA/CaHN-Btkxid/J (CBA/N) mice were purchased from Jackson Laboratory (Bar Harbor, ME, USA) and used for the immunization studies. These mice have a mutation in their Bruton's tyrosine kinase gene. Due to this mutation, these mice are unable to initiate a proper antibody response to Type II thymic-independent antigens (e.g., capsular polysaccharides), and are, thus, able to better mimic natural antibody responses in at-risk elderly or young populations. Mice were housed under specific pathogen-free conditions where all bedding, caging, water, and feed were sterilized prior to use. All studies were conducted with the approval of the Iowa State University Institutional Animal Care and Use Committee.

Immunization Protocols

Groups of 8–10 CBA/N mice were immunized subcutaneously at the nape of the neck with 0–20 μg PspA, 0–5 μg PspA encapsulated into 50–500 μg polyanhydride nanoparticles, and/or 50 μL of Imject Alum Adjuvant (ThermoFisher Scientific) and delivered in a total volume of 100 μL. Immunization groups for the individual studies (see **Tables 1** and **2**) comprised the following : (i) 25 μg soluble PspA alone, (ii) 25 μg PspA administered with 50 μL Imject Alum, (iii) 5 μg PspA encapsulated into 250 μg 50:50 CPTEG:CPH nanoparticles + 20 μg soluble PspA, (iv) 5 μg PspA encapsulated into 250 μg 20:80 CPH:SA nanoparticles + 20 μg soluble PspA, (v) 1 μg soluble PspA alone, (vi) 1 μg PspA administered with 50 μL Imject Alum, (vii) 1 μg PspA encapsulated into 50 μg 50:50 CPTEG:CPH nanoparticles, (viii) 0.5 μg PspA encapsulated into 25 μg 50:50 CPTEG:CPH nanoparticles + 25 μg blank 50:50 CPTEG:CPH nanoparticles + 0.5 μg soluble PspA, or (ix)

TABLE 1 | 25 μg Pneumococcal surface protein A (PspA)-containing single dose vaccine treatments groups.

Formulation	sPspA (μg)	ePspA (μg)
50:50 CPTEG:CPH PspA Nanovaccine	20	5
20:80 CPH:SA PspA Nanovaccine	20	5
sPspA + Alum	25	0
sPspA	25	0
Saline	0	0

Separate groups of mice were immunized s.c. and all formulations were delivered in 100 μL total volume. Soluble PspA is represented as sPspA, and nanoparticle-encapsulated PspA is represented as ePspA.

TABLE 2 | One-microgram pneumococcal surface protein A (PspA)-containing single dose vaccine treatments groups.

Formulation	sPspA (μg)	ePspA (μg)
PspA Nanovaccine	0	1
PspA Nanovaccine + sPspA	0.5	0.5
sPspA + Alum	1	0
sPspA	1	0
Saline	0	0

Separate groups of mice were immunized s.c. and all formulations were delivered in 100 μL total volume. Soluble PspA is represented as sPspA and nanoparticle-encapsulated PspA is represented as ePspA.

saline control. Blood was collected from mice *via* saphenous vein and serum was isolated following centrifugation (10,000 rcf for 10 min) at days 17 or 21 DPI. Serum was stored at −20°C until analysis could be performed.

S. pneumoniae Challenge

S. pneumoniae strain A66.1, of PspA family 1, clade 2 was used for challenge and grown as previously described (56, 57). Briefly, the bacteria was grown at 37°C for 18 h in filter-sterilized Todd-Hewitt broth with 0.5% yeast extract, and stored at −80°C at a concentration of 1×10^8 CFU/mL. Inoculum was diluted to a concentration of 2.5×10^4 CFU/mL in sterile PBS and 100 μL was administered intraveneously at 24 DPI. Mice were monitored three times per day for the duration of the challenge (14 days). Body temperatures and body condition scores were also recorded once per day. Mice were sacrificed when determined to be moribund or at 14 days post-challenge.

Anti-PspA Antibody Titer

Anti-PspA antibody titers were determined *via* an ELISA as described previously (37). Briefly, high-binding Costar 590 EIA/RIA microtiter plates (Corning) were coated overnight at 4°C with 0.5 μg/mL PspA. The blocking buffer for this assay comprised 2.5% (w/v) powdered milk dissolved in PBS-T and incubated for 2 h at 56°C to inactivate any endogenous phosphatase activity. PspA-coated plates were incubated with blocking solution for 2 h at room temperature before being washed three times with PBS-T. Serum obtained from immunized mice was added to the first well of a row at a dilution of 1:200 and serially diluted in PBS-T containing 1% (v/v) goat serum. Each serum sample was tested in duplicate. Following incubation overnight at 4°C, plates were washed three times with PBS-T after which secondary antibody was added at a dilution of 1 μg/mL. The secondary antibody used in these studies was alkaline phosphatase-conjugated goat anti-mouse IgG heavy and light chain (Jackson ImmunoResearch) and was incubated on the plates for 2 h at room temperature. Plates were then washed three times with PBS-T and alkaline phospatase substrate (Fisher Scientific, Pittsburgh, PA, USA) was added at a concentration of 1 mg/mL dissolved in 50 mM sodium carbonate, 2 mM magnesium chloride buffer at pH 9.3 for colorimetric development. Plates were analyzed after 30 min using a SpectraMax M3 microplate reader at a wavelength of 405 nm. Titer is reported as the reciprocoal of serum dilution at which optical density value was at least twice that of the saline group average plus two SDs.

Shelf Stability of Stored PspA Nanovaccine

Shelf stability of the PspA nanovaccine was assessed *via* ELISA and lethal challenge. 50:50 CPTEG:CPH nanoparticles encapsulating PspA were taken out of the freezer (−80°C) and stored as a dry powder formulation at 25°C (room temperature) in a glass desiccator containing drierite for 60 days prior to immunization. Soluble PspA was stored at 4°C and combined with Imject Alum prior to immunization. A separate group of nanoparticles were kept in the freezer over the course of this experiment as a freezer-stored standard control. Following room temperature storage, vaccine efficacy was evaluated by immunizing mice with a nanovaccine dose equivalent to 1 μg PspA per animal from one of the storage conditions above, soluble PspA adsorbed to Alum, or the saline control and assessing antibody titer *via* ELISA 21 DPI (see "Anti-PspA Antibody Titer" for details). Following lethal challenge with 2,500 CFU of *S. pneumoniae* (see *S. pneumoniae* challenge for details), survival was assessed over the next 24 days.

Statistical Analyses

Statistical analyses were performed using the Gehan–Breslow–Wilcoxon test and the one-way analysis of variance using Tukey's multiple comparisons test. A p-value ≤ 0.05 was considered statistically significant. All analyses were performed using GraphPad Prism v. 7.0 software.

RESULTS

Synthesis and Characterization of PspA-Encapsulated Polyanhydride Nanoparticles

The nanoparticle chemistries chosen for the current study were based on 50:50 CPTEG:CPH and 20:80 CPH:SA copolymers, consistent with our previous work, in which these chemistries were shown to provide protein structural stability and maintain the functional activity of PspA following release (37). The nanoparticles were synthesized using solid/oil/oil emulsion (54). The PspA release kinetics from these formulations are described in our previous work (37). Scanning electron photomicrographs of the nanoparticles revealed similar sizes for the two formulations, with sizes of 455 ± 175 and 422 ± 163 nm for 50:50 CPTEG:CPH and 20:80 CPH:SA nanoparticles, respectively (**Figure 1**). Zeta potential measurements of empty 20:80 CPH:SA and 50:50 CPTEG:CPH nanoparticles revealed that the particles had a negative surface charge, with zeta potentials of -41.9 ± 0.9 and -33.1 ± 5.1 mV, respectively, consistent with previous publications (45, 48, 58).

Immunization with PspA-Based Nanovaccines Induces Protective Antibody Response

Previously, it was demonstrated that mice vaccinated with PspA-based nanovaccines induced a robust humoral response; however, protective efficacy was not evaluated (37). In the current studies, separate groups of CBA/CaHN mice ($n = 8$ per

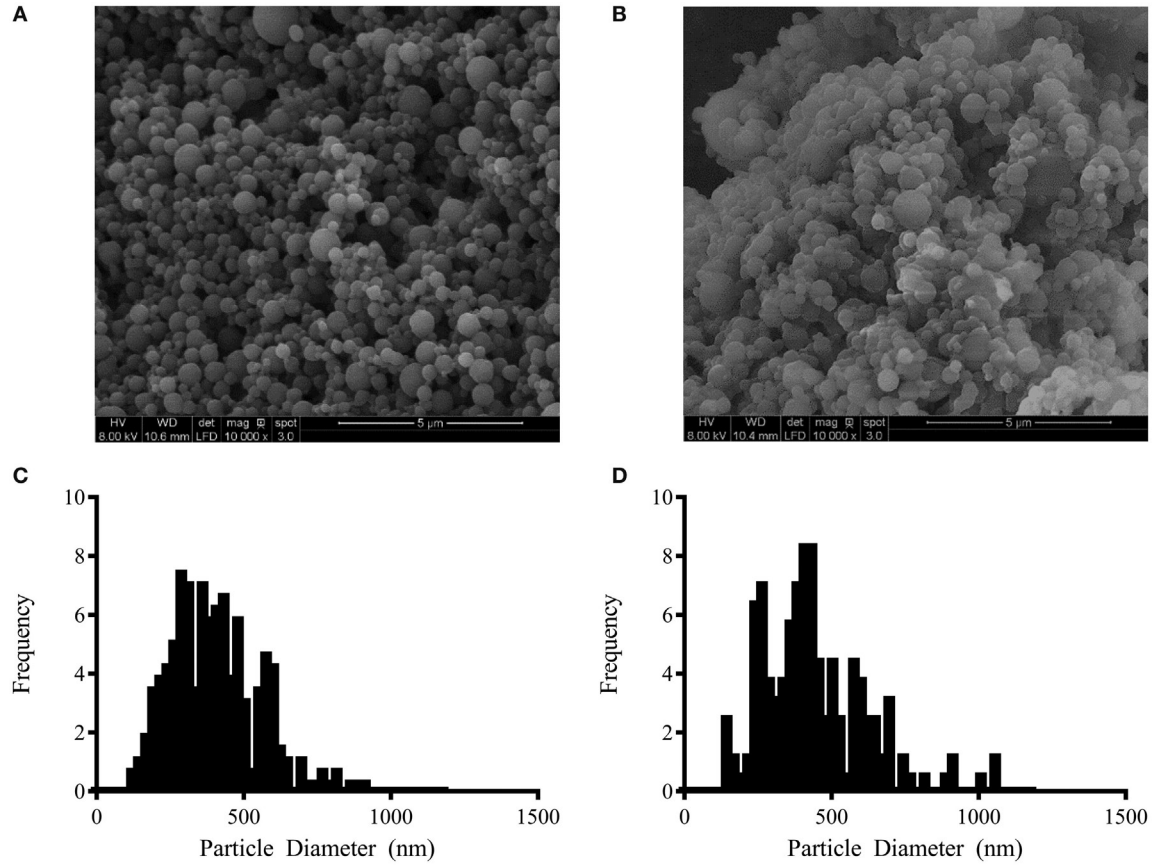

FIGURE 1 | Pneumococcal surface protein A nanovaccine characterization. Representative scanning electron photomicrographs of **(A)** 2% PspA-loaded (w/w) 20:80 CPH:SA nanoparticles and **(B)** 2% PspA-loaded (w/w) 50:50 CPTEG:CPH nanoparticles (scale bar = 5 μm). **(C)** Particle size distribution of 2% PspA-loaded (w/w) 20:80 CPH:SA nanoparticles (422 ± 163 nm). **(D)** Particle size distribution of 2% PspA-loaded (w/w) 50:50 CPTEG:CPH nanoparticles (455 ± 175 nm).

group) were immunized subcutaneously as follows: (i) 25 μg soluble PspA alone, (ii) 25 μg PspA administered with Imject Alum, (iii) PspA-containing 50:50 CPTEG:CPH nanoparticles, (iv) PspA-containing 20:80 CPH:SA nanoparticles, or (v) saline (**Table 1**). Both the nanovaccine formulations contained 5 μg of encapsulated PspA along with 20 μg of soluble protein, as shown in **Table 1**. Anti-PspA total IgG titers were evaluated at 17 DPI and there were no significant differences in titer between vaccinated groups (**Figure 2A**). Mice were challenged with a lethal dose of *S. pneumoniae* strain A66.1 at 24 DPI and survival was assessed over a period of 2 weeks. All PspA naïve (saline) mice succumbed to infection within 4 days, while all the immunized animals showed prolonged survival following challenge. At 14 days post-challenge, only 25% of the (non-adjuvanted) soluble PspA-immunized animals survived, whereas adjuvanting the protein with alum provided 100% protection. Immunization with the 20:80 CPH:SA nanovaccine resulted in 87% survival, while 100% of the animals immunized with 50:50 CPTEG:CPH nanovaccine were protected, as shown in **Figure 2B**. The survival data, in correlation with the antibody titers indicate that not only is PspA an effective immunogen, but induces protective immunity when delivered with an adjuvant. Though both nanoparticle chemistries protected animals from lethal challenge compared to saline, the 50:50 CPTEG:CPH PspA nanovaccine performed significantly ($p \leq 0.008$) better than soluble PspA (i.e., sPspA) alone. Based on these results, we selected the 50:50 CPTEG:CPH nanovaccine as our lead candidate for further evaluation.

PspA Nanovaccine Demonstrates Dose-Sparing Capabilities

Rational design of vaccines using subunit proteins involves considering total cost of the end product, as well as protein availability that potentially impacts vaccine shortages. Our previous work has shown that encapsulating a lowered dose of antigen into polyanhydride nanoparticles can induce a robust immune response (43). In the current studies, the ability of the nanovaccine to provide dose-sparing (i.e., 25-fold reduction) was evaluated by immunizing separate groups of CBA/N mice ($n = 8$ per group; see **Table 2**) subcutaneously using the following regimens: (i) 1 μg PspA encapsulated into 50:50 CPTEG:CPH nanoparticles (PspA Nanovaccine), (ii) 0.5 μg PspA encapsulated into 50:50 CPTEG:CPH nanoparticles plus 0.5 μg soluble PspA (PspA Nanovaccine + Soluble PspA), (iii) 1 μg soluble PspA administered with Imject Alum, (iv) 1 μg soluble PspA alone, and (v) saline alone (i.e., naïve control). Serum was collected at 21 DPI and analyzed

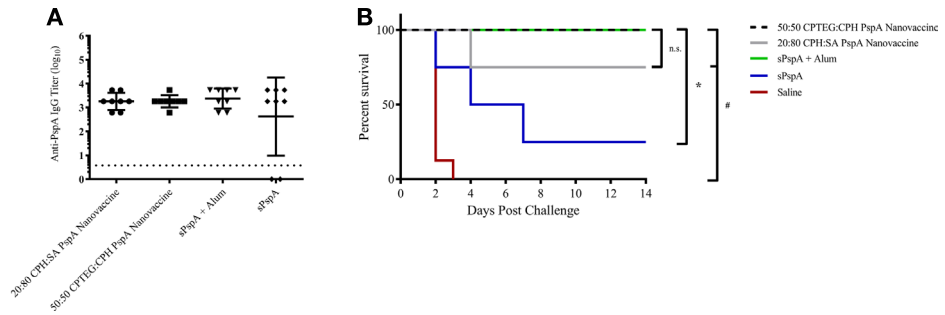

FIGURE 2 | Pneumococcal surface protein A (PspA) nanovaccines are capable of initiating protective immune responses. **(A)** Serum was collected from immunized mice (see **Table 1**) at 17 days post-immunization (DPI) and analyzed for total anti-PspA IgG (data is represented as $\log_{10}$) using ELISA. Dashed line represents background anti-PspA IgG levels in serum from the saline-immunized mice. **(B)** *S. pneumoniae* challenge was performed at 24 DPI by i.v. administration of 2,500 CFUs of A66.1 strain and survival was monitored for 14 days post-challenge. * indicates significance ($p \leq 0.0025$) compared to sPspA alone and # indicates significance ($p \leq 0.001$) compared to saline-treated mice. Data are representative of one independent experiment containing $n = 8$ mice per treatment group.

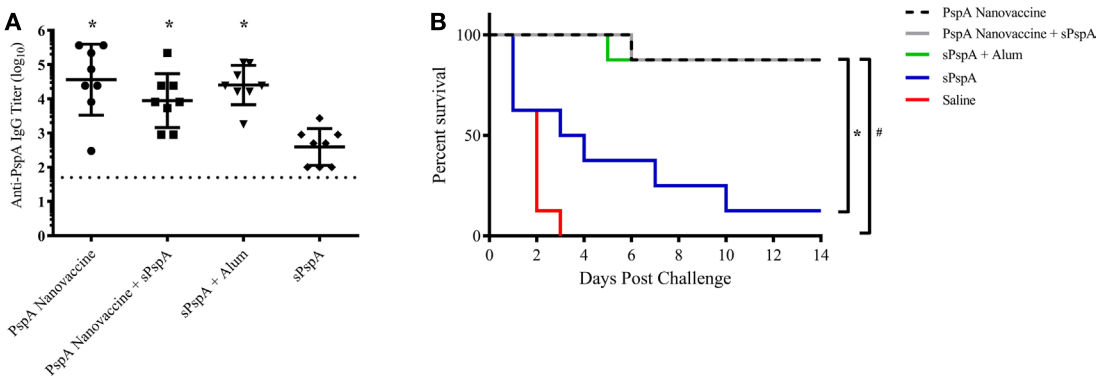

FIGURE 3 | Nanovaccines with 25-fold reduction in total protein provided protection against lethal challenge. **(A)** Serum was collected from immunized mice (see **Table 2**) at 21 days post-immunization (DPI) and analyzed for total anti-PspA IgG (data is represented as $\log_{10}$) using ELISA. Dashed line represents background anti-PspA IgG levels in the serum from the saline-immunized mice. * indicates significance ($p \leq 0.008$) compared to sPspA alone. **(B)** *S. pneumoniae* challenge was performed at 24 DPI by i.v. administration of 2,500 CFUs of A66.1 strain and survival was monitored for 14 days. * indicates significance ($p \leq 0.003$) compared to sPspA alone and # indicates significance ($p \leq 0.0002$) compared to saline-treated mice. Data are representative of one independent experiment containing $n = 8$ mice per treatment group.

for total anti-PspA IgG. Mice immunized with the nanovaccines or PspA + Alum showed significantly ($p \leq 0.008$) higher titers to PspA compared to soluble PspA alone (**Figure 3A**). Survival rates following lethal challenge showed significantly ($p \leq 0.001$) higher survival (87.5%) in mice immunized with both the nanovaccine formulations compared to animals immunized with soluble PspA (12%) (**Figure 3B**). Animals immunized with PspA adjuvanted with Alum performed similarly to the animals receiving the nanovaccine formulations. There were no observable differences in disease severity between the immunized animals, as measured by body condition scores and temperature (data not shown). In addition, soluble PspA administered in conjunction with 100 μg of empty 50:50 CPTEG:CPH nanoparticles, performed similarly to other adjuvanted groups, further indicating the ability for PspA to initiate a protective immune response when adjuvanted properly (data not shown). No significant differences in survival were observed between mice immunized with PspA fully encapsulated within the nanoparticles (i.e., PspA Nanovaccine) and animals that received half of the protein as a soluble bolus (i.e., PspA Nanovaccine + Soluble PspA). Eliminating the use of soluble PspA in the nanovaccine is beneficial when designing a shelf-stable dry powder formulation for the long-term storage of a PspA nanovaccine.

PspA Nanovaccine Maintains Efficacy following Room Temperature Storage

To evaluate the potential for a room temperature stored (i.e., non-refrigerated) PspA nanovaccine, 1 μg of PspA was encapsulated within 50 μg of 50:50 CPTEG:CPH nanoparticles (i.e., 2 wt.% loading) and stored at room temperature (25°C) and standard storage conditions (−80°C), as detailed in the Section "Materials and Methods" and as previously described (28). The PspA encapsulated nanovaccine was stored at −80°C (freezer stored) or at 25°C for 60 days. The soluble PspA was stored at 4°C

and mixed with Alum prior to immunization. Following storage, separate groups of mice (n = 8–10 per group) were immunized subcutaneously with the PspA nanovaccine stored at the different conditions or with alum-adjuvanted PspA and serum was collected and analyzed at 21 DPI. Storage conditions did not have a significant effect on anti-PspA IgG titers, with all of the PspA nanovaccines performing similarly (**Figure 4A**). Mice were then challenged with a lethal dose of *S. pneumoniae* at 24 DPI and survival was monitored for 2 weeks. All of the non-immunized mice succumbed to challenge within 4 days post challenge, while the nanovaccine-immunized mice presented with 60–70% survival with a single dose (**Figure 4B**). Once again, no significant differences were observed between the survival rates of mice immunized with the PspA nanovaccine stored at various conditions and those immunized with soluble PspA adjuvanted with Alum. These data indicate that the PspA nanovaccine is efficacious when stored both in the freezer or at room temperature for time periods up to 60 days and performs similarly to refrigerated PspA adjuvanted with Alum.

DISCUSSION

Streptococcus pneumoniae is a causative agent of debilitating bacterial pneumonia. While many existing vaccines have proven to be valuable in reducing overall global disease burden, none are without limitations. Newly developed vaccine strategies against *S. pneumoniae* have identified several novel antigens, including PspA. Anti-PspA antibodies have been observed, following natural colonization or infection in children (59, 60). Other studies have shown success against lethal intranasal or septic *S. pneumoniae* challenge by vaccinating with PspA, which further indicates its potential as an efficacious vaccine immunogen (22, 61).

Aluminum hydroxide (i.e., Alum)-based adjuvants are widely used because of their ability to promote Th2 immune responses (62). However, Alum-based vaccines are associated with higher levels of immunization site tissue reactogenicity (63, 64). Immunization-site tenderness and pain are the most commonly reported symptoms following immunization with vaccines containing Alum. Prevalence of these adverse reactions has been found to be directly associated with increased protein dose administered and decreased age of the vaccinated individuals (65–67). Previous work with polyanhydride nanovaccines has shown low-level tissue site inflammation and toxicity making them a safe alternative to traditional vaccine adjuvants (32, 33, 41). Therefore, nanovaccines may represent a safe and efficacious alternative to Alum-based vaccines, which have limitations associated with administration site reactogenicity and only promote humoral immune responses against PspA.

Work from other laboratories has shown limited success using nanotechnology-based vaccine platforms with PspA in various animal models though, to date, none of these studies have shown protection against lethal challenge with single-dose immunization (68–70). Previous work from our laboratories has indicated that encapsulation of PspA into polyanhydride nanoparticles is capable of retaining protein structure and function, which enabled initiation of a humoral immune response (37). Building upon these studies, PspA was encapsulated within both 50:50 CPTEG:CPH and 20:80 CPH:SA nanoparticle formulations in the current work. Both formulations produced nanoparticles of similar size and size distribution (**Figure 1**). The size, morphology, and size distribution of these particles were similar to those previously reported for these formulations (28, 30, 37, 42). Following subcutaneous immunization of mice with a single dose of either formulation, anti-PspA IgG antibodies were produced, in agreement with our previous findings (37). Following lethal septic challenge, both nanovaccine formulations (containing 25 μg PspA) were capable of conferring protective immunity in mice, with 87.5% survival in 20:80 CPH:SA nanovaccine-immunized mice and 100% protection in those that received the 50:50 CPTEG:CPH nanovaccine (**Figure 2**). Based on the increased protection and higher antibody titers observed following immunization with a single dose of the 50:50 CPTEG:CPH

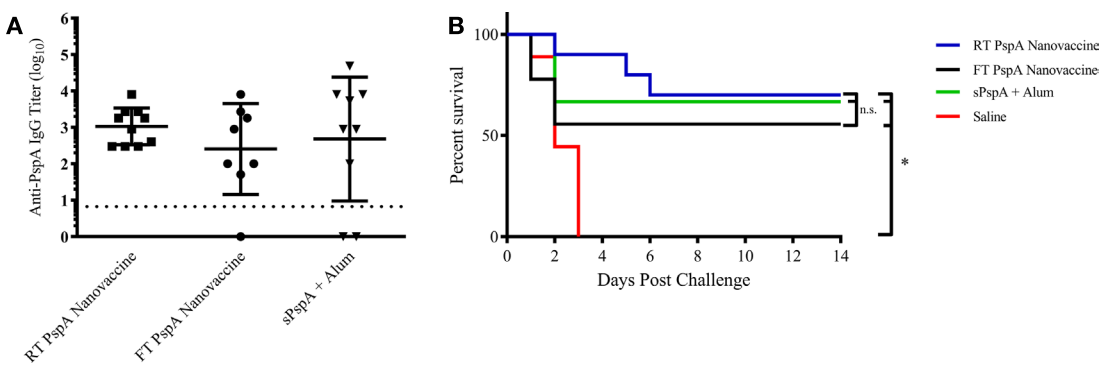

FIGURE 4 | Room temperature-stored Pneumococcal surface protein A (PspA) nanovaccine maintains efficacy after 60 days. **(A)** Serum was collected from groups of immunized mice at 21 days post-immunization (DPI) with vaccine stored at different conditions as indicated and analyzed for total anti-PspA IgG (data are represented as $\log_{10}$) using ELISA. Dashed line represents background anti-PspA IgG levels in the serum from the saline-immunized mice. **(B)** *S. pneumoniae* challenge was performed at 24 DPI by i.v. administration of 2,500 CFUs of A66.1 strain and survival was monitored for 14 days. * indicates significance ($p \leq 0.001$) compared to saline-treated mice. Data are representative of one independent experiment containing n = 8–10 mice per treatment group.

nanovaccine formulation, this chemistry was selected as the lead candidate nanovaccine.

Reducing the amount of protein necessary per dose can greatly reduce the cost associated with using a recombinant protein vaccine, thereby allowing for the production and storage of more doses. Most of the published reports evaluating PspA-based vaccine success immunized mice with a minimum of 5 μg of antigen plus an adjuvant and required multiple boosts (56, 61, 71, 72). Indeed, a recent report demonstrated complete protection in mice receiving 0.5 μg of PspA adjuvanted with poly(I:C) intranasally; however, the immunization schedule required three doses to provide protection (71). The need for a single dose vaccination regimen cannot be overstated from a patient compliance standpoint because according to the WHO, an estimated 29% of children aged 1 month–5 years die each year from vaccine preventable diseases, citing non-compliance with the immunization regimen as a key reason for lack of successful national vaccination programs (73). Therefore, single-dose vaccines can aid in improving patient compliance, reduce cost, and improve national immunization rates worldwide. Recent work from our laboratories has demonstrated that 25 μg of ovalbumin encapsulated into polyanhydride microparticles was able to elicit robust antibody titers equivalent to a 16× larger soluble dose of ovalbumin while 25 μg of soluble ovalbumin alone was unable to elicit detectable antibody responses (43). In order to corroborate these results with PspA, the dose of antigen evaluated was reduced 25-fold to 1 μg. Immunization with the 1 μg PspA-based 50:50 CPTEG:CPH nanovaccine formulation, both with and without soluble PspA, induced production of high anti-PspA IgG titers (**Figure 3A**), with very little reduction in overall antibody titer compared to the previous study with a 25 μg dose of PspA (i.e., data in **Figure 2**). Antibody titers were similar between mice immunized with 1 μg of soluble PspA administered with Alum or with the nanovaccine formulations, with the highest overall titers observed in mice immunized with the fully encapsulated nanovaccine formulation. When compared to soluble protein adjuvanted with Alum, mice immunized with the 50:50 CPTEG:CPH nanovaccine were similarly protected from lethal challenge. Furthermore, 87.5% of the animals challenged with the reduced dose PspA nanovaccine (with or without soluble PspA) were protected (**Figure 3B**). These data demonstrate that reducing the protein dose by 25-fold had little effect on survival, with both the fully encapsulated PspA nanovaccine and the nanovaccine administered with a soluble bolus providing significantly higher survival following lethal challenge, compared to soluble protein alone.

By eliminating the soluble protein component from vaccine formulations, nanovaccines can be stored as a dry powder outside of refrigeration with the potential for long-term shelf storage, thereby circumventing the cold chain. As it currently stands, all prequalified WHO vaccines require refrigeration (73). Nanovaccines may enable next-generation vaccines to be stored without the need for refrigeration (i.e., eliminating the cold chain), allowing for vaccines to be sent to remote locations in need for vaccination, resulting in reduced medical costs and productivity losses associated with disease (74). Previous work from our laboratories demonstrated that nanovaccines encapsulating PspA were able to retain protein structure and activity following release, and a nanovaccine encapsulating the Bacillus anthracis protective antigen (PA) released biologically and immunologically functional protein following storage at both room temperature and above after 4 months (28, 37). By contrast, aluminum salt-based adjuvants have been reported to alter the structure of proteins and decrease thermal stability following adsorption (75), and previous work from our laboratories has shown that PA adsorbed to alum lost its functional activity when stored for 4 months at refrigerated conditions or above (28). Following storage at room temperature for 60 days, the PspA nanovaccine was shown to be efficacious, as measured by antibody titer and survival (**Figure 4**). PspA adsorbed to alum performed similarly, however, because PspA is a stable protein with coiled structure, it is likely that differences may be observed between the efficacy of the nanovaccine and alum-based formulations following storage for an extended period of time, or at elevated temperature, and should be evaluated in future studies (22). As such, this work indicates that the PspA nanovaccine formulation can be stored as a dry powder for at least 60 days while maintaining its immunogenicity.

In summary, this work describes the design of a safe next-generation PspA-based pneumonia nanovaccine with dose-sparing, protective immunity, and enhanced room temperature storage. These studies are promising first steps with respect to establishing the polyanhydride nanovaccine platform as an alternative to traditional vaccines in terms of reduced cost (enabled by the dose sparing and single dose capabilities) and difficulties associated with transportation and storage of vaccines in developing countries (enabled by the superior room temperature storage capabilities).

ETHICS STATEMENT

This study was carried out in accordance with the recommendations of the Iowa State University Institutional Animal Care and Use Committee. The protocol was approved by the Iowa State University Institutional Animal Care and Use Committee.

AUTHOR CONTRIBUTIONS

DW-M, SH, and SK performed the experiments and analyzed the data. MW and BN, together with DW-M, SH, and SK, designed the experimental plan. All the authors participated in writing the manuscript.

FUNDING

The authors thank Dr. David McPherson of the University of Alabama at Birmingham for producing the recombinant PspA used in this work. The authors acknowledge financial support from NIH-NIAID (R56-AI075026) and the Nanovaccine Institute. BN acknowledges the support of the Vlasta Klima Balloun Faculty Chair.

REFERENCES

1. O'Brien KL, Wolfson LJ, Watt JP, Henkle E, Deloria-Knoll M, McCall N, et al. Burden of disease caused by *Streptococcus pneumoniae* in children younger than 5 years: global estimates. *Lancet* (2009) 374:893–902. doi:10.1016/S0140-6736(09)61204-6
2. Huang SS, Johnson KM, Ray GT, Wroe P, Lieu TA, Moore MR, et al. Healthcare utilization and cost of pneumococcal disease in the United States. *Vaccine* (2011) 29:3398–412. doi:10.1016/j.vaccine.2011.02.088
3. Jedrzejas MJ. Pneumococcal virulence factors : structure and function pneumococcal virulence factors: structure and function. *Microbiol Mol Biol Rev* (2001) 65:187–207. doi:10.1128/MMBR.65.2.187
4. Althouse BM, Hammitt LL, Grant L, Wagner BG, Reid R, Larzelere-Hinton F, et al. Identifying transmission routes of *Streptococcus pneumoniae* and sources of acquisitions in high transmission communities. *Epidemiol Infect* (2017) 145:2750–8. doi:10.1017/S095026881700125X
5. Mendy AL, Agbla SC, Odutola AA, Antonio M, Greenwood M, Sutherland JS, et al. Kinetics of antibodies against pneumococcal proteins and their relationship to nasopharyngeal carriage in the first two months of life. *PLoS One* (2017) 12(10):e0185824. doi:10.1371/journal.pone.0185824
6. Quintero B, Araque M, Van Der Gaast-De Jongh C, Escalona F, Correa M, Morillo-Puente S, et al. Epidemiology of *Streptococcus pneumoniae* and *Staphylococcus aureus* colonization in healthy Venezuelan children. *Eur J Clin Microbiol Infect Dis* (2011) 30:7–19. doi:10.1007/s10096-010-1044-6
7. Wyllie AL, Pannekoek Y, Bovenkerk S, van Engelsdorp Gastelaars J, Ferwerda B, van de Beek D, et al. Sequencing of the variable region of rpsB to discriminate between *Streptococcus pneumoniae* and other streptococcal species. *Open Biol* (2017) 7:170074. doi:10.1098/rsob.170074
8. Song J-H, Chang H-H, Suh JY, Ko KS, Jung S-I, Oh WS, et al. Macrolide resistance and genotypic characterization of *Streptococcus pneumoniae* in Asian countries: a study of the Asian Network for Surveillance of Resistant Pathogens (ANSORP). *J Antimicrob Chemother* (2004) 53:457–63. doi:10.1093/jac/dkh118
9. Grabenstein JD, Musey LK. Differences in serious clinical outcomes of infection caused by specific pneumococcal serotypes among adults. *Vaccine* (2014) 32:2399–405. doi:10.1016/j.vaccine.2014.02.096
10. Jacobs DM, Yung F, Hart E, Nguyen MNH, Shaver A. Trends in pneumococcal meningitis hospitalizations following the introduction of the 13-valent pneumococcal conjugate vaccine in the United States. *Vaccine* (2017) 35:6160–5. doi:10.1016/j.vaccine.2017.09.050
11. Bonten MJM, Huijts SM, Bolkenbaas M, Webber C, Patterson S, Gault S, et al. Polysaccharide conjugate vaccine against pneumococcal pneumonia in adults. *N Engl J Med* (2015) 372:1114–25. doi:10.1056/NEJMoa1408544
12. Marrie TJ, Tyrrell GJ, Majumdar SR, Eurich DT. Effect of age on the manifestations and outcomes of invasive pneumococcal disease in adults. *Am. J. Med* (2017) 131(1):.e1–100. doi:10.1016/j.amjmed.2017.06.039
13. Guevara M, Barricarte A, Gil-Setas A, García-Irure JJ, Beristain X, Torroba L, et al. Changing epidemiology of invasive pneumococcal disease following increased coverage with the heptavalent conjugate vaccine in Navarre. *Clin Microbiol Infect* (2009) 15:1013–9. doi:10.1111/j.1469-0691.2009.02904.x
14. Pletz MW, Maus U, Krug N, Welte T, Lode H. Pneumococcal vaccines: mechanism of action, impact on epidemiology and adaption of the species. *Int J Antimicrob Agents* (2008) 32:199–206. doi:10.1016/j.ijantimicag.2008.01.021
15. Vestjens SMT, Wagenvoort GHJ, Grutters JC, Meek B, Aldenkamp AF, Vlaminckx BJM, et al. Changes in pathogens and pneumococcal serotypes causing community-acquired pneumonia in The Netherlands. *Vaccine* (2017) 35:4112–8. doi:10.1016/j.vaccine.2017.06.049
16. Hausdorff WP, Hoet B, Schuerman L. Do pneumococcal conjugate vaccines provide any cross-protection against serotype 19A? *BMC Pediatr* (2010) 10:4. doi:10.1186/1471-2431-10-4
17. Kristian SA, Ota T, Bubeck SS, Cho R, Groff BC, Kubota T, et al. Generation and improvement of effector function of a novel broadly reactive and protective monoclonal antibody against pneumococcal surface protein A of *Streptococcus pneumoniae*. *PLoS One* (2016) 11:e0154616. doi:10.1371/journal.pone.0154616
18. Rolo D, Ardanuy C, Fleites A, Martín R, Liñares J. Diversity of pneumococcal surface protein A (PspA) among prevalent clones in Spain. *BMC Microbiol* (2009) 9:80. doi:10.1186/1471-2180-9-80
19. Weil-Olivier C, van der Linden M, de Schutter I, Dagan R, Mantovani L. Prevention of pneumococcal diseases in the post-seven valent vaccine era: a European perspective. *BMC Infect Dis* (2012) 12:207. doi:10.1186/1471-2334-12-207
20. Khan MN, Xu Q, Pichichero ME. Protection against *Streptococcus pneumoniae* invasive pathogenesis by a protein-based vaccine is achieved by suppression of nasopharyngeal bacterial density during influenza A virus coinfection. *Infect Immun* (2017) 85:e00530–16. doi:10.1128/IAI.00530-16
21. Pichichero ME. Pneumococcal whole-cell and protein-based vaccines: changing the paradigm. *Expert Rev Vaccines* (2017) 16:1181–90. doi:10.1080/14760584.2017.1393335
22. Khan N, Jan AT. Towards identifying protective B-cell epitopes: the PspA story. *Front Microbiol* (2017) 8:742. doi:10.3389/fmicb.2017.00742
23. Mehr S, Wood N. *Streptococcus pneumoniae* – a review of carriage, infection, serotype replacement and vaccination. *Paediatr Respir Rev* (2012) 13:258–64. doi:10.1016/j.prrv.2011.12.001
24. Zafar MA, Hamaguchi S, Zangari T, Cammer M, Weiser JN. Capsule type and amount affect shedding and transmission of *Streptococcus pneumoniae*. *mBio* (2017) 8:e989–917. doi:10.1128/mBio.00989-17
25. Darrieux M, Moreno AT, Ferreira DM, Pimenta FC, de Andrade ALSS, Lopes APY, et al. Recognition of pneumococcal isolates by antisera raised against PspA fragments from different clades. *J Med Microbiol* (2008) 57:273–8. doi:10.1099/jmm.0.47661-0
26. Goulart C, Darrieux M, Rodriguez D, Pimenta FC, Cristina Brandileone MC, Lucia de Andrade AS, et al. Selection of family 1 PspA molecules capable of inducing broad-ranging cross-reactivity by complement deposition and opsonophagocytosis by murine peritoneal cells. *Vaccine* (2010) 29:1634–42. doi:10.1016/j.vaccine.2010.12.074
27. Piao Z, Akeda Y, Takeuchi D, Ishii KJ, Ubukata K, Briles DE, et al. Protective properties of a fusion pneumococcal surface protein A (PspA) vaccine against pneumococcal challenge by five different PspA clades in mice. *Vaccine* (2014) 32:5607–13. doi:10.1016/j.vaccine.2014.07.108
28. Petersen LK, Phanse Y, Ramer-Tait AE, Wannemuehler MJ, Narasimhan B. Amphiphilic polyanhydride nanoparticles stabilize bacillus anthracis protective antigen. *Mol. Pharm* (2012) 9:874–82. doi:10.1021/mp2004059
29. Ross K, Adams J, Loyd H, Ahmed S, Sambol A, Broderick S, et al. Combination nanovaccine demonstrates synergistic enhancement in efficacy against influenza. *ACS Biomater Sci Eng* (2016) 2:368–74. doi:10.1021/acsbiomaterials.5b00477
30. Ulery BD, Kumar D, Ramer-Tait AE, Metzger DW, Wannemuehler MJ, Narasimhan B. Design of a protective single-dose intranasal nanoparticle-based vaccine platform for respiratory infectious diseases. *PLoS One* (2011) 6:e17642. doi:10.1371/journal.pone.0017642
31. Ulery BD, Petersen LK, Phanse Y, Kong CS, Broderick SR, Kumar D, et al. Rational design of pathogen-mimicking amphiphilic materials as nanoadjuvants. *Sci Rep* (2011) 1:198. doi:10.1038/srep00198
32. Adler AF, Petersen LK, Wilson JH, Torres MP, Thorstenson JB, Gardner SW, et al. High throughput cell-based screening of biodegradable polyanhydride libraries. *Comb Chem High Throughput Screen* (2009) 12:634–45.
33. Huntimer L, Ramer-Tait AE, Petersen LK, Ross KA, Walz KA, Wang C, et al. Evaluation of biocompatibility and administration site reactogenicity of polyanhydride-particle-based platform for vaccine delivery. *Adv Healthc Mater* (2013) 2:369–78. doi:10.1002/adhm.201200181
34. Vela-Ramirez JE, Goodman JT, Boggiatto PM, Roychoudhury R, Pohl NLB, Hostetter JM, et al. Safety and biocompatibility of carbohydrate-functionalized polyanhydride nanoparticles. *AAPS J* (2015) 17:256–67. doi:10.1208/s12248-014-9699-z
35. Brem H, Kader A, Epstein JI, Tamargo RJ, Domb A, Langer R, et al. Biocompatibility of a biodegradable, controlled-release polymer in the rabbit brain. *Sel Cancer Ther* (1989) 5:55–65. doi:10.1089/sct.1989.5.55
36. Brem H, Domb A, Lenartz D, Dureza C, Olivi A, Epstein JI. Brain biocompatibility of a biodegradable controlled release polymer consisting of anhydride copolymer of fatty acid dimer and sebacic acid. *J Control Release* (1992) 19:325–9. doi:10.1016/0168-3659(92)90087-8
37. Haughney SL, Petersen LK, Schoofs AD, Ramer-Tait AE, King JD, Briles DE, et al. Retention of structure, antigenicity, and biological function of pneumococcal surface protein A (PspA) released from polyanhydride nanoparticles. *Acta Biomater* (2013) 9:8262–71. doi:10.1016/j.actbio.2013.06.006

38. Renukaradhya GJ, Narasimhan B, Mallapragada SK. Respiratory nanoparticle-based vaccines and challenges associated with animal models and translation. *J Control Release* (2015) 219:622–31. doi:10.1016/j.jconrel.2015.09.047
39. Ross KA, Loyd H, Wu W, Huntimer L, Wannemuehler MJ, Carpenter S, et al. Structural and antigenic stability of H5N1 hemagglutinin trimer upon release from polyanhydride nanoparticles. *J Biomed Mater Res A* (2014) 102:4161–8. doi:10.1002/jbm.a.35086
40. Torres MP, Vogel BM, Narasimhan B, Mallapragada SK. Synthesis and characterization of novel polyanhydrides with tailored erosion mechanisms. *J Biomed Mater Res A* (2006) 76:102–10. doi:10.1002/jbm.a.30510
41. Vela Ramirez JE, Roychoudhury R, Habte HH, Cho MW, Pohl NLB, Narasimhan B. Carbohydrate-functionalized nanovaccines preserve HIV-1 antigen stability and activate antigen presenting cells. *J Biomater Sci Polym Ed* (2014) 25:1387–406. doi:10.1080/09205063.2014.940243
42. Haughney SL, Ross KA, Boggiatto PM, Wannemuehler MJ, Narasimhan B. Effect of nanovaccine chemistry on humoral immune response kinetics and maturation. *Nanoscale* (2014) 6:13770–8. doi:10.1039/C4NR03724C
43. Huntimer L, Wilson Welder JH, Ross K, Carrillo-Conde B, Pruisner L, Wang C, et al. Single immunization with a suboptimal antigen dose encapsulated into polyanhydride microparticles promotes high titer and avid antibody responses. *J Biomed Mater Res B Appl Biomater* (2013) 101:91–8. doi:10.1002/jbm.b.32820
44. Vela Ramirez JE, Tygrett LT, Hao J, Habte HH, Cho MW, Greenspan NS, et al. Polyanhydride nanovaccines induce germinal center B cell formation and sustained serum antibody responses. *J Biomed Nanotechnol* (2016) 12:1303–11. doi:10.1166/jbn.2016.2242
45. Carrillo-Conde B, Song E-H, Chavez-Santoscoy A, Phanse Y, Ramer-Tait AE, Pohl NLB, et al. Mannose-functionalized "pathogen-like" polyanhydride nanoparticles target C-type lectin receptors on dendritic cells. *Mol Pharm* (2011) 8:1877–86. doi:10.1021/mp200213r
46. Carrillo-Conde BR, Ramer-Tait AE, Wannemuehler MJ, Narasimhan B. Chemistry-dependent adsorption of serum proteins onto polyanhydride microparticles differentially influences dendritic cell uptake and activation. *Acta Biomater* (2012) 8:3618–28. doi:10.1016/j.actbio.2012.06.001
47. Chavez-Santoscoy AV, Roychoudhury R, Pohl NLB, Wannemuehler MJ, Narasimhan B, Ramer-Tait AE. Tailoring the immune response by targeting C-type lectin receptors on alveolar macrophages using "pathogen-like" amphiphilic polyanhydride nanoparticles. *Biomaterials* (2012) 33:4762–72. doi:10.1016/j.biomaterials.2012.03.027
48. Goodman JT, Vela Ramirez JE, Boggiatto PM, Roychoudhury R, Pohl NLB, Wannemuehler MJ, et al. Nanoparticle chemistry and functionalization differentially regulates dendritic cell-nanoparticle interactions and triggers dendritic cell maturation. *Part Part Syst Charact* (2014) 31:1269–80. doi:10.1002/ppsc.201400148
49. Kipper MJ, Wilson JH, Wannemuehler MJ, Narasimhan B. Single dose vaccine based on biodegradable polyanhydride microspheres can modulate immune response mechanism. *J Biomed Mater Res A* (2006) 76:798–810. doi:10.1002/jbm.a.30545
50. Petersen LK, Xue L, Wannemuehler MJ, Rajan K, Narasimhan B. The simultaneous effect of polymer chemistry and device geometry on the in vitro activation of murine dendritic cells. *Biomaterials* (2009) 30:5131–42. doi:10.1016/j.biomaterials.2009.05.069
51. Petersen LK, Ramer-Tait AE, Broderick SR, Kong C-S, Ulery BD, Rajan K, et al. Activation of innate immune responses in a pathogen-mimicking manner by amphiphilic polyanhydride nanoparticle adjuvants. *Biomaterials* (2011) 32:6815–22. doi:10.1016/j.biomaterials.2011.05.063
52. Phanse Y, Carrillo-Conde BR, Ramer-Tait AE, Roychoudhury R, Pohl NLB, Narasimhan B, et al. Functionalization of polyanhydride microparticles with di-mannose influences uptake by and intracellular fate within dendritic cells. *Acta Biomater* (2013) 9:8902–9. doi:10.1016/J.ACTBIO.2013.06.024
53. Torres MP, Wilson-Welder JH, Lopac SK, Phanse Y, Carrillo-Conde B, Ramer-Tait AE, et al. Polyanhydride microparticles enhance dendritic cell antigen presentation and activation. *Acta Biomater* (2011) 7:2857–64. doi:10.1016/j.actbio.2011.03.023
54. Ulery BD, Phanse Y, Sinha A, Wannemuehler MJ, Narasimhan B, Bellaire BH. Polymer chemistry influences monocytic uptake of polyanhydride nanospheres. *Pharm. Res* (2009) 26:683–90. doi:10.1007/s11095-008-9760-7
55. Mirza S, Benjamin WH, Coan PA, Hwang SA, Winslett AK, Yother J, et al. The effects of differences in pspA alleles and capsular types on the resistance of *Streptococcus pneumoniae* to killing by apolactoferrin. *Microb Pathog* (2016) 99:209–19. doi:10.1016/j.micpath.2016.08.029
56. Arulanandam BP, Lynch JM, Briles DE, Hollingshead S, Metzger DW. Intranasal vaccination with pneumococcal surface protein A and interleukin-12 augments antibody-mediated opsonization and protective immunity against *Streptococcus pneumoniae* infection. *Infect Immun* (2001) 69:6718–24. doi:10.1128/IAI.69.11.6718-6724.2001
57. Briles DE, Hollingshead SK, King J, Swift A, Braun PA, Park MK, et al. Immunization of humans with Recombinant Pneumococcal Surface Protein A (rPspA) elicits antibodies that passively protect mice from fatal infection with *Streptococcus pneumoniae* bearing heterologous PspA. *J Infect Dis* (2000) 182:1694–701. doi:10.1086/317602
58. Wafa EI, Geary SM, Goodman JT, Narasimhan B, Salem AK. The effect of polyanhydride chemistry in particle-based cancer vaccines on the magnitude of the anti-tumor immune response. *Acta Biomater* (2017) 50:417–27. doi:10.1016/j.actbio.2017.01.005
59. Lebon A, Verkaik NJ, Labout JAM, de Vogel CP, Hooijkaas H, Verbrugh HA, et al. Natural antibodies against several pneumococcal virulence proteins in children during the pre-pneumococcal-vaccine era: the generation R study. *Infect Immun* (2011) 79:1680–7. doi:10.1128/IAI.01379-10
60. Melin MM, Hollingshead SK, Briles DE, Lahdenkari MI, Kilpi TM, Käyhty HM. Development of antibodies to PspA families 1 and 2 in children after exposure to *Streptococcus pneumoniae*. *Clin Vaccine Immunol* (2008) 15:1529–35. doi:10.1128/CVI.00181-08
61. Daniels CC, Coan P, King J, Hale J, Benton KA, Briles DE, et al. The proline-rich region of pneumococcal surface proteins A and C contains surface-accessible epitopes common to all pneumococci and elicits antibody-mediated protection against sepsis. *Infect Immun* (2010) 78:2163–72. doi:10.1128/IAI.01199-09
62. Bungener L, Geeraedts F, Ter Veer W, Medema J, Wilschut J, Huckriede A. Alum boosts TH2-type antibody responses to whole-inactivated virus influenza vaccine in mice but does not confer superior protection. *Vaccine* (2008) 26:2350–9. doi:10.1016/j.vaccine.2008.02.063
63. Chen D, Kristensen D. Opportunities and challenges of developing thermostable vaccines. *Expert Rev Vaccines* (2009) 8:547–57. doi:10.1586/ERV.09.20
64. Levy O, Goriely S, Kollmann TR. Immune response to vaccine adjuvants during the first year of life. *Vaccine* (2013) 31(21):2500–5. doi:10.1016/j.vaccine.2012.10.016
65. Brady RC, Treanor JJ, Atmar RL, Keitel WA, Edelman R, Chen WH, et al. Safety and immunogenicity of a subvirion inactivated influenza A/H5N1 vaccine with or without aluminum hydroxide among healthy elderly adults. *Vaccine* (2009) 27:5091–5. doi:10.1016/j.vaccine.2009.06.057
66. Petrovsky N. Comparative safety of vaccine adjuvants: a summary of current evidence and future needs. *Drug Saf* (2015) 38(11):1059–74. doi:10.1007/s40264-015-0350-4
67. Willhite CC, Karyakina NA, Yokel RA, Yenugadhati N, Wisniewski TM, Arnold IMF, et al. Systematic review of potential health risks posed by pharmaceutical, occupational and consumer exposures to metallic and nanoscale aluminum, aluminum oxides, aluminum hydroxide and its soluble salts. *Crit Rev Toxicol* (2014) 44(Suppl 4):1–80. doi:10.3109/10408444.2014.934439
68. Fukuyama Y, Yuki Y, Katakai Y, Harada N, Takahashi H, Takeda S, et al. Nanogel-based pneumococcal surface protein A nasal vaccine induces microRNA-associated Th17 cell responses with neutralizing antibodies against *Streptococcus pneumoniae* in macaques. *Mucosal Immunol* (2015) 8(5):1144–53. doi:10.1038/mi.2015.5
69. Gyu Kong I, Sato A, Yuki Y, Nochi T, Takahashi H, Sawada S, et al. Nanogel-based pspa intranasal vaccine prevents invasive disease and nasal colonization by *streptococcus pneumoniae*. *Infect Immun* (2013) 81:1625–34. doi:10.1128/IAI.00240-13
70. Kunda NK, Alfagih IM, Miyaji EN, Figueiredo DB, Gonçalves VM, Ferreira DM, et al. Pulmonary dry powder vaccine of pneumococcal antigen loaded nanoparticles. *Int J Pharm* (2015) 495:903–12. doi:10.1016/J.IJPHARM.2015.09.034
71. Ezoe H, Akeda Y, Piao Z, Aoshi T, Koyama S, Tanimoto T, et al. intranasal vaccination with pneumococcal surface protein A plus poly(I:C) protects against secondary pneumococcal pneumonia in mice. *Vaccine* (2011) 29:1754–61. doi:10.1016/j.vaccine.2010.12.117

72. Tostes RO, Rodrigues TC, Da Silva JB, Schanoski AS, Oliveira MLS, Miyaji EN. Protection elicited by nasal immunization with recombinant pneumococcal surface protein A (rPspA) adjuvanted with whole-cell pertussis vaccine (wP) against co-colonization of mice with *Streptococcus pneumoniae*. *PLoS One* (2017) 12:e0170157. doi:10.1371/journal.pone.0170157
73. Walters AA, Krastev C, Hill AVS, Milicic A. Next generation vaccines: single-dose encapsulated vaccines for improved global immunisation coverage and efficacy. *J Pharm Pharmacol* (2015) 67:400–8. doi:10.1111/jphp.12367
74. Lee BY, Wedlock PT, Haidari LA, Elder K, Potet J, Manring R, et al. Economic impact of thermostable vaccines. *Vaccine* (2017) 35:3135–42. doi:10.1016/j.vaccine.2017.03.081
75. Jones LS, Peek LJ, Power J, Markham A, Yazzie B, Middaugh CR. Effects of adsorption to aluminum salt adjuvants on the structure and stability of model protein antigens. *J Biol Chem* (2005) 280:13406–14. doi:10.1074/jbc.M500687200

Conflict of Interest Statement: The authors declare that the research was conducted in the absence of any commercial or financial relationships that could be construed as a potential conflict of interest.

frontiers in Immunology

REVIEW
published: 07 March 2018
doi: 10.3389/fimmu.2018.00431

Lipid-Based Particles: Versatile Delivery Systems for Mucosal Vaccination against Infection

*Blaise Corthésy and Gilles Bioley**

R&D Laboratory, Division of Immunology and Allergy, Centre des Laboratoires d'Epalinges, Centre Hospitalier Universitaire Vaudois (CHUV), Lausanne, Switzerland

Vaccination is the process of administering immunogenic formulations in order to induce or harness antigen (Ag)-specific antibody and T cell responses in order to protect against infections. Important successes have been obtained in protecting individuals against many deleterious pathological situations after parenteral vaccination. However, one of the major limitations of the current vaccination strategies is the administration route that may not be optimal for the induction of immunity at the site of pathogen entry, i.e., mucosal surfaces. It is now well documented that immune responses along the genital, respiratory, or gastrointestinal tracts have to be elicited locally to ensure efficient trafficking of effector and memory B and T cells to mucosal tissues. Moreover, needle-free mucosal delivery of vaccines is advantageous in terms of safety, compliance, and ease of administration. However, the quest for mucosal vaccines is challenging due to (1) the fact that Ag sampling has to be performed across the epithelium through a relatively limited number of portals of entry; (2) the deleterious acidic and proteolytic environment of the mucosae that affect the stability, integrity, and retention time of the applied Ags; and (3) the tolerogenic environment of mucosae, which requires the addition of adjuvants to elicit efficient effector immune responses. Until now, only few mucosally applicable vaccine formulations have been developed and successfully tested. In animal models and clinical trials, the use of lipidic structures such as liposomes, virosomes, immune stimulating complexes, gas-filled microbubbles and emulsions has proven efficient for the mucosal delivery of associated Ags and the induction of local and systemic immune reponses. Such particles are suitable for mucosal delivery because they protect the associated payload from degradation and deliver concentrated amounts of Ags *via* specialized sampling cells (microfold cells) within the mucosal epithelium to underlying antigen-presenting cells. The review aims at summarizing recent development in the field of mucosal vaccination using lipid-based particles. The modularity ensured by tailoring the lipidic design and content of particles, and their known safety as already established in humans, make the continuing appraisal of these vaccine candidates a promising development in the field of targeted mucosal vaccination.

Keywords: mucosal, vaccination, lipidic particles, delivery system, infections

OPEN ACCESS

Edited by:
Rajko Reljic, St George's, University of London, United Kingdom

Reviewed by:
Vijay Panchanathan, Perdana University, Malaysia
Beatrice Jahn-Schmid, Medizinische Universität Wien, Austria

***Correspondence:**
Gilles Bioley
gilles.bioley@chuv.ch

Specialty section:
This article was submitted to Vaccines and Molecular Therapeutics, a section of the journal Frontiers in Immunology

Received: *22 December 2017*
Accepted: *19 February 2018*
Published: *07 March 2018*

Citation:
Corthésy B and Bioley G (2018) Lipid-Based Particles: Versatile Delivery Systems for Mucosal Vaccination against Infection. Front. Immunol. 9:431. doi: 10.3389/fimmu.2018.00431

INTRODUCTION

Vaccination is considered as one of the most successful medical actions and has greatly contributed to the improvement of world health. Indeed, it has strikingly reduced the prevalence of many infectious diseases, and thus helps nowadays to save millions of lives each year (1, 2). Vaccine administration aims at inducing and harnessing protective effector and memory

immunity, comprising neutralizing antibodies (Abs) together with cytotoxic and helper T cells (3) able to control subsequent challenge by the target pathogen. Live-attenuated or killed whole-pathogens have originally been administered for vaccination purposes, but due to safety concerns, including important reactogenicity and risks of reversion, the use of subunit vaccines is preferred. The latter are composed of recombinant or purified pathogen-derived antigenic entities, mostly depleted of innate immune stimulus, that require the co-administration of adjuvants and/or the use of delivery vehicles to achieve sufficient immunogenicity. Over the last decades, important pieces of work in the field of vaccine technology have allowed to rationally design and develop formulations that ensure efficient induction of immune responses (4). Synthetic micro-/nanoparticles, liposomes, immune stimulating complexes (ISCOMs), virosomes, virus-like particles, as well as emulsions, all offer several interesting attributes for vaccine delivery and have already proven efficient in parenteral (intramuscular or subcutaneous) vaccinations by inducing protection against infectious agents (5). These formulations have been designed to mimic biophysical and biochemical features of pathogens, thus ensuring efficient display and delivery of concentrated amounts of antigens (Ags) and adjuvants to innate and adaptive immune cells. Interestingly, this leads to reducing the number of injections required to elicit potent cellular and humoral immune responses with minimal cytotoxicity.

Despite important success in protecting individuals against many deleterious pathological situations, it remains that most of the licensed subunit vaccines are administered parenterally. However, except in previously infected individuals, such a route of administration only induces limited protective effect at the level of mucosal surfaces, the sites where the vast majority of pathogenic agents gain access to the host body (6). In addition to mechanical (epithelium covered with mucus) and chemical (anti-microbial peptides) barriers found at mucosae, adaptive humoral and cellular immunity is of prime importance to efficiently protect against pathogenic insults (7). Thus, to reinforce the efficiency of vaccination, the delivery of vaccine formulations directly to the mucosa represents an asset. It is now well accepted that immune responses have to be elicited locally to ensure efficient imprinting of effector and memory B and T cell homing to mucosal tissues where they will limit entry, colonization, and spreading of pathogens (8–11). Until now, the few licensed mucosal vaccines consist in administration of live-attenuated or killed whole-pathogens that raise similar safety concerns as for parenteral injection, while no subunit vaccines have been approved for human use. This is mainly due to technical difficulties inherent to the administration route and the physiology of the tissues where the vaccine formulations are applied. Identifying the most adequate vaccine formulation deliverable mucosally remains challenging due to (1) the fact that, in contrast to parenteral vaccination where injected Ags and adjuvants are directly in contact with antigen-presenting cells (APCs), Ag sampling has to be performed across the mucus and the epithelium first; (2) the deleterious acidic, proteolytic, and dynamic environment of the mucosal surfaces which impact the stability, integrity, and retention time of the applied Ags; and (3) the tolerogenic nature of the mucosa, which impairs induction of effector immunity to antigenic entities lacking sufficient immunostimulatory signals (12). Such hurdles may, however, be partially overcome thanks to recent progress made in the understanding of mucosal immunity and in the field of vaccine technology (6).

Apart from immunological and physiological aspects, one important point to be considered for vaccination is the compliance of the patients (13). For pediatric vaccination, administration has to be minimally invasive and easy to perform. The ability of vaccinating a large number of people in countries where endemic infections are present, but where access to medical infrastructures is limited, is of great importance as well. In this context, parenteral vaccination is not the most appropriate strategy as injections are invasive, painful and require trained/skilled medical staff for administration. Moreover, it poses problems related to the risks associated with infection at the site of injection, needle-stick injury, spreading of transmissible diseases, and disposal of used materials. Thus, there is an increasing demand for needle-free vaccination. As an example, mucosal vaccines display several advantages, such as ease of administration and self-delivery allowing mass vaccination, absence of needle-associated risks, and in some cases lower costs and simplified production due to absence of administration devices.

Until now, only few mucosally applicable subunit vaccine formulations have been developed and successfully tested (14), mainly because of the limited number of safe and efficient delivery systems and adjuvants available, coupled to the sometimes important amounts of Ag to be administered. This review will focus on lipid-based micro-/nanoparticles that possess several of the desired characteristics of an interesting Ag-delivery system for vaccination as they are biocompatible, can overcome physiological barriers at mucosae, promote Ag crossing of the epithelium and uptake by APCs, protect the associated payload, are adequate for incorporating adjuvants and may display mucoadhesive properties. In order to achieve the induction of protective anti-pathogen humoral and cellular responses at the relevant mucosal surfaces, the choice of the most potent administration route has to be carefully considered by taking into account the physiological and immunological features of the different target tissues (15). These aspects and the strategies to specifically target vaccines to the portals of entry across the epithelium and increase the efficiency of delivery will first be discussed. However, directing vaccines to the appropriate location is not sufficient to ensure optimal vaccination effect. The architecture, size, and surface chemistry of particles are of prime importance and can be manipulated to influence the intensity and type of immune responses. Physicochemical properties of lipid-based particles, Ag incorporation, mucoadhesion, and association with adjuvants will be discussed next. Examples of mucosal application of such formulations in animal models and their outcome will then be presented. Finally, an overview of the current evaluation of lipid particles and open challenges of mucosal vaccination in humans will be considered.

VACCINE SAMPLING AT MUCOSAL SURFACES AND THE SELECTION OF THE ROUTE OF ADMINISTRATION

When applying a vaccine formulation *via* any delivery route, the anatomical, functional, and immunological characteristics of the different tissues have to be considered (13). Indeed, the structure and spatial organization of the tissues, the presence of mucus and mechanisms to eliminate deposited materials/particles (e.g., peristaltism in the intestine and physical discharge in the respiratory tract), the pro-tolerogenic environment of mucosae and the presence and localization of particular immune cell subsets, especially dendritic cells (DCs), all impact on the outcome of vaccine administration (16). In addition, safety issues have to be considered. In this section, we will present the characteristics of the mucosal immune system in relationship with vaccination, the different mucosal administration routes, as well as the strategies under evaluation to increase the efficiency of vaccine delivery.

The Mucosal Immune System and Mucosal Vaccination

Mucosal surfaces are continuously exposed to, and challenged by, numerous environmental Ags present, for example, in food, air, or derived from pathogenic or commensal microorganisms in the lumen. On top of the epithelial barrier covered by mucus and the secretion of anti-microbial peptides, a specialized and complex immune network, called mucosa-associated lymphoid tissues, is involved in immunosurveillance of mucosal tissues (17). Lymphoid cells and effector molecules, such as secretory IgA (SIgA), the chief Ab molecule operating at mucosal surfaces (18), cytokines, and chemokines, tightly orchestrate protection against infections and maintenance of tolerance toward endogenous unharmful microorganisms. Sampling for such agents and their delivery to immune cells underneath the epithelial layer takes place *via* direct uptake by DCs within the epithelium (19–21) or across specialized epithelial cells named microfold (M) cells that are responsible for the selective transport of macromolecules, particulate Ags, and microorganisms (22, 23). Internalization *via* M cells occurs through different mechanisms (clathrin-coated endocytosis, actin-dependent phagocytosis, or macropinocytosis) depending on the nature of the Ags. M cells are present in (a) the follicle-associated epithelium that separates the intestinal lumen (apical side) from underlying immune cells (basolateral side) in Peyer's patches (PPs), (b) in intestinal isolated lymphoid follicles, (c) in nasopharynx-associated lymphoid tissues (NALT), and (d) in bronchial-associated lymphoid tissues (BALT) (24). Such structures are composed of innate and adaptive immune cells, including functionally different DC subsets, T, and B cells. DCs integrate signals derived from the sensing of the luminal environment, and release soluble factors, such as cytokines and chemokines, to orchestrate the generation of tightly controlled mucosal immunity locally or after migration in regional lymph nodes (LNs) (7). In addition, paracellular and transcellular uptake of macromolecules and small particles across the epithelia lead to their uptake by APCs outside inductive sites for induction of local immunity *via* regional LNs. By contrast, in the urogenital tract and in the oral cavity, the stratified epithelium does not contain M cells and sampling occurs by DCs interspersed within the tissue leading to induction of immune responses exclusively in draining LNs (15, 25, 26).

Upon encounter with microorganisms or vaccine formulations, mucosal DCs in combination with neighboring epithelial cells control the expression of specific homing receptors on primed lymphoid cells and modulate the type of ensuing immune response (8, 9, 27). Such imprinting relies on the expression of site-specific integrins and chemokine receptors by B and T cells and allows their transit *via* the lymph and through the blood to migrate to different mucosal sites. Recirculation of lymphocytes to the gut requires expression of α4β7 and CCR9, whereas migration to the airways, the oral cavity, and the reproductive tract relies on L-selectin and CCR10. In the case of pathogenic infections, danger signals generated by the sensing of microorganisms switch immune responses toward an effector type of response relying on both humoral and cellular arms to eliminate the infection (28). Immune exclusion and neutralization by SIgA, as well as production of Th1- or Th17-type cytokines that activate phagocytes and induction of cytotoxic T cells, all contribute to the protection of mucosal surfaces (29, 30). Therefore, the major aim of vaccines would be to elicit specific B and T cell responses at the relevant sites to induce specific SIgA that provide a first line of protection against invading pathogens, together with appropriate cellular immune responses to eliminate both the pathogen and pathogen-infected cells. For example, requirements for proper B cell isotype-switching and the generation of IgA responses include mainly the production of TGF-β, IL-6, retinoic acid, and IL-21 by PPs' cells, together with the CD40–CD40L interaction between T follicular helper cells and B cells (31). Thus, vaccine formulations for mucosal application have to be designed to best induce such immunological environment.

Administration Routes for Mucosal Vaccination

Each route of mucosal administration has its own characteristics and a balance between the pros and cons for each vaccine has to be considered, taking into account the pathogen to fight against and the formulation to be delivered. However, no standardized studies are available to directly compare safety, profile of induced immune responses, and efficiency of protection. In this section, we will consider the different mucosal administration routes. Oral and nasal/pulmonary are the most studied ones, but sublingual is now recognized as a promising way of vaccination. Vaginal and rectal delivery have also been studied, but more scarcely. Even though the most powerful response is usually elicited in the local inductive and adjacent tissues, the common mucosal immune system predicts that homing to distant mucosal tissues is possible (27). However, a certain degree of compartimentalization does not allow imprinted cells to migrate to every mucosal sites. Such flexibility allows to select for the most appropriate route of vaccination to induce protective immune responses at the desired site. Of note, some recent works demonstrated that transcutaneous immunizations have the potency to promote the induction of immune responses with the ability to traffic to the

gut and airways, although up to now with low consistency (32). However, this aspect will not be covered by this review and has been described elsewhere (33, 34).

Nasal administration represents a promising route for mucosal vaccination (35), because nasal tissues display a relatively large surface for Ag absorption covered with only a thin layer of mucus, and are highly vascularized. It does not require the delivery of high Ag doses (e.g., as compared to oral administration), is non-invasive and easily accessible for self-administration. Nasal vaccination allows the generation of a broad range of Ab and T cell responses at different mucosal sites, such as the upper (preferentially) and lower airway mucosae, the local secretions, the salivary glands, and the urogenital tract. It also elicits concomitant robust systemic immunity (15). However, in the nasal environment, the presence of proteases and the local pH, together with a relatively high mucoscillary clearance rate, may impact on the vaccine integrity and retention time, thus affecting the generation of immune responses. The major drawback concerns the safety of nasal administration, as physiological function such as smell perception might be altered by vaccine-induced inflammation and the close relationship with the brain might promote health problems. Thus, every vaccine candidate has to be evaluated carefully for safety. Sometimes achieved by nasal delivery or directly targeted, pulmonary immunization allows vaccine formulation to directly access the respiratory tract which is of interest due to its high permeability, its large surface area and the high density of APCs (alveolar macrophages, DCs, and B cells). This route of administration preferentially induces immune responses in the lower airways and has interestingly been shown to promote cellular and humoral responses in the gut. However, efficient delivery in the lung is not an easy task. Delivery *via* the nasal and pulmonary routes does not necessarily lead to similar outcomes: for example, pulmonary vaccination was shown to be more effective than its nasal counterpart at protecting against *Mycobacterium tuberculosis* infection, because different immune mechanisms were involved after one or the other administration route (36–38). Indeed, elevated levels of SIgA were produced in the lung after pulmonary vaccination, with equivalent responses observed in the nasal passage. In addition, IFN-γ production in the lung following pulmonary vaccination was important to fight against *M. tuberculosis*, whereas there was apparently no role for this cytokine in the nasal environment.

Oral administration represents an interesting strategy in terms of ease of delivery, patient compliance, and safety (39). However, due to the intrinsic high dilution of vaccine formulations and the harsh environment of the digestive tract, substantial amounts of Ags have to be administered. Indeed, the extremely low pH in the stomach, proteolytic enzymes and bile salts in the intestine, the presence of relatively thick one-layered mucus, and the overall low permeability of the intestine greatly affect the integrity and delivery of applied Ags. In this context, oral vaccines are likely to be more efficient if repeated doses are given, provided that adjuvants are incorporated to avoid tolerance induction (13). Oral administration is the most efficient delivery route to achieve induction of gut immunity, which is of high importance to fight against the large burden of enteropathogenic infections worldwide. Induction of immune responses in the colon, stomach, mammary, and salivary glands, as well as systemically, also takes place, but with limited robustness (15).

Sublingual immunization generates immune responses with similar profile and mucosal tropism as nasal delivery, i.e., vigorous and broadly disseminating mucosal and systemic IgA and IgG, as well as helper and cytotoxic T cell, responses (40), without many side effects (41), and formulation concerns associated with nasal or oral immunization (42). It is also easily accessible for self-administration. It has been shown to induce immune responses after administration of soluble Ags, particulate Ags, live/killed bacteria, and viruses (40). Sublingual delivery is interesting because the oral cavity has a milder environment that may not degrade vaccine components, and may, thus, not require large amounts of Ags. As an example, higher Ab responses were obtained in mice after sublingual, as compared to oral, administration with about 10–50 times less Ag applied (43). One limiting factor is the absence of Ag-sampling M cells in the oral cavity lined by a stratified epithelium and the relatively low number of DCs in the upper layer of oral tissues. However, vaccine formulations can be taken up by lingual tonsils for delivery into regional LNs and Langerhans cells in the oral epithelium have been shown to act as potent inducers of immunity (15). Several delivery systems (microneedles, liposomes, inactivated microorganisms) and adjuvants [toll-like receptor (TLR) ligands, cholera toxin (CT), mutants of heat labile toxin (LT) and CT] have been evaluated for sublingual vaccination and protective Th1-type responses in the lung, genital tract, and the gut, together with SIgA in the saliva, intestinal, and vaginal washes, have been obtained with different vaccine formulations (42–45).

Vaginal immunization elicits immune responses in the genital tissues and secretions, but is not efficient to induce systemic immunity. Despite relatively low pH, the vagina is a mild environment that does not impair Ag integrity and, thus, allows to limit the amount of Ag to be delivered (25). However, the presence of a stratified epithelium and the absence of inductive sites imply that induction of vaccine response *via* vaginal delivery requires specific adjuvanted formulations and DC subsets (46). In addition, the changes occurring in term of immunological functions during the estrous cycle complicate such immunization (47–49). Additional studies are required to better understand mucosal immunity in the urogenital tract and define specific requirements for vaccine formulations. Rectal immunization is able to induce potent immune responses in the small intestine and the colon, but not efficiently in the systemic compartment (15). Only limited studies are available to fully appreciate the potential of such an administration route for mucosal vaccination.

Targeted Delivery of Vaccine Ags

Not only do vaccine formulations have to resist the deleterious environment of some mucosal surfaces, but they also have to face an additional hurdle that is to cross the epithelium to gain access to underlying APCs. In this context, targeting the relatively low number of portals of entry at inducing sites, e.g., M cells that represent 1% of epithelial cells (5–10% of enterocytes within the follicular-associated epithelium), or DCs spread within the epithelium is an asset for efficient vaccination. DC targeting by the mean of C-type lectin receptors (DEC205, DC-SIGN, mannose receptor)

or specific Abs directed against DC markers has proven to be an efficient strategy to improve the potency of parenteral vaccination (50). Similar strategies have been developed for mucosal vaccination, such as targeting of Langerin on DCs of the oral cavity, the esophagus or the vaginal mucosa (51). FcRn expressed by airway and gut epithelial cells (52, 53), as well as some DC subsets (54), has also been demonstrated as an efficient strategy to deliver IgG-based complexes across the epithelium and to underlying DCs. Such an approach efficiently led to the induction of both CD4 and CD8 T cell effector responses (55–57). Galactosyl ceramide may function as a targeting moiety in the intestine, the rectum, and the endocervical mucosa (58), and the ganglioside GM1 molecule can be targeted by a specific peptide developed by phage display (59). As far as M cells are concerned, specific delivery can be achieved *via* different strategies: the tight junction molecule claudin-4 (60), the bacterial FimH receptor GlycoProtein-2 (61, 62), the complement C5a receptor and its ligand Co1 (63, 64), a M-cell-specific peptide referred to as CKS9 (65), or the unique glycosylation pattern involving α-1-fucose; for the later, the use of Ulex Europaeus Lectin-1, or a specific monoclonal Ab have been successfully demonstrated (66–68). However, in humans, the lack of expression of this particular sugar moiety on M cells (69), together with the extra-M cell expression of GP-2 (70), precludes the use of such strategies for specific targeting purposes. By contrast, a promising approach consists in coupling vaccine Ags with SIgA in order to induce M-cell-specific retrotransport across the epithelium and DC targeting *via* Dectin-1 in both mice and humans (71). This Ab molecule can potentially serve as a cargo for the controlled delivery of the associated payload as this occurs naturally with microorganisms sampled from the mucosal lumen (72). An additional advantage is the resistance of SIgA to protease degradation and its ability to anchor in mucus (18), two features that may improve both stability and retention time of the associated Ags.

FORMULATION CONSIDERATIONS

Particulated Ags have been designed to mimic the shape, size, and antigenic display of pathogens with the aim of improving vaccine efficiency (73). Ags associated with micro-/nanoparticles display increased depot effect upon administration, are better protected from degradation, and are more efficiently taken up by APCs and presented to B and T cells than soluble Ags (74). An important number of studies have evaluated the effect of particle properties (type of material, size and charge, Ag incorporation, or association of adjuvants) on the profile and strength of induced Ab and T cell responses. When composed of natural lipids, lipid-based particles have the advantage of being biocompatible. In addition, they are very flexible in terms of formulation, implying that lipid exchange within the particle shell is achievable, leading to modulation of their physico-chemical properties. This is of importance in the biological environment because all these parameters will influence the stability and immunological consequence of delivered particles. However, minor changes in the composition of the particle may impact on its efficiency and protective ability, meaning that any formulation needs to be individually evaluated *in vivo*.

Size and Charge of Particles

The size of particulate Ags has an impact on the type of immune responses that are generated because it influences the mechanism of uptake by APCs. Indeed, receptor-mediated endocytosis, pinocytosis, macropinocytosis, or phagocytosis, all lead to different ways of trafficking within the cells and, therefore, induce preferentially presentation *via* the MHC I or MHC II pathway for CD8 or CD4 T cell priming, respectively (75). Small particles (up to 200 nm) are sensed as viruses and are taken up by receptor-mediated endocytosis leading to predominant T cell responses, whereas larger particles (more than 500 nm) are taken up *via* micropinocytosis or phagocytosis to preferentially induce Ab responses (76). Similar size-dependent uptake by M cells or enterocytes takes place, leading to differential sampling of the particulated Ags. Other studies demonstrated that vesicles smaller than 250 nm induced a balance toward Th2-type of responses, whereas the opposite was observed for larger vesicles (77–79). Moreover, in the context of mucosal delivery, the size of the particles influences the tissue localization and the diffusion across the mucus. Following nasal administration, small particles are better transported across the nasal mucosa, whereas larger ones are better deposited in the respiratory tract to be taken up by alveolar macrophages (80, 81). In order to get access to the epithelium, both viscosity and pore size of mucus can impact on the penetration of vaccine components. Apparently, the average size of pores in the mucus is in between 200 and 500 nm, e.g., in the cervicovaginal and small intestinal mucus. This suggests that particles smaller than this cutoff freely diffuse across the mucus, whereas larger ones take more time to reach the epithelium or possibly never reach it (82, 83). One major point to be considered is that correlation between size and immunogenicity is difficult to strictly assess for lipid-based particles, because homogeneous and monodispersed preparations have been challenging to obtain, and when feasible, such preparations require technical issues that may dramatically increase the cost of vaccine formulations.

Diffusion across the mucus is not only governed by size of particulated Ags or mucus pores but also by chemical characteristics such as the surface charge of particles. Hydrophobic and electrostatic interactions mediated by particles aggregate mucus microstructure and impede diffusion of vaccines, while hydrophilic and neutral vaccine formulations promote mucus penetration (23). Mucoadhesion is promoted by positively charged particles that interact with negatively charged mucus. For example, electrostatic interactions between cationic lipids and the nasal mucosa promote enhanced contact time with the tissue, higher local concentration, and thus improved penetration of liposomes (84). Similarly, cationic particles better interact with negatively charged cell membranes, such as those of M cells and enterocytes, therefore limiting vaccine clearance and improving sampling *via* endocytosis or membrane fusion (85, 86); it also improves the uptake by DCs (87). However, cationic particles may have charge-dependent cytotoxicity against target cells; therefore, the density of cationic lipids within the particle shell has to be carefully defined and a tight balance between strong adhesion and safety has to be achieved (23). Interestingly, it seems that the presence of the mucus limits cytotoxicity (85), meaning that cationic particles keep their validity for mucosal vaccination.

Incorporation of Ag

There are different ways of associating Ags to lipid-based delivery systems and the choice depends mainly on the administration route and the nature of the Ags (88, 89). For oral administration, encapsulation seems favorable in terms of ensuing immune responses, because it prevents rapid degradation of the Ag within the gastrointestinal environment and, hence, increases its half-life (90). Encapsulation of Ags is relatively easy to perform during the manufacture process, but this may alter antigenic structures. By contrast, maintenance of the integrity of the Ags is less affected by the nasal route, suggesting that surface association *via* charge interaction is sufficient. Such an approach is technically not demanding, owing that opposite charges of either the particles or the Ags favors it (90). Alternatively, covalent binding at the surface of particles is achievable, although more complicated to perform; this precludes the undesired release of the payload that may occur within the tissue environment. In terms of immune response induction, encapsulation within liposomes preferentially induces IgG production, whereas surface display of the Ag induces both IgM and IgG responses (91), with elevated levels (92). In addition, Ag density at the surface of particles, as well as the Ag-to-lipid ratio, has been documented to influence the elicited immune responses following immunization (93, 94). This may suggest that both encapsulation and surface location of the Ag within the same formulation would promote optimal induction of T cell and B cell responses.

Apart from protein Ags, plasmid DNA coding for pathogen-derived Ags have been evaluated for vaccination (95, 96). Such strategy has an established record of efficacy in preclinical studies and can be safely used in humans, even in immunocompromised individuals. However, based on results obtained in the field of veterinary vaccination, naked DNA induces only weak immune responses. In order to improve immunogenicity, association of DNA with cationic liposomes leads to increased uptake by target cells and delivery into the nucleus. DNA immunization through the nasal or the oral route can effectively induce protective humoral and cellular immunity at related mucosal surfaces, but necessitates association with cationic delivery systems, presumably to increase mucus penetration, to reduce mucociliary clearance, and to improve permeation across the epithelium (97, 98). DNA sequences such as the canonical CpG motifs have been shown to display immunostimulatory properties. In a similar way, messenger RNA-based vaccines, when appropriately protected from ribonucleases are translated in the cytoplasm and do not require nuclear transport (99). This has been mainly evaluated with cationic lipid-based vesicles in the context of cancer immunotherapy, and the efficient nasal application of particle-associated mRNA has been demonstrated (100).

Mucoadhesive Properties

Upon mucosal administration, vaccine formulations are diluted in mucosal fluids and have to face bulk flow, leading to limited retention time and suboptimal access to the epithelium for sampling. Such deleterious effects can be compensated by incorporation of mucoadhesive and mucus-penetrating components. In this case, the surface structure of lipid-based particles has to be carefully designed to obtain an adequate balance between strong adhesion and mucus penetration. Some possible strategies are described below. The first one consists in incorporating polyethylene glycol (PEG) at the surface of particles. PEG has originally been used for systemic administration in order to avoid adsorption of plasma proteins and the formation of a corona that may mask targeting ligands, adjuvants, or Ags at the surface of particles (101). In addition, the presence of PEG increases the stability upon administration. A similar stabilization effect has been reported in the case of oral or sublingual delivery of liposomes (93, 102, 103). PEG is a hydrophilic component that has been reported to help particles to penetrate the nasal mucosa by preventing aggregation and thus facilitating diffusion across the mucosal barrier. Moreover, it can form hydrogen bonds with mucus leading to mucoadhesion, but also helps diffusion across the mucus; indeed, such intriguing bifunctionality has been correlated with the molecular weight of PEG. High molecular weight polymers (>PEG5000) are preferentially mucoadhesive whereas lower ones (PEG2000) better diffuse within the mucus (103–105). An additional non-negligible advantage of PEG is that it provides cryopreservative functions during particle manufacture.

The second strategy is to associate with micro-/nanoparticles some mucoadhesive components, such as chitosan (deacetylated chitin), alginate, polyvinyl alcohol, hyaluronan, or cellulose derivatives that all boost particle-based vaccination (106–108). Addition of bioadhesive components (xanthan gum or tramella) within formulations helps to increase the viscosity of the vaccine and, thus, the retention time at mucosal surfaces. The most studied mucoadhesive molecule is chitosan, whose relevant properties for mucosal vaccination are as follows: (1) it is a positively charged molecule that can interact with negatively charged mucus to improve adhesion; (2) it is a permeation enhancer due to its ability to transiently open epithelial tight junctions and, thus, improve Ag sampling (109); and (3) it has adjuvant properties, promoting induction of IFN-γ, IgG, and SIgA (110). Chitosan has been explored for delivery *via* oral, nasal, and pulmonary routes in association with liposomes leading to increased stability and mucoadhesion for absorption by mucosal surfaces (111). Interestingly, it did not demonstrate detrimental effects toward mucosal tissues (112).

Incorporation of Adjuvants

Several adjuvants have been evaluated during the last decades for mucosal vaccination (113). Essential properties of the ideal adjuvant include the following: to be effective with low-dose Ag; to be suitable with many different Ags; to be effective enough to reduce the number of vaccine administrations; to be able to induce long-term immune responses; and to display limited or absent toxicity. Innate immune triggers have been used as adjuvants as they have the capacity to elicit pro-inflammatory responses to recruit phagocytes, to enhance Ag presentation by APCs, and to activate APCs in order to generate the adequate environment for efficient priming of adaptive immunity. Studies in animals have demonstrated an important adjuvant effect of the *Vibrio cholerae* endotoxin CT and *Escherichia coli* LT, ensuring enhanced Ag permeation through the epithelium, enhanced targeting of M cells, increased Ag presentation by DCs and improved activation

of DCs (114); a direct effect on B and T cells has additionally been reported (15). However, such adjuvants are inadequate for human use because of their toxicity and unacceptable side effects, as for example: induction of deleterious inflammatory response leading to altered function of olfactory nerves or to Bell's palsy after nasal administration, and diarrhea symptoms after oral administration (115, 116). This has oriented research toward the generation of less toxic derivatives engineered by introduction of mutations in the A subunit of CT and LT (117–120). The most promising derivative is the double mutant LT (R192G/L211A, dmLT) that has no demonstrated side effects in animal application while retaining important adjuvant activity after oral or sublingual administration (121–123). Similar mutations R192G/L211A applied to CT similarly reduced its toxicity, although to a level still not acceptable for human use. Introduction of additional mutations within the amino acid 189–197 stretch recently demonstrated more safety with an ability to induce both Ab and T cell responses close to that of the non-mutated CT following nasal, oral, and sublingual vaccinations (124). An alternative approach is the use of the B subunit of LT or CT only. LTB and CTB are not very efficient *via* the oral route, however, nasal administration demonstrated some efficiency when the Ag was physically linked to the adjuvant resulting in increased uptake across the epithelium and by DCs (15). Fusion protein obtained by association of the A1 subunit of CT and *S. aureus* protein A derivative (CTA1-DD) proved efficient at boosting B cell responses after nasal administration (125). In another report, edema toxin from *Bacillus anthracis* and diphtheria toxoid within lipidic particles have been evaluated for nasal administration and showed efficient induction of immune responses leading to reduced bacterial load after pathogen challenge (126).

In parallel, evaluation of immunostimulatory molecules active for parenteral administration, such as TLR ligands, have been performed (113). CpG oligodeoxynucleotides (CpG), monophosphoryl lipid A (MPLA), and flagellin that are ligands for TLR-9, TLR-4, and TLR-5, respectively, have been administered orally or intranasally and demonstrated immunostimulatory properties for mucosal immune responses, including induction of SIgA (127–131). Pulmonary delivery of a *M. tuberculosis*-derived Ag together with CpG or MPLA promoted the generation of IFN-γ production in the lung; MPLA was more potent to induce IL-17 production and to decrease the bacterial load following challenge (132). Flagellin, expressed by different pathogenic bacteria, can indirectly stimulate local DCs following nasal delivery, and induce mucosal IgA responses and protection upon Influenza vaccine administration (133, 134). Alternatively, trehalose dibehenate (TDB), a synthetic analog of a *M. tuberculosis* cord factor known to interact with Mincle and promote Th1/Th17-type of responses (135), has also been shown to be effective by the nasal route (136). Saponin QS21 also demonstrated potent adjuvant effect when nasally administered (128, 129). In addition, STING ligands 3′3′-cGAMP, c-di-AMP, and c-di-GMP have been efficiently delivered *via* the nasal or the sublingual route to elicit Th1/Th17 responses and high-affinity SIgA (137). Activation of NKT cells by administration of α-galactosylceramide is also of interest for nasal, oral, and sublingual vaccination due to its ability to enhance immunogenicity of different mucosal vaccine formulations (138–140). All these adjuvants can be incorporated within lipid-based particles or associated at their surface depending on the localization of their cognate receptor in target cells. This has been successfully achieved and resulted in improved uptake by and activation of DCs (141). Moreover, cationic lipids *per se* have been shown to directly activate APCs (142).

LIPID-BASED PARTICLES FOR MUCOSAL VACCINATION

In order to induce efficient and protective immune responses by vaccination, not only the Ags and the adjuvants have to be carefully defined, but also an appropriate delivery system is of prime importance. When aiming at using mucosal routes of administration, they must be designed to resist chemical degradation by low pH, proteolytic enzymes, and the harsh environment of mucosal surfaces. Lipid-based particles represent interesting delivery systems to incorporate Ags and adjuvants, allowing targeted and concentrated delivery of relatively low amounts in tissues, together with limiting toxicity associated with potential spreading of the payload (**Figure 1**). Many lipid-based particles have been tested in animal models of immunization and/or infection and are reviewed below (**Table 1**). Advantages, limitations, and necessary refinements for use as effective mucosal vaccine are discussed sequentially.

Liposomes

The enormous potential of liposomes for drug delivery has been acknowledged for decades. Indeed, they display features including controlled release, protection from degradation, improved pharmacokinetics, increased circulation time, and targeting to specific tissues (143, 144). They have been progressively adapted for administration of diverse antigenic entities, such as proteins, peptides, and DNA, in order to produce vaccine formulations to fight against several viral and bacterial infections (89). Liposomes are spherical vesicles consisting in unilamellar or multilamellar shell of phospholipid bilayer(s) entrapping an aqueous core and range in size from tens of nanometers to several micrometers in diameter. The amphiphilic nature of phospholipids mediates self-assembling of liposomes in an aqueous environment leading to a bilayer configuration. They can incorporate both hydrophilic molecules encapsulated within the aqueous core and hydrophobic molecules hooked at their surface or inserted within the inner hydrophobic space of the lipid bilayer. Biocompatible neutral and anionic phospholipids, such as phosphatidyl cholines [e.g., distearoylphosphatidylcholine (DSPC)], and cholesterol, are the most commonly used constituents of the shell that ensures proper stability of the structure and improved immunogenicity of the formulation (145, 146). The length and degree of saturation of acyl chains influence both the permeability and the fluidity of the shell, leading to increased or decreased stability. Liposomes are versatile delivery systems that are interesting for vaccination formulations because their physicochemical properties can be modulated by altering their composition in lipids. Among possible modifications, pH titrable lipids to induce controlled release of payloads (147, 148) and synthetic cationic lipids to

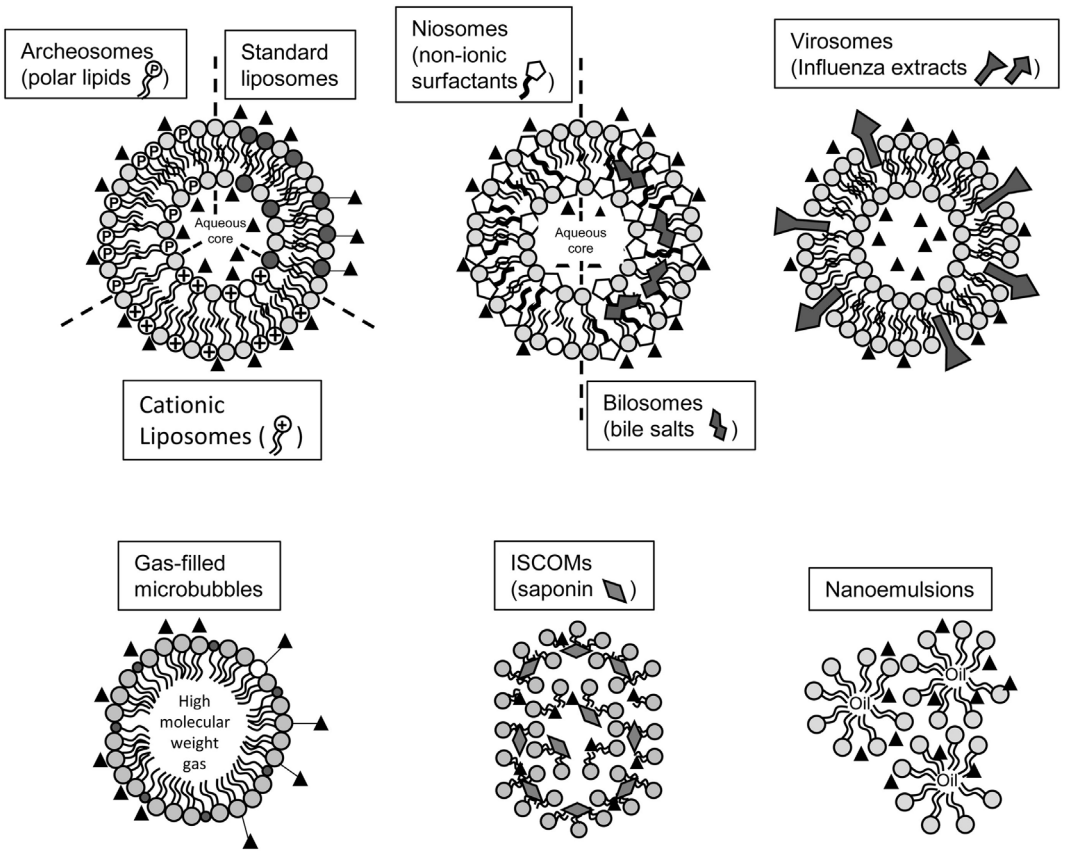

FIGURE 1 | Schematic representation of lipid-based particles evaluated for mucosal vaccination. Liposomes can be tailored to incorporate particular lipids (cationic lipids, polar lipids from Archea), Influenza extracts or non-ionic surfactants in order to improve stability and immunogenicity of vesicles. Other lipid-based structure incorporating saponin, entrapping inert high molecular gas, or composed of emulsions has been developed for vaccination purposes. Black triangles represent Ags. They can be entrapped in aqueous cores, entrapped in hybrophobic parts, associated at the surface of particles through electrostatic interactions, or covalently linked at the surface of particles. Not drawn on scale.

improve immunogenicity (90) have been generated. In addition, functionalization of liposomes with specific targeting moieties has emerged as a promising strategy to improve delivery. Vesicles bearing the DC-SIGN-specific ligand Lewis x glycan showed increased DC-targeting properties and subsequent activation of T cells, especially when adjuvanted (141) and IgG-coupled liposomes have demonstrated enhanced transmucosal transport in nasal tissues (55).

Cationic liposomes prepared with dioleoyltrimethylammoniumpropane (DOTAP), dimethyldioctadecylammonium bromide (DDA), dimethylaminoethane-carbamoyl (DC)-cholesterol have been successfully evaluated. Nasal administration of DDA-based liposomes induced greater local and vaginal IgA production as compared to vesicles without cationic lipid. Moreover, the incorporation of PEG further increased the observed immune responses (149). Similarly, delivery of cationic liposomes composed of DOTAP and DC-cholesterol *via* the nasal route allowed efficient uptake by DCs in NALT and subsequent induction of specific IgA and T cells in nasal tissues (150). The adjuvant CAF01 is a prime example of efficient cationic liposomes to be used for mucosal vaccination. Incorporation of both DDA and the immunostimulatory molecule TDB, has been evaluated in several animal models of infections with Influenza, *Chlamydia* and *M. tuberculosis* (151). In such context, the presence of the adjuvant had a substantial beneficial effect on immunogenicity (152). Nasal vaccination against Influenza or *Streptococcus pyogenes* with CAF01-based formulations allowed to generate mucosal effector T cell and IgA responses and to protect vaccinated animals (136, 153). Furthermore, preparation of liposomes with the cationic lipid ceramide carbamoylspermine efficiently stimulated systemic and mucosal immunity following intranasal administration (154). The use of cationic preparations is also an interesting approach for alternative forms of antigenic entities, as liposomes incorporating DOTAP and a plasmid DNA coding for a mycobacterial heat-shock protein given nasally induced local mucosal immune responses able to reduce *M. tuberculosis* load in the lung (155). Overall, liposome-based vaccination *via* the nasal route leads to the induction of robust immune responses whatever the nature of the Ag and its mode of incorporation. Thus, fine-tuning modulation of the profile of vaccine-elicited responses appears to depend on the composition of the formulation, including the type of lipids and/or the presence of adjuvants. Interestingly, most

TABLE 1 | Lipid-based formulations evaluated for mucosal vaccination in mouse models.

	Structure	Evaluated mucosal routes	Advantages	Stability	Limitations
Liposomes	Bilayer of phospholipids entrapping an aqueous core	Nasal, oral	Flexibility in lipid composition, ease of Ag/adjuvant incorporation, immunogenicity of cationic liposomes	Relatively low intrinsic stability for storage and after administration	Potent toxicity of cationic lipids (dose-dependent)
Archaeosomes	Liposomes composed of Archaea-derived polar lipids	Nasal, oral	Improved immunogenicity	Improved stability as compared to liposomes	Preparation of Archea lipids
Niosomes, bilosomes	Cholesterol-based liposomes with non-ionic surfactants and bile salts	Oral	Ease of manufacture	Improved stability as compared to liposomes	Low flexibility in lipid composition, low immunogenicity
Virosomes	Liposomes containing lipidic viral extracts	Nasal, sublingual	Immunogenic without addition of adjuvant	Good stability	Purification of Influenza extracts
ISCOMs	Cage-like structure made of cholesterol, phospholipids and Quil A saponin	Nasal, oral, vaginal	Self-adjuvanted due to saponin	Good stability	Difficult to incorporate non-lipidic Ags
Microbubbles	Monolayer of phospholipids/palmitic acid entrapping an inert gas	Nasal, oral	Flexibility in lipid composition	Limited stability upon reconstitution and administration	Difficult to entrap Ags
Emulsions	Oil-in-water nanosized droplets	Nasal, oral	Ease of manufacture, self-adjuvanted	Limited stability after administration	Low protection of Ag structure

liposomal preparations seem to be well tolerated, inducing only limited inflammatory responses, irritation, sneezing, or burning syndroms. Oral administration of liposomes has been documented, but its stability in the gastrointestinal tract remains the main concern. As already discussed in Section "Mucoadhesive Properties," promising approaches can be envisaged to improve the stability of liposomal preparations. Incorporation of mannose, chitosan, and PEG are all possible scenarios resulting in reinforced stability, better targeted delivery across the epithelium and to APCs, and improved immunogenicity. Stabilization of liposomes with layer-by-layer deposition of polyelectrolytes also increased the generation of Ab and T cell responses in mucosal tissues (156). The administration of multilamellar preparations is an alternative strategy. Finally, as discussed in Section "Administration Routes for Mucosal Vaccination," vaccination *via* the sublingual route is a promising development that requires to be further evaluated for liposomal preparations in the context of infectious diseases. For example, PEG-modified liposomes incorporating Influenza-derived Ags, together with the TLR-4 agonist CRX-601 as adjuvant, were effective at eliciting elevated levels of serum neutralizing Abs and mucosal IgA (103).

Liposome-Derivatives

Derivatives of liposomes have been explored to circumvent some of the drawbacks associated with liposomes and to improve their efficiency. For example, association of non-ionic surfactants with cholesterol or its derivatives to generate a structure called niosomes has allowed to increase the stability of the bilayer vesicles by preventing oxidation of the lipids (157). Addition of mannan at the surface of niosomes further increased the stability of the vesicles and helped to target specific receptors on APCs following oral administration. Vaccination with niosomes incorporating plasmid DNA coding for an Hepatitis B Ag induced SIgA production in the salivary and intestinal fluids, together with systemic Th1-type T cell responses (158). Moreover, incorporation of bile salts within niosome structures (bilosomes) has been shown to increase the stability of the vesicles and thus to improve oral delivery of peptides and proteins to the gut immune system (159, 160). Bile salts, such as deoxycholic acid or taurocholic acid, are amphiphatic molecules that can be easily incorporated within lipid bilayers and can promote the passage of lipophilic components across cell membranes (161). Thus, bilosomes have the ability to reinforce the biovailability of associated Ags mainly for oral vaccination (162). Different examples of bilosome application have been reported in association with Hepatitis B-derived Ags and Tetanus toxoid. In this context, induction of SIgA in mucosal secretions and IgA-positive plasma cells were observed (162–164) and showed elevated responses as compared to parenteral injection or use of niosomes without bile salts. An alternative approach is the inclusion of polar lipids with fully saturated isoprenoid chains extracted from Archaea to generate vesicles called archaeosomes or archaeal lipid mucosal vaccine adjuvant and delivery (AMVAD) (165). They have been shown to induce robust long-lasting protective Ab and T cell responses, including cytotoxic T lymphocytes responses after systemic injection (166). Advantages of such structures for mucosal vaccination comprise increased pH-dependent and thermal stability due to prevention of lipid oxidation and resistance to phospholipases and bile salts. In this context, mice immunized by the nasal route demonstrated sustained robust local and distant IgA responses in mucosal fluids, strong systemic IgG responses, and T cell responses (167). In addition, nasal vaccination with archaeosomes and cell-free extracts of *Francisella tularensis* led to reduced bacterial burden in the lung and spleen in a mouse model of tularemia (168). Oral immunization with archaeosomes is possible as well, although with higher amounts of Ags. Improved stability and retention

time of such vesicles has been observed in the intestine, leading to potent IgG and IgA production (169). One non-negligible drawback of this approach is the access to achaeal polar lipids, as the purification from Archaea is a relatively demanding process. Nevertheless, production of synthetic polar lipid structures is under development.

Virosomes

Virosomes are a special category of liposomes, where part of the lipid content is derived from viral components that self-assemble into an organized three-dimensional structure that mimics the antigenic structure of the original virus (170). Interestingly, they have been demonstrated to be immunogenic without further addition of adjuvants (171), although addition of immunopotentiating agents further improves their vaccine efficiency (172). Originally called immunopotentiating reconstituted Influenza virosomes, they harbor hemagglutinin and neuraminidase proteins from Influenza virus. These proteins target sialic acid on cell membranes, leading to fusion between the target cell and virosomes, followed by intracellular delivery of their payload. They exhibit similar flexibility and advantages as standard liposomes; however, the process to extract all the necessary components from Influenza virus is relatively complex. Virosomes have been mainly investigated for parenteral vaccination, but reports on their use for mucosal administration exist. They have been used as prime-boost vaccination strategy in a simian model of HIV infection, where intramuscular injections have been followed by nasal administration. It induced full protection against vaginal simian-HIV challenge that was correlated with the presence of mucosal IgA and IgG with blocking activity against virus transcytosis and neutralizing/Ab-dependent cellular cytotoxicity properties, respectively (173). In mice, nasal or sublingual administrations of adjuvanted virosomes were able to protect against Influenza and respiratory syncytial virus infections by promoting mucosal and systemic Ab responses, together with Th1-type cellular responses (174–176).

Gas-Filled Microbubbles

Gas-filled microbubbles are microsized spherical structures composed of a lipidic, denatured protein-based, or crosslinked polymer shell generally entrapping inert high molecular weight gases to ensure resistance to pressure once administered (177). Due to their strong echogenicity in presence of low ultrasound intensities, they are currently used for human application as intravenously delivered echo-contrast agents to more precisely visualize for example angiogenesis in malignant tumors, left ventricular opacification, and myocardial perfusion. In addition, cavitation induced by higher ultrasound application leads to the transient nonlethal permeability of the surrounding tissue (e.g., vascular barriers or cell membrane) allowing enhanced local on-demand extravasation and bioavailabilty of microbubble-associated payload (178). In the last decades, such a process, known as sonoporation, has received important attention in order to improve delivery of a wide range of therapeutic molecules, including chemotherapeutic agents, siRNA, miRNA, oligonucleotides, or plasmid DNA, to tumor or immune cells (177, 179). Typically, sonoporation has been used for improved delivery of Ags into DCs with the aim of boosting immune responses (180). Interestingly, lipid-based microbubbles can be taken up by APCs and deliver intracellularly their antigenic payload without ultrasound application, leading to processing and presentation of the Ag to responsive T cells (181, 182). Furthermore, microbubble-associated Ags can be injected parenterally as a vaccine formulation to elicit potent and long-lasting immune responses against systemic bacterial infection (183, 184). Lipid-based microbubbles are usually composed of phospholipids (e.g., DSPC) and palmitic acid, but tailored formulations can be prepared by incorporation of cationic lipids in their shell in order to better associate DNA (179). In addition, to improve the specificity of imaging and drug delivery, microbubbles can be targeted to particular tissues by linking cell-specific ligands or Abs has been developed at their surface (185, 186). Such aspects are of interest for mucosal vaccination using targeting strategies as discussed in Section "Targeted Delivery of Vaccine Ags." Moreover, adjuvants can be associated with microbubbles, which results in enhanced immunogenicity of the vaccine preparations. As an example, nasal delivery of α-galactosylceramide-adjuvanted microbubbles displaying the *Salmonella*-derived SseB Ag at their surface were able to induce potent IgA, IgM, and IgG humoral responses in the gut, which were associated with a Th1-/Th17-type cellular response. This resulted in a significant decrease in local and systemic bacterial load following oral infection with *Salmonella enterica* Typhimurium in prophylactically vaccinated mice; such effect was more potent than parenteral injection of the same microbubble formulation (140). Despite so far limited induction of local immune responses after oral administration, improvement of microbubble formulations may lead to enhanced immunogenicity. Moreover, sublingual administration remains to be tested owing to its valuable advantages in the context of mucosal vaccination. In recent years, nanosized bubbles have been developed that showed increased stability and extravasation following systemic administration, suggesting that such derivatives might be even more suitable for vaccination purposes (187).

Immune Stimulating Complexes

Immune stimulating complexes (ISCOMs) are negatively charged self-assembling pentagonal dodecahedrons cage-like rigid structures with a size of 30–40 nm. They can form spontaneously after mixing Ags with cholesterol, phospholipids (usually phosphatidylethanolamine and phosphatidylcholine), and the saponin Quil A extracted from the bark of *Quillaja saponaria* Molina tree. Interestingly, such formulation allows to reduce the toxicity associated with saponin administration, while retaining its adjuvant activity (188, 189). Proteins or glycoproteins that are normally anchored by a hydrophobic transmembrane sequence into the cell membrane can be incorporated as such. Non-amphipatic proteins or peptides have to be modified by attachment of a lipid tail (e.g., palmitic acid). Immunization with ISCOMs induced both Th1-type humoral and cellular responses, including cytotoxic T lymphocytes that are important to fight against intracellular pathogens (190). Several studies have reported potent induction of mucosal immune responses, including robust IgA production in nasal washes and the lung, after nasal/pulmonary vaccination with ISCOMs harboring antigenic entities from Influenza virus

(191–194), respiratory syncitial virus (195), Hepatitis B virus (196) and measles (197). Protective efficacy was observed as well after vaccination with an Influenza subunit vaccine composed of ISCOMs (198), adjuvanted ISCOM-based anti-*M. tuberculosis* and anti-Influenza vaccines (199, 200) and *Helicobacter pylori*-Ags delivered *via* ISCOMs (201). In some cases, such immunization proved more efficient than parenteral injection (196, 202). Production of ISCOMs with an alternative saponin, derived from *Quilaja brasiliensis*, also allowed to induce mucosal local and distant IgA production after nasal delivery of an OVA-based vaccine (203). In addition, incorporation of DNA plasmid within the ISCOM matrix elicited potent anti-*Haemophilus influenzae* cellular and Ab responses in the nasopharynx of nasally immunized animals (204). Oral administration of ISCOM-based vaccines has been evaluated (205, 206); however, it seems that the generation of intestinal IgA responses was limited (207). Although ISCOMs are self-adjuvanted delivery systems, incorporation of the adjuvant CTA1-DD within the structure allowed to induce robust mucosal IgA production and T cell proliferation, together with systemic responses, after nasal administration (208). Such an approach has also been evaluated *via* oral delivery. Potent systemic Th1-type immune responses were induced, but unfortunately the mucosal compartments were not analyzed (209). CTA1-DD/ISCOMs incorporating major outer membrane protein from *Chlamydia muridarum* have also been administered *via* the vaginal route. Vaccination induced limited Ab responses, but clearly detectable CD4 T cell responses in vaginal tissues. This led to protection against a bacterial challenge, as demonstrated by reduction in bacterial shedding from the genital tract (49). Overall, the use of ISCOMs as a delivery vehicle for mucosal vaccination finds its best applicable for nasal administration, even though the sublingual route remains to be explored. Nevertheless, the difficulties related to the use of hydrophilic Ags that have to be modified before incorporation within ISCOMs, together with the reported toxicity of saponin, somehow limits the wide use of such vaccination approach.

Others

Oil-in-water nanoemulsions disperse into nanosized droplets and exhibit long-term colloidal stability. They can encapsulate hydrophilic or hydrophobic payload, respectively, and have been tested for nasal vaccination. A nanoemulsion based on soybean oil and cetylpiridinium chloride (W805EC) has been shown to deliver its antigenic payload across ciliated nasal epithelial cells and to the regional LNs in the NALT through migrating activated DCs (210). *Via* TLR-2 and TLR-4, such vaccine formulation promoted the induction of robust Ab and Th1-/Th17-type cellular responses and when associated with inactivated Influenza vaccine, generated a protective immunity against Influenza challenge (211). Such an approach similarly proved efficient in animal models to fight against *M. tuberculosis*, Hepatitis B, and *Bacillus anthracis* infections, or to generate HIV-1-specific mucosal immune responses (212, 213). Improved stability of nanoemulsions for mucosal delivery can now be achieved by the double emulsion water-in-oil-in-water technology, which has been applied both nasally and orally and resulted in robust production of systemic IgG and mucosal IgA (214). Alternatively, coupling of lipopeptides with a polylysine core induces the formation of 5–15 nm particles that can promote the generation of systemic and mucosal IgG/IgA and T cell responses after nasal administration. In these conditions, protective responses have been obtained against *S. pyogenes* infection (215, 216).

HUMAN APPLICATION OF LIPID PARTICLES FOR MUCOSAL VACCINATION

Currently approved mucosal vaccines are composed of live-attenuated or killed whole-pathogen cells that offer relatively good efficacy, but cannot be administered to young infants, immunocompromised people and the elderly due to potential safety issues. The majority of mucosally administered vaccines in humans are delivered *via* the oral route and directed against enteric infections such as polio, cholera, typhoid fever, and rotavirus infection (14). Oral polio vaccine has been used for more than 50 years with great success and is a prototypical vaccine for polio eradication in many countries. Interestingly, it demonstrated improved efficacy as compared to an inactivated pathogen vaccine injected parenterally (217–219). Vivotif®, as well as Dukoral®, Shanchol™, Orochol®/Vaxchora™, and mORC-Vax™, are live-attenuated or whole-killed vaccines against *Salmonella*-induced typhoid fever or *Vibrio cholerae* infections, respectively (220–222). As expected based on preclinical studies in animal models, their protective efficacy has been correlated with effector immune responses present at mucosal surfaces (in most cases detection of SIgA in mucosal fluids) and induction of plasma cells expressing gut-homing molecules specific for the small intestine and the colon (223–225). In addition, and similar to observations in animal models, the choice of the administration route impacts on the tropism of the induced mucosal immune responses (226). Only FluMist®, a live-attenuated Influenza virus vaccine, is licensed for nasal administration (227). It demonstrates high level of protection against matched and mismatched viral strains in children and adults and proved more efficient than parenteral vaccination (228). Virus-specific mucosal IgA and systemic IgG responses with a possible role for cell-mediated immunity has been documented in vaccinated individuals (229). So far, the only adjuvant used for vaccinal application to mucosae is the B subunit of CT, which has been included in Dukoral® to improve the immunogenicity of the killed whole-pathogen *Vibrio cholerae* vaccine.

Despite many encouraging results obtained in proof-of-concept and preclinical animal models, a limited number of subunit vaccines based on lipidic delivery systems has been evaluated and/or approved for human use, especially for mucosal administration (**Table 2**) (230). Interestingly, in the context of mucosal vaccination, at least three formulations have been evaluated in early phase clinical trials. Nasal administration of the oil-in-water nanoemulsion W805EC combined with the approved inactivated systemic Influenza vaccine Fluzone® has demonstrated induction of IgA responses in nasal washes in a clinical evaluation (231). In addition, virosome-based and ISCOM-based Influenza vaccines are currently under development for administration *via* the nasal route (232, 233). Systemic injection of virosomes has been

TABLE 2 | Examples of licensed and in development lipid-based vaccines for human use.

	Admin. routes	Clinical situation	Safety, tolerability	Remarks
Liposomes	I.m. I.m. I.m.	Phase 3 trial of AS01 against malaria (239) Phase 3 trial of AS01 against varicella-zooster virus (240) Phase 1 trial of CAF01 against tuberculosis (230)	Safe and well tolerated Safe and well tolerated Unknown to date	Adjuvanted with saponin and monophosphoryl lipid A Evaluated in the elderly Cationic lipid-adjuvanted with trehalose dibehenate
Virosomes	I.m. I.n.	Licensed vaccines against Influenza and Hepatitis (234) Clinical evaluation against Influenza (232)	Safe and well tolerated Unknown to date	Additional formulations in preclinical stages
Immune stimulating complexes	I.m. I.m. I.m. I.n.	Phase 1 trial against HCV (243) Phase 1 trial against HPV (241, 242) Clinical evaluations against Influenza (189) Clinical evaluation against Influenza (233)	Safe, low-mild reactogenicity Safe, low reactogenicity Not reported Unknown to date	Tested in healthy adults and elderly
Microbubbles	I.v.	Not tested in the context of vaccination	Safe and well tolerated	Licensed use for ultrasound-based imaging
Emulsions	I.m. I.m. I.n.	Licensed vaccines against Influenza containing MF59 (236) Licensed vaccines against Influenza containing AS03 (237) Phase 1 clinical trial of W805EC (231)	Some levels of reactogenicity depending on formulations Well-tolerated, no significant adverse events	Additional formulations in clinical evaluation

I.m., intramuscular; I.n., intranasal; I.v., intravenous.

licensed for human vaccination against hepatitis A (Epaxal®) and Influenza (Inflexal V®) (234). Additional vaccines based on such technology have been tested in Phase 1 clinical trial for malaria and Influenza *via* the systemic route (232, 235). The advantage of such approach is that virosomes are self-adjuvanted, which is not the case for all other lipid-based delivery systems. Two Influenza vaccine formulations composed of squalene-based nanoemulsions (MF59® and AS03) are also approved for intramuscular injection in humans, with a particular focus on use in young children and elderly (236, 237). At least three additional strategies have been evaluated in humans. The most promising one is the use of the AS01 adjuvant, composed of liposomes made of highly unsaturated neutral phospholipids including MPLA and saponin QS21 (238). Successful phase III vaccination trials of such delivery system have been performed with the RTS,S/Mosquirix™ vaccine formulation against malaria (239) and the herpes-zooster vaccine (HZ/su) (240). CAF01 is an alternative formulation that is currently tested for parenteral vaccination against tuberculosis. Such liposomal bilayer preparation contains the cationic lipid DDA and the glycolipid TDB as immunostimulator (152). ISCOMs incorporating Ags E6 and E7 from HPV16 have been tested in women with cervical intraepithelial neoplasia and HIV-positive individuals with oncogenic HPV infections (241, 242). They demonstrated a safety profile and induced specific humoral and effector T cell responses. Similar results were obtained following vaccination with HCV-derived antigenic entities (243). Additional vaccine preparations based on lipidic constructs are currently evaluated to fight against pathogen infections, such as malaria, dengue fever, HIV, or Influenza (90, 230).

Nevertheless, the above-mentioned studies are mainly performed with systemically injected formulations and only rare mucosal applications have been assessed. The use of mucosal route of administration requires that anatomical, functional, and immunological characteristics are taken into consideration and differences between humans and animals may results in poor inter-species translation of promising results (13). An organized NALT similar to that present in mice is not found in humans. By contrast, alternative inductive sites in the form of immune nodules are present in humans in the upper nasal cavity, in the concha, and in Waldeyer's rings (adenoids, tonsils) (244). Pulmonary delivery of vaccines does not seem to be optimal as well, because BALT have only been reported in fetuses and young children, but not in healthy adults. In addition, the localization and phenotype of DCs in the nasal cavity and in the lung all differ between mice and humans. Taking into account these considerations, sublingual administration sounds like a promising strategy (42). Indeed, immunological and physiological organization of the oral cavity is similar in both mice and humans, with documented presence of the same DC subsets, such as Langerhans cells, capable of eliciting immunogenic or tolerogenic responses depending on the applied formulations. Vaccination *via* the sublingual route has been mostly evaluated in humans for allergen immunotherapy, and has been shown to induce systemic IgG (focus of allergy) (245). Therefore, evaluation of the mucosal vaccination approach to protect against infectious diseases is highly relevant and needs evaluation. In addition, although the gut immune system is relatively similar between both species, oral administration of subunit vaccines is further complicated due to the constraints related to the stability of formulations in the aggressive environment of the digestive tract. On the top of anatomical considerations, the age-related decline in the immune function, possibly related to the documented decrease in M cell differentiation with age, represents a drawback for immunization in eldery people.

CONCLUSION AND PERSPECTIVES

Although vaccination has led to the control of several diseases and has demonstrated substantial technological progresses, humans still suffer from infections leading to death and increasing health

costs. Many infectious diseases for which the development of effective vaccines is urgently needed include those transmitted through various mucosal routes that affect the gastrointestinal tract (*E. coli, Salmonella, Shigella, Vibrio cholerae, H. pylori*), the respiratory tract (Influenza, *M. tuberculosis*, respiratory syncitial virus) or are sexually transmitted (HIV, *Chlamydia*) (15). To date, parenteral vaccination represents an important part of the administered vaccines, despite the fact that they poorly induce mucosal immune responses. Furthermore, the requirement for sterile needles, their subsequent elimination, the associated cost, and the cold chain's requirement in many instances prompt a shift toward reduced frequencies of intramuscular vaccination. In addition, most of the currently licensed vaccines can only be administered over 2 years of age for safety reasons; similar considerations apply for immunodeficient individuals and elderly (13). Therefore, the mucosal application of subunit vaccines represents a sound alternative to broaden the target population that could benefit from vaccination. Cues into this direction include recent advances in the understanding of mucosal immunity as well as assessment of correlates of protection may help to develop promising mucosal vaccines; in this respect, design of novel effective delivery strategies will permit to achieve mucosal vaccines that induce protective neutralizing SIgA, together with CTLs and effector CD4 T cells mainly secreting IFN-γ and IL-17. Moreover, because they are considered as safe, subunit vaccines can certainly be administered to neonates and young infants who already possess a functional mucosal immune system (13).

Lipid-based particles fulfill the requirements for better efficiency, safety, low-dose Ag, and ease to handle logistically. They can deliver a wide range of antigenic entities upon mucosal delivery and can be tailored to obtain vaccine formulations with appropriate properties to address questions related to the mechanisms invlolved in the control of the pathogen and the route of administration. Robust and sustained induction of immune responses, comprising production of SIgA at mucosal surfaces, together with helper and cytotoxic T cells, often correlate with protection in defined animal models under study; this will undoubtly help to drive vaccine development toward the right direction. It remains that a strict comparative analysis of the formulations and administration routes to be used against a particular infectious disease is rarely performed within the same study. To contribute to the identification of such a missing piece in this complex puzzle would be an asset in order to optimize mucosal vaccination. The same lack of information must be filled up when one deals with the definition of the optimal dosing and schedule of administration to ensure efficient priming and boosting of immune responses aiming at reaching optimal magnitude and maintenance.

Some lipid-based preparations have the advantage of being lyophilized, thus allowing to simplify the logistics usually necessary for cold chain. Indeed, some of these formulations can be stored at room temperature for several months and can be administered in such form *via* the nasal, oral, or sublingual routes. Dry powder nasal vaccines have already been tested (246), oral delivery of capsules is not a problem (222), and many allergy-related immunotherapy tablets have been considered for sublingual administration (247). Moreover, lipid-based preparations can be aerosolized, which might represent an alternative procedure to keeping stable vaccine preparations. Overall, great expectations are coming from the lipid-based vaccine formulations currently evaluated in clinical trials in humans, which together with the different mechanisms of mucosal immunity recently unraveled, may likely favor the development of future mucosal vaccines suitable for a majority of individuals, thanks to the combinatorial flexibility offered by the nature of the constituents available.

AUTHOR CONTRIBUTIONS

BC and GB planned the manuscript and wrote sections of the manuscript. Both authors read and approved the submitted version of the manuscript.

FUNDING

This work was supported by the Swiss Science Research Foundation (grant 3100-156806 and grant 310030_175686 to BC).

REFERENCES

1. Andre FE. Vaccinology: past achievements, present roadblocks and future promises. *Vaccine* (2003) 21(7–8):593–5. doi:10.1016/S0264-410X(02)00702-8
2. Plotkin SA. Vaccines: past, present and future. *Nat Med* (2005) 11(4 Suppl):S5–11. doi:10.1038/nm1209
3. Pulendran B, Ahmed R. Immunological mechanisms of vaccination. *Nat Immunol* (2011) 12(6):509–17. doi:10.1038/ni.2039
4. Rueckert C, Guzman CA. Vaccines: from empirical development to rational design. *PLoS Pathog* (2012) 8(11):e1003001. doi:10.1371/journal.ppat.1003001
5. De Temmerman ML, Rejman J, Demeester J, Irvine DJ, Gander B, De Smedt SC. Particulate vaccines: on the quest for optimal delivery and immune response. *Drug Discov Today* (2011) 16(13–14):569–82. doi:10.1016/j.drudis.2011.04.006
6. Woodrow KA, Bennett KM, Lo DD. Mucosal vaccine design and delivery. *Annu Rev Biomed Eng* (2012) 14:17–46. doi:10.1146/annurev-bioeng-071811-150054
7. Lamichhane A, Azegamia T, Kiyonoa H. The mucosal immune system for vaccine development. *Vaccine* (2014) 32(49):6711–23. doi:10.1016/j.vaccine.2014.08.089
8. Iwata M, Hirakiyama A, Eshima Y, Kagechika H, Kato C, Song SY. Retinoic acid imprints gut-homing specificity on T cells. *Immunity* (2004) 21(4):527–38. doi:10.1016/j.immuni.2004.08.011
9. Mora JR, Iwata M, Eksteen B, Song SY, Junt T, Senman B, et al. Generation of gut-homing IgA-secreting B cells by intestinal dendritic cells. *Science* (2006) 314(5802):1157–60. doi:10.1126/science.1132742
10. Mora JR, Bono MR, Manjunath N, Weninger W, Cavanagh LL, Rosemblatt M, et al. Selective imprinting of gut-homing T cells by Peyer's patch dendritic cells. *Nature* (2003) 424(6944):88–93. doi:10.1038/nature01726
11. Neutra MR, Kozlowski PA. Mucosal vaccines: the promise and the challenge. *Nat Rev Immunol* (2006) 6(2):148–58. doi:10.1038/nri1777
12. Mestecky J, Russell MW, Elson CO. Perspectives on mucosal vaccines: is mucosal tolerance a barrier? *J Immunol* (2007) 179(9):5633–8. doi:10.4049/jimmunol.179.9.5633
13. Shakya AK, Chowdhury MYE, Tao W, Gill HS. Mucosal vaccine delivery: current state and a pediatric perspective. *J Control Release* (2016) 240:394–413. doi:10.1016/j.jconrel.2016.02.014
14. Lycke N. Recent progress in mucosal vaccine development: potential and limitations. *Nat Rev Immunol* (2012) 12(8):592–605. doi:10.1038/nri3251
15. Czerkinsky C, Holmgren J. Topical immunization strategies. *Mucosal Immunol* (2010) 3(6):545–55. doi:10.1038/mi.2010.55

16. Heritage PL, Underdown BJ, Arsenault AL, Snider DP, McDermott MR. Comparison of murine nasal-associated lymphoid tissue and Peyer's patches. *Am J Respir Crit Care Med* (1997) 156(4 Pt 1):1256–62. doi:10.1164/ajrccm.156.4.97-03017
17. Brandtzaeg P. Mucosal immunity: induction, dissemination, and effector functions. *Scand J Immunol* (2009) 70(6):505–15. doi:10.1111/j.1365-3083.2009.02319.x
18. Corthesy B. Multi-faceted functions of secretory IgA at mucosal surfaces. *Front Immunol* (2013) 4:185. doi:10.3389/fimmu.2013.00185
19. Lelouard H, Fallet M, de Bovis B, Meresse S, Gorvel JP. Peyer's patch dendritic cells sample antigens by extending dendrites through M cell-specific transcellular pores. *Gastroenterology* (2012) 142(3):592–601.e3. doi:10.1053/j.gastro.2011.11.039
20. Niess JH, Brand S, Gu X, Landsman L, Jung S, McCormick BA, et al. CX3CR1-mediated dendritic cell access to the intestinal lumen and bacterial clearance. *Science* (2005) 307(5707):254–8. doi:10.1126/science.1102901
21. Chieppa M, Rescigno M, Huang AY, Germain RN. Dynamic imaging of dendritic cell extension into the small bowel lumen in response to epithelial cell TLR engagement. *J Exp Med* (2006) 203(13):2841–52. doi:10.1084/jem.20061884
22. Brandtzaeg P. The gut as communicator between environment and host: immunological consequences. *Eur J Pharmacol* (2011) 668(Suppl 1):S16–32. doi:10.1016/j.ejphar.2011.07.006
23. Jia Y, Krishnan L, Omri A. Nasal and pulmonary vaccine delivery using particulate carriers. *Expert Opin Drug Deliv* (2015) 12(6):993–1008. doi:10.1517/17425247.2015.1044435
24. Corr SC, Gahan CC, Hill C. M-cells: origin, morphology and role in mucosal immunity and microbial pathogenesis. *FEMS Immunol Med Microbiol* (2008) 52(1):2–12. doi:10.1111/j.1574-695X.2007.00359.x
25. Iwasaki A. Antiviral immune responses in the genital tract: clues for vaccines. *Nat Rev Immunol* (2010) 10(10):699–711. doi:10.1038/nri2836
26. Song JH, Kim JI, Kwon HJ, Shim DH, Parajuli N, Cuburu N, et al. CCR7-CCL19/CCL21-regulated dendritic cells are responsible for effectiveness of sublingual vaccination. *J Immunol* (2009) 182(11):6851–60. doi:10.4049/jimmunol.0803568
27. Czerkinsky C, Holmgren J. Mucosal delivery routes for optimal immunization: targeting immunity to the right tissues. *Curr Top Microbiol Immunol* (2012) 354:1–18. doi:10.1007/82_2010_112
28. Laffont S, Siddiqui KR, Powrie F. Intestinal inflammation abrogates the tolerogenic properties of MLN CD103+ dendritic cells. *Eur J Immunol* (2010) 40(7):1877–83. doi:10.1002/eji.200939957
29. Corthesy B. Roundtrip ticket for secretory IgA: role in mucosal homeostasis? *J Immunol* (2007) 178(1):27–32. doi:10.4049/jimmunol.178.1.27
30. Mowat AM. Anatomical basis of tolerance and immunity to intestinal antigens. *Nat Rev Immunol* (2003) 3(4):331–41. doi:10.1038/nri1057
31. Fagarasan S, Kawamoto S, Kanagawa O, Suzuki K. Adaptive immune regulation in the gut: T cell-dependent and T cell-independent IgA synthesis. *Annu Rev Immunol* (2010) 28:243–73. doi:10.1146/annurev-immunol-030409-101314
32. Belyakov IM, Hammond SA, Ahlers JD, Glenn GM, Berzofsky JA. Transcutaneous immunization induces mucosal CTLs and protective immunity by migration of primed skin dendritic cells. *J Clin Invest* (2004) 113(7):998–1007. doi:10.1172/JCI20261
33. Gavillet BM, Mondoulet L, Dhelft V, Eberhardt CS, Auderset F, Pham HT, et al. Needle-free and adjuvant-free epicutaneous boosting of pertussis immunity: preclinical proof of concept. *Vaccine* (2015) 33(30):3450–5. doi:10.1016/j.vaccine.2015.05.089
34. Hirobe S, Okada N, Nakagawa S. Transcutaneous vaccines – current and emerging strategies. *Expert Opin Drug Deliv* (2013) 10(4):485–98. doi:10.1517/17425247.2013.760542
35. Bernocchi B, Carpentier R, Betbeder D. Nasal nanovaccines. *Int J Pharm* (2017) 530(1–2):128–38. doi:10.1016/j.ijpharm.2017.07.012
36. Vujanic A, Snibson KJ, Wee JL, Edwards SJ, Pearse MJ, Scheerlinck JP, et al. Long-term antibody and immune memory response induced by pulmonary delivery of the influenza Iscomatrix vaccine. *Clin Vaccine Immunol* (2012) 19(1):79–83. doi:10.1128/CVI.05265-11
37. Hodge LM, Simecka JW. Role of upper and lower respiratory tract immunity in resistance to mycoplasma respiratory disease. *J Infect Dis* (2002) 186(2):290–4. doi:10.1086/341280
38. Woolard MD, Hodge LM, Jones HP, Schoeb TR, Simecka JW. The upper and lower respiratory tracts differ in their requirement of IFN-gamma and IL-4 in controlling respiratory mycoplasma infection and disease. *J Immunol* (2004) 172(11):6875–83. doi:10.4049/jimmunol.172.11.6875
39. Soares E, Borges O. Oral vaccination through Peyer's patches: update on particle uptake. *Curr Drug Deliv* (2017). doi:10.2174/1567201814666170825153955
40. Cuburu N, Kweon MN, Song JH, Hervouet C, Luci C, Sun JB, et al. Sublingual immunization induces broad-based systemic and mucosal immune responses in mice. *Vaccine* (2007) 25(51):8598–610. doi:10.1016/j.vaccine.2007.09.073
41. Shim BS, Stadler K, Nguyen HH, Yun CH, Kim DW, Chang J, et al. Sublingual immunization with recombinant adenovirus encoding SARS-CoV spike protein induces systemic and mucosal immunity without redirection of the virus to the brain. *Virol J* (2012) 9:215. doi:10.1186/1743-422X-9-215
42. Kraan H, Vrieling H, Czerkinsky C, Jiskoot W, Kersten G, Amorij JP. Buccal and sublingual vaccine delivery. *J Control Release* (2014) 190:580–92. doi:10.1016/j.jconrel.2014.05.060
43. Song JH, Nguyen HH, Cuburu N, Horimoto T, Ko SY, Park SH, et al. Sublingual vaccination with influenza virus protects mice against lethal viral infection. *Proc Natl Acad Sci U S A* (2008) 105(5):1644–9. doi:10.1073/pnas.0708684105
44. Ma Y, Tao W, Krebs SJ, Sutton WF, Haigwood NL, Gill HS. Vaccine delivery to the oral cavity using coated microneedles induces systemic and mucosal immunity. *Pharm Res* (2014) 31(9):2393–403. doi:10.1007/s11095-014-1335-1
45. Zhen Y, Wang N, Gao Z, Ma X, Wei B, Deng Y, et al. Multifunctional liposomes constituting microneedles induced robust systemic and mucosal immunoresponses against the loaded antigens via oral mucosal vaccination. *Vaccine* (2015) 33(35):4330–40. doi:10.1016/j.vaccine.2015.03.081
46. Zhao X, Deak E, Soderberg K, Linehan M, Spezzano D, Zhu J, et al. Vaginal submucosal dendritic cells, but not Langerhans cells, induce protective Th1 responses to herpes simplex virus-2. *J Exp Med* (2003) 197(2):153–62. doi:10.1084/jem.20021109
47. Prabhala RH, Wira CR. Influence of estrous cycle and estradiol on mitogenic responses of splenic T- and B-lymphocytes. *Adv Exp Med Biol* (1995) 371A:379–81. doi:10.1007/978-1-4615-1941-6_78
48. Seavey MM, Mosmann TR. Estradiol-induced vaginal mucus inhibits antigen penetration and CD8(+) T cell priming in response to intravaginal immunization. *Vaccine* (2009) 27(17):2342–9. doi:10.1016/j.vaccine.2009.02.025
49. Marks E, Helgeby A, Andersson JO, Schon K, Lycke NY. CD4(+) T-cell immunity in the female genital tract is critically dependent on local mucosal immunization. *Eur J Immunol* (2011) 41(9):2642–53. doi:10.1002/eji.201041297
50. Kastenmuller W, Kastenmuller K, Kurts C, Seder RA. Dendritic cell-targeted vaccines – hope or hype? *Nat Rev Immunol* (2014) 14(10):705–11. doi:10.1038/nri3727
51. Iwasaki A. Mucosal dendritic cells. *Annu Rev Immunol* (2007) 25:381–418. doi:10.1146/annurev.immunol.25.022106.141634
52. Israel EJ, Taylor S, Wu Z, Mizoguchi E, Blumberg RS, Bhan A, et al. Expression of the neonatal Fc receptor, FcRn, on human intestinal epithelial cells. *Immunology* (1997) 92(1):69–74. doi:10.1046/j.1365-2567.1997.00326.x
53. Spiekermann GM, Finn PW, Ward ES, Dumont J, Dickinson BL, Blumberg RS, et al. Receptor-mediated immunoglobulin G transport across mucosal barriers in adult life: functional expression of FcRn in the mammalian lung. *J Exp Med* (2002) 196(3):303–10. doi:10.1084/jem.20020400
54. Zhu X, Meng G, Dickinson BL, Li X, Mizoguchi E, Miao L, et al. MHC class I-related neonatal Fc receptor for IgG is functionally expressed in monocytes, intestinal macrophages, and dendritic cells. *J Immunol* (2001) 166(5):3266–76. doi:10.4049/jimmunol.166.5.3266
55. Tiwari B, Agarwal A, Kharya AK, Lariya N, Saraogi G, Agrawal H, et al. Immunoglobulin immobilized liposomal constructs for transmucosal vaccination through nasal route. *J Liposome Res* (2011) 21(3):181–93. doi:10.3109/08982104.2010.498003
56. Pridgen EM, Alexis F, Kuo TT, Levy-Nissenbaum E, Karnik R, Blumberg RS, et al. Transepithelial transport of Fc-targeted nanoparticles by the neonatal fc receptor for oral delivery. *Sci Transl Med* (2013) 5(213):213ra167. doi:10.1126/scitranslmed.3007049
57. Yoshida M, Claypool SM, Wagner JS, Mizoguchi E, Mizoguchi A, Roopenian DC, et al. Human neonatal Fc receptor mediates transport of IgG into luminal

secretions for delivery of antigens to mucosal dendritic cells. *Immunity* (2004) 20(6):769–83. doi:10.1016/j.immuni.2004.05.007
58. Alfsen A, Bomsel M. HIV-1 gp41 envelope residues 650-685 exposed on native virus act as a lectin to bind epithelial cell galactosyl ceramide. *J Biol Chem* (2002) 277(28):25649–59. doi:10.1074/jbc.M200554200
59. Kim SH, Lee KY, Kim J, Park SM, Park BK, Jang YS. Identification of a peptide enhancing mucosal and systemic immune responses against EGFP after oral administration in mice. *Mol Cells* (2006) 21(2):244–50.
60. Rajapaksa TE, Bennett KM, Hamer M, Lytle C, Rodgers VG, Lo DD. Intranasal M cell uptake of nanoparticles is independently influenced by targeting ligands and buffer ionic strength. *J Biol Chem* (2010) 285(31):23739–46. doi:10.1074/jbc.M110.126359
61. Shima H, Watanabe T, Fukuda S, Fukuoka S, Ohara O, Ohno H. A novel mucosal vaccine targeting Peyer's patch M cells induces protective antigen-specific IgA responses. *Int Immunol* (2014) 26(11):619–25. doi:10.1093/intimm/dxu061
62. Ma T, Wang L, Yang T, Ma G, Wang S. M-cell targeted polymeric lipid nanoparticles containing a toll-like receptor agonist to boost oral immunity. *Int J Pharm* (2014) 473(1–2):296–303. doi:10.1016/j.ijpharm.2014.06.052
63. Kim SH, Seo KW, Kim J, Lee KY, Jang YS. The M cell-targeting ligand promotes antigen delivery and induces antigen-specific immune responses in mucosal vaccination. *J Immunol* (2010) 185(10):5787–95. doi:10.4049/jimmunol.0903184
64. Kim SH, Jung DI, Yang IY, Jang SH, Kim J, Truong TT, et al. Application of an M-cell-targeting ligand for oral vaccination induces efficient systemic and mucosal immune responses against a viral antigen. *Int Immunol* (2013) 25(11):623–32. doi:10.1093/intimm/dxt029
65. Jiang T, Singh B, Li HS, Kim YK, Kang SK, Nah JW, et al. Targeted oral delivery of BmpB vaccine using porous PLGA microparticles coated with M cell homing peptide-coupled chitosan. *Biomaterials* (2014) 35(7):2365–73. doi:10.1016/j.biomaterials.2013.11.073
66. Foster N, Clark MA, Jepson MA, Hirst BH. Ulex europaeus 1 lectin targets microspheres to mouse Peyer's patch M-cells in vivo. *Vaccine* (1998) 16(5):536–41. doi:10.1016/S0264-410X(97)00222-3
67. Manocha M, Pal PC, Chitralekha KT, Thomas BE, Tripathi V, Gupta SD, et al. Enhanced mucosal and systemic immune response with intranasal immunization of mice with HIV peptides entrapped in PLG microparticles in combination with Ulex Europaeus-I lectin as M cell target. *Vaccine* (2005) 23(48–49):5599–617. doi:10.1016/j.vaccine.2005.06.031
68. Nochi T, Yuki Y, Matsumura A, Mejima M, Terahara K, Kim DY, et al. A novel M cell-specific carbohydrate-targeted mucosal vaccine effectively induces antigen-specific immune responses. *J Exp Med* (2007) 204(12):2789–96. doi:10.1084/jem.20070607
69. Clark MA, Jepson MA, Simmons NL, Booth TA, Hirst BH. Differential expression of lectin-binding sites defines mouse intestinal M-cells. *J Histochem Cytochem* (1993) 41(11):1679–87. doi:10.1177/41.11.7691933
70. Giannasca PJ, Giannasca KT, Leichtner AM, Neutra MR. Human intestinal M cells display the sialyl Lewis A antigen. *Infect Immun* (1999) 67(2):946–53.
71. Rochereau N, Drocourt D, Perouzel E, Pavot V, Redelinghuys P, Brown GD, et al. Dectin-1 is essential for reverse transcytosis of glycosylated SIgA-antigen complexes by intestinal M cells. *PLoS Biol* (2013) 11(9):e1001658. doi:10.1371/journal.pbio.1001658
72. Rol N, Favre L, Benyacoub J, Corthesy B. The role of secretory immunoglobulin A in the natural sensing of commensal bacteria by mouse Peyer's patch dendritic cells. *J Biol Chem* (2012) 287(47):40074–82. doi:10.1074/jbc.M112.405001
73. Bachmann MF, Jennings GT. Vaccine delivery: a matter of size, geometry, kinetics and molecular patterns. *Nat Rev Immunol* (2010) 10(11):787–96. doi:10.1038/nri2868
74. Sun H, Pollock KG, Brewer JM. Analysis of the role of vaccine adjuvants in modulating dendritic cell activation and antigen presentation in vitro. *Vaccine* (2003) 21(9–10):849–55. doi:10.1016/S0264-410X(02)00531-5
75. Sahay G, Alakhova DY, Kabanov AV. Endocytosis of nanomedicines. *J Control Release* (2010) 145(3):182–95. doi:10.1016/j.jconrel.2010.01.036
76. Xiang SD, Scholzen A, Minigo G, David C, Apostolopoulos V, Mottram PL, et al. Pathogen recognition and development of particulate vaccines: does size matter? *Methods* (2006) 40(1):1–9. doi:10.1016/j.ymeth.2006.05.016
77. Mann JF, Shakir E, Carter KC, Mullen AB, Alexander J, Ferro VA. Lipid vesicle size of an oral influenza vaccine delivery vehicle influences the Th1/Th2 bias in the immune response and protection against infection. *Vaccine* (2009) 27(27):3643–9. doi:10.1016/j.vaccine.2009.03.040
78. Brewer JM, Tetley L, Richmond J, Liew FY, Alexander J. Lipid vesicle size determines the Th1 or Th2 response to entrapped antigen. *J Immunol* (1998) 161(8):4000–7.
79. Henriksen-Lacey M, Devitt A, Perrie Y. The vesicle size of DDA:TDB liposomal adjuvants plays a role in the cell-mediated immune response but has no significant effect on antibody production. *J Control Release* (2011) 154(2):131–7. doi:10.1016/j.jconrel.2011.05.019
80. Vila A, Sanchez A, Evora C, Soriano I, McCallion O, Alonso MJ. PLA-PEG particles as nasal protein carriers: the influence of the particle size. *Int J Pharm* (2005) 292(1–2):43–52. doi:10.1016/j.ijpharm.2004.09.002
81. Thomas C, Gupta V, Ahsan F. Particle size influences the immune response produced by hepatitis B vaccine formulated in inhalable particles. *Pharm Res* (2010) 27(5):905–19. doi:10.1007/s11095-010-0094-x
82. Lai SK, Wang YY, Hida K, Cone R, Hanes J. Nanoparticles reveal that human cervicovaginal mucus is riddled with pores larger than viruses. *Proc Natl Acad Sci U S A* (2010) 107(2):598–603. doi:10.1073/pnas.0911748107
83. Bajka BH, Rigby NM, Cross KL, Macierzanka A, Mackie AR. The influence of small intestinal mucus structure on particle transport ex vivo. *Colloids Surf B Biointerfaces* (2015) 135:73–80. doi:10.1016/j.colsurfb.2015.07.038
84. Kim TW, Chung H, Kwon IC, Sung HC, Jeong SY. In vivo gene transfer to the mouse nasal cavity mucosa using a stable cationic lipid emulsion. *Mol Cells* (2000) 10(2):142–7. doi:10.1007/s10059-000-0142-1
85. Ingvarsson PT, Rasmussen IS, Viaene M, Irlik PJ, Nielsen HM, Foged C. The surface charge of liposomal adjuvants is decisive for their interactions with the Calu-3 and A549 airway epithelial cell culture models. *Eur J Pharm Biopharm* (2014) 87(3):480–8. doi:10.1016/j.ejpb.2014.04.001
86. Korsholm KS, Agger EM, Foged C, Christensen D, Dietrich J, Andersen CS, et al. The adjuvant mechanism of cationic dimethyldioctadecylammonium liposomes. *Immunology* (2007) 121(2):216–26. doi:10.1111/j.1365-2567.2007.02560.x
87. Foged C, Arigita C, Sundblad A, Jiskoot W, Storm G, Frokjaer S. Interaction of dendritic cells with antigen-containing liposomes: effect of bilayer composition. *Vaccine* (2004) 22(15–16):1903–13. doi:10.1016/j.vaccine.2003.11.008
88. Watson DS, Endsley AN, Huang L. Design considerations for liposomal vaccines: influence of formulation parameters on antibody and cell-mediated immune responses to liposome associated antigens. *Vaccine* (2012) 30(13):2256–72. doi:10.1016/j.vaccine.2012.01.070
89. Heurtault B, Frisch B, Pons F. Liposomes as delivery systems for nasal vaccination: strategies and outcomes. *Expert Opin Drug Deliv* (2010) 7(7):829–44. doi:10.1517/17425247.2010.488687
90. Bernasconi V, Norling K, Bally M, Hook F, Lycke NY. Mucosal vaccine development based on liposome technology. *J Immunol Res* (2016) 2016:5482087. doi:10.1155/2016/5482087
91. Therien HM, Shahum E. Importance of physical association between antigen and liposomes in liposomes adjuvanticity. *Immunol Lett* (1989) 22(4):253–8. doi:10.1016/0165-2478(89)90161-2
92. Barnier-Quer C, Elsharkawy A, Romeijn S, Kros A, Jiskoot W. Adjuvant effect of cationic liposomes for subunit influenza vaccine: influence of antigen loading method, cholesterol and immune modulators. *Pharmaceutics* (2013) 5(3):392–410. doi:10.3390/pharmaceutics5030392
93. Minato S, Iwanaga K, Kakemi M, Yamashita S, Oku N. Application of polyethyleneglycol (PEG)-modified liposomes for oral vaccine: effect of lipid dose on systemic and mucosal immunity. *J Control Release* (2003) 89(2):189–97. doi:10.1016/S0168-3659(03)00093-2
94. Brewer MG, DiPiazza A, Acklin J, Feng C, Sant AJ, Dewhurst S. Nanoparticles decorated with viral antigens are more immunogenic at low surface density. *Vaccine* (2017) 35(5):774–81. doi:10.1016/j.vaccine.2016.12.049
95. Saade F, Petrovsky N. Technologies for enhanced efficacy of DNA vaccines. *Expert Rev Vaccines* (2012) 11(2):189–209. doi:10.1586/erv.11.188
96. Gregoriadis G, Bacon A, Caparros-Wanderley W, McCormack B. A role for liposomes in genetic vaccination. *Vaccine* (2002) 20(Suppl 5):B1–9. doi:10.1016/S0264-410X(02)00514-5
97. Henderson A, Propst K, Kedl R, Dow S. Mucosal immunization with liposome-nucleic acid adjuvants generates effective humoral and cellular immunity. *Vaccine* (2011) 29(32):5304–12. doi:10.1016/j.vaccine.2011.05.009

98. Wang D, Xu J, Feng Y, Liu Y, McHenga SS, Shan F, et al. Liposomal oral DNA vaccine (*Mycobacterium* DNA) elicits immune response. *Vaccine* (2010) 28(18):3134–42. doi:10.1016/j.vaccine.2010.02.058
99. Midoux P, Pichon C. Lipid-based mRNA vaccine delivery systems. *Expert Rev Vaccines* (2015) 14(2):221–34. doi:10.1586/14760584.2015.986104
100. Phua KK, Staats HF, Leong KW, Nair SK. Intranasal mRNA nanoparticle vaccination induces prophylactic and therapeutic anti-tumor immunity. *Sci Rep* (2014) 4:5128. doi:10.1038/srep05128
101. Palchetti S, Digiacomo L, Pozzi D, Peruzzi G, Micarelli E, Mahmoudi M, et al. Nanoparticles-cell association predicted by protein corona fingerprints. *Nanoscale* (2016) 8(25):12755–63. doi:10.1039/c6nr03898k
102. Iwanaga K, Ono S, Narioka K, Kakemi M, Morimoto K, Yamashita S, et al. Application of surface-coated liposomes for oral delivery of peptide: effects of coating the liposome's surface on the GI transit of insulin. *J Pharm Sci* (1999) 88(2):248–52. doi:10.1021/js980235x
103. Oberoi HS, Yorgensen YM, Morasse A, Evans JT, Burkhart DJ. PEG modified liposomes containing CRX-601 adjuvant in combination with methylglycol chitosan enhance the murine sublingual immune response to influenza vaccination. *J Control Release* (2016) 223:64–74. doi:10.1016/j.jconrel.2015.11.006
104. Lai SK, O'Hanlon DE, Harrold S, Man ST, Wang YY, Cone R, et al. Rapid transport of large polymeric nanoparticles in fresh undiluted human mucus. *Proc Natl Acad Sci U S A* (2007) 104(5):1482–7. doi:10.1073/pnas.0608611104
105. Huang Y, Leobandung W, Foss A, Peppas NA. Molecular aspects of muco- and bioadhesion: tethered structures and site-specific surfaces. *J Control Release* (2000) 65(1–2):63–71. doi:10.1016/S0168-3659(99)00233-3
106. Lai SK, Wang YY, Hanes J. Mucus-penetrating nanoparticles for drug and gene delivery to mucosal tissues. *Adv Drug Deliv Rev* (2009) 61(2):158–71. doi:10.1016/j.addr.2008.11.002
107. Augst AD, Kong HJ, Mooney DJ. Alginate hydrogels as biomaterials. *Macromol Biosci* (2006) 6(8):623–33. doi:10.1002/mabi.200600069
108. Rebelatto MC, Guimond P, Bowersock TL, HogenEsch H. Induction of systemic and mucosal immune response in cattle by intranasal administration of pig serum albumin in alginate microparticles. *Vet Immunol Immunopathol* (2001) 83(1–2):93–105. doi:10.1016/S0165-2427(01)00370-1
109. Chadwick S, Kriegel C, Amiji M. Nanotechnology solutions for mucosal immunization. *Adv Drug Deliv Rev* (2010) 62(4–5):394–407. doi:10.1016/j.addr.2009.11.012
110. Read RC, Naylor SC, Potter CW, Bond J, Jabbal-Gill I, Fisher A, et al. Effective nasal influenza vaccine delivery using chitosan. *Vaccine* (2005) 23(35):4367–74. doi:10.1016/j.vaccine.2005.04.021
111. Filipovic-Grcic J, Skalko-Basnet N, Jalsenjak I. Mucoadhesive chitosan-coated liposomes: characteristics and stability. *J Microencapsul* (2001) 18(1):3–12. doi:10.1080/026520401750038557
112. Kobayashi T, Fukushima K, Sannan T, Saito N, Takiguchi Y, Sato Y, et al. Evaluation of the effectiveness and safety of chitosan derivatives as adjuvants for intranasal vaccines. *Viral Immunol* (2013) 26(2):133–42. doi:10.1089/vim.2012.0057
113. McKee AS, Marrack P. Old and new adjuvants. *Curr Opin Immunol* (2017) 47:44–51. doi:10.1016/j.coi.2017.06.005
114. Pizza M, Giuliani MM, Fontana MR, Monaci E, Douce G, Dougan G, et al. Mucosal vaccines: non toxic derivatives of LT and CT as mucosal adjuvants. *Vaccine* (2001) 19(17–19):2534–41. doi:10.1016/S0264-410X(00)00553-3
115. Fukuyama Y, Okada K, Yamaguchi M, Kiyono H, Mori K, Yuki Y. Nasal administration of cholera toxin as a mucosal adjuvant damages the olfactory system in mice. *PLoS One* (2015) 10(9):e0139368. doi:10.1371/journal.pone.0139368
116. Mutsch M, Zhou W, Rhodes P, Bopp M, Chen RT, Linder T, et al. Use of the inactivated intranasal influenza vaccine and the risk of Bell's palsy in Switzerland. *N Engl J Med* (2004) 350(9):896–903. doi:10.1056/NEJMoa030595
117. Ryan EJ, McNeela E, Murphy GA, Stewart H, O'Hagan D, Pizza M, et al. Mutants of *Escherichia coli* heat-labile toxin act as effective mucosal adjuvants for nasal delivery of an acellular pertussis vaccine: differential effects of the nontoxic AB complex and enzyme activity on Th1 and Th2 cells. *Infect Immun* (1999) 67(12):6270–80.
118. Jakobsen H, Saeland E, Gizurarson S, Schulz D, Jonsdottir I. Intranasal immunization with pneumococcal polysaccharide conjugate vaccines protects mice against invasive pneumococcal infections. *Infect Immun* (1999) 67(8):4128–33.
119. Neidleman JA, Vajdy M, Ugozzoli M, Ott G, O'Hagan D. Genetically detoxified mutants of heat-labile enterotoxin from *Escherichia coli* are effective adjuvants for induction of cytotoxic T-cell responses against HIV-1 gag-p55. *Immunology* (2000) 101(1):154–60. doi:10.1046/j.1365-2567.2000.00090.x
120. Yamamoto S, Kiyono H, Yamamoto M, Imaoka K, Fujihashi K, Van Ginkel FW, et al. A nontoxic mutant of cholera toxin elicits Th2-type responses for enhanced mucosal immunity. *Proc Natl Acad Sci U S A* (1997) 94(10):5267–72. doi:10.1073/pnas.94.10.5267
121. Norton EB, Lawson LB, Freytag LC, Clements JD. Characterization of a mutant *Escherichia coli* heat-labile toxin, LT(R192G/L211A), as a safe and effective oral adjuvant. *Clin Vaccine Immunol* (2011) 18(4):546–51. doi:10.1128/CVI.00538-10
122. Norton EB, Bauer DL, Weldon WC, Oberste MS, Lawson LB, Clements JD. The novel adjuvant dmLT promotes dose sparing, mucosal immunity and longevity of antibody responses to the inactivated polio vaccine in a murine model. *Vaccine* (2015) 33(16):1909–15. doi:10.1016/j.vaccine.2015.02.069
123. Sjokvist Ottsjo L, Flach CF, Clements J, Holmgren J, Raghavan S. A double mutant heat-labile toxin from *Escherichia coli*, LT(R192G/L211A), is an effective mucosal adjuvant for vaccination against *Helicobacter pylori* infection. *Infect Immun* (2013) 81(5):1532–40. doi:10.1128/IAI.01407-12
124. Lebens M, Terrinoni M, Karlsson SL, Larena M, Gustafsson-Hedberg T, Kallgard S, et al. Construction and preclinical evaluation of mmCT, a novel mutant cholera toxin adjuvant that can be efficiently produced in genetically manipulated *Vibrio cholerae*. *Vaccine* (2016) 34(18):2121–8. doi:10.1016/j.vaccine.2016.03.002
125. Agren LC, Ekman L, Lowenadler B, Lycke NY. Genetically engineered nontoxic vaccine adjuvant that combines B cell targeting with immunomodulation by cholera toxin A1 subunit. *J Immunol* (1997) 158(8):3936–46.
126. Zaman M, Ozberk V, Langshaw EL, McPhun V, Powell JL, Phillips ZN, et al. Novel platform technology for modular mucosal vaccine that protects against *Streptococcus*. *Sci Rep* (2016) 6:39274. doi:10.1038/srep39274
127. McCluskie MJ, Davis HL. Oral, intrarectal and intranasal immunizations using CpG and non-CpG oligodeoxynucleotides as adjuvants. *Vaccine* (2000) 19(4–5):413–22. doi:10.1016/S0264-410X(00)00208-5
128. Boyaka PN, Marinaro M, Jackson RJ, van Ginkel FW, Cormet-Boyaka E, Kirk KL, et al. Oral QS-21 requires early IL-4 help for induction of mucosal and systemic immunity. *J Immunol* (2001) 166(4):2283–90. doi:10.4049/jimmunol.166.4.2283
129. Sasaki S, Sumino K, Hamajima K, Fukushima J, Ishii N, Kawamoto S, et al. Induction of systemic and mucosal immune responses to human immunodeficiency virus type 1 by a DNA vaccine formulated with QS-21 saponin adjuvant via intramuscular and intranasal routes. *J Virol* (1998) 72(6):4931–9.
130. Wang N, Wang T, Zhang M, Chen R, Niu R, Deng Y. Mannose derivative and lipid A dually decorated cationic liposomes as an effective cold chain free oral mucosal vaccine adjuvant-delivery system. *Eur J Pharm Biopharm* (2014) 88(1):194–206. doi:10.1016/j.ejpb.2014.04.007
131. Iho S, Maeyama J, Suzuki F. CpG oligodeoxynucleotides as mucosal adjuvants. *Hum Vaccin Immunother* (2015) 11(3):755–60. doi:10.1080/21645515.2014.1004033
132. Todoroff J, Lemaire MM, Fillee C, Jurion F, Renauld JC, Huygen K, et al. Mucosal and systemic immune responses to *Mycobacterium tuberculosis* antigen 85A following its co-delivery with CpG, MPLA or LTB to the lungs in mice. *PLoS One* (2013) 8(5):e63344. doi:10.1371/journal.pone.0063344
133. Van Maele L, Fougeron D, Janot L, Didierlaurent A, Cayet D, Tabareau J, et al. Airway structural cells regulate TLR5-mediated mucosal adjuvant activity. *Mucosal Immunol* (2014) 7(3):489–500. doi:10.1038/mi.2013.66
134. Hong SH, Byun YH, Nguyen CT, Kim SY, Seong BL, Park S, et al. Intranasal administration of a flagellin-adjuvanted inactivated influenza vaccine enhances mucosal immune responses to protect mice against lethal infection. *Vaccine* (2012) 30(2):466–74. doi:10.1016/j.vaccine.2011.10.058
135. Schoenen H, Bodendorfer B, Hitchens K, Manzanero S, Werninghaus K, Nimmerjahn F, et al. Cutting edge: mincle is essential for recognition and adjuvanticity of the mycobacterial cord factor and its synthetic analog trehalose-dibehenate. *J Immunol* (2010) 184(6):2756–60. doi:10.4049/jimmunol.0904013
136. Christensen D, Foged C, Rosenkrands I, Lundberg CV, Andersen P, Agger EM, et al. CAF01 liposomes as a mucosal vaccine adjuvant: in vitro and in vivo investigations. *Int J Pharm* (2010) 390(1):19–24. doi:10.1016/j.ijpharm.2009.10.043

137. Martin TL, Jee J, Kim E, Steiner HE, Cormet-Boyaka E, Boyaka PN. Sublingual targeting of STING with 3'3'-cGAMP promotes systemic and mucosal immunity against anthrax toxins. *Vaccine* (2017) 35(18):2511–9. doi:10.1016/j.vaccine.2017.02.064
138. Courtney AN, Nehete PN, Nehete BP, Thapa P, Zhou D, Sastry KJ. Alpha-galactosylceramide is an effective mucosal adjuvant for repeated intranasal or oral delivery of HIV peptide antigens. *Vaccine* (2009) 27(25–26):3335–41. doi:10.1016/j.vaccine.2009.01.083
139. Singh S, Nehete PN, Yang G, He H, Nehete B, Hanley PW, et al. Enhancement of mucosal immunogenicity of viral vectored vaccines by the NKT cell agonist alpha-galactosylceramide as adjuvant. *Vaccines (Basel)* (2014) 2(4):686–706. doi:10.3390/vaccines2040686
140. Pigny F, Lassus A, Terrettaz J, Tranquart F, Corthesy B, Bioley G. Intranasal vaccination with *Salmonella*-derived serodominant secreted effector protein B associated with gas-filled microbubbles partially protects against gut infection in mice. *J Infect Dis* (2016) 214(3):438–46. doi:10.1093/infdis/jiw162
141. Boks MA, Ambrosini M, Bruijns SC, Kalay H, van Bloois L, Storm G, et al. MPLA incorporation into DC-targeting glycoliposomes favours anti-tumour T cell responses. *J Control Release* (2015) 216:37–46. doi:10.1016/j.jconrel.2015.06.033
142. Lonez C, Bessodes M, Scherman D, Vandenbranden M, Escriou V, Ruysschaert JM. Cationic lipid nanocarriers activate toll-like receptor 2 and NLRP3 inflammasome pathways. *Nanomedicine* (2014) 10(4):775–82. doi:10.1016/j.nano.2013.12.003
143. Henriksen-Lacey M, Korsholm KS, Andersen P, Perrie Y, Christensen D. Liposomal vaccine delivery systems. *Expert Opin Drug Deliv* (2011) 8(4):505–19. doi:10.1517/17425247.2011.558081
144. Sessa G, Weissmann G. Phospholipid spherules (liposomes) as a model for biological membranes. *J Lipid Res* (1968) 9(3):310–8.
145. Watarai S, Han M, Tana, Kodama H. Antibody response in the intestinal tract of mice orally immunized with antigen associated with liposomes. *J Vet Med Sci* (1998) 60(9):1047–50. doi:10.1292/jvms.60.1047
146. Han M, Watarai S, Kobayashi K, Yasuda T. Application of liposomes for development of oral vaccines: study of in vitro stability of liposomes and antibody response to antigen associated with liposomes after oral immunization. *J Vet Med Sci* (1997) 59(12):1109–14. doi:10.1292/jvms.59.1109
147. Drummond DC, Zignani M, Leroux J. Current status of pH-sensitive liposomes in drug delivery. *Prog Lipid Res* (2000) 39(5):409–60. doi:10.1016/S0163-7827(00)00011-4
148. Nair S, Zhou F, Reddy R, Huang L, Rouse BT. Soluble proteins delivered to dendritic cells via pH-sensitive liposomes induce primary cytotoxic T lymphocyte responses in vitro. *J Exp Med* (1992) 175(2):609–12. doi:10.1084/jem.175.2.609
149. Yusuf H, Ali AA, Orr N, Tunney MM, McCarthy HO, Kett VL. Novel freeze-dried DDA and TPGS liposomes are suitable for nasal delivery of vaccine. *Int J Pharm* (2017) 533(1):179–86. doi:10.1016/j.ijpharm.2017.09.011
150. Tada R, Hidaka A, Iwase N, Takahashi S, Yamakita Y, Iwata T, et al. Intranasal immunization with DOTAP cationic liposomes combined with DC-cholesterol induces potent antigen-specific mucosal and systemic immune responses in mice. *PLoS One* (2015) 10(10):e0139785. doi:10.1371/journal.pone.0139785
151. Agger EM, Rosenkrands I, Hansen J, Brahimi K, Vandahl BS, Aagaard C, et al. Cationic liposomes formulated with synthetic mycobacterial cord-factor (CAF01): a versatile adjuvant for vaccines with different immunological requirements. *PLoS One* (2008) 3(9):e3116. doi:10.1371/journal.pone.0003116
152. Davidsen J, Rosenkrands I, Christensen D, Vangala A, Kirby D, Perrie Y, et al. Characterization of cationic liposomes based on dimethyldioctadecylammonium and synthetic cord factor from *M. tuberculosis* (trehalose 6,6'-dibehenate) – a novel adjuvant inducing both strong CMI and antibody responses. *Biochim Biophys Acta* (2005) 1718(1–2):22–31. doi:10.1016/j.bbamem.2005.10.011
153. Mortensen R, Christensen D, Hansen LB, Christensen JP, Andersen P, Dietrich J. Local Th17/IgA immunity correlate with protection against intranasal infection with *Streptococcus pyogenes*. *PLoS One* (2017) 12(4):e0175707. doi:10.1371/journal.pone.0175707
154. Joseph A, Itskovitz-Cooper N, Samira S, Flasterstein O, Eliyahu H, Simberg D, et al. A new intranasal influenza vaccine based on a novel polycationic lipid – ceramide carbamoyl-spermine (CCS) I. Immunogenicity and efficacy studies in mice. *Vaccine* (2006) 24(18):3990–4006. doi:10.1016/j.vaccine.2005.12.017
155. Rosada RS, de la Torre LG, Frantz FG, Trombone AP, Zarate-Blades CR, Fonseca DM, et al. Protection against tuberculosis by a single intranasal administration of DNA-hsp65 vaccine complexed with cationic liposomes. *BMC Immunol* (2008) 9:38. doi:10.1186/1471-2172-9-38
156. Harde H, Agrawal AK, Jain S. Tetanus toxoid-loaded layer-by-layer nano-assemblies for efficient systemic, mucosal, and cellular immunostimulatory response following oral administration. *Drug Deliv Transl Res* (2015) 5(5):498–510. doi:10.1007/s13346-015-0247-x
157. Mahale NB, Thakkar PD, Mali RG, Walunj DR, Chaudhari SR. Niosomes: novel sustained release nonionic stable vesicular systems – an overview. *Adv Colloid Interface Sci* (2012) 183-184:46–54. doi:10.1016/j.cis.2012.08.002
158. Jain S, Vyas SP. Mannosylated niosomes as carrier adjuvant system for topical immunization. *J Pharm Pharmacol* (2005) 57(9):1177–84. doi:10.1211/jpp.57.9.0012
159. Conacher M, Alexander J, Brewer JM. Oral immunisation with peptide and protein antigens by formulation in lipid vesicles incorporating bile salts (bilosomes). *Vaccine* (2001) 19(20–22):2965–74. doi:10.1016/S0264-410X(00)00537-5
160. Shukla A, Mishra V, Kesharwani P. Bilosomes in the context of oral immunization: development, challenges and opportunities. *Drug Discov Today* (2016) 21(6):888–99. doi:10.1016/j.drudis.2016.03.013
161. Holm R, Mullertz A, Mu H. Bile salts and their importance for drug absorption. *Int J Pharm* (2013) 453(1):44–55. doi:10.1016/j.ijpharm.2013.04.003
162. Shukla A, Singh B, Katare OP. Significant systemic and mucosal immune response induced on oral delivery of diphtheria toxoid using nano-bilosomes. *Br J Pharmacol* (2011) 164(2b):820–7. doi:10.1111/j.1476-5381.2011.01452.x
163. Mann JF, Scales HE, Shakir E, Alexander J, Carter KC, Mullen AB, et al. Oral delivery of tetanus toxoid using vesicles containing bile salts (bilosomes) induces significant systemic and mucosal immunity. *Methods* (2006) 38(2):90–5. doi:10.1016/j.ymeth.2005.11.002
164. Jain S, Harde H, Indulkar A, Agrawal AK. Improved stability and immunological potential of tetanus toxoid containing surface engineered bilosomes following oral administration. *Nanomedicine* (2014) 10(2):431–40. doi:10.1016/j.nano.2013.08.012
165. Patel GB, Chen W. Archaeal lipid mucosal vaccine adjuvant and delivery system. *Expert Rev Vaccines* (2010) 9(4):431–40. doi:10.1586/erv.10.34
166. Conlan JW, Krishnan L, Willick GE, Patel GB, Sprott GD. Immunization of mice with lipopeptide antigens encapsulated in novel liposomes prepared from the polar lipids of various archaebacteria elicits rapid and prolonged specific protective immunity against infection with the facultative intracellular pathogen, *Listeria monocytogenes*. *Vaccine* (2001) 19(25–26):3509–17.
167. Patel GB, Zhou H, Ponce A, Chen W. Mucosal and systemic immune responses by intranasal immunization using archaeal lipid-adjuvanted vaccines. *Vaccine* (2007) 25(51):8622–36. doi:10.1016/j.vaccine.2007.09.042
168. Patel GB, Zhou H, Ponce A, Harris G, Chen W. Intranasal immunization with an archaeal lipid mucosal vaccine adjuvant and delivery formulation protects against a respiratory pathogen challenge. *PLoS One* (2010) 5(12):e15574. doi:10.1371/journal.pone.0015574
169. Li Z, Zhang L, Sun W, Ding Q, Hou Y, Xu Y. Archaeosomes with encapsulated antigens for oral vaccine delivery. *Vaccine* (2011) 29(32):5260–6. doi:10.1016/j.vaccine.2011.05.015
170. Felnerova D, Viret JF, Gluck R, Moser C. Liposomes and virosomes as delivery systems for antigens, nucleic acids and drugs. *Curr Opin Biotechnol* (2004) 15(6):518–29. doi:10.1016/j.copbio.2004.10.005
171. Moser C, Amacker M, Kammer AR, Rasi S, Westerfeld N, Zurbriggen R. Influenza virosomes as a combined vaccine carrier and adjuvant system for prophylactic and therapeutic immunizations. *Expert Rev Vaccines* (2007) 6(5):711–21. doi:10.1586/14760584.6.5.711
172. Madhun AS, Haaheim LR, Nilsen MV, Cox RJ. Intramuscular matrix-M-adjuvanted virosomal H5N1 vaccine induces high frequencies of multifunctional Th1 CD4+ cells and strong antibody responses in mice. *Vaccine* (2009) 27(52):7367–76. doi:10.1016/j.vaccine.2009.09.044
173. Bomsel M, Tudor D, Drillet AS, Alfsen A, Ganor Y, Roger MG, et al. Immunization with HIV-1 gp41 subunit virosomes induces mucosal

antibodies protecting nonhuman primates against vaginal SHIV challenges. *Immunity* (2011) 34(2):269–80. doi:10.1016/j.immuni.2011.01.015
174. Pedersen GK, Ebensen T, Gjeraker IH, Svindland S, Bredholt G, Guzman CA, et al. Evaluation of the sublingual route for administration of influenza H5N1 virosomes in combination with the bacterial second messenger c-di-GMP. *PLoS One* (2011) 6(11):e26973. doi:10.1371/journal.pone.0026973
175. Ebensen T, Debarry J, Pedersen GK, Blazejewska P, Weissmann S, Schulze K, et al. Mucosal administration of cycle-di-nucleotide-adjuvanted virosomes efficiently induces protection against influenza H5N1 in mice. *Front Immunol* (2017) 8:1223. doi:10.3389/fimmu.2017.01223
176. Shafique M, Meijerhof T, Wilschut J, de Haan A. Evaluation of an intranasal virosomal vaccine against respiratory syncytial virus in mice: effect of TLR2 and NOD2 ligands on induction of systemic and mucosal immune responses. *PLoS One* (2013) 8(4):e61287. doi:10.1371/journal.pone.0061287
177. Lindner JR. Microbubbles in medical imaging: current applications and future directions. *Nat Rev Drug Discov* (2004) 3(6):527–32. doi:10.1038/nrd1417
178. Shapiro G, Wong AW, Bez M, Yang F, Tam S, Even L, et al. Multiparameter evaluation of in vivo gene delivery using ultrasound-guided, microbubble-enhanced sonoporation. *J Control Release* (2016) 223:157–64. doi:10.1016/j.jconrel.2015.12.001
179. Sennoga CA, Kanbar E, Auboire L, Dujardin PA, Fouan D, Escoffre JM, et al. Microbubble-mediated ultrasound drug-delivery and therapeutic monitoring. *Expert Opin Drug Deliv* (2017) 14(9):1031–43. doi:10.1080/17425247.2017.1266328
180. Oda Y, Suzuki R, Otake S, Nishiie N, Hirata K, Koshima R, et al. Prophylactic immunization with Bubble liposomes and ultrasound-treated dendritic cells provided a four-fold decrease in the frequency of melanoma lung metastasis. *J Control Release* (2012) 160(2):362–6. doi:10.1016/j.jconrel.2011.12.003
181. Bioley G, Bussat P, Lassus A, Schneider M, Terrettaz J, Corthesy B. The phagocytosis of gas-filled microbubbles by human and murine antigen-presenting cells. *Biomaterials* (2012) 33(1):333–42. doi:10.1016/j.biomaterials.2011.09.045
182. Bioley G, Lassus A, Bussat P, Terrettaz J, Tranquart F, Corthesy B. Gas-filled microbubble-mediated delivery of antigen and the induction of immune responses. *Biomaterials* (2012) 33(25):5935–46. doi:10.1016/j.biomaterials.2012.05.004
183. Bioley G, Zehn D, Lassus A, Terrettaz J, Tranquart F, Corthesy B. The effect of vaccines based on ovalbumin coupled to gas-filled microbubbles for reducing infection by ovalbumin-expressing *Listeria monocytogenes*. *Biomaterials* (2013) 34(21):5423–30. doi:10.1016/j.biomaterials.2013.04.005
184. Bioley G, Lassus A, Terrettaz J, Tranquart F, Corthesy B. Long-term persistence of immunity induced by OVA-coupled gas-filled microbubble vaccination partially protects mice against infection by OVA-expressing *Listeria*. *Biomaterials* (2015) 57:153–60. doi:10.1016/j.biomaterials.2015.04.008
185. Wu W, Wang Y, Shen S, Wu J, Guo S, Su L, et al. In vivo ultrasound molecular imaging of inflammatory thrombosis in arteries with cyclic Arg-Gly-Asp-modified microbubbles targeted to glycoprotein IIb/IIIa. *Invest Radiol* (2013) 48(11):803–12. doi:10.1097/RLI.0b013e318298652d
186. Bettinger T, Bussat P, Tardy I, Pochon S, Hyvelin JM, Emmel P, et al. Ultrasound molecular imaging contrast agent binding to both E- and P-selectin in different species. *Invest Radiol* (2012) 47(9):516–23. doi:10.1097/RLI.0b013e31825cc605
187. Cavalli R, Soster M, Argenziano M. Nanobubbles: a promising efficient tool for therapeutic delivery. *Ther Deliv* (2016) 7(2):117–38. doi:10.4155/tde.15.92
188. Sun HX, Xie Y, Ye YP. ISCOMs and ISCOMATRIX. *Vaccine* (2009) 27(33):4388–401. doi:10.1016/j.vaccine.2009.05.032
189. Morelli AB, Becher D, Koernig S, Silva A, Drane D, Maraskovsky E. ISCOMATRIX: a novel adjuvant for use in prophylactic and therapeutic vaccines against infectious diseases. *J Med Microbiol* (2012) 61(Pt 7):935–43. doi:10.1099/jmm.0.040857-0
190. Wilson NS, Yang B, Morelli AB, Koernig S, Yang A, Loeser S, et al. ISCOMATRIX vaccines mediate CD8+ T-cell cross-priming by a MyD88-dependent signaling pathway. *Immunol Cell Biol* (2012) 90(5):540–52. doi:10.1038/icb.2011.71
191. Jones PD, Tha Hla R, Morein B, Lovgren K, Ada GL. Cellular immune responses in the murine lung to local immunization with influenza A virus glycoproteins in micelles and immunostimulatory complexes (iscoms). *Scand J Immunol* (1988) 27(6):645–52. doi:10.1111/j.1365-3083.1988.tb02397.x
192. Coulter A, Harris R, Davis R, Drane D, Cox J, Ryan D, et al. Intranasal vaccination with ISCOMATRIX adjuvanted influenza vaccine. *Vaccine* (2003) 21(9–10):946–9. doi:10.1016/S0264-410X(02)00545-5
193. Wee JL, Scheerlinck JP, Snibson KJ, Edwards S, Pearse M, Quinn C, et al. Pulmonary delivery of ISCOMATRIX influenza vaccine induces both systemic and mucosal immunity with antigen dose sparing. *Mucosal Immunol* (2008) 1(6):489–96. doi:10.1038/mi.2008.59
194. Vujanic A, Wee JL, Snibson KJ, Edwards S, Pearse M, Quinn C, et al. Combined mucosal and systemic immunity following pulmonary delivery of ISCOMATRIX adjuvanted recombinant antigens. *Vaccine* (2010) 28(14):2593–7. doi:10.1016/j.vaccine.2010.01.018
195. Trudel M, Nadon F, Seguin C, Brault S, Lusignan Y, Lemieux S. Initiation of cytotoxic T-cell response and protection of Balb/c mice by vaccination with an experimental ISCOMs respiratory syncytial virus subunit vaccine. *Vaccine* (1992) 10(2):107–12. doi:10.1016/0264-410X(92)90026-G
196. Pandey RS, Dixit VK. Evaluation of ISCOM vaccines for mucosal immunization against hepatitis B. *J Drug Target* (2010) 18(4):282–91. doi:10.3109/10611860903450015
197. Hsu SC, Schadeck EB, Delmas A, Shaw M, Steward MW. Linkage of a fusion peptide to a CTL epitope from the nucleoprotein of measles virus enables incorporation into ISCOMs and induction of CTL responses following intranasal immunization. *Vaccine* (1996) 14(12):1159–66. doi:10.1016/0264-410X(95)00241-R
198. Lovgren K, Kaberg H, Morein B. An experimental influenza subunit vaccine (iscom): induction of protective immunity to challenge infection in mice after intranasal or subcutaneous administration. *Clin Exp Immunol* (1990) 82(3):435–9. doi:10.1111/j.1365-2249.1990.tb05467.x
199. Andersen CS, Dietrich J, Agger EM, Lycke NY, Lovgren K, Andersen P. The combined CTA1-DD/ISCOMs vector is an effective intranasal adjuvant for boosting prior *Mycobacterium bovis* BCG immunity to *Mycobacterium tuberculosis*. *Infect Immun* (2007) 75(1):408–16. doi:10.1128/IAI.01290-06
200. Eliasson DG, Helgeby A, Schon K, Nygren C, El-Bakkouri K, Fiers W, et al. A novel non-toxic combined CTA1-DD and ISCOMS adjuvant vector for effective mucosal immunization against influenza virus. *Vaccine* (2011) 29(23):3951–61. doi:10.1016/j.vaccine.2011.03.090
201. Skene CD, Doidge C, Sutton P. Evaluation of ISCOMATRIX and ISCOM vaccines for immunisation against *Helicobacter pylori*. *Vaccine* (2008) 26(31):3880–4. doi:10.1016/j.vaccine.2008.05.004
202. Sjolander A, Drane D, Maraskovsky E, Scheerlinck JP, Suhrbier A, Tennent J, et al. Immune responses to ISCOM formulations in animal and primate models. *Vaccine* (2001) 19(17–19):2661–5. doi:10.1016/S0264-410X(00)00497-7
203. Cibulski SP, Mourglia-Ettlin G, Teixeira TF, Quirici L, Roehe PM, Ferreira F, et al. Novel ISCOMs from *Quillaja brasiliensis* saponins induce mucosal and systemic antibody production, T-cell responses and improved antigen uptake. *Vaccine* (2016) 34(9):1162–71. doi:10.1016/j.vaccine.2016.01.029
204. Kodama S, Hirano T, Noda K, Umemoto S, Suzuki M. Nasal immunization with plasmid DNA encoding P6 protein and immunostimulatory complexes elicits nontypeable *Haemophilus influenzae*-specific long-term mucosal immune responses in the nasopharynx. *Vaccine* (2011) 29(10):1881–90. doi:10.1016/j.vaccine.2010.12.129
205. Kazanji M, Laurent F, Pery P. Immune responses and protective effect in mice vaccinated orally with surface sporozoite protein of *Eimeria falciformis* in ISCOMs. *Vaccine* (1994) 12(9):798–804. doi:10.1016/0264-410X(94)90288-7
206. Ghazi HO, Erturk M, Stannard LM, Faulkner M, Potter CW, Jennings R. Immunogenicity of influenza and HSV-1 mixed antigen ISCOMs in mice. *Arch Virol* (1995) 140(6):1015–31. doi:10.1007/BF01315412
207. Aguila A, Donachie AM, Peyre M, McSharry CP, Sesardic D, Mowat AM. Induction of protective and mucosal immunity against diphtheria by a immune stimulating complex (ISCOMS) based vaccine. *Vaccine* (2006) 24(24):5201–10. doi:10.1016/j.vaccine.2006.03.081
208. Helgeby A, Robson NC, Donachie AM, Beackock-Sharp H, Lovgren K, Schon K, et al. The combined CTA1-DD/ISCOM adjuvant vector promotes priming of mucosal and systemic immunity to incorporated antigens by specific targeting of B cells. *J Immunol* (2006) 176(6):3697–706. doi:10.4049/jimmunol.176.6.3697

209. Mowat AM, Donachie AM, Jagewall S, Schon K, Lowenadler B, Dalsgaard K, et al. CTA1-DD-immune stimulating complexes: a novel, rationally designed combined mucosal vaccine adjuvant effective with nanogram doses of antigen. *J Immunol* (2001) 167(6):3398–405. doi:10.4049/jimmunol.167.6.3398
210. Makidon PE, Belyakov IM, Blanco LP, Janczak KW, Landers J, Bielinska AU, et al. Nanoemulsion mucosal adjuvant uniquely activates cytokine production by nasal ciliated epithelium and induces dendritic cell trafficking. *Eur J Immunol* (2012) 42(8):2073–86. doi:10.1002/eji.201142346
211. Bielinska AU, Makidon PE, Janczak KW, Blanco LP, Swanson B, Smith DM, et al. Distinct pathways of humoral and cellular immunity induced with the mucosal administration of a nanoemulsion adjuvant. *J Immunol* (2014) 192(6):2722–33. doi:10.4049/jimmunol.1301424
212. Ahmed M, Smith DM, Hamouda T, Rangel-Moreno J, Fattom A, Khader SA. A novel nanoemulsion vaccine induces mucosal Interleukin-17 responses and confers protection upon *Mycobacterium tuberculosis* challenge in mice. *Vaccine* (2017) 35(37):4983–9. doi:10.1016/j.vaccine.2017.07.073
213. Makidon PE, Bielinska AU, Nigavekar SS, Janczak KW, Knowlton J, Scott AJ, et al. Pre-clinical evaluation of a novel nanoemulsion-based hepatitis B mucosal vaccine. *PLoS One* (2008) 3(8):e2954. doi:10.1371/journal.pone.0002954
214. Shahiwala A, Amiji MM. Enhanced mucosal and systemic immune response with squalane oil-containing multiple emulsions upon intranasal and oral administration in mice. *J Drug Target* (2008) 16(4):302–10. doi:10.1080/10611860801900082
215. Olive C, Schulze K, Sun HK, Ebensen T, Horvath A, Toth I, et al. Enhanced protection against *Streptococcus pyogenes* infection by intranasal vaccination with a dual antigen component M protein/SfbI lipid core peptide vaccine formulation. *Vaccine* (2007) 25(10):1789–97. doi:10.1016/j.vaccine.2006.11.031
216. Schulze K, Ebensen T, Chandrudu S, Skwarczynski M, Toth I, Olive C, et al. Bivalent mucosal peptide vaccines administered using the LCP carrier system stimulate protective immune responses against *Streptococcus pyogenes* infection. *Nanomedicine* (2017) 13(8):2463–74. doi:10.1016/j.nano.2017.08.015
217. Ogra PL. Mucosal immune response to poliovirus vaccines in childhood. *Rev Infect Dis* (1984) 6(Suppl 2):S361–8. doi:10.1093/clinids/6.Supplement_2.S361
218. Beale AJ. Efficacy and safety of oral poliovirus vaccine and inactivated poliovirus vaccine. *Pediatr Infect Dis J* (1991) 10(12):970–2.
219. Onorato IM, Modlin JF, McBean AM, Thoms ML, Losonsky GA, Bernier RH. Mucosal immunity induced by enhance-potency inactivated and oral polio vaccines. *J Infect Dis* (1991) 163(1):1–6. doi:10.1093/infdis/163.1.1
220. Levine MM, Chen WH, Kaper JB, Lock M, Danzig L, Gurwith M. PaxVax CVD 103-HgR single-dose live oral cholera vaccine. *Expert Rev Vaccines* (2017) 16(3):197–213. doi:10.1080/14760584.2017.1291348
221. Perry RT, Plowe CV, Koumare B, Bougoudogo F, Kotloff KL, Losonsky GA, et al. A single dose of live oral cholera vaccine CVD 103-HgR is safe and immunogenic in HIV-infected and HIV-noninfected adults in Mali. *Bull World Health Organ* (1998) 76(1):63–71.
222. Davitt CJ, Lavelle EC. Delivery strategies to enhance oral vaccination against enteric infections. *Adv Drug Deliv Rev* (2015) 91:52–69. doi:10.1016/j.addr.2015.03.007
223. Viret JF, Favre D, Wegmuller B, Herzog C, Que JU, Cryz SJ Jr, et al. Mucosal and systemic immune responses in humans after primary and booster immunizations with orally administered invasive and noninvasive live attenuated bacteria. *Infect Immun* (1999) 67(7):3680–5.
224. Sundstrom P, Lundin SB, Nilsson LA, Quiding-Jarbrink M. Human IgA-secreting cells induced by intestinal, but not systemic, immunization respond to CCL25 (TECK) and CCL28 (MEC). *Eur J Immunol* (2008) 38(12):3327–38. doi:10.1002/eji.200838506
225. Kantele A, Kantele JM, Savilahti E, Westerholm M, Arvilommi H, Lazarovits A, et al. Homing potentials of circulating lymphocytes in humans depend on the site of activation: oral, but not parenteral, typhoid vaccination induces circulating antibody-secreting cells that all bear homing receptors directing them to the gut. *J Immunol* (1997) 158(2):574–9.
226. Kantele A, Hakkinen M, Moldoveanu Z, Lu A, Savilahti E, Alvarez RD, et al. Differences in immune responses induced by oral and rectal immunizations with *Salmonella typhi* Ty21a: evidence for compartmentalization within the common mucosal immune system in humans. *Infect Immun* (1998) 66(12):5630–5.
227. Belshe RB, Mendelman PM, Treanor J, King J, Gruber WC, Piedra P, et al. The efficacy of live attenuated, cold-adapted, trivalent, intranasal influenzavirus vaccine in children. *N Engl J Med* (1998) 338(20):1405–12. doi:10.1056/NEJM199805143382002
228. Ambrose CS, Luke C, Coelingh K. Current status of live attenuated influenza vaccine in the United States for seasonal and pandemic influenza. *Influenza Other Respir Viruses* (2008) 2(6):193–202. doi:10.1111/j.1750-2659.2008.00056.x
229. Zakay-Rones Z. Human influenza vaccines and assessment of immunogenicity. *Expert Rev Vaccines* (2010) 9(12):1423–39. doi:10.1586/erv.10.144
230. Alving CR, Beck Z, Matyas GR, Rao M. Liposomal adjuvants for human vaccines. *Expert Opin Drug Deliv* (2016) 13(6):807–16. doi:10.1517/17425247.2016.1151871
231. Stanberry LR, Simon JK, Johnson C, Robinson PL, Morry J, Flack MR, et al. Safety and immunogenicity of a novel nanoemulsion mucosal adjuvant W805EC combined with approved seasonal influenza antigens. *Vaccine* (2012) 30(2):307–16. doi:10.1016/j.vaccine.2011.10.094
232. Mymetics SA. (2018). Available from: https://www.mymetics.com/
233. Drane D, Gittleson C, Boyle J, Maraskovsky E. ISCOMATRIX adjuvant for prophylactic and therapeutic vaccines. *Expert Rev Vaccines* (2007) 6(5):761–72. doi:10.1586/14760584.6.5.761
234. Moser C, Muller M, Kaeser MD, Weydemann U, Amacker M. Influenza virosomes as vaccine adjuvant and carrier system. *Expert Rev Vaccines* (2013) 12(7):779–91. doi:10.1586/14760584.2013.811195
235. Pedersen GK, Sjursen H, Nostbakken JK, Jul-Larsen A, Hoschler K, Cox RJ. Matrix M(TM) adjuvanted virosomal H5N1 vaccine induces balanced Th1/Th2 CD4(+) T cell responses in man. *Hum Vaccin Immunother* (2014) 10(8):2408–16. doi:10.4161/hv.29583
236. O'Hagan DT, Ott GS, De Gregorio E, Seubert A. The mechanism of action of MF59 – an innately attractive adjuvant formulation. *Vaccine* (2012) 30(29):4341–8. doi:10.1016/j.vaccine.2011.09.061
237. Garcon N, Morel S, Didierlaurent A, Descamps D, Wettendorff M, Van Mechelen M. Development of an AS04-adjuvanted HPV vaccine with the adjuvant system approach. *BioDrugs* (2011) 25(4):217–26. doi:10.2165/11591760-000000000-00000
238. Garcon N, Van Mechelen M. Recent clinical experience with vaccines using MPL- and QS-21-containing adjuvant systems. *Expert Rev Vaccines* (2011) 10(4):471–86. doi:10.1586/erv.11.29
239. Casares S, Brumeanu TD, Richie TL. The RTS,S malaria vaccine. *Vaccine* (2010) 28(31):4880–94. doi:10.1016/j.vaccine.2010.05.033
240. Lal H, Cunningham AL, Heineman TC. Adjuvanted herpes zoster subunit vaccine in older adults. *N Engl J Med* (2015) 373(16):1576–7. doi:10.1056/NEJMc1508392
241. Frazer IH, Quinn M, Nicklin JL, Tan J, Perrin LC, Ng P, et al. Phase 1 study of HPV16-specific immunotherapy with E6E7 fusion protein and ISCOMATRIX adjuvant in women with cervical intraepithelial neoplasia. *Vaccine* (2004) 23(2):172–81. doi:10.1016/j.vaccine.2004.05.013
242. Anderson JS, Hoy J, Hillman R, Barnden M, Eu B, McKenzie A, et al. A randomized, placebo-controlled, dose-escalation study to determine the safety, tolerability, and immunogenicity of an HPV-16 therapeutic vaccine in HIV-positive participants with oncogenic HPV infection of the anus. *J Acquir Immune Defic Syndr* (2009) 52(3):371–81. doi:10.1097/QAI.0b013e3181b7354c
243. Drane D, Maraskovsky E, Gibson R, Mitchell S, Barnden M, Moskwa A, et al. Priming of CD4+ and CD8+ T cell responses using a HCV core ISCOMATRIX vaccine: a phase I study in healthy volunteers. *Hum Vaccin* (2009) 5(3):151–7. doi:10.4161/hv.5.3.6614
244. Pabst R. Mucosal vaccination by the intranasal route. Nose-associated lymphoid tissue (NALT) – structure, function and species differences. *Vaccine* (2015) 33(36):4406–13. doi:10.1016/j.vaccine.2015.07.022
245. Allam JP, Novak N. Immunological mechanisms of sublingual immunotherapy. *Curr Opin Allergy Clin Immunol* (2014) 14(6):564–9. doi:10.1097/ACI.0000000000000118
246. Bahamondez-Canas TF, Cui Z. Intranasal immunization with dry powder vaccines. *Eur J Pharm Biopharm* (2018) 122:167–75. doi:10.1016/j.ejpb.2017.11.001

247. Passalacqua G, Canonica GW. Sublingual immunotherapy: focus on tablets. *Ann Allergy Asthma Immunol* (2015) 115(1):4–9. doi:10.1016/j.anai.2015.03.022

Conflict of Interest Statement: The authors declare that the research was conducted in the absence of any commercial or financial relationships that could be construed as a potential conflict of interest.

frontiers in Immunology

ORIGINAL RESEARCH
published: 12 March 2018
doi: 10.3389/fimmu.2018.00346

Mucosal Delivery of Fusion Proteins with *Bacillus subtilis* Spores Enhances Protection against Tuberculosis by Bacillus Calmette-Guérin

*Alastair Copland[1†], Gil R. Diogo[1†], Peter Hart[1†], Shane Harris[1], Andy C. Tran[1], Mathew J. Paul[1], Mahavir Singh[2], Simon M. Cutting[3] and Rajko Reljic[1]**

[1] St George's Medical School, London, United Kingdom, [2] Lionex GmbH, Braunschweig, Germany, [3] School of Biological Sciences, Royal Holloway University of London, Egham, United Kingdom

OPEN ACCESS

Edited by:
Jeffrey K. Actor, University of Texas Health Science Center at Houston, United States

Reviewed by:
Camille Locht, INSERM, France
Owen Kavanagh, York St John University, United Kingdom

***Correspondence:**
Rajko Reljic
rreljic@sgul.ac.uk

†These authors have contributed equally to this work.

Specialty section:
This article was submitted to Vaccines and Molecular Therapeutics, a section of the journal Frontiers in Immunology

Received: *13 November 2017*
Accepted: *07 February 2018*
Published: *12 March 2018*

Citation:
Copland A, Diogo GR, Hart P, Harris S, Tran AC, Paul MJ, Singh M, Cutting SM and Reljic R (2018) Mucosal Delivery of Fusion Proteins with Bacillus subtilis Spores Enhances Protection against Tuberculosis by Bacillus Calmette-Guérin. Front. Immunol. 9:346. doi: 10.3389/fimmu.2018.00346

Tuberculosis (TB) is the most deadly infectious disease in existence, and the only available vaccine, *Bacillus Calmette-Guérin* (BCG), is almost a century old and poorly protective. The immunological complexity of TB, coupled with rising resistance to antimicrobial therapies, necessitates a pipeline of diverse novel vaccines. Here, we show that *Bacillus subtilis* spores can be coated with a fusion protein 1 ("FP1") consisting of *Mycobacterium tuberculosis* (Mtb) antigens Ag85B, ACR, and HBHA. The resultant vaccine, Spore-FP1, was tested in a murine low-dose Mtb aerosol challenge model. Mice were primed with subcutaneous BCG, followed by mucosal booster immunizations with Spore-FP1. We show that Spore-FP1 enhanced pulmonary control of Mtb, as evidenced by reduced bacterial burdens in the lungs. This was associated with elevated antigen-specific IgG and IgA titers in the serum and lung mucosal surface, respectively. Spore-FP1 immunization generated superior antigen-specific memory T-cell proliferation in both $CD4^+$ and $CD8^+$ compartments, alongside bolstered Th1-, Th17-, and Treg-type cytokine production, compared to BCG immunization alone. $CD69^+CD103^+$ tissue resident memory T-cells (Trm) were found within the lung parenchyma after mucosal immunization with Spore-FP1, confirming the advantages of mucosal delivery. Our data show that Spore-FP1 is a promising new TB vaccine that can successfully augment protection and immunogenicity in BCG-primed animals.

Keywords: tuberculosis, spores, vaccine, immunity, adjuvants

INTRODUCTION

In 2015, tuberculosis (TB) overtook HIV/AIDS as the leading cause of death due to infection (1). This statistic contrasts starkly with the fact that the only available TB vaccine, *Mycobacterium bovis* Bacillus Calmette-Guérin (BCG), is the most widely administered vaccine in history (2), having been developed almost a century ago. The proposed reasons for the failure of BCG to adequately protect against TB are many and varied. They include (i) BCG sub-strain heterogeneity (3), (ii) pre-exposure of the host to environmental non-tubercle mycobacteria (4), (iii) a failure to prevent pulmonary infection (5), and (iv) limited protection in adults compared to children (6). Despite these limitations,

BCG is unlikely to be discontinued in clinical use. While its efficacy in many demographics is modest, there are accumulating data indicating that BCG may protect against non-TB diseases by training the innate immune system to respond non-specifically to diverse microbial threats (7, 8). A novel TB vaccine is therefore likely to supplement, rather than replace, BCG.

In 2011, the novel viral vector TB vaccine MVA85A, comprising Ag85A, was tested for safety and efficacy in a phase 2 clinical trial in South Africa, and it was found that parenteral administration of MVA85A in BCG-immunized infants offered no significant protection above that of BCG alone (9). The reasons for its failure are still unclear, since MVA85A protected against *Mycobacterium tuberculosis* (Mtb) in multiple animal models (10). But it is becoming increasingly apparent that the development pipeline for new TB vaccines will require technological diversity in order to maximize chances of success. In recent years, vaccines that are based upon particulate nano- or microscale delivery systems have made remarkable strides in both oncology and infectious diseases (11–13).

Bacillus subtilis is an environmental Gram-positive bacterium that is also found as a gut commensal in humans (14). Its spores have the desirable properties of being both safe and adjuvantic (15). But more importantly, they possess hydrophobic and electrostatic properties that allow them to readily bind protein antigens, making these spores pertinent to vaccine development as potential antigen delivery systems (16). The combination of intrinsic adjuvanticity and antigen-binding biophysical properties allows *B. subtilis* spores to act simultaneously as adjuvants and antigen carriers. Studies have shown that immunization of mice with *B. subtilis* spores coated with the influenza antigen M2e can induce strong antibody responses and protect against lethal challenge (17, 18). Similar findings have been observed in other immunization models, including immunogenicity against HIV and streptococci (19, 20). *B. subtilis* spores are thus an attractive platform for subunit vaccine enhancement.

We have previously shown that *B. subtilis* spores coated with TB antigens (21) or genetically engineered to express a TB antigen (22) can enhance protection against TB by BCG (prime-boost) in a mouse intranasal infection model. Although this provided a proof-of-principle framework for vaccine efficacy, the use of genetically modified components in a vaccine presents numerous regulatory barriers for clinical application (23). Here, we developed a novel TB vaccine—"Spore-FP1"—composed of *B. subtilis* spores non-covalently coated with a fusion protein (FP1) consisting of the antigens Ag85B, ACR and the epithelium-binding domain of HBHA ("FP1"). Ag85B and ACR were chosen to represent early and late stages of *Mtb* infection, respectively, while HBHA (heparin-binding domain only) was used for epithelial targeting in the lungs. Mucosal booster immunization with Spore-FP1 in BCG-primed mice enhanced protection in a low-dose aerosol Mtb challenge model, compared to BCG alone. The enhanced protection was concomitant with a wide array of boosted immunological parameters, including enhanced antigen-dependent T-cell proliferation and antibody production. Spore-FP1 is therefore a novel TB vaccine that has the potential to supplement pre-existing immunity conferred by BCG in human populations.

MATERIALS AND METHODS

Ethics Statement

All animals were used with approval from St. George's University of London Ethics Committee under an approved Home Office animal project license (70/7490) and used in accordance with the Animals (Scientific Procedures) Act 1986.

Mice and Immunizations

Female C57BL/6 mice were obtained from Charles River, UK, and were between 8 and 12 weeks of age before experimental use. For all bacterial challenge or immunogenicity experiments (except lung T-cell analysis), mice were immunized with 5×10^5 CFU BCG Pasteur (100 µL) subcutaneously or vehicle control. Intranasal booster immunizations consisted of 1×10^9 *B. subtilis* spores coated with 10 µg FP1 in 40 µL volumes per animal per dose, or vehicle control. These immunizations were performed under light anesthesia. For experiments involving dead spores, spores were autoclaved before protein adsorption. For some experiments, the adjuvant poly(I:C) (Sigma-Aldrich) was used intranasally at a dose of 20 µg.

Mice were infected with approximately 200 *M. tuberculosis* bacilli per animal delivered *via* low-dose aerosol, using a Biaera aerosol generator (Biaera Technologies). Infectious dose was routinely verified by standard plating techniques.

Bacteria and Colony Forming Unit Quantification

Bacillus Calmette-Guérin Pasteur and Mtb (strain H37Rv) were used for the *in vivo* experiments; these were kind gifts of Professor Juraj Ivanyi (King's College, London). Both strains were grown to log phase at 37°C in 7H10 broth (Becton Dickinson) supplemented with ADC (Becton Dickinson), 0.05% Tween-80 and Selectab (Mast Diagnostics). Bacteria were then enumerated by the standard CFU method on 7H11 agar plates [supplemented with OADC (Becton Dickinson), glycerol and Selectab (Mast Diagnostics)] and cryopreserved in liquid nitrogen until use.

Bacterial burden from mouse organs was assessed by CFU enumeration. Lung and spleen homogenates were prepared in a stomacher containing 0.1% Triton X-100. Homogenates were plated in technical duplicates (lungs) or singlets (spleens) on 7H11 agar supplemented with OADC, glycerol and Selectatab. CFUs were counted after a 3–4-week incubation at 37°C.

Vaccines and Immunization

Amino acid sequences of the Mtb proteins ACR, Ag85B (pos. 23–25), and HBHA (pos. 160–199) were connected via linker peptides (GGGSGGGS), and six histidine residues were added to the C-terminus resulting in FP1. The amino acid sequence of FP1 was retranslated to DNA considering the codon usage of *Escherichia coli* DH5α, the host strain for protein production. In order to enable site-directed cloning, restriction sites for *Nco*I and *Hind*III were added to the 5′ and 3′ end, respectively. The synthetic gene was provided by GenScript (USA) inserted in pUC57. The gene of FP1 was excised from this plasmid using the abovementioned restriction endonucleases and ligated to

expression vector pLEXWO481, an IPTG-inducible derivative of pMV261 (24), digested with the same enzymes as before. For production of FP1, the gene was expressed under control of lac-promoter while growing the host strain in APS medium at 30°C. Recombinant protein was isolated from inclusion bodies after denaturation in 8 M urea using metal chelate chromatography (Ni-NTA Superflow, Qiagen). Highly enriched FP1 was refolded by gel-filtration using sephadex G-200 material (GE Healthcare). Purity was assessed by fully automated SDS-PAGE with fluorimetric detection and densitometric purity (>97% purity). Western blots specific for component antigens were used to confirm the identity of the protein band. Endotoxin content was measured by LAL assay and determined to be <7 IU/mg. For formulation, FP1 was incubated with spores for 1 h at room temperature prior to the addition of polyI:C (if used). Vaccines were delivered immediately after formulation.

Antibody and Antigen Quantification

Antibody levels (IgA and IgG) in BAL and serum were quantified by ELISA. Antigens [Ag855, ACR; Lionex GmbH (Braunschweig, Germany)] were coated onto a plate at 2 μg/mL overnight, followed by blocking for 2 h with PBS containing 1% bovine serum albumin (BSA). BAL and serum were diluted 1:250 and 1:1,000, respectively, in PBS with 1% BSA and incubated on the plate in triplicate for 1 h at 37°C. Levels of IgA or IgG were detected using peroxidase-conjugated anti-mouse IgA or anti-mouse IgG (Sigma) and OPD substrate (Sigma). Plates were read on a Tecan200 plate-reader at 450 nm absorbance.

Assessment of protein loading onto spores and stability of final product was done by ELISA (quantifying unbound protein after adsorption) and by measuring charge and size using a ZetaSizer NanoZS (Malvern) according to manufacturer's instructions and proprietary software. Significance was tested with a paired *t*-test. For ELISA measurements, FP1 was coated onto plates at varying concentrations as described for the antibody measurements, followed by detection by a peroxidase-conjugated anti-His antibody (Sigma) in conjunction with OPD substrate. Plates were read as described above.

General Flow Cytometry

For most experiments, cells were first stained with Fixable Viability Dye eFluor® 780 (1:1,000 dilution; eBioscience) in the presence of Fc receptor blockade (TruStain, 1:500 dilution; Biolegend). For surface staining, cells were then stained in flow cytometry buffer (PBS containing 0.5% BSA and 0.1% sodium azide—all from Sigma-Aldrich) for 30–45 min at 4°C. For some experiments, cells were subsequently fixed in the appropriate fixative for 30 min at 4°C, and then stained in a permeabilization buffer for 45 min, followed by acquisition on a BD FACSCanto II, unless otherwise specified. For compensation matrices, UltraComp beads were used according to the manufacturer's instructions (eBioscience). Staining boundaries were determined by a combination of antibody titration, biological controls and fluorescence-minus-one samples.

Antigen-Presenting Cell (APC) Activation

Dendritic cells (DCs) were obtained according to a well-established protocol (25). Briefly, mouse femurs were aseptically flushed with complete RPMI (RPMI-1640 containing 100 U/mL penicillin/streptomycin, 2 mM L-glutamine, 10% fetal calf serum, and 50 μM 2-mercaptoethanol—all from Sigma-Aldrich) and the bone marrow cells were cultured in complete RPMI with 50 ng/mL GM-CSF (Peprotech) for 2 days, followed by complete removal of the liquid media containing non-adherent granulocytes, and replacement with fresh GM-CSF-supplemented media. Cells were then cultured for a further 3–4 days, and non-adherent and loosely adherent cells were gently detached. DCs were phenotyped by flow cytometry and were found to be>85% $CD11c^+$ and expressing high levels of MHC Class II. DCs were cryopreserved in 10% DMSO until use. For experiments involving macrophages, the J774 cell line was used. Macrophages were cultured in complete DMEM (from Sigma, see RPMI), and sub-cultured every 3 days at ~80% confluency. Cells were>99% $CD11b^+$ as assessed by flow cytometry.

To measure activation, APCs were stimulated for 48 h with *B. subtilis* spores at an MOI of 1, 10, or 100, or *E. coli* LPS (100 ng/mL; Sigma-Aldrich), and stained with a panel of antibodies: CCR7-PerCP/Cy5.5, CD80-APC, CD86-PE/Cy7, MHC Class I-FITC, MHC Class II-Brilliant Violet 510, PD-L1-Brilliant Violet 421, and PD-L2-PE—all from Biolegend. Supernatants were tested for IL-1β, IL-6, and TNF-α. IL-12p40 was detected by intracellular cytokine staining after 20 h stimulation of macrophages in the presence of 10 μg/mL brefeldin A (Sigma-Aldrich) using IL-12p40-PE (Biolegend) in flow cytometry buffer containing 0.5% saponin (Sigma-Aldrich). To detect transcription factor phosphorylation, macrophages were stimulated for 4 h and then fixed in 90% methanol as previously described (26), followed by staining with antibodies against phosphorylated forms of c-Jun (AP-1), NF-κB (p60), and IRF-3 (Cell Signaling).

T-Cell Proliferation

Splenocytes were obtained from mouse spleens that had been mechanically homogenized and treated with ACK lysis buffer (Sigma-Aldrich) to remove erythrocyte contamination. Splenocytes were cultured at 1×10^6/well in a 96-well plate. Cells were stimulated with 5 μg/mL recall antigen or 1 μg/mL α-CD3 (Biolegend) for 5–6 days, followed by surface staining with CD4-PerCP/Cy5.5, CD8-Brilliant Violet 510, CD44-FITC, CD62L-PE, and CD90.2-Brilliant Violet 421—all from Biolegend. Cells were then fixed and permeabilized using the eBioscience Foxp3/Transcription Factor Staining Buffer Set and stained with Ki67-APC.

Cytokine Quantification

Cytokines were measured by ELISA or Multiplex immunoassay. IL-1β, IL-6, and TNF-α in culture supernatant were measured by ELISA using eBioscience Ready-Set-Go kits according to the manufacturer's instructions. For IL-4, IL-10, IL-17A, and IFN-γ, a 4-plex multiplex immunoassay (Biolegend) was used according to manufacturer's instructions. Data was acquired on a BD FACSCanto, and analysis performed using Legendplex software (Biolegend).

Lung Cell Isolation and Analysis

For these experiments, mice were immunized with PBS or BCG (subcutaneously) or mucosally with the indicated vaccine

component. Lungs were perfused of blood by flushing PBS through the right ventricle. Tissue was then dissected into 1 mm pieces using a scalpel, followed by digestion in 1 mg/mL collagenase and 0.5 mg/mL DNase I (Roche). Cells were then passed through a 70 μm strainer (Becton Dickinson), contaminating erythrocytes were lysed, and mononuclear cells were stained for CD3-APC, CD4-PerCP/Cy5.5, CD8-Brilliant Violet 510, CD44-FITC, CD62L-PE, CD69-PE/Cy7, and CD103-Brilliant Violet 421—all from Biolegend.

Statistical Analysis

Statistical tests are described in the relevant figure legends. All analysis was performed using FlowJo v10, Microsoft Excel 2010 and GraphPad Prism 7.

RESULTS

Spores Can Effectively Bind to Mtb Fusion Proteins

We tested whether a biological carrier system, such as spores, could bind and facilitate carriage of the FP-1 fusion-protein. Spores were incubated with FP-1 prior to centrifugation to quantity the amount of free FP1 present in the supernatant after adsorption. Of 100 μg FP1, less than 2 μg free FP1 was detected in supernatants after adsorption indicating a high binding efficiency of over 98% ($n = 3$). To characterize the formulated Spore-FP1 vaccine, we assessed the size and charge of Spores either pre- or postadsorption using a ZetaSizer NanoZS. Size of the spores increased following FP-1 adsorption from 1,337 ± 13.8 to 1,389 ± 13.53 nm for naked and loaded spores, respectively ($n = 3$). Spores became marginally more negative when FP-1 was loaded, with charge decreasing from −47.13 ± 0.95 to −49.1 ± 0.44 mv ($n = 3$). While neither of the changes were significant, both trended toward significance ($p = 0.064$ and 0.068 for charge and size, respectively) and, in conjunction with the ELISA data, are suggestive of protein loading onto the spore surface. Importantly, FP1 loaded spores were moderately negatively charged and had a low polydispersity index (PDI = 0.237), indicating strong colloidal stability.

Spore-FP1 Can Enhance Bacterial Control Afforded by BCG

Mucosal vaccination against respiratory diseases offers distinct advantages over parenteral delivery routes, such as enhanced control of the pathogen, presumably due to localized immune effector cells (27). We therefore tested the ability of mucosally-delivered Spore-FP1 to enhance control of Mtb, compared to BCG immunization alone, in a "prime-boost" strategy. We hypothesized that a booster immunization with Spore-FP1 would lead to better protection than immunization with BCG alone. Mice were first primed with BCG or vehicle control, followed by two intranasal boosts with Spore-FP1. Mice were then challenged with ~100 CFU aerosolized Mtb, and bacterial burdens were quantified in the lungs and spleen. As shown in **Figure 1A**, mice immunized with BCG alone were better able to control Mtb compared to mock-immunized mice, as evidenced by reduced CFUs in the lungs (PBS CFUs: 5.54 ± 0.06; BCG CFUs: 4.84 ± 0.18, $p < 0.05$). When mice received the Spore-FP1 booster immunization, however, there was a significant improvement compared to BCG alone, with a near −1 log reduction in bacterial burden (Spore-FP1 CFUs: 4.10 ± 0.20, $p < 0.0001$ vs. PBS, $p < 0.05$ vs. BCG). In the spleens, BCG and Spore-FP1 offered comparable levels of protection, with both groups exhibiting significant protection compared to mock immunization ($p < 0.0001$). Next, Spore-FP1 was tested with codelivery of the adjuvant poly(I:C), a known inducer of the Th1 subset when used in the respiratory tract (28). As can be seen in the lungs (**Figure 1B**), Spore-FP1 was again able to induce significantly better protection than BCG ($p < 0.01$), with a trend—though not a statistically significant difference—for increased protection in the spleen ($p = 0.06$, BCG vs. Spore-FP1). These data collectively demonstrate that Spore-FP1 immunization could improve protection offered by BCG alone in multiple contexts, and therefore

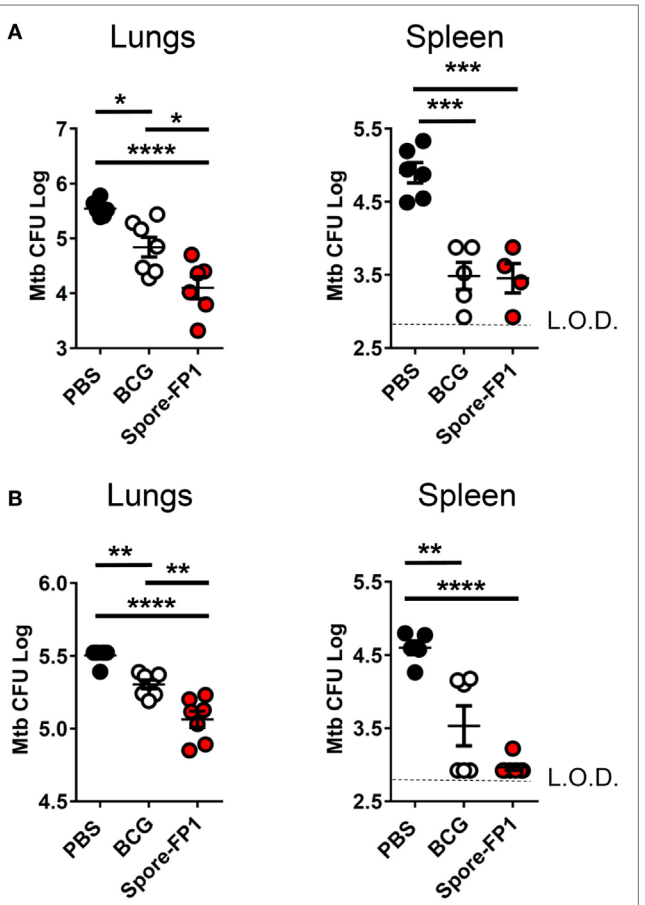

FIGURE 1 | Spore-FP1 protects against aerosol *Mycobacterium tuberculosis* (Mtb) challenge. Mice received a Bacillus Calmette-Guérin subcutaneous prime (except the PBS control group) followed by two intranasal boosts with Spore-FP1. After 3 weeks, bacterial burdens in the lungs and spleens were quantified by CFU counting on 7H11 plates across three dilution ranges. **(A)** Mice were immunized with Spore-FP1 alone. **(B)** Mice were immunized with Spore-FP1 in combination with the adjuvant poly(I:C). Results are expressed as mean ± SEM. Data are derived from $n = 4$–7 individual mice. Significance was tested against the by one-way ANOVA with Tukey's posttest, $^{*}p < 0.05$, $^{**}p < 0.01$, $^{***}p < 0.001$, and $^{****}p < 0.0001$.

we sought to uncover any immunological phenomena that could be associated with efficacy.

Spore-FP1 Enhances Antigen-Specific Antibody Production

Evidence suggests that antibodies may play a role in protecting against TB, either directly (Fab-mediated) or indirectly (Fc-mediated): monoclonal IgA therapy can reduce pulmonary Mtb burden (29), and adoptive transfer of antibodies from hosts with latent TB can improve macrophage functionality (30). We therefore probed whether Spore-FP was generating antibodies against Ag85B and ACR. Spore-FP1 immunization significantly enhanced titers of Ag85B-specific IgA in the BAL compared to PBS ($p < 0.05$), whereas there was no difference with BCG (**Figure 2A**). There was also a trend for increased levels of Ag85B-specific IgG induced by Spore-FP1. With regards to ACR-specific antibodies (**Figure 2B**), Spore-FP1 was able to significantly enhance levels of α-ACR IgG in the serum, compared to PBS ($p < 0.01$). However, there were no changes in the α-ACR IgA within the BAL.

Spore-FP1 Generates Abundant Tcm and Tem Cells with High Proliferative Capacity

The observation that Spore-FP1 immunization led to higher Mtb-specific IgG and IgA titers suggested that T-cell immunity was also being modulated. We hypothesized that Spore-FP1 was inducing stronger T-cell immunity than BCG alone, leading to enhanced antibody levels. To test this, splenocytes from immunized mice were assessed for the expression of the cell cycle and proliferation marker Ki67 after exposure to the recall antigens Ag85B, ACR and FP1. The Ki67$^+$ cells were then divided into naive (CD44^{lo}CD62L^{hi}), T central memory (Tcm; CD44^{hi}CD62L^{hi}) or T effector memory (Tem; CD44^{hi}CD62L^{lo}) phenotypes. As shown in **Figure 3**, as expected, there was minimal proliferation in the PBS group in response to all antigens, with a background level of ~3% Ki67$^+$ in memory cell subsets. There were modestly more proliferating cells in the BCG group, which is consistent with other studies showing that BCG induces a very small percentage of antigen-specific splenic T-cells (31, 32). For instance, there were 6.48% Ki67$^+$ CD4$^+$ Tem cells after ACR stimulation in this group, and a similar level in the CD8$^+$ Tem cells. However, in the Spore-FP1 group, there was a sharp overall increase in the percentage of Ki67$^+$ cells, with notable spikes (>20%) in proliferating CD8$^+$ Tcm and Tem cells in response to Ag85B. Similarly, Spore-FP1 had the highest percentage of CD4$^+$ Tem cells responding to Ag85B (>10%). Results for ACR in this group were more modest, but the trend remained consistent. These data support the ability of a mucosal vaccine to induce substantial T-cell responses at primary lymphoid sites.

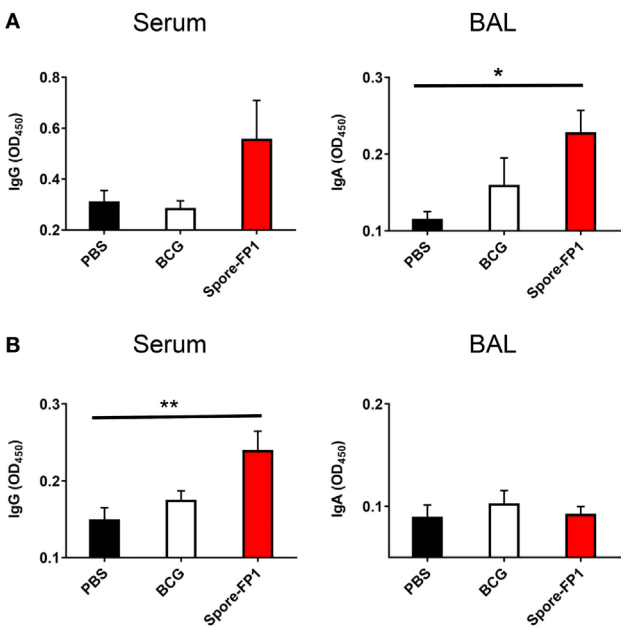

FIGURE 2 | Enhanced humoral immunity caused by Spore-FP1. Immunized mice were tested for the presence of antigen-specific IgG in the serum (1:1,000 dilution) and IgA in the BAL (1 mL PBS flush; 1:10 dilution) by ELISA, with optical density read at 450 nm in duplicate. **(A)** Levels of IgG and IgA specific to Ag85B. **(B)** Levels of IgG and IgA specific to ACR. Results are expressed as mean ± SEM. Data shown are derived from $n = 3$ individual mice and are representative of two independent experiments. Significance was tested against the unstimulated control by one-way ANOVA with Tukey's posttest, $^*p < 0.05$ and $^{**}p < 0.01$.

Spore-FP1 Immunization Results in a Mixed T-Cell Cytokine Profile

The increase in T-cell proliferation in response to mucosal immunization with Spore-FP1 led us to question which subsets of T helper cells and cytotoxic T-cells were responding to antigen. Therefore, splenocytes from immunized animals were cultured with recall antigens (Ag85B, ACR and FP1) and assessed for the production of IFN-γ, IL-4, IL-10, and IL-17A, which are secreted from Th1/Tc1, Th2/Tc2, Treg, and Th17/Tc17 subsets, respectively. We found (**Figure 4**) that there was muted cytokine production across all analytes in the BCG group when cells were stimulated with recall antigens, with the exception of minor IFN-γ secretion (570.36 pg/mL) after ACR pulsing. In the Spore-FP1 group, however, there was profound cytokine release in response to all three antigens. After Ag85B pulsing, Spore-FP1 splenocytes produced copious amounts of IFN-γ (3519.6 pg/mL), IL-10 (86.26 pg/mL), and IL-17A (1837.5 pg/mL), suggesting that Spore-FP1 immunization generated mixed T-cell subsets that were specific for Mtb antigens. Similar results were observed for FP1 antigen recall, and there were modest levels of cytokines for ACR. No IL-4 was detected in any of the groups.

Evidence of Tissue-Resident Memory T-Cells after Mucosal Immunization

Since Spore-FP1 was causing the development of antigen-specific T-cells in central lymphoid organs, we next interrogated the lungs for the presence of tissue-resident memory T-cells. Lungs were perfused and harvested from immunized animals, and then CD44^{hi} (i.e., memory) T-cells were assessed for the expression of tissue retention markers CD69 and CD103. As shown in **Figure 5**, PBS and BCG immunization induced minimal levels

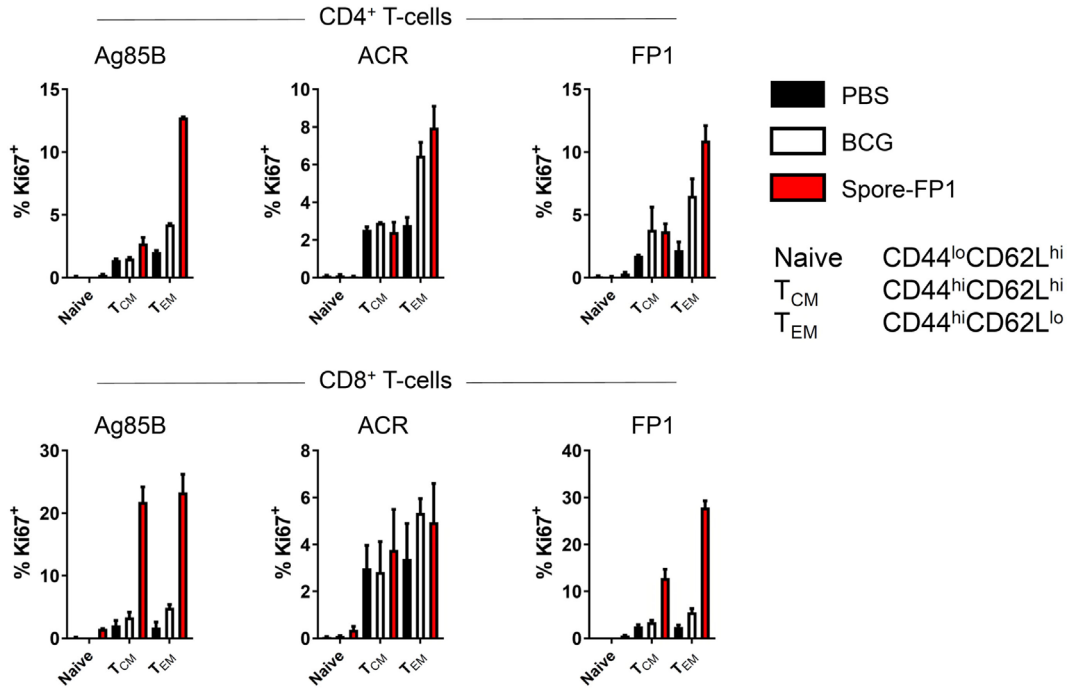

FIGURE 3 | Enhanced T-cell proliferation due to Spore-FP1. Splenocytes were incubated in technical duplicates with 5 μg/mL recall antigen for 5–6 days and proliferation was measured by Ki67 staining. A gating strategy of live cells→single cells→$CD3^+$→$CD4^+$/$CD8^+$ was used, followed by gating for $Ki67^+$ cells and determination of memory cell phenotype by expression of CD44 and CD62L. Results are expressed as mean ± SEM. Data are derived from $n = 3$ pooled spleens per group.

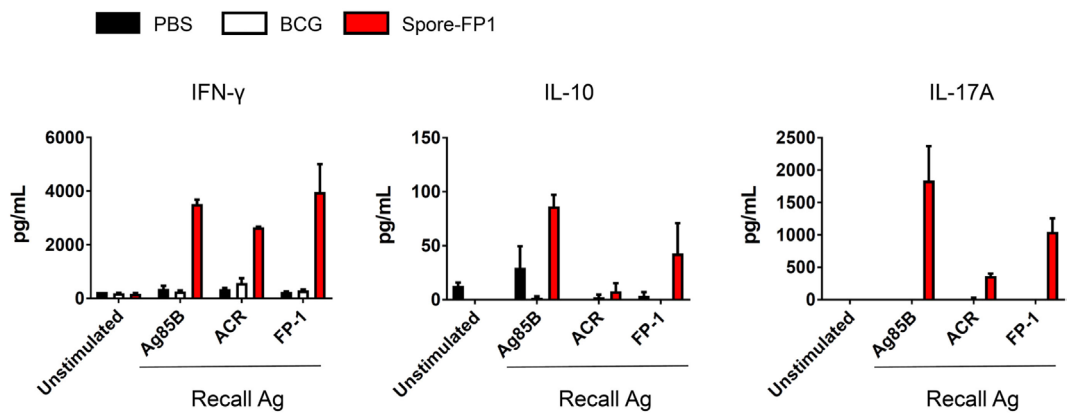

FIGURE 4 | Cytokine profiles during splenocyte antigen recall. Splenocytes from immunized mice were stimulated in technical duplicates with 5 μg/mL recall antigen for 5–6 days and T-cell cytokines were measured by multiplex flow cytometry. Results are expressed as mean ± SEM. Data are derived from $n = 3$ pooled spleens per group.

of these cells (<4% in both $CD4^+$ and $CD8^+$ T-cells), with only a minor increase induced by FP1 alone. Notably, the mucosal delivery of *B. subtilis* spores alone did not lead to the generation of Trm, while the full vaccine construct, Spore-FP1, was able to induce 14.9% $CD4^+$ and 12.5% $CD8^+$ Trm, respectively.

Bacillus Spores Activate Macrophages and DCs

Antigen-presenting cells are essential for the generation of T-cell immunity after immunization (33, 34). Empirical and systems biology approaches have revealed a correlation between APC activation by some antibody-inducing vaccines and protective immunity (35–37). Consequently, we next tested whether *B. subtilis* spores could activate DCs and macrophages (**Figure 6**). DCs and macrophages were pulsed with *B. subtilis* spores for 2 days at a range of MOIs and assessed for the upregulation of maturation markers. In DCs, spores significantly upregulated CD80, MHC Class I and CCR7 (CD80: $p < 0.05$, MHC Class I: $p < 0.001$, CCR7: $p < 0.01$), with strong trends for upregulation of CD86 and PD-L1 (**Figure 6A**). Interestingly, spores induced

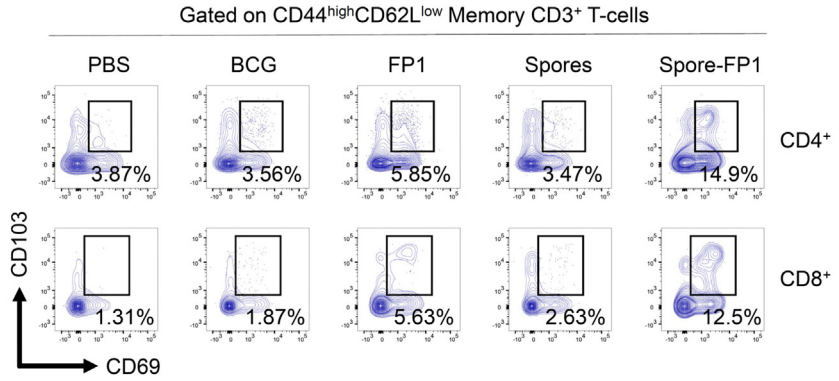

FIGURE 5 | Spore-FP1 induces enrichment of tissue resident memory cells. Mice were first immunized with Bacillus Calmette-Guérin for 6 weeks (except the PBS group) and then received two intranasal doses of either spores alone, fusion protein 1 (FP1) alone, or Spore-FP1. Lung parenchymal cells were assessed by flow cytometry for T-cell markers. A gating strategy of live cells→single cells→$CD3^+$→$CD4^+$/$CD8^+$→$CD44^{hi}CD62L^{lo}$ was used to measure the frequency of double-positive CD69/CD103 Trm. Data are derived from $n = 3$ pooled mice per group showing a representative plot.

the downregulation of MHC Class II and PD-L2. This may reflect the time-point at which the markers were measured, since Class II is known to be upregulated initially, followed by late-phase downregulation in activated DCs (38). In macrophages, spores were able to induce the upregulation of PD-L1 ($p < 0.05$), PD-L2 ($p < 0.001$), and CCR7 ($p < 0.001$), with similar trends for CD80, CD86, and MHC Class II. With regards to the production of proinflammatory cytokines, there was evidence of secretion of IL-6 and TNF-α at an MOI of 100 in DCs and macrophages (**Figure 6B**), albeit at lower levels compared to the positive control LPS. There was modest IL-1β production at the highest dose of spores. Next, we used intracellular cytokine staining to detect IL-12p40 production after spore exposure (**Figure 6C**). Spores were found to induce comparable levels of IL-12p40$^+$ APCs (23.3%) compared to LPS (18.3%). As expected, there was minimal production of IL-12p40 in unstimulated cells. Finally, we investigated three transcription factors downstream of Toll-like receptors (TLRs) to understand the cause of the phenotype. Intracellular flow cytometry at 4 h poststimulation (**Figure 6D**) revealed that *B. subtilis* spores were activating AP-1 (c-JUN), NF-κB and IRF-3 to a greater extent than LPS, suggesting engagement of both MyD88 and TRIF adaptors, in tandem with mitogen-activated protein kinase activity.

DISCUSSION

Tuberculosis is a disease defined by an immunological complexity that has hindered efforts toward vaccine development and allowed Mtb to persist perniciously across the globe. The cause of this complexity is a raft of exquisite immune evasion mechanisms that has evolved over thousands of years to manipulate host immunity. Therefore, at present, animal infection models are the most useful tool for predicting TB vaccine success (10).

We have previously reported that spores coated with Mtb antigens can provide good protection against Mtb in an intranasal infection model (21). A major limitation of this model, however, is that intranasal infection is not physiologically representative of natural Mtb infection. Furthermore, this study did not address whether such vaccine constructs could enhance pre-existing BCG-mediated immunity in the mouse model in a prime-boost immunization schedule. In the present study, we used a technologically superior low-dose aerosol Mtb challenge model to test the efficacy of a novel TB vaccine, Spore-FP1, on BCG-immunized mice, with the hypothesis that Spore-FP1 could boost the protection afforded by BCG. Spore-FP1 was designed to include antigens expressed during the early (Ag85B) and late (ACR) phases of Mtb infection, which could help to account for some of the observed dynamic changes in antigen expression during disease (39). Moreover, unlike previous studies, Spore-FP1 also contained a portion of the epithelium-binding domain of HBHA, which would encourage attachment to lung epithelium and dissemination of the vaccine (40).

Our most important finding was that intranasal immunization with Spore-FP1 in a BCG-primed mouse (i.e., the "prime-boost" strategy) could significantly enhance protection above that given by BCG alone. This effect was independent of any coadjuvants or whether the spores were viable or not. Bacterial burdens in the lungs were significantly reduced by the Spore-FP1 booster immunization compared to BCG alone. Interestingly, there was no statistically significant reduction in extra-pulmonary Mtb. This may reflect a limitation of detection in our assays, or at least an area of potential development for future utilization of spore vehicle systems. Distinct T-cell-derived cytokine patterns are known to exert dichotomous effects on bacterial burdens in the lungs and spleen (41), which may be the case here. Furthermore there was also a slight reduction in protective effect when Spore-FP1 was used with adjuvant. This may reflect ordinary biological variation between experiments, or perhaps non-optimal adjuvant choice, and will be the subject of future investigations.

To investigate immunological events associated with protection, we first evaluated antigen-dependent antibody production in serum and BAL. The role of antibodies in TB is contentious, although there have been recent reappraisals of the field generally in favor of their protective role (42). Mice immunized with Spore-FP1 were found to produce more Ag85B-specific IgG in the serum and IgA in the BAL than the BCG group; a similar

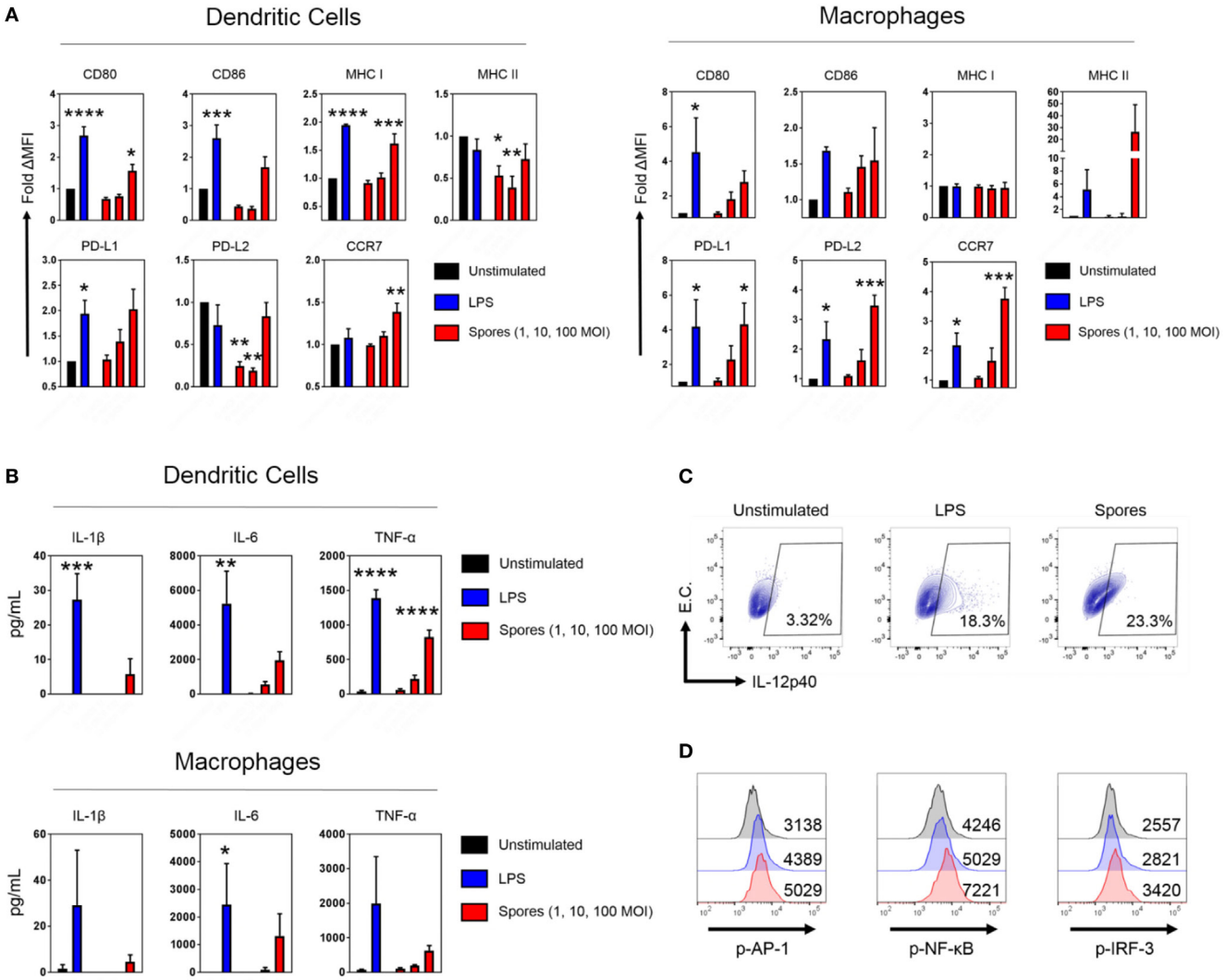

FIGURE 6 | *Bacillus subtilis* spores activate antigen-presenting cells. **(A)** Dendritic cells (DCs) (left) and macrophages (right) were stimulated in duplicate for 48 h with LPS (100 ng/mL) or *B. subtilis* spores (1, 10, and 100 MOI) and surface molecule expression was measured by flow cytometry on gated viable cells. MFI was normalized to the unstimulated control. **(B)** Cytokines from the supernatants were tested for proinflammatory cytokine production by ELISA. **(C)** Macrophages were stimulated for 20 h with LPS (100 ng/mL) or *B. subtilis* spores (100 MOI) in the presence of brefeldin A (10 μg/mL), followed by intracellular detection of IL-12p40. EC, empty channel. A representative experiment is shown. **(D)** Transcription factor phosphorylation levels were determined by PhosphoFlow. Macrophages were stimulated with 100 ng/mL LPS (blue histograms) or 100 MOI spores (red histograms) for 4 h and then fixed and stained. Some cells were left untreated (black histograms). Representative MFI values are plotted on the relevant histogram. Data are from three **(A–C)** or one **(D)** independent experiments. Results are expressed as mean ± SEM. Significance was tested against the unstimulated control by one-way ANOVA with Fisher's posttest, $^{*}p < 0.05$, $^{**}p < 0.01$, $^{***}p < 0.001$, and $^{****}p < 0.0001$.

trend was observed for ACR. These data strongly suggest that a Spore-FP1 boost immunization was better at inducing humoral immunity than a single BCG immunization.

T-cells are essential for protection against Mtb: Th1 cells prime macrophages for activation via IFN-γ (43), and Th17 cells can upregulate the production of antimicrobial peptides and lymphocyte chemoattractants (44, 45). Deficiency in either of these cytokines is extremely detrimental to the host during disease. It has been shown that during natural infection, Mtb can subvert the host immune system in order to restrict antigen presentation (46, 47). Hence a vaccine that enhances antigen presentation, and thus leads to a higher frequency of antigen-specific T-cells, is highly desirable. In our experiments, we observed a higher frequency of proliferating splenic T-cells in response to recall antigens in the Spore-FP1 group compared to mice that had only received BCG immunization. BCG is also able to restrict antigen presentation *in vivo* to a certain extent (47–49), and consistent with this fact, we observed minimal proliferative responses to Ag85B/ACR in BCG-immunized animals. Such small-magnitude responses in BCG-immunized mice are highly typical and described elsewhere in the literature, wherein cells specific for Ag85 typically represent ~0.1% of the total splenic polyclonal T-cell pool in cytokine capture assays (31, 32). In contrast to these constrained responses, Spore-FP1 was able to

induce a dramatically larger percentage of proliferating T-cells, indicating either a higher frequency of memory cells, or at the very least cells with a higher proliferative capacity. Many of the proliferating $CD8^+$ $Ki67^+$ cells were of the Tcm phenotype, which act as a "reservoir" of cells in primary and secondary lymphoid organs with high potential for differentiation into effector cells in distal sites. For chronic diseases such as TB that include T-cell exhaustion as a definitive mechanism of immune evasion (i.e., terminal differentiation), the generation of proliferative Tcm by a prophylactic vaccine offers a distinct advantage.

In line with proliferative responses, Spore-FP1 was also a potent inducer of IFN-γ, IL-10, and IL-17A release after splenocyte exposure to recall antigens. Thus, the antigen-specific cells were fully functional by producing effector cytokines during proliferation. It could be surmised that Spore-FP1 therefore induced a mixed Th1-Th17-Treg response. The absence of IL-4 release is interesting, and suggests that Spore-FP1 induced a T-cell skewing away from the Th2 to a Th1/Th17 phenotype. IL-4 is largely believed to be detrimental during Mtb infection, since it antagonizes the biological effects of IFN-γ to promote alternatively activated macrophages (50). The role of IL-10 in TB is more contentious. While IL-10 can hamper antimycobacterial immunity during BCG immunization (51), recent evidence from *Rhesus macaque* infection models has suggested that $CD4^+$ T-cells coexpressing a balance of pro- and anti-inflammatory cytokines are significantly associated with granuloma sterilization, possibly due to a reduction in "collateral damage" to the lung tissue (52). Furthermore, IL-10 is important for shielding $CD8^+$ memory T-cells from apoptosis in inflammatory contexts (53), and IL-10 deficient mice are highly susceptible to reinfection by intracellular pathogens (54). We believe that the T-cell profile induced by Spore-FP1 is therefore beneficial in the context of immunization.

It is worth noting that for both humoral and cellular immunogenicity, there was generally a greater response to Ag85B than to ACR. This is perhaps due to the fact that Ag85B is a strong immunodominant antigen (55) that has formed the basis of many new TB vaccines. Notably, however, ACR was still able to elicit potent IFN-γ production in splenocytes from Spore-FP1-immunized mice.

Alongside conventional T-cell activation signatures, we also observed a striking accumulation of gross $CD69^+CD103^+$ Trm in lung tissue after immunization with Spore-FP1. These cells are likely to be directed toward epitopes found within FP1, since the vehicle control (spores alone) failed to induce any appreciable quantities of these cells. As to why no Trm were directed against *B. subtilis* spores themselves, it may be that *B. subtilis,* as a mammalian commensal (56) (in the absence of a "foreign" antigen such as those included in FP1), can suppress the mobilization of effector T-cells that would lead to its own clearance. In support of this hypothesis, *B. subtilis* secretory products can induce a Foxp3-dependent tolerogenic environment in the gut (57), and consistent with this fact, we observed modest IL-10 responses from splenocytes exposed to recall antigen (although much lower than IFN-γ and IL-17A). A recent study has elegantly demonstrated that mucosal immunization with BCG—as opposed to parenteral immunization—leads to the accumulation of Trm in the pulmonary tissue (27). These cells are sufficient for protection, since adoptive transfer of Trm into BCG-naive mice protects against Mtb challenge. We speculate that the enrichment of this cell type in the lungs, induced by Spore-FP1 in our experiments, is playing a major role in the protection afforded by our novel vaccine.

Turning our attention to the innate immune system, we detected potent activation signatures in macrophages and DCs pulsed with *B. subtilis* spores. While it is known that *B. subtilis* spores can activate TLR-2→MyD88 downstream pathways, these studies have largely restricted maturation marker analysis to CD40 and MHC Class I and II expression on DCs (19, 58). Here, we showed for the first time that spores can also simultaneously induce CCR7, PD-L1 and PD-L2 upregulation. Since minimal T-cell priming occurs in the lung (59, 60), CCR7 expression will be critical for DCs that have taken up Spore-FP1 to migrate to the lung-draining lymph nodes and present antigen to naive T-cells. The upregulation of PD-L1 and PD-L2, on the other hand, may mitigate the overall inflammatory response, which is an important boon for mucosal delivery. In justification of this notion, PD-L1 blockade during antigen delivery into the lungs leads to exacerbated irritation and inflammation via Treg depletion, which is ameliorated upon immune reconstitution (61). Underscoring all of these phenotypic characteristics was the observation that IRF-3 was phosphorylated alongside NF-κB upon APC stimulation with spores. These data allude to a novel activation pathway besides the TLR-2→MyD88 axis, which is driving APC activation by *B. subtilis* spores, and has hitherto remained unexplored. This proposition warrants further biochemical investigation.

To conclude, we have shown that Spore-FP1 can enhance protection offered by BCG and also activate multiple arms of the innate and adaptive immune systems. These data demonstrate the potential applicability of Spore-FP1 as a TB vaccine, but also offer fresh insights into the mechanisms of *B. subtilis* spores as a vaccine development platform.

ETHICS STATEMENT

The animal work was reviewed and approved by St George's University of London Ethics Committee for animal experimentation and studies performed under a valid UK Home Office Project Licence.

AUTHOR CONTRIBUTIONS

AC, PH, and GD performed most of the immunization and MTB challenge experiments. SH and ACT performed *in vitro* immunogenicity experiments. MS provided recombinant proteins. SC provided spores. MP performed immunological evaluations. RR conceived the study and wrote up the manuscript with AC.

FUNDING

This study was funded by the European Commission H2020 grant no. 643558 awarded to the EMI-TB Consortium.

REFERENCES

1. Churchyard G, Kim P, Shah NS, Rustomjee R, Gandhi N, Mathema B, et al. What we know about tuberculosis transmission: an overview. *J Infect Dis* (2017) 216:S629–35. doi:10.1093/infdis/jix362
2. Dye C. Making wider use of the world's most widely used vaccine: bacille Calmette-Guerin revaccination reconsidered. *J R Soc Interface* (2013) 10:20130365. doi:10.1098/rsif.2013.0365
3. Castillo-Rodal AI, Castanon-Arreola M, Hernandez-Pando R, Calva JJ, Sada-Diaz E, Lopez-Vidal Y. *Mycobacterium bovis* BCG substrains confer different levels of protection against *Mycobacterium tuberculosis* infection in a BALB/c model of progressive pulmonary tuberculosis. *Infect Immun* (2006) 74:1718–24. doi:10.1128/IAI.74.3.1718-1724.2006
4. Poyntz HC, Stylianou E, Griffiths KL, Marsay L, Checkley AM, Mcshane H. Non-tuberculous mycobacteria have diverse effects on BCG efficacy against *Mycobacterium tuberculosis*. *Tuberculosis (Edinb)* (2014) 94:226–37. doi:10.1016/j.tube.2013.12.006
5. Moliva JI, Turner J, Torrelles JB. Prospects in *Mycobacterium bovis* bacille Calmette et Guerin (BCG) vaccine diversity and delivery: why does BCG fail to protect against tuberculosis? *Vaccine* (2015) 33:5035–41. doi:10.1016/j.vaccine.2015.08.033
6. Mangtani P, Abubakar I, Ariti C, Beynon R, Pimpin L, Fine PE, et al. Protection by BCG vaccine against tuberculosis: a systematic review of randomized controlled trials. *Clin Infect Dis* (2014) 58:470–80. doi:10.1093/cid/cit790
7. Kleinnijenhuis J, Quintin J, Preijers F, Joosten LA, Ifrim DC, Saeed S, et al. Bacille Calmette-Guerin induces NOD2-dependent nonspecific protection from reinfection via epigenetic reprogramming of monocytes. *Proc Natl Acad Sci U S A* (2012) 109:17537–42. doi:10.1073/pnas.1202870109
8. de Castro MJ, Pardo-Seco J, Martinon-Torres F. Nonspecific (heterologous) protection of neonatal BCG vaccination against hospitalization due to respiratory infection and sepsis. *Clin Infect Dis* (2015) 60:1611–9. doi:10.1093/cid/civ144
9. Tameris MD, Hatherill M, Landry BS, Scriba TJ, Snowden MA, Lockhart S, et al. Safety and efficacy of MVA85A, a new tuberculosis vaccine, in infants previously vaccinated with BCG: a randomised, placebo-controlled phase 2b trial. *Lancet* (2013) 381:1021–8. doi:10.1016/S0140-6736(13)60177-4
10. McShane H, Williams A. A review of preclinical animal models utilised for TB vaccine evaluation in the context of recent human efficacy data. *Tuberculosis (Edinb)* (2014) 94:105–10. doi:10.1016/j.tube.2013.11.003
11. Hamdy S, Molavi O, Ma Z, Haddadi A, Alshamsan A, Gobti Z, et al. Co-delivery of cancer-associated antigen and toll-like receptor 4 ligand in PLGA nanoparticles induces potent CD8+ T cell-mediated anti-tumor immunity. *Vaccine* (2008) 26:5046–57. doi:10.1016/j.vaccine.2008.07.035
12. Moon JJ, Suh H, Li AV, Ockenhouse CF, Yadava A, Irvine DJ. Enhancing humoral responses to a malaria antigen with nanoparticle vaccines that expand Tfh cells and promote germinal center induction. *Proc Natl Acad Sci U S A* (2012) 109:1080–5. doi:10.1073/pnas.1112648109
13. Kanekiyo M, Wei CJ, Yassine HM, Mctamney PM, Boyington JC, Whittle JR, et al. Self-assembling influenza nanoparticle vaccines elicit broadly neutralizing H1N1 antibodies. *Nature* (2013) 499:102–6. doi:10.1038/nature12202
14. Hong HA, Khaneja R, Tam NM, Cazzato A, Tan S, Urdaci M, et al. *Bacillus subtilis* isolated from the human gastrointestinal tract. *Res Microbiol* (2009) 160:134–43. doi:10.1016/j.resmic.2008.11.002
15. Barnes AG, Cerovic V, Hobson PS, Klavinskis LS. *Bacillus subtilis* spores: a novel microparticle adjuvant which can instruct a balanced Th1 and Th2 immune response to specific antigen. *Eur J Immunol* (2007) 37:1538–47. doi:10.1002/eji.200636875
16. Wiencek KM, Klapes NA, Foegeding PM. Hydrophobicity of *Bacillus* and *Clostridium* spores. *Appl Environ Microbiol* (1990) 56:2600–5.
17. Zhao G, Miao Y, Guo Y, Qiu H, Sun S, Kou Z, et al. Development of a heat-stable and orally delivered recombinant M2e-expressing *B. subtilis* spore-based influenza vaccine. *Hum Vaccin Immunother* (2014) 10:3649–58. doi:10.4161/hv.36122
18. Lega T, Weiher P, Obuchowski M, Nidzworski D. Presenting influenza A M2e antigen on recombinant spores of *Bacillus subtilis*. *PLoS One* (2016) 11:e0167225. doi:10.1371/journal.pone.0167225
19. de Souza RD, Batista MT, Luiz WB, Cavalcante RC, Amorim JH, Bizerra RS, et al. *Bacillus subtilis* spores as vaccine adjuvants: further insights into the mechanisms of action. *PLoS One* (2014) 9:e87454. doi:10.1371/journal.pone.0087454
20. Tavares Batista M, Souza RD, Paccez JD, Luiz WB, Ferreira EL, Cavalcante RC, et al. Gut adhesive *Bacillus subtilis* spores as a platform for mucosal delivery of antigens. *Infect Immun* (2014) 82:1414–23. doi:10.1128/IAI.01255-13
21. Reljic R, Sibley L, Huang JM, Pepponi I, Hoppe A, Hong HA, et al. Mucosal vaccination against tuberculosis using inert bioparticles. *Infect Immun* (2013) 81:4071–80. doi:10.1128/IAI.00786-13
22. Sibley L, Reljic R, Radford DS, Huang JM, Hong HA, Cranenburgh RM, et al. Recombinant *Bacillus subtilis* spores expressing MPT64 evaluated as a vaccine against tuberculosis in the murine model. *FEMS Microbiol Lett* (2014) 358:170–9. doi:10.1111/1574-6968.12525
23. Frey J. Biological safety concepts of genetically modified live bacterial vaccines. *Vaccine* (2007) 25:5598–605. doi:10.1016/j.vaccine.2006.11.058
24. Stover CK, De La Cruz VF, Fuerst TR, Burlein JE, Benson LA, Bennett LT, et al. New use of BCG for recombinant vaccines. *Nature* (1991) 351:456–60. doi:10.1038/351456a0
25. Inaba K, Inaba M, Romani N, Aya H, Deguchi M, Ikehara S, et al. Generation of large numbers of dendritic cells from mouse bone marrow cultures supplemented with granulocyte/macrophage colony-stimulating factor. *J Exp Med* (1992) 176:1693–702. doi:10.1084/jem.176.6.1693
26. Bending D, Giannakopoulou E, Lom H, Wedderburn LR. Synovial regulatory T cells occupy a discrete TCR niche in human arthritis and require local signals to stabilize FOXP3 protein expression. *J Immunol* (2015) 195:5616–24. doi:10.4049/jimmunol.1500391
27. Perdomo C, Zedler U, Kuhl AA, Lozza L, Saikali P, Sander LE, et al. Mucosal BCG vaccination induces protective lung-resident memory T cell populations against tuberculosis. *MBio* (2016) 7:e1686–1616. doi:10.1128/mBio.01686-16
28. Trumpfheller C, Caskey M, Nchinda G, Longhi MP, Mizenina O, Huang Y, et al. The microbial mimic poly IC induces durable and protective CD4+ T cell immunity together with a dendritic cell targeted vaccine. *Proc Natl Acad Sci U S A* (2008) 105:2574–9. doi:10.1073/pnas.0711976105
29. Balu S, Reljic R, Lewis MJ, Pleass RJ, Mcintosh R, Van Kooten C, et al. A novel human IgA monoclonal antibody protects against tuberculosis. *J Immunol* (2011) 186:3113–9. doi:10.4049/jimmunol.1003189
30. Lu LL, Chung AW, Rosebrock TR, Ghebremichael M, Yu WH, Grace PS, et al. A functional role for antibodies in tuberculosis. *Cell* (2016) 167:433–43.e414. doi:10.1016/j.cell.2016.08.072
31. Goonetilleke NP, Mcshane H, Hannan CM, Anderson RJ, Brookes RH, Hill AV. Enhanced immunogenicity and protective efficacy against *Mycobacterium tuberculosis* of bacille Calmette-Guerin vaccine using mucosal administration and boosting with a recombinant modified vaccinia virus Ankara. *J Immunol* (2003) 171:1602–9. doi:10.4049/jimmunol.171.3.1602
32. Wozniak TM, Ryan AA, Britton WJ. Interleukin-23 restores immunity to *Mycobacterium tuberculosis* infection in IL-12p40-deficient mice and is not required for the development of IL-17-secreting T cell responses. *J Immunol* (2006) 177:8684–92. doi:10.4049/jimmunol.177.12.8684
33. Jung S, Unutmaz D, Wong P, Sano G, De Los Santos K, Sparwasser T, et al. In vivo depletion of CD11c+ dendritic cells abrogates priming of CD8+ T cells by exogenous cell-associated antigens. *Immunity* (2002) 17:211–20. doi:10.1016/S1074-7613(02)00365-5
34. Fahlen-Yrlid L, Gustafsson T, Westlund J, Holmberg A, Strombeck A, Blomquist M, et al. CD11c(high)dendritic cells are essential for activation of CD4+ T cells and generation of specific antibodies following mucosal immunization. *J Immunol* (2009) 183:5032–41. doi:10.4049/jimmunol.0803992
35. Querec T, Bennouna S, Alkan S, Laouar Y, Gorden K, Flavell R, et al. Yellow fever vaccine YF-17D activates multiple dendritic cell subsets via TLR2, 7, 8, and 9 to stimulate polyvalent immunity. *J Exp Med* (2006) 203:413–24. doi:10.1084/jem.20051720
36. Li S, Rouphael N, Duraisingham S, Romero-Steiner S, Presnell S, Davis C, et al. Molecular signatures of antibody responses derived from a systems biology study of five human vaccines. *Nat Immunol* (2014) 15:195–204. doi:10.1038/ni.2789
37. Kazmin D, Nakaya HI, Lee EK, Johnson MJ, Van Der Most R, Van Den Berg RA, et al. Systems analysis of protective immune responses to RTS,S malaria vaccination in humans. *Proc Natl Acad Sci U S A* (2017) 114:2425–30. doi:10.1073/pnas.1621489114
38. Villadangos JA, Cardoso M, Steptoe RJ, Van Berkel D, Pooley J, Carbone FR, et al. MHC class II expression is regulated in dendritic cells independently

of invariant chain degradation. *Immunity* (2001) 14:739–49. doi:10.1016/S1074-7613(01)00148-0
39. Moguche AO, Musvosvi M, Penn-Nicholson A, Plumlee CR, Mearns H, Geldenhuys H, et al. Antigen availability shapes T cell differentiation and function during tuberculosis. *Cell Host Microbe* (2017) 21:695–706.e695. doi:10.1016/j.chom.2017.05.012
40. Pethe K, Alonso S, Biet F, Delogu G, Brennan MJ, Locht C, et al. The heparin-binding haemagglutinin of *M. tuberculosis* is required for extrapulmonary dissemination. *Nature* (2001) 412:190–4. doi:10.1038/35084083
41. Sakai S, Kauffman KD, Sallin MA, Sharpe AH, Young HA, Ganusov VV, et al. CD4 T cell-derived IFN-gamma plays a minimal role in control of pulmonary *Mycobacterium tuberculosis* infection and must be actively repressed by PD-1 to prevent lethal disease. *PLoS Pathog* (2016) 12:e1005667. doi:10.1371/journal.ppat.1005667
42. Jacobs AJ, Mongkolsapaya J, Screaton GR, Mcshane H, Wilkinson RJ. Antibodies and tuberculosis. *Tuberculosis (Edinb)* (2016) 101:102–13. doi:10.1016/j.tube.2016.08.001
43. Herbst S, Schaible UE, Schneider BE. Interferon gamma activated macrophages kill mycobacteria by nitric oxide induced apoptosis. *PLoS One* (2011) 6:e19105. doi:10.1371/journal.pone.0019105
44. Liang SC, Tan XY, Luxenberg DP, Karim R, Dunussi-Joannopoulos K, Collins M, et al. Interleukin (IL)-22 and IL-17 are coexpressed by Th17 cells and cooperatively enhance expression of antimicrobial peptides. *J Exp Med* (2006) 203:2271–9. doi:10.1084/jem.20061308
45. Gopal R, Monin L, Slight S, Uche U, Blanchard E, Fallert Junecko BA, et al. Unexpected role for IL-17 in protective immunity against hypervirulent *Mycobacterium tuberculosis* HN878 infection. *PLoS Pathog* (2014) 10:e1004099. doi:10.1371/journal.ppat.1004099
46. Bold TD, Banaei N, Wolf AJ, Ernst JD. Suboptimal activation of antigen-specific CD4+ effector cells enables persistence of *M. tuberculosis* in vivo. *PLoS Pathog* (2011) 7:e1002063. doi:10.1371/journal.ppat.1002063
47. Grace PS, Ernst JD. Suboptimal antigen presentation contributes to virulence of *Mycobacterium tuberculosis* in vivo. *J Immunol* (2016) 196:357–64. doi:10.4049/jimmunol.1501494
48. Pecora ND, Fulton SA, Reba SM, Drage MG, Simmons DP, Urankar-Nagy NJ, et al. *Mycobacterium bovis* BCG decreases MHC-II expression in vivo on murine lung macrophages and dendritic cells during aerosol infection. *Cell Immunol* (2009) 254:94–104. doi:10.1016/j.cellimm.2008.07.002
49. Sakai S, Kawamura I, Okazaki T, Tsuchiya K, Uchiyama R, Mitsuyama M. PD-1-PD-L1 pathway impairs T(h)1 immune response in the late stage of infection with *Mycobacterium bovis* bacillus Calmette-Guerin. *Int Immunol* (2010) 22:915–25. doi:10.1093/intimm/dxq446
50. Buccheri S, Reljic R, Caccamo N, Ivanyi J, Singh M, Salerno A, et al. IL-4 depletion enhances host resistance and passive IgA protection against tuberculosis infection in BALB/c mice. *Eur J Immunol* (2007) 37:729–37. doi:10.1002/eji.200636764
51. Pitt JM, Stavropoulos E, Redford PS, Beebe AM, Bancroft GJ, Young DB, et al. Blockade of IL-10 signaling during *Bacillus* Calmette-Guerin vaccination enhances and sustains Th1, Th17, and innate lymphoid IFN-gamma and IL-17 responses and increases protection to *Mycobacterium tuberculosis* infection. *J Immunol* (2012) 189:4079–87. doi:10.4049/jimmunol.1201061
52. Gideon HP, Phuah J, Myers AJ, Bryson BD, Rodgers MA, Coleman MT, et al. Variability in tuberculosis granuloma T cell responses exists, but a balance of pro- and anti-inflammatory cytokines is associated with sterilization. *PLoS Pathog* (2015) 11:e1004603. doi:10.1371/journal.ppat.1004603
53. Laidlaw BJ, Cui W, Amezquita RA, Gray SM, Guan T, Lu Y, et al. Production of IL-10 by CD4(+) regulatory T cells during the resolution of infection promotes the maturation of memory CD8(+) T cells. *Nat Immunol* (2015) 16:871–9. doi:10.1038/ni.3224
54. Belkaid Y, Piccirillo CA, Mendez S, Shevach EM, Sacks DL. CD4+CD25+ regulatory T cells control *Leishmania major* persistence and immunity. *Nature* (2002) 420:502–7. doi:10.1038/nature01152
55. Huygen K. The immunodominant T-cell epitopes of the mycolyl-transferases of the antigen 85 complex of *M. tuberculosis*. *Front Immunol* (2014) 5:321. doi:10.3389/fimmu.2014.00321
56. Salzman NH, De Jong H, Paterson Y, Harmsen HJ, Welling GW, Bos NA. Analysis of 16S libraries of mouse gastrointestinal microflora reveals a large new group of mouse intestinal bacteria. *Microbiology* (2002) 148:3651–60. doi:10.1099/00221287-148-11-3651
57. Paynich ML, Jones-Burrage SE, Knight KL. Exopolysaccharide from *Bacillus subtilis* induces anti-inflammatory M2 macrophages that prevent T cell-mediated disease. *J Immunol* (2017) 198:2689–98. doi:10.4049/jimmunol.1601641
58. Aps LR, Diniz MO, Porchia BF, Sales NS, Moreno AC, Ferreira LC. *Bacillus subtilis* spores as adjuvants for DNA vaccines. *Vaccine* (2015) 33:2328–34. doi:10.1016/j.vaccine.2015.03.043
59. Belz GT, Bedoui S, Kupresanin F, Carbone FR, Heath WR. Minimal activation of memory CD8+ T cell by tissue-derived dendritic cells favors the stimulation of naive CD8+ T cells. *Nat Immunol* (2007) 8:1060–6. doi:10.1038/ni1505
60. Pastva AM, Mukherjee S, Giamberardino C, Hsia B, Lo B, Sempowski GD, et al. Lung effector memory and activated CD4+ T cells display enhanced proliferation in surfactant protein A-deficient mice during allergen-mediated inflammation. *J Immunol* (2011) 186:2842–9. doi:10.4049/jimmunol.0904190
61. Gollwitzer ES, Saglani S, Trompette A, Yadava K, Sherburn R, Mccoy KD, et al. Lung microbiota promotes tolerance to allergens in neonates via PD-L1. *Nat Med* (2014) 20:642–7. doi:10.1038/nm.3568

Conflict of Interest Statement: Author MS was employed by company Lionex. All other authors declare no competing interests.

frontiers in Immunology

ORIGINAL RESEARCH
published: 20 March 2018
doi: 10.3389/fimmu.2018.00562

Trimethyl Chitosan Nanoparticles Encapsulated Protective Antigen Protects the Mice Against Anthrax

*Anshu Malik, Manish Gupta, Rajesh Mani, Himanshu Gogoi and Rakesh Bhatnagar**

Molecular Biology and Genetic Engineering Laboratory, School of Biotechnology, Jawaharlal Nehru University, New Delhi, India

Anthrax is an era old deadly disease against which there are only two currently available licensed vaccines named anthrax vaccine adsorbed and precipitated (AVP). Though they can provide a protective immunity, their multiple side-effects owing to their ill-defined composition and presence of toxic proteins (LF and EF) of *Bacillus anthracis,* the causative organism of anthrax, in the vaccine formulation makes their widespread use objectionable. Hence, an anthrax vaccine that contains well-defined and controlled components would be highly desirable. In this context, we have evaluated the potential of various vaccine formulations comprising of protective antigen (PA) encapsulated trimethyl-chitosan nanoparticles (TMC-PA) in conjunction with either CpG-C ODN 2395 (CpG) or Poly I:C. Each formulation was administered *via* three different routes, viz., subcutaneous (SC), intramuscular (IM), and intraperitoneal in female BALB/c mice. Irrespective of the route of immunization, CpG or Poly I:C adjuvanted TMC-PA nanoparticles induced a significantly higher humoral response (total serum IgG and its isotypes viz., IgG1, IgG2a, and IgG2b), compared to their CpG or Poly I:C PA counterparts. This clearly demonstrates the synergistic behavior of CpG and Poly I:C with TMC nanoparticles. The adjuvant potential of TMC nanoparticles could be observed in all the three routes as the TMC-PA nanoparticles by themselves induced IgG titers ($1–1.5 \times 10^5$) significantly higher than both CpG PA and Poly I:C PA groups ($2–8 \times 10^4$). The effect of formulations on T-helper (T_h) cell development was assessed by quantifying the Th1-dependant (TNF-α, IFN-γ, and IL-2), Th2-dependant (IL-4, IL-6, and IL-10), and Th17-type (IL-17A) cytokines. Adjuvanation with CpG and Poly I:C, the TMC-PA nanoparticles triggered a Th1 skewed immune response, as suggested by an increase in the levels of total IgG2a along with IFN-γ cytokine production. Interestingly, the TMC-PA group showed a Th2-biased immune response. Upon challenge with the *B. anthracis* Ames strain, CpG and Poly I:C adjuvanted TMC-PA nanoparticles immunized *via* the SC and IM routes showed the highest protective efficacy of ~83%. Altogether, the results suggest that CpG or Poly I:C adjuvanted, PA-loaded TMC nanoparticles could be used as an effective, non-toxic, second generation subunit-vaccine candidate against anthrax.

Keywords: anthrax, vaccine, protective antigen, trimethylchitosan nanoparticles, CpG, PolyI:C

OPEN ACCESS

Edited by:
África González-Fernández, Centro de Investigaciones Biomédicas (CINBIO), Spain

Reviewed by:
Noemi Csaba, Universidade de Santiago de Compostela, Spain
Arun Kumar, Linköping University, Sweden

***Correspondence:**
Rakesh Bhatnagar
rakeshbhatnagar@jnu.ac.in

Specialty section:
This article was submitted to Vaccines and Molecular Therapeutics, a section of the journal Frontiers in Immunology

Received: *18 December 2017*
Accepted: *06 March 2018*
Published: *20 March 2018*

Citation:
Malik A, Gupta M, Mani R, Gogoi H and Bhatnagar R (2018) Trimethyl Chitosan Nanoparticles Encapsulated Protective Antigen Protects the Mice Against Anthrax. Front. Immunol. 9:562. doi: 10.3389/fimmu.2018.00562

INTRODUCTION

Bacillus anthracis, a Gram-positive microorganism, is the cause of an acute disease Anthrax. It can form spores, which could remain dormant for years and accidental exposure by inhalation may result in death (1). Although inhalational anthrax has been reported to have a high fatality rate near to 100%, few deaths have also been documented due to cutaneous and gastrointestinal anthrax (2).

It is also recognized for many bioterror attacks in history, including the famous 2001 bioterror attack of anthrax spores in the US (3). A prophylactic approach would be the best way to cease the disease and protect people against any bioterror attack. The currently existing vaccines BioThrax (also known as anthrax vaccine adsorbed) and anthrax vaccine precipitated (AVP) are the only licensed vaccines present globally (4). The major caveats of these vaccines are the presence of toxic proteins [lethal factor (LF) and edema factor (EF)] and the undefined composition of anthrax proteins (5). At present, only the high-risk population such as defense personnel are vaccinated with BioThrax. However, there have been several reports of reactogenicity in such individuals (6). Another drawback associated with this vaccine is the cumbersome dosing schedule, which comprises of multiple initial doses and subsequent annual boosters for sustained immunity (7).

In recent times, the focus has shifted to second generation subunit vaccines where the composition is pharmaceutically defined, and highly immunogenic proteins are taken into account making it safer for the mass use. In case of anthrax, *B. anthracis,* the causative organism of anthrax, secrete two toxins comprised of three proteins: the protective antigen (PA), the LF, and the EF. The edema toxin (PA + EF) causes edema and lethal toxin (PA + LF) causes death in animals (8). PA has always been the choice of antigen as it binds to the host receptor and binds to LF and EF to make lethal toxin and edema toxin, which eventually cause the toxicity in the host (9). Hence, the antibodies against PA have been shown to protect against aerosolized *B. anthracis* Ames spore challenge (10).

A soluble antigen when injected alone has less residence time and often lack essential danger signals necessary to provoke dendritic cells and consequently, T-cells. To surpass these limitations, antigen encapsulation into particulate system helps by increasing the retention time of the antigen in the host system and creating a depot, which releases the antigen into the system for a longer duration in a controlled manner (11, 12). The susceptibility of particles to be phagocytized by the macrophages is 1,000–10,000 times more efficient, and it also allows multimeric antigen presentation and delivery to antigen-presenting cells (APCs), in comparison to the soluble antigens (13).

The intervention of natural, biodegradable polymers-based encapsulation carriers makes them reasonably safe to employ for vaccine delivery (14, 15). Poly (lactic-co-glycolic acid) and chitosan are the most studied among them. Chitosan is derived from chitin, which is a ubiquitous natural polymer and is soluble in water under acidic conditions. Chitosan particles are usually positively charged and irregular in shape. However, they are susceptible to dissociation with ionic fluctuations and unstable at physiological pH. Several chemically modified (at functional groups -OH and -NH2) derivatives of chitosan have been studied. For instance, trimethyl-chitosan (TMC) is preferred over chitosan due to its stability at several pH ranges and its positive surface charge and has been utilized for vaccine delivery against influenza and Hepatitis B (14, 16–21).

Trimethyl-chitosan as well as chitosan have also been claimed to possess mucoadhesive and intrinsic adjuvant properties, and evidently, its nanoparticles can stimulate *in vitro* T-cell maturation and proliferation (22). Furthermore, it also possesses the ability to open tight junctions and cross epithelial barriers by redistributing the cytoskeletal F-actin and ZO-1 tight junction protein (23–26). The precursor of TMC and chitosan, chitin, has also been demonstrated to be a size-dependent pathogen-associated molecular pattern (PAMP) and shown to interact and activate the macrophages through different TLRs and dectin-1 (27, 28).

In addition to TMC nanoparticles, we sought to investigate further whether the immune response of nanoparticles could be synergistically improved upon addition of an adjuvant. Alum or aluminum salts-based adjuvants are currently licensed by FDA for human use and are most commonly employed in combination with several antigens. Despite this, they too suffer from various shortcomings such as variable antigen adsorption, induction of weak T-cell-mediated immune response, poor maturation of APCs, and intermittent occurrence of hypersensitivity reactions (29–31). Hence, PAMP-based adjuvants CpG-C ODN 2395 and Poly I:C were used in the study, which has been documented to provide protective immunity against anthrax infection (32, 33). CpG interacts with the TLR9 receptor and initiates a cascade of immuno-stimulatory signaling events culminating in secreting various cytokines and chemokines. This, in turn, causes maturation, differentiation, and proliferation of several immune cell types and eventually perpetuates a pro-inflammatory and TH1-biased immune response (34, 35). Similarly, the interaction of Poly I:C with TLR-3 induces dendritic cells maturation and is also reported to promote the *in vitro* survival of activated CD4+ cells and *in vivo* survival of antigen-activated CD8+ cells (36–39). Cytokines also perform a crucial part in the generation of humoral and cell-mediated immunity, and hence were examined in this study post immunization. The inflammatory Th1 cytokines, comprising of IFN-γ, TNF, and IL-2, stimulate predominantly cell-mediated immunity and T-cell proliferation, along with T-helper cell differentiation (40, 41). Immune modulating Th2 cytokines, such as IL-4, IL-6, and IL-10, support humoral immunity and adaptive immunity, mediate allergic diseases, and regulate chronic infections (42, 43).

The following parameters are known to affect the immune response elicited by the particulate-antigen delivery system: (i) administration route, (ii) booster administration, and the interval between boosters (iii) delivery system and amount of antigen, (iv) inclusion of immune modulating molecules like toll-like receptors (TLRs) ligands. Hence, in this study, we evaluated the vaccine potential of various TMC-PA nano-formulations with adjuvants through subcutaneous (SC), intramuscular (IM), and intraperitoneal (IP) delivery platforms. The protective efficacy of the various TMC-PA vaccine formulations was also assessed.

MATERIALS AND METHODS

Materials

Chitosan (75–85% deacetylated, mol wt 50–190 kDa), Sodium tripolyphosphate (TPP), Poly I:C and Tween 80 were purchased from Sigma (Sigma, India). CpG-C ODN 2395 was purchased from Hycult Biotech Pvt. Ltd. All other materials used were of the analytical or pharmaceutical grade.

Preparation of TMC Form Chitosan

Trimethyl-chitosan was derived from chitosan as described previously by Muzarelli and Tanfani and Verheul et al. (17, 44), with some modifications. To begin with, for formic acid–formaldehyde methylation (Eschweiler-Clarke), 3 g of chitosan was dissolved in 10 ml of formic acid, 10 ml of formaldehyde, and 60 ml distilled water added one by one in a round bottom flask. Under reflux condensing conditions, it was heated in an oil bath at 70°C for 118 h, under constant magnetic stirring. The resultant viscous liquid was evaporated and treated with 1N NaOH to increase its pH to 12. The so-formed dimethyl-chitosan (DMC) was washed with distilled water and then dissolved in 25 ml of 1-methyl-2-pyrrolidinone in the presence of 0.5 ml of iodomethane. It was heated up to 40°C on an oil bath under constant magnetic stirring for overnight. The solution was then dissolved in ethanol/diethyl ether mixture (50:50) resulting in the precipitation of TMC. The precipitated TMC was separated by centrifugation and washed thrice with diethyl ether. After complete evaporation of diethyl-ether, TMC was dissolved in 50 ml of 10% NaCl and dialyzed against deionized water for 3 days. After dialysis, TMC was lyophilized to obtain a dried powder form. ^{1}H-nuclear magnetic resonance (^{1}H-NMR) spectroscopy was done to assess the presence of trimethyl groups in chitosan. The degree of quaternization (DQ) of the end product was estimated by:

$$\mathrm{DQ}(\%) = \frac{[(\mathrm{CH_3})_3]}{[\mathrm{H}]} \times 1/9 \times 100 \quad (1)$$

Preparation of PA-loaded TMC Nanoparticles (TMC-PA)

The nanoparticles were prepared by using the ionic gelation method as described previously (22, 45). A schematic representation of the preparation process is illustrated by Figure S1 in Supplementary Material. Briefly, 10 mg of TMC was dissolved in 5 ml 10 mM HEPES (pH 7.4), and PA was also prepared in the same buffer (8 mg/ml). The protein was dissolved in the TMC solution achieving a final concentration of 0.1 mg/ml under constant stirring. While continuous stirring (350 rpm), 1 ml of the crosslinking agent, TPP solution (1.7 mg/ml) was added to the TMC-PA solution drop by drop to induce ionic complexation. Weight ratio TMC:PA:TPP of 10:0.5:1.7 was taken to get the desired size of particles. An opalescent dispersion forms after TPP addition indicating the formation of nanoparticles. The nanoparticles were collected by centrifugation at 12,000 rpm for 15 min on a 10 µl glycerol bed. The particles were stored at −20°C until further use. The supernatant obtained was used for Micro BCA protein estimation. The protein encapsulation efficiency of the particles was further calculated by using Eq. 2:

$$\text{Encapsulation efficiency}(\%) = \frac{\text{weight of encapsulated protein}}{\text{weight of total protein used for encapsulation}} \times 100 \quad (2)$$

For size analysis, a separate batch of nanoparticles was prepared with a minor modification. 0.05% of Tween 80 was added after dissolving TMC in the HEPES buffer.

Physical Characterization and *In Vitro* Release Profile of TMC-PA Nanoparticles

The particles were dissolved in HEPES buffer pH 7.4 to measure the size, polydispersity index and zeta potential of the particles with the help of a Nanosizer ZS apparatus (Malvern Instruments, Malvern, UK). For scanning electron microscopic (SEM) imaging, particles were coated on a carbon tape on an aluminum stub and then coated with gold particles at 2 kV for 200 s under inert Argon condition. SEM images were captured using an electron microscope [Zeiss EVO40 (Carl Zeiss, Thornwood, NY, USA)]. For transmission electron microscopy [JEM 2100 F (Jeol Ltd., Tokyo, Japan), Electron Microscopy Sciences, Hatfield, PA] the nanoparticles dissolved in HEPES buffer were dropped (20 µl) on a copper mesh grid (46). After evaporating the buffer, the grid was inserted in the instrument and imaging was done in a high vacuum, at 200 kV and direct magnification of 3,000X.

For the *in vitro* protein release profile of the nanoparticles, a definite amount of particles were dissolved in 1× PBS and were stirred at 100 rpm at 37°C in several aliquots. Each aliquot was taken out from stirring at a specific time point and was centrifuged to spin down the nanoparticles, and the supernatant was taken to estimate the protein released by the nanoparticles in that specific time interval. Consequently, at different time points (2, 4, 6, 8, 10, 12, 24, 48, and 96 h), the release of protein was measured to assess the release of nanoparticles. The protein release was monitored for 96 h.

In Vivo Immunological Study

Mice were obtained from National Centre for Laboratory Animal Sciences, NIN, Hyderabad, India, and were maintained in animal holding room of BSL3 laboratory. All the animal experiments including challenge studies were performed in compliance with Institutional Animal Ethics Committee (Jawaharlal Nehru University) and Council for the Purpose of Control and Supervision of Experiments on Animals (CPCSEA, Ministry of Social Justice and Empowerment, Government of India). Female Balb/c mice (6–8 weeks of age) were immunized with the placebo nanoparticles (Blank NP), TMC-PA nanoparticles (TMC-PA), TMC-PA nanoparticles in combination with CpG (CpG TMC-PA), and Poly I:C (Poly I:C TMC-PA) ($n = 21$ per group). All these formulations were administered in mice *via* SC, IM and IP routes. The amount of PA administered with every formulation was 20 µg/mice. CpG (20 µg/mice) as well as Poly I:C (10 µg/mice) were mixed with the nanoparticles right before the administration into mice. After an initial prime dose, two successive booster doses were given at an interval of 7 and 15 days, respectively (as depicted in Figure S2 in Supplementary Material). Sera were collected on 28th and 42nd day and stored at −80°C until further use. The sera samples were then used for the estimation of total IgG, IgG1, and IgG2a endpoint antibody titer against PA (anti-PA) by ELISA. Administration routes used

in the study and the corresponding volume of dose injected into each animal are detailed in Table S1 in Supplementary Material.

Cytokine Analysis

After 42 days of primary immunization, three mice from each group were sacrificed, and their spleens were crushed to make a single cell suspension. 10^6 cells were seeded in each well of a 96-well round bottom (Nunc) plate. The cells were stimulated with PA (10 μg/ml) to induce the production of cytokines in the supernatant. Unstimulated and Con A (5 μg/well) treated cells were taken as negative and positive control, respectively. After 48 h of stimulation, the supernatant was collected from each well and was used for cytokine measurement using CBA (Cytometric Bead Array) Mouse Th1/Th2/Th17 Cytokine Kit (BD Biosciences), according to manufacturer instructions. The data were acquired on a BD LSR™ II flow cytometer (Becton Dickinson) and analyzed using the FCAP Array software V3.0 (Becton 519 Dickinson).

Survival Assay/Protective Efficacy Studies

At 43rd day, remaining mice in each group were challenged with 0.5×10^3 spores of *B. anthracis* Ames strain. As a control, 20 μg of PA adsorbed on alum was subcutaneously injected into a separate mice group ($n = 12$) and then challenged simultaneously. Mice were monitored for 15 days for death events in each group. Survival curve was plotted to compare the efficiency of protection in vaccinated mice groups over control blank nanoparticle immunized mice group.

Statistical Analysis

The results are reported as mean ± SE post data preparation and statistical analysis using GraphPad Prism v6.05 software. The statistical significance of antibody titer and cytokine level data was calculated by using one-way ANOVA, followed by Tukey's multiple comparisons test. The survival curve for anthrax spore challenge experiment was evaluated using Kaplan–Meier survival estimates (GraphPad Prism, La Jolla, CA, USA). Statistically significant differences between the groups are highlighted by following denotations: * for P-value <0.05, ** for P-values <0.01, *** for P-values <0.001, and **** for P-values <0.0001.

RESULTS

NMR Characterization of the Trimethyl Chitosan

First, a dimethyl derivative of chitosan (DMC) was obtained with formic acid and formaldehyde treatment. Followed by derivation of TMC from DMC, ^{1}H-NMR spectrum was analyzed for the presence of trimethyl group in chitosan. The peak present at 3.33 ppm represents the trimethyl group incorporated into the polymer at the -NH2 group of chitosan, imparting a positive charge to the polymer (Figure S3 in Supplementary Material). The final product was completely soluble in water, and the NMR was carried out by dissolving the final product in D_2O. The DQ calculated by the Eq. 1 above was 80.4 ± 5.2%. Negligible O-methylation was observed in the product as seen in the NMR profile.

PA Encapsulated Nanoparticles Preparation

TMC-PA nanoparticles were prepared by ionic gelation method with the help of TPP anion. The particles were in the nanometer range with an average particle size of 254 ± 24 nm as depicted in **Figure 1D**. The particles shape and morphology was observed by SEM and TEM as shown in **Figures 1A,B**, and the nanoparticles were found to be smooth in texture but irregular in shape. The encapsulation efficiency of the particles was found to be 78.33 ± 4.75%. The polydispersity index of the particles was found to be 0.2 indicating fine homogeneity of the particles. **Figure 1E** reveals the zeta potential of the protein-loaded nanoparticles was found to be 8.84 ± 0.25 mV, which confirmed that the particles carried a positive charge.

In Vitro Antigen Release

The antigen release profile of the TMC-PA nanoparticles was taken into account to estimate the amount of protein released from the particles over a specified period. The release of protein was studied until 96 h, illustrated in **Figure 1C**. Around 30% of the protein was released in the first 6 h only, and approximately 55% of the protein was released within first 24 h. Afterward, protein release was quite slow, and in next 24 h, only 7% protein was released. For the next 24 h also, only 8% release was observed. Therefore, in the later period, the release was slow and consistent inferring that remaining 30% of the protein would also be released at the same pace at these conditions. This suggests that at physiological pH, PA would be completely released within a week from the particles. Since 50% of the protein was burst released in the first 24 h; therefore, for immunization studies, 20 μg of protein encapsulating nanoparticles were used per mice. The encapsulated protein was analyzed on SDS polyacrylamide upon dissolution of the nanoparticles with 1% NaCl. The protein was observed at its molecular weight of 83KDa, and no protein degradation was observed, as seen in **Figure 1F**.

Immune Response Generated in Mice by TMC-PA Alone and Upon Adjuvanation with CpG and Poly I:C

The immune response was elucidated in terms of the total IgG titer raised against the antigen. Since the mice were immunized *via* three routes: subcutaneous, IM, and IP; therefore, the comparison between different groups was also carried out within one frame of the route at a time.

Total IgG Titer

Figure 2 illustrates the highly elevated total IgG titer in almost all the vaccinated mice groups when compared to only PA vaccinated control mice. In all three routes, the descending order for the titers was CpG TMC-PA > Poly I:C TMC-PA > TMC-PA > Poly I:C PA > CpG PA. It could be seen that CpG and Poly I:C adjuvanation increased the total IgG titer from TMC-PA group significantly in almost all the three routes. In the subcutaneous route, the total IgG titer of the CpG TMC-PA group was significantly ($P < 0.0001$) higher than Poly I:C TMC-PA group on the 28th day (1.45-fold higher), whereas on 42nd day, the two titers were

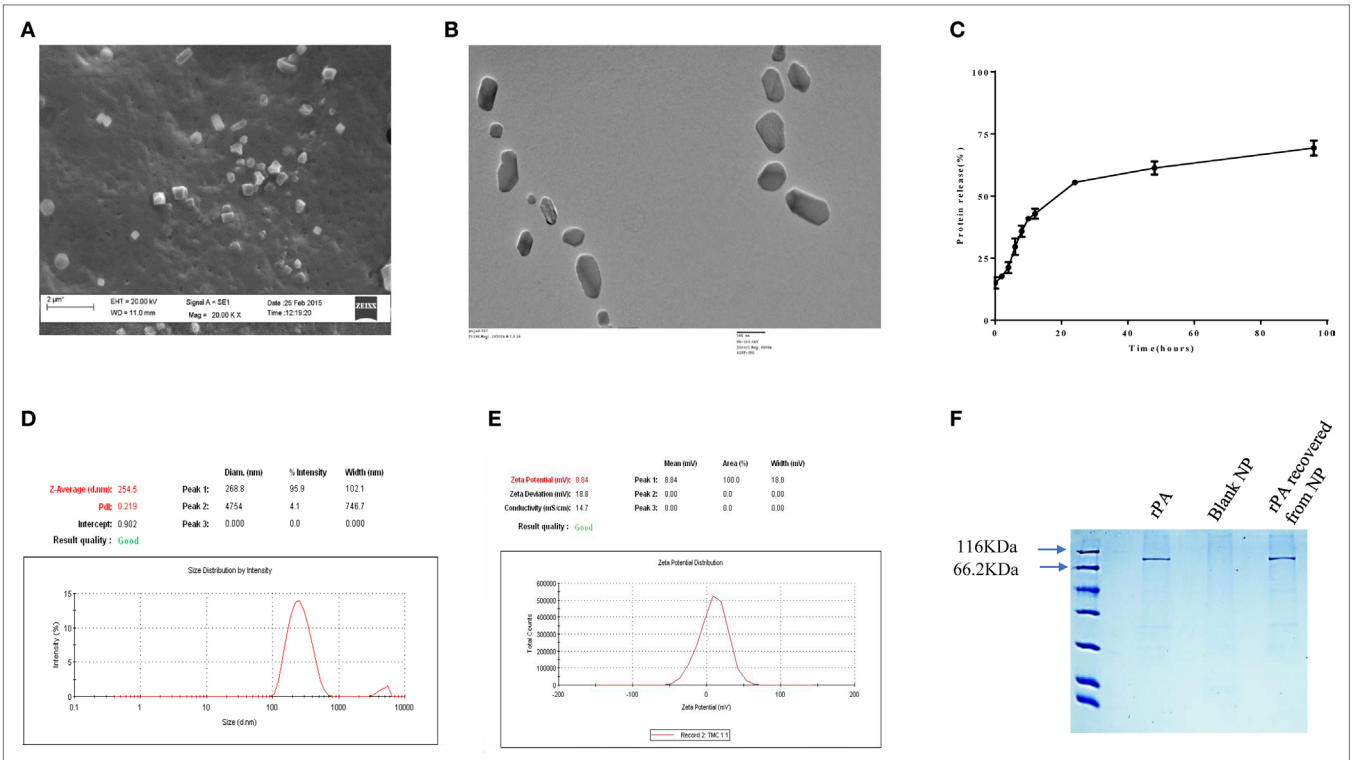

FIGURE 1 | Physical characterization of nanoparticles. **(A)** scanning electron microscopic and **(B)** TEM micrographs, **(C)** *in vitro* release profile of protective antigen (PA) protein from Trimethyl-chitosan (TMC)-PA nanoparticles after suspension and incubation at 37°C in PBS (50 mg/ml, pH7.4) for indicated time periods and the released protein estimation by micro-BCA assay. **(D)** Particle size distribution (DLS) and **(E)** zeta potential of TMC nanoparticles encapsulating PA. **(F)** SDS PAGE analysis of the purified recombinant PA and the PA recovered from TMC-PA nanoparticles.

not significantly different. However in IM route, on both 28th and the 42nd day, the total IgG titer of CpG TMC-PA group is significantly ($P < 0.01$ and $P < 0.0001$, respectively) higher than Poly I:C TMC-PA group (1.44-fold on the 28th day and 1.5-fold on the 42nd day). Also, the TMC-PA, CpG TMC-PA, and Poly I:C TMC-PA groups showed significantly higher titer than the only PA group. These results elucidate the potential of TMC in mediating a very good humoral response in comparison to the only protein group and upon adjuvanation with CpG or Poly I:C, it increased in a synergistic manner. In all the three routes, the TMC-PA group showed significantly higher titer than CpG PA group and Poly I:C PA group ($P < 0.0001$). This shows that the TMC acts as a strong and better adjuvant in the form of nanoparticles with the PA protein and CpG as well Poly I:C adjuvanation improves the immune response mounted by TMC-PA alone.

IgG Isotypes

The levels of IgG1 (**Figure 3**) were higher in all TMC-PA containing groups in comparison to other groups, and this pattern was similar for all the three routes. On 28th and 42nd day, the TMC-PA group showed the highest titer in SC and IM route. However, for IP route, Poly I:C TMC-PA group showed the highest titer on both 28th and 42nd day followed by the TMC-PA group. The Poly I:C PA and CpG PA groups showed substantially lower levels of IgG1 in comparison to the other nanoformulation vaccinated groups at both the time points and all the routes ($P < 0.0001$).

In case of IgG2a subtype (**Figure 4**), among all routes, on the 28th and 42nd day, the Poly I:C TMC-PA and CpG TMC-PA groups showed the highest titers. The TMC-PA, CpG PA, and Poly I:C PA groups showed significantly lower titers when compared to the CpG and Poly I:C adjuvated TMC-PA groups, through all the routes, and at 42nd day, there was no significant difference in their titers as well, except in SC route. IgG isotypes have been of importance as to determine the Th biasness of the immune response. TMC has been reported to have a Th2-directing effect on the immune response, whereas CpG and Poly I:C have been reported to have a Th1 biasing effect on the immune response.

Cytokine Release and Th1/Th2 Immune Response in Mice Groups

CpG TMC-PA Group

Based on the cytokine levels and the levels of IgG isotypes (IgG1 and IgG2a), it was seen that CpG TMC-PA SC/IM/IP groups of mice developed a dominant Th1-biased immune response. By 42nd day, the ratio of IgG2a vs IgG1 was found to be 2.4 for SC route, 2.3 for IM route, and 2.3 for IP route (**Figures 3** and **4**). The IFN-γ levels for these groups for SC, IM, and IP routes were highest among all the groups with no significant difference between them (**Figure 5A**). IL-4 levels for this group were <10 pg/ml for all three routes with no significant difference among them (**Figure 5D**). Similarly, IL-10 levels were <150 pg/ml and IL-6 levels were ~200 pg/ml, with no significant difference among all

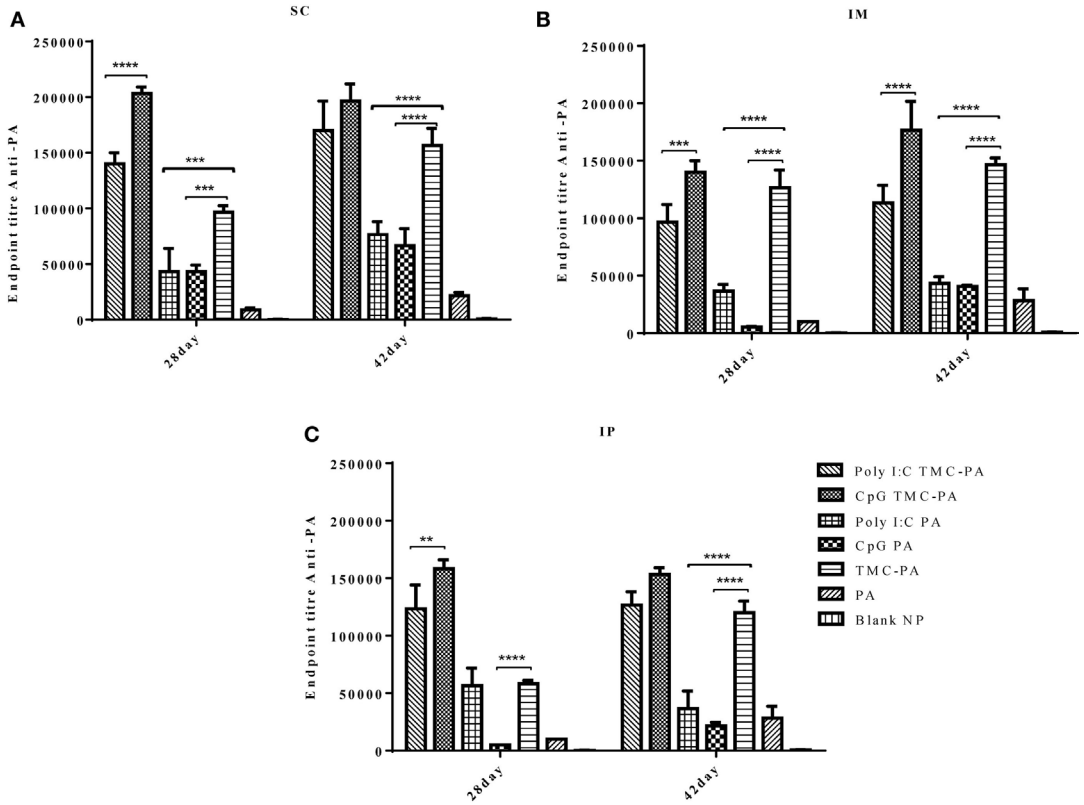

FIGURE 2 | Serum antiprotective antigen (PA) total IgG endpoint titer. Female Balb/c mice (6–8 weeks of age; $n = 21$) were immunized with 1× PBS, PA, trimethyl-chitosan (TMC) NP-PA, Poly IC PA, Poly I:C TMC NP-PA, CpG PA, and CpG TMC NP-PA *via* three routes: subcutaneous (SC), intramuscular (IM), and intraperitoneal (IP) with a prime dose and two booster doses with an interval of 7 and 15 days, respectively. The mice were bled on 28th and 42nd day and sera samples were collected from all mice. Serial dilutions of sera from each group were analyzed for anti-PA total IgG titer for **(A)** SC route, **(B)** IM route, and **(C)** IP route. Statistically significant differences between the groups are highlighted (* for *P*-value <0.05, ** for *P*-values <0.01, *** for *P*-values <0.001 and **** for *P*-values <0.0001).

three routes (**Figures 5E,F**). TNF-α level for the SC, IM, and IP routes were ~500 pg/ml, with no significant difference between different routes (**Figure 5B**). However, IL-2 levels for IM route were significantly higher ($P < 0.0001$) than SC and IP routes (**Figure 5C**).

CpG PA Group

This group also showed a Th1-skewed response as the ratio of IgG2a:IgG1 for SC, IM, and IP routes were 2.1, 1.8, and 1.7, respectively at 42nd day (**Figures 3** and **4**). The IFN-γ levels were significantly different between SC vs IM route ($P < 0.0001$) and SC vs IP route ($P < 0.0001$); however, no significant difference was observed between IM vs IP routes (**Figure 5A**). The Th2 cytokine IL-4 was observed to have very low levels (<10 pg/ml) supporting the Th1 biasness (**Figure 5D**). TNF-α levels for SC, IM, and IP routes were ~400 pg/ml (**Figure 5B**). The IL-2 levels of the SC route were significantly higher in comparison to IM ($P < 0.0001$) and IP ($P < 0.0001$) routes (**Figure 5C**). IL-10 and IL-6 levels for all three routes were <160 pg/ml, with no significant difference amongst the three routes (**Figures 5E,F**).

Poly I:C TMC-PA Group

At 42nd day, the ratios of IgG2a:IgG1 for SC, IM, and IP routes were 3.2, 3.0, and 2.5, respectively, suggesting a dominant Th1 response (**Figures 3** and **4**). In contrast, the IFN-γ and IL-4 levels do not support a strong Th-1 response (**Figures 5A,D**). Similarly, the levels of TNF-α and IL-2 were relatively low and exhibited no significant difference between the routes (**Figure 5B**). Both IL-10 and IL-6 levels were relatively higher with the IL-10 levels of IP route significantly higher than SC ($P < 0.0001$) and IM route ($P < 0.001$) (**Figures 5E,F**). The IL-6 levels for SC, IM and IP routes also revealed a highly significant inter-route difference ($P < 0.0001$) (**Figure 5F**).

Poly I:C PA Group

At 42nd day, the ratios of IgG2a:IgG1 for SC, IM, and IP routes were 1.9, 1.6, and 1.4, respectively, suggesting a moderate Th1 response (**Figures 3** and **4**). Similarly, the IFN-γ levels were relatively high showing a significant difference between SC vs IM route ($P < 0.001$) and SC vs IP ($P < 0.01$) routes whereas the IL-4 levels for all routes were >20 pg/ml, also suggesting a moderate Th-1 response (**Figures 5A,D**). The levels of TNF-α for the IM route were significantly higher than SC ($P < 0.001$) and IP ($P < 0.0001$) routes (**Figure 5B**). The IL-2 levels of IM and IP routes were found to be significantly higher ($P < 0.0001$) than SC route (**Figure 5C**). In contrast to the moderate Th-1 response demonstrated by above parameters, IL-10 values of SC and IP

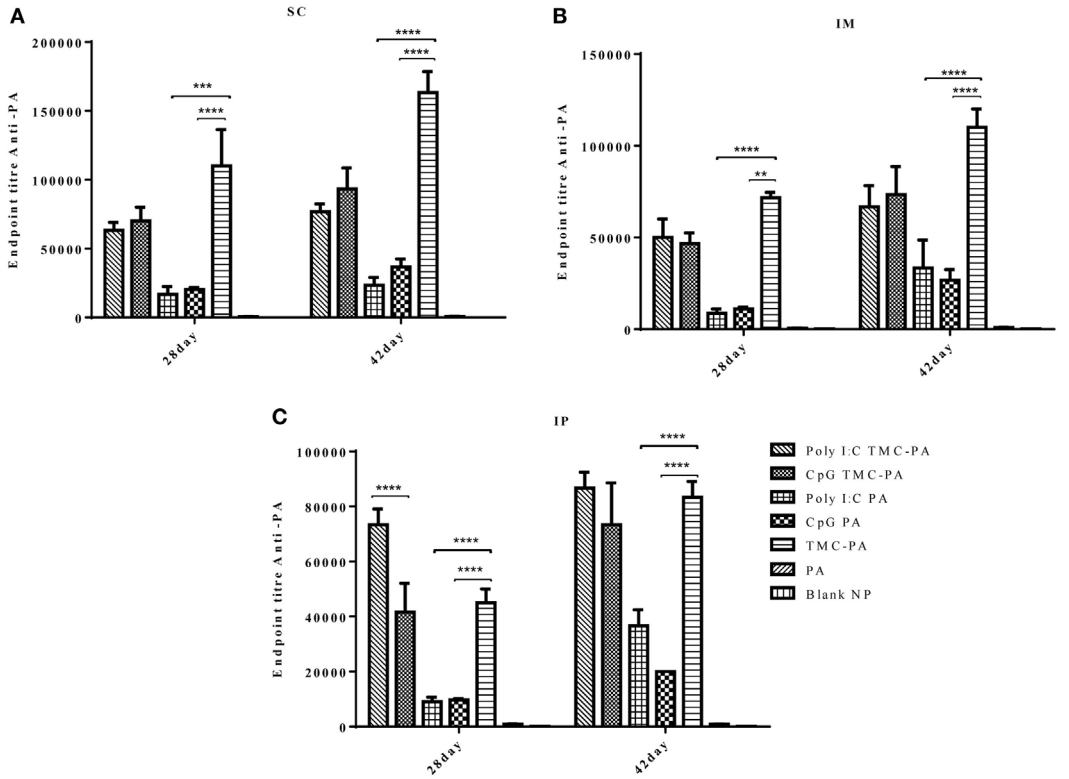

FIGURE 3 | Serum antiprotective antigen (PA) IgG1 endpoint titer. Female Balb/c mice (6–8 weeks of age; $n = 21$) were immunized with 1× PBS, PA, TMC NP-PA, Poly IC PA, Poly I:C TMC NP-PA, CpG PA, and CpG TMC NP-PA *via* three routes: subcutaneous (SC), intramuscular (IM), and intraperitoneal (IP) with a prime dose and two booster doses with an interval of 7 and 15 days, respectively. The mice were bled on 28th and 42nd day and sera samples were collected from all mice. Serial dilutions of sera from each group were analyzed for anti-PA IgG1 titer for **(A)** SC route, **(B)** IM route, and **(C)** IP route. Statistically significant differences between the groups are highlighted (* for *P*-value <0.05, ** for *P*-values <0.01, *** for *P*-values <0.001, and **** for *P*-values <0.0001).

routes were higher, whereas IM route response was moderate (**Figure 5E**). The IL-6 levels for all three routes were observed to be <350 pg/ml (**Figure 5F**).

TMC-PA Group

At 42nd day, the ratios of IgG1:IgG2a for SC, IM, and IP routes were 2.9, 3.5, and 1.6, respectively, suggesting a dominant Th2 response (**Figures 3** and **4**). However, IFN-γ levels and IL-4 levels suggest a Th1 biased immune response (**Figures 5A,D**). As the values of IL-10 and IL-6 fall in the range of 500–1,200 pg/ml, it suggests a Th2 response, which is also supported by low levels (<500 pg/ml) of TNF-α and IL-2 (**Figures 5B–F**).

IL-17 A Cytokine

Figure 5G illustrates that the highest levels of IL-17A were observed in the TMC-PA IP group, followed by Poly:IC TMC PA IP group and Poly:IC TMC PA IM being ~4,000 pg/ml. The Poly:IC PA SC and TMC-PA SC groups produced similar levels of this cytokine. Poly:IC PA IP and Poly:IC TMC PA SC groups secreted ~1,000 pg/ml of IL-17. All the remaining groups secreted relatively lower amount of cytokine.

Survival Curve

After 6 weeks of immunization, all the mice groups were challenged with 0.5×10^3 spores of *B. anthracis* Ames strain. The mice were monitored for 2 weeks to observe the protective efficacy of different formulations as shown in **Figure 6**. The mice vaccinated with Alum and PA were taken as a positive control and exhibited a survival of 83.3%, which was the maximum of all the groups examined. The CpG TMC-PA SC, Poly I:C TMC-PA SC, and Poly I:C TMC-PA IM groups also showed a survival rate of 83.3%, equivalent to the positive control used. Except for the blank nanoparticles and only PA-treated groups, all other mice groups showed a survival rate of more than 50%. The TMC-PA SC group showed a survival of 75% and the TMC-PA IM and TMC-PA IP groups showed a survival of 66.6%. Our study demonstrates that the SC route of immunization showed a better survival rate in comparison to the other two routes.

DISCUSSION

The need to expand the arsenal of adjuvants and development of new subunit vaccine against anthrax with fewer side effects has set out an exploration of the natural, biodegradable polymers with enhanced bioavailability. This study investigated a novel combination of TMC nanoparticles with PA as a potential vaccine candidate against anthrax. To the best of author's knowledge, this novel approach has not been reported to-date.

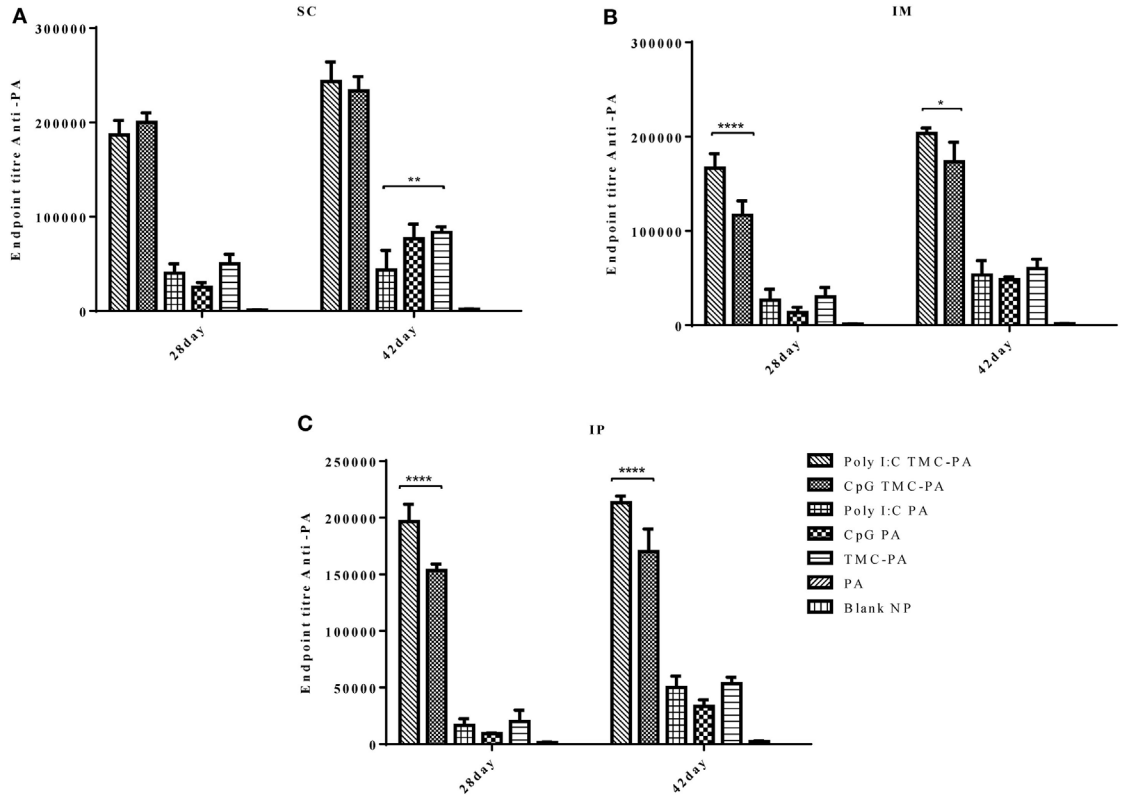

FIGURE 4 | Serum antiprotective antigen (PA) IgG2a endpoint titer. Female Balb/c mice (6–8 weeks of age; $n = 21$) were immunized with 1× PBS, PA, trimethyl-chitosan (TMC) NP-PA, Poly IC PA, Poly I:C TMC NP-PA, CpG PA, and CpG TMC NP-PA *via* three routes: subcutaneous (SC), intramuscular (IM), and intraperitoneal (IP) with a prime dose and two booster doses with an interval of 7 and 15 days, respectively. The mice were bled on 28th and 42nd day, and sera samples were collected from all mice. Serial dilutions of sera from each group were analyzed for anti-PA IgG2a titer for **(A)** SC route, **(B)** IM route, and **(C)** IP route. Statistically significant differences between the groups are highlighted (* for *P*-value <0.05, ** for *P*-values <0.01, *** for *P*-values <0.001, and **** for *P*-values <0.0001).

The preparation of TMC and its nanoparticles, its subsequent characterization of physicochemical properties, and *in vitro* release kinetics was studied before performing the murine studies. The synthesis of TMC polymer followed an intermediate step of formation of dimethyl chitosan. This method was adapted to avoid the O-methylation of the chain and chain scission which occurs commonly due to prolonged harsh conditions during the preparation of TMC. A DQ of >30% and lower extent of O-methylation enhances the water solubility of TMC. This property of TMC was leveraged for the preparation of PA-loaded TMC nanoparticles at pH 7 in HEPES buffer (17, 44). The TPP-based ionic gelation method follows the principle of complexation of oppositely charged molecules (protonated amine of TMC and TPP anion), resulting in the formation of nanoparticles (19, 47, 48). Unlike the widely used methods utilizing organic solvents and high temperature, the ionic gelation method is very mild, and thus we did not observe any degradation products in the SDS PAGE analysis (49–51).

The average size of PA-loaded TMC nanoparticles (254 nm) was found to be suitable for an efficient uptake by APCs. As the TMC nanoparticles were positively charged at physiological pH, an electrostatic interaction with the negatively charged cell membrane is highly likely. This is in alignment with a previously reported study where insulin, ovalbumin (OVA), and tetanus toxoid-based chitosan nanoparticles were shown to have a similar particle size, charge distribution (47, 52–54). In terms of the release kinetics of protein, the observed pattern of an initial burst release followed by a controlled release is also supported by other studies (52, 53). Thus, the *in vitro* antigen release study confirms the long-term antigen-releasing capacity of PA-TMCs without any protein degradation post-encapsulation.

After successful preparation and characterization of TMC nanoparticles, mice studies were conducted. Although the nasal route has been extensively explored for TMC nanoparticle-based immunization (19, 23, 47, 52, 55), we did not achieve a satisfactory immune response modulation. This could potentially be attributed to the large size of TMC-PA nanoparticles and subsequently its poor diffusion across the epithelial layer covering nasal-associated lymphoid tissue. In a similar instance, Boonyo et al. and Hagenaars et al. reported a subdued intranasal immune response for an OVA and HI-loaded TMC nanoparticle system (52, 55). Thus, the SC, IM, and IP routes were subsequently pursued for immunization.

The results of our study, as evident from **Figures 2–6**, demonstrated an effective immune response for TMC nanoparticles by all three routes (SC, IM, and IP). The striking results were that the TMC-PA groups *via* all routes were able to produce a sufficient amount of anti-PA titer as well as provided nearly 60–70%

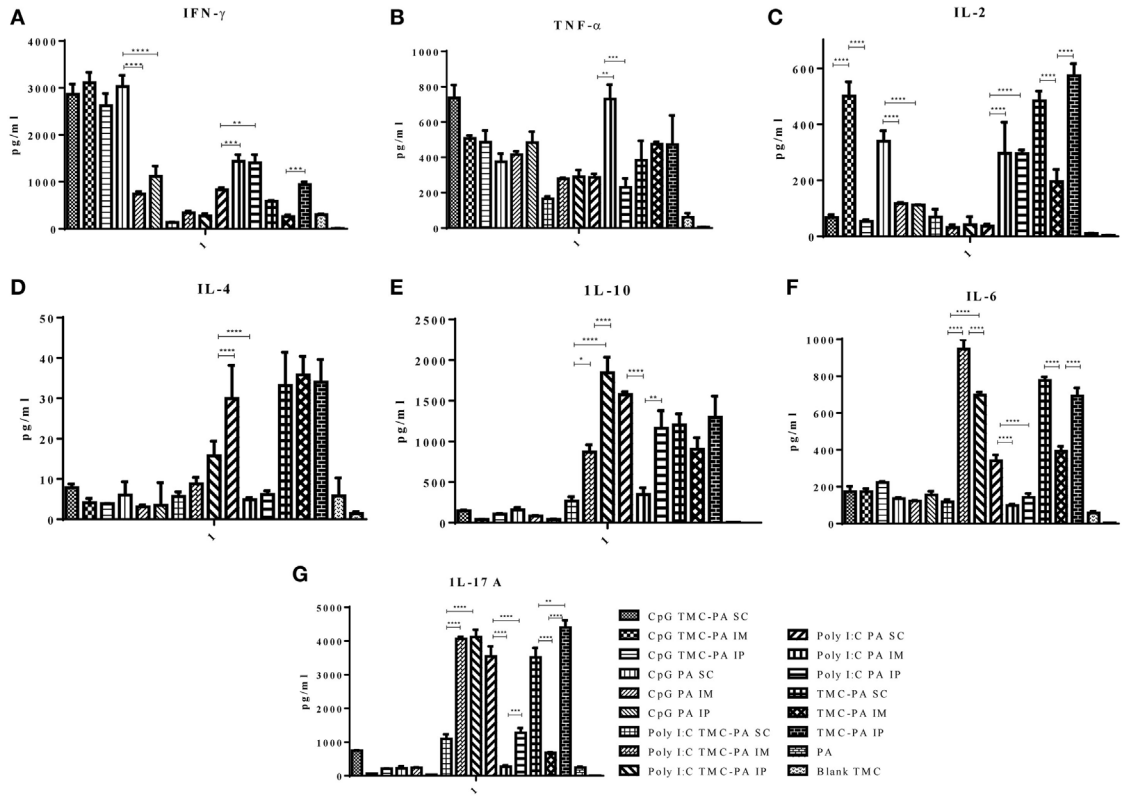

FIGURE 5 | Cytokine levels. Female Balb/c mice (6–8 weeks of age; $n = 21$) were immunized with 1× PBS, PA, Trimethyl-chitosan (TMC) NP-protective antigen (PA), Poly IC PA, Poly I:C TMC NP-PA, CpG PA, and CpG TMC NP-PA *via* three routes: subcutaneous (SC), intramuscular (IM), and intraperitoneal (IP) with a prime dose and two booster doses with an interval of 7 and 15 days, respectively. 42 days after the primary immunization, mice ($n = 3$) from each group were sacrificed, and their spleen single cell suspension was used for **(A)** IFN-γ, **(B)** TNF-α, **(C)** IL-2, **(D)** IL-4, **(E)** IL-10, **(F)** IL-6, and **(G)** IL-17A cytokines analysis. Statistically significant differences between the groups are highlighted (* for *P*-value <0.05, ** for *P*-values <0.01, *** for *P*-values <0.001, and **** for *P*-values <0.0001).

protection in anthrax challenged mice. More interestingly, the adjuvants CpG and Poly I:C behaved synergistically with TMC-PA in terms of generating an elevated anti-PA antibody titer and survival efficacy of nearly 70–80%. However, SC route was found be more effective in generating the highest IgG titer. Such response could be attributed to longer persistence, slower clearance, and prolonged antigen presentation after SC administration (56). Consequently, we could relate to the large number of vaccines, which are currently being administered *via* SC route like mumps, rubella, yellow fever, Japanese encephalitis, measles, Haemophilus influenza type b, inactivated polio vaccine, and *S. pneumonia* (25, 56).

In line with the previously reported studies, the TMC-PA group generated a Th2-biased immune response (25, 34). On the other hand, Poly I:C and CpG are reportedly Th1 biasing adjuvants (57–60). CpG alone has been reported to establish a Th1-biased immune response with several antigens (61–63). In this study, Poly I:C administration modulated the immune response toward Th1 with PA and TMC-PA nanoparticles. Supporting the earlier evidence, the CpG PA groups generated a Th1 response *via* all the three routes. Despite the fact that the PA is a Th2 biased antigen and TMC is also a Th2 biased adjuvant, the CpG adjuvated TMC-PA-treated groups also generated a dominant Th1 response *via* all the three routes. This observation is supported by Slütter and Jiskoot (34), which reported that the TMC-CpG nanoparticles encapsulating OVA as an antigen generated a 10-fold higher Ig2a titer than the TMC-TPP nanoparticles encapsulating OVA, thus provoked a strong Th1 response. The same report also revealed that the antigen-stimulated splenocytes secreted elevated levels of IFN-γ. This was also observed in our study that the CpG PA and CpG adjuvated TMC-PA groups showed highest levels of IFN-γ. In another study by Wang et al., virus-like particles encapsulating CpG-gold nanoparticle conjugates elicited a strong IFN-γ secretion (64). Therefore, we conclude that CpG enhances the production of IFN-γ, upon adjuvanation with an antigen. However, the levels of IL-4 produced by the splenocytes were low for all the groups, but the TMC-PA group relatively secreted the highest IL-4 irrespective of the route of immunization. Although, the CD4+ and CD8+ T-cell count gives a clear indication about the Th1 or Th2 response, but in this study, we did not analyze these parameters. However, the cytokines levels do indicate the direction of biasness of the immune response.

IL-17 T-helper cells are well known to serve as a bridge between innate and acquired immunity. Upon sensing the cytokines in the mucosal sites, the memory effector subset of Th17 cells can transform into Th1 or Th2 phenotype. IL-17A is the hallmark cytokine of the proinflammatory Th cell subset of Th17. As evident from **Figure 5**, Poly I:C PA and Poly I:C TMC-PA groups generated

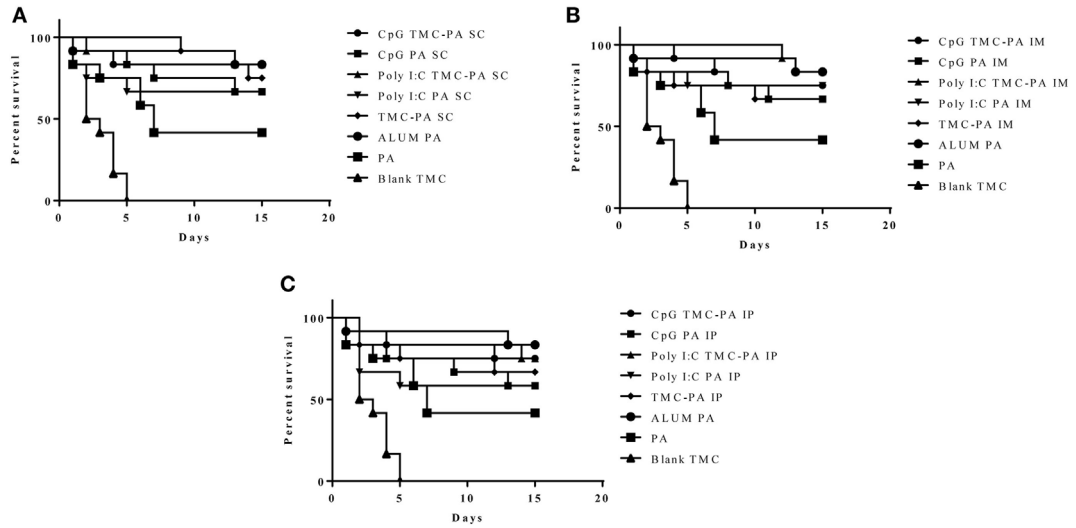

FIGURE 6 | Survival curve. Female Balb/c mice (6–8 weeks) were immunized with 1X PBS, Protective Antigen (PA), Trimethyl-chitosan (TMC) NP-PA, Poly IC PA, Poly I:C TMC NP-PA, CpG PA and CpG TMC NP-PA *via* three routes: **(A)** subcutaneous (SC), **(B)** intramuscular (IM), and **(C)** intraperitoneal (IP) with a prime dose and two booster doses with an interval of 7 and 15 days, respectively. At 43rd day, mice in each group ($n = 12$) were challenged with 0.5×10^3 spores of Ames strain of *Bacillus anthracis*. Mice were monitored for 15 days for death events in each group. Survival curve was plotted to compare the efficiency of protection in vaccinated mice groups over control placebo nanoparticle immunized mice group. As a control, 20 μg PA adsorbed on Alum (group named as ALUMN PA) was subcutaneously injected into a separate mice group ($n = 12$). The survival curve for anthrax spore challenge experiments was evaluated using Kaplan–Meier survival estimates (GraphPad Prism, La Jolla, CA, USA).

high levels of IL-17A. The TMC-PA group also secreted high levels of IL-17A, except the IM route. In a study by Holm et al., Poly I:C was reported to stimulate the production of IL-17A and IL-21 directly and consequently, drive the human naïve CD4+ T-cells differentiation, whereas CpG did not affect IL-17A on either mRNA or protein level (65). Similarly, Vultaggio et al. reported a positive correlation between Poly I:C and 1L-17A production (66). The chitin-based adjuvants have also been reported to be an immune response modulator (67) with a size-dependent response on macrophage IL-17A production (28). Thus, the growing scientific evidence indicates that TMC plays a role in stimulating IL-17A production. However, the mechanism of action remains unclear and need further exploration.

CpG and Poly I:C are PAMP-based adjuvants and act by initiating a cascade of innate immune system stimulation by interacting with TLR-3 and TLR-9, respectively. However, the immune modulation mechanism behind TMC nanoparticles remains elusive. We hypothesize that this immune-modulated response is due to the positively charged TMC nanoparticles, which might act as "danger signal" for dendritic cells.

In conclusion, the PA-loaded TMC nanoparticles as well as CpG and Poly I:C adjuvanted TMC-PA formulations elicited strong IgG antibody response *via* SC, IM, and IP routes in mice. However, the SC route showed the strongest response for IgG titer and survival efficacy. The TMC nanoparticle formulations were able to protect the mice against anthrax challenge and were comparable in protective efficacy to alum. In our opinion, TMC-based formulations possess a great potential as a vaccine candidate against anthrax, and further studies are needed to explore its adjuvant mechanisms.

ETHICS STATEMENT

All mice experiments were performed in compliance with Institutional Animal Ethics Committee (Jawaharlal Nehru University) and Council for the Purpose of Control and Supervision of Experiments on Animals (CPCSEA, Ministry of Social Justice and Empowerment, Government of India). Mice were housed in the individually ventilated animal caging system.

AUTHOR CONTRIBUTIONS

Experiments conceptualized and designed by AM. Performed by AM, MG, and RM. Data analysis by AM. Wrote the article: AM, HG, and RB. Supervised by RB.

ACKNOWLEDGMENTS

We would like to thank all the members of the laboratory for thoughtful and lively discussions during this work. The author AM would like to thank Council of Scientific and Industrial Research (CSIR), India, Department of Biotechnology (DBT), India, and JC Bose fellowship for providing financial support during this research term.

SUPPLEMENTARY MATERIAL

The Supplementary Material for this article can be found online at https://www.frontiersin.org/articles/10.3389/fimmu.2018.00562/full#supplementary-material.

REFERENCES

1. Turnbull PC; World Health Organization. *Guidelines for the Surveillance and Control of Anthrax in Humans and Animals*. Geneva, Switzerland: World Health Organization, Department of Communicable Diseases Surveillance and Response (1998).
2. Kamal S, Rashid AM, Bakar M, Ahad M. Anthrax: an update. *Asian Pac J Trop Biomed* (2011) 1(6):496–501. doi:10.1016/S2221-1691(11)60109-3
3. Jernigan DB, Raghunathan PL, Bell BP, Brechner R, Bresnitz EA, Butler JC, et al. Investigation of bioterrorism-related anthrax, United States, 2001: epidemiologic findings. *Emerg Infect Dis* (2002) 8(10):1019. doi:10.3201/eid0810.020353
4. Plotkin S, Grabenstein JD. Countering anthrax: vaccines and immunoglobulins. *Clin Infect Dis* (2008) 46(1):129–36. doi:10.1086/523578
5. Taft SC, Weiss AA. Neutralizing activity of vaccine-induced antibodies to two *Bacillus anthracis* toxin components, lethal factor and edema factor. *Clin Vaccine Immunol* (2008) 15(1):71–5. doi:10.1128/CVI.00321-07
6. Strom BL, Durch JS, Zwanziger LL, Joellenbeck LM. *The Anthrax Vaccine: Is It Safe? Does It Work?* Washington, DC: National Academies Press (2002).
7. Friedlander AM, Welkos S, Ivins B. Anthrax vaccines. In: Koehler T, editor. *Anthrax*. Frederick, MD: Springer (2002). p. 33–60.
8. Brossier F, Mock M. Toxins of *Bacillus anthracis*. *Toxicon* (2001) 39(11): 1747–55. doi:10.1016/S0041-0101(01)00161-1
9. Liu S, Moayeri M, Leppla SH. Anthrax lethal and edema toxins in anthrax pathogenesis. *Trends Microbiol* (2014) 22(6):317–25. doi:10.1016/j.tim.2014.02.012
10. Mikszta JA, Sullivan VJ, Dean C, Waterston AM, Alarcon JB, Dekker JP III, et al. Protective immunization against inhalational anthrax: a comparison of minimally invasive delivery platforms. *J Infect Dis* (2005) 191(2):278–88. doi:10.1086/426865
11. Irvine DJ, Swartz MA, Szeto GL. Engineering synthetic vaccines using cues from natural immunity. *Nat Mater* (2013) 12(11):978–90. doi:10.1038/nmat3775
12. Gregory AE, Titball R, Williamson D. Vaccine delivery using nanoparticles. *Front Cell Infect Microbiol* (2013) 3:13. doi:10.3389/fcimb.2013.00013
13. Peek LJ, Middaugh CR, Berkland C. Nanotechnology in vaccine delivery. *Adv Drug Deliv Rev* (2008) 60(8):915–28. doi:10.1016/j.addr.2007.05.017
14. Amidi M, Mastrobattista E, Jiskoot W, Hennink WE. Chitosan-based delivery systems for protein therapeutics and antigens. *Adv Drug Deliv Rev* (2010) 62(1):59–82. doi:10.1016/j.addr.2009.11.009
15. Danhier F, Ansorena E, Silva JM, Coco R, Le Breton A, Préat V. PLGA-based nanoparticles: an overview of biomedical applications. *J Control Release* (2012) 161(2):505–22. doi:10.1016/j.jconrel.2012.01.043
16. Verheul RJ, Amidi M, van Steenbergen MJ, van Riet E, Jiskoot W, Hennink WE. Influence of the degree of acetylation on the enzymatic degradation and in vitro biological properties of trimethylated chitosans. *Biomaterials* (2009) 30(18):3129–35. doi:10.1016/j.biomaterials.2009.03.013
17. Verheul RJ, Amidi M, van der Wal S, van Riet E, Jiskoot W, Hennink WE. Synthesis, characterization and in vitro biological properties of O-methyl free N, N, N-trimethylated chitosan. *Biomaterials* (2008) 29(27):3642–9. doi:10.1016/j.biomaterials.2008.05.026
18. Hagenaars N, Mania M, de Jong P, Que I, Nieuwland R, Slütter B, et al. Role of trimethylated chitosan (TMC) in nasal residence time, local distribution and toxicity of an intranasal influenza vaccine. *J Control Release* (2010) 144(1):17–24. doi:10.1016/j.jconrel.2010.01.027
19. Amidi M, Romeijn SG, Verhoef JC, Junginger HE, Bungener L, Huckriede A, et al. N-trimethyl chitosan (TMC) nanoparticles loaded with influenza subunit antigen for intranasal vaccination: biological properties and immunogenicity in a mouse model. *Vaccine* (2007) 25(1):144–53. doi:10.1016/j.vaccine.2006.06.086
20. Verheul RJ, Hagenaars N, van Es T, van Gaal EV, de Jong PH, Bruijns S, et al. A step-by-step approach to study the influence of N-acetylation on the adjuvanticity of N, N, N-trimethyl chitosan (TMC) in an intranasal nanoparticulate influenza virus vaccine. *Eur J Pharm Sci* (2012) 45(4):467–74. doi:10.1016/j.ejps.2011.10.001
21. Tafaghodi M, Saluja V, Kersten GF, Kraan H, Slütter B, Amorij J-P, et al. Hepatitis B surface antigen nanoparticles coated with chitosan and trimethyl chitosan: impact of formulation on physicochemical and immunological characteristics. *Vaccine* (2012) 30(36):5341–8. doi:10.1016/j.vaccine.2012.06.035
22. Slütter B, Plapied L, Fievez V, Sande MA, des Rieux A, Schneider Y-J, et al. Mechanistic study of the adjuvant effect of biodegradable nanoparticles in mucosal vaccination. *J Control Release* (2009) 138(2):113–21. doi:10.1016/j.jconrel.2009.05.011
23. Bal SM, Slütter B, Verheul R, Bouwstra JA, Jiskoot W. Adjuvanted, antigen loaded N-trimethyl chitosan nanoparticles for nasal and intradermal vaccination: adjuvant-and site-dependent immunogenicity in mice. *Eur J Pharm Sci* (2012) 45(4):475–81. doi:10.1016/j.ejps.2011.10.003
24. Hagenaars N, Verheul RJ, Mooren I, de Jong PH, Mastrobattista E, Glansbeek HL, et al. Relationship between structure and adjuvanticity of N, N, N-trimethyl chitosan (TMC) structural variants in a nasal influenza vaccine. *J Control Release* (2009) 140(2):126–33. doi:10.1016/j.jconrel.2009.08.018
25. Bal SM, Slütter B, van Riet E, Kruithof AC, Ding Z, Kersten GF, et al. Efficient induction of immune responses through intradermal vaccination with N-trimethyl chitosan containing antigen formulations. *J Control Release* (2010) 142(3):374–83. doi:10.1016/j.jconrel.2009.11.018
26. Slütter B, Soema PC, Ding Z, Verheul R, Hennink W, Jiskoot W. Conjugation of ovalbumin to trimethyl chitosan improves immunogenicity of the antigen. *J Control Release* (2010) 143(2):207–14. doi:10.1016/j.jconrel.2010.01.007
27. Da Silva CA, Chalouni C, Williams A, Hartl D, Lee CG, Elias JA. Chitin is a size-dependent regulator of macrophage TNF and IL-10 production. *The J Immunol* (2009) 182(6):3573–82. doi:10.4049/jimmunol.0802113
28. Da Silva CA, Hartl D, Liu W, Lee CG, Elias JA. TLR-2 and IL-17A in chitin-induced macrophage activation and acute inflammation. *J Immunol* (2008) 181(6):4279–86. doi:10.4049/jimmunol.181.6.4279
29. Tomljenovic L, Shaw CA. Aluminum vaccine adjuvants: are they safe? *Curr Med Chem* (2011) 18(17):2630–7. doi:10.2174/092986711795933740
30. Petrovsky N, Aguilar JC. Vaccine adjuvants: current state and future trends. *Immunol Cell Biol* (2004) 82(5):488–96. doi:10.1111/j.0818-9641.2004.01272.x
31. Lindblad EB. Aluminium compounds for use in vaccines. *Immunol Cell Biol* (2004) 82(5):497–505. doi:10.1111/j.0818-9641.2004.01286.x
32. Kachura MA, Hickle C, Kell SA, Sathe A, Calacsan C, Kiwan R, et al. A CpG-Ficoll nanoparticle adjuvant for anthrax protective antigen enhances immunogenicity and provides single-immunization protection against inhaled anthrax in monkeys. *J Immunol* (2016) 196(1):284–97. doi:10.4049/jimmunol.1501903
33. Sloat BR, Cui Z. Nasal immunization with anthrax protective antigen protein adjuvanted with polyriboinosinic–polyribocytidylic acid induced strong mucosal and systemic immunities. *Pharm Res* (2006) 23(6):1217–26. doi:10.1007/s11095-005-9078-7
34. Slütter B, Jiskoot W. Dual role of CpG as immune modulator and physical crosslinker in ovalbumin loaded N-trimethyl chitosan (TMC) nanoparticles for nasal vaccination. *J Control Release* (2010) 148(1):117–21. doi:10.1016/j.jconrel.2010.06.009
35. Friede M, Aguado M. Need for new vaccine formulations and potential of particulate antigen and DNA delivery systems. *Adv Drug Deliv Rev* (2005) 57(3):325–31. doi:10.1016/j.addr.2004.10.001
36. Bardel E, Doucet-Ladeveze R, Mathieu C, Harandi AM, Dubois B, Kaiserlian D. Intradermal immunisation using the TLR3-ligand poly (I: C) as adjuvant induces mucosal antibody responses and protects against genital HSV-2 infection. *npj Vaccines* (2016) 1:16010.
37. Alexopoulou L, Holt AC, Medzhitov R, Flavell RA. Recognition of double-stranded RNA and activation of NF-κB by Toll-like receptor 3. *Nature* (2001) 413(6857):732–8. doi:10.1038/35099560
38. Gelman AE, Zhang J, Choi Y, Turka LA. Toll-like receptor ligands directly promote activated CD4+ T cell survival. *J Immunol* (2004) 172(10):6065–73. doi:10.4049/jimmunol.172.10.6065
39. Salem ML, Kadima AN, Cole DJ, Gillanders WE. Defining the antigen-specific T-cell response to vaccination and poly (I: C)/TLR3 signaling: evidence of enhanced primary and memory CD8 T-cell responses and antitumor immunity. *J Immunother* (2005) 28(3):220–8. doi:10.1097/01.cji.0000156828.75196.0d
40. Wei H, Tan K, Sun R, Yin L, Zhang J, Pu Y. Aberrant production of Th1/Th2/Th17-related cytokines in serum of C57BL/6 mice after short-term formaldehyde exposure. *Int J Environ Res Public Health* (2014) 11(10):10036–50. doi:10.3390/ijerph111010036
41. Hoyer KK, Dooms H, Barron L, Abbas AK. Interleukin-2 in the development and control of inflammatory disease. *Immunol Rev* (2008) 226(1):19–28. doi:10.1111/j.1600-065X.2008.00697.x

42. Hofmann SR, Ettinger R, Zhou Y-J, Gadina M, Lipsky P, Siegel R, et al. Cytokines and their role in lymphoid development, differentiation and homeostasis. *Curr Opin Allergy Clin Immunol* (2002) 2(6):495–506. doi:10.1097/00130832-200212000-00004
43. Jones SA. Directing transition from innate to acquired immunity: defining a role for IL-6. *J Immunol* (2005) 175(6):3463–8. doi:10.4049/jimmunol.175.6.3463
44. Muzzarelli RA, Tanfani F. The N-permethylation of chitosan and the preparation of N-trimethyl chitosan iodide. *Carbohydr Polym* (1985) 5(4):297–307. doi:10.1016/0144-8617(85)90037-2
45. Slütter B, Bal S, Keijzer C, Mallants R, Hagenaars N, Que I, et al. Nasal vaccination with N-trimethyl chitosan and PLGA based nanoparticles: nanoparticle characteristics determine quality and strength of the antibody response in mice against the encapsulated antigen. *Vaccine* (2010) 28(38):6282–91. doi:10.1016/j.vaccine.2010.06.121
46. Manish M, Rahi A, Kaur M, Bhatnagar R, Singh S. A single-dose PLGA encapsulated protective antigen domain 4 nanoformulation protects mice against *Bacillus anthracis* spore challenge. *PLoS One* (2013) 8(4):e61885. doi:10.1371/journal.pone.0061885
47. Amidi M, Romeijn SG, Borchard G, Junginger HE, Hennink WE, Jiskoot W. Preparation and characterization of protein-loaded N-trimethyl chitosan nanoparticles as nasal delivery system. *J Control Release* (2006) 111(1):107–16. doi:10.1016/j.jconrel.2005.11.014
48. Vila A, Sánchez A, Janes K, Behrens I, Kissel T, Jato JLV, et al. Low molecular weight chitosan nanoparticles as new carriers for nasal vaccine delivery in mice. *Eur J Pharm Biopharm* (2004) 57(1):123–31. doi:10.1016/j.ejpb.2003.09.006
49. Xu Y, Du Y, Huang R, Gao L. Preparation and modification of N-(2-hydroxyl) propyl-3-trimethyl ammonium chitosan chloride nanoparticle as a protein carrier. *Biomaterials* (2003) 24(27):5015–22. doi:10.1016/S0142-9612(03)00408-3
50. Calvo P, Remuñan-López C, Vila-Jato JL, Alonso MJ. Chitosan and chitosan/ethylene oxide-propylene oxide block copolymer nanoparticles as novel carriers for proteins and vaccines. *Pharm Res* (1997) 14(10):1431–6. doi:10.1023/A:1012128907225
51. Mao S, Bakowsky U, Jintapattanakit A, Kissel T. Self-assembled polyelectrolyte nanocomplexes between chitosan derivatives and insulin. *J Pharm Sci* (2006) 95(5):1035–48. doi:10.1002/jps.20520
52. Boonyo W, Junginger HE, Waranuch N, Polnok A, Pitaksuteepong T. Chitosan and trimethyl chitosan chloride (TMC) as adjuvants for inducing immune responses to ovalbumin in mice following nasal administration. *J Control Release* (2007) 121(3):168–75. doi:10.1016/j.jconrel.2007.05.025
53. Siddhapura K, Harde H, Jain S. Immunostimulatory effect of tetanus toxoid loaded chitosan nanoparticles following microneedles assisted immunization. *Nanomedicine* (2016) 12(1):213–22. doi:10.1016/j.nano.2015.10.009
54. Mukhopadhyay P, Mishra R, Rana D, Kundu PP. Strategies for effective oral insulin delivery with modified chitosan nanoparticles: a review. *Prog Polym Sci* (2012) 37(11):1457–75. doi:10.1016/j.progpolymsci.2012.04.004
55. Hagenaars N, Mastrobattista E, Verheul RJ, Mooren I, Glansbeek HL, Heldens JG, et al. Physicochemical and immunological characterization of N, N, N-trimethyl chitosan-coated whole inactivated influenza virus vaccine for intranasal administration. *Pharm Res* (2009) 26(6):1353–64. doi:10.1007/s11095-009-9845-y
56. Hickling J, Jones K, Friede M, Zehrung D, Chen D, Kristensen D. Intradermal delivery of vaccines: potential benefits and current challenges. *Bull World Health Organ* (2011) 89(3):221–6. doi:10.2471/BLT.10.079426
57. Jin B, Wang RY, Qiu Q, Sugauchi F, Grandinetti T, Alter HJ, et al. Induction of potent cellular immune response in mice by hepatitis C virus NS3 protein with double-stranded RNA. *Immunology* (2007) 122(1):15–27. doi:10.1111/j.1365-2567.2007.02607.x
58. Salaun B, Greutert M, Romero P. Toll-like receptor 3 is necessary for dsRNA adjuvant effects. *Vaccine* (2009) 27(12):1841–7. doi:10.1016/j.vaccine.2009.01.044
59. Trumpfheller C, Caskey M, Nchinda G, Longhi MP, Mizenina O, Huang Y, et al. The microbial mimic poly IC induces durable and protective CD4+ T cell immunity together with a dendritic cell targeted vaccine. *Proc Natl Acad Sci U S A* (2008) 105(7):2574–9. doi:10.1073/pnas.0711976105
60. Navabi H, Jasani B, Reece A, Clayton A, Tabi Z, Donninger C, et al. A clinical grade poly I: C-analogue (Ampligen®) promotes optimal DC maturation and Th1-type T cell responses of healthy donors and cancer patients in vitro. *Vaccine* (2009) 27(1):107–15. doi:10.1016/j.vaccine.2008.10.024
61. Weeratna RD, Brazolot Millan CL, McCluskie MJ, Davis HL. CpG ODN can re-direct the Th bias of established Th2 immune responses in adult and young mice. *FEMS Immunol Med Microbiol* (2001) 32(1):65–71. doi:10.1111/j.1574-695X.2001.tb00535.x
62. Millan CLB, Weeratna R, Krieg AM, Siegrist C-A, Davis HL. CpG DNA can induce strong Th1 humoral and cell-mediated immune responses against hepatitis B surface antigen in young mice. *Proc Natl Acad Sci U S A* (1998) 95(26):15553–8. doi:10.1073/pnas.95.26.15553
63. Chu RS, Targoni OS, Krieg AM, Lehmann PV, Harding CV. CpG oligodeoxynucleotides act as adjuvants that switch on T helper 1 (Th1) immunity. *J Exp Med* (1997) 186(10):1623–31. doi:10.1084/jem.186.10.1623
64. Wang Y, Wang Y, Kang N, Liu Y, Shan W, Bi S, et al. Construction and immunological evaluation of CpG-Au@ HBc virus-like nanoparticles as a potential vaccine. *Nanoscale Res Lett* (2016) 11(1):1–9. doi:10.1186/s11671-016-1554-y
65. Holm CK, Petersen CC, Hvid M, Petersen L, Paludan SR, Deleuran B, et al. TLR3 ligand polyinosinic: polycytidylic acid induces IL-17A and IL-21 synthesis in human Th cells. *J Immunol* (2009) 183(7):4422–31. doi:10.4049/jimmunol.0804318
66. Vultaggio A, Nencini F, Pratesi S, Petroni G, Romagnani S, Maggi E. Poly (I: C) promotes the production of IL-17A by murine CD1d-driven invariant NKT cells in airway inflammation. *Allergy* (2012) 67(10):1223–32. doi:10.1111/j.1398-9995.2012.02876.x
67. Da Silva CA, Pochard P, Lee CG, Elias JA. Chitin particles are multifaceted immune adjuvants. *Am J Respir Crit Care Med* (2010) 182(12):1482–91. doi:10.1164/rccm.200912-1877OC

Conflict of Interest Statement: The authors declare that the research was conducted in the absence of any commercial or financial relationships that could be construed as a potential conflict of interest.

frontiers in Immunology

ORIGINAL RESEARCH
published: 18 April 2018
doi: 10.3389/fimmu.2018.00783

Carbonate Apatite Nanoparticles Act as Potent Vaccine Adjuvant Delivery Vehicles by Enhancing Cytokine Production Induced by Encapsulated Cytosine-Phosphate-Guanine Oligodeoxynucleotides

*Hideki Takahashi[1], Kazuki Misato[1], Taiki Aoshi[2,3], Yasuyuki Yamamoto[4], Yui Kubota[5], Xin Wu[5], Etsushi Kuroda[6,7], Ken J. Ishii[6,7], Hirofumi Yamamoto[5] and Yasuo Yoshioka[1,4,8,9]**

[1] Vaccine Creation Project, BIKEN Innovative Vaccine Research Alliance Laboratories, Research Institute for Microbial Diseases, Osaka University, Suita, Japan, [2] Vaccine Dynamics Project, BIKEN Innovative Vaccine Research Alliance Laboratories, Research Institute for Microbial Diseases, Osaka University, Suita, Japan, [3] Vaccine Dynamics Project, BIKEN Center for Innovative Vaccine Research and Development, The Research Foundation for Microbial Diseases of Osaka University, Suita, Japan, [4] Vaccine Creation Project, BIKEN Center for Innovative Vaccine Research and Development, The Research Foundation for Microbial Diseases of Osaka University, Suita, Japan, [5] Division of Health Sciences, Department of Molecular Pathology, Graduate School of Medicine, Osaka University, Suita, Japan, [6] Laboratory of Adjuvant Innovation, Center for Vaccine and Adjuvant Research, National Institutes of Biomedical Innovation, Health and Nutrition, Ibaraki, Japan, [7] Laboratory of Vaccine Science, WPI Immunology Frontier Research Center, Osaka University, Suita, Japan, [8] Laboratory of Nano-Design for Innovative Drug Development, Graduate School of Pharmaceutical Sciences, Osaka University, Suita, Japan, [9] Global Center for Medical Engineering and Informatics, Osaka University, Suita, Japan

OPEN ACCESS

Edited by:
Rajko Reljic,
St George's, University of London, United Kingdom

Reviewed by:
Sylvie Fournel,
Université de Strasbourg, France
Michael Schotsaert,
Icahn School of Medicine at Mount Sinai, United States

***Correspondence:**
Yasuo Yoshioka
y-yoshioka@biken.osaka-u.ac.jp

Specialty section:
This article was submitted to Vaccines and Molecular Therapeutics, a section of the journal Frontiers in Immunology

Received: 28 December 2017
Accepted: 28 March 2018
Published: 18 April 2018

Citation:
Takahashi H, Misato K, Aoshi T, Yamamoto Y, Kubota Y, Wu X, Kuroda E, Ishii KJ, Yamamoto H and Yoshioka Y (2018) Carbonate Apatite Nanoparticles Act as Potent Vaccine Adjuvant Delivery Vehicles by Enhancing Cytokine Production Induced by Encapsulated Cytosine-Phosphate-Guanine Oligodeoxynucleotides. Front. Immunol. 9:783. doi: 10.3389/fimmu.2018.00783

Vaccine adjuvants that can induce not only antigen-specific antibody responses but also Th1-type immune responses and $CD8^+$ cytotoxic T lymphocyte responses are needed for the development of vaccines against infectious diseases and cancer. Of many available adjuvants, oligodeoxynucleotides (ODNs) with unmethylated cytosine-phosphate-guanine (CpG) motifs are the most promising for inducing the necessary immune responses, and these adjuvants are currently under clinical trials in humans. However, the development of novel delivery vehicles that enhance the adjuvant effects of CpG ODNs, subsequently increasing the production of cytokines such as type-I interferons (IFNs), is highly desirable. In this study, we demonstrate the potential of pH-responsive biodegradable carbonate apatite (CA) nanoparticles as CpG ODN delivery vehicles that can enhance the production of type-I IFNs (such as IFN-α) relative to that induced by CpG ODNs and can augment the adjuvant effects of CpG ODNs *in vivo*. In contrast to CpG ODNs, CA nanoparticles containing CpG ODNs (designated CA-CpG) induced significant IFN-α production by mouse dendritic cells and human peripheral blood mononuclear cells *in vitro*; and production of interleukin-12, and IFN-γ was higher in CA-CpG-treated groups than in CpG ODNs groups. In addition, treatment with CA-CpG resulted in higher cytokine production in draining lymph nodes than did treatment with CpG ODNs *in vivo*. Furthermore, vaccination with CA-CpG plus an antigen, such as ovalbumin or influenza virus hemagglutinin, resulted in higher antigen-specific antibody

responses and CD8+ cytotoxic T lymphocyte responses *in vivo*, in an interleukin-12- and type-I IFN-dependent manner, than did vaccination with the antigen plus CpG ODNs; in addition, the efficacy of the vaccine against influenza virus was higher with CA-CpG as the adjuvant than with CpG ODNs as the adjuvant. These data show the potential of CA nanoparticles to serve as CpG ODN delivery vehicles that increase the production of cytokines, especially IFN-α, induced by CpG ODNs and thus augment the efficacy of CpG ODNs as adjuvants. We expect that the strategy reported herein will facilitate the design and development of novel adjuvant delivery vehicles for vaccines.

Keywords: adjuvant, cytosine-phosphate-guanine oligodeoxynucleotide, influenza virus, interferon-α, nanoparticle, vaccine

INTRODUCTION

As the recent Ebola virus outbreak and past worldwide influenza pandemics have demonstrated, infectious diseases are a serious global health problem (1). Vaccines are the most efficient way to prevent infectious diseases, and as a result of immunological innovations such as the development of checkpoint inhibitors, vaccines are also expected to be effective against cancer in the coming years (2).

There are various types of vaccines, including attenuated live vaccines, inactivated whole vaccines, and protein- or peptide-based subunit vaccines (3–5), and they all have various advantages and disadvantages. For example, although attenuated live vaccines can generate strong adaptive immunity, the pathogens in these vaccines have the potential to cause infectious disease in rare cases, especially in individuals with compromised immune systems (3–5). In contrast, protein- or peptide-based subunit vaccines are much safer than attenuated live vaccines and inactivated whole vaccines; however, when used alone, subunit vaccines evoke only weak adaptive immunity. The efficacy of subunit vaccines can be improved by using adjuvants (6). Aluminum salts (alum) are the most widely used adjuvants and are present in many important vaccines, including the diphtheria–tetanus–pertussis-inactivated poliomyelitis vaccine, the pneumococcal conjugate vaccine, and hepatitis B vaccine in humans (7). Unfortunately, although alum induces strong Th2-type immune responses, it cannot induce Th1-type immune responses or CD8+ cytotoxic T lymphocyte (CTL) responses, which are necessary for vaccines against infectious diseases such as influenza virus, hepatitis C, and malaria as well as for cancer vaccines designed to eliminate infected or malignant cells (8). Therefore, the development of adjuvants that can induce Th1-type immune responses and CD8+ CTL responses is necessary.

Oligodeoxynucleotides (ODNs) with unmethylated cytosine-phosphate-guanine (CpG) motifs, which act as Toll-like receptor 9 (TLR9) agonists, are among the most effective adjuvants for inducing Th1-type immune responses and CD8+ CTL responses (9). CpG ODNs, which are short single-stranded synthetic DNA fragments containing immunostimulatory CpG motifs, bind to TLR9 at endosomes after being taken up by B cells and dendritic cells (DCs). This binding initiates an innate immune response characterized by the production of cytokines that can promote Th1-type immune responses. Therefore, CpG ODNs are expected to be useful as vaccine adjuvants and immunotherapeutic agents against infectious diseases and cancer (9). In fact, in Phase II clinical trials, a hepatitis B vaccine with CpG ODNs as an adjuvant has demonstrated superiority to a currently licensed hepatitis B virus vaccine with alum as an adjuvant (10, 11). There are at least four types of CpG ODNs, each of which has a different structure and different physical and immunostimulatory properties (9). Of the various types, D-type CpG ODNs (also known as A-type CpG ODNs) and K-type CpG ODNs (also known as B-type CpG ODNs) are the major types for experimental and clinical uses. D-type CpG ODNs can induce plasmacytoid DCs to produce massive amounts of type-I interferons (IFNs) such as IFN-α. IFN-α is important for the activation and cytotoxicity of natural killer T cells (12), for CD8+ T-cell activation (13), and for the maturation of DCs, thus indicating the importance of adjuvants that can induce IFN-α production. D-type CpG ODNs self-assemble into multimers because of their palindromic and poly-G sequences, and these multimers are important for IFN-α induction (14). However, uncontrollable aggregation hinders the clinical utility of D-type CpG ODNs. In contrast, K-type CpG ODNs can activate the production of interleukin (IL)-6 by B cells and DCs but only weakly induce IFN-α production by plasmacytoid DCs. These differences in cytokine production between D-type and K-type CpG ODNs are thought to be the reason for their different adjuvant effects in the treatment of some infectious diseases. For example, K-type CpG ODNs induce better antibody production and cytokine responses than D-type CpG ODNs when used in a malaria vaccine in cynomolgus monkeys (15), whereas D-type CpG ODNs elicit better immune responses than K-type CpG ODNs in a leishmania vaccine in rhesus monkeys (16). In addition, when used as a monotherapeutic for leishmaniasis, D-type CpG ODNs have better therapeutic effects than K-type CpG ODNs (17). Therefore, the design of CpG ODN-based adjuvants with the functions of both D-type and K-type CpG ODNs would be highly desirable.

Abbreviations: alum, aluminum salts; CA, carbonate apatite; CpG, cytosine-phosphate-guanine; CTL, cytotoxic T lymphocyte; DCs, dendritic cells; ELISA, enzyme-linked immunosorbent assays; FCS, fetal calf serum; HRP, Horseradish peroxidase; IFNs, interferons; Ifnar2, IFN-α/β receptor 2; IL, interleukin; ODNs, oligodeoxynucleotides; OVA, ovalbumin; PBMCs, peripheral blood mononuclear cells; SV, ether-treated hemagglutinin antigen-enriched virion-free split vaccine; TLR9, toll-like receptor 9.

To design such multifunctional CpG ODNs, researchers have tried to use multimerization to give K-type CpG ODNs the ability to induce IFN-α production. There are two main methods for multimerizing K-type CpG ODNs: the use of biological molecules and the use of synthetic particles. With regard to the former, several types of peptides (e.g., antimicrobial peptide LL37 and Tat peptide) and β-glucan have been used to enhance the ability of K-type CpG ODNs to induce IFN-α production and to increase their adjuvant activity both *in vitro* and *in vivo* (18–20). In contrast, only limited data are available on the use of synthetic particles to enhance the adjuvant activity of K-type CpG ODNs *in vivo* by giving them the ability to induce IFN-α production, although the encapsulation of K-type CpG ODNs in, or their conjugation with, various types of particles has been shown to enhance IFN-α production *in vitro* (14, 21, 22). Therefore, the development of novel particles that contain encapsulated K-type CpG ODNs and can induce IFN-α production would be useful and would facilitate investigations of the relationship between IFN-α production *in vitro* and vaccine effects *in vivo*.

Among the synthetic particles that have been studied to date, pH-sensitive carbonate apatite (CA) particles have been shown to serve as efficient intracellular delivery vehicles for small molecules, as well as for DNA, RNA, and proteins (23–25). For example, the DNA transfection efficiency of CA nanoparticles is 10–100 times that of a general transfection reagent, Lipofectamine, and calcium phosphate precipitation in mammalian cells *in vitro* (23). Furthermore, Yamamoto and colleagues recently developed CA nanoparticles of 10–20 nm diameters by modifying the process by which the nanoparticles were generated (26). Wu et al. reported a simple method for generating CA nanoparticles in which siRNA is encapsulated with high efficiency (26). The resulting CA nanoparticles are highly stable at pH 7.4 but quickly degrade in acidic environments such as endosomal compartments in cells. These siRNA-containing CA nanoparticles show dramatic antitumor effects after intravenous administration and are nontoxic in mice and monkeys (26). These facts suggest that CA nanoparticles have the potential to serve as CpG ODN delivery vehicles owing to their high encapsulation efficiency, low cost, biodegradability, safety, and biocompatibility.

In this study, we show the usefulness of CA nanoparticles as CpG ODN delivery vehicles that give K-type CpG ODNs the ability to induce IFN-α production. We found that CA nanoparticles containing K-type CpG ODNs (designated CA-CpG) showed stronger antigen-specific antibody responses and $CD8^+$ CTL responses than those of K-type CpG ODNs, and when mice were vaccinated with the nanoparticles in combination with an antigen, the preventive vaccine effects against influenza virus were better than those of the antigen plus K-type CpG ODNs. This is the first report of the use of pH-responsive biodegradable CA nanoparticles to improve the cytokine production pattern of K-type CpG ODNs and enhance their adjuvant activity.

MATERIALS AND METHODS

Reagents

K-type CpG ODNs (CpG K3: 5′-atcgactctcgagcgttctc-3′) and Alexa 488-labeled K-type CpG ODNs (Alexa 488-labeled CpG K3) were purchased from GeneDesign (Osaka, Japan). EndoGrade endotoxin-free ovalbumin (OVA) (<0.1 EU/mg protein) purchased from Hyglos GmbH (Bayern, Germany) was used for immunization. Grade V OVA purchased from Sigma-Aldrich (St. Louis, MO, USA) was used for enzyme-linked immunosorbent assays (ELISA). Horseradish peroxidase (HRP)-conjugated goat anti-mouse IgG and IgG1 antibodies were purchased from Merck Millipore (Darmstadt, Germany). HRP-conjugated goat anti-mouse IgG2c was purchased from GeneTex, Inc. (Irvine, CA, USA). Alhydrogel adjuvant 2% (alum) was purchased from InvivoGen (San Diego, CA, USA).

Mice

C57BL/6J mice were purchased from SLC (Kyoto, Japan). *IFN-α/β receptor 2 (Ifnar2)-Il-12 p40* double-deficient mice have been described previously (27) and were kindly provided by Dr. Ishii (National Institutes of Biomedical Innovation, Health and Nutrition, Ibaraki, Osaka, Japan). Mice were used at 7 to 8 weeks of age and were housed in a room with a 12-h-light/12-h-dark cycle (lights on at 8:00 am, lights off at 8:00 pm) with access to food and water. All animal experiments were performed in accordance with institutional guidelines of Osaka University for the ethical treatment of animals (protocol number H26-11-0).

Synthesis of CA Nanoparticles and CA-CpG

Carbonate apatite nanoparticles and CA-CpG were prepared as described previously (26). We incubated a 25 mL solution of $NaHCO_3$ (44 mM), NaH_2PO_4 (0.9 mM), and $CaCl_2$ (1.8 mM) (pH 7.5) without or with 1.9, 5.6, 16.7, 50, or 150 μg of K-type CpG ODNs at 37°C for 30 min. The solution was then centrifuged at 12,000 rpm for 3 min, and the pellet was dissolved in saline containing 0.5% mouse serum. The resulting solution of CA nanoparticles or CA-CpG was sonicated in a water bath for 10 min. For determination of the amount of endotoxin, the collected CA-CpG was dissolved in 1 mL of 0.02 M ethylenediaminetetraacetic acid and the amount of endotoxin was determined by means of a Toxicolor LS-50M kit (Seikagaku Corporation, Tokyo, Japan). CA-CpG was found to include <0.2 EU/mL of endotoxin.

Efficiency of K-Type CpG ODN Encapsulation Into CA Nanoparticles

For determination of the K-type CpG ODN encapsulation efficiency, the collected CA-CpG was dissolved in 1 mL of 0.02 M ethylenediaminetetraacetic acid and the amount of K-type CpG ODNs was determined with a Qubit ssDNA Assay Kit (Thermo Fisher Scientific, Waltham, MA, USA).

Properties of CA-CpG and CA Nanoparticles

The size distributions of CA nanoparticles and CA-CpG were analyzed with a Zetasizer Nano ZS (Malvern Instruments, Malvern, Worcestershire, UK). Specifically, the mean diameters and particle size distributions of the nanoparticles in mouse

serum albumin (Sigma-Aldrich) were measured by means of a dynamic light-scattering method using capillary cells. The size distributions of both types of nanoparticles were also analyzed by atomic force microscopy conducted with a scanning probe microscope (SPM-9500, Shimadzu, Kyoto, Japan) operated in dynamic mode and equipped with a microcantilever (OMCL-AC240TS-R3, Olympus, Tokyo, Japan).

Preparation and Stimulation of Mouse Bone Marrow-Derived DCs and Human Peripheral Blood Mononuclear Cells

To generate bone marrow-derived DCs, we isolated bone marrow cells from the femurs of C57BL/6J mice and cultured the cells for 7 days with 100 ng/mL human Flt-3L (PeproTech, Rocky Hill, NJ, USA). Cells were seeded at a density of 5×10^5 cells/well in a 96-well flat-bottom culture plate (Nunc, Roskilde, Denmark) and were cultured in complete RPMI medium (RPMI 1640 supplemented with 10 vol% fetal calf serum (FCS), penicillin, and streptomycin). These cells were stimulated with K-type CpG ODNs or CA-CpG for 24 h. Supernatants were subjected to ELISA to determine the levels of IFN-α (PBL Assay Science, Piscataway, NJ, USA), IFN-γ (BioLegend, San Diego, CA, USA), and IL-12 p40 (BD Biosciences, San Jose, CA, USA) according to the manufacturer's instructions. Human peripheral blood mononuclear cells (PBMCs) were obtained from two healthy adult male Japanese volunteers (26 years of age) with informed consent. After the PBMCs were prepared with Ficoll, they were plated at a concentration of 1×10^7 cells/mL in a 96-well flat-bottom culture plate and maintained in complete RPMI medium. They were stimulated with K-type CpG ODNs or CA-CpG for 24 h. Supernatants were subjected to ELISA to determine the levels of pan-IFN-α and IFN-γ according to the manufacturers' instructions. All experiments using human PBMCs were approved by the Institutional Review Board of the Research Institute for Microbial Diseases, Osaka University.

Cellular Uptake of CA-CpG and K-Type CpG ODNs

Mouse bone marrow-derived DCs (1×10^7 cells/mL in a 96-well flat-bottom culture plate) were treated with Alexa 488-labeled K-type CpG ODNs (1.25 μg CpG ODNs/mL) or CA nanoparticles containing Alexa 488-labeled K-type CpG ODNs (CA-Alexa 488-CpG; 1.25 μg CpG ODNs/mL) for 10, 30, 90, 120, or 180 min. Cells were stained with 0.4 w/v% trypan blue solution (Wako, Osaka, Japan) to quench any Alexa 488-labeled K-type CpG ODNs bound to the cell surface, and then the cells were analyzed by means of flow cytometry (NovoCyte Flow Cytometer, ACEA Bioscience, San Diego, CA, USA). To separate various subsets of DCs from the collected cells, we incubated the cells with anti-mouse CD16/CD32 antibody (TONBO biosciences, San Diego, CA, USA), anti-mouse B220 antibody (BioLegend), anti-CD11c antibody (BioLegend), and anti-CD11b antibody (BioLegend) in the absence of trypan blue. In this way, the DCs were separated into the following subsets: $B220^+$ $CD11c^+$ plasmacytoid DCs, $CD11b^+$ $CD11c^+$ conventional DCs, and $CD11b^-$ $CD11c^+$ conventional DCs.

Biodistribution of CpG ODNs *In Vivo*

C57BL/6J mice were treated with saline, Alexa 488-labeled K-type CpG ODNs (8 or 40 μg CpG ODNs/mouse), or CA-Alexa 488-CpG (8 μg CpG ODNs/mouse) into the ear pinna. Twenty-four hours after administration, draining lymph nodes were collected. To prepare single-cell suspensions, we incubated the draining lymph nodes with 5 μg/mL collagenase D (Wako, Tokyo, Japan) for 60 min at 37°C. We used flow cytometry to analyze the uptake of CpG ODNs by cells in draining lymph nodes.

In Vivo Activation of Lymph Node Cells

C57BL/6J mice were treated with K-type CpG ODNs (8 or 40 μg CpG ODNs/mouse) or CA-CpG (8 μg CpG ODNs/mouse) into the ear pinna. Twenty-four hours after administration, draining lymph nodes were collected. To prepare single-cell suspensions, we incubated the draining lymph nodes with collagenase D (5 μg/mL) for 60 min at 37°C. Prepared cells were incubated for 8 h, culture supernatants were collected, and cytokines were measured by means of ELISA.

Immunization

C57BL/6J mice were treated with OVA (100 μg/mouse) without or with K-type CpG ODNs (10 or 50 μg CpG ODNs/mouse) or OVA with CA-CpG (10 μg CpG/mouse) subcutaneously at the base of the tail at days 0 and 14. Using hematocrit capillary tubes (Terumo, Tokyo, Japan), we obtained blood samples from the retro-orbital venous plexus at day 21 and centrifuged the samples at $3{,}000 \times g$ at 4°C. The resulting plasma was stored at −80°C until analysis. To investigate the adjuvant effects of CA-CpG administered by another route, we treated C57BL/6J mice with OVA (80 μg/mouse) without or with K-type CpG ODNs (8 or 40 μg CpG ODNs/mouse) or OVA with CA-CpG (8 μg CpG/mouse) into the ear pinna at days 0 and 7, and we obtained blood samples at day 14.

Detection of OVA-Specific Antibodies

The levels of OVA-specific antibodies in plasma were determined by means of ELISA. To detect OVA-specific IgG, IgG1, and IgG2c, we coated ELISA plates (Corning, Corning, NY, USA) with OVA in carbonate buffer (10 μg/mL) overnight at 4°C. The coated plates were incubated with PBS containing 10% FCS. Plasma samples were diluted with PBS containing 10% FCS, and the dilutions were added to the OVA-coated plates. After incubation with plasma for 2 h, the coated plates were incubated with an HRP-conjugated goat anti-mouse IgG, IgG1, or IgG2c solution for 1 h at room temperature. After incubation, the color was developed with tetramethyl benzidine (Moss, Pasadena, MD, USA), the reaction was stopped with 2 N H_2SO_4, and the $OD_{450-570}$ was measured on a microplate reader (Power Wave HT, BioTek, Winooski, VT, USA).

Detection of OVA-Specific $CD8^+$ CTL Induction

C57BL/6J mice were treated with OVA (80 μg/mouse) without or with K-type CpG ODNs (8 or 40 μg CpG ODNs/mouse) or CA-CpG (8 μg CpG ODNs/mouse) into the ear pinna. Draining

lymph nodes were collected at day 7, and lymph node cells were prepared for determination of $OVA_{257–264}$-specific $CD8^+$ CTL responses. Lymph node cells (1×10^6 cells) were added to the wells of a 96 half-well plate and then stimulated with $OVA_{257–264}$ peptide (SIINFEKL, final concentration 5 μg/mL) for 24 h at 37°C. After the incubation, the concentration of IFN-γ in the supernatants was analyzed by means of ELISA. For the tetramer assay, lymph node cells (1×10^6 cells) were stained with purified anti-mouse CD16/CD32 antibody and then with the phycoerythrin-labeled H-$2K^b$/$OVA_{257–264}$ tetramer (MBL, Aichi, Japan). Fluorescein isothiocyanate-conjugated CD8α (Abcam, Cambridge, UK), allophycocyanin-conjugated CD44 (BioLegend), and 7-amino-actinomycin D (BioLegend) were then added. The number of $CD8\alpha^+$ $CD44^+$ $tetramer^+$ cells was determined by flow cytometry.

Vaccine Against Influenza Virus

C57BL/6J mice were treated with ether-treated hemagglutinin antigen-enriched virion-free split vaccine (SV; strain A/California/7/2009, H1N1, 0.5 μg/mouse) without or with K-type CpG ODNs (10 or 50 μg CpG ODNs/mouse), CA-CpG (10 μg CpG ODNs/mouse), CA nanoparticles, or alum at days 0 and 14. At day 21, we obtained blood samples from the retro-orbital venous plexus and centrifuged the samples at 3,000 × *g* at 4°C; the resulting plasma was stored at −80°C until analysis. To detect SV-specific IgG, IgG1, and IgG2c, we coated ELISA plates with SV in carbonate buffer (10 μg/mL) overnight at 4°C. The coated plates were incubated with PBS containing 10% FCS. Plasma samples were diluted with PBS containing 10% FCS, and the dilutions were added to the SV-coated plates. After incubation with plasma for 2 h, the coated plates were incubated with a solution of HRP-conjugated goat anti-mouse IgG, IgG1, or IgG2c for 1 h at room temperature. After incubation, the color was developed with tetramethyl benzidine, the reaction was stopped with 2 N H_2SO_4, and $OD_{450–570}$ was measured on a microplate reader. For analysis of hemagglutination inhibition (HI) titers, plasma samples were incubated with RDE (II) (DENKA SEIKEN, Tokyo, Japan) for 18 h at 37°C and then heated at 56°C for 30 min to deactivate the enzyme. To avoid nonspecific hemagglutination, plasma samples were treated with guinea pig red blood cells for 1 h at room temperature, and the supernatants were serially diluted 2-fold in microtiter plates. An equal volume of influenza virus (strain A/California/7/2009, H1N1) was added to each well, and the plates were incubated for 1 h at room temperature. Guinea pig red blood cells were added and allowed to settle for 1 h at 4°C. The HI titer was determined from the dilution of the last well that contained non-agglutinated guinea pig red blood cells. Moreover, immunized mice were challenged intranasally with 7.2×10^3 pfu (10-LD50) of influenza virus (strain A/PR/8/34, H1N1) (28). Body weights and survival rates of challenged mice were monitored for 14 days. Ether-treated hemagglutinin antigen-enriched virion-free split vaccine and influenza virus were kindly provided by the Research Foundation for Microbial Diseases of Osaka University, Suita, Japan.

Weight of Tissues

K-type CpG ODNs (10 or 50 μg CpG ODNs/mouse) or CA-CpG (10 μg CpG ODNs/mouse) was administered to C57BL/6J mice subcutaneously at the base of the tail at days 0, 2, and 4. Twenty-four hours after the final administration, the entire spleen, the entire liver, and draining lymph nodes were isolated and weighed.

Statistical Analyses

Statistical analyses were performed with GraphPad Prism (GraphPad Software, San Diego, CA, USA). All data are presented as mean with SD or SEM. Significant differences between control groups and experimental groups were determined by means of Dunnett's test, Tukey's test, or Student's *t*-test. A p value of <0.05 was considered to indicate statistical significance.

RESULTS

CA-CpG Had High CpG ODN Encapsulation Efficiency

We evaluated the usefulness of CA nanoparticles as CpG ODN delivery vehicles. We began by determining the amount of K-type CpG ODNs encapsulated in CA-CpG. We found that the amount of K-type CpG ODNs used to generate CA-CpG affected the efficiency with which the K-type CpG ODNs was encapsulated in CA-CpG (**Figure 1A**). When we used 50 μg K-type CpG ODNs, the encapsulation efficiency was high (58%). Therefore, we used CA-CpG prepared with 50 μg K-type CpG ODNs for subsequent experiments. Dynamic light scattering showed that both the empty CA nanoparticles and CA-CpG were uniform and monodispersed, with hydrodynamic diameters ranging from 30 to 40 nm, respectively (**Figure 1B**). In addition, we confirmed that CA-Alexa 488-CpG was also uniform and monodispersed, with hydrodynamic diameters ranging from 30 to 40 nm, as was the case for both the empty CA nanoparticles and CA-CpG (data not shown). Atomic force microscopy showed that the sizes of the CA nanoparticles and CA-CpG ranged from 13 to 25 nm (**Figure 1C**). These results suggest that we successfully generated nanosize CA-CpG with high encapsulation efficiency for K-type CpG ODNs.

CA-CpG Induced IFN-α Production and Enhanced the Production of Other Cytokines in Mouse DCs and Human PBMCs

To determine the immunostimulatory effects of CA-CpG on DCs, we treated mouse-derived DCs with CA-CpG or K-type CpG ODNs *in vitro* and measured cytokine levels in the supernatants by means of ELISA (**Figure 2A**). DCs stimulated with CA-CpG produced substantial amounts of not only IFN-γ and IL-12 p40 but also IFN-α, whereas K-type CpG ODNs did not induce cytokine production at the tested doses. In human PBMCs, higher levels of IFN-α and IFN-γ were produced in response to CA-CpG than in response to K-type CpG ODNs (**Figure 2B**). These data suggest that CA-CpG might be superior to K-type CpG ODNs as an adjuvant. In addition, they suggest that CA-CpG has some characteristics of D-type CpG ODNs, because IFN-α is known to be a D-type CpG ODN-specific cytokine.

A

Added CpG ODNs (μg)	Encapsulation efficiency (%)
1.9	42
5.6	51
16.7	48
50	58
150	37

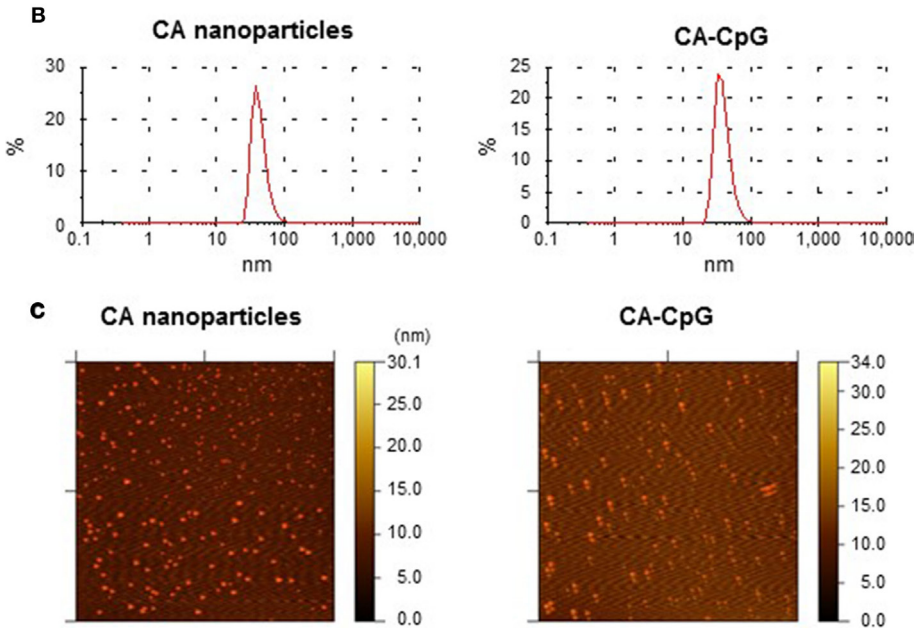

FIGURE 1 | Encapsulation efficiency and size distribution of carbonate apatite (CA)-cytosine-phosphate-guanine (CpG). **(A)** The use of various amounts of K-type CpG oligodeoxynucleotides (ODNs) to generate CA-CpG showed that encapsulation efficiency was highest at 50 μg CpG ODNs. **(B,C)** The size distribution of CA-CpG was determined by dynamic light scattering **(B)** and atomic force microscopy **(C)**. CA-CpG was roughly the same size as CA nanoparticles that did not contain K-type CpG ODNs.

Pattern of CA-CpG Uptake by DCs Differed From That of K-Type CpG ODNs *In Vitro*

To elucidate the mechanism of the immunostimulatory effects of CA-CpG, we compared the cellular internalization of CA-CpG and K-type CpG ODNs in mouse DCs by using Alexa 488-labeled K-type CpG ODNs. DCs were treated with CA-Alexa 488-CpG or with Alexa 488-labeled K-type CpG ODNs, and cells were stained with trypan blue solution to quench any Alexa 488-labeled K-type CpG ODNs bound to the cell surface, so that only internalized K-type CpG ODNs were detected during flow cytometry (**Figures 3A–C**). The amount of Alexa 488-labeled K-type CpG ODNs in DCs treated with CA-Alexa 488-CpG or Alexa 488-labeled K-type CpG ODNs increased over time, and at 90, 120, and 180 min after treatment the groups treated with Alexa 488-labeled K-type CpG ODNs had more cells that were positive for K-type CpG ODNs than did the groups treated with CA-Alexa 488-CpG (**Figures 3A,B**). For more precise analysis, the fractions that were positive for CpG ODNs were divided into two fractions, one with low fluorescence and one with high fluorescence; then we again compared the groups treated with CA-Alexa 488-CpG and the groups treated with Alexa 488-labeled K-type CpG ODNs (**Figures 3A,C**). In the low-fluorescence fraction, at 90, 120, and 180 min after treatment, the groups treated with Alexa 488-labeled K-type CpG ODNs had more cells that were positive for K-type CpG ODNs than did the CA-Alexa 488-CpG-treated groups. In contrast, in the high-fluorescence fraction at all time points, the CA-Alexa 488-CpG-treated groups had significantly more cells that were positive for K-type CpG ODNs than did the groups treated with Alexa 488-labeled K-type CpG ODNs. On the basis of these results, we speculated that certain subsets of DCs might have taken up CA-CpG more efficiently than others. To evaluate this possibility, we categorized DCs into the following subsets: $B220^+$ $CD11c^+$ plasmacytoid DCs, $CD11b^+$ $CD11c^+$ conventional DCs, and $CD11b^-$ $CD11c^+$ conventional DCs. Then we analyzed the CpG ODN-positive cells in each subset at both 37°C and 4°C, so that we could evaluate nonspecific binding of CA-Alexa 488-CpG or Alexa 488-labeled K-type CpG ODNs to the cell surface (**Figure 3D**). There were fewer CpG ODN-positive cells at 4°C

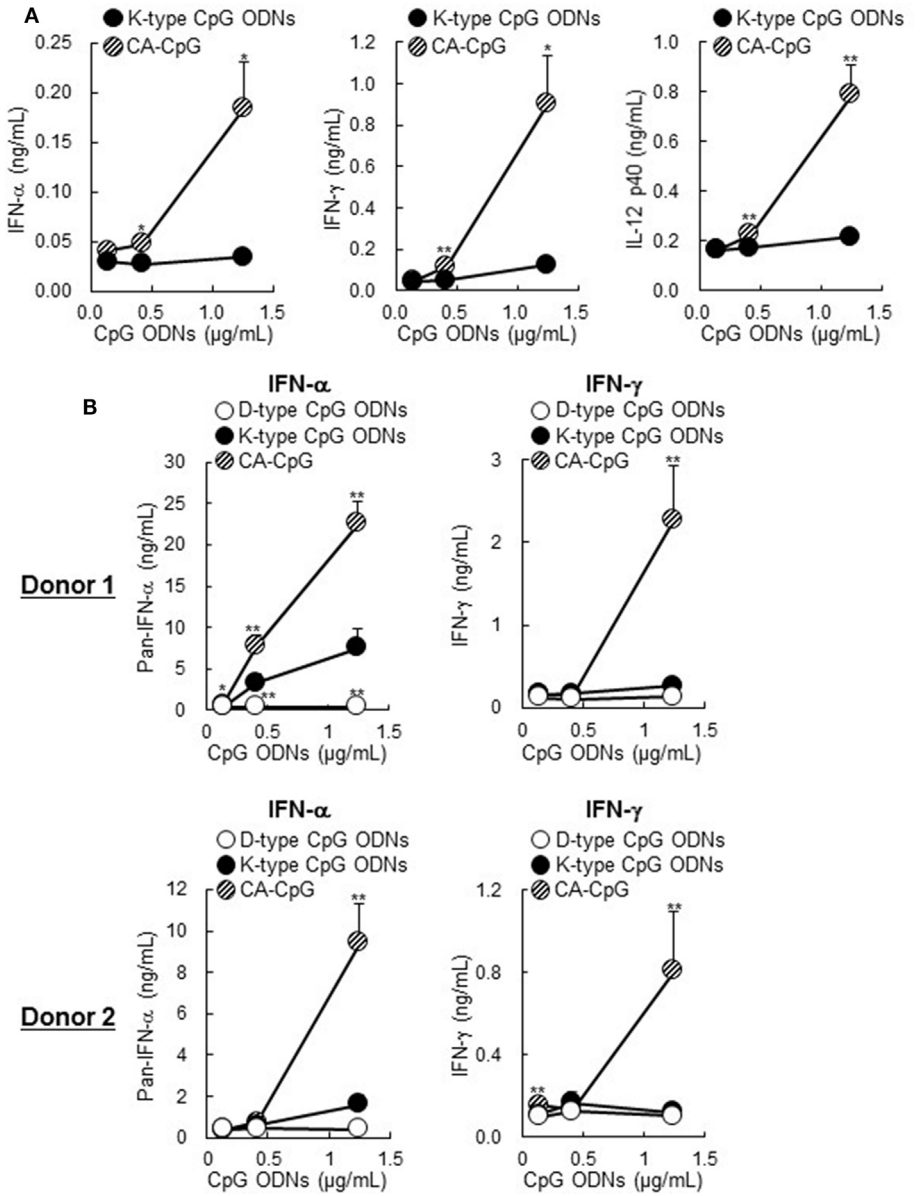

FIGURE 2 | Cytokine production induced by carbonate apatite (CA)-cytosine-phosphate-guanine (CpG) in mouse-derived dendritic cells (DCs) and human peripheral blood mononuclear cells (PBMCs). Mouse-derived DCs **(A)** and human PBMCs **(B)** were treated with several concentrations (adjusted for CpG oligodeoxynucleotides (ODN) concentration) of CA-CpG, K-type CpG ODNs, or D-type CpG ODNs for 24 h, and the cytokine concentrations in the supernatants were then measured by ELISA. **(A)** In DCs, CA-CpG induced higher IFN-α, IFN-γ, and IL-12 p40 production than did K-type CpG ODNs, $n = 4$ per group. **(B)** In PBMCs, CA-CpG induced higher levels of pan-IFN-α and IFN-γ production than did K-type or D-type CpG ODNs, $n = 5$ per group. These data suggest that CA-CpG has some characteristics of D-type CpG ODNs. Data are given as mean ± SD. $^{*}p < 0.05$, $^{**}p < 0.01$ vs. K-type CpG ODN-treated group as indicated by Student's *t*-test **(A)** or Dunnett's test **(B)**.

than at 37°C, indicating that the binding of CA-CpG or K-type CpG ODNs on the cell surface could be ignored in this assay. At 37°C, in all the subsets of DCs, the number of CpG ODN-positive cells in the CA-CpG-treated groups was lower than that in the K-type CpG ODN-treated groups (**Figure 3D**), indicating that CA-CpG was taken up into all the subsets of DCs equally, as was the case for the K-type CpG ODNs.

CA-CpG Enhanced Cytokine Production *In Vivo*

Generally, the delivery of an adjuvant to lymph nodes, and specifically to DCs in lymph nodes, is important for the efficient induction of adaptive immunity. However, the efficiency with which CA-CpG delivers CpG ODNs to DCs in lymph nodes is unknown. Therefore, to assess the distribution and uptake of

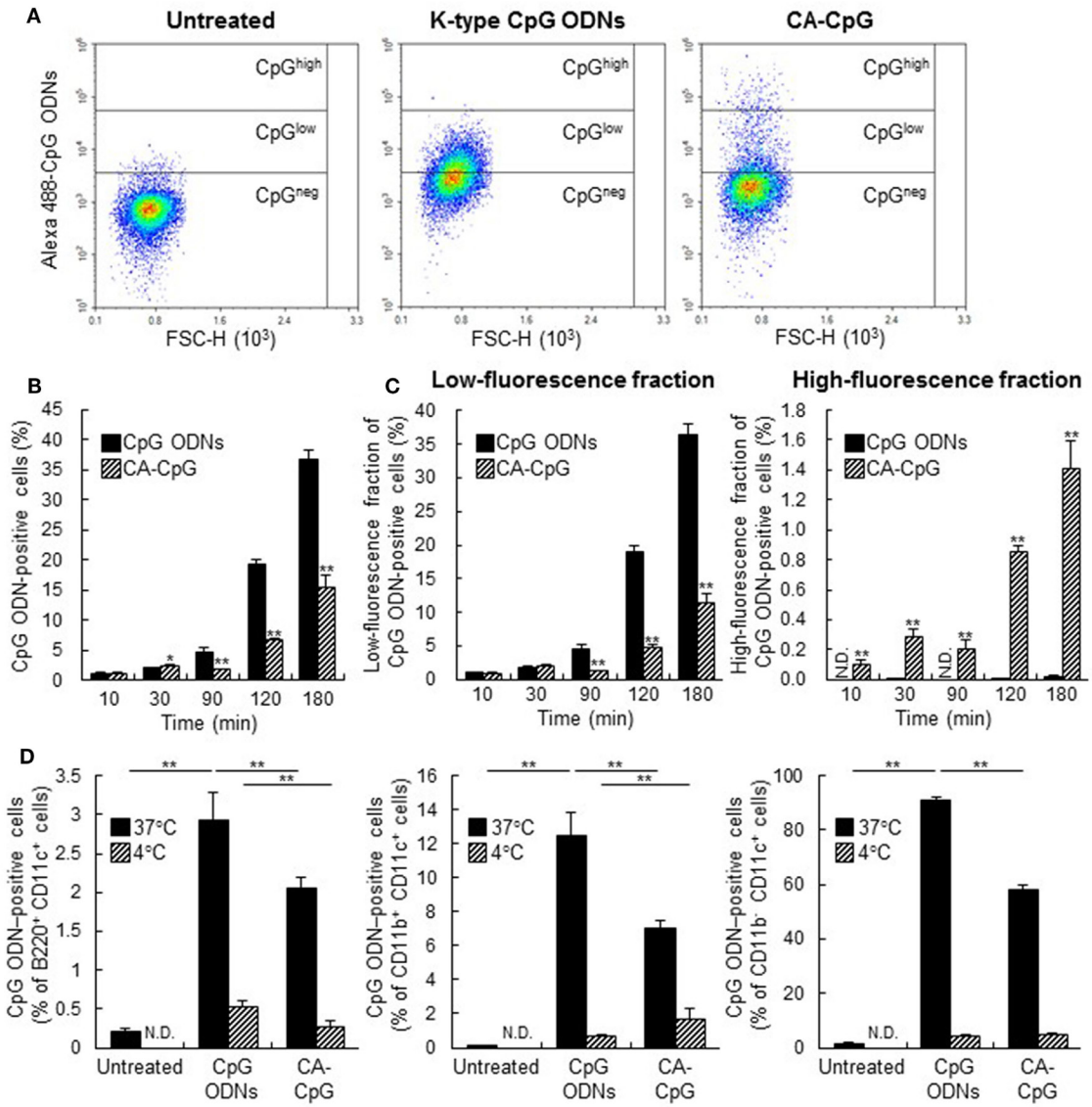

FIGURE 3 | Cellular uptake of carbonate apatite (CA)-cytosine-phosphate-guanine (CpG). **(A–C)** Comparison of cellular uptake patterns of CA-CpG and K-type CpG oligodeoxynucleotides (ODNs). Mouse-derived dendritic cells (DCs) were treated with CA-Alexa 488-CpG or Alexa 488-labeled K-type CpG ODNs. At various time points after treatment, K-type CpG ODNs internalized in DCs were measured by flow cytometry after trypan blue quenching. **(A)** Representative dot plots show Alexa 488-labeled CpG ODNs in DCs vs. forward scatter (FSC-A). **(B)** Quantification of fluorescence revealed that uptake of CA-CpG into DCs was lower than uptake of K-type CpG ODNs, $n = 5$ per group. **(C)** Separation of the dot plots for the CpG ODN-positive fraction in panel **(A)** into graphs for high-fluorescence and low-fluorescence fractions revealed that the number of CpG ODNs taken up by each DC in the CA-CpG-treated groups was larger than that in the K-type CpG ODN-treated groups, $n = 5$ per group. **(D)** Subsets of DCs that took up CA-CpG. Mouse-derived DCs were treated with CA-Alexa 488-CpG or Alexa 488-labeled K-type CpG ODNs for 3 h at 4°C or 37°C. Uptake of CA-Alexa 488-CpG or Alexa 488-labeled K-type CpG ODNs into each subset of DCs was measured by flow cytometry without trypan blue quenching, $n = 5$ per group. Data are given as mean ± SD. $^*p < 0.05$, $^{**}p < 0.01$ vs. K-type CpG ODN-treated group as indicated by Student's *t*-test **(B,C)** or Dunnett's test **(D)**. ND, not detected.

CA-CpG into lymph nodes, we measured the quantity of CpG ODN-positive cells in draining lymph nodes by flow cytometry after administration of CA-Alexa 488-CpG or Alexa 488-labeled K-type CpG ODNs to mice (**Figure 4A**). Whereas in the group treated with Alexa 488-labeled K-type CpG ODNs at 40 μg CpG ODNs/mouse (the positive control), large proportions of the lymph node cells were CpG ODN-positive, there were no significant differences between the proportions of CpG ODN-positive cells in the groups treated with CA-Alexa 488-CpG at 8 μg CpG ODNs/mouse and the groups treated with Alexa 488-labeled K-type CpG ODNs at 8 μg CpG ODNs/mouse at any time point. These results suggest that the CA nanoparticles did not increase the number of CpG ODNs taken up by DCs in lymph nodes.

Next, to determine the immunostimulatory effects of CA-CpG *in vivo*, we measured cytokine production in draining lymph nodes after CA-CpG administration (**Figure 4B**).

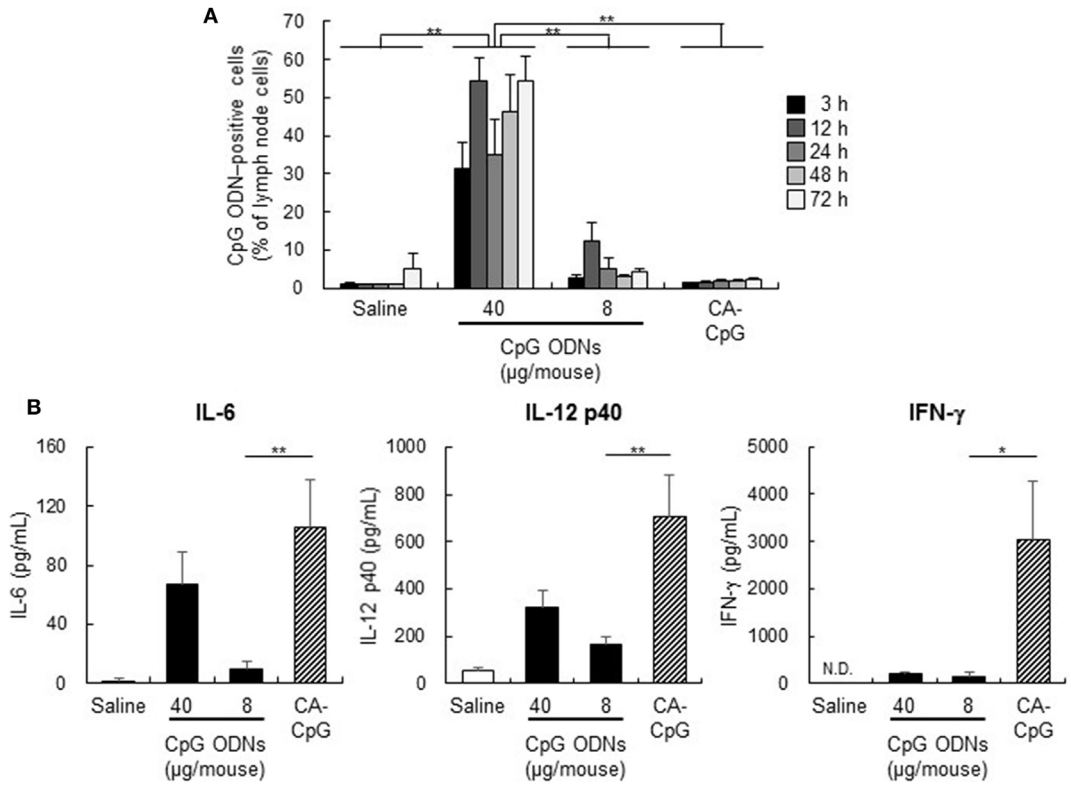

FIGURE 4 | Biodistribution of carbonate apatite (CA)-cytosine-phosphate-guanine (CpG) *in vivo* and cytokine production induced by CA-CpG in draining lymph nodes. **(A)** Biodistribution of CA-CpG *in vivo*. Mice were treated with CA-Alexa 488-CpG or Alexa 488-labeled K-type CpG oligodeoxynucleotides (ODNs) into the ear pinna, and internalization of K-type CpG ODNs by cells in draining lymph nodes was measured by flow cytometry at the indicated time points after trypan blue quenching. Treatment with CA-CpG did not increase the number of cells that internalized CpG ODNs, $n = 5$ per group. **(B)** Cytokine production induced by CA-CpG in draining lymph nodes. CA-CpG (8 μg CpG ODNs/mouse) or K-type CpG ODNs (8 or 40 μg CpG ODNs/mouse) were administered into the ear pinna. After 24 h, lymph node cells in draining lymph nodes were harvested and cultured for 8 h, and the levels of IL-6, IL-12 p40 and IFN-γ in the culture supernatants were evaluated. CA-CpG induced higher levels of cytokine production than did K-type CpG ODNs, $n = 5$ per group. Data are given as mean ± SEM. $^*p < 0.05$, $^{**}p < 0.01$ as indicated by Tukey's test **(A)** or vs. K-type CpG ODNs (8 μg CpG ODNs/mouse)-treated group as indicated by Dunnett's test **(B)**. ND, not detected.

We found that production of the cytokines IL-6, IL-12 p40, and IFN-γ in draining lymph nodes was substantially higher after treatment with CA-CpG than after treatment with K-type CpG ODNs (**Figure 4B**). These data suggest that CA-CpG markedly enhanced innate immune activation responses, such as cytokine production, relative to K-type CpG ODNs both *in vitro* and *in vivo*.

CA-CpG Enhanced Antigen-Specific Antibody Responses and CD8$^+$ CTL Responses *In Vivo*

To evaluate the *in vivo* effects of the use of CA-CpG as a vaccine adjuvant in mice, we assessed antibody responses and CD8$^+$ CTL responses following co-administration of CA-CpG or K-type CpG ODNs with OVA, a model protein antigen. Mice were immunized with OVA plus CA-CpG (10 μg CpG ODNs/mouse) or OVA plus K-type CpG ODNs (10 or 50 μg CpG ODNs/mouse) subcutaneously at the base of the tail. As a positive control, we used alum, which is widely used throughout the world as an adjuvant for human vaccines. Seven days after the final immunization, the levels of OVA-specific total IgG, IgG1, and IgG2c antibodies in plasma were analyzed by ELISA (**Figure 5A**). Levels of antigen-specific IgG subclasses reflect the subset of CD4$^+$ T cells that are induced by vaccination, with production of IgG1 and IgG2c corresponding to Th2- and Th1-type responses, respectively. Although mice immunized with OVA plus alum showed high levels of total IgG and IgG1 production, mice immunized with OVA plus CA-CpG or OVA plus K-type CpG ODNs produced high levels not only of total IgG and IgG1 but also of IgG2c. Mice immunized with OVA plus CA-CpG (10 μg CpG ODNs/mouse) produced significantly higher levels of OVA-specific total IgG, IgG1, and IgG2c than did mice immunized with OVA plus K-type CpG ODNs (10 μg CpG ODNs/mouse). Antibody production in groups treated with OVA plus CA-CpG (10 μg CpG ODNs/mouse) was comparable to that in groups treated with OVA plus K-type CpG ODNs (50 μg CpG ODNs/mouse).

Next, to evaluate the adjuvant effects of CA-CpG when administered by a different route, we immunized mice with OVA plus CA-CpG or OVA plus K-type CpG ODNs into the ear pinna and then measured OVA-specific antibody responses (**Figure 5B**). As was the case for immunization subcutaneously at the base of the

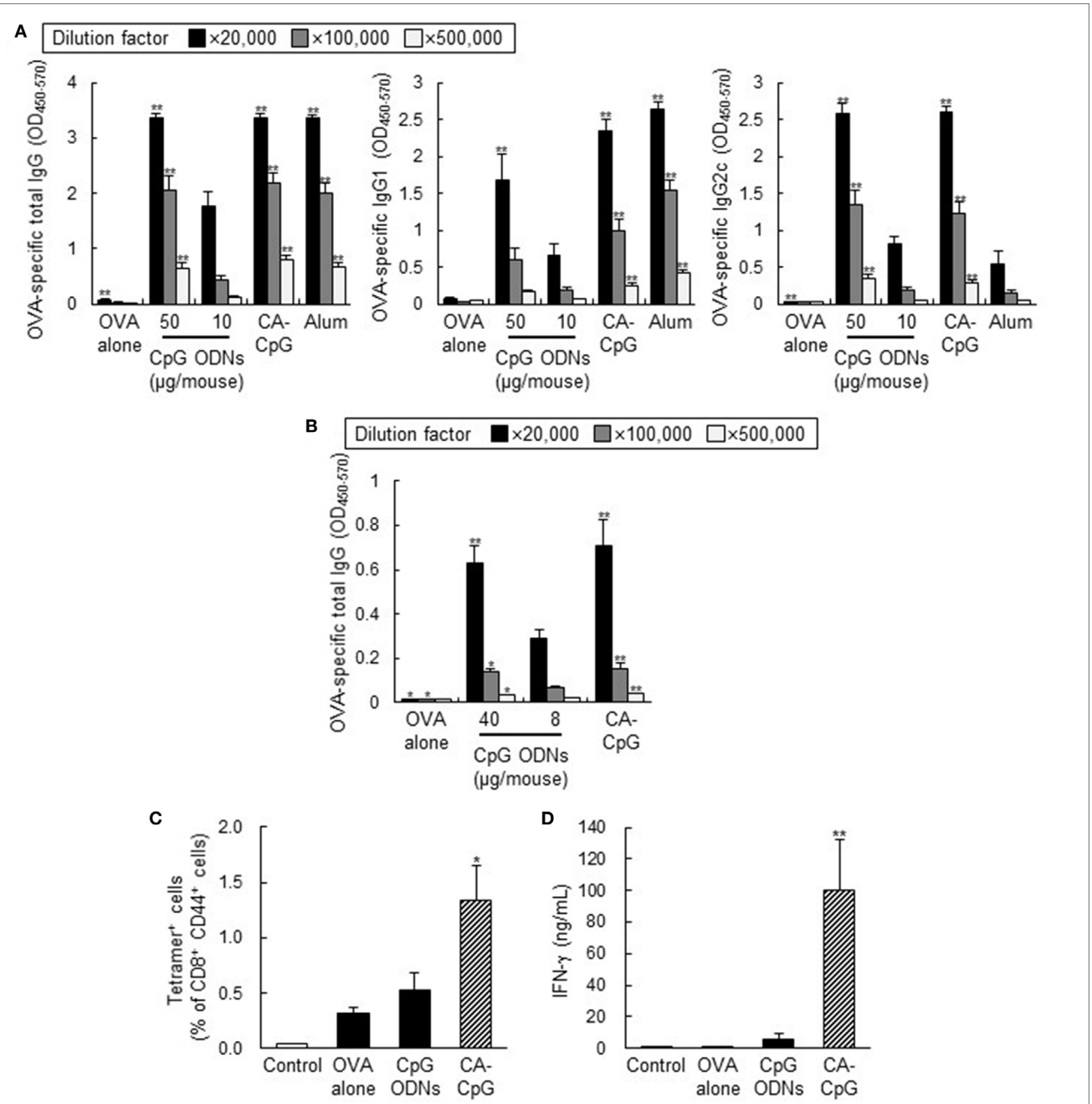

FIGURE 5 | Adjuvant effects of carbonate apatite (CA)-cytosine-phosphate-guanine (CpG) in mice. Mice were immunized subcutaneously at the base of the tail **(A)** or into the ear pinna **(B–D)** with ovalbumin (OVA) plus CA-CpG at 10 μg CpG oligodeoxynucleotides (ODNs)/mouse **(A)** or 8 μg CpG ODNs/mouse **(B–D)**; with OVA plus K-type CpG ODNs at 10 or 50 μg CpG ODNs/mouse **(A)**, at 8 or 40 μg CpG ODNs/mouse **(B)**, or at 8 μg CpG ODNs/mouse **(C,D)**; or with OVA plus alum. **(A,B)** OVA-specific antibody responses. Levels of OVA-specific total IgG, IgG1, and IgG2c in plasma were evaluated by ELISA 7 days after the final immunization, $n = 5$ per group. **(C,D)** $CD8^+$ cytotoxic T lymphocyte (CTL) responses. $OVA_{257–264}$-specific $CD8^+$ CTL responses were monitored by means of a tetramer assay in untreated mice and in mice immunized with OVA alone, with OVA plus K-type CpG ODNs, or with CA-CpG **(C)**, $n = 5$ per group. Lymph node cells were stimulated with $OVA_{257–264}$ peptide, and the concentration of IFN-γ in supernatants was analyzed by ELISA **(D)**, $n = 5$ per group. The data in this figure suggest that a simple mixture containing CA-CpG and an antigen-induced antigen-specific antibody responses and $CD8^+$ CTL responses that were superior to those induced by K-type CpG ODNs and alum, thus demonstrating the potential of CA-CpG as a vaccine adjuvant. Data are given as mean ± SEM. $^*p < 0.05$, $^{**}p < 0.01$ vs. K-type CpG ODNs (10 or 8 μg CpG ODNs/mouse)-treated group as indicated by Dunnett's test.

tail, the level of OVA-specific total IgG induced by immunization with OVA plus CA-CpG (8 μg CpG ODNs/mouse) was significantly higher than the level induced by immunization with OVA plus K-type CpG ODNs (8 μg CpG ODNs/mouse) and was comparable to the level induced by administration of OVA plus K-type CpG ODNs (40 μg CpG ODNs/mouse).

Clearance of viruses is known to require not only antibody responses but also strong $CD8^+$ CTL responses, which are characterized by IFN-γ production by $CD8^+$ T cells. To investigate the ability of CA-CpG to induce OVA-specific $CD8^+$ CTL responses, we vaccinated mice with OVA plus CA-CpG and then examined the frequency of H-$2K^b$/$OVA_{257–264}$ tetramer$^+$ $CD8^+$ T cells (**Figure 5C**) and measured the production of H-$2K^b$/$OVA_{257–264}$-specific IFN-γ (**Figure 5D**). The frequency of H-$2K^b$/$OVA_{257–264}$ tetramer$^+$ $CD8^+$ T cells induced by OVA plus CA-CpG was significantly higher than the frequency induced by OVA plus K-type CpG ODNs (**Figure 5C**). Furthermore, the production of $OVA_{257–264}$-specific IFN-γ induced by OVA plus CA-CpG was significantly higher than that induced by immunization with OVA plus K-type CpG ODNs (**Figure 5D**). Taken together, these results suggest that, *in vivo*, CA-CpG stimulated antigen-specific antibody responses and $CD8^+$ CTL responses more effectively than did K-type CpG ODNs.

CA-CpG Showed Strong Adjuvant Effects and Preventive Effects in Murine Influenza Models

We examined the vaccine adjuvant effects of CA-CpG by using clinically relevant influenza vaccination models in mice. Mice were immunized with A/California/7/2009 (H1N1) SV plus CA-CpG (10 μg CpG ODNs/mouse), K-type CpG ODNs (10 or 50 μg/mouse), CA nanoparticles, or Alum. The levels of SV-specific total IgG, IgG1, and IgG2c antibodies in plasma were analyzed by ELISA after the final immunization (**Figures 6A,B**). Mice immunized with SV plus CA-CpG (10 μg CpG ODNs/mouse) showed significantly higher levels of SV-specific total IgG, IgG1, and IgG2c than did mice immunized with OVA plus K-type CpG ODNs (10 and 50 μg CpG ODNs/mouse). The levels of SV-specific total IgG and IgG2c in mice treated with SV plus CA-CpG were significantly higher than those in mice treated with SV plus alum, whereas there was no difference in SV-specific IgG1 levels between these two groups of mice. The levels of total IgG and IgG1 in mice treated with SV plus CA nanoparticles were higher than the levels in mice treated with SV alone but were significantly lower than the levels in CA-CpG-treated mice. Next, we examined the neutralizing potential of these antibodies by using the HI assay against influenza virus A/California/7/2009 (**Figure 6C**), because this assay is widely used to evaluate anti-influenza virus neutralizing and protective antibodies. The HI titers showed the same trends as the levels of SV-specific total IgG, and mice immunized with SV plus CA-CpG had significantly higher HI titers than did mice immunized with SV plus K-type CpG ODNs (10 μg CpG ODNs/mouse). After the final immunization, we challenged the immunized mice with mouse-adapted influenza virus A/PR/8/34 (H1N1), which is a heterologous influenza virus from the one used as a vaccine antigen. Weights and survival rates of the infected mice were observed every day for 2 weeks (**Figure 6D**). Much greater pathogenesis was observed in the mice immunized without an adjuvant or with alum than in the mice co-immunized with CA-CpG or K-type CpG ODNs (10 or 50 μg CpG ODNs/mouse), as indicated by survival rate and weight loss. All mice died within 10 days after viral infection in the groups that received SV alone or SV plus alum, and 80% of the mice immunized with SV plus CA nanoparticles died within 7 days. Although only 40% of the mice immunized with SV plus K-type CpG ODNs (10 μg CpG ODNs/mouse) survived 14 days after challenge, 80% of mice immunized with SV plus CA-CpG (10 μg CpG ODNs/mouse) or K-type CpG ODNs (50 μg/mouse) survived, and they regained body weight more rapidly. These results indicate that CA-CpG is a potent vaccine adjuvant that protects against viral infection better than K-type CpG ODNs or alum.

Adjuvant Effects of CA-CpG Depended on Both IFN-α and IL-12

Activation of $CD8^+$ CTL responses requires T-cell activation by DCs via costimulatory signals and cytokine-mediated signals. For example, IFN-α and IL-12 work as critical survival signals that expand and differentiate effector $CD8^+$ T cells (29–31). Therefore, to elucidate the involvement of IFN-α and IL-12 in antibody responses and $CD8^+$ CTL responses induced by CA-CpG, we treated mice deficient in both *Ifnar2* and *Il-12 p40* with OVA plus CA-CpG (**Figure 7**). The levels of OVA-specific total IgG, IgG1, and IgG2c in these double-deficient mice immunized with OVA plus CA-CpG tended to be lower than the levels in wild-type mice (**Figure 7A**). In addition, the frequency of H-$2K^b$/$OVA_{257–264}$ tetramer$^+$ $CD8^+$ T cells in the double-deficient mice tended to be lower than that in the wild-type mice (**Figure 7B**). These results suggest that CA-CpG enhanced both Th1-type humoral and cellular immune responses *via* the IFN-α pathway, the IL-12 pathway, or both.

Adverse Effects of CpG ODNs Were Not Enhanced by CA-CpG

Cytosine-phosphate-guanine ODNs are known to cause splenomegaly and to disrupt splenic microarchitecture in mice after repeated administration (32). To assess the adverse effects of CA-CpG, we treated mice three times every other day with CA-CpG or K-type CpG ODNs and then measured tissue weights (**Figure 8**). No significant differences in liver weight were observed between the groups. In contrast, spleen weights and draining lymph node weights in mice treated with K-type CpG ODNs at 50 μg CpG ODNs/mouse were higher than those in mice treated with CA-CpG (10 μg CpG ODNs/mouse), although the difference was statistically significant only for spleen weights. The effects of CA-CpG (10 μg CpG ODNs/mouse) were almost the same as those of K-type CpG ODNs at 10 μg CpG ODNs/mouse. These results suggest that CA-CpG improved the efficacy of CpG ODNs without enhancing their adverse effects.

DISCUSSION

Because systemic dissemination of CpG ODNs away from the site of injection occurs rapidly after administration, high doses of CpG ODNs are required for induction of vaccine effects, thus increasing the risk of adverse events (33). Therefore, the development of easy to fabricate, high encapsulation capacity CpG ODN delivery vehicles that enhance the adjuvant activity

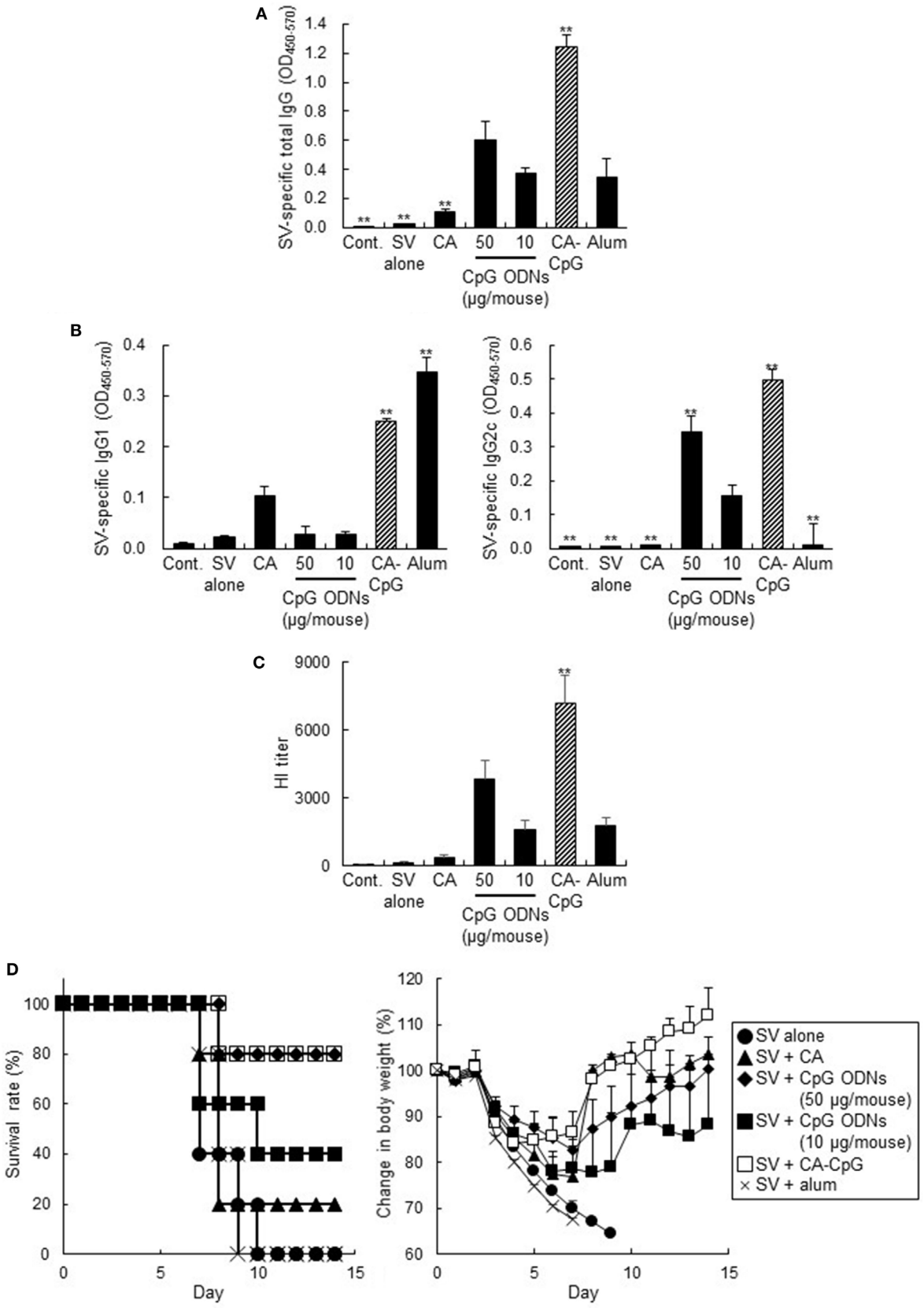

FIGURE 6 | Continued

FIGURE 6 | Vaccine adjuvant effect of carbonate apatite (CA)-cytosine-phosphate-guanine (CpG) against influenza virus. Mice were immunized subcutaneously at the base of the tail with SV alone or with SV plus CA nanoparticles that did not contain CpG oligodeoxynucleotides (ODNs), with SV plus K-type CpG ODNs (10 or 50 μg CpG/mouse), with SV plus CA-CpG (10 μg CpG/mouse), or with SV plus alum. **(A,B)** SV-specific antibody responses. Levels of SV-specific total IgG **(A)**, IgG1 **(B)**, and IgG2c **(B)** in plasma were evaluated by ELISA 7 days after the final immunization. **(C)** Hemagglutination inhibition (HI) assay. HI titers in plasma samples were evaluated 7 days after the final immunization. **(D)** Preventive effects against influenza virus. Fourteen days after the final immunization, mice were challenged with a 10-LD_{50} dose of influenza virus A/PR/8 (H1N1). Body weights and survival rates were monitored for the next 14 days. The data in this figure suggest that CA-CpG acted as an influenza vaccine adjuvant in mice. $n = 5$ per group. Data are given as mean ± SEM. $^{**}p < 0.01$ vs. K-type CpG ODNs (10 μg CpG ODNs/mouse)-treated group as indicated by Dunnett's test.

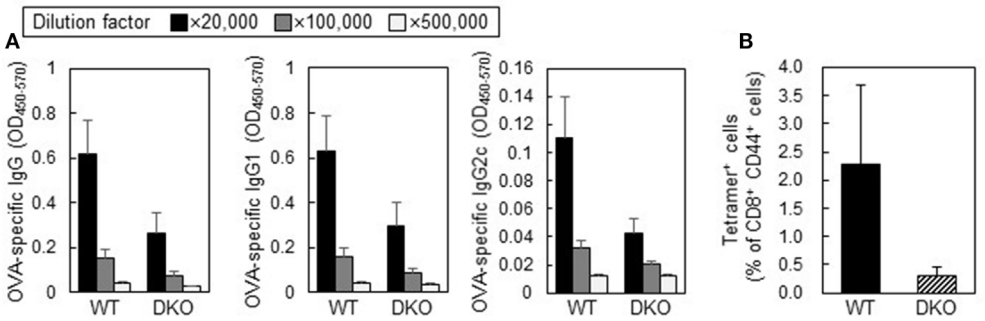

FIGURE 7 | Adjuvant activities of carbonate apatite (CA)-cytosine-phosphate-guanine (CpG) in *IFN-α/β receptor 2 (Ifnar2)* and *Il-12 p40* double-deficient mice (DKO mice). Wild-type (WT) mice or DKO mice were immunized subcutaneously at the base of the tail with ovalbumin (OVA) plus CA-CpG (10 μg CpG/mouse) at days 0 and 14. **(A)** OVA-specific antibody responses. Levels of OVA-specific total IgG, IgG1, and IgG2c in plasma were evaluated by ELISA 7 days after the final immunization, $n = 5$ per WT group and $n = 4$ per DKO group. **(B)** $CD8^+$ cytotoxic T lymphocyte (CTL) responses. $OVA_{257–264}$-specific $CD8^+$ CTL responses were monitored in mice by tetramer assay 7 days after the final immunization, $n = 5$ per WT group and $n = 4$ per DKO group.

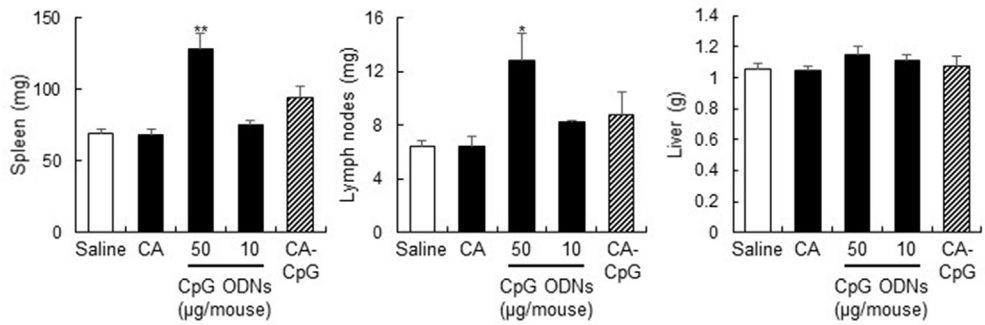

FIGURE 8 | Strong adjuvant effects of carbonate apatite (CA)-cytosine-phosphate-guanine (CpG) without splenomegaly. Mice were treated with CA-CpG (10 μg CpG oligodeoxynucleotides (ODNs)/mouse), CA nanoparticles or K-type CpG ODNs (10 or 50 μg CpG ODNs/mouse) subcutaneously at the base of the tail at days 0, 2, and 4. Twenty-four hours after the final administration, the spleen, liver, and lymph nodes were weighed. CA-CpG did not induce splenomegaly; in contrast, a high dose of K-type CpG ODNs did induce splenomegaly, $n = 5$ per group. Data are given as mean ± SEM. $^{*}p < 0.05$, $^{**}p < 0.01$ vs. saline-treated group as indicated by Tukey's test.

of CpG ODNs and reduce their adverse effects is necessary. In addition, after cellular uptake, the delivery vehicle must degrade rapidly *via* an endosomal or lysosomal processing pathway so that the CpG ODNs can bind to endosomal TLR9. Several types of particle-based delivery vehicles have been reported, including cationized gelatin nanoparticles (34), calcium phosphate nanoparticles (35), poly(lactic-*co*-glycolic acid) nanoparticles (36, 37), Ficoll nanoparticles (38), poly(propylene sulfide) nanoparticles (39), and liposomes (40, 41). However, there have been no reports suggesting that these particles can enhance the adjuvant activity of K-type CpG ODNs by giving them the ability to induce IFN-α production *in vivo*. We showed here that CA nanoparticles can serve as K-type CpG ODN delivery vehicles and that they enhance the adjuvant activity of K-type CpG ODNs by inducing IFN-α production both *in vitro* and *in vivo*.

Carbonate apatite nanoparticles have been shown to efficiently encapsulate siRNA (26). In this study, we showed that CA nanoparticles can also encapsulate K-type CpG ODNs, with an

encapsulation efficiency of about 60% (**Figure 1A**). Researchers have tried to enhance the adjuvant activity of CpG ODNs by encapsulating them in microparticles and nanoparticles, but the encapsulation efficiency has been very low (42–44). Because CpG ODNs are negatively charged, cationic materials such as protamine and chitosan have been used to bind CpG ODNs and facilitate their incorporation into particles. For example, Fisher et al. showed that CpG ODNs could be encapsulated with approximately 90% efficiency into protamine-coated poly(lactic-*co*-glycolic acid) particles, whereas the encapsulation efficiency was only 8% for bare particles (43). Peine et al. (44) and Zhang et al. (42) showed that CpG ODNs could be encapsulated with 30% efficiency into acetalated dextran particles and poly(lactic-*co*-glycolic acid) particles, respectively, without the use of cationic materials, by optimization of the conditions used to generate the particles. These results suggest that encapsulation of CpG ODNs into CA nanoparticles with relatively high efficiency can be achieved without the use of cationic materials.

Here, we showed that, compared with K-type CpG ODNs, CA-CpG induced higher levels of cytokine production in mouse DCs and human PBMCs (**Figure 2**). Notably, IFN-α production induced by CA-CpG was not only higher than that induced by K-type CpG ODNs but also higher than that induced by D-type CpG ODNs. Because IFN-α is a D-type CpG ODN-specific cytokine, these results suggest that CA-CpG-encapsulated K-type CpG ODNs gained characteristics of D-type CpG ODNs without losing their K-type CpG ODN characteristics. Many studies have shown that the difference between the cytokine production patterns induced by K-type and D-type CpG ODNs might be due to differences in their subcellular distribution in DCs (45, 46). It has been suggested that K-type CpG ODNs localize to late endosomes after cellular internalization and activate the IFN regulatory factor 5 pathway *via* TLR9, whereas D-type CpG ODNs localize to early endosomes and activate the IFN regulatory factor 7 pathway *via* TLR9 (47). In fact, a change in the localization of K-type CpG ODNs to early endosomes by the use of cationic liposomes has been shown to induce IFN-α production (47). In contrast, a new model was recently proposed in which adaptor protein 3-mediated TLR9 trafficking to lysosome-related organelles is essential for the induction of IFN-α production (48); this model suggests that the mechanisms of IFN-α production are more complicated than previously thought. Therefore, we cannot determine the precise relationship between the cellular localization of CA-CpG and its potential to induce IFN-α production. However, several studies have demonstrated that the particle size of CA-CpG affects its intracellular trafficking and localization. For example, small particles (<200 nm) are rapidly transported to late lysosomes, which have an acidic environment; whereas large particles (>500 nm) are localized in nearly neutral environments such as early endosomes and phagosomes (49, 50). These size-related differences may be the result of particle size-dependent differences in cellular internalization pathways (51). Therefore, we speculate that CA-CpG may localize in lysosome-related organelles, not in early endosomes, and may release CpG ODNs, which then induce IFN-α production. However, further study is required to clarify the exact cellular localization of CA-CpG.

In this study, we showed that, *in vitro*, CA-CpG was taken up by fewer DCs than were K-type CpG ODNs (**Figures 3A,B**). However, the number of CpG ODNs taken up by each DC was larger than the number of K-type CpG ODNs taken up by each DC, probably because CpG ODNs were condensed into a small space in the CA-CpG (**Figures 3A,C**). The greater uptake of CpG ODNs by cells treated with CA-CpG than by cells treated with K-type CpG ODNs might result in higher cytokine production in the former than in the latter.

With regard to the biodistribution of particles *in vivo*, several studies have suggested that small nanoparticles (<100 nm or <200 nm, depending on the study) can be trafficked to draining lymph nodes preferentially and can be taken up by DCs in lymph nodes, whereas larger particles (>100 nm or >200 nm, depending on the study) tend to be deposited at the injection site. These results suggest that nanoparticles <100 nm might be optimal for enhancing the efficacy of antigen and adjuvant delivery vehicles (52–54). We showed that the proportion of DCs that took up CpG ODNs in draining lymph nodes in CA-CpG-treated mice (8 μg CpG ODNs/mouse) was almost the same as the proportion in K-type CpG ODN-treated mice (8 μg CpG ODNs/mouse) (**Figure 4A**). However, cytokine production by lymph node cells was higher after administration of CA-CpG (8 μg CpG ODNs/mouse) than after administration of K-type CpG ODNs (8 μg CpG ODNs/mouse) (**Figure 4B**). These data suggest that, *in vivo* as well as *in vitro*, CA-CpG strongly induced cytokine production even though the number of CpG ODN-positive DCs was lower. It is not clear whether CpG ODN-positive individual DCs in the draining lymph nodes of CA-CpG-treated mice took up larger amounts of CpG ODNs than did individual DCs in the draining lymph nodes of K-type CpG ODN-treated mice. Further investigation of the biodistribution of CA-CpG *in vivo* is necessary.

The antigen (OVA and SV)-specific antibody responses (**Figures 5A,B** and **6**) and $CD8^+$ CTL responses (**Figures 5C,D**) induced by CA-CpG were superior to those induced by K-type CpG ODNs. The strength of the antigen-specific immune responses induced by CA-CpG was significantly higher than the strength of the responses induced by the same dose of K-type CpG ODNs and was almost the same as the strength of the responses induced by a dose of K-type CpG ODNs that was five times high. However, unlike K-type CpG ODNs (50 μg CpG ODNs/mouse), CA-CpG (10 μg CpG ODNs/mouse) did not induce splenomegaly, which suggests that CA-CpG may be a superior CpG ODN delivery vehicle in that it has better vaccine adjuvant effects than K-type CpG ODNs, without enhanced adverse effects (**Figure 8**). Many nanomaterials have the potential to enhance adaptive immunity, that is, they have adjuvant effects (55, 56). In this study, we found that the antibody responses in mice treated with SV plus CA nanoparticles without K-type CpG ODNs were slightly higher than the responses in mice treated with SV alone (**Figures 6A,B**). In contrast, the responses in mice treated with SV plus CA nanoparticles without K-type CpG ODNs were significantly lower than the responses in CA-CpG-treated mice (**Figures 6A,B**). These data suggest that the adjuvant activity of CA nanoparticles alone was low. In addition, we showed that CA-CpG performed better against influenza virus infection than did the

same dose of K-type CpG ODNs or alum (**Figure 6D**). Following influenza infection, not only neutralizing antibodies but also $CD8^+$ CTL responses play crucial roles in eliminating the virus and preventing viral persistence (57, 58). Furthermore, vaccines that induce $CD8^+$ CTL responses are expected to show efficacy against influenza virus, because $CD8^+$ CTL responses can provide cross-subtype or heterosubtypic protection (57, 58). Therefore, enhancement of $CD8^+$ CTL responses by CA-CpG might lead to the development of a vaccine with strong protective effects against not only homologous but also heterologous influenza viruses. Taken together, these data suggest that CA-CpG can be used as a potent adjuvant for protein-based vaccines such as influenza SVs.

We showed that the enhancement of antibody responses and $CD8^+$ CTL responses induced by CA-CpG tended to be negated in *Ifnar2*- and *Il-12 p40* double-deficient mice. We showed that CA-CpG induced the production of IFN-α and IL-12 in DCs more strongly than did K-type CpG ODNs *in vitro* (**Figure 2**). Previously, Kobiyama et al. showed that IFN-α and IL-12 are produced from plasmacytoid DCs and $CD8\alpha^+$ DCs, respectively, *in vitro* after stimulation with a complex consisting of CpG ODNs and β-glucan (19, 27). Furthermore, these investigators also showed that both IFN-α and IL-12 are indispensable for the induction of Th1-type antibody responses and $CD8^+$ CTL responses induced by the CpG ODN complex (19, 27). These findings suggest that IFN-α produced by plasmacytoid DCs or IL-12 produced by $CD8\alpha^+$ DCs, or both, play important roles in the strong immune responses induced by CA-CpG.

In summary, we have shown that CpG ODNs encapsulated in CA nanoparticles as delivery vehicles induce enhanced cytokine production—especially IFN-α production—relative to that induced by CpG ODNs alone. Furthermore, we have shown CA-CpG is a potent adjuvant for protein-based subunit vaccines. We believe that the use of CA-CpG can improve the efficacy of influenza vaccines, such as vaccines for pandemic influenza and influenza vaccines for use among the elderly. In addition, CA-CpG may be superior to CpG ODNs as an adjuvant for vaccines against cancer, because CA-CpG can induce not only antigen-specific antibody responses but also $CD8^+$ CTL responses. Thus, we believe that the novel pH-responsive CA nanoparticles reported herein have the potential to open up new avenues of research on vaccine adjuvant delivery vehicles. In addition, our results can be expected to lead to an improved understanding of the mechanisms of adjuvant effects and to the development novel particles or adjuvant delivery vehicles designed to improve vaccine efficacy.

ETHICS STATEMENT

All animal experiments were performed in accordance with the institutional guidelines of Osaka University for the ethical treatment of animals. All experiments using human peripheral blood mononuclear cells were approved by the Institutional Review Board of the Research Institute for Microbial Diseases, Osaka University.

AUTHOR CONTRIBUTIONS

HT, TA, HY, and YY designed the experiments and interpreted the results. HT, KM, YYamamoto, and YK performed the experiments. HT, KM, YYamamoto, YK, and YY collected and analyzed the data. XW, EK, and KI provided technical support and conceptual advice. HT and YY wrote the manuscript. YY supervised the study.

ACKNOWLEDGMENTS

We thank Dr. Yasuyuki Gomi (The Research Foundation for Microbial Diseases of Osaka University) and Dr. Toshihiro Akaike (Foundation for Advancement of International Science).

FUNDING

This study was supported by a grant from the Japan Society for the Promotion of Science (no. JP17H04009 to YYoshioka).

REFERENCES

1. Cohen J. Unfilled vials. *Science* (2016) 351(6268):16–9. doi:10.1126/science.351.6268.16
2. van der Burg SH, Arens R, Ossendorp F, van Hall T, Melief CJ. Vaccines for established cancer: overcoming the challenges posed by immune evasion. *Nat Rev Cancer* (2016) 16(4):219–33. doi:10.1038/nrc.2016.16
3. Plotkin SA. Vaccines: the fourth century. *Clin Vaccine Immunol* (2009) 16(12):1709–19. doi:10.1128/CVI.00290-09
4. Jones LH. Recent advances in the molecular design of synthetic vaccines. *Nat Chem* (2015) 7(12):952–60. doi:10.1038/nchem.2396
5. Bobbala S, Hook S. Is there an optimal formulation and delivery strategy for subunit vaccines? *Pharm Res* (2016) 33(9):2078–97. doi:10.1007/s11095-016-1979-0
6. Steinhagen F, Kinjo T, Bode C, Klinman DM. TLR-based immune adjuvants. *Vaccine* (2011) 29(17):3341–55. doi:10.1016/j.vaccine.2010.08.002
7. Baylor NW, Egan W, Richman P. Aluminum salts in vaccines – US perspective. *Vaccine* (2002) 20(Suppl 3):S18–23. doi:10.1016/S0264-410X(02)00166-4
8. Yewdell JW. Designing CD8+ T cell vaccines: it's not rocket science (yet). *Curr Opin Immunol* (2010) 22(3):402–10. doi:10.1016/j.coi.2010.04.002
9. Shirota H, Klinman DM. Recent progress concerning CpG DNA and its use as a vaccine adjuvant. *Expert Rev Vaccines* (2014) 13(2):299–312. doi:10.1586/14760584.2014.863715
10. Sablan BP, Kim DJ, Barzaga NG, Chow WC, Cho M, Ahn SH, et al. Demonstration of safety and enhanced seroprotection against hepatitis B with investigational HBsAg-1018 ISS vaccine compared to a licensed hepatitis B vaccine. *Vaccine* (2012) 30(16):2689–96. doi:10.1016/j.vaccine.2012.02.001
11. Janssen RS, Mangoo-Karim R, Pergola PE, Girndt M, Namini H, Rahman S, et al. Immunogenicity and safety of an investigational hepatitis B vaccine with a toll-like receptor 9 agonist adjuvant (HBsAg-1018) compared with a licensed hepatitis B vaccine in patients with chronic kidney disease. *Vaccine* (2013) 31(46):5306–13. doi:10.1016/j.vaccine.2013.05.067
12. Marschner A, Rothenfusser S, Hornung V, Prell D, Krug A, Kerkmann M, et al. CpG ODN enhance antigen-specific NKT cell activation via plasmacytoid dendritic cells. *Eur J Immunol* (2005) 35(8):2347–57. doi:10.1002/eji.200425721
13. Huber JP, Farrar JD. Regulation of effector and memory T-cell functions by type I interferon. *Immunology* (2011) 132(4):466–74. doi:10.1111/j.1365-2567.2011.03412.x
14. Kerkmann M, Costa LT, Richter C, Rothenfusser S, Battiany J, Hornung V, et al. Spontaneous formation of nucleic acid-based nanoparticles is responsible for high interferon-alpha induction by CpG-A in plasmacytoid dendritic cells. *J Biol Chem* (2005) 280(9):8086–93. doi:10.1074/jbc.M410868200
15. Tougan T, Aoshi T, Coban C, Katakai Y, Kai C, Yasutomi Y, et al. TLR9 adjuvants enhance immunogenicity and protective efficacy of the SE36/AHG malaria vaccine in nonhuman primate models. *Hum Vaccin Immunother* (2013) 9(2):283–90. doi:10.4161/hv.22950

16. Verthelyi D, Kenney RT, Seder RA, Gam AA, Friedag B, Klinman DM. CpG oligodeoxynucleotides as vaccine adjuvants in primates. *J Immunol* (2002) 168(4):1659–63. doi:10.4049/jimmunol.168.4.1659
17. Verthelyi D, Gursel M, Kenney RT, Lifson JD, Liu S, Mican J, et al. CpG oligodeoxynucleotides protect normal and SIV-infected macaques from *Leishmania* infection. *J Immunol* (2003) 170(9):4717–23. doi:10.4049/jimmunol.170.9.4717
18. Lande R, Gregorio J, Facchinetti V, Chatterjee B, Wang YH, Homey B, et al. Plasmacytoid dendritic cells sense self-DNA coupled with antimicrobial peptide. *Nature* (2007) 449(7162):564–9. doi:10.1038/nature06116
19. Kobiyama K, Aoshi T, Narita H, Kuroda E, Hayashi M, Tetsutani K, et al. Nonagonistic Dectin-1 ligand transforms CpG into a multitask nanoparticulate TLR9 agonist. *Proc Natl Acad Sci U S A* (2014) 111(8):3086–91. doi:10.1073/pnas.1319268111
20. Gungor B, Yagci FC, Tincer G, Bayyurt B, Alpdundar E, Yildiz S, et al. CpG ODN nanorings induce IFNalpha from plasmacytoid dendritic cells and demonstrate potent vaccine adjuvant activity. *Sci Transl Med* (2014) 6(235):235ra61. doi:10.1126/scitranslmed.3007909
21. Kerkmann M, Lochmann D, Weyermann J, Marschner A, Poeck H, Wagner M, et al. Immunostimulatory properties of CpG-oligonucleotides are enhanced by the use of protamine nanoparticles. *Oligonucleotides* (2006) 16(4):313–22. doi:10.1089/oli.2006.16.313
22. Chinnathambi S, Chen S, Ganesan S, Hanagata N. Binding mode of CpG oligodeoxynucleotides to nanoparticles regulates bifurcated cytokine induction via toll-like receptor 9. *Sci Rep* (2012) 2:534. doi:10.1038/srep00534
23. Chowdhury EH, Maruyama A, Kano A, Nagaoka M, Kotaka M, Hirose S, et al. pH-sensing nano-crystals of carbonate apatite: effects on intracellular delivery and release of DNA for efficient expression into mammalian cells. *Gene* (2006) 376(1):87–94. doi:10.1016/j.gene.2006.02.028
24. Hossain S, Stanislaus A, Chua MJ, Tada S, Tagawa Y, Chowdhury EH, et al. Carbonate apatite-facilitated intracellularly delivered siRNA for efficient knockdown of functional genes. *J Control Release* (2010) 147(1):101–8. doi:10.1016/j.jconrel.2010.06.024
25. Tada S, Chowdhury EH, Cho CS, Akaike T. pH-sensitive carbonate apatite as an intracellular protein transporter. *Biomaterials* (2010) 31(6):1453–9. doi:10.1016/j.biomaterials.2009.10.016
26. Wu X, Yamamoto H, Nakanishi H, Yamamoto Y, Inoue A, Tei M, et al. Innovative delivery of siRNA to solid tumors by super carbonate apatite. *PLoS One* (2015) 10(3):e0116022. doi:10.1371/journal.pone.0116022
27. Kobiyama K, Temizoz B, Kanuma T, Ozasa K, Momota M, Yamamoto T, et al. Species-dependent role of type I IFNs and IL-12 in the CTL response induced by humanized CpG complexed with beta-glucan. *Eur J Immunol* (2016) 46(5):1142–51. doi:10.1002/eji.201546059
28. Tamura S, Samegai Y, Kurata H, Nagamine T, Aizawa C, Kurata T. Protection against influenza virus infection by vaccine inoculated intranasally with cholera toxin B subunit. *Vaccine* (1988) 6(5):409–13. doi:10.1016/0264-410X(88)90140-5
29. Curtsinger JM, Valenzuela JO, Agarwal P, Lins D, Mescher MF. Type I IFNs provide a third signal to CD8 T cells to stimulate clonal expansion and differentiation. *J Immunol* (2005) 174(8):4465–9. doi:10.4049/jimmunol.174.8.4465
30. Haring JS, Badovinac VP, Harty JT. Inflaming the CD8+ T cell response. *Immunity* (2006) 25(1):19–29. doi:10.1016/j.immuni.2006.07.001
31. Keppler SJ, Rosenits K, Koegl T, Vucikuja S, Aichele P. Signal 3 cytokines as modulators of primary immune responses during infections: the interplay of type I IFN and IL-12 in CD8 T cell responses. *PLoS One* (2012) 7(7):e40865. doi:10.1371/journal.pone.0040865
32. Heikenwalder M, Polymenidou M, Junt T, Sigurdson C, Wagner H, Akira S, et al. Lymphoid follicle destruction and immunosuppression after repeated CpG oligodeoxynucleotide administration. *Nat Med* (2004) 10(2):187–92. doi:10.1038/nm987
33. Scheiermann J, Klinman DM. Clinical evaluation of CpG oligonucleotides as adjuvants for vaccines targeting infectious diseases and cancer. *Vaccine* (2014) 32(48):6377–89. doi:10.1016/j.vaccine.2014.06.065
34. Bourquin C, Anz D, Zwiorek K, Lanz AL, Fuchs S, Weigel S, et al. Targeting CpG oligonucleotides to the lymph node by nanoparticles elicits efficient antitumoral immunity. *J Immunol* (2008) 181(5):2990–8. doi:10.4049/jimmunol.181.5.2990
35. Knuschke T, Sokolova V, Rotan O, Wadwa M, Tenbusch M, Hansen W, et al. Immunization with biodegradable nanoparticles efficiently induces cellular immunity and protects against influenza virus infection. *J Immunol* (2013) 190(12):6221–9. doi:10.4049/jimmunol.1202654
36. Demento SL, Bonafe N, Cui W, Kaech SM, Caplan MJ, Fikrig E, et al. TLR9-targeted biodegradable nanoparticles as immunization vectors protect against West Nile encephalitis. *J Immunol* (2010) 185(5):2989–97. doi:10.4049/jimmunol.1000768
37. Tacken PJ, Zeelenberg IS, Cruz LJ, van Hout-Kuijer MA, van de Glind G, Fokkink RG, et al. Targeted delivery of TLR ligands to human and mouse dendritic cells strongly enhances adjuvanticity. *Blood* (2011) 118(26):6836–44. doi:10.1182/blood-2011-07-367615
38. Kachura MA, Hickle C, Kell SA, Sathe A, Calacsan C, Kiwan R, et al. A CpG-ficoll nanoparticle adjuvant for anthrax protective antigen enhances immunogenicity and provides single-immunization protection against inhaled anthrax in monkeys. *J Immunol* (2016) 196(1):284–97. doi:10.4049/jimmunol.1501903
39. de Titta A, Ballester M, Julier Z, Nembrini C, Jeanbart L, van der Vlies AJ, et al. Nanoparticle conjugation of CpG enhances adjuvancy for cellular immunity and memory recall at low dose. *Proc Natl Acad Sci U S A* (2013) 110(49):19902–7. doi:10.1073/pnas.1313152110
40. Gursel I, Gursel M, Ishii KJ, Klinman DM. Sterically stabilized cationic liposomes improve the uptake and immunostimulatory activity of CpG oligonucleotides. *J Immunol* (2001) 167(6):3324–8. doi:10.4049/jimmunol.167.6.3324
41. Shivahare R, Vishwakarma P, Parmar N, Yadav PK, Haq W, Srivastava M, et al. Combination of liposomal CpG oligodeoxynucleotide 2006 and miltefosine induces strong cell-mediated immunity during experimental visceral leishmaniasis. *PLoS One* (2014) 9(4):e94596. doi:10.1371/journal.pone.0094596
42. Zhang XQ, Dahle CE, Weiner GJ, Salem AK. A comparative study of the antigen-specific immune response induced by co-delivery of CpG ODN and antigen using fusion molecules or biodegradable microparticles. *J Pharm Sci* (2007) 96(12):3283–92. doi:10.1002/jps.20978
43. Fischer S, Schlosser E, Mueller M, Csaba N, Merkle HP, Groettrup M, et al. Concomitant delivery of a CTL-restricted peptide antigen and CpG ODN by PLGA microparticles induces cellular immune response. *J Drug Target* (2009) 17(8):652–61. doi:10.1080/10611860903119656
44. Peine KJ, Bachelder EM, Vangundy Z, Papenfuss T, Brackman DJ, Gallovic MD, et al. Efficient delivery of the toll-like receptor agonists polyinosinic:polycytidylic acid and CpG to macrophages by acetalated dextran microparticles. *Mol Pharm* (2013) 10(8):2849–57. doi:10.1021/mp300643d
45. Leifer CA, Medvedev AE. Molecular mechanisms of regulation of toll-like receptor signaling. *J Leukoc Biol* (2016) 100(5):927–41. doi:10.1189/jlb.2MR0316-117RR
46. Majer O, Liu B, Barton GM. Nucleic acid-sensing TLRs: trafficking and regulation. *Curr Opin Immunol* (2017) 44:26–33. doi:10.1016/j.coi.2016.10.003
47. Honda K, Ohba Y, Yanai H, Negishi H, Mizutani T, Takaoka A, et al. Spatiotemporal regulation of MyD88-IRF-7 signalling for robust type-I interferon induction. *Nature* (2005) 434(7036):1035–40. doi:10.1038/nature03547
48. Sasai M, Linehan MM, Iwasaki A. Bifurcation of toll-like receptor 9 signaling by adaptor protein 3. *Science* (2010) 329(5998):1530–4. doi:10.1126/science.1187029
49. Brewer JM, Pollock KG, Tetley L, Russell DG. Vesicle size influences the trafficking, processing, and presentation of antigens in lipid vesicles. *J Immunol* (2004) 173(10):6143–50. doi:10.4049/jimmunol.173.10.6143
50. Tran KK, Shen H. The role of phagosomal pH on the size-dependent efficiency of cross-presentation by dendritic cells. *Biomaterials* (2009) 30(7):1356–62. doi:10.1016/j.biomaterials.2008.11.034
51. Rejman J, Oberle V, Zuhorn IS, Hoekstra D. Size-dependent internalization of particles via the pathways of clathrin- and caveolae-mediated endocytosis. *Biochem J* (2004) 377(Pt 1):159–69. doi:10.1042/BJ20031253
52. Reddy ST, Rehor A, Schmoekel HG, Hubbell JA, Swartz MA. In vivo targeting of dendritic cells in lymph nodes with poly(propylene sulfide) nanoparticles. *J Control Release* (2006) 112(1):26–34. doi:10.1016/j.jconrel.2006.01.006
53. Reddy ST, van der Vlies AJ, Simeoni E, Angeli V, Randolph GJ, O'Neil CP, et al. Exploiting lymphatic transport and complement activation in nanoparticle vaccines. *Nat Biotechnol* (2007) 25(10):1159–64. doi:10.1038/nbt1332
54. Manolova V, Flace A, Bauer M, Schwarz K, Saudan P, Bachmann MF. Nanoparticles target distinct dendritic cell populations according to their size. *Eur J Immunol* (2008) 38(5):1404–13. doi:10.1002/eji.200737984

55. Kuroda E, Coban C, Ishii KJ. Particulate adjuvant and innate immunity: past achievements, present findings, and future prospects. *Int Rev Immunol* (2013) 32(2):209–20. doi:10.3109/08830185.2013.773326
56. Yoshioka Y, Kuroda E, Hirai T, Tsutsumi Y, Ishii KJ. Allergic responses induced by the immunomodulatory effects of nanomaterials upon skin exposure. *Front Immunol* (2017) 8:169. doi:10.3389/fimmu.2017.00169
57. Askonas BA, Taylor PM, Esquivel F. Cytotoxic T cells in influenza infection. *Ann N Y Acad Sci* (1988) 532:230–7. doi:10.1111/j.1749-6632.1988.tb36342.x
58. Laidlaw BJ, Decman V, Ali MA, Abt MC, Wolf AI, Monticelli LA, et al. Cooperativity between CD8+ T cells, non-neutralizing antibodies, and alveolar macrophages is important for heterosubtypic influenza virus immunity. *PLoS Pathog* (2013) 9(3):e1003207. doi:10.1371/journal.ppat.1003207

Conflict of Interest Statement: The following authors have conflict of interests to declare. TA, Y Yamamoto, and Y Yoshioka are employed by The Research Foundation for Microbial Diseases of Osaka University. HY and Y Yoshioka have filed a patent application related to the content of this manuscript. The other authors have no conflicts of interest to declare.

frontiers in Immunology

ORIGINAL RESEARCH
published: 19 April 2018
doi: 10.3389/fimmu.2018.00791

Polymeric Nanocapsules for Vaccine Delivery: Influence of the Polymeric Shell on the Interaction With the Immune System

Mercedes Peleteiro[1†], Elena Presas[2,3†], Jose Vicente González-Aramundiz[3,4], Beatriz Sánchez-Correa[1,5], Rosana Simón-Vázquez[1], Noemi Csaba[2,3], María J. Alonso[2,3] and África González-Fernández[1*]*

[1] Inmunología, Centro de Investigaciones Biomédicas (CINBIO) (Centro Singular de Investigación de Galicia), Instituto de Investigación Sanitaria Galicia Sur, Universidade de Vigo, Vigo, Spain, [2] Department of Pharmacy and Pharmaceutical Technology, School of Pharmacy, University of Santiago de Compostela, Santiago de Compostela, Spain, [3] Center for Research in Molecular Medicine and Chronic Diseases (CIMUS), University of Santiago de Compostela, Santiago de Compostela, Spain, [4] Departamento de Farmacia, Facultad de Química, Pontificia Universidad Católica de Chile, Santiago, Chile, [5] Immunology Unit, University of Extremadura, Cáceres, Spain

OPEN ACCESS

Edited by:
Urszula Krzych,
Walter Reed Army Institute of Research, United States

Reviewed by:
Thorsten Demberg,
Immatics Biotechnologies, Germany
Serge Muyldermans,
Vrije Universiteit Brussel, Belgium

***Correspondence:**
María J. Alonso
mariaj.alonso@usc.es;
África González-Fernández
africa@uvigo.es

[†]These authors have contributed equally to this work.

Specialty section:
This article was submitted to Vaccines and Molecular Therapeutics, a section of the journal Frontiers in Immunology

Received: 18 January 2018
Accepted: 29 March 2018
Published: 19 April 2018

Citation:
Peleteiro M, Presas E, González-Aramundiz JV, Sánchez-Correa B, Simón-Vázquez R, Csaba N, Alonso MJ and González-Fernández Á (2018) Polymeric Nanocapsules for Vaccine Delivery: Influence of the Polymeric Shell on the Interaction With the Immune System. Front. Immunol. 9:791. doi: 10.3389/fimmu.2018.00791

The use of biomaterials and nanosystems in antigen delivery has played a major role in the development of novel vaccine formulations in the last few decades. In an effort to gain a deeper understanding of the interactions between these systems and immunocompetent cells, we describe here a systematic *in vitro* and *in vivo* study on three types of polymeric nanocapsules (NCs). These carriers, which contained protamine (PR), polyarginine (PARG), or chitosan (CS) in the external shell, and their corresponding nanoemulsion were prepared, and their main physicochemical properties were characterized. The particles had a mean particle size in the range 250–450 nm and a positive zeta potential (~30–40 mV). The interaction of the nanosystems with different components of the immune system were investigated by measuring cellular uptake, reactive oxygen species production, activation of the complement cascade, cytokine secretion profile, and MAP kinases/nuclear factor κB activation. The results of these *in vitro* cell experiments showed that the NC formulations that included the arginine-rich polymers (PR and PARG) showed a superior ability to trigger different immune processes. Considering this finding, protamine and polyarginine nanocapsules (PR and PARG NCs) were selected to assess the association of the recombinant hepatitis B surface antigen (rHBsAg) as a model antigen to evaluate their ability to produce a protective immune response in mice. In this case, the results showed that PR NCs elicited higher IgG levels than PARG NCs and that this IgG response was a combination of anti-rHBsAg IgG1/IgG2a. This work highlights the potential of PR NCs for antigen delivery as an alternative to other positively charged nanocarriers.

Keywords: nanocapsules, vaccination, antigen, adjuvant, hepatitis B, rHBsAg, nanovaccines

INTRODUCTION

Vaccination is one of the most cost-effective health interventions for the prophylaxis of infectious diseases. Conventional vaccines use inactivated or attenuated pathogens—or even subunits of these organisms, such as toxoids and carbohydrates—as antigens (1). Unfortunately, the immune protection provided by these subunit vaccines, even with classical adjuvants, i.e., alum, is often insufficient.

Moreover, these vaccines suffer from additional problems, such as limited storage stability and the need for multiple-dose injection schemes to achieve effective protection. Thus, vaccine development has been required to move toward a new generation of vaccines that could provide better and more sustainable protective immune responses (2).

Interest in the use of innovative antigens such as recombinant proteins, peptides, or nucleic acids has increased in the last few decades (3–5). In spite of the many advantages of these new vaccine prototypes, including an enhanced immunogenicity/risk ratio profile and easier manufacture, the development of improved adjuvants that may enhance the potency of these vaccines has become essential. Several inmunostimulant molecules (i.e., cytokines, toll-like receptor ligands, toxins, or saponins) and antigen delivery systems (i.e., virosomes, emulsions, or nanoparticles) are among the potential adjuvants studied in this scope. In particular, the use of nanosystems has attracted significant attention, especially for vaccines requiring an improvement in cell-mediated immune responses (6).

Polymer- and lipid-based nanoparticles have been the most widely explored nanosystems in vaccination. It has already been reported that nanostructures are able to enhance both B and T cell responses due to their similarity with viruses in terms of size and surface properties (7). In addition, due to their prolonged presentation to the immune system, these nanostructures can induce long-lasting immune responses, thereby offering the possibility of decreasing the number of doses required to achieve protective antibody levels. Moreover, nanoparticle formulations have shown the ability to avoid overactivation of the immune response and, simultaneously, to trigger the production of pro-inflammatory cytokines (8).

Our group has developed a number of antigen delivery technologies and validated them using rHBsAg as a model antigen. Namely, we have produced various chitosan-based nanocarriers, including chitosan-coated PLGA nanoparticles (9), CS nanoparticles (10), and CS nanocapsules (NCs) (11). More recently, we also developed arginine-rich based (PARG and PR) NCs (12) and nanoparticles including different anionic polymers (dextran sulfate and alginate) (13). Overall, the *in vivo* administration of these nanocarriers through nasal or parenteral routes has led to significant IgG responses in mice (11, 14). Interestingly, the differences obtained in the elicited immune responses highlighted the importance of the composition of the nanosystem, especially concerning the type of biopolymer exposed on the nanoparticle surface.

The aim of the work described here was to gain an understanding of the role of the polymeric shell of NCs in their interaction with immune cells. For this purpose, three types of NCs with different coating polymers (PARG, PR, and CS), and the corresponding nanoemulsion (NE), were compared in a systematic study. This included the *in vitro* evaluation of cellular uptake, the reactive oxygen species (ROS) production, the activation of the complement cascade, the cytokine secretion profile, the MAP kinases/nuclear factor κB (NFκB) activation, and gene expression. The influence of size, composition of the outer shell layer, and superficial charge in these processes were analyzed, and the two most promising prototypes were selected to perform *in vivo* studies with the rHBsAg antigen. In addition to the systematic study, the four different prototypes were converted into freeze-dried products, to enhance the stability of the formulations under storage and avoid the need of the maintenance of the cold chain. The physicochemical characterization of the resulting products is disclosed in Supplementary Material.

MATERIALS AND METHODS

Materials

Three polymers were used: protamine from Yuki Gosei Kogyo, Ltd. Company (Japan), chitosan hydrochloride salt (Protasan UP CL113 deacetylation degree of 75–90%, M_w: 125 kDa) was purchased from NovaMatrix (Sandvika, Norway) and polyarginine (PARG) (M_w 5–15 kDa) was obtained from Sigma-Aldrich (Barcelona, Spain). Miglyol® 812, a mixture of three different triglycerides of medium chain fatty acids, was obtained from Sasol GmbH (Witten, Germany). Recombinant hepatitis B surface antigen (rHBsAg) (M_w 24 kDa) in an aqueous suspension [0.16 mg/mL in phosphate-buffered saline (PBS)] was kindly donated by Shantha Biotechnics Limited (Hyderabad, India). PEG-stearate (Simulsol® M52) was purchased from Invitrogen (UK). Cobra venom factor (CVF) was supplied by Quidel Corporation (USA), and the PVDF membranes were obtained from Bio-Rad (USA).

Aluminum hydroxide, sodium hydroxide, rhodamine 6G, Triton 100x, PBS, 5-bromo-4-chloro-3-indolyl phosphate (BCIP), glycerol, sodium cholate, 2′,7-dichlorofluorescein diacetate (DCFH-DA), lipopolysaccharide (LPS), phorbol myristate acetate (PMA), and phytohemagglutinin (PHA) were all obtained from Sigma-Aldrich (USA).

Cell culture media (DMEM and RPMI 1640) and the antibiotics penicillin and streptomycin were supplied by Gibco (Life Technologies, Scotland). Heat inactivated fetal bovine serum (FBS) and Accutase® were purchased from PAA Laboratories (Austria), and Ficoll-Hypaque was obtained from GE Healthcare (Sweden).

Antibodies

Enzyme-Linked Immunosorbent Assay (ELISA) for Recombinant Hepatitis B Antigen (rHBsAg)

Enzyme-linked immunosorbent assay kit (Murex HBsAg Version 3) was obtained from Murex Biotech Ltd. (Dartford, UK), and the polyclonal chicken antibodies against HBsAg were purchased from Abcam (UK). Mouse and rabbit antibodies against HBsAg used in the ELISA test were purchased from Acris Antibodies GmbH (Hiddenhausen, Germany) and Biokit (Barcelona, Spain), respectively. Secondary mouse antibodies against IgG, IgG1, IgG2a conjugated with horseradish peroxidase (HRP) were acquired from Southern Biotech (USA).

Western Blot and ELISA for Complement Factors (C3 and C5)

Polyclonal secondary antibodies used in the Western blot assay were purchased from Dako (Glostrup, Denmark), and the monoclonal antibody (mAb) against complement factor C3 was obtained from Abcam (UK). Human C5a ELISA Kit II BD

OptEIA™ used for the detection of complement factor C5 was purchased from BD Biosciences Pharmingen (CA, USA).

Flow Cytometry: Cell Markers and Cytokines

Monoclonal antibodies for flow cytometry assays were anti-CD3-PECy5.5, anti-CD19-PECy5.5 (Southern Biotech, AL, USA), anti-HLA-DR-FITC (Beckman Coulter, USA), and anti-CD71-PE (NIT Zipper, Nanoimmunotech, Spain).

Cytokine detection was performed with the FlowCytomix kit Th1/Th2 from eBioscience (San Diego, CA, USA).

Analysis of Kinase Routes by Western Blot

Rabbit monoclonal antihuman p-extracellular signal-regulated kinase (ERK), p-p38, p-SAP/JNK, IKBα, and goat anti-rabbit IgG-HRP antibodies used for the Western blot analysis were supplied by Cell Signaling Tech. (Danvers, MA, USA), and the anti-GAPDH antibody was obtained from Sigma-Aldrich (Barcelona, Spain).

Nanoparticle Preparation

Nanocapsules were prepared using the solvent displacement technique previously described by our research group (15). Briefly, a mixture of 12 mg of PEG-st and 5 mg of sodium cholate was dissolved in 0.750 mL of ethanol, followed by the addition of 62.5 μL of Miglyol® 812 to the previous mixture. The volume of the organic phase was increased by adding 4.25 mL of acetone. This organic phase was added to an aqueous phase composed of 10 mL of a solution of 0.05% w/v of PR, PARG, or CS for the preparation of the PR and CS NCs or 10 mL of milliQ water in the case of the control, uncoated NE. In all cases, the nanostructures were spontaneously formed upon diffusion of the solvents. The nanostructures were isolated by ultracentrifugation of the samples at 61,690 *g* for 1 h at 15°C (Optoma TM L-90K Ultracentrifuge, Beckman Coulter, USA).

Physicochemical Characterization of the Nanostructures

The hydrodynamic diameter and polydispersity index (PDI) of the NCs and the corresponding NE were measured by photon correlation spectroscopy. Zeta potential was determined by laser-Doppler anemometry (Zetasizer®, NanoZS, Malvern Instruments, Malvern, UK). Samples were measured after diluting in milliQ water (970 μL of water: 30 μL of NCs) or in 1 mM KCl for size and zeta potential, respectively.

Fluorescent Labeling of the Nanocarriers

Nanocapsules were prepared as described in Section "Nanoparticle Preparation" by adding an aliquot of the chromophores to the oily phase. Rhodamine B, rhodamine 6G, and DiD (1,1′-dioctadecyl-3,3,3′,3′-tetramethylindodicarbocyanine, 4-chlorobenzenesulfonate salt) were selected as fluorescent markers at two different concentrations (10 and 50 μg/mL dissolved in ethanol), evaluating both the influence of the nature of the chromophore and its concentration. The evaluation of the encapsulation efficiency of the chromophores was carried out indirectly by quantifying the non-encapsulated fluorophore remaining in the undernatants after the centrifugation step. Rhodamines were measured at an emission wavelength of 590 nm (LB 940 Multimode Reader Mithras, Berthold Technologies GmbH & Co KG, Germany); UV–VIS spectroscopy at $\lambda = 646$ nm (Du-BoLife Science UV/VIS Beckman Coulter) was used to quantify DiD. The three different fluorophores were incorporated into the NE, PR and CS NCs, assuming no differences in the release and the encapsulation efficiency between the PR and the PARG NCs. The evaluation of the loading efficiency and release profile of the different fluorescent dyes are disclosed in Supplementary Material (Supplementary Figure 1 and Supplementary Table 1).

Association of Hepatitis B Surface Antigen (rHBsAg) With the NCs

PR and PARG NCs, prepared as described in Section "Nanoparticle preparation," were incubated with rHBsAg in equal volumes at a mass ratio of 4:1 (theoretical concentration of the cationic polymer adsorbed on the NC surface:rHBsAg) to achieve adsorption onto the polymeric corona. The process was performed under mild conditions (RT, 1 h), and the loaded NCs were subsequently isolated (30 min, 12,872 *g*, 15°C). The amount of rHBsAg associated to the NCs was indirectly quantified by measuring the concentration of antigen remaining in the undernatant after the ultracentrifugation step. An ELISA commercial kit was used to quantify the rHBsAg concentration in the samples, according to the manufacturer's instructions. The association efficiency for rHBsAg (A.E.%) was calculated indirectly as the difference between the concentration of free antigen detected in the supernatant and the total concentration in the initial suspension.

Freeze Drying of the NCs

To obtain a lyophilized product, preliminary studies were carried out to determine the best conditions to preserve the original physicochemical properties of the prototypes upon reconstitution (Supplementary Figure 2). The conversion into a dry powder was performed using a freeze-drying process (Genesis SQ Freeze dryer, Virtis, USA) (11). The studies were conducted with aliquots of the four nanosystems in a range of concentrations (0.25–1% w/v) both with and without cryoprotectant (glucose, trehalose, and sucrose at 5 and 10% w/v). Based on the results obtained, and to standardize the process conditions for the four prototypes, a solution of each of the different nanosystems (0.75% w/v) was frozen overnight at −20°C in the presence of sucrose as cryoprotectant (10% w/v). Subsequently, the samples were transferred to the lyophilizer (Genesis SQ Freeze Drier, Virtis, USA) and submitted to an initial drying step for 24 h at −35°C and 2–10 mTorr followed by a second and a third drying step (24 h, 0°C and 16 h, 20°C, respectively). After the process, the freeze-dried cake had an overall good aspect and could be resuspended swiftly in ultrapure water.

Activation of the Complement Cascade

The activation of the complement cascade upon contact with the different nanostructures was analyzed by two methods: degradation of the complement C3 factor by Western blot and

quantification of the C5a levels by ELISA. A pool of human plasma from healthy donors was incubated with different concentrations of nanosystems (10, 100, and 1,000 μg/mL of the constituent polymer and the corresponding amount of NE) and veronal buffer (pH 7.4). An aliquot of 50 μL of each formulation and controls were incubated at 37°C for 1 h. CVF and PBS were used as positive and negative controls, respectively. After the incubation step, samples were centrifuged at 16,000 *g* for 30 min to separate the nanosystems from the other components.

Qualitative Determination by Western Blot

After the centrifugation step, supernatants containing the complement proteins were loaded onto a 10% SDS-PAGE gel and transferred to a PVDF membrane with the Transblot-Turbo Transfer System (Bio-Rad, Hercules, CA, USA). Membranes were blocked overnight at 4°C with TBST with 5% of non-fat dried milk. Membranes were then incubated with a mouse mAb against human C3 (1:1,000) (90 min, RT). A secondary incubation step was performed under the same conditions (90 min, RT) with secondary polyclonal goat anti-mouse IgG antibodies conjugated with alkaline phosphatase (1:2,000). Intensive washes were carried out between all steps. Membranes were revealed with BCIP. To quantify the degradation, the intensity of the lower band was normalized to the negative control, where some basal C3 degradation was observed.

Quantitative Determination by ELISA

An ELISA assay was performed using the Human C5a ELISA Kit II to confirm the activation of the complement cascade quantifying C5a factor levels. Briefly, standards and samples were added for 2 h at RT to the wells previously coated with an mAb against the C5a factor. After several washes, wells were incubated for 1 h with a mixture of biotinylated antihuman C5a antibody and streptavidin-HRP. Intensive washes were performed between all these steps. To detect the presence of the antibody-antigen complexes, TMB Substrate Reagent was added. After 30 min of incubation, the reaction was stopped, and the absorbance was measured at 450 nm.

In Vitro Cell Studies

Cells

Raw 264.7 (mouse macrophage cell line), Jurkat (human leukemic T-cell line), Hmy (human B lymphoblast cell line), and HL60 (human promyelocytic leukemia cell line) were purchased from ATCC (American Type Culture Collection, Middlesex, UK). All lines were cultured in RPMI supplemented with 10% (v/v) of heated-inactivated FBS, 2 mM glutamine, and 100 U/mL of penicillin/streptomycin, at 37°C in a 5% CO_2 atmosphere. Cells were split every other day to maintain 70–80% confluent cultures.

Human peripheral blood mononuclear cells (hPBMCs) were obtained from three healthy voluntary donors. To separate mononuclear cells, 15 mL of EDTA-anticoagulated blood was diluted with 15 mL of PBS and centrifuged (180 *g*, 30 min, 20°C) through a Ficoll-Hypaque gradient using a 7:3 ratio (diluted blood:ficoll). Mononuclear cells were collected at the interface between the ficoll and the plasma and washed twice by centrifugation (100 *g*, 5 min, 20°C) with complete medium.

Cell Viability Assay: xCELLigence® System

An xCELLigence® RTCA DP Instrument (Roche Diagnostics, Penzberg, Germany) was used according to the manufacturer's instructions to analyze cell viability. Raw 264.7 cells were cultured at a density of 1.5×10^4 cells/well with 200 μL of RPMI supplemented with 10% FBS until they reached the exponential phase (37°C and 5% CO_2) (around 18 h). The different prototypes were added in a range of six different concentrations from 250 to 7.8 μg/mL. As negative controls, cell culture media and the blank nanosystems were added to the wells. The impedance was monitored at 15 min intervals for 72 h.

Cellular Uptake by Macrophages

To evaluate the internalization of the nanosystems by fluorescence microscopy, 1×10^5 of Raw 264.7 cells were seeded in an NUNC 96-Well Optical-Bottom Plates with Coverglass Base (Thermo Fisher Scientific, Langenselbold, Germany) with RPMI 10% FBS in the presence and absence of the fluorescent prototypes at 10 and 50 μg/mL of the constituent polymer and the corresponding amount of NE for 30 min. Three washes were performed to remove the excess nanosystems, and cells were observed with an inverted fluorescence microscope (IX50, Olympus Optical Co. GmbH, Hamburg, Germany).

A similar protocol was followed to perform the flow cytometry analysis. In this case, after incubation with the fluorescently labeled prototypes followed by three washes with PBS, cells were detached using Accutase® (10 min, 37°C and 5% CO_2). Finally, cells were washed once with complete medium to inactivate Accutase®, and the suspension was analyzed by flow cytometry (Accuri Cytometers, Ann Arbor, MI, USA).

A kinetic and more detailed study of the internalization was carried out by Confocal Laser Scanning Microscopy (Leica SP5) using the High Content Screening Automation HCS A module and the LAS AF MATRIX software. Images were acquired every 5 min during 3 h.

Cytokine Profile Evaluation

Cytokine production was assessed by incubating 2×10^5 hPBMCs during 24 h in 96-well plates (37°C, 5% CO_2) in the presence of the prototypes at two different concentrations: 10 and 100 μg/mL. As negative and positive controls, cells were incubated with complete medium or with a combination of a solution of 1 μg/mL of LPS and 10 μg/mL of PHA, respectively. After 24 h, the plate was centrifuged (100 *g*, 5 min, 4°C), and supernatants were collected and stored at −20°C before analysis. The cytokine levels (IL-12p70, INFγ, IL-2, IL-10, Il-8, IL-6, IL-4, IL-5, IL-1β, TNFα, and TNF β) were quantified using the FlowCytomix kit Th1/Th2 according to the manufacturer's instructions. Briefly, 25 μL of antibody-coated microspheres was incubated with 25 μL of culture supernatants and 50 μL of biotin-conjugated secondary antibodies (2 h, RT) using a microplate shaker. After several washes, 50 μL of streptavidin conjugated to phycoerythrin and 100 μL of PBS-T were added to the preparation and incubated on a microplate shaker (1 h, RT). Finally, phycoerythrin-bound

beads were studied by flow cytometry (FC500, Beckman Coulter, Miami, FL, USA), and data were analyzed using FlowCytomix Pro 3.0 Software (eBioscience, San Diego, CA, USA).

ROS Production

The production of intracellular ROS was detected by measuring the oxidation of 2′,7-dichlorofluorescein diacetate (DCFH-DA). This marker can be oxidized by ROS and converted to a fluorescent compound.

The human promyeloblast cell line HL60 was used to evaluate the production of ROS. 2.5×10^5 cells were cultured in 24-well plates in contact with 10 or 100 μg/mL of the different prototypes after 1 and 12 h. As negative and positive controls, complete medium and a solution of 10 μM of PMA were used, respectively. After this incubation step, cells were collected and centrifuged (100 *g*, 5 min) and resuspended in PBS containing 5 μM of DCFH-DA. Afterward, the samples were incubated at 37°C during 30 min. Finally, cells were washed twice with PBS and analyzed by flow cytometry (Accuri Cytometers, Ann Arbor, MI, USA). The median of the fluorescence intensity was normalized to the negative control.

Activation Markers

Changes in the pattern of expression of membrane markers were studied in hPBMCs (CD3, CD19, CD71, and HLA-DR). 2×10^5 cells were seeded in a 96-well plate and incubated with and without the nanosystems at two different concentrations (10 and 100 μg/mL of the constituent polymer and the corresponding amount of the NE) during 24 h. As a positive control, a solution of 10 μg/mL of PHA was used. Cells were labeled with the antibodies during 30 min at 4°C. In a final, the cells were washed twice with PBS and analyzed by flow cytometry (FC500, Beckman Coulter, Miami, FL, USA).

Routes of Activation. MAP Kinases and NFκB

The study of the signaling pathway activation (ERK1/2, p38, SAPK/JNK and NFκB) was performed with the human tumoral cell lines Jurkat and Hmy. These two cell lines were incubated with 10 μg/mL of the constituent polymer of PR NCs and PARG NCs for 1 and 3 h.

To perform the Western blot analysis, cells were washed with PBS and then suspended in a lysis buffer (Tris–HCl 10 mM, pH 8, NaCl 150 mM, EDTA 2.5 mM and 1% NP-40) containing a protease and phosphatase inhibitor (Complete Mini and PhosphoStop from Roche Ltd., Basel, Switzerland). Cell lysates were centrifuged (16,000 *g*, 4°C, 5 min) using an Eppendorf 5415R centrifuge (Eppendorf AG, Hamburg, Germany) to remove cell residues.

Cell extracts were loaded onto a 10% SDS-PAGE gel and transferred to a PVDF membrane using the Transblot-Turbo Transfer System (Bio-Rad, Hercules, CA, USA). PVDF membranes were blocked with 5% of non-fat dried milk in TBST (1 h, RT). Membranes were washed and incubated overnight at 4°C with specific rabbit monoclonal antihuman p-ERK, p-, and p-SAP/JNK antibodies to determine the phosphorylation of ERK, p38, and SAP/JNK kinases (dilutions from 1:10,000 to 1:20,000 in TBST) and with anti IKBα (1:10,000), which is the NFκB inhibitor, to evaluate its activation indirectly. After intensive washes, membranes were incubated with the anti-GAPDH antibody as internal control (1:40,000) for 1 h at RT. Goat anti-rabbit IgG antibodies conjugated to HRP diluted 1:50,000 in TBST with 2.5% of skimmed milk were used as secondary antibodies.

Membranes were revealed with the Clarity Western ECL Substrate (Bio-Rad Laboratories Inc.), and the protein bands were analyzed and quantified using the ChemiDoc XRS imaging system (Bio-Rad Laboratories Inc.).

In Vivo Studies

Animals

Female BALB/c mice (4–5 weeks old) were housed in filter-top cages with a 12 h light/12 h dark cycle with a constant temperature environment of 22°C. Food and water were provided *ad libitum*.

Groups of five animals were randomly distributed and immunized twice (0 and 28 days) with 60 μL of PR NCs or PARG NCs incorporating 10 μg of rHBsAg. The injection was performed intramuscularly (i.m.) in the hind leg of the mouse and rHBsAg adsorbed to aluminum hydroxide was used as a positive control. Aluminum hydroxide and rHBsAg solutions were incubated in a volumetric ratio of 3:1 (rHBsAg:alum) for 30 min at 4°C under moderate agitation. The suspension was centrifuged (10,000 *g*, 10 min, 4°C), and the pellet was resuspended in a suitable volume of isotonic saline solution. Blood samples were collected from the mouse maxillary vein at 6 and 10 weeks for the quantification of HBsAg-specific antibodies.

Quantification of rHBsAg-Specific IgG and IgG Subtypes by ELISA

96-Well plates were coated with rHBsAg diluted in carbonate buffer (pH 9.6) at a concentration of 5 μg/mL and incubated overnight at 4°C. The plates were then blockaded with PBS-BSA 1% for 1 h at 37°C to reduce the non-specific interactions. A mouse monoclonal IgG anti-HBsAg was used to quantify the levels of specific rHBsAg IgG: the μg/mL of the specific IgG were converted into international units using a solution of anti-HBsAg rabbit IgG with a known concentration into mIU/mL. The controls and a pool of serum samples from each group were serially diluted and incubated for 2 h at 37°C. Two secondary antibodies (goat anti-mouse and anti-rabbit IgG conjugated with HRP) were added and incubated with the samples for 1 h at 37°C. Bound antibodies were revealed with 2,2′-azino-bis(3-ethylbenzothiazoline-6-sulfonic acid) (ABTS), and the optical density was read at 405 nm.

To calculate the ratio IgG1/IgG2a, a pool of sera collected from the immunized mice were analyzed using the same ELISA protocol, but using the goat anti-mouse IgG1 and IgG2a (conjugated to HRP) as secondary antibodies.

Restimulation of Splenocytes *Ex Vivo* for Quantitative PCR (qPCR) Gene Expression Assays

Changes in gene expression were evaluated by qPCR using TaqMan® Gene Expression Assays for several genes and the TaqMan® Fast Advanced Master Mix from Life Technologies™.

The qPCR was performed in a 7900HT Fast Real-Time PCR System (AB, Life Technology Co.).

Mice previously immunized with two intramuscular doses (0, 4 weeks) were sacrificed at the end of the study (11 weeks after the first immunization). To obtain cell suspensions, spleens were removed under sterile conditions, and cells were dissociated by gentle teasing in complete medium (DMEM with 10% FBS) and filtered with a cell strainer (Falcon, NJ, USA). The suspension was centrifuged (100 *g*, 5 min), and the pellet was resuspended in 7 mL of DMEM. The same protocol followed to obtain hPBMCs was carried out to eliminate spleen erythrocytes and granulocytes.

Mononuclear cells separated by gradient centrifugation at a concentration of 5×10^6 cells/mL were restimulated with 10 µg/mL of rHBsAg for 12 or 24 h. RNA was extracted and purified using the ReliaPrep™ RNA Miniprep Systems kit (Promega), and genomic DNA was eliminated with the same kit. The cDNA was synthetized using the Maxima First Strand cDNA Synthesis kit (Thermo Fisher Scientific Inc.). To check the optimal concentration of cDNA per sample, a qPCR for GAPDH was previously performed at different dilutions.

Data from three mice per group were normalized to the internal control GAPDH, and ΔΔCt was calculated using as a baseline the control data from mice immunized with PBS 1× and restimulated *in vitro* with rHBsAg. These data were averaged, and relative quantification (RQ) was calculated.

Statistical Analysis

Results are presented as Mean ± SD. Statistical comparisons were made by the Mann–Whitney *U* test for *in vivo* experiments and *T* test for *in vitro* experiments. The accepted level of significance was a p value < 0.05.

Ethical Issues

Institutional ethics approval to work with human samples from healthy donors was obtained from the Ethics Committee for Clinical Research (Xunta de Galicia, Spain, 2013/272). All participants included in the study gave their written informed consent.

All protocols developed with mice were adapted from the guidelines of the Spanish regulations (Royal Decree 53/2013) regarding the use of animals in scientific research and under the approval of the Ethical Committee of the University of Vigo.

RESULTS AND DISCUSSION

Development and Characterization of Polymeric NCs

The method selected for the preparation of the nanostructures was the solvent displacement technique previously described by our research group (16). The procedure is based on the nanoprecipitation of the lipid components upon the diffusion of a polar solvent into an aqueous phase, where the cationic polymer interacts with the oily nanodroplet cores, thus forming a polymeric coating that surrounds the oily core. Polycationic NCs made of CS (11, 14), PARG (17) and PR (12) with different oil/surfactant ratios were previously developed by our research group. In this work, the type and the ratio of the lipidic constituents were adjusted to develop nanocarriers with the identical oily core composition but varying the polymeric surface coatings. As a result, three different NC formulations and the corresponding negatively charged NE were developed (**Table 1**). As expected, the three NC formulations had a positive zeta potential and their size varied depending on the nature of the polymer shell. PR and PARG NCs presented zeta potential values close to +30 mV, whereas the value for CS NCs was higher (+47 mV), probably due to the presence of a larger number of positive groups on their surface. With respect to the particle size, PR or PARG NCs had similar sizes, within the range 250–300 nm, and a low PDI (0.2 and 0.1, respectively). By contrast, CS NCs had a larger size and higher PDI (456 ± 2; 0.3). This result can be explained by the different entanglement of the tensioactive agents (PEG-stearate and sodium cholate) with the cationic polymers at the interface of the oily cores. In fact, CS NCs with reduced sizes could also be produced by adjusting the surfactant composition (11).

Loading of rHBsAg Antigen Onto the NCs

Based on the results obtained in the different cellular studies, PR and PARG NCs were selected for loading with rHBsAg. The incorporation of the antigen into the nanostructure surface was attributed to electrostatic forces occurring between the cationic polypeptide of the polymer coating and the negatively charged antigen (−20 mV), as well as to hydrophobic interactions between the antigen and the tensioactive molecules. To associate rHBsAg to the NC surface, the antigen solution was incubated with the previously isolated NCs (11). The mass ratio selected was 4:1 (theoretical concentration of the cationic polymer adsorbed into

TABLE 1 | Physicochemical characterization of the selected nanocapsules (NCs).

Formulation	Abbreviation	Size (nm)	PDI	Zeta potential (mV)	rHBAg association (%)
Nanoemulsion	NE	264 ± 10	0.2	−23 ± 2	–
Chitosan nanocapsules	CS NCs	456 ± 2	0.3	+47 ± 2	–
Protamine nanocapsules	PR NCs	274 ± 4	0.2	+27 ± 4	–
rHBsAg-loaded protamine nanocapsules	PR NCs-rHBsAg	358 ± 20	0.3	+5 ± 4	74 ± 5
Polyarginine nanocapsules	PARG NCs	251 ± 2	0.1	+30 ± 2	–
rHBsAg-loaded polyarginine nanocapsules	PARG NCs-rHBsAg	320 ± 8	0.3	+15 ± 1	70 ± 7

PDI, polydispersity index; HBsAg, hepatitis B surface antigen.

the NC surface:rHBsAg). Quantification of the non-associated antigen was performed by ELISA. Both prototypes showed an association efficiency greater than 70% (**Table 1**). Regarding the physicochemical properties of the nanostructures, the association of the antigen to the NC surface led to a size increase and a decrease in the zeta potential. These changes support the presence of the antigen on the NC surface, a location that would theoretically facilitate recognition by antigen-presenting cells (18, 19).

Activation of the Complement Cascade

The complement system is one of the most important constituents of the innate humoral system. It includes different serum proteins that are activated in cascade upon contact with different stimuli. Three different routes (classic, alternative, and lectins) can activate this system, and the degradation of the C3 is a common step in all of them. The stimulation and the consequent activation of the cascade can promote phagocytosis processes, it can mediate inflammation, and it is involved in the recognition and clearance of pathogens (20). The complement serves as a first line of defense, and it plays an important role in promoting antigen-specific responses by enhancing both B- and T-cell immunity (21). In fact, the bioactivity of alum (the most used adjuvant in vaccines worldwide) is strongly related to its ability to activate the complement cascade (22).

Analysis of the C3 degradation by Western blot showed that PR NCs slightly induced the activation of the complement cascade. The highest rate of activation was achieved at the highest concentration tested (1 mg/mL of theoretical concentration of protamine), and the degradation rate was double that found in the negative control (**Figure 1**). This result was confirmed by ELISA using the quantification of the C5a factor levels, which were two times higher in the plasma exposed to the NCs than in the untreated negative control (data not shown).

It has been previously reported that the nanoparticle surface composition plays a crucial role in the complement cascade activation: the presence of a high surface density of amino groups in the polymer chain can enhance the interaction with the C3b α-chain (23). PR and PARG are guanidine-rich polymers, and they would be expected to activate the complement cascade. By contrast, the results on the complement activation properties of chitosan reported to date are quite variable (24, 25), probably due to the different types and sources of chitosan on the market. In our case, activation was not observed after contact between this polymer and the complement cascade proteins.

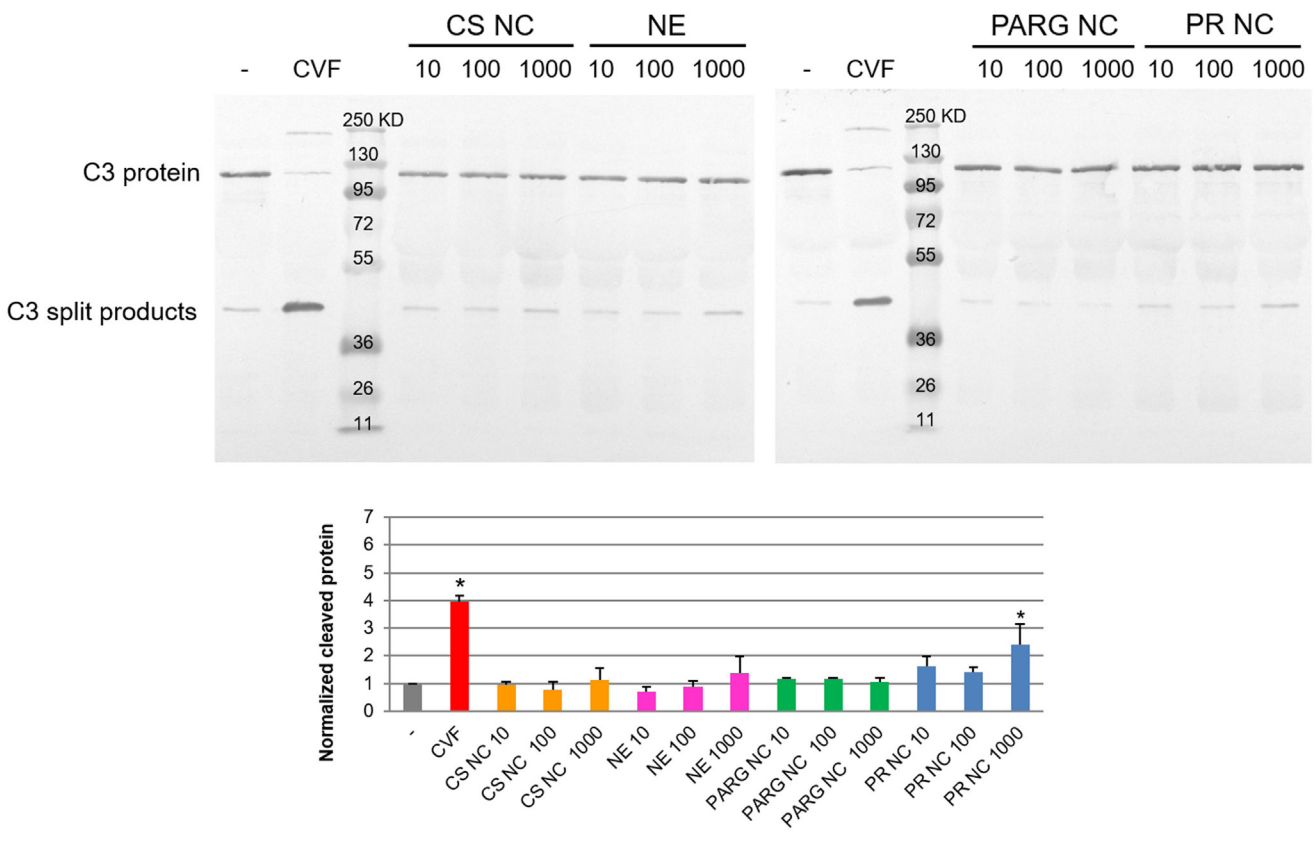

FIGURE 1 | Complement activation of human plasma induced by the nanostructures. Different concentrations of the prototypes were tested by Western blot: 10, 100, and 1,000 μg/mL. Phosphate-buffered saline and cobra venom factor (CVF) were selected as negative and positive controls. Abbreviations: NE, nanoemulsion; CS NC, chitosan nanocapsule; PARG NC, polyarginine nanocapsule; PR NC: protamine nanocapsule. Bands corresponding to the C3 protein and C3 split products are indicated. Molecular weight controls are expressed in kilodalton. The lower graph corresponds to the intensity of the lower band (C3 cleaved) normalized to the negative control. The median ± SD is represented ($n = 3$). *Significant differences between negative and positive (CVF) controls or nanocapsule treatments.

Western blot analysis showed that only PR NCs, and not PARG NCs, were able to achieve significant levels of the C3 split products at the highest concentration tested. This finding suggests that another mechanism, besides the interaction with the C3b α-chain, may be contributing to the activation of the complement cascade. This difference could also be attributed to a higher percentage of adsorption of the PR when compared with the PARG. Further investigation need to be perform to validate this hypothesis. Although little is known about the mechanism of complement activation induced by arginine-rich polymers, it has previously been reported that PR, which is commonly used to neutralize the effect of heparin after cardiopulmonar bypass, can induce complement cascade activation through the classic route when heparin–PR complexes are formed (26).

In Vitro Cell Studies

Cell Viability

Six different concentrations of the nanosystems (from 250 to 7.8 μg/mL) were used to evaluate the cell viability. As shown in **Figure 2**, a dose-dependent trend was observed for all formulations. PARG NCs reduced cell viability to a greater extent than the other prototypes, with an IC50 close to 30 μg/mL, followed by PR NCs > NE > CS NCs. A major reduction in the cell viability has been previously reported with NCs presenting PARG in the surface composition, being this toxicity reported as dose dependent and influenced by the composition of the nucleus (27). In addition, it has previously been reported that the toxic effect induced by nanoparticles decreases with increasing particle size (28). This may explain why CS NCs are the prototype that reduces less the cell viability. In the case of the NE, this prototype was only able to reduce the cell viability at the higher concentrations tested: the negative charge on the surface may play an important role in the reduction of cell viability (29, 30).

Cellular Uptake and ROS Production by Macrophages

Fluorescence microscopy and flow cytometry results (**Figure 3**) indicate that all prototypes were efficiently internalized by the cells in a dose-dependent manner. A real-time uptake study using Confocal Laser Scanning Microscopy and the High Content Screening Automation HCS A module was performed by incubating macrophages with fluorescent NCs during 90 min. All of the prototypes were quickly internalized, and the fluorescence was detected after 15 min from the starting time point of the experiment (**Figure 4**). The fluorescence intensity increased up to the last time point of the experiment.

It has been reported in the literature that particulate delivery systems are commonly taken up by phagocytic cells and that this internalization is dependent on particle size, composition, and surface charge (31–33). In general, charged large particles are internalized more rapidly than small neutral particles, with the cationic prototypes being particularly prone to uptake within

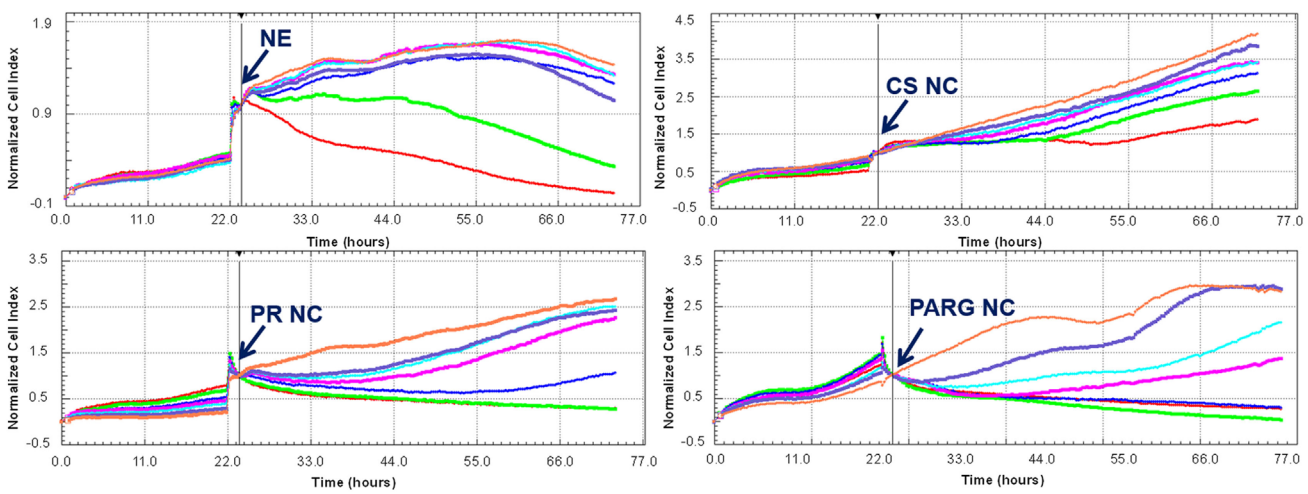

PROTOTYPE	IC50 (μg/mL)
NE	114,7
CS NC	235,4
PR NC	59,22
PARG NC	26,7

FIGURE 2 | Effect of the prototypes on the viability of Raw 264.7 cells. Cells were cultured until their exponential phase, and then the nanostructures were added (indicated with an arrow) at different concentrations. IC50 was calculated with RTCA Software 1.2.1. Abbreviations: NE, nanoemulsion; CS NC, chitosan nanocapsule; PR NC, protamine nanocapsule; PARG NC, polyarginine nanocapsule.

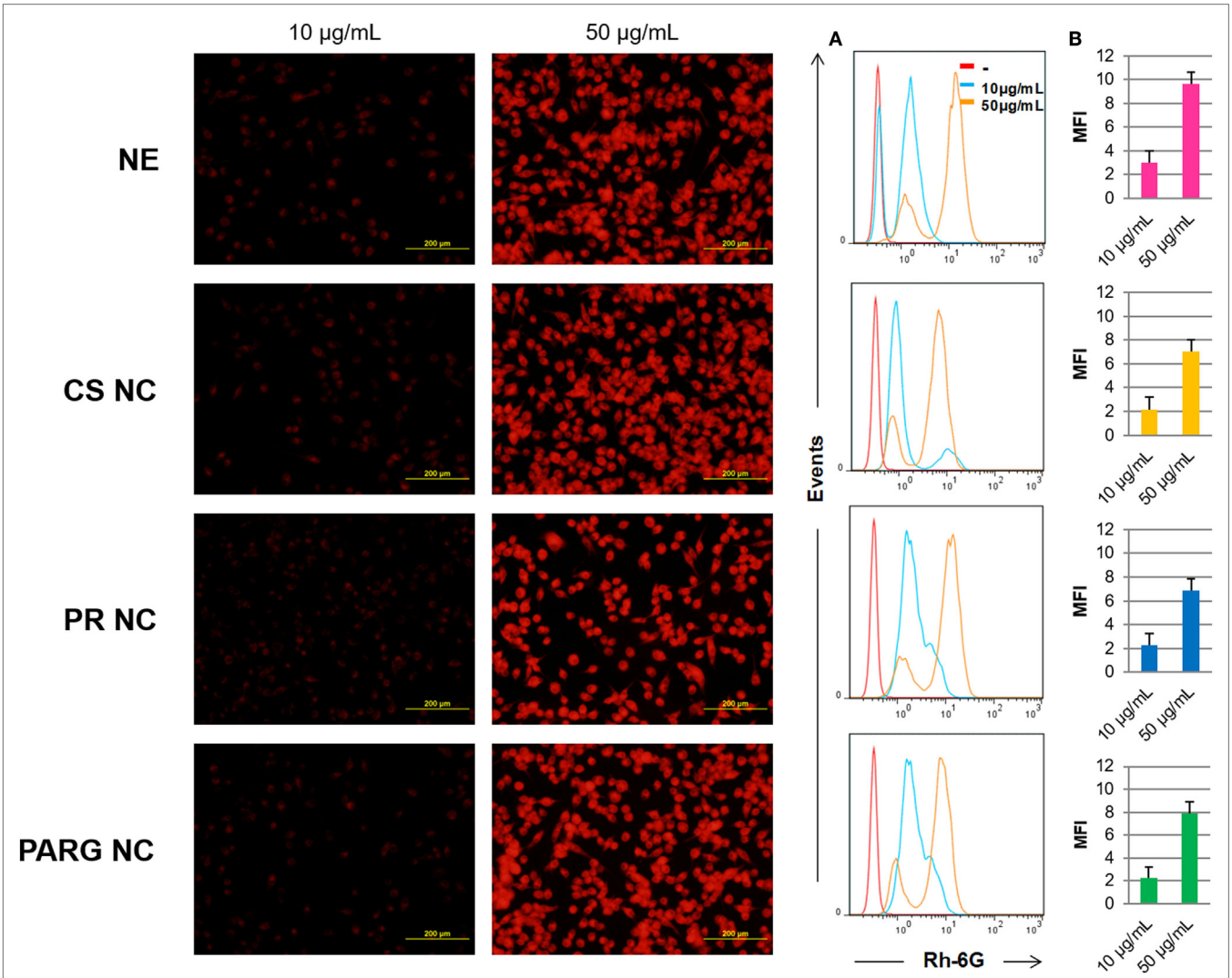

FIGURE 3 | Internalization of the fluorescent nanostructures by Raw 264.7 cells. Left: cells incubated with the fluorescent prototypes (images taken on a fluorescence microscope) at 10 and 50 µg/mL. Right: cells analyzed by flow cytometry **(A)** by histograms **(B)** by the median of the fluorescence intensity (MFI). Abbreviations: NE, nanoemulsion; CS NC, chitosan nanocapsule; PR NC, protamine nanocapsule; PARG NC, polyarginine nanocapsule.

charged systems (34). In this study, all the formulations are charged, positively or negatively, and have proven to be efficiently internalized. The charge, regardless of its sign, may have facilitated capture by macrophages: while cationic nanoparticles would have easily interacted with anionic cell surfaces, the internalization of anionic NEs may have occurred through the non-specific binding of the particles on cationic domains followed by endocytosis (35). It has been described in other polymeric nanomaterials, that once they are internalized in endosomes, they go to lysosome where they are processed. They can induce ROS production, and eventually, trigger the immune response (36–38). In addition, it has been reported that ROS production by the dendritic cells plays an important role in the antigen presentation in that it stimulates the cross-presentation in these cells and therefore it enhances the $CD8^+$ T lymphocyte responses (39). As a consequence, ROS production in the promyelocytic cell line HL60 was studied as a measure of cell activation after the internalization of these prototypes, where the cell activation was at the same time an indicator of the initiation of the adaptive immune response.

The ROS production was studied after cell exposure to nanostructures during 1 or 12 h (Figure S3 in Supplementary Material). All the prototypes induced the production of ROS in a dose- and time-dependent manner. It has been previously reported that the induction of ROS by inorganic nanoparticles could be a mechanism for the promotion of cell death (40). However, little is known about ROS production by polymeric nanoparticles as a mechanism of cell defense against infections.

Cytokine Profile Evaluation

Cytokines are peptides, small proteins, or glycoproteins that play an important regulatory role in several biological processes. They

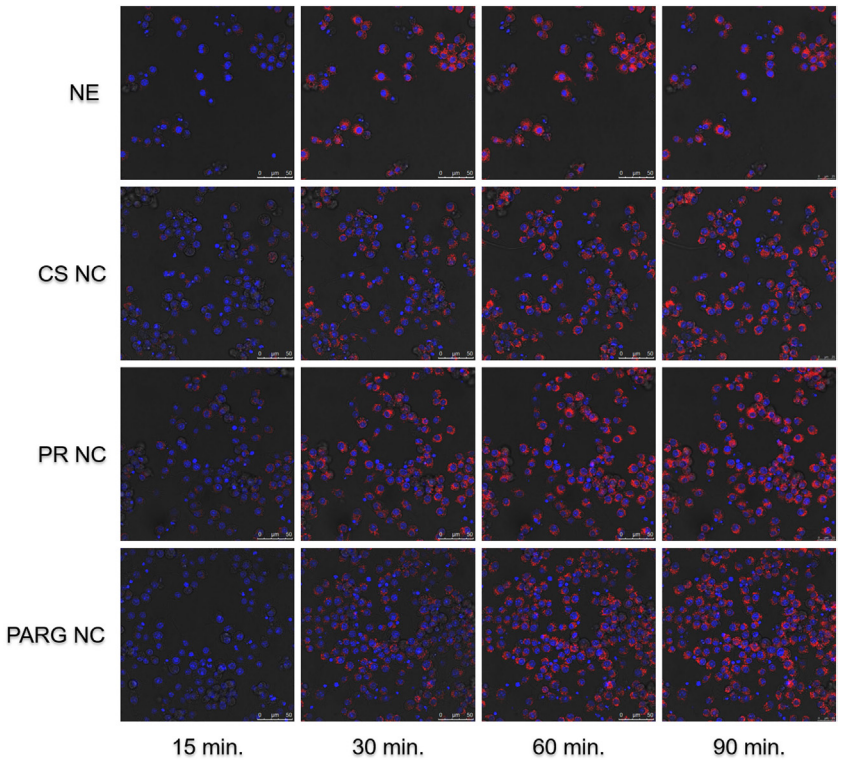

FIGURE 4 | Kinetic internalization study of the labeled nanostructures performed on a confocal microscope [red channel: rhodamine 6G (labeled nanocapsules); blue channel: DAPI (nucleus)]. Raw 264.7 cells were incubated in the presence of the nanosystems, and images were acquired every 5 min. Images at 15, 30, 60, and 90 min are shown. Abbreviations: NE, nanoemulsion nanocapsule; CS NC, chitosan nanocapsule; PR NC, protamine nanocapsule; PARG NC, polyarginine nanocapsule.

are produced mainly by immune cells, but also by several other cell types. Cytokines are the main messengers between cells of the immune system and they regulate the innate and adaptive responses and also modulate the inflammatory response (41). In this study, our main goal was to investigate if the NCs, to be used as antigen carriers, are inherently able to stimulate cytokine secretion by hPBMCs.

It can be seen from the results in **Table 2** that the PR and PARG NCs have a slightly greater tendency to induce the production of pro-inflammatory cytokines than CS NCs or the control NE. The main difference was observed in the secretion of TNFα, where two out of the three donors responded in the case of PR and PARG NCs, only one out of three donors was positive for CS NCs, and no positive response was observed for the control NEs. Although these responses are not remarkable, they are in agreement with previous studies in which it was found that protamine and PARG are able to induce the production of TNFα; PR was included in a nanoparticulate form and incorporated CpG (42), while in the case of PARG it was the bulk material (43). On the other hand, it has also been reported that cationic particles are more efficient at inducing inflammatory responses than anionic or neutral particles (34). This observation is consistent with the overall cytokine profiles observed for the three types of NCs. By contrast, the anionic NE was only able to induce the production of IL-8, a cytokine that is basally produced at high levels (**Table 2**). The differences in the cytokine secretion profiles for the three cationic prototypes could be explained by the smaller size of PR and PARG NCs when compared with CS NCs: the higher specific surface area may contribute to a more efficient interaction with the mononuclear cells (44).

The cytokine profile induced by PR and PARG prototypes is dominated by IL-6, Il-1β, IL-8, and TNFα (at the highest dose tested). All of these cytokines are mainly produced by macrophages when they are exposed to inflammatory stimuli (45). While IL-8 is a potent chemotactic factor for lymphocytes and neutrophils that is often released during phagocytosis, IL-6 induces B cell differentiation and increases antibody titers (46, 47). In addition, IL-1β is released upon activation of macrophages *via* Caspase 1 pathway, and similarly to this one, TNFα is also an endogenous pyrogen that is produced and released at the early stages of the immune response to infections (45). Both prototypes have proved to be efficiently internalized by phagocytic cells (**Figures 3** and **4**), hence a high internalization rate during the first steps of the immune response may have contributed to the activation of human monocytes, leading to the release of all these pro-inflammatory cytokines generating an adequate scenario to initiate a specific immune response.

Activation Markers

Human CD71 (transferrin receptor) and class II molecules of the major histocompatibility complex (HLA-DR) are membrane markers that can be modulated during cell activation. Transferrin receptor is expressed at different levels in many cell types and increases its expression in activated cells such as T and B lymphocytes, because this mechanism is used to import extracellular iron for metabolic needs (48, 49). HLA-DR is constitutively expressed in B cells and it has been shown to be down regulated under certain stimuli. The modulation of this marker changes depending on the stage of differentiation of the B cells upon its activation. While an increase during the first contact with stimuli is commonly observed, a decrease occurs during the last steps of differentiation (50–52). On the other hand, T cells do not express HLA-DR unless they are activated (53).

The expression of the activation markers CD71 (transferrin receptor) and HLA-DR in T (as $CD3^+$) and B (as $CD19^+$) cells incubated with the different nanostructures at two different doses (10 and 100 μg/mL) was evaluated by flow cytometry (**Figure 5**). The results indicate that only PARG NCs were able to increase the percentage of $CD71^+HLA\text{-}DR^+$ T cells and also the expression of CD71 in B cells. Furthermore, PARG NCs induced the modulation of HLA-DR in B cells. While this effect seems to correlate to cell activation, it cannot be excluded that a cytotoxic effect could have been the responsible for this modulation in the expression of these markers as consequence of exposure to damage-associated molecular patterns (DAMPs, danger signals, or alarmins). In fact, these molecules have been described as the possible responsibles for the adjuvant effect of other molecules such as alum (54).

These results are in agreement with the cytokine data, where PARG NCs induced the production of different cytokines in hPBMCs. A synergistic effect of all of these cytokines may play a crucial role in the lymphocyte activation and subsequently in the modulation of markers such as CD71 or HLA-DR.

TABLE 2 | Cytokine production by human peripheral blood mononuclear cells incubated with nanocapsules at two doses (10 and 100 μg/mL).

		μg/mL	NE	CS NCs	PR NCs	PARG	LPS-PHA
Th1 profile	IL-2	10	–	–	–	–	++
		100	–	–	–	++1/3	
	IL-12p70	10	–	–	–	–	+++
		100	–	–	–	–	
	IFN γ	10	–	–	–	++1/3	+++
		100	–	–	–	–	
	TNF β	10	–	–	–	–	+
		100	–	–	–	–	
	TNF α	10	–	–	–	–	+++
		100	–	+1/3	+2/3	+2/3	
Th2 profile	IL 4	10	–	–	–	–	+
		100	–	–	–	–	
	IL 5	10	–	–	–	–	+
		100	–	–	++1/3	++1/3	
	IL 10	10	–	–	–	–	++
		100	–	–	+1/3	+1/3	
Other pro-inflammatory cytokines	IL 1β	10	–	–	–	–	+
		100	–	+1/3	+	+	
	IL 6	10	–	–	–	–	+++
		100	+1/3	++	+++	++	
	IL 8	10	+1/3	–	+1/3	+2/3	+
		100	+	+	+	+	

NE, nanoemulsion; CS NC, chitosan nanocapsule; PR NC, protamine nanocapsule; PARG NC, polyarginine nanocapsule.

The positive control was lipopolysaccharide (LPS) (1 μg/mL) with phytohemagglutinin (PHA) (10 μg/mL).

+: 1–10; ++: 10–100; +++: 100–1,000; ++++: >1,000-fold higher than negative control (cells incubated in culture media).

+N/tested: number of positive responsive persons/three donors tested.

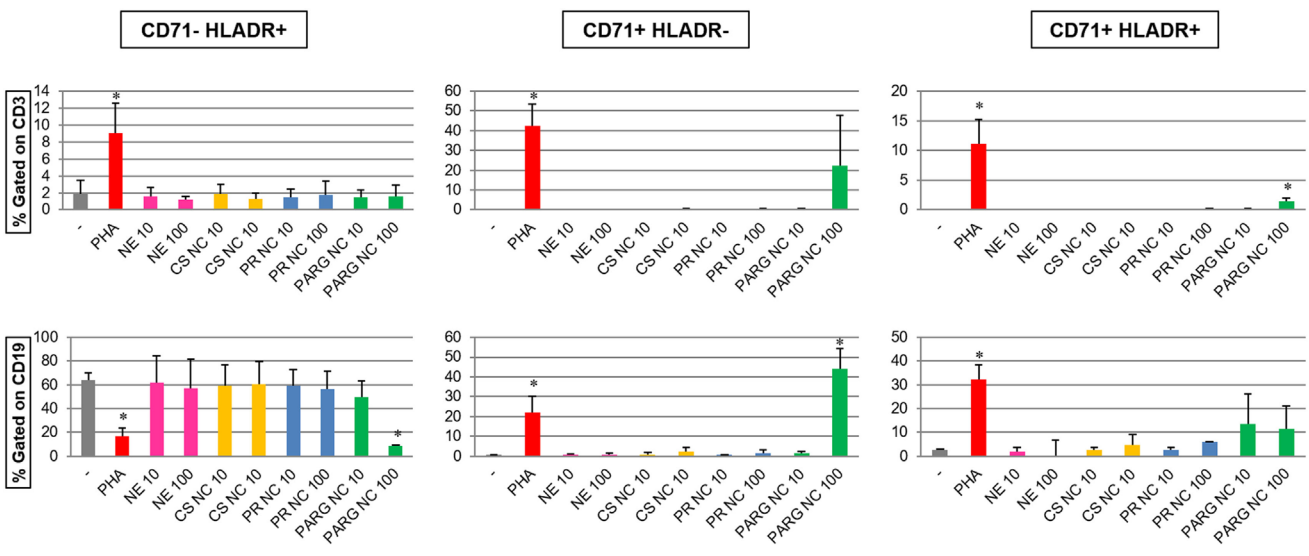

FIGURE 5 | Modulation of activation markers (CD71 and HLA-DR) in gated T ($CD3^+$) and B ($CD19^+$) lymphocytes (top and bottom graphs, respectively) from human peripheral blood mononuclear cells (hPBMCs) incubated with the prototypes (at 10 and 100 μg/mL). Percentages of $CD71^-HLADR^+$, $CD71^+HLADR^-$, and $CD71^+HLADR^+$ cells are represented. The results are the average of three independent experiments with hPBMCs from three different healthy donors (*$p < 0.05$).

Routes of Activation. MAP Kinases

Mitogen-activated protein kinases (MAPKs) are a protein family that is involved in several processes such as gene expression, mitosis, cell migration, metabolism, and programmed cell death. MAPKs are activated through the phosphorylation of certain residues and, in turn, they activate their target proteins, including other protein kinases, transcription factors, or cytoskeleton proteins.

The MAPK families that are most widely reported in the literature are the ERK, the c-Jun NH2-terminal kinases (JNK), and the p38 family. While ERKs are involved in the regulation of processes such as mitosis or meiosis, JNK are mainly involved in the control of programmed cell death or apoptosis. On the other hand, p38 participates in the immune response activation (55). In addition, the NFκB is a transcription factor that plays an important role in the regulation of certain immune responses by modulating the expression of receptors or surface adhesion molecules, inflammatory cytokines, and chemokines. Furthermore, it is involved in the response to stress signals and in cell survival (56, 57).

In this study, we investigated the capacity of PR and PARG NCs to induce the secretion of MAPK and NFκB in two different cell lines, namely, the Jurkat (human leukemic T-cell line) and the Hmy (human B Lymphoblast cell line) cell lines. It has previously been reported that activation of the NFκB pathway leads to the degradation of the IKBα inhibitor and therefore a decrease in IKBα was expected in these cells.

The Western blot analysis only showed a slight increase in the phosphorylation levels of the p38 family after 3 h in contact with PARG NCs (**Figure 6**). Considering Hmy and Jurkat cell lines as representative B and T cells, respectively, of the main PBMCs, this result could correlate with the observed capacity of these NCs to induce the production of Il-1β, IL-6 and IL-8 in human PBMC, as it is known that the p38 family is activated in response to different inflammatory cytokines and the triggering of different immune responses (55, 58, 59). In addition, p-p38 has also been shown to be involved in the proliferation of Th1 cells (60). This explains why p38 is activated mainly by PARG NCs, as this NCs formulation showed a Th1 profile characterized by the production of TNFα.

In the case of ERK, both prototypes, PR and PARG NCs, induced its activation in Hmy and Jurkat cells, with this effect being time dependent only in Jurkat cells (**Figure 6**). ERK is activated in response to several cytokines, and it is involved not only in cell survival but also in cell differentiation (55). In addition, ERK phosphorylation is an important step during both T and B cell activation (61, 62) and in the Th2 differentiation process (63).

Regarding p-SAP/JNK, activation was not detected upon contact with any of these prototypes (**Figure 6**). This fact can be explained by the pro-apoptotic activity of the p-SAP/JNK family:

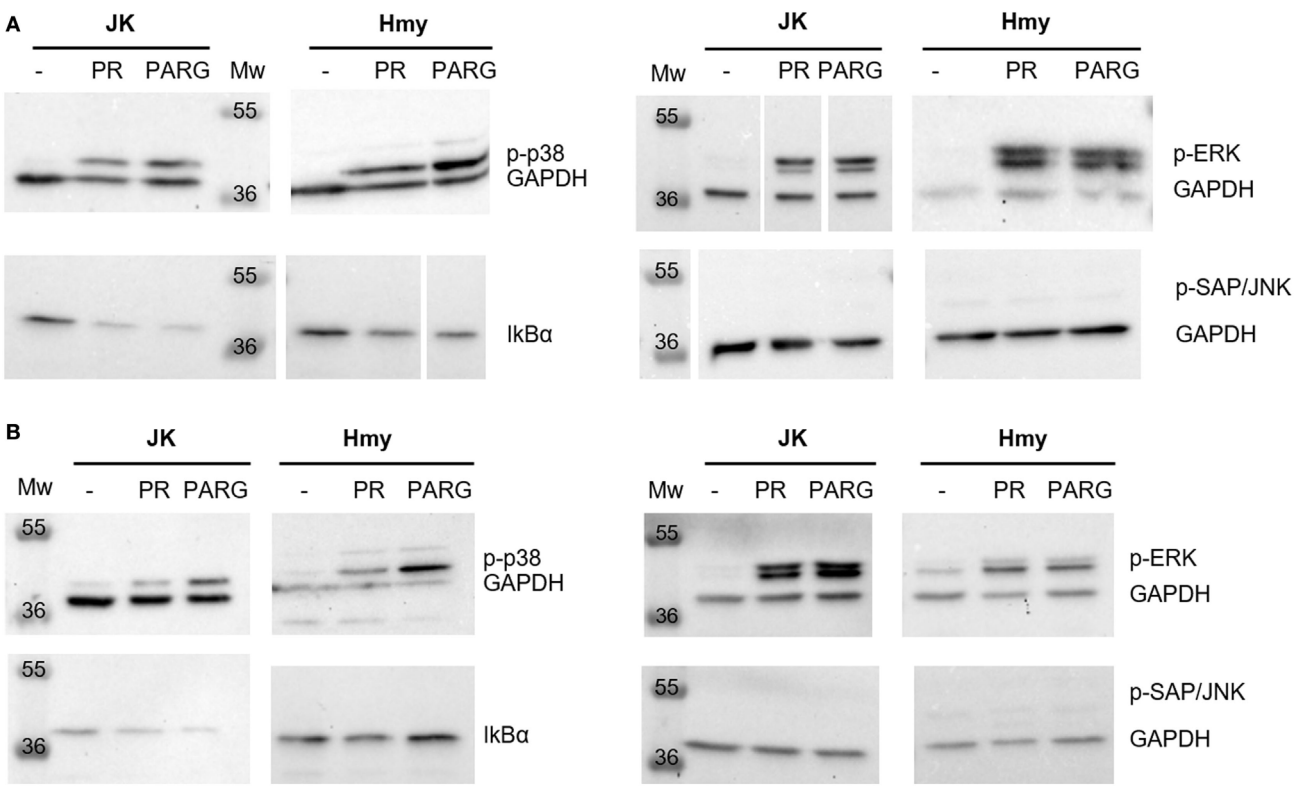

FIGURE 6 | Reduction in IκBα expression and activation of mitogen-activated protein kinases [p-extracellular signal-regulated kinase (ERK), p38, and p-SAP/c-Jun NH2-terminal kinases (JNK)] and the nuclear factor κB pathway in Jurkat and Hmy cell lines induced by PR NCs and PARG NCs after 1 h **(A)** or 3 h **(B)** of incubation. GAPDH was used as a loading control. White space between lanes shows the cut point in membranes.

the lack of activation was expected (58, 64) since none of the prototypes showed a cytotoxic effect at low doses and in short periods of time.

The activation of NFκB was detected by the decrease in its IkBα inhibitor levels (**Figure 6**). This fact was observed in both Jurkat and Hmy cells and with both protamine NCs and PARG NCs. NFκB is activated by a wide range of signals such as antigen receptors, pattern-recognition receptors, and different TNF and IL-1 receptors. This activation regulates not only the innate but also the adaptive immunity and different inflammatory responses (65). The decrease in the IkBα levels in both Jurkat and Hmy cell lines upon contact with this immune stimulator was expected considering that this transcription factor is essential to trigger some processes related to immune cell activation.

In light of the results obtained, it can be concluded that PR and PARG NCs are able to induce the phosphorylation of p38 and ERK, as well as the degradation of IκBα in both T and B cell lines, with PARG NCs having a slightly superior activation capacity.

Overall, data obtained by *in vitro* studies, postulate PR and PARG NCs as the most promising prototypes as antigen delivery systems. On the other hand, NE and CS NC have not demonstrated to be strong inducers of immune responses and do not activate the complement cascade, thus they could be useful as carriers intended to avoid the immune system recognition, for example to target cells for gene therapy (66).

In Vivo Studies

Taking into account the results obtained in the *in vitro* studies, PARG and PR NCs were selected for the *in vivo* evaluation of their capacity to induce the production of an immune response against a model antigen, rHBsAg. To this end, groups of five Balb/C female mice were intramuscularly immunized with two doses of rHBsAg adsorbed onto PR NCs and PARG NCs or alum. The humoral-specific immune response (anti-rHBsAg serum IgG) and the type of immune response elicited (measured by the IgG1/IgG2a ratio) were both analyzed. In addition, a panel of several genes involved in immune responses was studied *ex vivo* in cells from immunized mice.

Immune Response Elicited by Immunostimulating rHBsAg-Loaded NCs

It can be seen from the results in **Figure 7** that PR NCs and PARG NCs were able to elicit antigen-specific antibody levels at 6 weeks after immunization, with levels close to 400 and 130 mIU/mL, respectively. These levels increased slightly to 500 and 200 mIU/mL, respectively, after 10 weeks. It is worthy to note that in both cases, seroprotection levels (>100 mUI/mL) were achieved, although this increase was not as high as the one observed in control mice immunized with alum-rHBsAg (from 1,100 to 1,600 mUI/mL) (**Figure 7**).

Despite the response induced by the marketed alum-rHBsAg vaccine was much higher, the average levels achieved by PR NCs and PARG NCs were over 100 mIU/mL, which has been established as the threshold of antibody protective levels in humans (67). It can also be stated that PR NCs showed better immunostimulant properties than PARG NCs as they induced higher specific antibody levels in mice (5/5). This difference can be explained by the higher ability of PR NCs to activate the complement cascade compared with PARG NCs, which may play a crucial role in the adjuvant effect of the NC. Thus, independently on the NCs under study, the immune response induced by both prototypes could be due to a combination of several routes such as p38 and ERK. Moreover, the lack of a strong activation of the

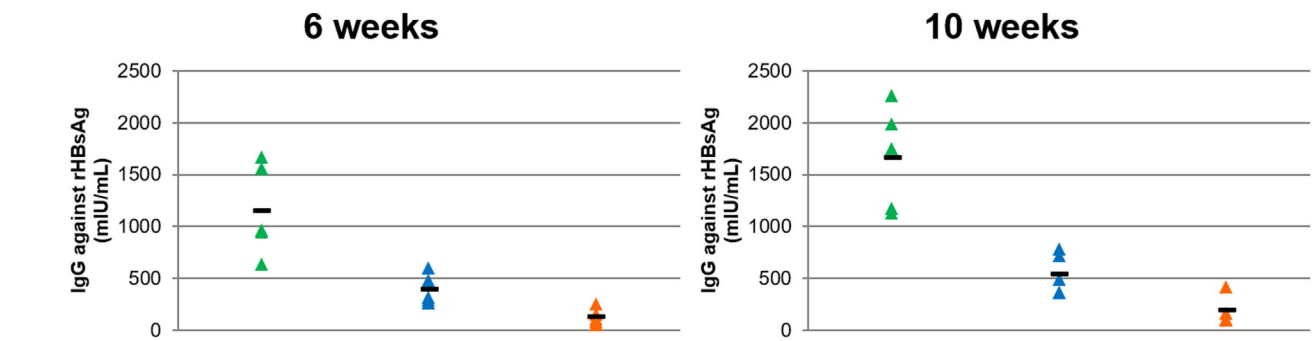

	6 weeks			10 weeks		
	Alum-rHBsAg	PR NC-rHBsAg	PARG NC-rHBsAg	Alum-rHBsAg	PR NC-rHBsAg	PARG NC-rHBsAg
Nº mice with IgG>100mIU/mL	5/5	5/5	3/5	5/5	5/5	4/5
Ratio IgG1/IgG2a	5,1	2,3	2,6	2,3	2,3	1,7

FIGURE 7 | Systemic immune response upon intramuscular immunization with rHBsAg PR NCs and PARG NCs. The top graphs represent individual IgG concentrations of anti-HBsAg (expressed in mUI/mL) in each mouse (triangles) and the average of five mice (dash) at 6 weeks (left graph) and 10 weeks (right graph) after the first administration. The number of mice with antibody levels over 100 mIU/mL and the IgG1/IgG2a ratios at different time points are also represented in the lower table.

NFκB pathway could be related to the moderate *in vivo* immune response obtained in the presence of NCs.

Modulation of the Immune Response

To determine the type of response induced by these prototypes, the IgG1/IgG2a ratio was calculated for both prototypes. These two IgGs were selected because while the IgG2a subtype is related to cellular immune responses mediated by Th1 lymphocytes, IgG1 is mostly produced after Th2 activation, which mediates the humoral immune response.

Both humoral and cellular responses were elicited by both prototypes. The highest levels detected for Th2, with ratios ranging from 2.6 to 1.7. While this ratio did not change over time for PR NCs, it decreased slightly for PARG NCs, which indicates that an increase in Th1 response had occurred (**Figure 7**). This finding is in agreement with the combination of cytokines produced by hPBMCs upon contact with PARG NCs and also due to the activation of both p-ERK and p-p38, which are commonly involved in Th2 and Th1 responses, respectively (60, 63). The same trend was observed in the control group, although in this case the initial IgG1/IgG2a ratio was higher (close to 5). This is in agreement with the known fact that alum is a very effective Th2 activator (68).

Gene Expression Assays in Restimulated Splenocytes From Immunized Mice

To understand the mechanism involved in the immunostimulant properties of PARG NCs and PR NCs, the expression of different genes was studied by qPCR. For this purpose, splenocytes from immunized mice were restimulated with the HBsAg during 12 or 24 h. RNA from these cells was extracted to analyze the expression of genes involved in apoptosis and inflammation (Caspase 1, 3, 8, and 9; Fas and Bcl2) of different cytokines (IL-10, 1L-4, IL-2, INF-γ, IL-6, TNF-α, IL-1β, and IL-17) and of certain activation markers (CD74, B2M, CD71, CD69, CD154, CD80, and CD86). The results of these studies are summarized in **Table 3**, and the values highlighted in red show an increase in the RQ value greater than 2. Significant differences were only registered for IL17A in mice immunized with PR NCs-HBsAg both 12 and 24 h after restimulation. A minor increase was also observed in IL-1β levels in the same group after 24 h of restimulation.

IL-17A is a cytokine produced by Th17 cells and by other immune cells, including γδ T cells, NKT cells, NK cells, neutrophils, and eosinophils. In fact, one of its functions is to connect innate and adaptive immune responses. IL-17A is a pro-inflammatory cytokine that induces the production of other cytokines and chemokines, which are crucial in the recruitment, activation, and migration of neutrophils to the site of inflammation. It has been reported that this cytokine is also involved in the development of germinal centers (GC) (69). IL-1β, which is produced through the NALP3 inflammasome route and whose release can be initiated by the complement cascade activation (70), is one of the major mediators of inflammation and it is the main known endogenous pyrogen. IL-1β is also very important in the initiation of innate immune responses and, as a consequence, it has a critical role in the control of pathogenic infections (71). Both cytokines IL-17

TABLE 3 | Changes in the expression of selected genes in splenocytes from mice immunized with alum-rHBsAg, PRNC-rHBsAg, and PARGNC-rHBsAg restimulated for 12 or 24 h with rHBsAg.

Gene	Name	RQ (12 h)			RQ (24 h)		
		Alum-rHBsAg	PRNC-rHBsAg	PARGNC-rHBsAg	Alum-rHBsAg	PRNC-rHBsAg	PARGNC-rHBsAg
B2M	Beta-2-microglobulin	0.93	0.71	0.91	0.98	1.28	0.82
TNF	Tumor necrosis factor	1.12	0.95	1.16	1.16	1.38	0.74
IL10	Interleukin 10	0.80	0.69	0.89	0.76	1.17	0.65
IL4	Interleukin 4	1.10	0.73	0.88	1.07	1.62	0.79
IL2	Interleukin 2	1.28	0.92	0.96	0.92	1.58	0.73
INFγ	Interferon gamma	0.92	1.03	1.19	0.84	1.26	0.69
IL6	Interleukin 6	0.93	0.81	1.04	0.89	1.24	0.72
IL1β	Interleukin 1 beta	1.68	1.34	1.40	1.20	2.06	1.13
IL17A	Interleukin 17A	1.72	2.30	0.91	2.18	3.11	0.46
CASP1	Caspase 1	0.94	0.81	1.01	1.43	1.36	1.05
CASP3	Caspase 3	0.88	0.80	0.91	1.33	1.26	0.88
CASP8	Caspase 8	1.02	0.80	0.92	1.18	1.14	0.89
CASP9	Caspase 9	0.82	0.77	0.83	1.43	1.25	0.91
Bcl 2	B-cell lymphoma 2	0.73	0.68	0.83	1.11	1.00	0.81
FADD	Fas-associated protein with death domain	0.91	0.76	0.74	1.74	1.21	0.89
CD154	Cluster of differentiation 154	0.63	0.64	0.70	0.92	0.94	0.72
CD69	Cluster of differentiation 69	1.12	0.91	0.99	1.24	0.90	0.65
CD74	Cluster of differentiation 74	0.91	0.96	1.09	1.48	1.35	1.06
TFRC	Transferrin receptor	0.88	0.80	0.90	0.96	1.32	0.90
CD86	Cluster of differentiation 86	1.09	0.83	0.94	0.02	1.50	1.00
CD80	Cluster of differentiation 80	0.69	0.91	0.88	1.19	1.30	0.79

Values in this table represent the RQ with respect to the control (splenocytes from mice immunized with phosphate-buffered saline 1× and restimulated in vitro with rHBsAg) calculated from independent data for 3 mice per group.

RQ values greater than 2 are represented in red (% CV of ΔCt < 25).

RQ, relative quantification; PR NC, protamine nanocapsule; PARG NC, polyarginine nanocapsule; rHBsAg, recombinant hepatitis B surface antigen.

and IL-1 have been proposed as the main mediators of the adjuvant effect of several vaccines (72–74). The induction of IL-17 and IL-1β production by PR NCs in cells from immunized mice may have an important role in initiating the immune response after vaccination. These could induce an inflammatory response that would create the appropriate environment for the development of a specific immune response.

PR NCs have proved to be efficient antigen carriers *in vivo* using the HBsAg as a model antigen. We postulate that the incorporation of immunostimulant molecules into this formulation, such as imiquimod, CpG, polyI:C (13, 14, 75), could lead to the design of a prototype able to induce an enhanced immune response, even stronger than that induced by alum, and also to an effective system that could modulate this immune response toward a Th1 profile.

CONCLUSION

The results underline the potential of arginine-rich NCs as antigen delivery carriers. The systematic analysis performed in this study provides valuable information regarding the feasibility of modulating the immunostimulatory properties of NCs by selecting the nature of the polymer shell. This information could help in the design and development of novel nanocarriers for vaccine delivery, taking as a starting point the physicochemical properties of PR NCs, which was the prototype that showed the best immunological profile in the *in vivo* evaluation.

ETHICS STATEMENT

Institutional ethics approval to work with human samples from healthy donors was obtained from the Ethics Committee for Clinical Research (Xunta de Galicia, Spain, 2013/272). All participants included in the study gave their written informed consent. All protocols developed with mice were adapted from the guidelines of the Spanish regulations (Royal Decree 53/2013) regarding the use of animals in scientific research and under the approval of the Ethical Committee of the University of Vigo.

AUTHOR CONTRIBUTIONS

MP and EP have contributed to the design, acquisition, analysis, and interpretation of data; the drafting and the revision of the work. JG-A, BS-C, and RS-V have contributed to the design, acquisition, analysis, and interpretation of data for the work. NC, MA, and ÁG-F have contributed to the design, the drafting, and the revision of the work.

ACKNOWLEDGMENTS

This work was supported by the Spanish Ministry of Economy and Competitiveness (SAF2011-30337-C02-02 and BIO2014-53091-C3-1-R). Financial support from the Xunta de Galicia (Centro singular de investigación de Galicia 2016–2019 and Grupo de referencia competitiva, ED431C 2016041) and the European Union (European Regional Development Fund—ERDF) is gratefully acknowledged. The authors would like to thank Jesús Méndez from CACTI facilities of the University of Vigo. MP acknowledges fellowships from the Spanish Ministry of Education (FPU predoctoral grants program).

SUPPLEMENTARY MATERIAL

The Supplementary Material for this article can be found online at https://www.frontiersin.org/articles/10.3389/fimmu.2018.00791/full#supplementary-material.

REFERENCES

1. Delany I, Rappuoli R, De Gregorio E. Vaccines for the 21st century. *EMBO Mol Med* (2014) 6(6):708–20. doi:10.1002/emmm.201403876
2. Cordeiro AS, Alonso MJ. Recent advances in vaccine delivery. *Pharm Pat Anal* (2015) 5(1):49–73. doi:10.4155/ppa.15.38
3. Skwarczynski M, Toth I. Recent advances in peptide-based subunit nanovaccines. *Nanomedicine* (2014) 9(17):2657–69. doi:10.2217/nnm.14.187
4. Guan S, Rosenecker J. Nanotechnologies in delivery of mRNA therapeutics using nonviral vector-based delivery systems. *Gene Ther* (2017) 24(3):133–43. doi:10.1038/gt.2017.5
5. Karch CP, Burkhard P. Vaccine technologies: from whole organisms to rationally designed protein assemblies. *Biochem Pharmacol* (2016) 120:1–14. doi:10.1016/j.bcp.2016.05.001
6. Kalam MA, Khan AA, Alshamsan A. Non-invasive administration of biodegradable nano-carrier vaccines. *Am J Transl Res* (2017) 9(1):15–35.
7. Bachmann MF, Jennings GT. Vaccine delivery: a matter of size, geometry, kinetics and molecular patterns. *Nat Rev Immunol* (2010) 10(11):787–96. doi:10.1038/nri2868
8. Marciani DJ. Vaccine adjuvants: role and mechanisms of action in vaccine immunogenicity. *Drug Discov Today* (2003) 8(20):934–43. doi:10.1016/S1359-6446(03)02864-2
9. Paolicelli P, Prego C, Sanchez A, Alonso MJ. Surface-modified PLGA-based nanoparticles that can efficiently associate and deliver virus-like particles. *Nanomedicine* (2010) 5(6):843–53. doi:10.2217/nnm.10.69
10. Prego C, Paolicelli P, Díaz B, Vicente S, Sánchez A, González-Fernández Á, et al. Chitosan-based nanoparticles for improving immunization against hepatitis B infection. *Vaccine* (2010) 28(14):2607–14. doi:10.1016/j.vaccine.2010.01.011
11. Vicente S, Diaz-Freitas B, Peleteiro M, Sanchez A, Pascual DW, Gonzalez-Fernandez A, et al. A polymer/oil based nanovaccine as a single-dose immunization approach. *PLoS One* (2013) 8(4):e62500. doi:10.1371/journal.pone.0062500
12. González-Aramundiz JV, Presas E, Dalmau-Mena I, Martínez-Pulgarín S, Alonso C, Escribano JM, et al. Rational design of protamine nanocapsules as antigen delivery carriers. *J Control Release* (2017) 245:62–9. doi:10.1016/j.jconrel.2016.11.012
13. Correia-Pinto JF, Peleteiro M, Csaba N, González-Fernández Á, Alonso MJ. Multi-enveloping of particulated antigens with biopolymers and immunostimulant polynucleotides. *J Drug Deliv Sci Technol* (2015) 30(Pt B):424–34. doi:10.1016/j.jddst.2015.08.010
14. Vicente S, Peleteiro M, Díaz-Freitas B, Sanchez A, González-Fernández Á, Alonso MJ. Co-delivery of viral proteins and a TLR7 agonist from polysaccharide nanocapsules: a needle-free vaccination strategy. *J Control Release* (2013) 172(3):773–81. doi:10.1016/j.jconrel.2013.09.012
15. Calvo P. Novel hydrophilic chitosan-polyethylene oxide nanoparticles as protein carriers. *J Appl Polym Sci* (1997) 63(1):125–32. doi:10.1002/(SICI)1097-4628(19970103)63:1<125::AID-APP13>3.0.CO;2-4
16. Calvo P, Remuñán-López C, Vila-Jato JL, Alonso MJ. Development of positively charged colloidal drug carriers: Chitosan-coated polyester nanocapsules and submicron-emulsions. *Colloid and Polymer Science* (1997) 275(1):46–53.

17. Lozano MV, Lollo G, Alonso-Nocelo M, Brea J, Vidal A, Torres D, et al. Polyarginine nanocapsules: a new platform for intracellular drug delivery. *J Nanopart Res* (2013) 15(3):1–14. doi:10.1007/s11051-013-1515-7
18. Jones KS. Biomaterials as vaccine adjuvants. *Biotechnol Prog* (2008) 24(4): 807–14. doi:10.1002/btpr.10
19. Burgdorf S, Kautz A, Bohnert V, Knolle PA, Kurts C. Distinct pathways of antigen uptake and intracellular routing in CD4 and CD8 T cell activation. *Science* (2007) 316(5824):612–6. doi:10.1126/science.1137971
20. Wilson MR, Gaumer HR, Salvaggio JE. Activation of the alternative complement pathway and generation of chemotactic factors by asbestos. *J Allergy ClinImmunol* (1977) 60(4):218–22. doi:10.1016/0091-6749(77) 90133-6
21. Reddy ST, van der Vlies AJ, Simeoni E, Angeli V, Randolph GJ, O'Neil CP, et al. Exploiting lymphatic transport and complement activation in nanoparticle vaccines. *Nat Biotechnol* (2007) 25(10):1159–64. doi:10.1038/nbt1332
22. Gupta RK. Aluminum compounds as vaccine adjuvants. *Adv Drug Deliv Rev* (1998) 32(3):155–72. doi:10.1016/S0169-409X(98)00008-8
23. Moghimi SM, Andersen AJ, Ahmadvand D, Wibroe PP, Andresen TL, Hunter AC. Material properties in complement activation. *Adv Drug Deliv Rev* (2011) 63(12):1000–7. doi:10.1016/j.addr.2011.06.002
24. Minami S, Suzuki H, Okamoto Y, Fujinaga T, Shigemasa Y. Chitin and chitosan activate complement via the alternative pathway. *Carbohydr Polym* (1998) 36(2):151–5. doi:10.1016/S0144-8617(98)00015-0
25. Marchand C, Bachand J, Perinet J, Baraghis E, Lamarre M, Rivard GE, et al. C3, C5, and factor B bind to chitosan without complement activation. *J Biomed Mater Res A* (2010) 93(4):1429–41. doi:10.1002/jbm.a.32638
26. Cavarocchi NC, Schaff HV, Orszulak TA, Homburger HA, Schnell WA, Pluth JR. Evidence for complement activation by protamine-heparin interaction after cardiopulmonary bypass. *Surgery* (1985) 98(3):525–31.
27. Gonzalez-Paredes A, Torres D, Alonso MJ. Polyarginine nanocapsules: a versatile nanocarrier with potential in transmucosal drug delivery. *Int J Pharm* (2017) 529(1):474–85. doi:10.1016/j.ijpharm.2017.07.001
28. Park MV, Neigh AM, Vermeulen JP, de la Fonteyne LJ, Verharen HW, Briedé JJ, et al. The effect of particle size on the cytotoxicity, inflammation, developmental toxicity and genotoxicity of silver nanoparticles. *Biomaterials* (2011) 32(36):9810–7. doi:10.1016/j.biomaterials.2011.08.085
29. Goodman CM, McCusker CD, Yilmaz T, Rotello VM. Toxicity of gold nanoparticles functionalized with cationic and anionic side chains. *Bioconjug Chem* (2004) 15(4):897–900. doi:10.1021/bc049951i
30. El Badawy AM, Silva RG, Morris B, Scheckel KG, Suidan MT, Tolaymat TM. Surface charge-dependent toxicity of silver nanoparticles. *Environ Sci Technol* (2011) 45(1):283–7. doi:10.1021/es1034188
31. Xiang SD, Scholzen A, Minigo G, David C, Apostolopoulos V, Mottram PL, et al. Pathogen recognition and development of particulate vaccines: does size matter? *Methods* (2006) 40(1):1–9. doi:10.1016/j.ymeth.2006.05.016
32. Zaki NM, Nasti A, Tirelli N. Nanocarriers for cytoplasmic delivery: cellular uptake and intracellular fate of chitosan and hyaluronic acid-coated chitosan nanoparticles in a phagocytic cell model. *Macromol Biosci* (2011) 11(12):1747–60. doi:10.1002/mabi.201100156
33. He C, Hu Y, Yin L, Tang C, Yin C. Effects of particle size and surface charge on cellular uptake and biodistribution of polymeric nanoparticles. *Biomaterials* (2010) 31(13):3657–66. doi:10.1016/j.biomaterials.2010.01.065
34. Dobrovolskaia MA, McNeil SE. Immunological properties of engineered nanomaterials. *Nat Nanotechnol* (2007) 2(8):469–78. doi:10.1038/nnano.2007.223
35. Zaman M, Good MF, Toth I. Nanovaccines and their mode of action. *Methods* (2013) 60(3):226–31. doi:10.1016/j.ymeth.2013.04.014
36. Gao J, Ochyl LJ, Yang E, Moon JJ. Cationic liposomes promote antigen cross-presentation in dendritic cells by alkalizing the lysosomal pH and limiting the degradation of antigens. *Int J Nanomedicine* (2017) 12:1251–64. doi:10.2147/IJN.S125866
37. Liu L, Ma P, Wang H, Zhang C, Sun H, Wang C, et al. Immune responses to vaccines delivered by encapsulation into and/or adsorption onto cationic lipid-PLGA hybrid nanoparticles. *J Control Release* (2016) 225:230–9. doi:10.1016/j.jconrel.2016.01.050
38. Vatansever F, de Melo WC, Avci P, Vecchio D, Sadasivam M, Gupta A, et al. Antimicrobial strategies centered around reactive oxygen species – bactericidal antibiotics, photodynamic therapy, and beyond. *FEMS Microbiol Rev* (2013) 37(6):955–89. doi:10.1111/1574-6976.12026
39. Kotsias F, Hoffmann E, Amigorena S, Savina A. Reactive oxygen species production in the phagosome: impact on antigen presentation in dendritic cells. *Antioxid Redox Signal* (2013) 18(6):714–29. doi:10.1089/ars.2012.4557
40. Auffan M, Rose J, Bottero J-Y, Lowry GV, Jolivet J-P, Wiesner MR. Towards a definition of inorganic nanoparticles from an environmental, health and safety perspective. *Nat Nanotechnol* (2009) 4(10):634–41. doi:10.1038/nnano.2009.242
41. Vilček J, Feldmann M. Historical review: cytokines as therapeutics and targets of therapeutics. *Trends Pharmacol Sci* (2004) 25(4):201–9. doi:10.1016/j.tips.2004.02.011
42. Kerkmann M, Lochmann D, Weyermann J, Marschner A, Poeck H, Wagner M, et al. Immunostimulatory properties of CpG-oligonucleotides are enhanced by the use of protamine nanoparticles. *Oligonucleotides* (2006) 16(4):313–22. doi:10.1089/oli.2006.16.313
43. Yang Y, Wolfram J, Fang X, Shen H, Ferrari M. Polyarginine induces an antitumor immune response through binding to toll-like receptor 4. *Small* (2014) 10(7):1250–4. doi:10.1002/smll.201302887
44. Kreuter J, Berg U, Liehl E, Soliva M, Speiser PP. Influence of the particle size on the adjuvant effect of particulate polymeric adjuvants. *Vaccine* (1986) 4(2):125–9. doi:10.1016/0264-410X(86)90051-4
45. Arango Duque G, Descoteaux A. Macrophage cytokines: involvement in immunity and infectious diseases. *Front Immunol* (2014) 5:491. doi:10.3389/fimmu.2014.00491
46. Akira S, Hirano T, Taga T, Kishimoto T. Biology of multifunctional cytokines: IL 6 and related molecules (IL 1 and TNF). *FASEB J* (1990) 4(11):2860–7. doi:10.1096/fasebj.4.11.2199284
47. Koch A, Polverini P, Kunkel S, Harlow L, DiPietro L, Elner V, et al. Interleukin-8 as a macrophage-derived mediator of angiogenesis. *Science* (1992) 258(5089):1798–801. doi:10.1126/science.1281554
48. Fonseca AM, Porto G, Uchida K, Arosa FA. Red blood cells inhibit activation-induced cell death and oxidative stress in human peripheral blood T lymphocytes. *Blood* (2001) 97:3152–60. doi:10.1182/blood.V97.10.3152
49. Rosa D, Saletti G, De Gregorio E, Zorat F, Comar C, D'Oro U, et al. Activation of naïve B lymphocytes via CD81, a pathogenetic mechanism for hepatitis C virus-associated B lymphocyte disorders. *Proc Natl Acad Sci U S A* (2005) 102(51):18544–9. doi:10.1073/pnas.0509402102
50. Rizzo L. Differential modulatory effect of IL-5 on MHC class II expression by macrophages and B cells. *Braz J Med Biol Res* (1991) 25(5):509–13.
51. Hunakova L, Sedlak J, Chorvath B. Phorbol ester-induced modulation of cell surface antigens on U-937 cells in protein-free medium: effect of protein kinase and calmodulin inhibitors. *Neoplasma* (1992) 40(3): 141–6.
52. Smith KG, Hewitson TD, Nossal G, Tarlinton DM. The phenotype and fate of the antibody-forming cells of the splenic foci. *Eur J Immunol* (1996) 26(2):444–8. doi:10.1002/eji.1830260226
53. Biancotto A, Iglehart SJ, Vanpouille C, Condack CE, Lisco A, Ruecker E, et al. HIV-1-induced activation of CD4+ T cells creates new targets for HIV-1 infection in human lymphoid tissue ex vivo. *Blood* (2008) 111:699–704. doi:10.1182/blood-2007-05-088435
54. Svensson A, Sandberg T, Siesjö P, Eriksson H. Sequestering of damage-associated molecular patterns (DAMPs): a possible mechanism affecting the immune-stimulating properties of aluminium adjuvants. *Immunol Res* (2017) 65(6):1164–75. doi:10.1007/s12026-017-8972-5
55. Johnson GL, Lapadat R. Mitogen-activated protein kinase pathways mediated by ERK, JNK, and p38 protein kinases. *Science* (2002) 298(5600):1911–2. doi:10.1126/science.1072682
56. Li X, Stark GR. NFκB-dependent signaling pathways. *Exp Hematol* (2002) 30(4):285–96. doi:10.1016/S0301-472X(02)00777-4
57. Shih VF-S, Tsui R, Caldwell A, Hoffmann A. A single NF[kappa]B system for both canonical and non-canonical signaling. *Cell Res* (2011) 21(1):86–102. doi:10.1038/cr.2010.161
58. Junttila MR, Li S-P, Westermarck J. Phosphatase-mediated crosstalk between MAPK signaling pathways in the regulation of cell survival. *FASEB J* (2008) 22(4):954–65. doi:10.1096/fj.06-7859rev
59. Ashwell JD. The many paths to p38 mitogen-activated protein kinase activation in the immune system. *Nat Rev Immunol* (2006) 6(7):532–40. doi:10.1038/nri1865

60. Rincón M, Enslen H, Raingeaud J, Recht M, Zapton T, Su MSS, et al. Interferon-γ expression by Th1 effector T cells mediated by the p38 MAP kinase signaling pathway. *EMBO J* (1998) 17(10):2817–29. doi:10.1093/emboj/17.10.2817
61. Carr EL, Kelman A, Wu GS, Gopaul R, Senkevitch E, Aghvanyan A, et al. Glutamine uptake and metabolism are coordinately regulated by ERK/MAPK during T lymphocyte activation. *J Immunol* (2010) 185(2):1037–44. doi:10.4049/jimmunol.0903586
62. Brummer T, Shaw PE, Reth M, Misawa Y. Inducible gene deletion reveals different roles for B-Raf and Raf-1 in B-cell antigen receptor signalling. *EMBO J* (2002) 21(21):5611–22. doi:10.1093/emboj/cdf588
63. Yamashita M, Kimura M, Kubo M, Shimizu C, Tada T, Perlmutter RM, et al. T cell antigen receptor-mediated activation of the Ras/mitogen-activated protein kinase pathway controls interleukin 4 receptor function and type-2 helper T cell differentiation. *Proc Natl Acad Sci U S A* (1999) 96(3):1024–9. doi:10.1073/pnas.96.3.1024
64. Tournier C, Hess P, Yang DD, Xu J, Turner TK, Nimnual A, et al. Requirement of JNK for stress-induced activation of the cytochrome c-mediated death pathway. *Science* (2000) 288(5467):870–4. doi:10.1126/science.288.5467.870
65. Vallabhapurapu S, Karin M. Regulation and function of NF-κB transcription factors in the immune system. *Annu Rev Immunol* (2009) 27:693–733. doi:10.1146/annurev.immunol.021908.132641
66. Cullis PR, Hope MJ. Lipid nanoparticle systems for enabling gene therapies. *Mol Ther* (2017) 25(7):1467–75. doi:10.1016/j.ymthe.2017.03.013
67. Shouval D. Hepatitis B vaccines. *J Hepatol* (2003) 39(Suppl 1):S70–6. doi:10.1016/S0168-8278(03)00152-1
68. Brewer JM. (How) do aluminium adjuvants work? *Immunol Lett* (2006) 102(1):10–5. doi:10.1016/j.imlet.2005.08.002
69. Korn T, Bettelli E, Oukka M, Kuchroo VK. IL-17 and Th17 Cells. *Annu Rev Immunol* (2009) 27:485–517. doi:10.1146/annurev.immunol.021908.132710
70. Laudisi F, Spreafico R, Evrard M, Hughes TR, Mandriani B, Kandasamy M, et al. Cutting edge: the NLRP3 inflammasome links complement-mediated inflammation and IL-1β release. *J Immunol* (2013) 191:1006–10. doi:10.4049/jimmunol.1300489
71. Martinon F, Tschopp J. Inflammatory caspases: linking an intracellular innate immune system to autoinflammatory diseases. *Cell* (2004) 117(5):561–74. doi:10.1016/j.cell.2004.05.004
72. Khader SA, Bell GK, Pearl JE, Fountain JJ, Rangel-Moreno J, Cilley GE, et al. IL-23 and IL-17 in the establishment of protective pulmonary CD4+ T cell responses after vaccination and during *Mycobacterium tuberculosis* challenge. *Nat Immunol* (2007) 8(4):369–77. doi:10.1038/ni1449
73. Higgins SC, Jarnicki AG, Lavelle EC, Mills KHG. TLR4 mediates vaccine-induced protective cellular immunity to bordetella pertussis: role of IL-17-producing T cells. *J Immunol* (2006) 177(11):7980–9. doi:10.4049/jimmunol.177.11.7980
74. Sharp FA, Ruane D, Claass B, Creagh E, Harris J, Malyala P, et al. Uptake of particulate vaccine adjuvants by dendritic cells activates the NALP3 inflammasome. *Proc Natl Acad Sci U S A* (2009) 106(3):870–5. doi:10.1073/pnas.0804897106
75. Gómez JMM, Fischer S, Csaba N, Kündig TM, Merkle HP, Gander B, et al. A protective allergy vaccine based on CpG- and protamine-containing PLGA microparticles. *Pharm Res* (2007) 24(10):1927–35. doi:10.1007/s11095-007-9318-0

Conflict of Interest Statement: The authors declare that the research was conducted in the absence of any commercial or financial relationships that could be construed as a potential conflict of interest.

frontiers in Immunology

ORIGINAL RESEARCH
published: 02 May 2018
doi: 10.3389/fimmu.2018.00934

Mucosal Immunity and Protective Efficacy of Intranasal Inactivated Influenza Vaccine Is Improved by Chitosan Nanoparticle Delivery in Pigs

*Santosh Dhakal[1], Sankar Renu[1], Shristi Ghimire[1], Yashavanth Shaan Lakshmanappa[1], Bradley T. Hogshead[1], Ninoshkaly Feliciano-Ruiz[1], Fangjia Lu[2], Harm HogenEsch[2], Steven Krakowka[3], Chang Won Lee[1] and Gourapura J. Renukaradhya[1]**

[1] Food Animal Health Research Program, Department of Veterinary Preventive Medicine, The Ohio State University, Wooster, OH, United States, [2] Department of Comparative Pathobiology, College of Veterinary Medicine, Purdue University, West Lafayette, IN, United States, [3] Department of Veterinary Biosciences, The Ohio State University, Columbus, OH, United States

OPEN ACCESS

Edited by:
África González-Fernández, Centro de Investigaciones Biomédicas (CINBIO), Spain

Reviewed by:
Jose Crecente-Campo, Centro de Investigación en Medicina Molecular y Enfermedades Crónicas (CiMUS), Spain
Rong Hai, University of California, Riverside, United States

***Correspondence:**
Gourapura J. Renukaradhya
gourapura.1@osu.edu

Specialty section:
This article was submitted to Vaccines and Molecular Therapeutics, a section of the journal Frontiers in Immunology

Received: *21 January 2018*
Accepted: *16 April 2018*
Published: *02 May 2018*

Citation:
Dhakal S, Renu S, Ghimire S, Shaan Lakshmanappa Y, Hogshead BT, Feliciano-Ruiz N, Lu F, HogenEsch H, Krakowka S, Lee CW and Renukaradhya GJ (2018) Mucosal Immunity and Protective Efficacy of Intranasal Inactivated Influenza Vaccine Is Improved by Chitosan Nanoparticle Delivery in Pigs. Front. Immunol. 9:934. doi: 10.3389/fimmu.2018.00934

Annually, swine influenza A virus (SwIAV) causes severe economic loss to swine industry. Currently used inactivated SwIAV vaccines administered by intramuscular injection provide homologous protection, but limited heterologous protection against constantly evolving field viruses, attributable to the induction of inadequate levels of mucosal IgA and cellular immune responses in the respiratory tract. A novel vaccine delivery platform using mucoadhesive chitosan nanoparticles (CNPs) administered through intranasal (IN) route has the potential to elicit strong mucosal and systemic immune responses in pigs. In this study, we evaluated the immune responses and cross-protective efficacy of IN chitosan encapsulated inactivated SwIAV vaccine in pigs. Killed SwIAV H1N2 (δ-lineage) antigens (KAg) were encapsulated in chitosan polymer-based nanoparticles (CNPs-KAg). The candidate vaccine was administered twice IN as mist to nursery pigs. Vaccinates and controls were then challenged with a zoonotic and virulent heterologous SwIAV H1N1 (γ-lineage). Pigs vaccinated with CNPs-KAg exhibited an enhanced IgG serum antibody and mucosal secretory IgA antibody responses in nasal swabs, bronchoalveolar lavage (BAL) fluids, and lung lysates that were reactive against homologous (H1N2), heterologous (H1N1), and heterosubtypic (H3N2) influenza A virus strains. Prior to challenge, an increased frequency of cytotoxic T lymphocytes, antigen-specific lymphocyte proliferation, and recall IFN-γ secretion by restimulated peripheral blood mononuclear cells in CNPs-KAg compared to control KAg vaccinates were observed. In CNPs-KAg vaccinated pigs challenged with heterologous virus reduced severity of macroscopic and microscopic influenza-associated pulmonary lesions were observed. Importantly, the infectious SwIAV titers in nasal swabs [days post-challenge (DPC) 4] and BAL fluid (DPC 6) were significantly ($p < 0.05$) reduced in CNPs-KAg vaccinates but not in KAg vaccinates when compared to the unvaccinated challenge controls. As well, an increased frequency of T helper memory cells and increased levels of recall IFNγ secretion by tracheobronchial lymph nodes cells were observed. In summary, chitosan SwIAV nanovaccine delivered by IN route elicited strong cross-reactive mucosal IgA and

cellular immune responses in the respiratory tract that resulted in a reduced nasal viral shedding and lung virus titers in pigs. Thus, chitosan-based influenza nanovaccine may be an ideal candidate vaccine for use in pigs, and pig is a useful animal model for preclinical testing of particulate IN human influenza vaccines.

Keywords: swine influenza virus, chitosan nanoparticles, mucosal immune response, intranasal vaccination, pigs

INTRODUCTION

Influenza is caused by influenza A virus (IAV) of *Orthomyxoviridae* family. It is an economically important disease in the global pig industry (1, 2). Virulent swine IAV (SwIAV) infection leads to acute febrile respiratory disease which is often complicated with secondary bacterial infections (3). SwIAV increases its genetic diversity through frequent antigenic drift and antigenic shift. So far, H1N1, H1N2, and H3N2 subtypes are the major SwIAV circulating in pig populations (4). Since epithelial cells lining the porcine respiratory tract bear receptors for both avian and human IAVs, pigs can be infected with IAV from different hosts, and this event favors genetic assortment and adaptation of novel influenza strains of zoonotic and even pandemic potential (5). The pandemic H1N1 virus of 2009 and the more recent "H3N2 variant" virus in the USA are recent examples of swine-origin IAVs which cause infection and resultant pulmonary disease in humans (6, 7). Controlling influenza in pigs through vaccination serves dual benefits by protecting economic loss in swine industry and preventing possible public health risk that these reassorted SwIAVs pose for humans.

Swine influenza vaccines are commercially available. These are multivalent whole-inactivated virus (WIV) vaccines that are administered intramuscularly (IM) (8). The WIV vaccines provide protection against homologous virus infections but do not induce adequate heterologous immunity against constantly evolving IAVs that develop by point mutation(s) (8, 9). Moreover, the IM route used for WIV vaccines does not elicit adequate mucosal immune responses which are essential for providing cross-protective immunity against multitude of variant IAVs (10, 11). Intranasal (IN) vaccine that targets mucosal immune system of the respiratory tract can be a useful alternative to the current IM influenza vaccines used in pigs. Nasal mucosal vaccination not only induces strong protective immune responses at mucosal sites in the respiratory tract but also enhances immunity at distal mucosal and systemic sites (12, 13).

Biodegradable and biocompatible polymer-based nanoparticle (NP) formulation(s) provide an innovative strategy of vaccine antigen delivery to mucosal sites (14). Particulate vaccines facilitate antigen uptake by professional antigen-presenting cells (APCs), maintain slow and sustained antigen release, prevent the antigen(s) from undesirable enzymatic degradation, and potentiate the levels of protective immunity (14, 15). Different types of NPs are investigated for IN delivery of influenza vaccine antigens. For example, IN immunization in mice using liposome-based DNA and subunit influenza nanovaccines are shown to elicit mucosal, cellular, and humoral immune responses (16, 17). Poly(lactic-co-glycolic) acid (PLGA) NP-entrapped highly conserved H1N1 influenza virus peptides administered IN enhances the epitope-specific T cell response and protective efficacy in pigs (18). Ferritin-based IN influenza nanovaccine is shown to enhance mucosal secretary IgA and T cell response and confers homo- and heterosubtypic protection in mice (19). In our previous study, killed SwIAV antigen (KAg) encapsulated in PLGA polymer-based NP and delivered IN induced a robust cross-reactive cell-mediated immune response associated with a significant clearance of challenge heterologous virus from the lungs of pigs (20). In another study, the encapsulation of KAg in polyanhydride polymer-based NP also enhanced the cross-reactive cell-mediated immune response against SwIAV (21). However, both PLGA and polyanhydride polymer-based NP SwIAV vaccines used IN in these studies failed to elicit mucosal IgA and systemic IgG antibody responses, most likely due to their biased ability to induce strong T helper 1 (Th1) but not T helper 2 (Th2) responses. This Th1-biased response failed to reduce the nasal virus shedding in pigs (20, 21).

In the present study, we used chitosan, a natural mucoadhesive polymer derived NPs (CNPs) for the encapsulation of SwIAV KAg (CNPs-KAg) and performed a heterologous vaccine challenge trial in nursery pigs. Due to its cationic nature, chitosan binds readily to mucosal surfaces. Chitosan also possesses adjuvant properties, a feature which promotes immune activation (22). Previous studies have shown that CNPs form an attractive platform for mucosal vaccine delivery. For example, live Newcastle disease virus (NDV) encapsulated in CNPs and delivered through oral and IN route in chickens induced a higher secretary IgA antibody response in intestinal mucosa and enhanced the protective efficacy against highly virulent NDV strain challenge infection (23). Similarly, influenza subunit/split virus vaccine delivered in CNPs by IN route improves systemic and mucosal antibody and cell-mediated immune responses in mice (24–26). Hence, we hypothesized that IN delivery of chitosan-based nanovaccine would enhance both mucosal antibody and cellular immune responses and provide better protective immunity against SwIAV in pigs compared to soluble IN-inactivated vaccine. Our results demonstrated that CNPs-KAg IN vaccination improved mucosal IgA response in the entire respiratory tract and also elicited cell-mediated immune response against different subtypes of SwIAV, resulting in a reduced nasal viral shedding and an infectious virus burden in the pulmonary parenchyma.

MATERIALS AND METHODS

SwIAV Propagation and Inactivation

Field isolates of IAVs A/Swine/OH/FAH10-1/10 (H1N2) (27), A/Swine/OH/24366/2007 (H1N1) (28), and A/Turkey/OH/313053/2004 (H3N2) (29) were propagated in Madin–Darby

canine kidney (MDCK) cells. The H1N2 A/Swine/OH/FAH10-1/10 (H1N2-OH10) was used for CNPs-KAg vaccine preparation and H1N1 A/Swine/OH/24366/2007 (H1N1-OH7) was used for the virulent virus challenge infection. The H3N2 A/Turkey/OH/313053/2004 (H3N2-OH4) was used together with H1N2-OH10 and H1N1-OH7 for *ex vivo* cross-reactive immune analysis. The H1N2-OH10 vaccine virus and H1N1-OH7 challenge virus are heterologous to each other with 77% HA gene identity, whereas H3N2-OH4 virus, originally isolated from turkeys, is heterosubtypic to other two SwIAVs with HA gene identity of 63% (27–29). For vaccine preparation, cell culture fluid of H1N2-OH10 virus grown in MDCK cells was harvested and subjected to sucrose gradient ultracentrifugation. The virus pellet was suspended in phosphate-buffered saline (PBS), titrated for infectious virus titer, and inactivated by using binary ethyleneimine (Sigma, MO, USA) as described previously (20).

Preparation of Chitosan-Based Nanovaccine and *In Vitro* Characterization

Chitosan NPs-loaded-killed SwIAV antigen (KAg) (CNPs-KAg) formulation was prepared by the ionic gelation method as described previously (23, 30–32) with some modifications. Briefly, 1.0% (w/v) low-molecular weight chitosan polymeric (Sigma, MO, USA) solution was prepared in an aqueous solution of 4.0% acetic acid under magnetic stirring until the solution became clear. The chitosan solution was sonicated; pH was adjusted to 4.3 and filtered *via* a 0.44-µm syringe filter. Five milliliters of 1.0% chitosan solution was added to 5.0-mL deionized water and incubated with 3.0-mg SwIAV KAg dissolved in 1.0 mL 3-(N-morpholino) propanesulfonic acid (MOPS) buffer at pH 7.4. Consequently, 2.5 mL of 1.0% (w/v) tripolyphosphate (TPP) (Sigma, MO, USA) dissolved in 2.5-mL deionized water was added into the chitosan polymer solution with continuous magnetic stirring at room temperature (RT) (22°C). The formulated SwIAV nanovaccine was centrifuged at 10,000 rpm for 10 min, dispersed in MOPS buffer at pH 7.4, lyophilized with a cryoprotectant, and stored at −80°C.

Particle size and zeta potential of empty and vaccine antigen-loaded NPs were measured after dispersion in PBS (pH 7.4) and stored at 4°C for at least 30 h by dynamic light-scattering (DLS) method using a zeta-sizer coupled with an MPT-2 titrator (Malvern) as described previously (33). During each vaccination, CNPs-KAg were freshly prepared and used. The morphology of NPs was obtained by using the cold field emission Hitachi S-4700 scanning electron microscope (SEM) (20). Briefly, the powder form of NPs was loaded on to aluminum stubs and coated with platinum prior to examination under the microscope. Protein loading efficiency in CNPs-KAg was estimated indirectly by determining the difference between the initial amount of protein used for loading CNPs and the protein left in the supernatant (23). *In vitro* protein release profile in CNPs-KAg suspended in PBS for up to 15 days was estimated and expressed as the cumulative percentage release of SwIAV antigen at each time point as described previously (20). In brief, CNPs-KAg suspended in 500 µL PBS (pH 7.4) in triplicate in eppendorf tubes was incubated at 37°C in a revolving roller apparatus. At indicated time point, tubes were centrifuged, supernatant collected, and pellet was resuspended in fresh 500 µL PBS. Protein released on to the supernatant was estimated by micro-BCA protein assay kit (Thermo Scientific, MA, USA) and expressed as the percentage of cumulative protein released over the initial amount at time zero in particles.

In Vitro Uptake of CNPs-KAg by APCs

Peripheral blood mononuclear cells (PBMCs) isolated from 9- to 10-week-old pigs were used for the *in vitro* antigen uptake study. Cells were suspended in enriched-Roswell Park Memorial Institute medium and seeded on to 1 million cells/well in 96-well cell culture plates. After overnight incubation at 37°C in 5% CO_2, unattached cells were removed. The attached monocyte/macrophage cells were treated with SwIAV KAg or CNPs-KAg containing the antigen at 10 µg/mL concentration for 10, 30, and 150 min. After the indicated period of incubation, the cells were fixed with 80% acetone, stained with IAV nucleoprotein-specific antibody (CalBioreagents, CA, USA) followed by Alexa Fluor 488 conjugated goat anti-mouse IgG antibody (Life technologies, OR, USA). Cells were evaluated under fluorescent microscope (Olympus IX70) and photomicrographs were taken (20×). For evaluation of SwIAV antigen uptake from CNPs-KAg-treated porcine monocyte/macrophages prepared from three pigs, PBMCs separately were incubated in 48-well plates seeded with 2×10^6 cells per well overnight as described above. Cells were treated with KAg or CNPs-KAg at SwIAV antigen concentration 10 µg/mL for 10, 30, and 150 min. A positive control was MDCK cells infected with SwIAV H1N2-OH10 at multiplicity of infection (MOI) 1 for 12 h. After the indicated period of treatment, cells were fixed using 1% paraformaldehyde (PFA), permeabilized, and stained with IAV nucleoprotein-specific antibody (CalBioreagents, CA, USA) followed by treatment with goat anti-mouse IgG Alexa Flour 488 conjugated secondary antibody. We acquired 50,000 events in BD Aria II flow cytometer (BD Biosciences, CA, USA) and the data analyzed by using the FlowJo software (Tree Star, OR, USA).

In Vitro Generation and Stimulation of Porcine Dendritic Cells (DCs)

Porcine monocyte-derived dendritic cells (MoDCs) were prepared from PBMCs isolated from seven pigs as described previously (34) with few modifications. Briefly, 25 million PBMCs per mL were seeded in each well of six-well culture plates. After overnight incubation at 37°C in a 5% CO_2 incubator, non-adherent cells were discarded and adhered cells were treated with GM-CSF (25 ng/mL) and interleukin (IL-4) (10 ng/mL) cytokines. Half of the culture media was replaced on every third day. On day 7, the plate was centrifuged at 2,000 RPM at 4°C for 5 min and the supernant was harvested gently, and the generated immature MoDCs were stimulated in the same plate without seeding into fresh plates with medium only, LPS control (10 µg/mL), KAg (10 µg/mL), and CNPs-KAg containing 10 µg/mL of KAg for 48 h. The culture supernatant was harvested, and the levels of innate, pro-inflammatory and Th1 cytokines, IFN-α, TNF-α, IL-1β, IL-12, IL-6, and IL-10 were estimated by ELISA as described previously (35).

Experimental Design

Cesarean-delivered colostrum-deprived and bovine colostrum-fed influenza antibody-free Large White-Duroc crossbred piglets were raised in our BSL2 animal facility at OARDC. Piglets at 4 weeks

of age (male and female) were randomly assigned into one of the three experimental groups and kept in separate isolation rooms (**Table 1**). The first IN vaccination was performed at 5 weeks of age and the second IN booster vaccination at 8 weeks of age. All piglets receiving virulent SwIAV were challenged at 10 weeks of age. Separate groups of pigs were vaccinated IN with DMEM (Gibco) or with 1×10^7 $TCID_{50}$ equivalent of KAg or CNPs-KAg suspended in 2 mL DMEM by IN mist as described previously (20). The challenge infection was done using heterologous H1N1-OH7 SwIAV (6×10^6 $TCID_{50}$) in 2 mL, divided into 1 mL administered IN and 1 mL intratracheally as described previously (18, 20, 21).

Serum samples were collected at days post-vaccination (DPV) 21 and 35. The rectal temperatures were recorded daily from day post-challenge (DPC) 0 onward, and nasal swab samples were collected at DPC 0, DPC 4, and DPC 6. Pigs were euthanized at DPC 6, and serum and bronchoalveolar lavage (BAL) fluid were collected. During necropsy, lungs were examined for macroscopic pneumonic lesions and scored as described previously (20). Lung lysates were prepared by homogenization of 1.0 g of lung tissue collected from the right apical lobe (20). Nasal swabs, sera, BAL fluid, and lung lysate samples were stored at −80°C until processed for antibody and virus titration. The PBMCs were isolated from blood at DPV 35/DPC 0 and DPC 6 (20). Mononuclear cells were harvested from tracheobronchial lymph nodes (TBLN-MNCs) at DPC 6 as described previously (35).

Antibody Titration

Hemagglutination inhibition (HI) antibody titers against IAVs H1N1-OH7, H1N2-OH10, and H3N2-OH4 in sera and BAL fluid samples were determined as described previously (20). The SwIAV-specific IgG and IgA antibodies in nasal swabs, sera, BAL fluids, and lung lysates were determined by ELISA (20). Briefly, 96-well plates (Greiner bio-one, NC, USA) were coated overnight with respective pre-titrated IAV antigen (5 μg/mL) and blocked with 5% skim milk powder containing 0.05% Tween-20 for 2 h at RT. After washing, fivefold dilutions of nasal swab, serum, BAL fluid, and lung lysate samples in PBS containing 2.5% skim milk powder and 0.05% Tween-20 were added to marked duplicate wells, incubated for 2 h at RT, washed, and horse radish peroxidase-conjugated goat anti-pig IgA (Bethyl Laboratories Inc., TX, USA) or goat anti-pig IgG (KPL, MD, USA) was added. Finally, the antigen and antibody interaction were detected by using 1:1 mixture of peroxidase substrate solution B and TMB peroxidase substrate (KPL, MD, USA). The reaction was stopped using 1.0 M phosphoric acid, and optical density was measured at 450 nm using Spectramax microplate reader (Molecular devices, CA, USA).

TABLE 1 | Experimental design showing different vaccine groups.

Experimental groups	Pig no.	First vaccination (DPV 0)	Second vaccination (DPV 21)	Day of challenge (DPV 35/ DPC 0)
Unvaccinated	3	DMEM	DMEM	H1N1-OH7
KAg	4	Inactivated H1N2-OH10	Inactivated H1N2-OH10	H1N1-OH7
CNPs-KAg	5	Inactivated H1N2-OH10 encapsulated in chitosan nanoparticle (CNP)	Inactivated H1N2-OH10 encapsulated in CNP	H1N1-OH7

Antigen-Specific Cell Proliferation Assay

The PBMCs isolated at DPV 35/DPC 0 were cultured together with H1N1-OH7, H1N2-OH10, or H3N2-OH4 SwIAV at 0.1 MOI and incubated at 37°C in 5% CO_2 incubator for 72 h. Antigen-specific lymphocyte proliferation was determined by using the cell titer 96 aqueous non-radioactive proliferation assay kit (Promega, WI, USA). The cell proliferative response was compared among groups using lymphocyte stimulation index values as described previously (20).

Cytokine ELISA

The PBMCs isolated at DPC 0 and TBLN-MNCs at DPC 6 were cultured with H1N2-OH10, H1N1-OH7, or H3N2-OH4 SwIAV at 0.1 MOI. After 72 h of stimulation, the supernatant was collected and interferon gamma (IFNγ) secretion was determined by ELISA as described previously (20). Similarly, the production of interleukin-6 (IL-6) in BAL fluid collected at DPC 6 was determined by ELISA (35).

Virus Titration

Viral titers contained in nasal swabs and BAL fluids were determined in a 10-fold dilution of the samples in DMEM containing TPCK-trypsin (1 μg/mL). The samples were transferred to quadruplicate 96-well cell culture plate wells containing overnight cultured monolayers of MDCK cells and incubated for 72 h, 37°C, 5.0% CO_2. Cells were fixed with acetone and immunostained with IAV nucleoprotein-specific antibody (#M058, CalBioreagents, CA, USA) followed by Alexa Fluor 488 conjugated goat anti-mouse IgG (H + L) antibody (Life technologies, OR, USA). Virus replication in cells was determined by using immunofluorescence technique as described previously (20).

Histopathology of Lungs

For histopathological analysis of pulmonary tissues, 10% formalin-inflated apical, cardiac, and diaphragmatic lobes were collected and further emulsion-fixed in 10% neutral buffered formalin. Five-micrometer sections of formalin-fixed, paraffin-embedded apical, cardiac, and diaphragmatic lung lobes were stained with hematoxylin and eosin (H&E) as previously described (20). The H&E-stained tissue sections were examined for microscopic changes of interstitial pneumonia, peribronchial and perivascular accumulation of mononuclear cells, bronchial exudates, and epithelial changes related to influenza infection. All these parameters were scored by a board-certified veterinary pathologist (SK) who was not provided with any vaccination history of pig groups in a scale of 0 (no change compared from normal) to 3 (marked changes from normal) as described previously (20).

Flow Cytometry

The PBMCs isolated at DPC 0 and TBLN-MNCs at DPC 6 were immunostained for T lymphocyte subset phenotyping as described previously (20). Antibodies used in the flow cytometry were anti-porcine CD3 (Southernbiotech, AL, USA), CD4α (Southernbiotech, AL, USA), CD8α (Southernbiotech, AL,

USA), and CD8β (BD Biosciences, CA, USA). Briefly, the cells were blocked with 2% pig serum in fluorescence-activated cell sorting (FACS) buffer and surface labeled with pig lymphocyte-specific purified, biotin or fluorochrome-conjugated antibodies or their respective antibody isotypes. Cells were fixed using 1% PFA, washed, suspended in FACS buffer, and acquired using BD Aria II flow cytometer (BD Biosciences, CA, USA). Data analysis was done using FlowJo software (Tree Star, OR, USA).

Quantitative Reverse Transcription PCR (RT-qPCR)

Total RNA was extracted from PBMCs at DPC 0 and TBLN at DPC 6 using TRIzol reagent (Invitrogen, CA, USA) as per the manufacturer's instructions. NanoDrop™ 2000c Spectrophotometer (Thermo Fisher Scientific, MA, USA) was used to determine the concentration and purity of RNA. cDNA was prepared from 1 µg of total RNA using the QuantiTect Reverse Transcription Kit (AIAGEN). Primers of housekeeping gene (β actin) and target genes (T-bet and GATA-3) used in this experiment were described previously (36). The mRNA expression was analyzed by 7500 Real-Time qPCR system (Applied Biosystems, CA, USA) using the qScript™ One-Step SYBR Green qRT-PCR kit, Low ROX™ (Quantabio, MA, USA). The target gene expression level was normalized with housekeeping gene levels, and the fold change was determined by comparative $2^{-\Delta\Delta C}$T method (37).

Statistical Analysis

Statistical analysis was performed by using non-parametric Kruskal–Wallis test followed by Dunn's *post hoc* test using the software GraphPad Prism 5 (GraphPad Software, Inc., CA, USA). Pig rectal temperature data were analyzed by repeated measure

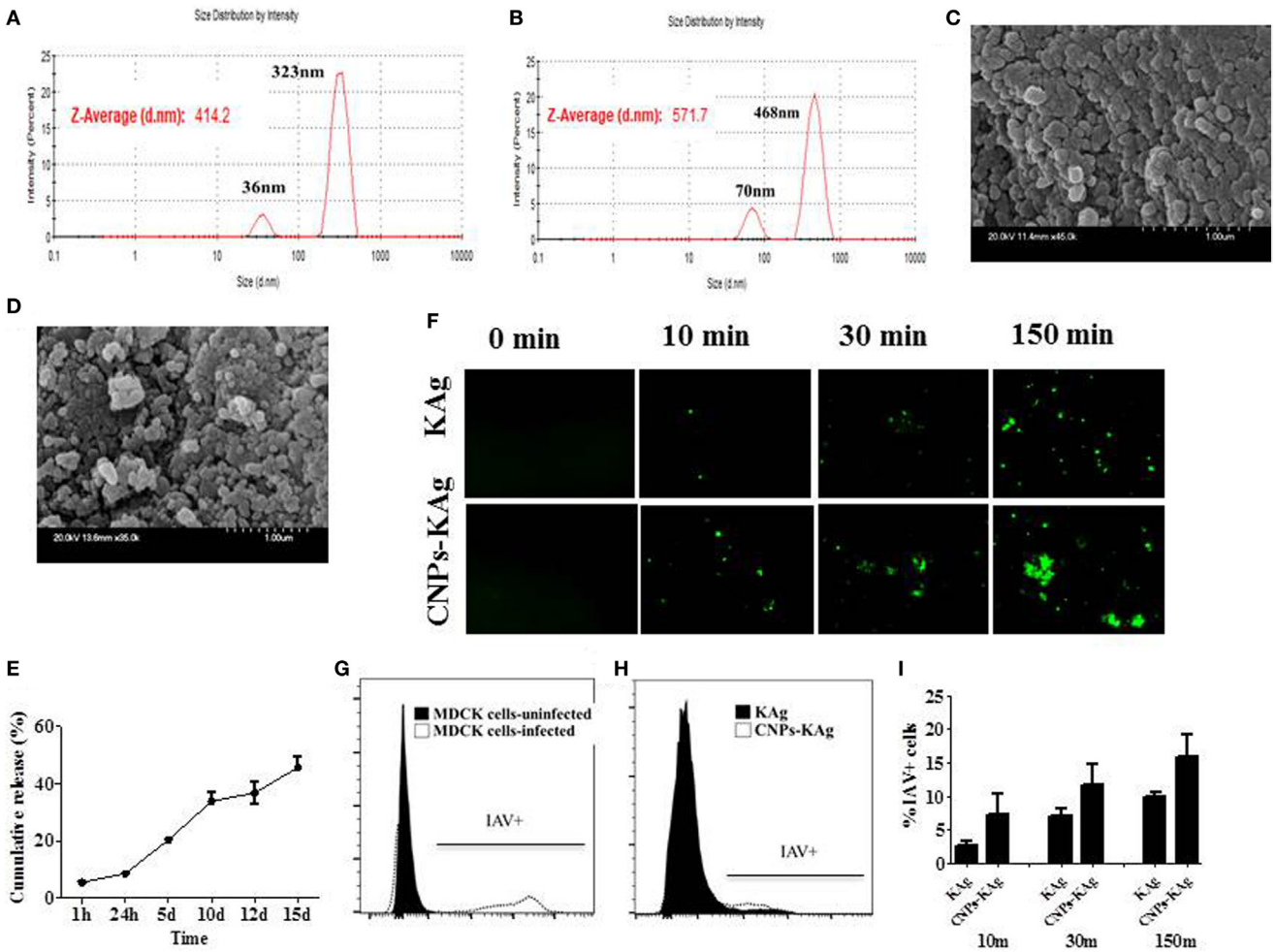

FIGURE 1 | *In vitro* characteristics of chitosan nanoparticles (CNPs)-KAg. Diameter of **(A)** empty CNPs and **(B)** swine influenza A virus (SwIAV)-killed antigen (KAg)-loaded CNPs (CNPs-KAg) determined by dynamic light scattering. Scanning electron microscope (SEM) images of **(C)** empty CNPs and **(D)** CNPs-KAg. **(E)** Release of KAg from CNPs-KAg suspended in phosphate-buffered saline over a period of 15 days. **(F)** Uptake of soluble SwIAV KAg or CNPs-KAg formulation by monocytes/macrophages at indicated time points determined by fluorescent microscopy (Olympus, IX70, 20× magnifications). The frequency of monocytes/macrophages uptaken SwIAV KAg treated with soluble antigen or CNPs-KAg determined by flow cytometry: **(G)** SwIAV-infected Madin-Darby canine kidney (MDCK) cells as positive control; **(H)** a representative picture of SwIAV KAg or CNPs-KAg uptake by porcine monocytes/macrophages after 150 min treatment; and **(I)** percentage of cells with internalized SwIAV antigen at 10, 30, and 150 min treatment.

ANOVA using Friedman test followed by Dunn's pairwise comparison. Cytokine data (**Figure 2**) between two groups were analyzed by Mann–Whitney test. A *p*-value of less than 0.05 was considered to be statistically significant. The infectious virus titer was determined using Reed and Muench method. Data were presented as the mean ± SEM of three to five pigs except for the HI titers which were expressed as the geometric mean with 95% confidence interval.

RESULTS

Characterization of CNPs-KAg Vaccine Candidate

The encapsulation efficiency of SwIAV KAg in chitosan nanovaccine formulation was 67%. This result was comparable to the encapsulation efficiency of chitosan NPs entrapped with *Salmonella* outer membrane protein antigens (70%) (Renu et al., 2018, manuscript under review). As determined by DLS, the average size of the empty (**Figure 1A**) and antigen-loaded (**Figure 1B**) NPs was 414.2 and 571.7 nm, respectively. Empty NPs showed two peaks at 36 (~10%) and 323 nm (~90%) with polydispersity index (PDI) of 0.39. Likewise, antigen-loaded NPs also had two peaks at 70 (~15%) and 468 nm (~85%) with PDI of 0.60. Data show that the CNPs-KAg were polydispersed in nature. SEM analysis showed that the morphology of the empty NPs was spherical with a smooth surface (**Figure 1C**), while antigen-loaded NPs had a relatively rough and irregular surface (**Figure 1D**). The surface charge of empty and antigen-loaded chitosan NPs was +1.88 and +1.69 mV, respectively. We observed 6% burst release, i.e., surface-associated antigen release during the first 1 h, and on an average, 9% of antigen was released after 24 h of incubation. Further, a slow and sustained release of antigen was observed with a cumulative release of approximately 46% after 15 days (**Figure 1E**).

To determine whether chitosan encapsulation of KAg enhances the uptake of antigen by APCs, we prepared monocyte/macrophages from PBMCs and allowed for interaction with KAg or CNPs-KAg and stopped the reaction at three different time points. Internalization of CNPs-KAg vaccine by monocytes/macrophages was observed within 10 min of treatment indicated by a higher number of influenza-specific fluorescent signals compared to KAg treatment (**Figure 1F**). Further, the uptake of CNPs-KAg was substantially increased after 30 and 150 min post treatment compared to control KAg-treated cells. We also performed flow cytometry analysis of monocyte/macrophages treated with KAg

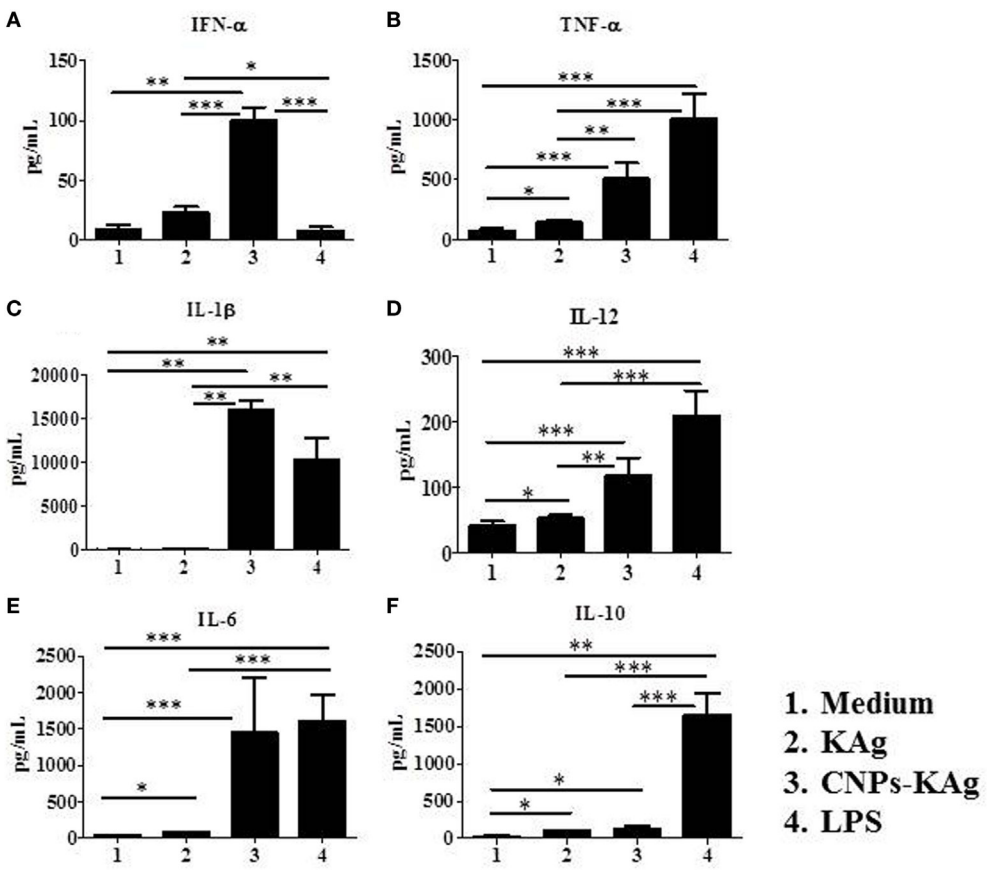

FIGURE 2 | Production of innate, pro-inflammatory and T helper 1 cytokines by porcine MoDCs treated for 48 h with medium, KAg, chitosan nanoparticles (CNPs)-KAg or LPS control. Levels of cytokines **(A)** IFN-α, **(B)** TNF-α, **(C)** interleukin (IL)-1β, **(D)** IL-12, **(E)** IL-6, and **(F)** IL-10 were estimated in stimulated cell culture supernatant by ELISA. Data represent mean value of seven pig-derived DCs ± SEM. Statistical analysis between two groups was carried out using Mann–Whitney test. Asterisk refers to statistical significant difference between the indicated two pig groups. $^{*}p < 0.05$, $^{**}p < 0.01$, and $^{***}p < 0.001$.

or CNPs-KAg to determine the frequency of specific uptake of influenza antigens in APCs. MDCK cells infected with SwIAV H1N2-OH10 were used as positive control (**Figure 1G**) and a representative picture of flow cytometry analysis of KAg or CNPs-KAg uptake by monocyte/macrophages is also shown (**Figure 1H**). In soluble KAg-treated cells, an average of 2.7, 7.1, and 10.1% cells positive for influenza antigen, and in CNPs-KAg-treated cells, 7.2, 11.7, and 16% cells with uptaken influenza antigen after 10, 30, and 150 min of incubation were noticed, respectively (**Figure 1I**). These data clearly demonstrated that CNPs-KAg was efficiently internalized by pig APCs better than soluble antigens.

CNPs-KAg Formulation Induced the Secretion of Cytokines by Porcine MoDCs *In Vitro*

In order to elucidate the adjuvant property of chitosan NPs in porcine APCs, we treated porcine MoDCs with medium and LPS as control to compare the effect of soluble KAg and CNPs-KAg treatment in inducing the secretion of different cytokines. As expected, the medium control cells had very little secretion of all the detected cytokines, while LPS treatment induced the production of all the analyzed cytokines except IFN-α (**Figures 2A–F**). Cells treated with KAg secreted significantly higher levels of pro-inflammatory cytokines TNF-α (**Figure 2B**) and IL-6 (**Figure 2E**) and Th1 cytokine IL-12 (**Figure 2D**) compared to medium control. In DCs treated with CNPs-KAg, the production of innate IFN-α (**Figure 2A**), TNF-α (**Figure 2B**), IL-1β (**Figure 2C**), and IL-12 (**Figure 2D**) was significantly higher in CNPs-KAg-treated compared to that in soluble KAg-treated cells. In CNPs-KAg-treated cells, the production of IL-6 (**Figure 2E**) and Th2 cytokine IL-10 (**Figure 2F**) was higher than medium control cells, but not significantly higher compared to KAg-treated cells. Our *in vitro* DCs treatment data suggest that chitosan nanovaccine formulation has a potent adjuvant effect on porcine DCs.

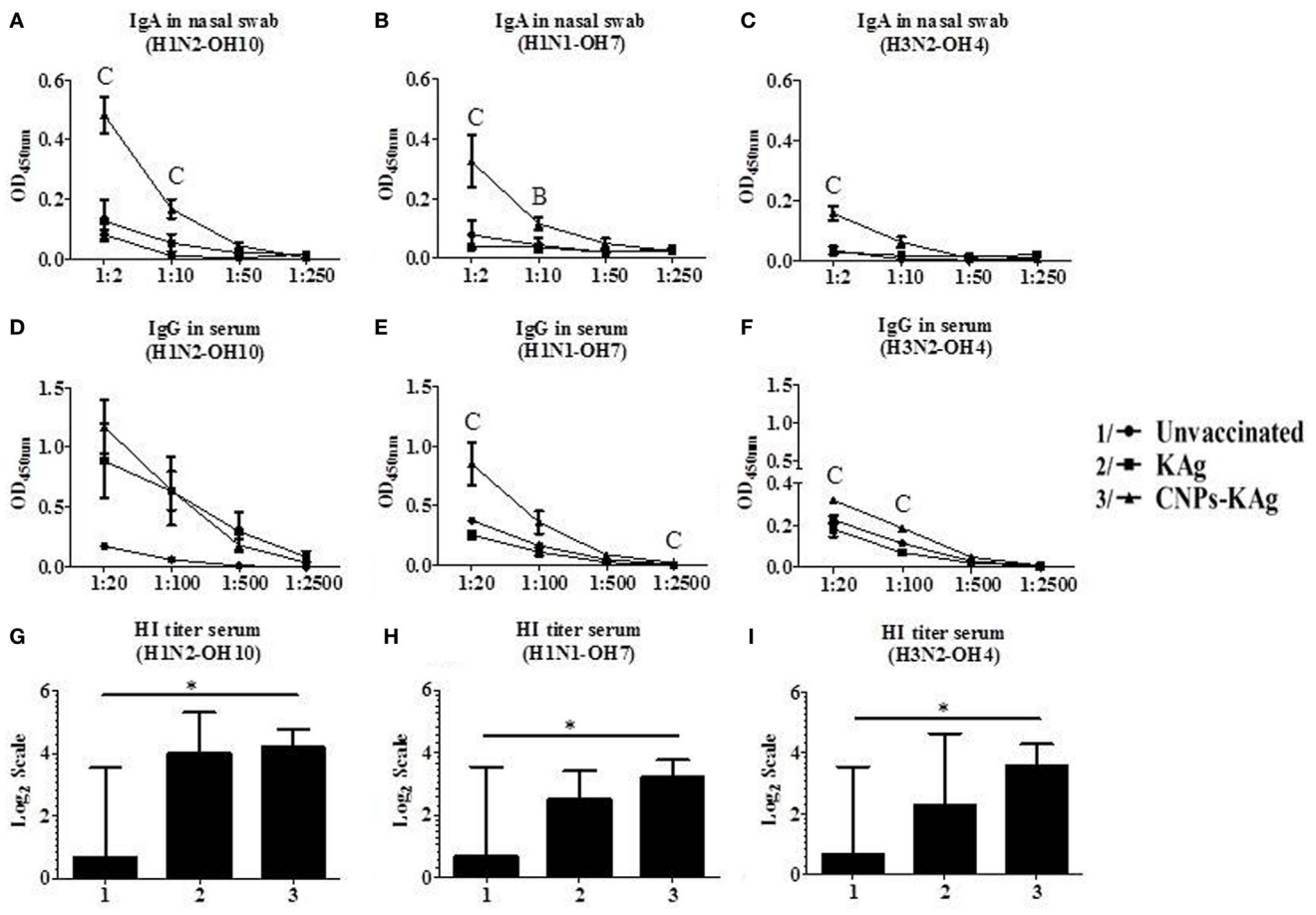

FIGURE 3 | Antibody response after chitosan nanoparticles (CNPs)-KAg prime-boost vaccination at day post-vaccination 35/day post-challenge 0 (DPV 35/DPC 0) in pigs. Mucosal secretory IgA antibody response in nasal swab, systemic IgG antibody, and hemagglutination inhibition (HI) titers in serum samples against **(A,D,G)** H1N2-OH10, **(B,E,H)** H1N1-OH7, and **(C,F,I)** H3N2-OH4 influenza A virus (IAVs). Data represent the mean value of three to five pigs ± SEM. Statistical analysis was carried out using Kruskal–Wallis test followed by Dunn's *post hoc* test. Asterisk refers to statistical significant difference between the indicated two pig groups (*$p < 0.05$). In antibody dilution curves **(A–F)**, A, B, and C refer to significant difference between unvaccinated vs KAg vaccinates, unvaccinated vs CNPs-KAg vaccinates, and KAg vs CNPs-KAg vaccinates, respectively, at the indicated dilution.

CNPs-KAg Vaccine Augmented the IAV-Specific Mucosal Antibody Response in the Respiratory Tract of Pigs

Secretary IgA antibody levels in nasal swab samples collected after IN prime-boost vaccination at DPV 35/DPC 0 were significantly higher ($p < 0.05$) in CNPs-KAg-vaccinated pigs compared to those in pigs receiving soluble KAg when tested against the homologous H1N2-OH10 (**Figure 3A**), heterologous H1N1-OH7 (**Figure 3B**), and heterosubtypic H3N2-OH4 IAVs (**Figure 3C**). A significant difference in antibody response was observed between CNPs-KAg and KAg vaccinates in serial twofold diluted nasal swab samples (**Figures 3A–C**). These data suggest that the CNPs-KAg IN delivery induced an enhanced cross-reactive mucosal secretary IgA antibody response in pigs. Specific IgG antibody response in sera after prime-boost vaccination in KAg-vaccinated pigs against the vaccine virus was comparable to the CNPs-KAg vaccine group (**Figure 3D**). A significantly higher ($p < 0.05$) cross-reactive IgG response was observed in CNPs-KAg vaccinates against heterologous H1N1-OH7 (**Figure 3E**) and heterosubtypic H3N2-OH10 (**Figure 3F**) IAVs compared to KAg-vaccinated animals. In CNPs-KAg-vaccinated pig sera, IAV-specific HI antibody titers against H1N2-OH10 (**Figure 3G**), H1N1-OH7 (**Figure 3H**), and H3N2-OH4 (**Figure 3I**) were significantly higher ($p < 0.05$) compared to mock pig group. The HI titers in CNPs-KAg vaccinates were around twofold higher compared to KAg vaccinates against heterologous (**Figure 3H**) and heterosubtypic (**Figure 3I**) IAVs, but the data were not statistically significant ($p > 0.05$). The expression of Th2-specific transcription factor GATA-3 mRNA in PBMCs of pigs at DPV 35/DPC 0 was 4- and 1.5-fold higher in CNPs-KAg-vaccinated pigs compared to that in unvaccinated control ($p < 0.05$) and KAg-vaccinated pigs ($p > 0.05$) (**Figure 4A**). The expression of Th1-specific transcription factor T-bet in PBMCs was not significantly different among the pig groups (**Figure 4B**).

The mucosal IgA response in pigs post-challenge at DPC 6 was determined, and the data indicate that specific IgA in CNPs-KAg-vaccinated pig group was significantly higher ($p < 0.05$) compared to unvaccinated-challenged animals and remarkably higher compared to KAg-vaccinated and -challenged animals against all three IAV subtypes in nasal swabs (**Figures 5A–C**), BAL fluids (**Figures 5D–F**), and lung lysates (**Figures 5G–I**). These data indicated the secretion of robust mucosal IgA antibody in the upper respiratory tract (nasal swabs), lower respiratory tract (BAL fluids), and lung parenchyma (lung lysates) of pigs. Similarly, systemic IgG antibody response in serum at DPC 6 was also enhanced in the CNPs-KAg vaccinates compared to that in unvaccinated ($p < 0.05$) and KAg-vaccinated and virus-challenged animals (**Figures 6A–C**). However, HI antibody titers in BAL fluid at DPC 6 were comparable between KAg and CNPs-KAg vaccinates (**Figures 6D–F**).

CNPs-KAg Vaccine Enhanced Systemic-Specific Cell-Mediated Immune Response Against IAVs

To understand the role of chitosan delivered IAV nanovaccine in the induction of specific cell-mediated immune response after IN vaccinations, isolated PBMCs at DPV 35 were restimulated with H1N2-OH10, H1N1-OH7, and H3N2-OH4 viruses. The harvested cell culture supernatants were analyzed for IFNγ secretion, and significantly higher ($p < 0.05$) levels of IFNγ in homologous H1N2-OH10 virus restimulated CNPs-KAg compared to soluble KAg-vaccinated pigs were observed (**Figure 7A**). Though not statistically significant, the IFNγ recall response in heterologous and heterosubtypic viruses restimulated cells was noticeably of higher levels in CNPs-KAg vaccinates than in KAg-vaccinated pigs (**Figures 7B,C**). The average IFNγ amounts in CNPs-KAg vaccine group against H1N1-OH7 and H3N2-OH4 viruses were 463 and 332 pg/mL compared to 91 and 16 pg/mL in KAg vaccinates, respectively (**Figures 7B,C**). We also performed phenotyping of PBMCs isolated at DPC 0 by flow cytometry. The frequency of cytotoxic T cells (CTLs) in CNPs-KAg-vaccinated pigs (average: 18.1%) was higher compared to that in KAg-vaccinated (average: 15.7%, $p > 0.05$) and unvaccinated pigs (average: 13.4%, $p < 0.05$) (**Figure 7D**). This finding is consistent with enhanced IFNγ response in CNPs-KAg-vaccinated pigs, as activated CTLs are one of the major T cell subsets which secrete high levels of antiviral cytokine IFNγ. In addition, in PBMCs at DPC 0, virus-specific cell proliferation was detected in an increased trend upon restimulation with homologous (**Figure 7E**) and heterologous (**Figure 7F**), but not with heterosubtypic (**Figure 7G**) viruses in CNPs-KAg-vaccinated pigs. Overall, these data suggested the

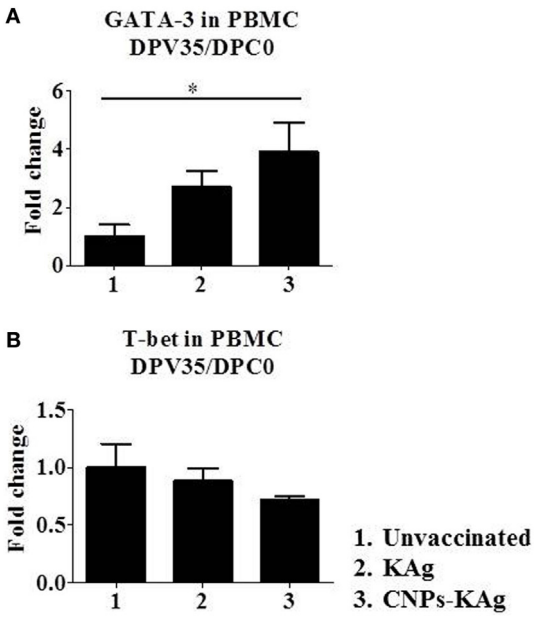

FIGURE 4 | Expression of T helper 1 (Th1) and T helper 2 (Th2) response inducing specific transcription factors after prime-boost vaccination in pigs. The expression of **(A)** Th2 transcription factor GATA-3 and **(B)** Th1 transcription factor T-bet in peripheral blood mononuclear cells of pigs at day post-vaccination (DPV) 35/day post-challenge (DPC) 0 were determined by quantitative reverse transcription PCR (qRT-PCR). Data represent the mean value of three to five pigs ± SEM. Statistical analysis was carried out using Kruskal–Wallis test followed by Dunn's *post hoc* test. Asterisk refers to the statistical significant difference between the indicated two pig groups. *$p < 0.05$.

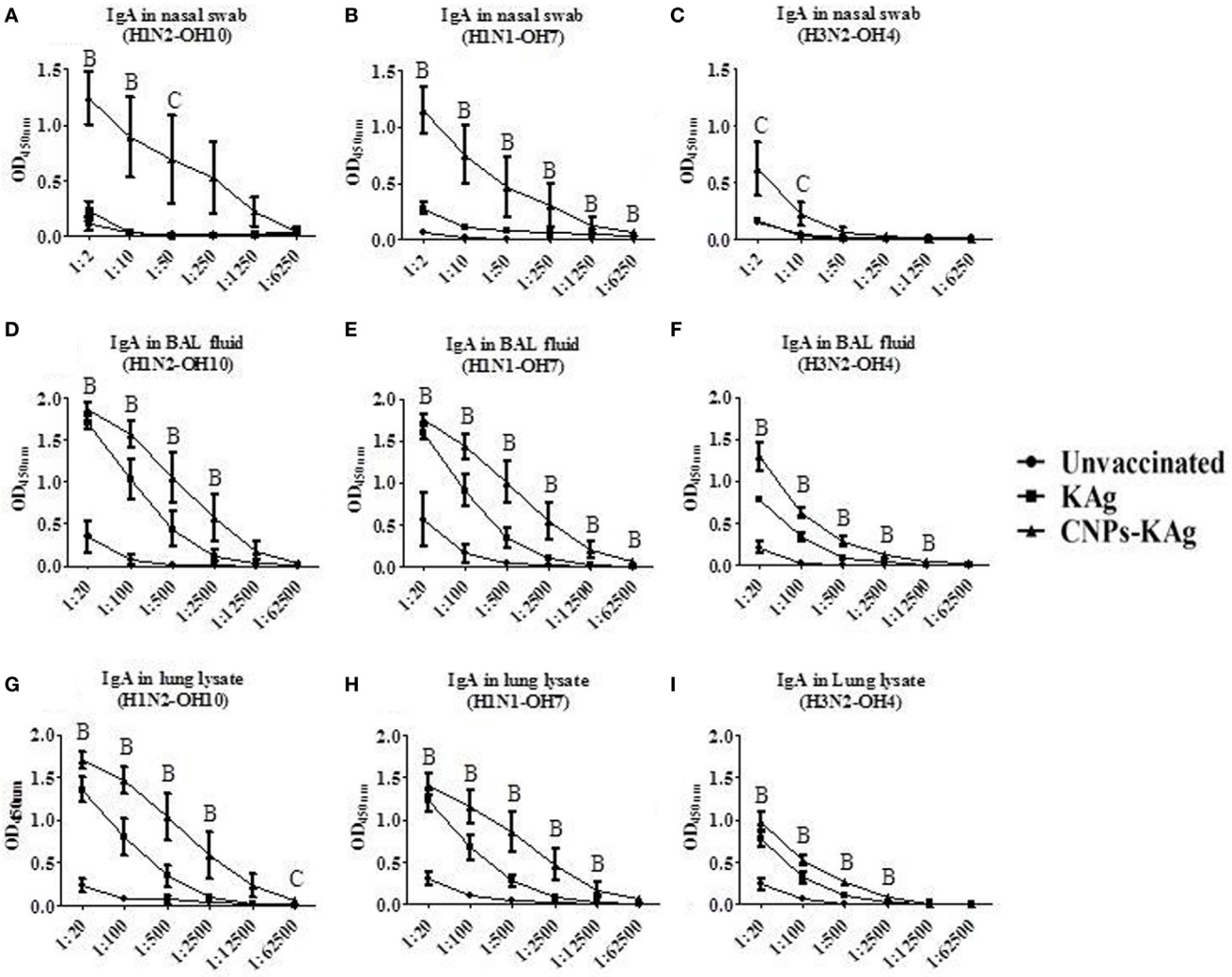

FIGURE 5 | Mucosal IgA antibody response in the respiratory tract of pigs vaccinated with chitosan nanoparticles (CNPs)-KAg at day post-challenge 6. Specific IgA antibody response in nasal swab, bronchoalveolar lavage (BAL) fluid, and lung lysate samples against H1N2-OH10 **(A,D,G)**, H1N1-OH7 **(B,E,H)**, and H3N2-OH4 **(C,F,I)** influenza A virus (IAVs). Data represent the mean value of three to five pigs ± SEM at all indicated dilutions. Statistical analysis was carried out using Kruskal–Wallis test followed by Dunn's *post hoc* test where A, B, and C refer to significant difference ($p < 0.05$) between unvaccinated vs KAg vaccinates, unvaccinated vs CNPs-KAg vaccinates, and KAg vs CNPs-KAg vaccinates, respectively, at the indicated dilution.

presence of superior cross-reactive effector memory lymphocyte response in pigs induced by chitosan encapsulation of inactivated SwIAV antigen.

CNPs-KAg Vaccine Reduced the Inflammatory Changes in the Lungs of Virulent and Heterologous Virus-Challenged Pigs

Rectal temperature of pigs was recorded daily post-challenge until euthanized. Pigs in all groups had fever (≥104°F) for the first 2 days after challenge. However, there was no statistical difference in temperature profile among the pig groups (**Figure 8A**). Macroscopic pulmonary lesions were scored for percent consolidation induced by influenza infection and observed lower pulmonary consolidation in CNPs-KAg vaccinates (mean score 15) compared to KAg (mean score 17) and unvaccinated animals (mean score 19) (**Figure 8B**), but the data were not statistically significant ($p > 0.05$). Microscopic pulmonary lesions were subjectively scored on H&E-stained lung sections where a score of 0 = no change from normal, 1 = minimal change from normal, 2 = moderate change from normal, and 3 = severe change from normal (**Figure 8C**). The mean scores of interstitial pneumonia (2, 1.6, and 0.8), peribronchial inflammation (2, 1.8, and 1.8), perivascular inflammation (1.6, 0.3, and 0.5), bronchial exudates (0.7, 0.1, and 0.2), and epithelial changes (0.3, 0.3, and 0.1) were observed in virus-challenged unvaccinated, KAg, and CNPs-KAg vaccinates, respectively. All the microscopic evaluation of pulmonary tissues was conducted by a board-certified veterinary pathologist. A moderate reduction in inflammatory changes was observed in both the

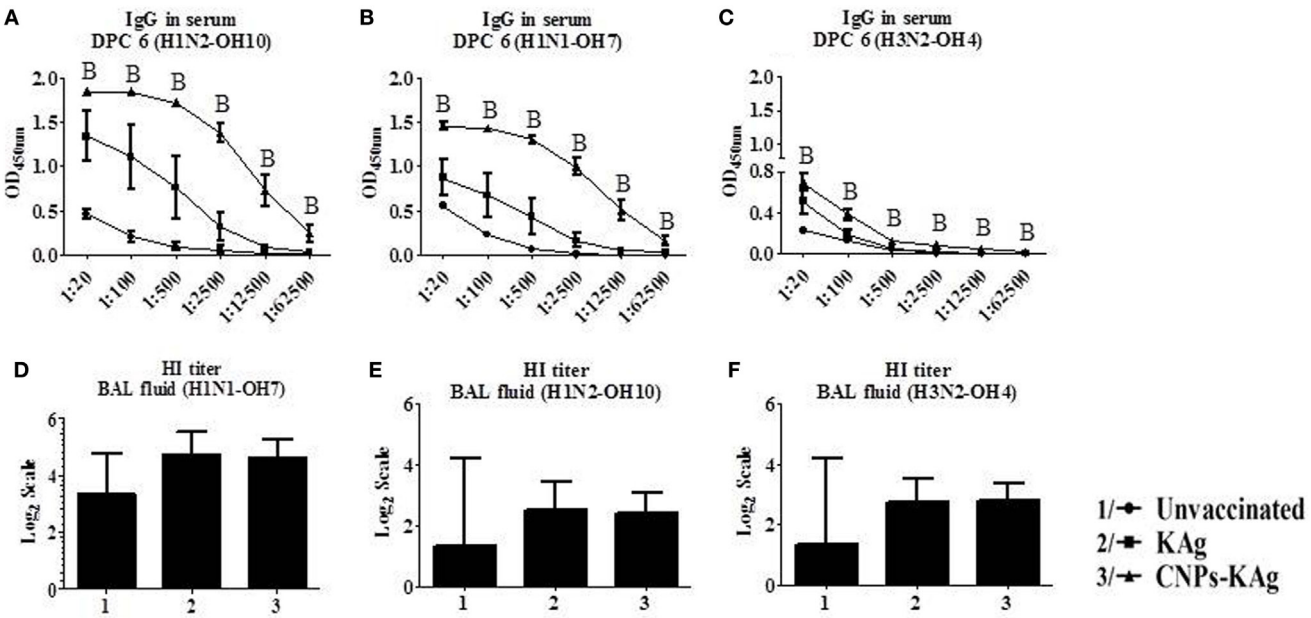

FIGURE 6 | Serum IgG response and bronchoalveolar lavage (BAL) fluid hemagglutination inhibition (HI) antibody titers in pigs vaccinated with chitosan nanoparticles (CNPs)-KAg at day post-challenge 6. Specific IgG antibody response in serum and BAL fluid HI titers against H1N2-OH10 **(A,E)**, H1N1-OH7 **(B,D)**, and H3N2-OH10 **(C,F)** influenza A virus (IAVs). Data represent the mean value of three to five pigs ± SEM. Statistical analysis was carried out using Kruskal–Wallis test followed by Dunn's *post hoc* test. Asterisk refers to the statistical significant difference between the indicated two pig groups (*$p < 0.05$). In antibody dilution curves **(A–C)**, A, B, and C refers to significant difference between unvaccinated vs KAg vaccinates, unvaccinated vs CNPs-KAg vaccinates, and KAg vs CNPs-KAg vaccinates, respectively, at the indicated dilution.

vaccinated pig groups when compared to the lesion scores in the unvaccinated and challenged group. In particular, the interstitial pneumonia and epithelial changes were much reduced in CNPs-KAg group compared to those in soluble KAg-vaccinated pigs.

We also evaluated the levels of pro-inflammatory cytokine IL-6 secretion in the BAL fluid and observed relatively lower levels in CNPs-KAg-vaccinated pigs, consistent with the lower macroscopic and microscopic lung lesions (**Figure 8D**).

CNPs-KAg Vaccine Enhanced the Mucosal Cellular Immune Response in the Tracheobronchial Lymph Nodes of Virulent and Heterologous Virus-Challenged Pigs

In the CNPs-KAg-vaccinated pigs, the frequency of CTLs, IFNγ, and specific lymphocyte proliferation index values were augmented in PBMCs (**Figure 7**). The cell-mediated immune response in the lung draining TBLN was also examined in these vaccinated pigs. Our data demonstrated a significantly higher ($p < 0.05$) secretion of IFNγ by TBLN-MNCs restimulated with vaccine (H1N2-OH10) and challenge (H1N1-OH7) viruses in CNPs-KAg, but not in KAg-vaccinated compared to mock group (**Figures 9A,B**). Cells similarly stimulated with heterosubtypic (H3N2-OH4) IAV showed an increase in IFNγ secretion in CNPs-KAg-vaccinated pig group but this increase was not statistically significant (**Figure 9C**). We performed flow cytometry analysis of TBLN-MNCs isolated at DPC 6 and observed a significantly higher ($p < 0.05$) frequency of T helper/memory cells ($CD3^+CD4^+CD8\alpha^+$), one of the principle contributors of IFNγ production in pigs (18), in CNPs-KAg-vaccinated pig group compared to that in unvaccinated and challenged animals (**Figure 9D**). The expression of Th1 and Th2 transcription factors mRNA level in TBLN collected at DPC 6 was analyzed. Consistent with augmented cellular response in TBLN-MNCs of CNPs-KAg-vaccinated pigs, in frozen TBLN tissues mRNA, the expression of the Th1-specific transcription factor T-bet was significantly higher ($p < 0.05$) in CNPs-KAg compared to KAg vaccinates (**Figure 9E**). The expression of Th2 transcription factor GATA-3 mRNA was not increased in TBLN (**Figure 9F**).

CNPs-KAg Vaccine Reduced Virus Shedding in the Nasal Cavity and Also Pulmonary Viral Titers in SwIAV-Challenged Pigs

We observed a significantly reduced ($p < 0.05$) challenge virus shedding at DPC 4 from the nasal passage of CNPs-KAg vaccinates compared to that of unvaccinated and challenged animals (**Figure 10A**). By DPC 6, infectious virus was detected in the nasal passage of only one of five pigs (20%) vaccinated with CNPs-KAg vaccine, while all pigs in KAg-vaccinated and unvaccinated groups were shedding virus ranging from $10^{2.5}$ to $10^{3.3}$ $TCID_{50}$/mL (**Figure 10B**). The average virus titers in nasal swab at DPC 6 in unvaccinated, KAg-, and CNPs-KAg-vaccinated and -challenged pigs were $10^{2.8}$, $10^{2.5}$, and $10^{0.5}$ $TCID_{50}$/mL, respectively (**Figure 10B**). Similarly, the virus titer in BAL fluid

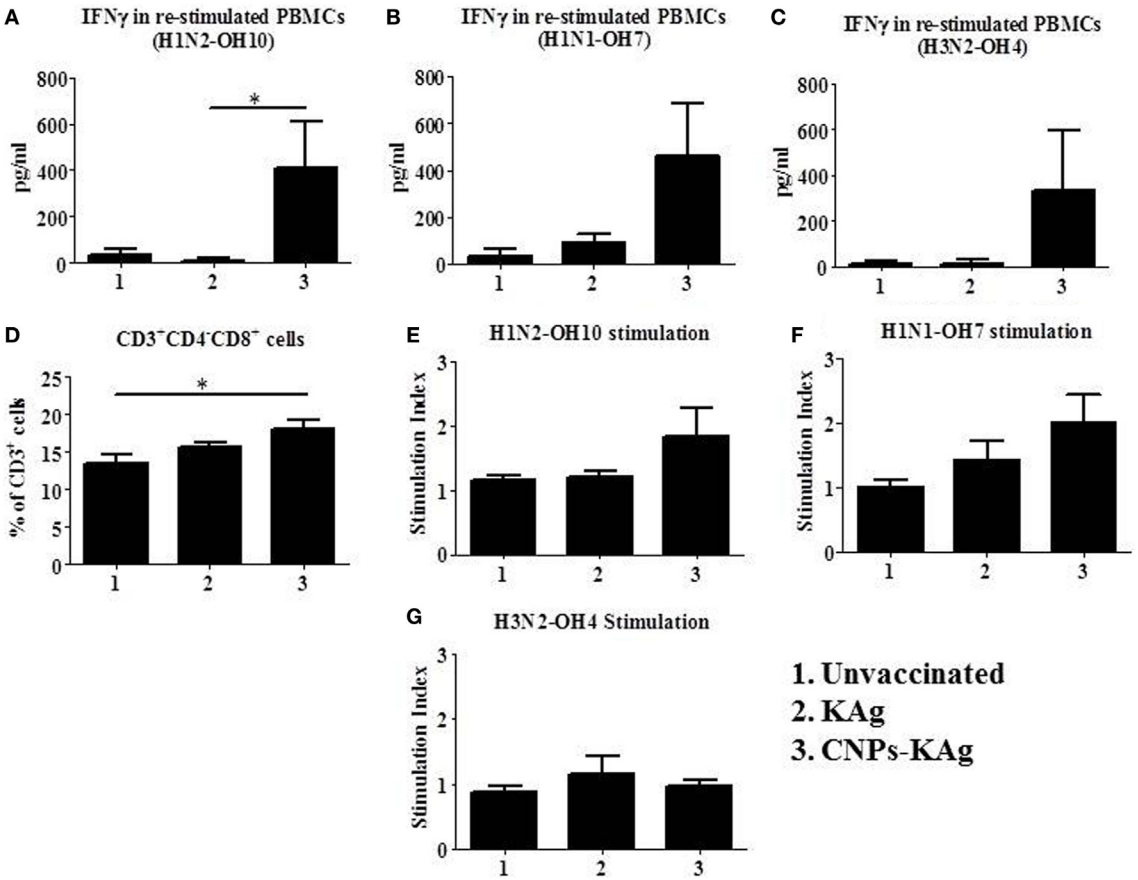

FIGURE 7 | Cell-mediated immune response after prime-boost vaccination was enhanced in chitosan nanoparticles (CNPs)-KAg-vaccinated pigs at pre-challenge days post-vaccination (DPV) 35/ day post-challenge (DPC) 0. Peripheral blood mononuclear cells (PBMCs) isolated from blood were stimulated with different variant influenza A virus (IAVs). IFNγ secretion in the culture supernatant and antigen-specific lymphocyte proliferation was determined after 72 h of stimulation with **(A,E)** H1N2-OH10, **(B,F)** H1N1-OH7, and **(C,G)** H3N2-OH4 IAVs. **(D)** Flow cytometry analysis of PBMCs showed enhanced frequency of CTLs ($CD3^+CD4^-CD8\alpha\beta^+$) in CNPs-KAg-vaccinated pigs. Data represent the mean value of three to five pigs ± SEM. Statistical analysis was carried out using Kruskal–Wallis test followed by Dunn's *post hoc* test. Asterisk refers to the statistical significant difference between the indicated two pig groups (*$p < 0.05$).

on DPC 6 was significantly reduced ($p < 0.05$) in CNPs-KAg but not in KAg group compared to unvaccinated virus challenge pigs (**Figure 10C**). The average virus titers in BAL fluid at DPC 6 in unvaccinated, KAg-, and CNPs-KAg-vaccinated and IAV-challenged pig groups were $10^{6.3}$, 10^5, and 10^3 $TCID_{50}$/mL, respectively.

DISCUSSION

Chitosan is a natural polymer synthesized by deacetylation of chitin, one of the most abundant polysaccharides in nature (38). Chitosan forms an attractive excipient for drug and vaccine delivery as it bears biocompatible, biodegradable, mucoadhesive, polycationic, and immunomodulatory properties (38, 39). Chitosan is often coupled with TPP, a polyanion that helps in the encapsulation of the biochemical agents through ionotropic gelation. The chitosan and TPP (CS/TPP) NPs formulation in mice were shown to induce both cell-mediated (Th1) and humoral (Th2) immune responses when immunized through IN route against *Streptococcus equi* (40). Similarly, tetanus toxoid loaded in CS/TPP NPs IN delivered in rat was efficiently transported through the nasal epithelium, and in mice, it induced a long-lasting systemic and mucosal antibody response compared to soluble antigen (41). Mice immunized through IN route using CS/TPP-based influenza split virus vaccine were shown to induce a higher systemic and mucosal antibody response than soluble antigens and also enhanced the cell-mediated immune response indicated by an increased IFNγ-secreting cell frequency in spleen (25). Unlike the preparation of PLGA and polyanhydride NPs, the process of preparing CNPs does not need any organic solvents and thus involves a simple and mild procedure protecting sensitive biochemical agents including proteins and provides scope for the easy modification of particles (42–45).

In this study, we prepared chitosan-based influenza nanovaccine using TPP by ionotropic gelation technique. The resulting NPs were around 500 nm in diameter which is adequate for efficient uptake by APCs (18, 20, 21, 46). The size of NPs was slightly increased after antigen loading like reported earlier (47). But the

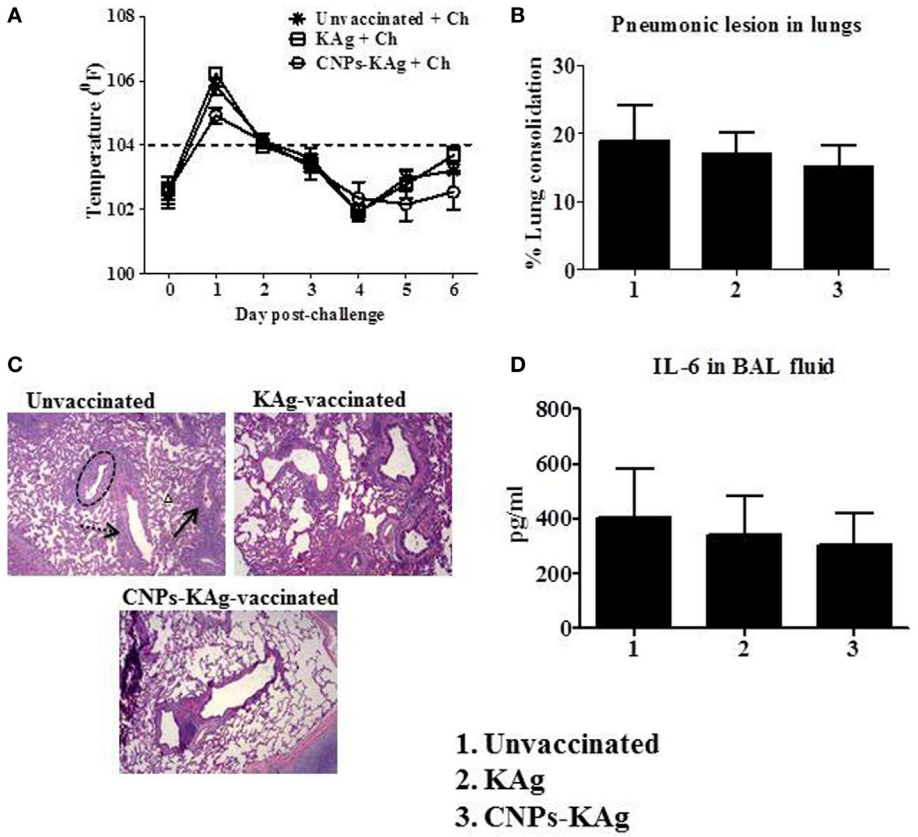

FIGURE 8 | Clinical and pathological changes in pigs vaccinated with chitosan nanoparticles (CNPs)-KAg post-challenge. **(A)** Rectal temperature was recorded daily after challenge until the day of necropsy. **(B)** Gross pneumonic lesions in lungs determined at day post-challenge (DPC) 6. **(C)** Representative Hematoxylin and eosin (H&E)-stained lung pictures showing bronchial exudates (dotted black circle), perivascular inflammation (black arrow), peribronchial inflammation (dashed black arrow), and interstitial pneumonia (small black triangle). **(D)** Secretion of cytokine interleukin (IL-6) in bronchoalveolar lavage (BAL) fluid. Data represent the mean value of three to five pigs ± SEM.

surface charge of our NPs did not change much with or without antigen loading, and the charge (+2.84 mV) was comparable to NPs entrapped with NDV, which was also loaded in CS:TPP at 2:1 ratio formulation like our CNPs-KAg (23). We evaluated the stability of CNPs-KAg NPs suspended in physiological buffer until 30 h maintained at 4°C. For vaccination of pigs, CNPs-KAg was freshly prepared and maintained on ice until delivered IN (1–2 h) which ensured the stability of NPs vaccine.

For better stability and long-term storage of NP vaccines, the surface charge should be highly negative or positive (38, 48). But our CNPs-KAg NPs were polydispersed in nature and had a weak positive surface charge, suggesting that further improvements to our CNPs-KAg formulation are required through optimization of the ratio of CS:TPP:KAg to ensure better physicochemical properties. The optimal CS:TPP:KAg combination should yield a higher positive surface charge, monodispersed nature, relatively smaller size NPs (100–300 nm), and stable for a long time at different storage conditions. The encapsulation efficiency of KAg in chitosan NPs formulation was 67%, higher than the encapsulation efficiency of H1N2-OH10 KAg (~50–55%) in PLGA and polyanhydride NPs (20, 21). The higher encapsulation efficiency of vaccine antigens is desirable to reduce the cost of vaccine production. The protein release from CNPs-KAg was slower than previously reported similar CS/TPP NPs formulation, wherein close to 50% of NDV antigens were released from CNPs within the first 3 days (23). CNP encapsulation enhances the antigen uptake by APCs, increases the expression of activation markers, and secretion of pro-inflammatory cytokines by APCs (49). As expected, SwIAV antigens delivered in chitosan NPs were efficiently internalized by porcine APCs compared to soluble KAg, and importantly, induced the higher production of innate, pro-inflammatory, and Th1 cytokines compared to soluble KAg.

Induction of strong mucosal immunity is associated with an increased breadth of protective efficacy against influenza, and inactivated IM vaccines do not elicit high levels of antigen-specific mucosal IgA antibody response in the respiratory tract (10, 11). Moreover, IM influenza vaccines in pigs have a limitation of not being effective in the presence of maternal-derived antibody (MDA) (50). However, successful IN vaccination has a potential to overcome MDA interference because of the induction of robust local mucosal immunity in the respiratory tract with minimal MDA interference (51). Chitosan is an attractive

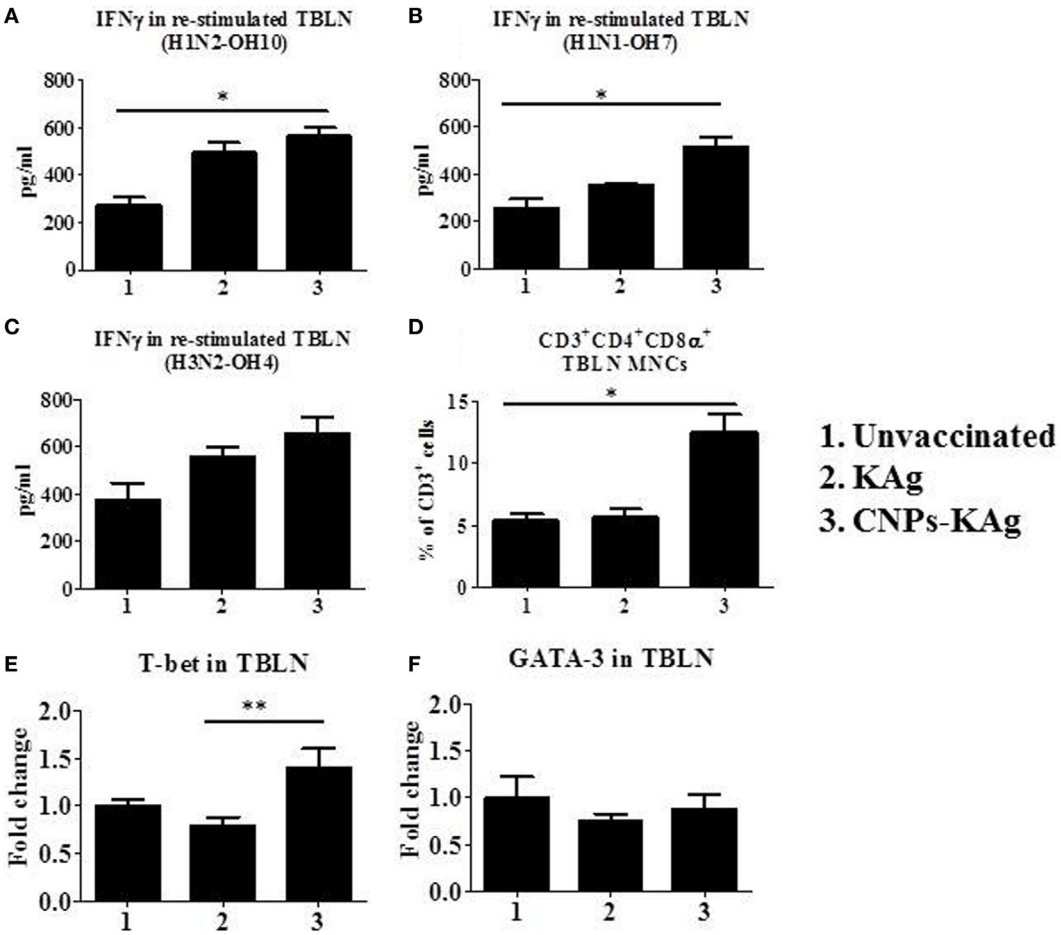

FIGURE 9 | Cell-mediated immune response in TBLN-MNCs of pigs vaccinated with chitosan nanoparticles (CNPs)-KAg at day post-challenge (DPC) 6. TBLN-MNCs isolated on the day of necropsy were stimulated with different variant swine influenza A viruses (SwIAVs), and secreted IFNγ into the culture supernatant was measured by cytokine ELISA against **(A)** H1N2-OH10, **(B)** H1N1-OH7, and **(C)** H3N2-OH4 influenza A virus (IAVs). **(D)** The frequency of T helper (Th)/memory cells ($CD3^+CD4^-CD8\alpha^+$) in TBLN-MNCs of CNPs-KAg-vaccinated pigs was analyzed by flow cytometry. The expression of Th1 **(E)** and Th2 **(F)** transcription factors were also determined in TBLN at DPC 6. Data represent the mean value of three to five pigs ± SEM. Statistical analysis was carried out using Kruskal–Wallis test followed by Dunn's *post hoc* test. Asterisk refers to the statistical significant difference between the indicated two pig groups (*$p < 0.05$).

polymer for IN immunization (22). It enhances the absorption of vaccine particles across the nasal epithelium (52). Further, when compared to aqueous chitosan solution, insulin-loaded CNPs (300–400 nm diameter) increased the nasal absorption of insulin (53). Due to the positive charge of chitosan, it can interact with anionic components such as sialic acid of glycoproteins on epithelial cell surfaces, thereby prolonging local retention time and decreasing antigen clearance on mucosal surfaces. In addition to its bioadhesive properties, chitosan enhances paracellular and intracellular transport of particulate antigens into the subepidermal space for optimal contact with APCs and other cells associated with immune responses (54, 55). In mice, the IN delivery of CNP-based hepatitis B vaccine enhances the mucosal IgA antibody response (56, 57). Other murine studies have shown that IN immunization with chitosan-based nanovaccine formulations induces robust mucosal and systemic antibody responses against *Pneumococcus* spp., *Diphtheria* spp., and *Bordetella* spp. (58–60).

An influenza subunit vaccine coadministered IN with chitosan delivery system enhanced both mucosal and systemic antibody response in mice (61). The IN delivery of chitosan-delivered DNA vaccine against *Coxsackievirus* in mice enhanced the secretion of both serum IgG and mucosal IgA as well as CTLs activity in spleen (62). Consistent with the previous studies in mice (58–60, 63), the prime-boost vaccination of CNPs-KAg in pigs improved the IgA antibody secretion in the nasal passage and lungs. Importantly, robust secreted antibodies were cross-reactive against heterologous and heterosubtypic IAV and helped in significant reduction in nasal virus shedding and lung load of a heterologous challenge virus. In a previous experiment, PLGA-SwIAV KAg nanovaccine failed to reduce nasal virus shedding in spite of inducing a robust-specific cell-mediated immune response and reducing virus load in the lungs of most of the pigs. This anomaly was likely due to the inability of PLGA-encapsulated vaccine to induce mucosal IgA response (20). Similarly, polyanhydride-SwIAV KAg nanovaccine also

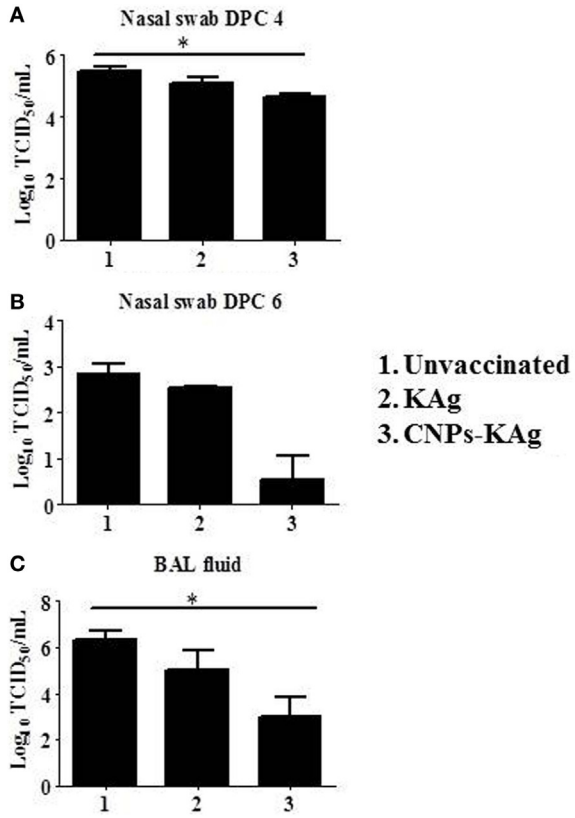

FIGURE 10 | Infectious challenge swine influenza A virus (SwIAV) H1N1 titer in the respiratory tract of chitosan nanoparticles (CNPs)-KAg-vaccinated and influenza A virus (IAV)-challenged pigs. Titers of challenge SwIAV shedding through nostrils at **(A)** day post-challenge (DPC) 4 and **(B)** DPC 6, and in bronchoalveolar lavage (BAL) fluid at DPC 6 **(C)** determined by using cell culture technique. Data represent the mean value of three to five pigs ± SEM. Statistical analysis was carried out using Kruskal–Wallis test followed by Dunn's *post hoc* test. Asterisk refers to the statistical significant difference between the indicated two pig groups ($^*p < 0.05$).

enhanced specific cell-mediated immunity but did not enhance mucosal antibody responses and hence did not significantly reduce the nasal virus shedding (21). Like earlier murine studies (64, 65), IN vaccination with CNPs-KAg also induced influenza-specific systemic IgG antibody and HI titers.

Cell-mediated immunity is of prime importance for providing complete protection against intracellular pathogens. The Th1 cytokine IFN-γ is a critical cytokine involved in antiviral responses (66, 67). Chitosan is superior to alum adjuvant in enhancing the cell-mediated immune responses (68). It also induces type I IFN secretion from immature DCs which helps in DC maturation and generation of Th1-mediated cellular immune responses (69). In this study, enhanced IFNγ secretion by activated lymphocytes in a recall response with genetically variant IAVs was observed in both PBMCs and TBLN-MNCs of CNPs-KAg-vaccinated pigs. The observed spike in IFNγ recall response was associated with an enhanced virus-specific cellular response both at mucosal sites and systemically. Activated T cell subsets such as T helper and CTLs and innate NK cells are the sources of IFNγ (70). The prime-boost vaccination schedule employed in this study with CNPs-KAg increased the CTLs in PBMC cultures, the major source of IFNγ, the cytokine that helps in clearing virus from infected cells (67).

Another important T cell subset in pigs is T helper/memory cells ($CD3^+CD4^+CD8\alpha^+$) (71) which possesses cytolytic function and also secretes IFNγ. The protective response against pseudorabies virus infection has been attributed to the increased frequency of T helper/memory cells (71, 72). The frequency of T helper/memory cells in TBLN-MNCs was significantly enhanced in CNPs-KAg-vaccinated pigs. Thus, both T helper/memory and CTLs appear to contribute substantially in improving the cross-protective cellular immune response in pigs vaccinated with chitosan-based influenza nanovaccine.

In conclusion, the mucoadhesive chitosan-based IAV nanovaccine formulation delivered as IN mist augmented cross-reactive T and B lymphocytes response in pigs at both mucosal (upper and lower respiratory tracts and regional lymph nodes—TBLN) and systemic (blood) sites by augmenting secretary IgA, systemic IgG, and T cell responses against highly variant IAVs. This augmented virus-specific cross-reactive immune response resulted in a reduced nasal virus shedding, reduced viral titers in the pulmonary parenchyma, and relatively reduced inflammatory changes in the lungs. Thus, our study indicates that chitosan IAV nanovaccine might be an ideal vaccine candidate against constantly evolving influenza infections in swine herds. Future studies will focus on the optimization of CS:TPP:KAg combination to ensure a monodispersed nature, a higher positive charge, and better stability of CNPs-KAg vaccine. In our future vaccine challenge studies, the efficacy of IN CNPs-KAg vaccine will also be compared with commercial IM-killed and IN-modified live IAV vaccines, and in MDA positive piglets against variant field IAV isolates.

ETHICS STATEMENT

This animal study was carried out in strict accordance with the recommendations by Public Health Service Policy, United States Department of Agriculture Regulations, the National Research Council's Guide for the Care and Use of Laboratory Animals, and the Federation of Animal Science Societies' Guide for the Care and Use of Agricultural Animals in Agricultural Research and Teaching. We followed all relevant institutional, state, and federal regulations and policies regarding animal care and use at The Ohio State University. All the pigs were maintained, samples collected, and euthanized, and all efforts were made to minimize the suffering of pigs. This study was carried out in accordance with the approved protocol of the Institutional Animal Care and Use Committee at The Ohio State University (Protocol number 2014A00000099).

AUTHOR CONTRIBUTIONS

SD and GR conceived and designed the project. SD, SR, CL, and GR performed the experiments, analyzed the data, and composed the manuscript. Vaccination trial in pigs, sample collection, and laboratory experiments were supported by SG, YL, BH, and NF-R. FL and HH worked on *in vitro* characterization of NPs. SK

provided the pathological analysis of the pulmonary tissues of pigs. All the authors provided critical feedback on the manuscript prior to publication and have agreed to the final content.

ACKNOWLEDGMENTS

We are thankful to Dr. Juliette Hanson, Megan Strother, Sara Tallmadge, Hyesun Jang, John M. Ngunjiri, and Mohamed Elaish for their help in animal studies. We also thank Dr. Tea Meulia, Horst Leona, and the team at MCIC, OARDC, for their help in SEM analysis.

FUNDING

This work was supported by OARDC OSU industry match grant and Agriculture and Food Research Initiative Competitive Grant No. 2013-67015-20476 from the USDA National Institute of Food and Agriculture.

REFERENCES

1. Dykhuis HC, Painter T, Fangman T, Holtkamp D. Assessing production parameters and economic impact of swine influenza, PRRS and *Mycoplasma hyopneumoniae* on finishing pigs in a large production system. *Proceedings of AASV Annual Meeting*. Denver, Colorado (2012). p. 75–6.
2. Crisci E, Mussa T, Fraile L, Montoya M. Review: influenza virus in pigs. *Mol Immunol* (2013) 55:200–11. doi:10.1016/j.molimm.2013.02.008
3. Janke BH. Clinicopathological features of swine influenza. *Curr Top Microbiol Immunol* (2013) 370:69–83. doi:10.1007/82_2013_308
4. Vincent AL, Ma W, Lager KM, Janke BH, Richt JA. Swine influenza viruses a North American perspective. *Adv Virus Res* (2008) 72:127–54. doi:10.1016/S0065-3527(08)00403-X
5. Ito T, Couceiro JN, Kelm S, Baum LG, Krauss S, Castrucci MR, et al. Molecular basis for the generation in pigs of influenza A viruses with pandemic potential. *J Virol* (1998) 72:7367–73.
6. Vincent A, Awada L, Brown I, Chen H, Claes F, Dauphin G, et al. Review of influenza A virus in swine worldwide: a call for increased surveillance and research. *Zoonoses Public Health* (2014) 61:4–17. doi:10.1111/zph.12049
7. Schicker RS, Rossow J, Eckel S, Fisher N, Bidol S, Tatham L, et al. Outbreak of influenza A(H3N2) variant virus infections among persons attending agricultural fairs housing infected swine—Michigan and Ohio, July-August 2016. *MMWR Morb Mortal Wkly Rep* (2016) 65:1157–60. doi:10.15585/mmwr.mm6542a1
8. Vincent AL, Perez DR, Rajao D, Anderson TK, Abente EJ, Walia RR, et al. Influenza A virus vaccines for swine. *Vet Microbiol* (2017) 206:35–44. doi:10.1016/j.vetmic.2016.11.026
9. Van Reeth K, Ma W. Swine influenza virus vaccines: to change or not to change—that's the question. *Curr Top Microbiol Immunol* (2013) 370:173–200. doi:10.1007/82_2012_266
10. Tamura S, Kurata T. Defense mechanisms against influenza virus infection in the respiratory tract mucosa. *Jpn J Infect Dis* (2004) 57:236–47.
11. van Riet E, Ainai A, Suzuki T, Hasegawa H. Mucosal IgA responses in influenza virus infections; thoughts for vaccine design. *Vaccine* (2012) 30:5893–900. doi:10.1016/j.vaccine.2012.04.109
12. Neutra MR, Kozlowski PA. Mucosal vaccines: the promise and the challenge. *Nat Rev Immunol* (2006) 6:148–58. doi:10.1038/nri1777
13. Kim SH, Jang YS. The development of mucosal vaccines for both mucosal and systemic immune induction and the roles played by adjuvants. *Clin Exp Vaccine Res* (2017) 6:15–21. doi:10.7774/cevr.2017.6.1.15
14. Mishra N, Goyal AK, Tiwari S, Paliwal R, Paliwal SR, Vaidya B, et al. Recent advances in mucosal delivery of vaccines: role of mucoadhesive/biodegradable polymeric carriers. *Expert Opin Ther Pat* (2010) 20:661–79. doi:10.1517/13543771003730425
15. Mahapatro A, Singh DK. Biodegradable nanoparticles are excellent vehicle for site directed in-vivo delivery of drugs and vaccines. *J Nanobiotechnology* (2011) 9:1–11. doi:10.1186/1477-3155-9-55
16. Babai I, Samira S, Barenholz Y, Zakay-Rones Z, Kedar E. A novel influenza subunit vaccine composed of liposome-encapsulated haemagglutinin/neuraminidase and IL-2 or GM-CSF. II. Induction of TH1 and TH2 responses in mice. *Vaccine* (1999) 17:1239–50. doi:10.1016/S0264-410X(98)00347-8
17. Wang D, Christopher ME, Nagata LP, Zabielski MA, Li H, Wong JP, et al. Intranasal immunization with liposome-encapsulated plasmid DNA encoding influenza virus hemagglutinin elicits mucosal, cellular and humoral immune responses. *J Clin Virol* (2004) 31(Suppl 1):S99–106. doi:10.1016/j.jcv.2004.09.013
18. Hiremath J, Kang KI, Xia M, Elaish M, Binjawadagi B, Ouyang K, et al. Entrapment of H1N1 influenza virus derived conserved peptides in PLGA nanoparticles enhances T cell response and vaccine efficacy in pigs. *PLoS One* (2016) 11:e0151922. doi:10.1371/journal.pone.0151922
19. Qi M, Zhang XE, Sun X, Zhang X, Yao Y, Liu S, et al. Intranasal nanovaccine confers homo- and hetero-subtypic influenza protection. *Small* (2018) 14:e1703207. doi:10.1002/smll.201703207
20. Dhakal S, Hiremath J, Bondra K, Lakshmanappa YS, Shyu DL, Ouyang K, et al. Biodegradable nanoparticle delivery of inactivated swine influenza virus vaccine provides heterologous cell-mediated immune response in pigs. *J Control Release* (2017) 247:194–205. doi:10.1016/j.jconrel.2016.12.039
21. Dhakal S, Goodman J, Bondra K, Lakshmanappa YS, Hiremath J, Shyu DL, et al. Polyanhydride nanovaccine against swine influenza virus in pigs. *Vaccine* (2017) 35:1124–31. doi:10.1016/j.vaccine.2017.01.019
22. van der Lubben IM, Verhoef JC, Borchard G, Junginger HE. Chitosan for mucosal vaccination. *Adv Drug Deliv Rev* (2001) 52:139–44. doi:10.1016/S0169-409X(01)00197-1
23. Zhao K, Chen G, Shi XM, Gao TT, Li W, Zhao Y, et al. Preparation and efficacy of a live Newcastle disease virus vaccine encapsulated in chitosan nanoparticles. *PLoS One* (2012) 7:e53314. doi:10.1371/journal.pone.0053314
24. Amidi M, Romeijn SG, Verhoef JC, Junginger HE, Bungener L, Huckriede A, et al. N-trimethyl chitosan (TMC) nanoparticles loaded with influenza subunit antigen for intranasal vaccination: biological properties and immunogenicity in a mouse model. *Vaccine* (2007) 25:144–53. doi:10.1016/j.vaccine.2006.06.086
25. Sawaengsak C, Mori Y, Yamanishi K, Mitrevej A, Sinchaipanid N. Chitosan nanoparticle encapsulated hemagglutinin-split influenza virus mucosal vaccine. *AAPS PharmSciTech* (2014) 15:317–25. doi:10.1208/s12249-013-0058-7
26. Liu Q, Zheng X, Zhang C, Shao X, Zhang X, Zhang Q, et al. Conjugating influenza a (H1N1) antigen to n-trimethylaminoethylmethacrylate chitosan nanoparticles improves the immunogenicity of the antigen after nasal administration. *J Med Virol* (2015) 87:1807–15. doi:10.1002/jmv.24253
27. Ali A, Khatri M, Wang L, Saif YM, Lee CW. Identification of swine H1N2/pandemic H1N1 reassortant influenza virus in pigs, United States. *Vet Microbiol* (2012) 158:60–8. doi:10.1016/j.vetmic.2012.02.014
28. Yassine HM, Khatri M, Zhang YJ, Lee CW, Byrum BA, O'Quin J, et al. Characterization of triple reassortant H1N1 influenza A viruses from swine in Ohio. *Vet Microbiol* (2009) 139:132–9. doi:10.1016/j.vetmic.2009.04.028
29. Yassine HM, Al-Natour MQ, Lee CW, Saif YM. Interspecies and intraspecies transmission of triple reassortant H3N2 influenza A viruses. *Virol J* (2007) 4:129. doi:10.1186/1743-422X-4-129
30. Calvo P, Remunan-Lopez C, Vila-Jato JL, Alonso MJ. Chitosan and chitosan/ethylene oxide-propylene oxide block copolymer nanoparticles as novel carriers for proteins and vaccines. *Pharm Res* (1997) 14:1431–6. doi:10.1023/A:1012128907225
31. Mirzaei F, Mohammadpour Dounighi N, Avadi MR, Rezayat M. A new approach to antivenom preparation using chitosan nanoparticles containing echiscarinatus venom as a novel antigen delivery system. *Iran J Pharm Res* (2017) 16:858–67.
32. Debnath SK, Saisivam S, Debanth M, Omri A. Development and evaluation of chitosan nanoparticles based dry powder inhalation formulations of prothionamide. *PLoS One* (2018) 13:e0190976. doi:10.1371/journal.pone.0190976
33. Lu F, Mencia A, Bi L, Taylor A, Yao Y, Hogenesch H. Dendrimer-like alpha-d-glucan nanoparticles activate dendritic cells and are effective vaccine adjuvants. *J Control Release* (2015) 204:51–9. doi:10.1016/j.jconrel.2015.03.002

34. Nedumpun T, Ritprajak P, Suradhat S. Generation of potent porcine monocyte-derived dendritic cells (MoDCs) by modified culture protocol. *Vet Immunol Immunopathol* (2016) 182:63–8. doi:10.1016/j.vetimm.2016.10.002
35. Dwivedi V, Manickam C, Dhakal S, Binjawadagi B, Ouyang K, Hiremath J, et al. Adjuvant effects of invariant NKT cell ligand potentiates the innate and adaptive immunity to an inactivated H1N1 swine influenza virus vaccine in pigs. *Vet Microbiol* (2016) 186:157–63. doi:10.1016/j.vetmic.2016.02.028
36. Meurens F, Berri M, Auray G, Melo S, Levast B, Virlogeux-Payant I, et al. Early immune response following *Salmonella enterica* subspecies enterica serovar Typhimurium infection in porcine jejunal gut loops. *Vet Res* (2009) 40:5. doi:10.1051/vetres:2008043
37. Livak KJ, Schmittgen TD. Analysis of relative gene expression data using real-time quantitative PCR and the 2(-Delta Delta C(T)) method. *Methods* (2001) 25:402–8. doi:10.1006/meth.2001.1262
38. Illum L, Jabbal-Gill I, Hinchcliffe M, Fisher AN, Davis SS. Chitosan as a novel nasal delivery system for vaccines. *Adv Drug Deliv Rev* (2001) 51:81–96. doi:10.1016/S0169-409X(01)00171-5
39. Wang JJ, Zeng ZW, Xiao RZ, Xie T, Zhou GL, Zhan XR, et al. Recent advances of chitosan nanoparticles as drug carriers. *Int J Nanomedicine* (2011) 6:765–74. doi:10.2147/IJN.S17296
40. Figueiredo L, Cadete A, Goncalves LM, Corvo ML, Almeida AJ. Intranasal immunisation of mice against *Streptococcus equi* using positively charged nanoparticulate carrier systems. *Vaccine* (2012) 30:6551–8. doi:10.1016/j.vaccine.2012.08.050
41. Vila A, Sanchez A, Janes K, Behrens I, Kissel T, Vila Jato JL, et al. Low molecular weight chitosan nanoparticles as new carriers for nasal vaccine delivery in mice. *Eur J Pharm Biopharm* (2004) 57:123–31. doi:10.1016/j.ejpb.2003.09.006
42. Astete CE, Sabliov CM. Synthesis and characterization of PLGA nanoparticles. *J Biomater Sci Polym Ed* (2006) 17:247–89. doi:10.1163/156856206775997322
43. Torres MP, Vogel BM, Narasimhan B, Mallapragada SK. Synthesis and characterization of novel polyanhydrides with tailored erosion mechanisms. *J Biomed Mater Res A* (2006) 76:102–10. doi:10.1002/jbm.a.30510
44. Peniche H, Peniche C. Chitosan nanoparticles: a contribution to nanomedicine. *Polym Int* (2011) 60:883–9. doi:10.1002/pi.3056
45. Rampino A, Borgogna M, Blasi P, Bellich B, Cesaro A. Chitosan nanoparticles: preparation, size evolution and stability. *Int J Pharm* (2013) 455:219–28. doi:10.1016/j.ijpharm.2013.07.034
46. Foged C, Brodin B, Frokjaer S, Sundblad A. Particle size and surface charge affect particle uptake by human dendritic cells in an *in vitro* model. *Int J Pharm* (2005) 298:315–22. doi:10.1016/j.ijpharm.2005.03.035
47. Satzer P, Svec F, Sekot G, Jungbauer A. Protein adsorption onto nanoparticles induces conformational changes: particle size dependency, kinetics, and mechanisms. *Eng Life Sci* (2016) 16:238–46. doi:10.1002/elsc.201500059
48. Yu W, Xie H. A review on nanofluids: preparation, stability mechanisms, and applications. *J Nanomater* (2012) 2012:435873. doi:10.1155/2012/435873
49. Koppolu B, Zaharoff DA. The effect of antigen encapsulation in chitosan particles on uptake, activation and presentation by antigen presenting cells. *Biomaterials* (2013) 34:2359–69. doi:10.1016/j.biomaterials.2012.11.066
50. Wesley RD, Lager KM. Overcoming maternal antibody interference by vaccination with human adenovirus 5 recombinant viruses expressing the hemagglutinin and the nucleoprotein of swine influenza virus. *Vet Microbiol* (2006) 118:67–75. doi:10.1016/j.vetmic.2006.07.014
51. Zhang F, Peng B, Chang H, Zhang R, Lu F, Wang F, et al. Intranasal immunization of mice to avoid interference of maternal antibody against H5N1 infection. *PLoS One* (2016) 11:e0157041. doi:10.1371/journal.pone.0157041
52. Illum L, Farraj NF, Davis SS. Chitosan as a novel nasal delivery system for peptide drugs. *Pharm Res* (1994) 11:1186–9. doi:10.1023/A:1018901302450
53. Fernandez-Urrusuno R, Calvo P, Remunan-Lopez C, Vila-Jato JL, Alonso MJ. Enhancement of nasal absorption of insulin using chitosan nanoparticles. *Pharm Res* (1999) 16:1576–81. doi:10.1023/A:1018908705446
54. Artursson P, Lindmark T, Davis SS, Illum L. Effect of chitosan on the permeability of monolayers of intestinal epithelial cells (Caco-2). *Pharm Res* (1994) 11:1358–61. doi:10.1023/A:1018967116988
55. Dodane V, Amin Khan M, Merwin JR. Effect of chitosan on epithelial permeability and structure. *Int J Pharm* (1999) 182:21–32. doi:10.1016/S0378-5173(99)00030-7
56. Borges O, Cordeiro-Da-Silva A, Tavares J, Santarem N, De Sousa A, Borchard G, et al. Immune response by nasal delivery of hepatitis B surface antigen and codelivery of a CpG ODN in alginate coated chitosan nanoparticles. *Eur J Pharm Biopharm* (2008) 69:405–16. doi:10.1016/j.ejpb.2008.01.019
57. Lebre F, Borchard G, Faneca H, Pedroso De Lima MC, Borges O. Intranasal administration of novel chitosan nanoparticle/DNA complexes induces antibody response to hepatitis B surface antigen in mice. *Mol Pharm* (2016) 13:472–82. doi:10.1021/acs.molpharmaceut.5b00707
58. Jabbal-Gill I, Fisher AN, Rappuoli R, Davis SS, Illum L. Stimulation of mucosal and systemic antibody responses against *Bordetella pertussis* filamentous haemagglutinin and recombinant pertussis toxin after nasal administration with chitosan in mice. *Vaccine* (1998) 16:2039–46. doi:10.1016/S0264-410X(98)00077-2
59. McNeela EA, O'Connor D, Jabbal-Gill I, Illum L, Davis SS, Pizza M, et al. A mucosal vaccine against diphtheria: formulation of cross reacting material (CRM(197)) of diphtheria toxin with chitosan enhances local and systemic antibody and Th2 responses following nasal delivery. *Vaccine* (2000) 19:1188–98. doi:10.1016/S0264-410X(00)00309-1
60. Xu J, Dai W, Wang Z, Chen B, Li Z, Fan X. Intranasal vaccination with chitosan-DNA nanoparticles expressing pneumococcal surface antigen a protects mice against nasopharyngeal colonization by *Streptococcus pneumoniae*. *Clin Vaccine Immunol* (2011) 18:75–81. doi:10.1128/CVI.00263-10
61. Bacon A, Makin J, Sizer PJ, Jabbal-Gill I, Hinchcliffe M, Illum L, et al. Carbohydrate biopolymers enhance antibody responses to mucosally delivered vaccine antigens. *Infect Immun* (2000) 68:5764–70. doi:10.1128/IAI.68.10.5764-5770.2000
62. Xu W, Shen Y, Jiang Z, Wang Y, Chu Y, Xiong S. Intranasal delivery of chitosan-DNA vaccine generates mucosal SIgA and anti-CVB3 protection. *Vaccine* (2004) 22:3603–12. doi:10.1016/j.vaccine.2004.03.033
63. Renegar KB, Small PA Jr. Immunoglobulin A mediation of murine nasal anti-influenza virus immunity. *J Virol* (1991) 65:2146–8.
64. Etchart N, Wild F, Kaiserlian D. Mucosal and systemic immune responses to measles virus haemagglutinin in mice immunized with a recombinant vaccinia virus. *J Gen Virol* (1996) 77(Pt 10):2471–8. doi:10.1099/0022-1317-77-10-2471
65. Bergquist C, Johansson EL, Lagergard T, Holmgren J, Rudin A. Intranasal vaccination of humans with recombinant cholera toxin B subunit induces systemic and local antibody responses in the upper respiratory tract and the vagina. *Infect Immun* (1997) 65:2676–84.
66. Samuel CE. Antiviral actions of interferons. *Clin Microbiol Rev* (2001) 14:778–809, table of contents. doi:10.1128/CMR.14.4.778-809.2001
67. La Gruta NL, Turner SJ. T cell mediated immunity to influenza: mechanisms of viral control. *Trends Immunol* (2014) 35:396–402. doi:10.1016/j.it.2014.06.004
68. Mori A, Oleszycka E, Sharp FA, Coleman M, Ozasa Y, Singh M, et al. The vaccine adjuvant alum inhibits IL-12 by promoting PI3 kinase signaling while chitosan does not inhibit IL-12 and enhances Th1 and Th17 responses. *Eur J Immunol* (2012) 42:2709–19. doi:10.1002/eji.201242372
69. Carroll EC, Jin L, Mori A, Munoz-Wolf N, Oleszycka E, Moran HBT, et al. The vaccine adjuvant chitosan promotes cellular immunity *via* DNA sensor cGAS-STING-dependent induction of type I interferons. *Immunity* (2016) 44:597–608. doi:10.1016/j.immuni.2016.02.004
70. Farrar MA, Schreiber RD. The molecular cell biology of interferon-gamma and its receptor. *Annu Rev Immunol* (1993) 11:571–611. doi:10.1146/annurev.iy.11.040193.003035
71. Zuckermann FA. Extrathymic CD4/CD8 double positive T cells. *Vet Immunol Immunopathol* (1999) 72:55–66. doi:10.1016/S0165-2427(99)00118-X
72. De Bruin TG, Van Rooij EM, De Visser YE, Bianchi AT. Cytolytic function for pseudorabies virus-stimulated porcine CD4+ CD8dull+ lymphocytes. *Viral Immunol* (2000) 13:511–20. doi:10.1089/vim.2000.13.511

Conflict of Interest Statement: The authors declare that the research was conducted in the absence of any commercial or financial relationships that could be construed as a potential conflict of interest.

frontiers in Immunology

ORIGINAL RESEARCH
published: 17 May 2018
doi: 10.3389/fimmu.2018.01093

Chaperna-Mediated Assembly of Ferritin-Based Middle East Respiratory Syndrome-Coronavirus Nanoparticles

*Young-Seok Kim[1,2], Ahyun Son[1], Jihoon Kim[1,2], Soon Bin Kwon[1,2], Myung Hee Kim[3], Paul Kim[1,2], Jieun Kim[4], Young Ho Byun[1], Jemin Sung[1,2], Jinhee Lee[1,2], Ji Eun Yu[1,2], Chan Park[1,2], Yeon-Sook Kim[5], Nam-Hyuk Cho[6,7], Jun Chang[3] and Baik L. Seong[1,2]**

[1] Department of Biotechnology, College of Life Sciences and Biotechnology, Yonsei University, Seoul, South Korea, [2] Vaccine Translational Research Center, Yonsei University, Seoul, South Korea, [3] Graduate School of Pharmaceutical Sciences, Ewha Womans University, Seoul, South Korea, [4] Life Science and Biotechnology, Underwood International College, Yonsei University, Seoul, South Korea, [5] Division of Infectious Diseases, Department of Internal Medicine, Chungnam National University School of Medicine, Daejeon, South Korea, [6] Department of Microbiology and Immunology, Seoul National University College of Medicine, Seoul, South Korea, [7] Department of Biomedical Sciences, Seoul National University College of Medicine, Seoul, South Korea

OPEN ACCESS

Edited by:
Rajko Reljic,
University of London,
United Kingdom

Reviewed by:
Pietro Speziale,
Università degli studi
di Pavia, Italy
Rong Hai,
University of California,
Riverside, United States
Jamie Mann,
University of Western Ontario,
Canada

***Correspondence:**
Baik L. Seong
blseong@yonsei.ac.kr

Specialty section:
This article was submitted to
Vaccines and Molecular
Therapeutics,
a section of the journal
Frontiers in Immunology

Received: 29 December 2017
Accepted: 01 May 2018
Published: 17 May 2018

Citation:
Kim Y-S, Son A, Kim JH, Kwon SB, Kim MH, Kim P, Kim JE, Byun YH, Sung JM, Lee JH, Yu JE, Park C, Kim Y-S, Cho N-H, Chang J and Seong BL (2018) Chaperna-Mediated Assembly of Ferritin-Based Middle East Respiratory Syndrome-Coronavirus Nanoparticles. Front. Immunol. 9:1093. doi: 10.3389/fimmu.2018.01093

The folding of monomeric antigens and their subsequent assembly into higher ordered structures are crucial for robust and effective production of nanoparticle (NP) vaccines in a timely and reproducible manner. Despite significant advances in *in silico* design and structure-based assembly, most engineered NPs are refractory to soluble expression and fail to assemble as designed, presenting major challenges in the manufacturing process. The failure is due to a lack of understanding of the kinetic pathways and enabling technical platforms to ensure successful folding of the monomer antigens into regular assemblages. Capitalizing on a novel function of RNA as a molecular chaperone (chaperna: chaperone + RNA), we provide a robust protein-folding vehicle that may be implemented to NP assembly in bacterial hosts. The receptor-binding domain (RBD) of Middle East respiratory syndrome-coronavirus (MERS-CoV) was fused with the RNA-interaction domain (RID) and bacterioferritin, and expressed in *Escherichia coli* in a soluble form. Site-specific proteolytic removal of the RID prompted the assemblage of monomers into NPs, which was confirmed by electron microscopy and dynamic light scattering. The mutations that affected the RNA binding to RBD significantly increased the soluble aggregation into amorphous structures, reducing the overall yield of NPs of a defined size. This underscored the RNA-antigen interactions during NP assembly. The sera after mouse immunization effectively interfered with the binding of MERS-CoV RBD to the cellular receptor hDPP4. The results suggest that RNA-binding controls the overall kinetic network of the antigen folding pathway in favor of enhanced assemblage of NPs into highly regular and immunologically relevant conformations. The concentration of the ion Fe^{2+}, salt, and fusion linker also contributed to the assembly *in vitro*, and the stability of the NPs. The kinetic "pace-keeping" role of chaperna in the super molecular assembly of antigen monomers holds promise for the development and delivery of NPs and virus-like particles as recombinant vaccines and for serological detection of viral infections.

Keywords: nanoparticle, virus-like particle, chaperone, ferritin, Middle East respiratory syndrome coronavirus, receptor-binding domain, Lysyl-tRNA synthetase, RNA-interacting domain of human LysRS

INTRODUCTION

Various types of viral vaccines have been developed over the last century with a wide spectrum of efficacy and safety (1, 2). The manufacturing of most conventional vaccines—live attenuated, inactivated, or subunit vaccines—invariably require the culturing of infectious viruses in cell substrates (3). Despite dedicated efforts, conventional cell culture often fails to produce sufficient amounts of virus for evaluating the immunogenicity, protective efficacy, and safety of viral vaccines. Moreover, some emerging viruses cause high-mortality rates, without options for treatment or prophylaxis, necessitating their manipulation, and manufacture under stringent bio-safety environment (4). Not surprisingly, alternative technologies that circumvent these limitations are a high priority in the areas of vaccine development and production. Nanoparticles (NPs), virus-like particles (VLPs), and assembly of multimeric peptides each provide attractive platforms for vaccine design (5).

Virus-like particles and NPs structurally resemble infectious virions, but are non-infectious due to the lack of viral genomes. Recombinant surface antigens from natural virions are assembled into highly ordered conformations as empty particles devoid of genetic material. Antigenic epitopes are presented on the multivalent and highly repetitive outer structure of the NPs, which leads to the crosslinking of B-cell receptors and the induction of long-lasting immune responses (6–8). By mimicking the morphology of the natural infectious virions, the regularly assembled particles are highly immunogenic, and are amenable to diagnostic and prophylactic exploitation. Among the simplest targets are the VLPs of non-enveloped viruses, such as hepatitis E virus or human papilloma virus, and are composed purely of viral capsid proteins (9–11).

In contrast to non-enveloped viruses, where virion assembly is exclusive to capsid proteins, enveloped viruses (e.g., coronavirus or flavivirus), require an additional membrane component for assembly into mature virions. Consequently, in enveloped VLPs, the assembly of matrix proteins provides a molecular scaffold, and viral antigens are embedded into lipid membranes. Different types of glycoproteins may be embedded in the lipid membrane as target antigens for generating immunological responses (12). However, this process requires multiple proteins (surface antigens and matrix proteins), and the enveloped VLPs are not structurally uniform and are difficult to characterize. A promising alternative is to present the target antigens on the surfaces of self-assembled NPs, which, in lieu of lipid membranes, serve as the macromolecular scaffold for the presentation of the antigens of interest.

In developing NP vaccines, consideration should be given regarding the selection of a robust and faithful system for NP assembly that enables the cost-effective development and delivery of vaccines in a timely manner. Structure-based approaches *in silico* and their underlying principles are relatively advanced for NP assembly (13–15). Most of the approaches consider the thermodynamic stability of the final assembled NPs, without due recognition for the kinetic complexities controlling regular assemblage over random interactions that lead to misfolded aggregations. Therefore, it is not surprising that most engineered NPs are refractory to soluble expression, which presents practical challenges in production, both at a laboratory-scale and in commercial manufacturing processes. This problem becomes augmented when expressed in bacterial hosts because of a lack of folding assistance in the bacterial cytoplasm for viral antigens. Therefore, due to advantages in assisted folding, post-translational modifications, and the possibility of generating multiple-component NPs and VLPs, eukaryotic hosts such as yeast, insects, and mammalian cells have been favored over bacterial hosts (16–18). However, these systems are significantly more expensive than bacterial systems, are more time-consuming, and the down-stream processes are usually more complex. Moreover, the purification of VLPs from insect cell systems poses a challenge due to similar physicochemical properties between the VLPs and the baculoviruses (1, 16). Bacterial systems, if available, would provide a cost-effective means to develop and deliver vaccines, as well as sero-diagnostic antigen kits used to diagnose-specific infection diseases.

Middle East respiratory syndrome (MERS) was first reported in Saudi Arabia in 2012 and has caused multiple cases of infection with high mortality in Europe and Asia (19, 20). MERS is caused by MERS-coronavirus (MERS-CoV), which can be transmitted from camels to humans, and from humans to other humans (21, 22). Worldwide transmission is increasing in direct household and community-wide transmission, as well as in nosocomial settings, as exemplified in a 2015 outbreak in Korea (23, 24). Neither effective vaccines nor therapeutic interventions are currently available. Because of this, assembly of MERS-CoV antigens into immunologically relevant conformation as NPs would be of interest and may be helpful in developing vaccines, sero-diagnostic tools, and therapeutic monoclonal antibodies.

In the current study, we present a novel bacterial NP of MERS-CoV antigen using ferritin as a molecular scaffold for self-assembly. Ferritin, which is present in most living organisms, has 24 identical subunits that spontaneously self-assemble and form NP complexes with internal and external diameters of 8 and 12 nm, respectively (25, 26). Previous studies show that ferritins of *Helicobacter pylori* from a human isolate can be used as scaffold for HIV and influenza NP vaccines, using eukaryotic host cells such as human embryonic kidney cells (HEK293F or HEK293S) (27, 28). Likewise, bacterioferritin (FR), which self-assembles into nanocages with octahedral symmetry, has also been evaluated as a potential drug delivery system (29). However, viral antigens of human pathogens are prone to misfolding into aggregates, which necessitates chemical refolding of the insoluble aggregates in order to regain solubility and to allow regular assembly of the antigen (30, 31). In addition, displaying antigens on the surface of multi-molecularly assembled scaffolds in bacterial hosts remains a daunting challenge.

We hypothesized that NPs displaying the receptor-binding domain (RBD) of the spike protein from MERS-CoV could be produced in a bacterial system by harnessing the function of a molecular chaperone. Conventionally, protein folding and the prevention of non-functional aggregation have been ascribed to molecular chaperones (32–34). Recently, it has been shown that RNA molecules are able to provide novel functions as molecular chaperones (35–37). Based on novel findings, the concept of

chaperna (chaperone + RNA) function was established (38). In this report, chaperna function was harnessed for the folding and assembly of hybrid ferritin monomers into NPs using a bacterial expression system. We also demonstrated that the biophysical properties, including solubility, yield, and stability of MERS-CoV NPs, could be improved by properly controlling the RNA-binding affinity, and the concentrations of Fe^{2+} and salts. The chaperna-based NP assembly may prove to be a versatile tool for developing and delivering recombinant vaccines and for serological detection of emerging/re-emerging viruses.

MATERIALS AND METHODS

Ethics Statement

All animal research was performed according to the guidelines of Ministry of Food and Drug Safety of Republic of Korea. All experiments were approved by the YLARC Institutional Animal Care and Use Committee (IACUC; permit number: IACUC-A-201710-377-01). Six-week-old female BALB/c mice were purchased from ORIENT BIO Inc. (Seoul, Korea). Sera from the recovered MERS patients were used after ethical approval granted by the institutional review boards of Chungnam National University Hospital (IRB no. 2015-08-029) and Seoul National University Hospital (IRB no. 1509-103-705). This study was performed in accordance with the ethical standards laid down in the 1964 declaration of Helsinki and all subsequent revisions. Informed consent was obtained from all patients participated in this study.

Construction of Expression Vectors

The expression vector pGE-hRID(3) was constructed from the parental vector pGE-LysRS (3) (39). The pGE-LysRS(3) vector was enzymatically cut with NdeI and KpnI. The PCR product of hRID, which carries the TEV protease cleavage site and a 6-histidine tag at the C-terminus, was cut using the same restriction enzymes and the digested fragment inserted into the vector to generate pGE-hRID(3). FR (Genebank accession No. NC_000913.3) DNA was synthesized by, and purchased from, COSMO GENETECH (Korea). The DNA was cleaved with SalI and HindIII, and inserted into pGE-hRID(3) to generate hRID(3)-FR. The receptor binding domain (RBD), N-terminal residues 367–606, of the MERS-CoV S protein (GenBank accession No. AFS88936.1), was generated by gene synthesis, cut with KpnI and SalI, and inserted into hRID-FR to generate pGE-hRID(3)-RBD-FR. Linker SSG or ASG was inserted into the C-terminus of the RBD using overlapping PCR, cleaved with KpnI and SaI, and ligated into hRID-FR, generating pGE-hRID(3)-RBD-[SSG]-FR or pGE-hRID(3)-RBD-[ASG]-FR, respectively. The schematic diagrams of each expression vector are illustrated in **Figure 1B**. The genes of mutant hRID(2 m) (K19A and K23A) and hRID(9 m) (K19A, K23A, R24A, K27A, K30A, K31A, K35A, K38A, and K40A) were generated by gene synthesis, cleaved with NdeI and KpnI, and inserted into pGE-hRID(3)-RBD-FR, generating pGE-hRID(2 m)-RBD-FR and pGE-hRID(9 m)-RBD-FR, respectively. The mutation sites and amino acid sequences of the mutants are shown in Table S1 in Supplementary Material.

Protein Expression and Purification

The resulting expression vectors were transformed into the *Escherichia coli* strain SHuffle® T7. The cells were grown in 50 ml of LB medium with ampicillin (50 μg/ml) at 30°C overnight. Each type of transformant was inoculated into 500 ml of LB medium with ampicillin, grown at 30°C until an optical density (OD_{600}) of 0.6–0.8 was reached. Protein expression was induced with 1 mM IPTG for 12 h. Each sample was harvested by centrifugation, lysed by sonication in lysis buffer (50 mM Tris–HCl, pH 7.5; 10% glycerol; 2 mM 2-mercaptoethanol; and 0.1% Tween-20). The soluble fraction of each lysate was purified on a Ni-affinity Histrap™ HP column by ATKA prime (GE Healthcare) and concentrated with Centriprep™ (Merck Millipore Ltd.). The purified proteins were treated with TEV protease to remove the fusion partner hRID. The assembled NPs were purified by gel filtration on 10/300 Superose™ 6 Increase columns (GE Healthcare).

Homology Modeling and Trimer Simulation of RBD-FR

A homology model for the fusion complex of MERS-CoV RBD and FR was generated by MODELER, version 9.16 (Sali Lab of California) (13) using data from protein data base (PDB) for MERS-CoV RBD (PDB ID code 4kqz) and bacterial ferritin (PDB ID code 1bcf) as templates. The linker domains were improved using refinements in the loop domain (40). Energy-stable models of RBD-FR, RBD-[SSG]-FR, RBD-[ASG]-FR, and RBD-[D6]-FR for trimer structure formation were predicted using Multimer Docking software, ClusPro (ABC Group and Structural Bioinformatics Lab Boston University and Stony Brook University). The thermodynamic stabilities were calculated using the Cluspro formula for Coefficient Weights ($E = 0.40\text{Erep} + -0.40\text{Eatt} + 600\text{Eelec} + 1.00\text{EDARS}$) (41, 42).

Characterization of NPs Using Transmission Electron Microscopy (TEM) and Cryo-Electron Microscopy (cryo-EM)

To examine the size and structure of the purified NPs, microscopic evaluations using TEM and cryo-EM were performed. For TEM analysis, a drop of the NPs was placed onto a formvar/carbon-coated TEM grid (SPL). The grid was negatively stained with 2% uranyl acetate, dried, and examined using a JEM-1011 electron microscope (JEOL) at an accelerating voltage of 80 kV. The particle sizes were calculated using Camera-Megaview III (Soft imaging system-Germany) for measuring the NPs in random image fields. For cryo-EM, the NPs were placed onto plasma-treated formvar/carbon 200 copper grid (EMS) and negatively stained with 2% uranyl acetate. The grid was accelerated at 200 kV with an FEI CryoTecnai F20 cryo-EM microscope made available through the Korean Institute of Science and Technology. The NPs were examined and photographed in high resolution.

Dynamic Light Scattering (DLS)

Nanoparticle samples (3 ml) were placed into a Dispo-H cell, and analyzed using a Zeta-potential & Particle size Analyzer (ELS-2000ZS; Otsuka Electronics). The intensity distribution diameter

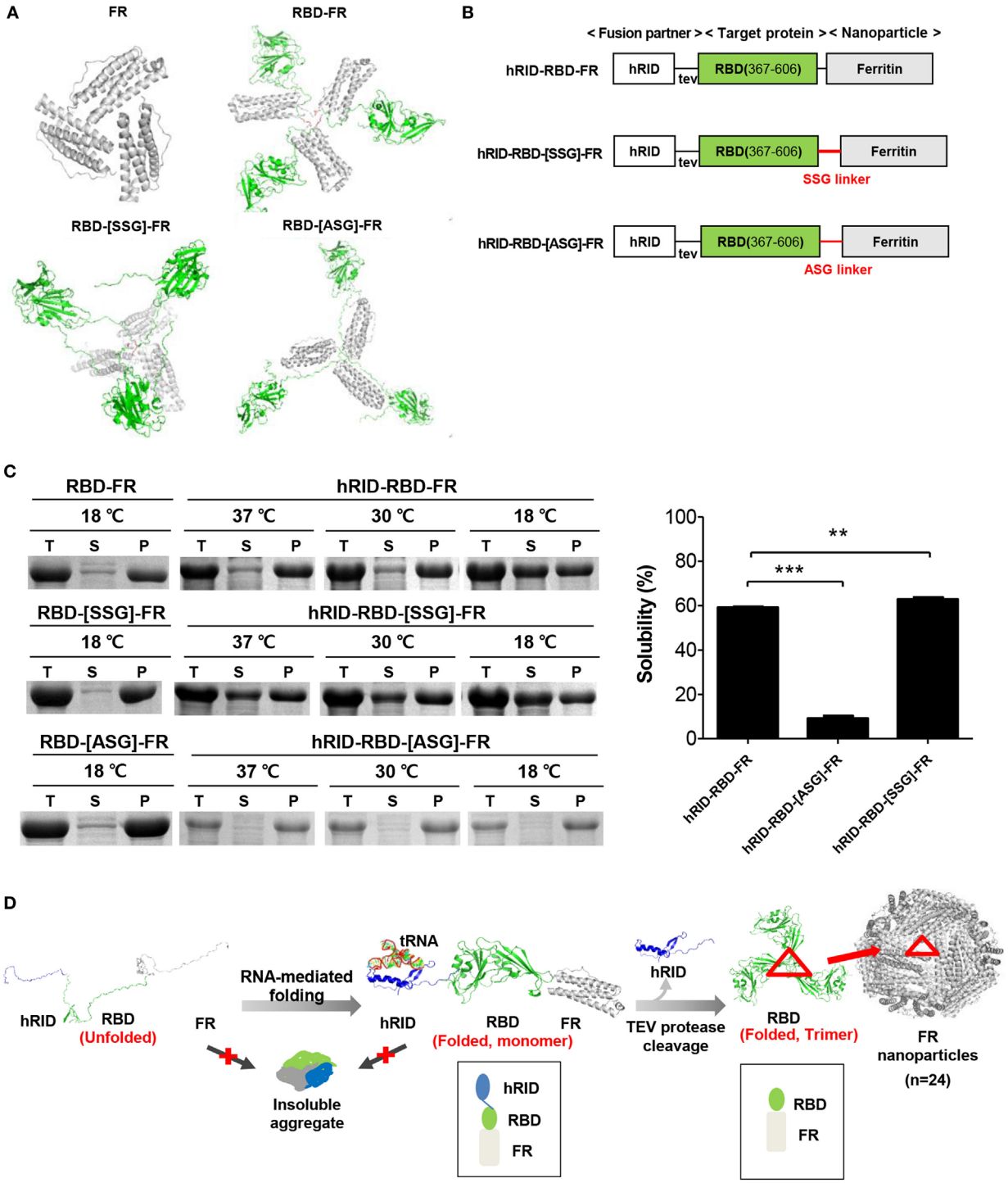

FIGURE 1 | Design and soluble expression of Middle East respiratory syndrome-coronavirus (MERS-CoV) receptor-binding domain (RBD) nanoparticles (NPs) using the chaperna-based expression platform. **(A)** Computational modeling of FR, RBD-FR, RBD-[SSG]-FR, and RBD-[ASG]-FR. The hRID domain, RBD, FR, and linkers are colored as blue, green, gray, and red, respectively. **(B)** Schematic diagram of the expression vector system. The two linkers are shown in red, and tev indicates the TEV protease recognition site. **(C)** Expression of hRID-RBD-FR in the presence or absence of the hRID fusion partner and linkers. The proteins were expressed at various temperatures (37, 30, and 18°C) and the cell lysates were separated into total (T), soluble (S), and insoluble (P) fractions by centrifugation (left panel). The solubility of each protein expressed at 18°C was measured by a gel densitometer and the data were summarized and shown in the right panel ($n = 3$). Statistical significance (**$p < 0.01$, ***$p < 0.001$) was indicated for the samples compared with the control using a two-tailed Student's t-test. **(D)** Illustration of MERS-CoV RBD-FR NPs using the chaperna-based hRID fusion partner. The hRID facilitated folding of the aggregation-prone RBD-FR through interaction with RNA. The monomer of RBD-FR formed a properly folded trimeric structure by cleaving hRID with TEV protease. Eight trimers assembled and formed into MERS-CoV-like NPs. Red triangles indicate the RBD trimer on the FR NPs.

of the NPs was measured twice at 25°C in water as a solvent with the sample accumulation time at 200 s.

Effect of Salt and Fe^{2+} Concentrations on NP Assembly and Stability

Cultured cells (3 ml) were lysed with lysis buffer in the presence of various concentrations of NaCl (0, 50, 100, 150, 200, 225, 250, 275, and 300 mM) to evaluate the intracellular proteins. All samples were performed in triplicate. The cell lysates were separated into soluble and insoluble fractions by centrifugation, and the protein stabilities analyzed by sodium dodecyl sulfate-polyacrylamide gel electrophoresis (SDS-PAGE). Thus, the proteins from cell lysates (500 ml culture) were purified using HisPur™ Ni-NTA Resin (Thermo Fisher Scientific) in buffer A depending on NaCl concentration (0–300 mM). To evaluate the effects on Fe^{2+} on NP formation, cells were cultured in LB media with various concentrations of Fe^{2+} (0, 200, 500, and 1,000 μM). NP formation was examined by size exclusion chromatography (SEC), SDS-PAGE, TEM, and DLS at the various concentrations of NaCl or Fe^{2+}.

Analysis of Protein Stability and RNA Binding

The cells were harvested, sonicated with lysis buffer, and separated into soluble and pellet fractions by centrifugation. Target proteins in the soluble fraction were purified using HisPur™ Ni-NTA Resin (Thermo Fisher Scientific), following the manufacturer's instruction. T (total lysate), S (soluble fraction), P (pellet fraction), W (wash fraction), and E (the elution fraction were analyzed by SDS-PAGE. Co-purification of the nucleic acids and proteins in the wash and elute were analyzed on a native agarose gel. The nucleic acids were visualized with ethidium bromide (EtBr), and the proteins with Coomassie staining.

RNase A Treatment

Cultured cells (10 ml) were harvested using the same method described above. The cells were lysed with 500 μl of protein extraction reagent B-PER™ II (Thermo scientific) and separated into soluble and pellet fractions by centrifuged 12,000 rpm for 10 m. A 200 μl aliquot of each soluble fraction was further treated with 250 μg/ml of RNase A (iNtRON Biotechnology) and incubated at 37°C for 15 min. The nuclease treated samples were clarified by centrifugation at 12,000 rpm for 15 min and the soluble supernatants and the pelleted precipitates were analyzed on an SDS-PAGE gel followed by western blot analysis.

hDPP4-Binding Enzyme-Linked Immunosorbent Assay (ELISA)

To confirm the proper folding of RBD-FR and its variant (RBD-[SSG]-FR), the binding of the purified proteins with the MERS-Cov receptor hddp4 was performed by ELISA. FR only and phosphate-buffered saline (PBS) were used as negative controls. Nunc 96-well microtiter immunoplates (Thermo Fisher Scientific) were coated with 100 ng/well of hDPP4 proteins (Abcam) and incubated at 4°C overnight. The plates were washed and blocked with 150 μl/well of blocking buffer (1% BSA) for 1 h at room temperature. RBD (SSG linker, WT, 2 m, or 9 m)-FR (100 ng/well) were added for 2 h at 37°C. An anti-penta His antibody (100 μl/well; Qiagen) was serially diluted (1/100 to 1/12,800) in TBST [50 mM Tris–Cl (pH 7.4), 0.05% Tween-20], added to the wells, and incubated for 1 h at 37°C. A secondary goat anti-mouse IgG antibody conjugated with HRP in a 100-μl volume (1:5,000, Sigma-Aldrich) was added and incubated for 1 h at 37°C. The plates were washed three times with TBST at the end of each step. After washing, 100 μl/well of substrate TMB solution (BD Biosciences) were added to the well and the plates were incubated at 37°C for 30 min in the dark. 50 μl of stop solution (2 N H_2SO_4) was added to the well to stop the colorimetric reaction, and the absorbance at 450 nm was measured using an ELISA reader, FLUOstar OPTIMA (BMG LABTECH).

Serological Detection of MERS-CoV Infection

Each well of a 96-well microplates (NUNC, Roskilde, Denmark) was coated with 250 ng of four proteins [RBD-[SSG]-FR, RBD-FR(WT), RBD-FR(2 m), and RBD-FR(9 m)] and incubated overnight at 4°C. MERS-CoV RBD protein (MERS-RBD-005P; eEnzyme) was used as a positive control. Following each subsequent step, the wells were washed three times with buffer (0.05% TWEEN-20-PBS; Sigma-Aldrich, St. Louis, MO, USA). The coating antigens were removed, and the wells were blocked with PBST (5% skim milk in PBS and Tween-20) for 1 h at 37°C. After 2 h, the blocking solution was removed. Twofold serially diluted sera from four patients (CNNH-0709, 0809, 1009, and 1309) were added to each well and incubated at 37°C for 2 h. The antigen-coated wells were incubated with peroxidase-conjugated goat anti-human IgG antibody (KPL, SeraCare Life Sciences, Milford, MA, USA) at 37°C for 1 h. The primary antibody was removed and 3,3′,5,5′-tetramethylbenzidine (TMB; Sigma-Aldrich) was added to each well as colorimetric substrate. Immediately after treatment of the reactions with stopping solution (Sigma-Aldrich), the OD was read at 450 nm.

Mouse Immunization and Sera Collection

Six-week-old female BALB/c mice were immunized with 20 μg/mouse of the RBD-FR, RBD-[SSG]-FR, or RBD protein generated as described above, or with commercially available MERS-CoV RBD protein (MERS-RBD-005P; eEnzyme) as antigen in BSL-2 facility in YLARC. Antigens were diluted in PBS. For the first group, equal volume of MF59 adjuvant (AddaVax, Cat. No vac-adx-10) (43) was mixed by pipetting. For the other group, equal volume of antigens and alum adjuvant (Thermo Fisher Scientific) were mixed by pipetting following the manufacturers' protocol. PBS plus adjuvant and FR were used as negative controls. The immunized mice were boosted twice with intramuscular injections on days 14 and 28. Mice were anesthetized on days 27 and 41 for ocular bleeding from the orbital sinus (Figure S10 in Supplementary Material). Immune sera were processed by centrifugation of the collected blood at 12,000 × *g* for 30 min. The spleen and the BALF (bronchoalveolar lavage) were obtained at 7 days after the last immunization from sacrificed mice. BALF was taken by washing the airways with 1 ml of PBS.

Flow Cytometric Analysis

T-cell population from immunized mice were analyzed by Flow cytometric analysis (43, 44). The spleens were taken at 7 days after the last immunization from the sacrificed mice. To obtain single-cell suspensions, the tissues were homogenized and passed through 70 μm cell strainers (SPL). After centrifugation, erythrocytes were removed by Red Blood Cell Lysing Buffer (Sigma). The cells were washed and resuspended in Iscove's Modified Dulbecco's Media containing 10% FBS. For intracellular cytokine staining, the splenocytes were stimulated with 10 μg/ml RBD protein or phorbol myristate acetate/ionomycin in the presence 10 ng/ml recombinant human IL-2 (BioLegend) and Brefeldin A (1:1,000; eBioscience) at 37°C for 5 h. After stimulation, the cells were blocked with rat anti-mouse CD16/CD32 (BD Biosciences) and surface stained with anti-CD8 (FITC, clone 53-6.7; BioLegend) and anti-CD4 (PE/Cy7, clone GK1.5; BioLegend) at 4°C for 30 min. The stained cells were fixed in FACS lysing solution (BD Biosciences) at room temperature for 20 min, and permeabilized with FACS buffer (0.5% FBS, 0.1% NaN3 in PBS) containing 0.5% saponin (Sigma) at room temperature for 15 min. Then, the cells were stained with anti-IFN-γ (PE, clone XMG1.2; BioLegend) and anti-TNF-α (APC, clone MP6-XT22; BioLegend) at room temperature for 40 min. All data were collected by BD LSR Fortessa (BD Biosciences) and analyzed with FlowJo software (Tree Star Inc., Ashland, OR, USA).

Competition ELISA Between RBD Protein and hDPP4 Receptor

Competition ELISA was performed to determine whether MERS-CoV antigen [RBD-[SSG]-FR, RBD-FR, RBD, and FR (negative control)]-immunized mouse serum inhibited binding of RBD protein to hDPP4 receptor (45, 46). 500 ng/well hDPP4 protein (Abcam) was coated on Nunc 96-well microtiter immunoplates (Thermo Fisher Scientific) and incubated overnight at 4°C. Plates were washed and blocked with 150 μl/well of blocking buffer [5% skim milk in PBS and Tween-20 (PBST)] for 1 h at 37°C. At the same time, mouse sera immunized with RBD, RBD-[SSG]-FR, RBD-FR, and FR were serially diluted (1/10 to 1/160) with 500 ng/well RBD protein (MERS-RBD-005P; eEnzyme) in TBST [50 mM Tris-Cl (pH 7.4), 0.05% Tween-20], added to new wells, and incubated for 1 h at 37°C. 100 μl solution was added to each well at 37°C and incubated for 2 h. After that, 100 μl of anti-6xHis tag antibody conjugated with horseradish peroxidase (1:1,000, Thermo Fisher Scientific) was added to each well and incubated for 1 h at 37°C. Plates were washed three times with TBST, and 100 μl/well of substrate TMB solution (BD Biosciences) was incubated at 37°C for 30 min in the dark. 50 μl of stop solution (2 N H_2SO_4) was added to the well to stop the color reaction and measure the absorbance at 450 nm using an ELISA reader FLUOstar OPTIMA (BMG LABTECH).

RESULTS

The hRID Facilitated the Solubility of MERS-CoV RBD-FR

The spike glycoprotein (S) of MERS-CoV was used for the generation of MERS-CoV-like NPs. S protein forms trimers, resulting in large spikes on the virus envelope (47). It is challenging to express the full-sized S protein (~200 kDa) in *E. coli*. Thus, the S1 domain of S protein (~80 kDa), which includes the receptor-binding ability, was used. Our initial attempt to express the S1 domain, either as S1 or as an S1-FR fusion protein, failed; the expression level and solubility of the protein was below the lower limit of detection by SDS-PAGE and western blotting (Figure S1 in Supplementary Material). We therefore used the RBD (367–606 a.a.) of the S1 protein, which has a pivotal function as illustrated in **Figure 1B** (48, 49). When expressed alone in *E. coli*, the RBD is not able to form the trimeric assembly (unpublished observation), due to the lack of the HR2 domain within the S2 domain (50). To overcome this problem, FR was used as scaffold for the assembly. FR is a spherical NP whose subunits form trimers that subsequently result in octahedral structures composed of 24 identical subunits (51). We therefore performed computational modeling to evaluate the potential of FR as scaffold for trimer formation of the RBD.

Possible trimer formation was analyzed by computational modeling using MODELER (13, 52) and ClusPro (41, 42). Various linkers, including SSG, ASG, and D6, were introduced between the RBD and FR with a goal to minimize steric hindrance between the two domains so as to enhance trimer and NP formation. *In silico* analysis showed energy-stable trimeric models of RBD-FR, RBD-[SSG]-FR, and RBD-[ASG]-FR, whereas RBD-D6-FR failed to form a trimeric structure (**Figure 1A**). The RBD-[SSG]-FR was predicted to be the most stable and well-structured compared with RBD-FR and RBD-[ASG]-FR. Initial testing of the RBD-FR constructs without hRID fusion showed that none of the constructs were solubly expressed, even under low-temperature culture conditions (**Figure 1C**) (10.5 and 8.8%, for RBD-FR and RBD-[SSG]-FR, respectively). In addition, the yield of purified RBD-FR from a 2 l culture was only 30 μg of protein. Because of the low-soluble expression of MERS-CoV RBD, we fused hRID to the N-terminus of RBD-FR as a chaperna-based fusion partner (**Figure 1B**). We previously confirmed that by using chaperna, the globular domain of influenza hemagglutinin (HA) is efficiently assembled into a trimeric complex with an immunologically relevant conformation (Yang et al., *in press*). As shown in **Figure 1C**, the hRID fusion significantly increased the solubility of both RBD-FR (59.1%) and RBD-[SSG]-FR (62.83%), indicating that the chaperna platform effectively increased both the solubility and the folding of its fused target proteins. Because of the poor expression level and low solubility of the RBD-[ASG]-FR construct (**Figure 1C**), further experiments were performed using only the RBD-FR and RBD-[SSG]-FR constructs.

The SSG Linker Increased the Proper Assembly of MERS-CoV RBD NPs

After purification of the soluble proteins (Figure S2 in Supplementary Material), we determined the potential effects of using hRID as a fusion partner for the self-assembly of the NPs. As shown in Figure S3 in Supplementary Material, hRID-RBD-FR failed to form NPs. Because of this, we performed TEV protease cleavage of the hRID. Removal of the hRID domain facilitated the self-assembly of the RBD-FR monomers, and also eliminated the immune response against the non-self hRID domain in

BALB/c mice (Figure S4 in Supplementary Material). After hRID cleavage, RBD-FR and RBD-[SSG]-FR were purified using SEC (**Figure 2A**). As expected, RBD-[SSG]-FR assembled into properly formed NPs (1,080 kDa) more efficiently than did RBD-FR NPs, which were mainly detected in the void-volume fractions, suggesting they were irregularly assembled soluble aggregates. The size of the RBD-[SSG]-FR NPs was further confirmed by TEM. TEM images of the RBD-[SSG]-FR NP structures showed hollow, spherical particles that were more compact than the RBD-FR NPs. The average diameter of the RBD-[SSG]-FR NPs was 28–30 nm (**Figure 2B**). In contrast, DLS analysis of the RBD-FR NP structure without the SSG linker appeared to be smaller with an average intensity diameter of 26.3 nm, and this compared with RBD-[SSG]-FR that had an average intensity distribution diameter of 30.5 nm (**Figure 2C**). Consistent with the SEC analysis, RBD-FR without a fusion partner was mostly produced in a soluble aggregated form. Therefore, we identified that the protein folding did not occur properly without hRID, and the formation of NPs was confirmed by both SEC and SDS-PAGE analyses. As shown in Figure S5 in Supplementary Material, the purified NPs retained their stability over an extended period of time at various temperatures (25, 4, and −20°C). Thus, these results indicate that the SSG linker allowed the RBD-FR to generate properly assembled NPs. It should also be noted that the efficiency of protein folding and NPs formation may be further enhance through appropriate linker selection.

NaCl Concentration Had a Pivotal Role in Assembly of RBD-[SSG]-FR NPs

It has been reported that ionic strength plays an important role in the stability and self-assembly of ferritins (53, 54). We examined the effect of salt concentration on the formation and stability of the RBD-[SSG]-FR NPs at various concentrations (0–300 mM). Consistent with the previous studies, the stability of the protein was highly affected by the concentration of NaCl in the lysis buffer by SDS-PAGE (**Figure 3A**) ($n = 3$). The solubility of the protein significantly decreased as the concentration of NaCl increased from 0 to 100 mM, with the solubility being about 8.79-fold lower at 100 mM compared with 0 mM. Unlike previous studies, the solubility of the protein was gradually recovered at higher NaCl concentrations (>100 mM); the solubility at 300 mM was 1.45-fold higher than at 0 mM. Furthermore, the yield of soluble of protein per liter of culture increased in a salt concentration-dependent manner (**Figure 3B**).

To further investigate the effect of salt concentration, the physicochemical and morphological properties of the RBD-[SSG]-FR protein were examined by SEC, TEM, and DLS. In 50 mM NaCl, most of the protein was aggregated during the purification process, and the purified protein failed to form spherical structures, but instead, existed predominantly as 45 kDa monomers (**Figures 3C,D**; Figure S6 in Supplementary Material). In contrast, the protein that was lysed in 0 mM NaCl and purified in 200 mM NaCl, developed well-structured NPs according to TEM and DLS analyses (**Figures 3C,D**; Figure S6 in Supplementary Material). However, based on SEC analysis, at high-salt concentrations (>250 mM), the protein failed to form stable structures with the proteins being eluted predominantly in the void volume, suggesting they were soluble aggregates under the high-salt concentrations (**Figure 3C**).

Transmission electron microscopy images under the various salt concentrations clearly supported the conclusion, showing that the tendency for aggregation was dependent on the salt concentration (**Figure 3D**). Taken together, the results underscored the importance of salt concentration on the solubility of monomers and the quality of multimeric assembly of hybrid NPs.

Fe^{2+} Had an Effect on the NPs Formation and Stability

Ferritin has an intrinsic ability to interact with Fe^{2+} to form ferritin-iron cores (55). Thus, it was worth investigating the effect of Fe^{2+} on the assembly and stability of RBD-[SSG]-FR NPs. Cells were grown in LB medium with various concentrations of Fe^{2+}. As shown in **Figure 4A**, the yield of purified protein was significantly increased from cultures with 500 μM Fe^{2+}, reflecting a 2.7-fold increase compared with similar cultures 0 μM Fe^{2+}. The cell growth and purification yield at 1,000 μM Fe^{2+} were slightly decreased, presumably due to the toxicity of ferric acid. NP formation under the various concentrations of Fe^{2+} was analyzed by SEC (**Figure 4B**). Consistent with the previous results, the proteins were eluted mainly in the fractions expected for the size of assembled NPs (1,080 kDa).

Of note, the ratio between NPs and soluble aggregates in the SEC analysis showed that NP formation was facilitated at high concentrations of Fe^{2+} (**Figure 4B**). The formation of RBD-[SSG]-FR NPs at an Fe^{2+} concentration of 1,000 μM was confirmed by TEM (**Figure 4C**) and DLS (**Figure 4D**). The TEM analysis clearly showed that the morphology of the proteins was more compact, and probably highly stable, when assembled at high Fe^{2+} concentrations (500 μM) than at lower concentrations (0 μM) (**Figure 4C**). As shown in **Figure 4D**, the average diameter of NPs examined by DLS was 25.1 nm at high Fe^{2+} concentration (500–1,000 μM) and 27.7–32.2 nm at lower concentration (0–200 μM). These results suggest that both Fe^{2+} and salts concentrations influenced the efficiency and quality of the regular assembly of hybrid ferritin monomers into NPs.

RNA Binding Was a Key Factor for the Solubility of Hybrid Ferritin

Our previous studies show that an RNA–protein interaction is crucial for transducing the chaperone function of RNA into the folding of client proteins (38). Consistent with that, our present study showed that RNA facilitated the folding of its interacting proteins. The solubility of hRID(WT)-RBD-FR was 5.69-fold higher than RBD-FR without hRID fusion (**Figure 1**), strongly supporting the previous studies. In addition, the solubility of RBD alone was completely insoluble (**Figure 5B**; Figure S7 in Supplementary Material). It has been shown that the positively charged residues of lysine moieties in hRID contribute to tRNA binding (56). In the current study, the tRNA binding induced the intrinsically disordered protein (IDP) status of hRID to form alpha-helical structures (**Figure 5A**). Thus, two RNA-binding

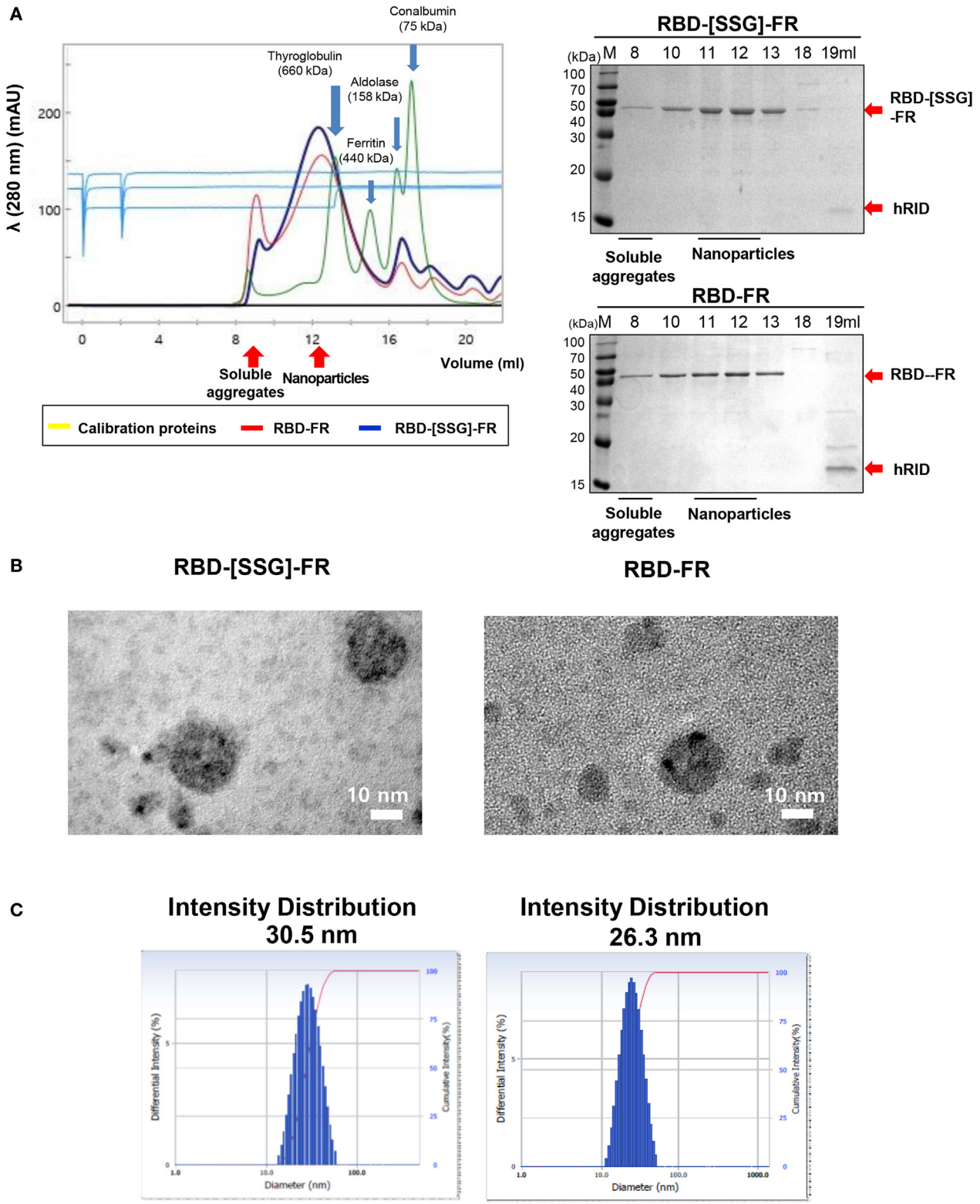

FIGURE 2 | Analysis of Middle East respiratory syndrome-coronavirus receptor-binding domain (RBD) nanoparticle formation. **(A)** Size exclusion chromatography (SEC) of RBD-[SSG]-FR (blue) and RBD-FR (red) using Superose 6 Increase 10/300 GL. Blue arrows indicate the four eluted calibration proteins (yellow) with each size of the proteins were shown with the arrows. The eluted fractions were analyzed on sodium dodecyl sulfate-polyacrylamide gel electrophoresis (right panel). Red arrows indicate the purified target protein and the separated hRID. **(B)** Negative-stained transmission electron microscopy images of RBD-[SSG]-FR and RBD-FR. **(C)** The intensity distribution diameter of RBD-[SSG]-FR and RBD-FR as determined by dynamic light scattering.

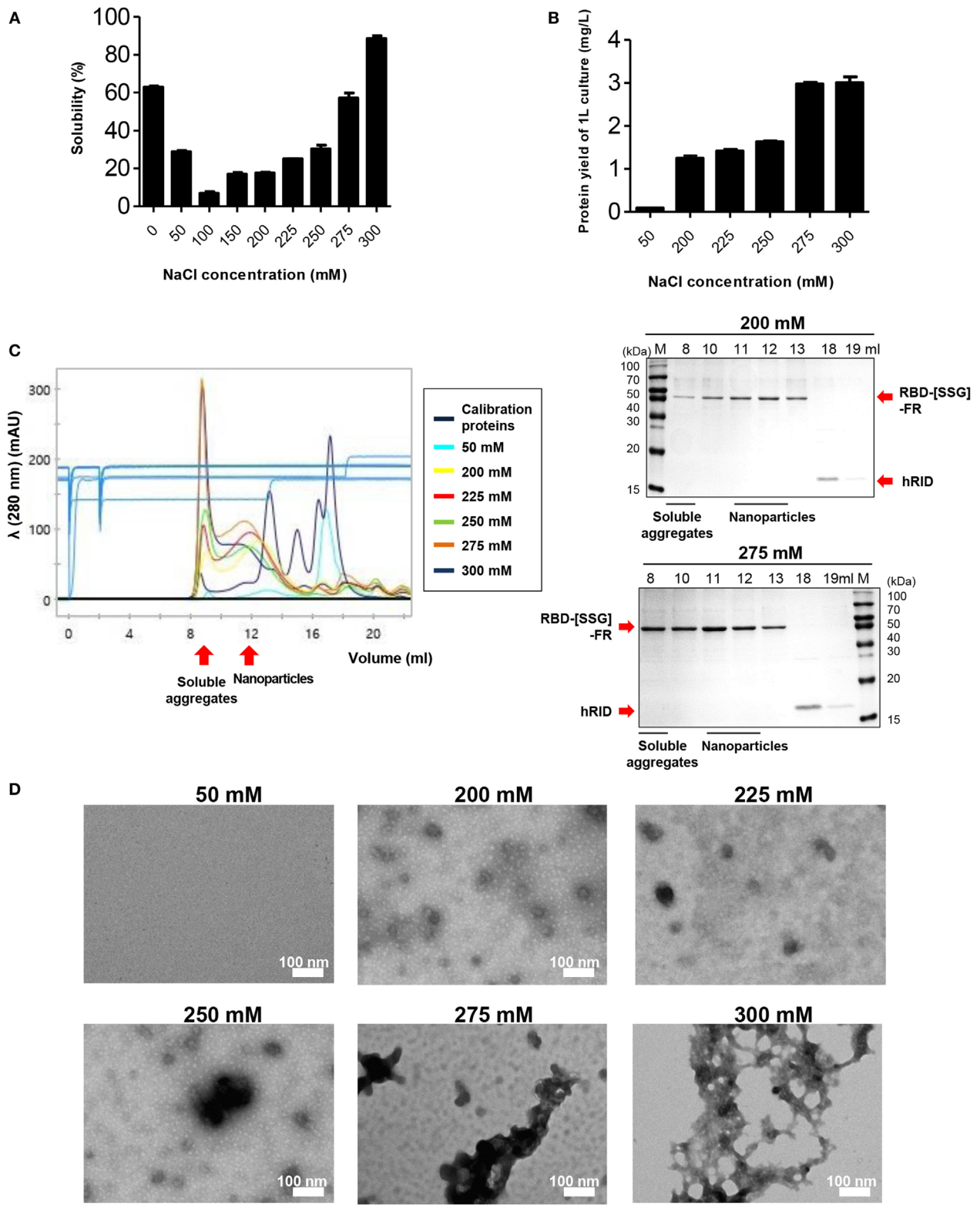

FIGURE 3 | The effect of NaCl concentration on the assembly and stability of receptor-binding domain (RBD) nanoparticles (NPs). **(A)** Solubility of RBD-[SSG]-FR at various NaCl concentrations (0, 50, 100, 150, 200, 225, 250, 275, and 300 mM) was analyzed on sodium dodecyl sulfate-polyacrylamide gel electrophoresis and the data obtained from three independent experiments are summarized. **(B)** Purification yields (milligram per liter) of RBD-[SSG]-FR from 1-l cultures at various concentrations of NaCl (50, 200, 225, 250, 275, and 300 mM). The data are shown as the mean ± SD from duplicate experiments. The purified proteins from **(B)** were used for confirming NP formation of RBD-[SSG]-FR by size exclusion chromatography **(C)**, transmission electron microscopy **(D)**.

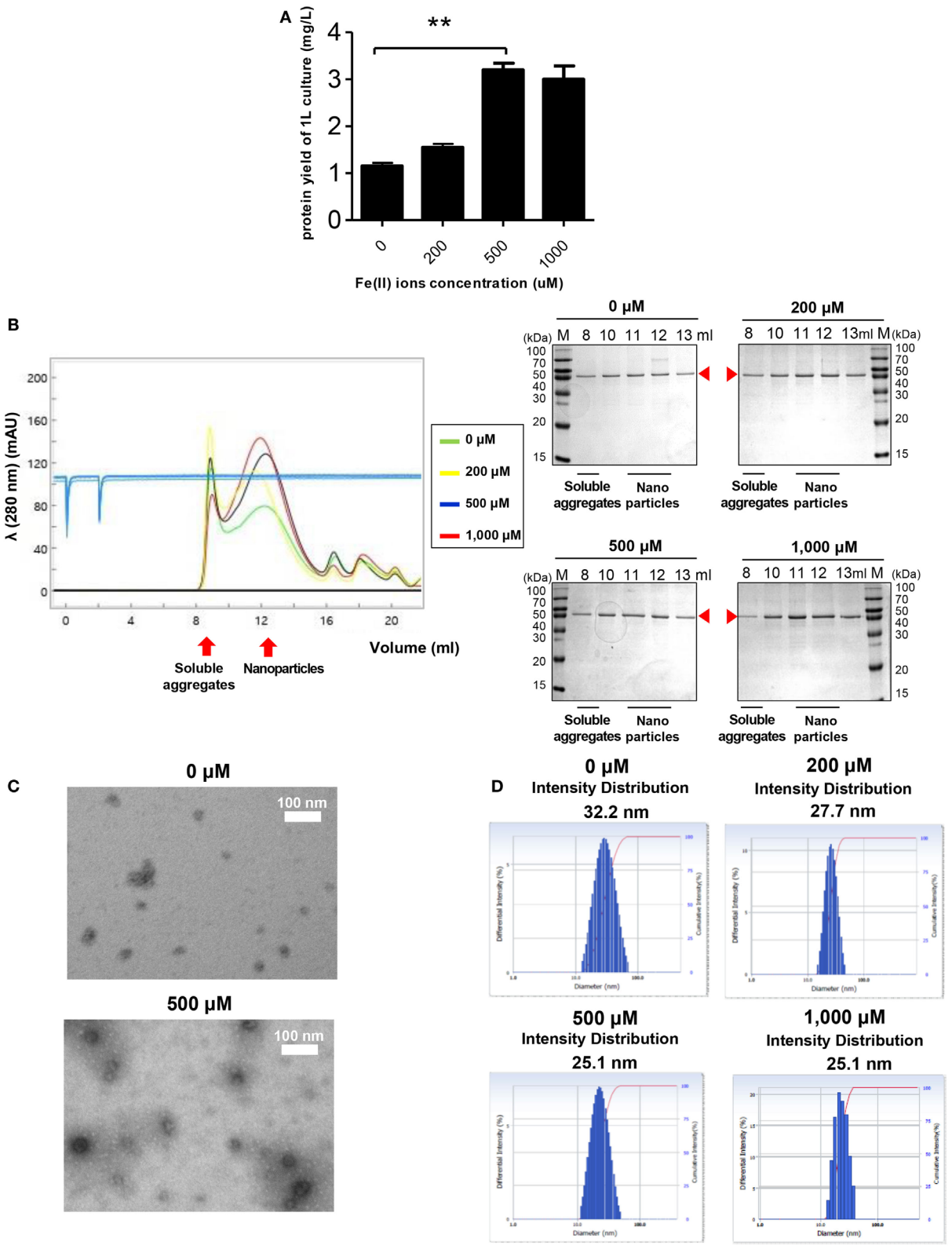

FIGURE 4 | The effect of Fe^{2+} on the stability and nanoparticle (NP) formation of receptor-binding domain (RBD)-[SSG]-FR. **(A)** Purification yields of RBD-[SSG]-FR from cell culture at various concentrations of Fe^{2+} (0, 200, 500, and 1,000 mM). The data are presented as mean ± SD of duplicate experiments. All *p*-values were determined using Student's two-tailed tests (**$p < 0.01$). After purification, the NPs were examined by size exclusion chromatography **(B)**, transmission electron microscopy **(C)**, and dynamic light scattering **(D)**. Arrowheads in **(B)** indicate the eluted RBD-[SSG]-FR.

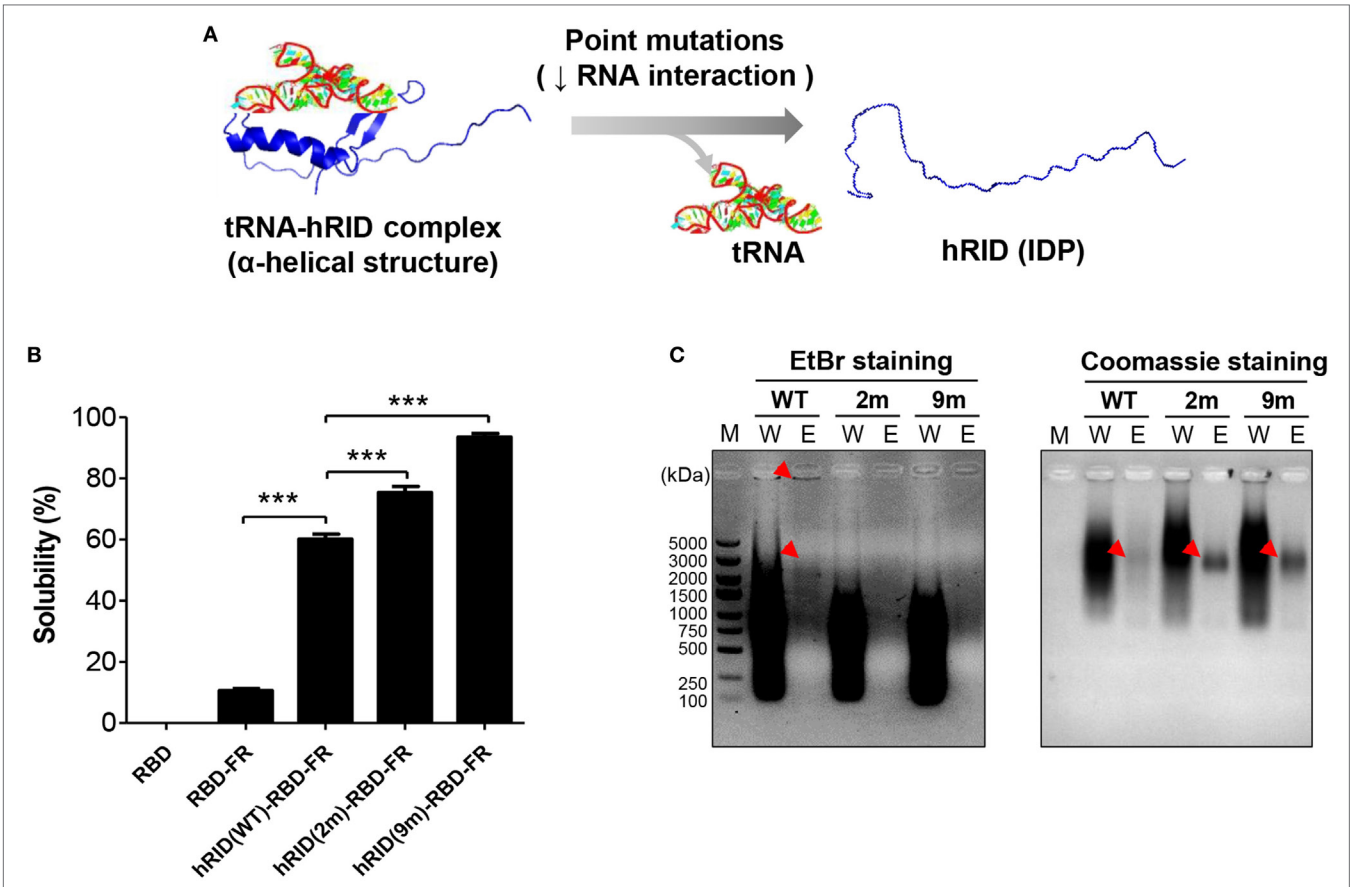

FIGURE 5 | Verifying the role of RNA in protein solubility and stability. **(A)** Schematic illustration of the hRID structure with and without tRNA binding. Mutant hRID with impaired tRNA binding failed to form the specific structure and remained disordered, whereas wild-type hRID interacted with tRNA and formed α-helical structures. **(B)** The solubility of receptor-binding domain (RBD), RBD-FR, hRID(WT)-RBD-FR, hRID(2 m)-RBD-FR, and hRID(9 m)-RBD-FR was analyzed on sodium dodecyl sulfate-polyacrylamide gel electrophoresis and summarized. The data obtained from three independent experiments were used (***$p < 0.001$). **(C)** Identification of RNAs co-purified with hRID(WT, 2 m, or 9 m)-RBD-FR. The arrowheads on the ethidium bromide-stained gel and coomassie blue-stained gel represent the co-purified RNAs and purified proteins, respectively. The molecular weight marker (M), wash fraction (W), and elution fraction (E), are indicated. Each soluble fraction from cell lysates was purified using Hispur™ Ni-NTA Resin.

mutants, double-mutant hRID (K19A and K23A) and nona-mutant hRID (K19A, K23A, R24A, K27A, K30A, K31A, K35A, K38A, and K40A) were constructed (Table S1 in Supplementary Material). The total *E. coli* lysate (T) was fractionated into the soluble fraction (S) and the pellet fraction (P) by centrifugation. As expected, both RBD and RBD-FR without fusion to hRID domain, were refractory to being produced as soluble proteins (**Figure 5B**). Interestingly, the solubility of the RNA-binding mutants did not decrease, but actually increased to 75.3% for the 2 m mutant and 93.4% for the 9 m mutant compared with wild-type protein at 60.1% (**Figure 5B**). Considering that hRID is relatively unstructured in the absence of tRNA binding, the results are consistent with previous reports that the fusion with IDPs promotes the solubility of target proteins (57–59). Following purification of wild-type hRID-RBD-FR (hRID(WT)-RBD-FR), electrophoretic mobility shift assays showed that greater amounts of nucleic acids were co-purified with hRID(WT)-RBD-FR protein than with the mutant hRID-RBD-FRs (2 and 9 m) under non-denaturing conditions (**Figure 5C**). The relative ratio of nucleic acid based on EtBr staining and proteins based on Coomassie staining in the eluted fraction confirmed the reduced affinity of mutants to nucleic acids.

To test if RNA had a role in maintaining the stability of the target proteins, the lysates were treated with RNase A to eliminate RNA, and the solubility of each protein was analyzed by SDS-PAGE and western blotting. The soluble fractions of the lysates (S) were incubated at 37°C in the presence and absence of RNase A and the samples were further separated into soluble fraction (SS′) and insoluble fraction (SP′) by centrifugation. As shown in the left panel of **Figure 6**, RNase A treatment completely abolished the effect of RNA on protein solubility as compared with the control (RNase A−) or with samples prior to RNase treatment. Parallel experiments with the 2 and 9 m mutants showed much less RNA co-purified with the proteins, confirming the reduced affinity to nucleic acids and the complete depletion of RNA by RNase A treatment (**Figure 6**, left panel). Remarkably, the solubility of hRID(WT)-RBD-FR was greatly

reduced by depletion of RNA as reflected in the ratio of [SS′]/[SP′] [0.1 and 0.4 for RNase (+) and RNase (−), respectively] by both Coomassie staining and western blot analyses (**Figure 6**, right panel). However, the solubility of the mutants (2 and 9 m), was not significantly affected by RNase A treatment, probably due to their lower affinity to RNA (**Figure 6**, right panel). Taken together, the results demonstrate that hRID(WT)-RBD-FR maintained a strong affinity for RNA, and that affinity was pivotal for maintaining the solubility of the protein.

RNA-Binding Facilitated NP Assembly and Prevented Formation of Soluble Aggregates

To further define the RNA dependence of solubility of the ferritin hybrids (**Figure 6**), we investigated if the RNA binding had a role in the formation of NPs. RBD-FR and the various hRID-RBD-FR (WT, 2, and 9 m) proteins were purified by nickel-affinity chromatography (Figure S2 in Supplementary Material) and their physicochemical properties analyzed by SEC (**Figure 7A**), TEM (**Figure 7B**), and DLS (**Figure 7C**). The soluble yields of RBD-FR (hRID fusion) was approximately 1.6 mg/l of culture, representing greater than 1,000-fold higher levels than its hRID (−) counterpart (~15 μg/l culture), again confirming the role of hRID as a robust enhancer for solubility and assembly. It was striking to note that the two mutant proteins, despite high solubility (**Figure 5B**), were detected at disproportionately higher amounts in the void fractions of SEC, indicating that they failed to form NPs of a defined size, and existed predominantly as soluble aggregates (**Figure 7A**). However, hRID(WT)-RBD-FR predominantly formed NPs of a defined size (~1,080 kDa). It is also interesting to note that there was a slight shift of the RNA-binding mutants (2 and 9 m) in the elution pattern, suggesting a larger size of NPs compared with wild-type NPs. Overall, the ratio between soluble aggregates in the void volume and the NPs of defined size clearly showed that RNA binding was crucial for assembly of the monomers into NPs. As a control, RBD-FR (without hRID fusion) existed predominantly as soluble aggregates (Figure S8 in Supplementary Material). Consistent with these results, EM analysis confirmed well-structured NPs by hRID(WT)-RBD-FR, compared to largely aggregated structures by the mutant proteins (**Figure 7B**). Even if multi-molecular structure was formed, the structure becomes unstable, mostly as soluble aggregates. Consistently, the intensity distribution diameter of the wild-type protein, as estimated by DLS analysis, was 25 nm compared with larger sizes of hRID(2 m) at 34.2, 519.2 nm and hRID(9 m) at 52, 717.7 nm (**Figure 7C**; Figure S9 in Supplementary Material). It is conceivable that soluble aggregates may shield the exposed 6-histidine tag, resulting in a decreased binding affinity to Nickel resins and elution in earlier fractions compared with WT protein (Figure S2 in Supplementary Material). Taken together, the data demonstrate that RNA binding prevented aggregation into irregular conformations and guided the self-assembly of the hybrid ferritin monomers into NPs of a stable structure.

Wild-Type Proteins Showed Strong-Binding Ability to Both the hDPP4 Receptor Protein and MERS-CoV Infected Patient Sera

The immunological properties of ferritin NPs were analyzed by ELISA. The hDDP4 (human DPP4) receptor has been previously identified as the receptor for MERS-CoV human infection (46). Therefore, using hDPP4 as a coating antigen, ELISA-binding assays between RBD NPs and the receptor were performed (**Figure 8**). FR without RBD fusion failed to bind, and was similar to the PBS negative control. Strikingly, the binding ability increased in the same order as the RNA-binding ability (hRID(WT) > 2 m > 9 m), with highest absorbance observed in the WT with the SSG linker (hRID(WT)-RBD-[SSG]-FR). The results show that the conformation of RBD in the WT NPs better resembled the protective antigen of MERS-CoV RBD from 293 cells, compared with the RNA-binding mutants 2 and 9 m. Again, judicious choice of linker between the ferritin carrier and the antigen was important for receptor binding and was reflected in its importance for NP assembly into a stable conformation (**Figure 2**). Finally, the ELISA results for NP against human patients was investigated using the sera from four MERS-CoV-infected patients (**Figure 9**). Six different proteins, including five recombinant NPs (hRID(WT)-RBD-FR, hRID(2 m)-RBD-FR, hRID(9 m)-RBD-FR, hRID(WT)-RBD-[SSG]-FR, and FR), and MERS-CoV RBD protein were compared by ELISA using them as capture antigens. Strong ELISA signals were detected for the four recombinant NPs and MERS-CoV RBD from 293 cells (positive control). The WT form consistently showed a higher response than the RNA-binding mutants (hRID(WT) > 2 m > 9 m), with hRID(WT)-RBD-[SSG]-FR being the best binder among constructs tested. These results address to the utility of the *E. coli* assembled MERS-CoV RBD-FR NPs as useful tools for sero-diagnosis of MERS-CoV infection. Taken together, the results confirmed the immunologically relevant conformation of the MERS-CoV RBD displayed on the hybrid ferritin particles, and the crucial role of RNA in controlling the kinetic pathway for the assembly of viral antigen monomers into stable NPs.

Immunization of MERS-CoV NPs Induces RBD-Specific Antibodies

To evaluate the immunogenicity of ferritin-based NPs, BALB/c mice ($n = 5$) were immunized with RBD, RBD-FR, and RBD-[SSG]-FR NPs antigens. The tRNAs were found to be removed from the hRID protein during the purification process. Before immunization, potential RNA contamination in the purified proteins was determined by gel electrophoresis. As shown in Figure S11 in Supplementary Material, RNA was below detection level, if any, after several purification steps, compared with the proteins purified in the first step. Previously, MF59-adjuvated and alum-adjuvated MERS-CoV antigen have been reported to increase the antibody and T-cell responses in mice (44, 60). Thus, the first group and second group were immunized twice with 20.0 μg of antigen containing the equal volume of alum

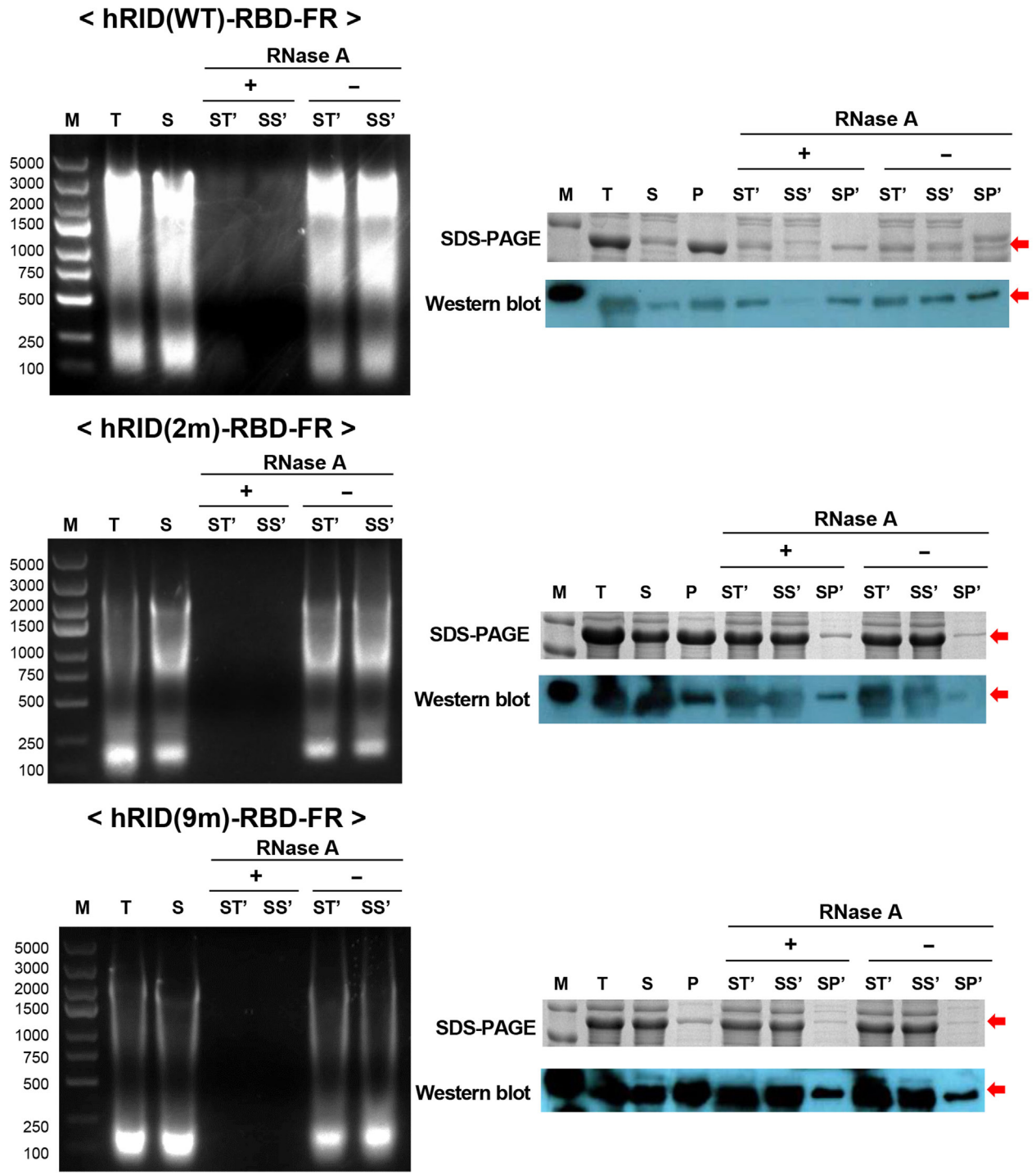

FIGURE 6 | RNA's function to maintain protein stability. The effect of RNase A treatment on the solubility of hRID(WT, 2, and 9 m)-receptor-binding domain (RBD)-FR. RNA elimination by RNase A was analyzed on an agarose gel (left). Following RNase A treatment, the soluble fraction (S) was further separated into total (ST′), soluble (SS′), and insoluble (SP′) fractions and analyzed by sodium dodecyl sulfate-polyacrylamide gel electrophoresis (SDS-PAGE) (right, upper panel) and western blot (right, lower panel).

and MF59, respectively (Figure S10 in Supplementary Material). After collecting serum, the RBD-specific IgG titer was analyzed by ELISA. Alum adjuvanted RBD-[SSG]-FR NPs and RBD-FR NPs induced 14-fold and 16-fold higher ($p < 0.0001$) than RBD (**Figure 10A**). The antibody titers of MF59 adjuvanted RBD-[SSG]-FR NPs and RBD-FR NPs were 4.5- and 3-fold

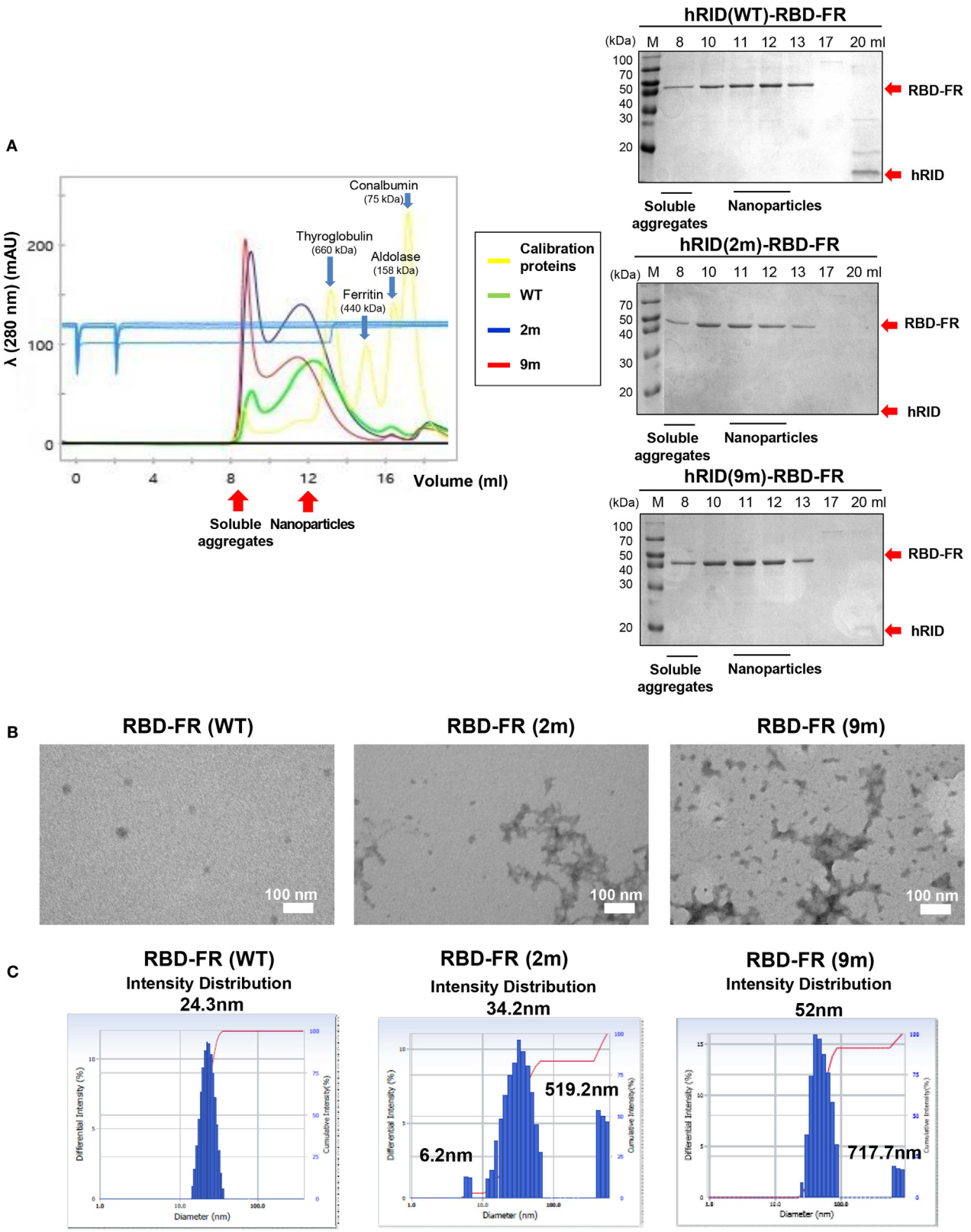

FIGURE 7 | Elucidation of RNA-mediated nanoparticle (NP) formation of receptor-binding domain (RBD)-FR. **(A)** Size exclusion chromatography analysis of RBD-FR NPs purified from the TEV protease-cleaved hRID(WT, 2, or 9 m)-RBD-FR. The fractions (11–12 ml) estimated as NPs were further analyzed by transmission Electron Microscopy **(B)** and dynamic light scattering **(C)**.

higher than RBD, respectively. The antibody responses by RBD-FR and RBD-[SSG]-FR NPs were much stronger than the RBD in all antibody subtypes tested (IgG1, IgG2a, and IgG2b) (**Figures 10B–D**). As a test of mucosal immune responses, the RBD-specific IgA antibody levels from BALF were also analyzed by ELISA (**Figure 10E**). MF59 adjuvanted RBD-[SSG]-FR NPs presented significantly higher OD values than RBD and FR (negative control). These results suggested that RBD-[SSG]-FR NPs induces local mucosal immune response stronger than RBD. In addition, it was confirmed that antibody responses of IgG, IgG1 (Th1), IgG2a, and IgG2b (Th2) against MF59-adjuvated antigens were higher than those from alum-adjuvated antigens. In contrast, PBS and FR control groups failed to, or only weakly induce an antibody response against RBD protein. These results suggest that FR-based NPs significantly enhance various antibody responses than monomeric antigens.

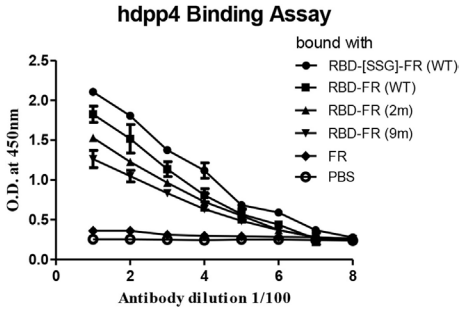

FIGURE 8 | Enzyme-linked immunosorbent assay analysis of receptor-binding domain (RBD)-FR bound with hDPP4 receptor protein. Each purified protein shown in Figure S2 in Supplementary Material and size exclusion chromatography was used to explore hDPP4 receptor-binding affinity to the protein. All data are shown as mean ± SD from triplicate samples. FR alone and phosphate-buffered saline were used as negative controls.

Specific Cellular Immune Responses Were Induced by MERS-CoV NPs

The cellular immune responses were investigated in mice immunized with protein (RBD, RBD-FR, RBD-[SSG]-FR) and FR (negative control). Splenocytes of mice ($n = 4$) were harvested 1 week after the last immunization, stimulated with

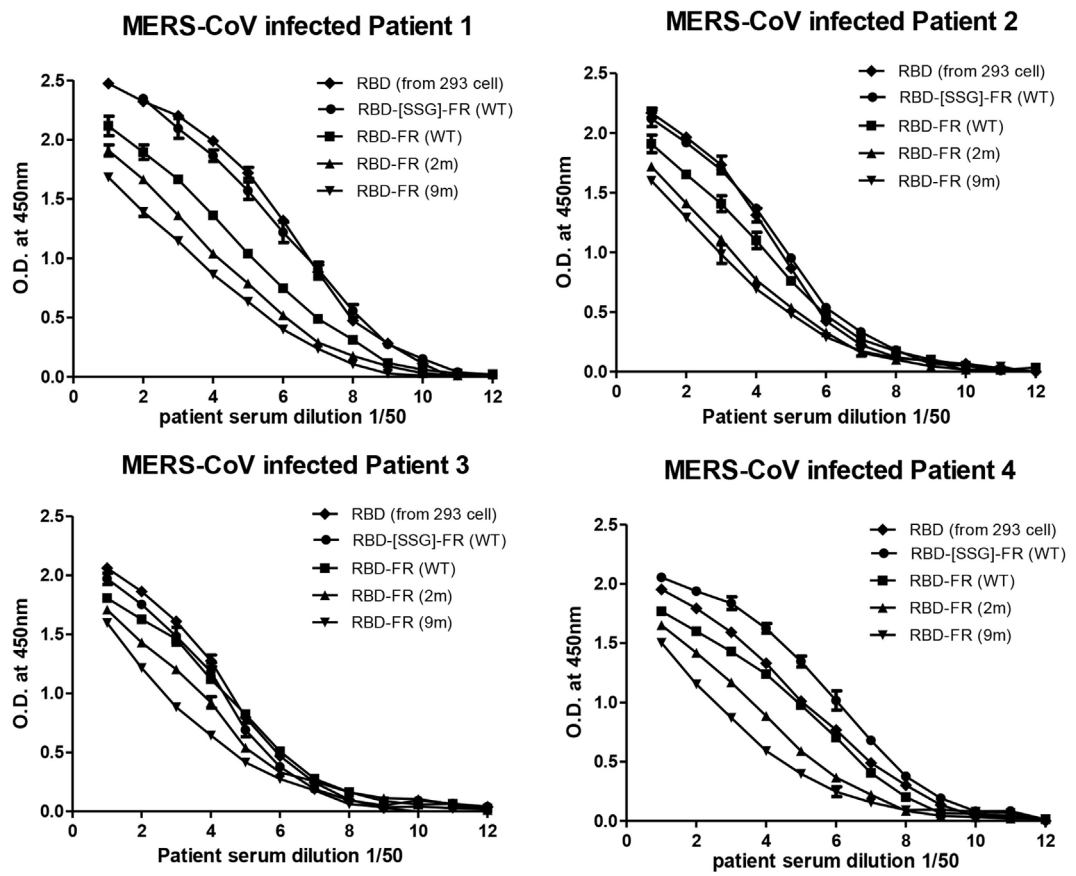

FIGURE 9 | Sero-diagnosis of Middle East respiratory syndrome-coronavirus-infected patients using receptor-binding domain (RBD)-FR nanoparticles. The purified proteins shown in Figure S2 in Supplementary Material were used as coating antigens. FR alone and infected cell lysates were used as negative and positive controls, respectively. Virus-infected sera from four patients were serially diluted from 1:100 (twofold dilution). All data are presented as mean ± SD of duplicate samples.

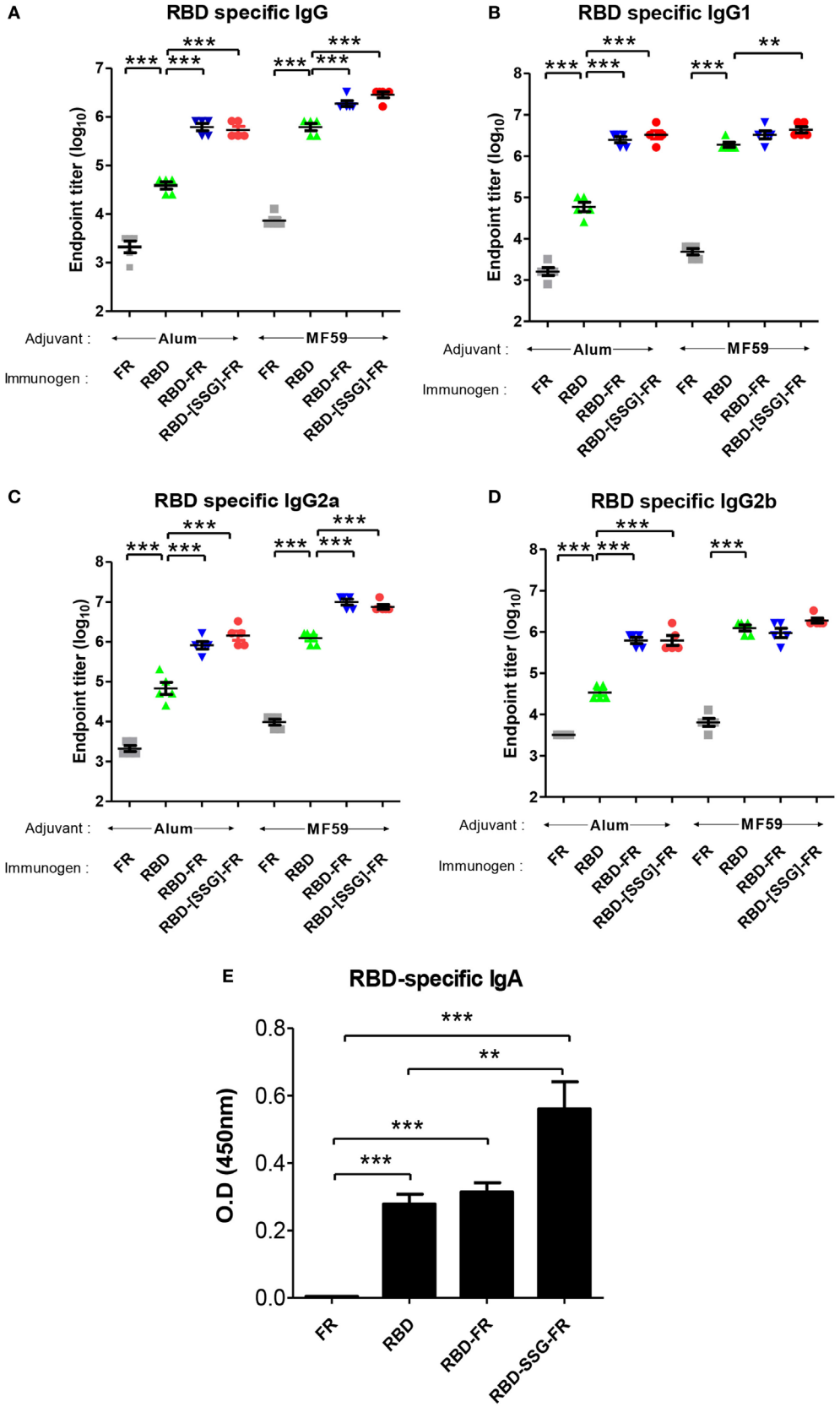

FIGURE 10 | Continued

FIGURE 10 | Immune responses in receptor-binding domain (RBD) nanoparticles (NPs) immunized mice ($n = 5$). Endpoint titer of IgG **(A)**, IgG1 **(B)**, IgG2a **(C)**, and IgG2b **(D)** antibody binding to Middle East respiratory syndrome-coronavirus RBD were detected using mice serum after two immunizations. RBD-specific antibodies were detected after immunizations of RBD NPs, RBD, FR with adjuvant (alum and MF59) using enzyme-linked immunosorbent assay. **(E)**. RBD-specific IgA antibodies were detected using BALF (diluted 1:8) after immunization of protein with MF59. OD, optical density. Each endpoint titer was shown by individual. All error bars were shown as mean ± SD ($n = 5$) and all p-values were obtained using Student's two-tailed tests (**$p < 0.01$, ***$p < 0.001$).

RBD protein, and analyzed for cytokines by flow cytometry. In the RBD-immunized group, IFN-γ and TNF-α-producing $CD4^+$ T-cell responses were detected at low levels. However, IFN-γ and TNF-α-producing $CD4^+$ T cells were significantly increased in RBD-FR and RBD-[SSG]-FR-immunized groups compared with RBD and FR-immunized group (Figure S12 in Supplementary Material). These results demonstrated that the RBD NPs vaccination induced antigen-specific $CD4^+$ T cells that produced IFN-γ and TNF-α upon antigen stimulation.

Anti-NPs Serum Effectively Blocked RBD Protein Binding to the hDPP4 Receptor

Middle East respiratory syndrome-coronavirus infection is mediated by the interaction of RBD and the host receptor hDPP4 (45, 46). As a correlate of protection, a competition ELISA was performed to investigate whether antibodies generated from NPs immunization were able to interfere with the binding to hDPP4. Thus, after incubation of RBD protein with mouse serum (1:10), the binding of serum-mixed samples to hDPP4 protein was measured. As shown in **Figure 11**, RBD-[SSG]-FR, RBD-FR, and RBD-immunized sera strongly abolished the binding of RBD to hDPP4 receptor (93.3, 82.2, and 75.67%, respectively). Interestingly, the relative efficiency of interference correlates with that of NP assemblage (**Figure 11**). In contrast, the FR-immunized mouse serum (negative control) failed to inhibit the interaction. Taking together, these results demonstrate that immunization of NPs greatly stimulates MERS-CoV-specific antibody response that effectively interferes with the cellular receptor binding, suggesting its possibility as a vaccine. However, protection efficacy should ultimately be tested in a live virus challenge model.

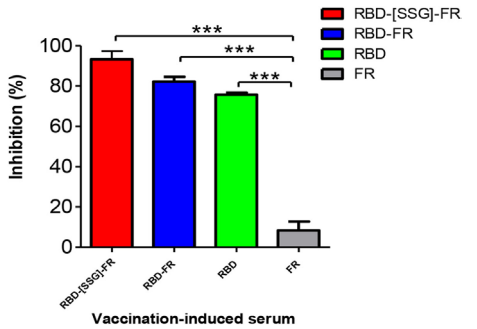

FIGURE 11 | Nanoparticles-immunized mouse serum inhibited interaction between Middle East respiratory syndrome-coronavirus receptor-binding domain (RBD) and hDPP4 receptor. Competition enzyme-linked immunosorbent assay showed that anti-RBD mouse sera (1:10, from mice immunized with RBD-[SSG]-FR, RBD-FR, and RBD) blocked binding between RBD (5 μg/ml) and hDPP4 receptor (5 μg/ml). FR-immunized mouse serum (1:10) was used as a negative control. All sera were serially diluted from 1:10 (twofold dilution). All data are presented as mean ± SD ($n = 5$) and p-values were obtained using Student's two-tailed tests (***$p < 0.001$).

DISCUSSION

Having key immunologic features, like a highly repetitive nanostructure, provides a designing principle for NPs in inducing potent and long-lasting antibody responses. For VLPs of non-enveloped viruses, assembly is made purely by capsid proteins. For enveloped viruses, however, additional membrane components and matrix proteins are required to display the target antigens on the surface of assembled VLPs. A promising alternative is to present target antigen on the surfaces of self-assembled NPs, which, in lieu of lipid membranes and matrix proteins, serve as a macromolecular scaffold for the presentation of antigens of interest (61). Ferritins, as a substitute for matrix proteins and membranes, have been used as scaffold for the regular assembly of target antigens. However, ferritin-based NPs have been produced only in host cells of mammalian or insect origin (28, 62). Previously, we showed that influenza HA could be assembled in a soluble, trimeric, and immunologically relevant conformation by exploiting chaperna activity (63). The present study is the first report of using RNAs as molecular chaperone for supra-molecular structures. Here, we present a novel bacterial system for NP assembly of hybrid ferritin displayed surface antigens from MERS-CoV. The NPs reacted strongly with sera derived from MERS-CoV-infected patients (**Figure 9**) confirming their utility in sero-diagnosis of infection. Moreover, the antisera, generated from immunization of mice, were able to interfere with the binding to the cellular receptor hDPP4 (**Figure 8**), in part of essential protective immune responses. The efficiency of receptor-binding inhibition (**Figure 11**), as well as the ability for inducing the mucosal responses (**Figure 10E**), correlated with the regular assembly of NPs as examined by DLS or EM (**Figure 2**), confirming that presentation of antigenic epitopes on a multivalent and highly repetitive structure is indeed important for the quality of immune responses. Overall, the quality of NPs and consequent immune responses were governed by the RNA-mediated assembly of antigens.

We hypothesized that chaperna function could be harnessed for presenting target antigens as highly repetitive nanostructures (**Figure 1D**). The hRID is the N-terminal domain of hLysRS and was previously identified as a nucleic acid-binding domain (**Figure 5**) (63). In this report, the hRID was exploited as a transducer for chaperna function (TCF) by serving as a docking-tag for cellular RNA for the folding/assembly of the hybrid FR containing client antigen proteins [RBD of MERS-CoV (**Figure 1D**)]. The advantage of using hRID as a TCF

could be many fold. First, hRID is small (8.3 kDa), monomeric, and was flexible enough to allow the access of site-specific protease for the removal of hRID (Figure S3 in Supplementary Material). Of note, hRID belongs to IDPs, which switches into stabile α-helixes upon binding with tRNAs. Second, the bound RNA, due to its highly negative charge, may resist uncontrolled intermolecular interactions among monomers into amorphous aggregation. Finally, even the naked hRID (in the absence of RNA binding), due to its intrinsically flexible nature, may not pose physical hindrance to multiple interactions among monomers, enabling assembly into stable super-structures, upon removal of the hRID. Thus, the potential "pace-making" function harnessed with the RNA molecule, allows a regular assembly of monomers as highly repetitive nanostructures. Consequently, in the current study, hybrid FR was produced in soluble forms, could be purified by one-step affinity chromatography, and most remarkably, assembled into NPs of defined sizes upon removal of the hRID (Figure S2 in Supplementary Material). Consistent with the principles of design, the loss of RNA binding by hRID significantly hampered the regular assembly of the ferritin monomers and increased the amount of non-functional misfolded proteins as soluble aggregates (**Figure 7**). Thus, the overall yield, as well as the quality of NPs, were dependent on the chaperna function transduced by the hRID, which in turn was mediated by interaction with cellular RNAs (likely to be tRNAs).

The driving and controlling factors for *de novo* assembly of biomolecules are poorly understood. Historically, host factors like GroEL/S were initially discovered as molecular chaperones for supporting viral growth in *E. coli* and supporting the assembly of viral capsid proteins (64, 65). Moreover, GroEL/S also cooperates with RbcX in plant cells for the assembly of multi-component RUBISCO, which is the most abundant protein in the biosphere responsible for photosynthesis (66). Therefore, it is intriguing that RNA could provide such a robust folding/assembly of a supra-molecular structure. We recently confirmed that the present strategy could be successfully applied to the assembly of bacterially synthesized monomers of norovirus into VLPs composed of 180 monomers (unpublished observation, Seong, B.L.). Whether RNA can substitute for, or collaborate with pre-existing protein-based molecular chaperones remains an exciting avenue for future investigations. It should be noted that the defined versatile functions are being expanded for RNA molecules. As an engineered system for harnessing chaperna function, the present report may prove to be the tip of an iceberg for pivotal function of RNA molecules as chaperones for the folding and supra-molecular assembly of proteins in living organisms (36, 38).

Various factors were identified as important for efficient assembly of MERS-CoV NPs. As an extrinsic factor, the binding affinity of hRID to cellular RNAs was crucial for the assembly and the quality of the assembled NPs (**Figure 7**). As intrinsic factors, the concentration of salts and Fe^{2+} also influenced the assembly and stability of NPs (**Figures 3** and **4**). The ionic strength played an important role in the stability and self-assembly of ferritins, and aggregation increased with increasing concentrations of NaCl (54). The assembly of the hybrid MERS-CoV NPs revealed an interesting change in salt dependence, with 200–225 mM NaCl buffer as optimal condition as confirmed by EM and DLS analyses (**Figure 3**). The change in salt dependence was probably due to the presence of electrostatic interactions among RBD domains (54, 67). The dependence on Fe^{2+} was not surprising considering that ferritin has an intrinsic ability to interact with Fe^{2+} to form ferritin-iron cores (55). Based on our experience, to enhance the quality of NPs, it is advisable to control Fe^{2+} concentrations, both during the culturing of the bacterial cells and during the purification of the soluble monomer proteins (**Figure 4**). First, the yield of the purified protein was increased in the presence of 500 μM Fe^{2+} (**Figure 4B**), up to 2.7-fold greater compared with the control conditions lacking Fe^{2+}. Second, the ratio between NPs and soluble aggregates in SEC showed that NPs formation was facilitated at high concentrations of Fe^{2+}, and resulted in a more compact morphology under EM (**Figures 4B,C**). Thus, both the overall yield and the quality of NPs were governed by their intrinsic ability to interact with Fe^{2+}. Finally, our data show that the presence and the nature of the linker between the ferritin and the RBD antigen was also important to the assembly of NPs. It is possible that a linker with flexibility and sufficient length would accommodate the steric requirements for assembly of multimeric NPs. However, it is difficult to precisely predict the effect of the linker, and therefore it is advisable to screen multiple constructs during the early stages of testing the assembly of NPs displaying antigens of interest.

In conclusion, the chaperna-based antigen assembly platform holds promise for the development and delivery of NP-based vaccines to enhance RBD-specific antibody responses, and the serological detection of emerging viruses. Various types of designing principles have advanced the structure-based approaches to NP assembly (61, 68). However, most of the *in silico* methods consider the thermodynamic stability of the final assembled NPs, but not necessarily the kinetic pathways leading to their successful folding into regular assemblages. Consequently, most NPs are refractory to soluble expression and fail to assemble as designed, resulting in significant, and practical challenges in the manufacturing process. The chaperna-mediated folding and the "pace-keeping" assembly of monomers into higher ordered structures will enable faithful production of NP and VLP-based vaccines against emerging and re-emerging viral infections.

ETHICS STATEMENT

This study was carried out in accordance with the recommendations of "Ministry of Food and Drug Safety (MFDS) of Republic of Korea." The protocol was approved by the "YLARC Institutional Animal Care and Use Committee (IACUC; permit number: IACUC-A-201710-377-01)."

AUTHOR CONTRIBUTIONS

Y-SK and BS designed the research study. Y-SK, AS, and BS wrote the manuscript. Y-SK performed overall experiments. JHK, JEK, SK, YB, and JS conducted the research study. JL and JY provided

technical assistance and vector. PK developed the necessary software for performing analyzing computer data. CP provide technical assistance to conduct RNase A treatment experiments. YK and NC provide patients sera infected with MERS-CoV. MK and JC analyzed cellular immune response by flow cytometry.

ACKNOWLEDGMENTS

We thank J. I. Kim and M.-S. Park at Korea University Medical School for providing information on sero-diagnosis of MERS-CoV-infected patient. We thank Y. H. Jang for information on cellular immune analyses.

FUNDING

This study was supported by grants from the Ministry of Health & Welfare, Republic of Korea (grant numbers HI13C0826 and HI15C2934) and the National Research Foundation of Korea (2014M3A9E4064743).

SUPPLEMENTARY MATERIAL

The Supplementary Material for this article can be found online at https://www.frontiersin.org/articles/10.3389/fimmu.2018.01093/full#supplementary-material.

REFERENCES

1. Jeong H, Seong BL. Exploiting virus-like particles as innovative vaccines against emerging viral infections. *J Microbiol* (2017) 55(3):220–30. doi:10.1007/s12275-017-7058-3
2. Wong S-S, Webby RJ. Traditional and new influenza vaccines. *Clin Microbiol Rev* (2013) 26(3):476–92. doi:10.1128/CMR.00097-12
3. Ulmer JB, Valley U, Rappuoli R. Vaccine manufacturing: challenges and solutions. *Nat Biotechnol* (2006) 24(11):1377–83. doi:10.1038/nbt1261
4. Gunther S, Feldmann H, Geisbert TW, Hensley LE, Rollin PE, Nichol ST, et al. Management of accidental exposure to Ebola virus in the biosafety level 4 laboratory, Hamburg, Germany. *J Infect Dis* (2011) 204(Suppl 3):S785–90. doi:10.1093/infdis/jir298
5. Gregory AE, Titball R, Williamson D. Vaccine delivery using nanoparticles. *Front Cell Infect Microbiol* (2013) 3:13. doi:10.3389/fcimb.2013.00013
6. Bachmann MF, Jennings GT. Vaccine delivery: a matter of size, geometry, kinetics and molecular patterns. *Nat Rev Immunol* (2010) 10(11):787–96. doi:10.1038/nri2868
7. Kushnir N, Streatfield SJ, Yusibov V. Virus-like particles as a highly efficient vaccine platform: diversity of targets and production systems and advances in clinical development. *Vaccine* (2012) 31(1):58–83. doi:10.1016/j.vaccine.2012.10.083
8. Bachmann MF, Rohrer UH, Kundig TM, Burki K, Hengartner H, Zinkernagel RM. The influence of antigen organization on B cell responsiveness. *Science* (1993) 262(5138):1448–51. doi:10.1126/science.8248784
9. Guu TS, Liu Z, Ye Q, Mata DA, Li K, Yin C, et al. Structure of the hepatitis E virus-like particle suggests mechanisms for virus assembly and receptor binding. *Proc Natl Acad Sci U S A* (2009) 106(31):12992–7. doi:10.1073/pnas.0904848106
10. Hagensee ME, Yaegashi N, Galloway DA. Self-assembly of human papillomavirus type 1 capsids by expression of the L1 protein alone or by coexpression of the L1 and L2 capsid proteins. *J Virol* (1993) 67(1):315–22.
11. Roden R, Wu T-C. How will HPV vaccines affect cervical cancer? *Nat Rev Cancer* (2006) 6(10):753–63. doi:10.1038/nrc1973
12. Kang S-M, Kim M-C, Compans RW. Virus-like particles as universal influenza vaccines. *Expert Rev Vaccines* (2012) 11(8):995–1007. doi:10.1586/erv.12.70
13. Webb B, Sali A. Comparative protein structure modeling using MODELLER. *Curr Protoc Bioinformatics* (2014) 47:561–32. doi:10.1002/0471250953.bi0506s47
14. Raman S, Machaidze G, Lustig A, Aebi U, Burkhard P. Structure-based design of peptides that self-assemble into regular polyhedral nanoparticles. *Nanomedicine* (2006) 2(2):95–102. doi:10.1016/j.nano.2006.04.007
15. Martí-Renom MA, Stuart AC, Fiser A, Sánchez R, Melo F, Šali A. Comparative protein structure modeling of genes and genomes. *Annu Rev Biophys Biomol Struct* (2000) 29(1):291–325. doi:10.1146/annurev.biophys.29.1.291
16. Zeltins A. Construction and characterization of virus-like particles: a review. *Mol Biotechnol* (2013) 53(1):92–107. doi:10.1007/s12033-012-9598-4
17. Lopez-Sagaseta J, Malito E, Rappuoli R, Bottomley MJ. Self-assembling protein nanoparticles in the design of vaccines. *Comput Struct Biotechnol J* (2016) 14:58–68. doi:10.1016/j.csbj.2015.11.001
18. Fang N, Frazer IH, Fernando GJ. Differences in the post-translational modifications of human papillomavirus type 6b major capsid protein expressed from a baculovirus system compared with a vaccinia virus system. *Biotechnol Appl Biochem* (2000) 32(1):27–33. doi:10.1042/BA20000001
19. Zaki AM, Van Boheemen S, Bestebroer TM, Osterhaus AD, Fouchier RA. Isolation of a novel coronavirus from a man with pneumonia in Saudi Arabia. *New Engl J Med* (2012) 367(19):1814–20. doi:10.1056/NEJMoa1211721
20. Engler O, Klingström J, Aliyev E, Niederhauser C, Fontana S, Strasser M, et al. Middle East respiratory syndrome coronavirus (MERS-CoV) serology in major livestock species in an affected region in Jordan, June to September 2013. *Euro Surveill* (2013) 18(50):20662. doi:10.2807/1560-7917.ES2013.18.50.20662
21. Memish ZA, Cotten M, Meyer B, Watson SJ, Alsahafi AJ, Al Rabeeah AA, et al. Human infection with MERS coronavirus after exposure to infected camels, Saudi Arabia, 2013. *Emerg Infect Dis* (2014) 20(6):1012. doi:10.3201/eid2006.140402
22. Breban R, Riou J, Fontanet A. Interhuman transmissibility of Middle East respiratory syndrome coronavirus: estimation of pandemic risk. *Lancet* (2013) 382(9893):694–9. doi:10.1016/S0140-6736(13)61492-0
23. Choi JY. An outbreak of middle east respiratory syndrome coronavirus infection in South Korea, 2015. *Yonsei Med J* (2015) 56(5):1174. doi:10.3349/ymj.2015.56.5.1174
24. Ki M. 2015 MERS outbreak in Korea: hospital-to-hospital transmission. *Epidemiol Health* (2015) 37:e2015033. doi:10.4178/epih/e2015033
25. Yariv J, Kalb A, Sperling R, Bauminger E, Cohen S, Ofer S. The composition and the structure of bacterioferritin of *Escherichia coli*. *Biochem J* (1981) 197(1):171–5. doi:10.1042/bj1970171
26. Zhang Y, Orner BP. Self-assembly in the ferritin nano-cage protein superfamily. *Int J Mol Sci* (2011) 12(8):5406–21. doi:10.3390/ijms12085406
27. He L, de Val N, Morris CD, Vora N, Thinnes TC, Kong L, et al. Presenting native-like trimeric HIV-1 antigens with self-assembling nanoparticles. *Nat Commun* (2016) 7:12041. doi:10.1038/ncomms12041
28. Yassine HM, Boyington JC, McTamney PM, Wei C-J, Kanekiyo M, Kong W-P, et al. Hemagglutinin-stem nanoparticles generate heterosubtypic influenza protection. *Nat Med* (2015) 21(9):1065–70. doi:10.1038/nm.3927
29. Todd TJ, Zhen Z, Xie J. Ferritin nanocages: great potential as clinically translatable drug delivery vehicles? *Nanomedicine* (2013) 8(10):1555–7. doi:10.2217/nnm.13.141
30. Clark EDB. Refolding of recombinant proteins. *Curr Opin Biotechnol* (1998) 9(2):157–63. doi:10.1016/S0958-1669(98)80109-2
31. Lilie H, Schwarz E, Rudolph R. Advances in refolding of proteins produced in *E. coli*. *Curr Opin Biotechnol* (1998) 9(5):497–501. doi:10.1016/S0958-1669(98)80035-9
32. Hendrick J, Hartl F. The role of molecular chaperones in protein folding. *FASEB J* (1995) 9(15):1559–69. doi:10.1096/fasebj.9.15.8529835
33. Hartl FU, Hayer-Hartl M. Molecular chaperones in the cytosol: from nascent chain to folded protein. *Science* (2002) 295(5561):1852–8. doi:10.1126/science.1068408
34. Bukau B, Horwich AL. The Hsp70 and Hsp60 chaperone machines. *Cell* (1998) 92(3):351–66. doi:10.1016/S0092-8674(00)80928-9
35. Choi SI, Ryu K, Seong BL. RNA-mediated chaperone type for de novo protein folding. *RNA Biol* (2009) 6(1):21–4. doi:10.4161/rna.6.1.7441
36. Son A, Choi SI, Han G, Seong BL. M1 RNA is important for the in-cell solubility of its cognate C5 protein: implications for RNA-mediated protein folding. *RNA Biol* (2015) 12(11):1198–208. doi:10.1080/15476286.2015.1096487

37. Horowitz S, Bardwell JC. RNAs as chaperones. *RNA Biol* (2016) 13(12): 1228–31. doi:10.1080/15476286.2016.1247147
38. Kim JM, Choi HS, Seong BL. The folding competence of HIV-1 Tat mediated by interaction with TAR RNA. *RNA Biol* (2017) 14(7):926–37. doi:10.1080/15476286.2017.1311455
39. Choi SI, Han KS, Kim CW, Ryu K-S, Kim BH, Kim K-H, et al. Protein solubility and folding enhancement by interaction with RNA. *PLoS One* (2008) 3(7):e2677. doi:10.1371/journal.pone.0002677
40. Fiser A, Do RK, Sali A. Modeling of loops in protein structures. *Protein Sci* (2000) 9(9):1753–73. doi:10.1110/ps.9.9.1753
41. Comeau SR, Gatchell DW, Vajda S, Camacho CJ. ClusPro: a fully automated algorithm for protein-protein docking. *Nucleic Acids Res* (2004) 32(Web Server issue):W96–9. doi:10.1093/nar/gkh354
42. Kozakov D, Hall DR, Xia B, Porter KA, Padhorny D, Yueh C, et al. The ClusPro web server for protein-protein docking. *Nat Protoc* (2017) 12(2):255–78. doi:10.1038/nprot.2016.169
43. Lee J-Y, Chang J. Universal vaccine against respiratory syncytial virus A and B subtypes. *PLoS One* (2017) 12(4):e0175384. doi:10.1371/journal.pone.0175384
44. Tang J, Zhang N, Tao X, Zhao G, Guo Y, Tseng C-TK, et al. Optimization of antigen dose for a receptor-binding domain-based subunit vaccine against MERS coronavirus. *Hum Vaccin Immunother* (2015) 11(5):1244–50. doi:10.1080/21645515.2015.1021527
45. Du L, Kou Z, Ma C, Tao X, Wang L, Zhao G, et al. A truncated receptor-binding domain of MERS-CoV spike protein potently inhibits MERS-CoV infection and induces strong neutralizing antibody responses: implication for developing therapeutics and vaccines. *PLoS One* (2013) 8(12):e81587. doi:10.1371/journal.pone.0081587
46. Raj VS, Mou H, Smits SL, Dekkers DH, Müller MA, Dijkman R, et al. Dipeptidyl peptidase 4 is a functional receptor for the emerging human coronavirus-EMC. *Nature* (2013) 495(7440):251. doi:10.1038/nature12005
47. Xia S, Liu Q, Wang Q, Sun Z, Su S, Du L, et al. Middle East respiratory syndrome coronavirus (MERS-CoV) entry inhibitors targeting spike protein. *Virus Res* (2014) 194:200–10. doi:10.1016/j.virusres.2014.10.007
48. Lu G, Hu Y, Wang Q, Qi J, Gao F, Li Y, et al. Molecular basis of binding between novel human coronavirus MERS-CoV and its receptor CD26. *Nature* (2013) 500(7461):227–31. doi:10.1038/nature12328
49. Wang N, Shi X, Jiang L, Zhang S, Wang D, Tong P, et al. Structure of MERS-CoV spike receptor-binding domain complexed with human receptor DPP4. *Cell Res* (2013) 23(8):986–93. doi:10.1038/cr.2013.92
50. Lu L, Liu Q, Zhu Y, Chan K-H, Qin L, Li Y, et al. Structure-based discovery of Middle East respiratory syndrome coronavirus fusion inhibitor. *Nat Commun* (2014) 5:3067. doi:10.1038/ncomms4067
51. Kilic MA, Spiro S, Moore GR. Stability of a 24-meric homopolymer: comparative studies of assembly-defective mutants of *Rhodobacter capsulatus* bacterioferritin and the native protein. *Protein Sci* (2003) 12(8):1663–74. doi:10.1110/ps.0301903
52. Sanchez R, Sali A. Evaluation of comparative protein structure modeling by MODELLER-3. *Proteins* (1997) (Suppl 1):50–8. doi:10.1002/(SICI)1097-0134(1997)1+<50::AID-PROT8>3.0.CO;2-S
53. Worwood M. Ferritin. *Blood Rev* (1990) 4(4):259–69. doi:10.1016/0268-960X(90)90006-E
54. Sun W, Jiao C, Xiao Y, Wang L, Yu C, Liu J, et al. Salt-dependent aggregation and assembly of *E coli*-expressed ferritin. *Dose Response* (2016) 14(1):1559325816632102. doi:10.1177/1559325816632102
55. Theil EC. Ferritin protein nanocages use ion channels, catalytic sites, and nucleation channels to manage iron/oxygen chemistry. *Curr Opin Chem Biol* (2011) 15(2):304–11. doi:10.1016/j.cbpa.2011.01.004
56. Yiadom KPAB, Hammamieh R, Ukpabi N, Tsang P, Yang DCH. A peptide from the extension of Lys-tRNA synthetase binds to transfer RNA and DNA. *Peptides* (2003) 24(7):987–98. doi:10.1016/S0196-9781(03)00188-8
57. Santner AA, Croy CH, Vasanwala FH, Uversky VN, Van YY, Dunker AK. Sweeping away protein aggregation with entropic bristles: intrinsically disordered protein fusions enhance soluble expression. *Biochemistry* (2012) 51(37):7250–62. doi:10.1021/bi300653m
58. Oldfield CJ, Dunker AK. Intrinsically disordered proteins and intrinsically disordered protein regions. *Annu Rev Biochem* (2014) 83:553–84. doi:10.1146/annurev-biochem-072711-164947
59. Dyson HJ, Wright PE. Intrinsically unstructured proteins and their functions. *Nat Rev Mol cell biol* (2005) 6(3):197–208. doi:10.1038/nrm1589
60. Zhang N, Channappanavar R, Ma C, Wang L, Tang J, Garron T, et al. Identification of an ideal adjuvant for receptor-binding domain-based subunit vaccines against Middle East respiratory syndrome coronavirus. *Cell Mol Immunol* (2016) 13(2):180. doi:10.1038/cmi.2015.03
61. Yang W, Guo W, Chang J, Zhang B. Protein/peptide-templated biomimetic synthesis of inorganic nanoparticles for biomedical applications. *J Mater Chem B* (2017) 5(3):401–17. doi:10.1039/C6TB02308H
62. Kanekiyo M, Wei CJ, Yassine HM, McTamney PM, Boyington JC, Whittle JR, et al. Self-assembling influenza nanoparticle vaccines elicit broadly neutralizing H1N1 antibodies. *Nature* (2013) 499(7456):102–6. doi:10.1038/nature12202
63. Yang SW, Jang YH, Kwon SB, Lee YJ, Chae W, Byun YH, et al. Harnessing an RNA-mediated chaperone for the assembly of influenza hemagglutinin in an immunologically relevant conformation. *FASEB J* (2018) 32(5):2658–75. doi:10.1096/fj.201700747RR
64. Georgopoulos CP, Hendrix RW, Casjens SR, Kaiser AD. Host participation in bacteriophage lambda head assembly. *J Mol Biol* (1973) 76(1):45–60. doi:10.1016/0022-2836(73)90080-6
65. Sternberg N. Properties of a mutant of *Escherichia coli* defective in bacteriophage lambda head formation (groE). I. Initial characterization. *J Mol Biol* (1973) 76(1):1–23. doi:10.1016/0022-2836(73)90079-X
66. Liu C, Young AL, Starling-Windhof A, Bracher A, Saschenbrecker S, Rao BV, et al. Coupled chaperone action in folding and assembly of hexadecameric Rubisco. *Nature* (2010) 463(7278):197–202. doi:10.1038/nature08651
67. Date MS, Dominy BN. Modeling the influence of salt on the hydrophobic effect and protein fold stability. *Commun Comput Phys* (2015) 13(1):90–106. doi:10.4208/cicp.290711.121011s
68. Kanekiyo M, Bu W, Joyce MG, Meng G, Whittle JR, Baxa U, et al. Rational design of an Epstein-Barr virus vaccine targeting the receptor-binding site. *Cell* (2015) 162(5):1090–100. doi:10.1016/j.cell.2015.07.043

Conflict of Interest Statement: The authors declare that the research was conducted in the absence of any commercial or financial relationships that could be construed as a potential conflict of interest.

frontiers in Immunology

REVIEW
published: 04 October 2018
doi: 10.3389/fimmu.2018.02224

Nanoparticle Vaccines Against Infectious Diseases

Rashmirekha Pati[1], *Maxim Shevtsov*[2,3,4] *and Avinash Sonawane*[1,5]*

[1] School of Biotechnology, KIIT University, Bhubaneswar, India, [2] Institute of Cytology of the Russian Academy of Sciences (RAS), St. Petersburg, Russia, [3] Klinikum Rechts der Isar, Technical University of Munich, Munich, Germany, [4] First Pavlov State Medical University of St.Petersburg, St. Petersburg, Russia, [5] Discipline of Biosciences and Biomedical Engineering, Indian Institute of Technology Indore, Indore, India

Due to emergence of new variants of pathogenic micro-organisms the treatment and immunization of infectious diseases have become a great challenge in the past few years. In the context of vaccine development remarkable efforts have been made to develop new vaccines and also to improve the efficacy of existing vaccines against specific diseases. To date, some vaccines are developed from protein subunits or killed pathogens, whilst several vaccines are based on live-attenuated organisms, which carry the risk of regaining their pathogenicity under certain immunocompromised conditions. To avoid this, the development of risk-free effective vaccines in conjunction with adequate delivery systems are considered as an imperative need to obtain desired humoral and cell-mediated immunity against infectious diseases. In the last several years, the use of nanoparticle-based vaccines has received a great attention to improve vaccine efficacy, immunization strategies, and targeted delivery to achieve desired immune responses at the cellular level. To improve vaccine efficacy, these nanocarriers should protect the antigens from premature proteolytic degradation, facilitate antigen uptake and processing by antigen presenting cells, control release, and should be safe for human use. Nanocarriers composed of lipids, proteins, metals or polymers have already been used to attain some of these attributes. In this context, several physico-chemical properties of nanoparticles play an important role in the determination of vaccine efficacy. This review article focuses on the applications of nanocarrier-based vaccine formulations and the strategies used for the functionalization of nanoparticles to accomplish efficient delivery of vaccines in order to induce desired host immunity against infectious diseases.

Keywords: nanoparticles, vaccine development, human diseases, targeted vaccine delivery, antigens

OPEN ACCESS

Edited by:
Nahid Ali,
Indian Institute of Chemical Biology, India

Reviewed by:
Randy A. Albrecht,
Icahn School of Medicine at Mount Sinai, United States
Michael Schotsaert,
Icahn School of Medicine at Mount Sinai, United States
Katie Louise Flanagan,
RMIT University, Australia

***Correspondence:**
Avinash Sonawane
asonawane@iiti.ac.in

Specialty section:
This article was submitted to Vaccines and Molecular Therapeutics, a section of the journal Frontiers in Immunology

Received: *13 April 2018*
Accepted: *07 September 2018*
Published: *04 October 2018*

Citation:
Pati R, Shevtsov M and Sonawane A (2018) Nanoparticle Vaccines Against Infectious Diseases. Front. Immunol. 9:2224. doi: 10.3389/fimmu.2018.02224

INTRODUCTION

In twenty-first Century, infectious diseases have emerged as a serious threat to the health of millions of people across the globe (1). According to the World Health Organization (WHO) report for 2016, ∼3.2 million deaths have occurred due to lower respiratory infections and 1.4 million from tuberculosis alone worldwide (2). Over the past few decades, many new infectious diseases have emerged and few old diseases re-emerged, which were once considered to be no longer a threat to the human being (3–5). Collectively, these diseases account for millions of deaths that cause enormous impact on the global socio-economical and health-care sectors. The major challenges to combat such diseases are that for many of them, there are no effective drugs available.

One of the plausible approaches could be based on the application of nanocarrier based vaccination (6). However, there are still no effective vaccines available against some of the most prevalent diseases including immune deficiency syndrome (AIDS) and tuberculosis. This underlines an urgent need for the development of desired vaccines against these diseases. Some of the important aspects of any optimal vaccine includes (i) safety, (ii) stability, and (iii) the ability to elicit durable and adequate immune response with a minimum number of doses (7–9). Presently, different generation vaccines such as attenuated or killed whole organisms (*first generation*), subunit (*second generation*) and RNA or DNA vaccines (*third generation*) are used to elicit protective immunity against diseases (10–12). Despite several advantages of RNA or DNA vaccines such as minimal risk of infection, ability to elicit immune response against specific pathogen and cost effective (13); there are a number of challenges associated with the efficient delivery of these vaccine molecules to the target sites and the requirement of the prime-boost vaccination regimens with other immunogenic agents. These includes premature degradation of molecules and the inability to translate into a functional immunogen (14). Similarly, protein based vaccines are used successfully against several infectious diseases such as *Haemophilus influenza* type b, diphtheria, tetanus, acellular pertusis, meningococcus and pneumococcus (15), however they require an adjuvant to potentiate their immunogenicity, and also encounter early degradation after exposure to hostile milieu. Introduced recombinant protein-based vaccines (e.g., recombinant hemagglutinin vaccine for influenza) further enhance the immunity toward infection indicating the applicability of the recombinant technology for the vaccine production (16). To overcome these hurdles, an efficient vaccine delivery system is required which not only delivers the vaccine molecules to the target site to evoke enduring immune responses but also has minimal side effects and requires less doses. Moreover, there is an increasing need to develop new generation composite vaccine molecules that will act as immunogen as well as an adjuvant. Nanotechnology based formulations offer numerous advantages for the development of new generation vaccines. Nanocarrier based delivery system can protect the vaccines from premature degradation, improve stability, has good adjuvant properties, and also assists in targeted delivery of an immunogen to the antigen presenting cells (APCs). There are several mechanisms by which vaccines can be delivered to the specific sites using nanocarriers. Vaccine antigens can be encapsulated within the nanocarriers or decorated on their surface (**Figure 1**). Encapsulation within the nanoparticles (NPs) can protect the antigen from premature protease degradation and elicit sustainable release, whereas the surface adsorption facilitates their interaction with cognate surface receptors such as toll like receptors (TLRs) of APCs (17). Nanocarrier based delivery systems provide a suitable route of administration of vaccine molecules and enhance cellular uptake thereby resulting in robust innate, humoral, cellular as well as mucosal immune responses when compared with unconjugated antigens. This review mainly focuses on the potential use of nano delivery systems as novel vaccine strategies for the induction of innate as well as adaptive immune responses against infectious diseases.

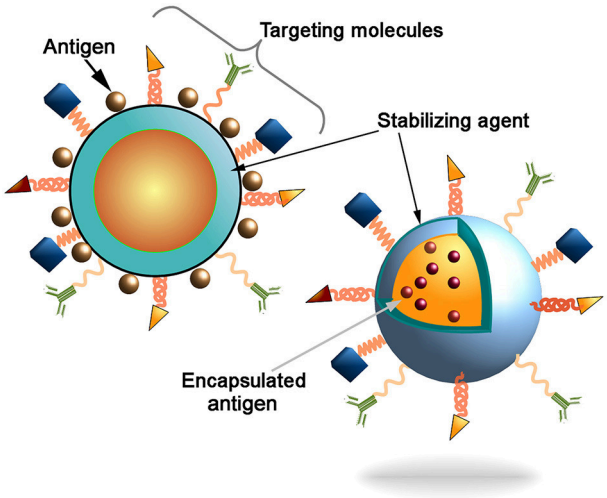

FIGURE 1 | Schematic representation of the nanocarriers. Antigen can be conjugated to the nanoparticles surface or incapsulated into core of the particles. Decoration of the nanoparticles surface with targeting molecules (e.g., antibodies, Fab-fragments, peptides, etc) could further increase the delivery of particles into the antigen presenting cells (APCs) to induce innate and adaptive immune responses.

KEY CELLULAR COMPONENTS OF THE IMMUNE SYSTEM

The immune system is composed of a collection of mobile cells that traffic throughout the body as well as reside at the site of entry (i.e., skin, respiratory, gastrointestinal, and genital tracts) in search of invading pathogens. These cells belong to two major types of innate and adaptive immune system. The innate immune cells like macrophages and neutrophils rapidly respond to the pathogens by recognizing pathogen surface moieties, phagocytosis, and the elimination of pathogens through activation of different antibacterial effector functions. Similarly, two major components of the adaptive immunity i.e., T and B-cells are important for the generation of cell mediated and humoral immune responses, respectively. T cells including $CD4^+$ helper T cells secrete different cytokines to modulate the functions of B cells, whereas $CD8^+$ T cells recognize and destroy virally infected cells. Antibodies produced by the B cells can further neutralize the invading microbes or clear infected cell or opsonized pathogens through cell-mediated systems. APCs, in particular dendritic cells (DCs) and macrophages, migrate through the body to sample, process and present the antigens to T-cells to activate cellular immune responses. These cells express various surface receptors to recognize cognate ligands and danger signals to trigger activation of different signaling pathways that eventually lead to the activation of T-cells (18). After sampling the antigens, DCs migrate from the peripheral tissues into the draining lymph nodes to activate naive T-cells (19), whereas macrophages after ingestion of antigens increase their lysosomal degradative machinery to enhance the antigen presentation to activate helper T cells.

TYPES OF NANO-IMMUNO ACTIVATORS

Some NPs are themselves able to stimulate different immune cells to boost the host immunity. The size, shape and surface chemistry of NPs (described below in more detail) are important factors that determine their potential to activate immune responses. In general, NPs are able to stimulate immune reactions by increasing the synthesis of defense genes and inflammatory reactions (20). Various types of NPs like gold, carbon, dendrimers, polymers and liposomes have the capability to induce cytokine and antibody responses (21–26). This was observed in the case of administration of empty PEGylated liposomes, which were able to elicit IgM response in an *in-vivo* model. (27, 28). Besides their potential to deliver various immune stimulators to the specific sites as well as into the deep tissues where vaccine molecules alone may not able to reach, these NPs have also been exploited as adjuvants to augment immunogenicity of vaccine candidates. Nano-immuno stimulators are the nano scale (20–100 nm) vaccine particles that can improve the vaccine efficacy *in vivo* better than bulk molecules (20, 29). Some of the known nano-immuno stimulators that have been used for this specific purpose are inorganic NPs (iron and silica) (30, 31), polymeric NPs (chitosan, PLGA, PVPONAlk, γ-PGA) (32–37), liposomes (cholesterol and lipids) (33, 38) and virus like particles (VLPs) (39, 40). Different types of NPs used to deliver antigens to give protection against different diseases have been listed in **Table 1**.

Inorganic NPs

Some biocompatible inorganic NPs such as gold, carbon and silica have been exploited in the vaccine delivery studies (50, 79–81). These NPs can be synthesized in various shapes, size and surface modified forms. Some of the viral antigens were successfully delivered using inorganic NPs as carriers. This caused increase in antigen stability by protecting them from premature degradation by proteolytic enzymes. Delivery of viral and bacterial antigens using gold NPs was also found to induce quite robust host immune responses against influenza, immunodeficiency virus, foot and mouth, and tuberculosis diseases in mice (51, 52, 82, 83). Encapsulation of plasmid DNA that encode mycobacterial hsp65 antigen in gold NPs exhibited significant reduction in the *Mycobacterium tuberculosis,* causative agent of human tuberculosis, burden in infected mice (52, 82). Few studies have used hollow mesosporous silica, nanotube and spherical forms of carbon NPs as adjuvants to improve the immunogenicity and delivery of protein and peptide antigens against viral infections (79, 83, 84). Silica based NPs contain abundant silanol groups that can be utilized to introduce specific functional groups on their surface to gain access for vaccine molecules into target cells (84–86). The major advantages of inorganic NPs include low production cost, reproducibility and safety in application.

Polymeric NPs

In recent years, polymeric NPs have received great attention for their applications in the delivery of a number of vaccines. This is primarily due to their ease in preparation, biodegradability, biocompatibility, reduced cytotoxicity, and the possibility to fine-tune surface properties as needed (87). Moreover, it is relatively easy to control the rate of vaccine release by altering the composition or ratio of co-polymers during the NP synthesis process (87). The most commonly used polymeric NPs for vaccine delivery are poly (lactic-*co*-glycolic acid; PLGA) or poly (lactic acid; PLA). PLGA NPs have already been tried in the delivery of a broad range of antigens, including hydrophobic antigens (34, 35), hepatitis-B virus antigens (54), *Bacillus anthracis* (41), tetanus toxoid (35), and ovalbumin (88). The use of PLGA conjugated antigens exhibited strong immuno-stimulatory property by inducing cytokine and nitric oxide production against mycobacteria infection (89). In addition to synthetic polymers, some natural biopolymers such as alginate, pullans, inulins, and chitosan have been used as adjuvants (90–93). Inulin, a known activator of the complement cascade (94), conferred better protection against hepatitis B and influenza viruses (92, 93). Similarly, chitosan NPs were demonstrated as nanocarrier molecules for HBV antigens (55), DNA vaccine (56), and Newcastle disease vaccine (42). The delivery of PLGA and chitosan NP conjugated vaccine molecules enhanced the immune responses at the mucosal site (95, 96). Our recent study also showed that delivery of *M. tuberculosis* lipids using biocompatible chitosan NPs was able to induce significant humoral as well as cellular immune responses when compared to lipids alone in mice (43). We also found that intraperitoneal administration of these conjugates showed better activation of splenic T-cells. Another study by de Titta et al. has shown that intradermal administration of CpG conjugated polymeric NPs increased dendritic cell activation by several fold, exhibited comparable vaccine efficacy at ∼400 times lower dose, and also caused enduring cellular immunity in comparison to free CpG (97). These desired properties along with already known reduced toxicity and biocompatibility under both *in vitro* and *in vivo* conditions make polymeric NPs plausible candidates for further preclinical pharmacokinetics and therapeutic applications (98).

Liposomes

In addition to polymeric NPs, liposomes are the second most widely explored vaccine and drug delivery vehicle in the nanomedicine field. The synthesis of liposomes is a spontaneous process, where hydration of lipids enables the lipid bilayer formation around an aqueous core (99). So far, different types of liposomes, including unilamellar or multilamellar vesicles composed of biodegradable phospholipids (e.g., phosphatidylserine, phosphatidylcholin and cholesterol) were included in the vaccine studies (100). Liposomes deliver vaccines by fusion with the target cell membrane (101).The structurally flexible and versatile liposomes are able to encapsulate both hydrophilic and hydrophobic substances. The hydrophilic molecules can be incorporated into the aqueous core, while hydrophobic molecules are encased within the phospholipid bilayer. Earlier reports have shown that delivery of antigenic proteins entrapped in multilamellar lipid vesicles elicit strong T and B-cell responses (102). Similarly antigenic peptides conjugated to phosphatidylserine (PS)-liposomes were readily

TABLE 1 | List of antigens delivered by using different nanocarriers for the treatment of different diseases.

Antigen	Nanocarrier used	Disease	References
AGAINST BACTERIAL INFECTION			
Antigenic protein	Poly(D,L-lactic-co-glycolic acid) nanospheres	Anthrax	(41)
DNA encoding T cell epitopes of Esat-6 and FL	Chitosan Nanoparticle	Tuberculosis	(42)
Mycobacterium lipids	Chitosan Nanoparticle	Tuberculosis	(43)
Polysaccharides	Liposomes	Pneumonia	(44)
Bacterial toxic and parasitic protein	Liposomes	Cholera and Malaria	(45)
Fusion protein	Liposomes	*Helicobacter pylori* infection	(46)
Antigenic protein	Nanoemulsion	Cystic fibrosis	(47)
Antigenic protein	Nanoemulsion	Anthrax	(48)
Mycobacterium fusion protein	Liposome	Tuberculosis	(49)
AGAINST VIRAL INFECTION			
Antigenic protein	Chitosan Nanoparticles	Hepatitis B	(33)
Viral protein	Gold Nanoparticles	Foot and mouth disease	(50)
Membrane protein	Gold Nanoparticles	Influenza	(51)
Viral plasmid DNA	Gold Nanoparticles	HIV	(52)
Tetanus toxoid	Poly(D,L-lactic-co-glycolic acid) nanospheres	Tetanus	(53)
Hepatitis B surface antigen	Poly(D,L-lactic-co-glycolic acid) nanospheres	Hepatitis B	(54)
Hepatitis B surface antigen	Alginate coated chitosan Nanoparticle	Hepatitis B	(55)
Live virus vaccine	Chitosan Nanoparticles	Newcastle disease	(56)
Capsid protein	VLPs	Norwalk virus infection	(57)
Capsid protein	VLPs	Norwalk virus infection	(58)
Influenza virus structural protein	VLPs	Influenza	(59–64)
Nucleocapsid protein	VLPs	Hepatitis	(65)
Fusion protein	VLPs	Human papilloma virus	(39, 40, 66–68)
Multiple proteins	VLPs	Rotavirus	(69, 70)
Virus proteins	VLPs	Blue tongue virus	(71)
Enveloped single protein	VLPs	HIV	(72–75)
Viral protein	Polypeptide Nanoparticles	Corona virus for Severe acute respiratory syndrome (SARS)	(76)
AGAINST PARASITIC INFECTION			
Merozoite surface protein	Iron oxide Nanoparticles	Malaria	(30)
Epitope of *Plasmodium berghei* circumsporozoite protein.	Polypeptide Nanoparticles	Rhodent mamarial parasitic infection	(77)
Surface protein from *Eimeria falciformis* sporozoites	ISCOMs	Diarrhea	(78)

internalized by APCs to potentiate T-helper cell mediated immune responses (103) and delivery of heat shock protein encoding vaccine DNA using liposomes elicited strong protective immunity against fungal infection (104). Because of their foreseen applications, several liposome based vaccine nano-formulations have been approved for clinical trials against intracellular pathogens, including viruses and *M. tuberculosis* (105). One such study already demonstrated the potency of liposomal aerosol carriers in the generation of protective immunity against *M. tuberculosis* infection (106, 107). Other studies have tried a combination of dimethyl dioctadecyl ammonium (DDA) lipid based liposomes and various immunomodulators to enhance immunity against influenza, chlamydia, erythrocytic-stage malaria, and tuberculosis infections (108–112). In the context of DNA vaccines, lipid-DNA complexes have been successfully delivered to the lungs of monkeys (101).

VLPs (Virus Like Particles)

There are several reports that adequately proved applications of VLPs as a vaccine carrier, and also their ability to stimulate the host immune responses (113–115). VLPs are composed of self-assembled viral membrane that forms a monomeric complex displaying a high density of epitopes (115, 116). Interestingly, VLPs can also be engineered to express additional proteins either by fusion of proteins with the particles or by endogenous expression of multiple antigens (113, 117). It is also possible to chemically couple non-protein antigens and small organic molecules onto the viral surface to produce bioconjugates with VLPs (118, 119). Due to these distinct features, VLPs can provide protection not only against virus, but also against heterologous antigens (116). A specific immune response was successfully generated after the delivery of an antigen using virus capsid protein SV40 in mammalian cells (120). VLPs were also found to increase the immunogenicity of weak antigens. For example

Salmonella typhi membrane antigen, influenza A M2 protein and H1V1 Nef gonadotropin releasing hormone (GnRH) assembled VLPs produced strong antigen specific humoral as well as cellular immune responses (121, 122). It is presumed that the use of VLP based nanoformulations could enable the antigens to achieve conformations resembling to native antigen structure, thus it may result in better stimulation of the host immune response (122).

Dendrimers

Dendrimers are three dimensional, mono-dispersed and hyperbranched nano structures that are made up of a mixture of amines and amides. Few studies have explored the application of dendrimers in the delivery of different antigenic molecules. The most commonly used dendrimers for vaccine delivery are polypropyleneimine (PPI) and polyamido amine (PAMAM) dendrimers. A single dose of dendrimer encapsulated multiple antigens was found to produce strong antibody and T-cell responses against Ebola virus, H1N1 influenza, and *Toxoplasma gondii* (123). This generation of robust immune response was found to be due to efficient uptake of dendrimers by the host cells. Similarly a significant increase in the vaccine efficacy of HIV transactivator of transcription (TAT) based DNA vaccine was observed due to enhanced cellular uptake of PMAM dendrimer (124). Hence, the possibility to tailor the dendrimers to attain certain biological and physico-chemical properties, and also the feasibility to conjugate several ligands to the single molecule have made dendrimers promising candidates for the development of new generation vaccines with enhanced immunogenic properties.

DELIVERY OF IMMUNE STIMULATORS USING NANOCARRIERS

Cytokines

Cytokines are known as important signaling molecules secreted by different cells in response to external stimuli. Some of the cytokines are able to activate immune cells to generate protective immunity against several diseases. However, cytokines are mostly susceptible to early degradation that subdue their participation in the generation of host immunity. Moreover, uncontrolled release of cytokines as immune responders may sometimes lead to harmful side effects (125). To overcome these limitations, several studies have attempted to synthesize engineered nanocarriers to achieve effective and controlled delivery of cytokines to the target sites. This approach was found to reduce their toxicity, improve circulation time and antigen specific T-cell responses in comparison to free cytokines (126, 127). Incorporation of granulocyte macrophage colony stimulating factor (GM-CSF) and interferon alpha (IFN-α) into nano-carriers exhibited great application in cancer therapy (128, 129). Nano-carrier conjugated cytokines also showed great potential in the treatment of infectious diseases. For example, IL-12 encapsulated microspheres induced strong protective immunity against tuberculosis (130). This effect was due to production of high antibody titers as a result of sustained and controlled release of IL-12 from the microspheres in immunized mice (130).

Toll Like Receptor Agonists

Like cytokines, several toll-like receptor (TLR) agonists were also explored as immune activators to augment immune surveillance mechanisms. Different immune effector cells such as macrophages, B-cells and DCs express different types of TLRs, which are known to interact with specific pathogen associated molecular patterns (PAMPs). These specific interactions eventually initiate downstream signaling cascades to ensure the elimination or generation of immunity against pathogens (131, 132). Conjugation of TLR specific agonists on nanocarriers helps to target the molecules to specific immune cells and therefore reduce the possibility of systemic biodistribution. One such study has shown that conjugation of TLR-7/8 agonist on nano polymers caused efficient internalization by APCs and also prolonged the T cell responses (133). Administration of NPs loaded with vaccine peptide antigen and TLR-7 and 9 ligands were also found to induce strong memory and effector $CD8^+$ T-cell response (134). Another study has shown that conjugation of TLR-8 agonist to a polymer nanocarrier increased activation and maturation of naive DCs due to selective endocytosis and prolonged release of an immunogen by the nanocarrier inside DCs (135). Moreover, intradermal injection of CpG and antigen encapsulated polymeric NPs were rapidly drained into the lymph nodes to activate DCs (97). These studies indicate that NPs can be used as a tool to appropriately target presentation of antigens to T and B-cell rich lymphoid organs.

Nucleic Acids

The genetic molecules such as DNA, plasmids and RNA can also act as immuno-stimulants. Due to these characteristics, in addition to less risk to cause disease particularly in immunocompromised individuals, these genetic materials are considered as promising candidates for the development of next generation vaccines. After administration, the plasmid vector translocates to the nucleus to initiate transcription of recombinant genes using the host cellular machinery. A recombinant DNA segment encoding HspX-PPE44-esxV fusion antigen of *M. tuberculosis* showed great potential as a new tuberculosis DNA vaccine candidate (136). A similar type of study has been conducted in the past where the vaccination of DNA or RNA constructs expressing mycobacterium antigens were capable of inducing humoral as well as cellular immune responses (137). Likewise, plasmids harboring genes encoding for viral antigen have been encapsulated into alginate nanocarriers and targeted against viral infections (138).

IMPORTANCE OF PHYSICOCHEMICAL PROPERTIES IN DESIGNING NANO-IMMUNO FORMULATIONS

In order to improve their delivery and vaccine characteristics, different approaches have been practiced to conjugate vaccine molecules to different nanocarriers. Vaccine molecules can be surface conjugated, encapsulated or surface adsorbed with the nanocarriers. Antigen adsorption on the nanocarrier is simply based on the presence of a charge or hydrophobic interactions

between NPs and the candidate molecule (139, 140). This type of interaction is usually non-covalent, which may lead to rapid dissociation of antigens from nanocarriers depending upon the external milieu such as pH, ionic strength, temperature, and the antigen hydrophobicity. On the other hand, encapsulation and chemical conjugation of antigen to nanocarriers is more stable due to strong interactions and chemical bond formation between the target molecule and the nanocarrier. Further, antigens can also be encapsulated into nanocarriers by simple mixing reaction during the synthesis. In this case, the antigens are released only after partial or complete dissociation of the nanocarrier (141). These processes have already been used with silica and gold NPs (142). Similarly, chitosan and dextran sulfate NPs were used for the preparation of cationic and anionic antigenic formulations. Some viral antigens are known to bind to both positive as well as negative charged NPs through immobilization process and hydrogen bonds (143). The immobilization process depends on the charge, pH, ratio of NPs and antigens, and the protein partition coefficient between the solution and the colloid (143). Several antigens were successfully delivered to the target sites by chemical conjugation, adsorption and encapsulation to soft nanocarriers like VLPs, liposomes and immune stimulating complexes (ISCOM) (144–147). ISCOMs are a class of adjuvant formulations that consist of saponins, cholesterol and phospholipids in specific ratios. Antigens can be formulated into ISCOMs directly (148) or after the surface modification (149, 150). Since ISCOM particles are negatively charged, direct conjugation of most of the soluble proteins is a limiting factor. Nanocarriers can augment immunogenicity of a molecule. For example, influenza antigen H1N1 conjugated chitosan NPs and *Yersinia pestis* F1-antigen coated gold NPs (AuNPs) produced higher levels of antibody and cytokine responses in comparison to mice administered with unconjugated antigens (151).This was found to be due to stabilization and increased immunogenicity of vaccine antigens due to conjugation with NPs.

Another important aspect in the development of nano-immuno formulations is that they improve antigen delivery and presentation (152). In this context, NP shape, size and surface charge are key factors that affect NP circulation, biodistribution, bioavailability and specificity by crossing biological barriers. Besides these factors, particle geometry such as surface to volume ratio plays an important role in the determination of immunogen release and degradation kinetics (153, 154). Here, the importance of different physicochemical parameters such as size, shape, surface area, porosity, hydrophobicity, hydrophilicity and crystallinity in the interaction between NPs and the target cell is discussed.

Size

The size of NPs determines the mode of cellular uptake and specificity (155, 156). PLGA NPs of large size (1, 7 and 17 μm) showed reduced internalization rate in comparison to smaller NPs (300 nm) (157). The size of NPs also determines the cellular specificity and migration. Smaller NPs (20–200 nm) were readily endocytosed by the resident DCs, whereas larger size (500–2,000 nm) NPs were effectively taken up by the migratory DCs (158). NPs of less than 200 nm size were drained into the lymph nodes (159), while particles up to 20 nm range were suitably transported to the APCs (152, 160). Notably, NP curvature also affects the cellular interaction and phagocytosis rate (161). NPs of 150 nm diameter and 450 nm height showed more cellular uptake as compared to the particles having 1,200 × 200 nm size. Of note the size of NPs was also found to influence the activation of signaling pathways. A study has demonstrated that smaller NPs are able to alter the cell signaling processes more efficaciously than the large NPs (31).

Surface Charge

Vaccine loaded NPs can also be targeted to specific sites by modifying the NP surface charge. Delivery of such NPs at appropriate sites elicit strong immune responses against antigens. NP surface charge is responsible for the interaction with congnate surface molecules present on the target cells. This was exemplified from the observation that cationic polysterene NPs were efficiently internalized by the APCs in comparison to neutral surface charged NPs. This may be due to electrostatic interactions between the cationic NPs with anionic cell membranes (162, 163). Interestingly, pulmonary instillation of cationic and anionic NPs showed similar endocytosis rate in macrophages and draining lymph nodes, however cationic formulations showed more expression of *Ccl2* and *Cxc10* chemokines that caused more recruitment and maturation of CD11b DCs in comparison to anionic NPs in the lung (125, 156). Similarly, neutral silica-silane shell polymer NPs were less effective in the activation of innate immune cells (128). These studies clearly indicate appropriate surface modifications of NPs may help to generate stronger immunological responses against specific infection.

Shape

Beside size and surface charge, NP shape is also a critical determinant in the cellular interaction, intracellular trafficking and the rate of antigen release inside the host cells (79, 141). Spherical gold NPs were actively internalized by bone marrow derived dendritic cells in comparison to rod shaped particles of similar dimensions (33, 34), and that spherical NPs were able to induce strong immune response than cube or rod shaped NPs (164). Another study reported that worm-like particles were impaired in phagocytosis as compared to spherical NPs (151). These distinctions were ascribed to the differences in contact area between NPs and the target cell membrane. The shape of NPs also determines the localization of NPs inside the host cells. This was demonstrated by the fact that although nano rods and nano sheets were internalized via clathrin mediated endocytosis, nano rods were particularly delivered to the nucleus while nano-sheet were retained in the cytoplasm (146, 147, 155). This is an important aspect in the context of improving antigen processing and presentation to T-cells. It is well established that enhanced antigen processing and presentation can be achieved if the candidate molecules are delivered to the lysosomal compartment of the cells.

Hydrophobicity

Hydrophobicity of NPs plays a significant role in the interaction with soluble proteins and immune cells through recognition of hydrophobic moieties (165). Previous studies have shown that

hydrophobic polymeric NPs are strong inducers of cytokines and co-stimulatory molecules than hydrophilic polymeric NPs (53, 105, 166). Exposure to hydrophobic NPs showed enhanced activation of DCs by inducing the expression of CD86 co-stimulatory molecules when compared with hydrophilic ones. Similar observations were reported in other innate immune cells, in which hydrophobic NPs were able to activate these cells by up-regulating the expression of proinflammatory cytokine encoding genes (102), and also facilitated opsonization process by increasing the adsorption of immunoglobulins on the cell surfaces (103). However, other studies have reported that polyethylene glycol coating (PEGylation) reduced the interaction of NPs with immune receptors (50, 80). This property is considered useful in the prevention of non-specific adsorption of proteins on NPs and thereby prevent their up-take by APCs (50). Such non-specific adsorption of proteins and their uptake by phagocytic cells can also be preventing by the incorporation of an alkyl linker between the PEG and thiol moieties on NPs (80).

Surface Modification

Surface modification of NPs alters ligand specificity and interaction with APCs (160). Conjugation of CD47 molecules on the surface of NPs modulated the down-stream signaling cascades and also reduced NP internalization by phagocytic cells (131). Functionalization of NPs with TLR-7, TLR-8, and TLR-9 agonists increased cytokine production and the expression of immunoregulatory genes (132–134). Similarly, conjugation of poly (methyl vinyl ether-co-maleic anhydride; PVMA), TLR2, and TLR4 agonists, and galactose polymer to NPs were shown to activate the complement pathway as a result of stable binding to C3b complement factor (139, 142). Further, lipoprotein-like NPs showed LPS scavenging activity, thereby resulting in the inhibition of TLR-4 dependent inflammatory responses (140). Overall, these studies strongly demonstrated that tuning of physico-chemical properties of NPs could be used as a fundamental tool to target vaccine molecules to specific sites to induce desired immune responses.

IMPLICATIONS OF THE NANOCARRIERS IN THE VACCINE DEVELOPMENT

Emerging studies have proved that nanocarriers can be useful mediators in the development of vaccines against various diseases. In this context, it is important to develop NP formulations that can deliver immunogens to APCs especially DCs to induce effective antigen-specific T-cell responses (**Figure 2**). Several nanocarriers have been shown to specifically activate DCs to effectuate anti-tumor or anti-viral immune responses (167–170). Zhu et al. proposed that nano-TiO_2 and Fe_3O_4-TiO_2 particles could function as a useful vector to promote vaccine delivery in immune cells (168). Co-incubation of nano-TiO_2 and Fe_3O_4-TiO_2 with DCs resulted in an increased production of TNF-α, and also upregulated the expression of CD80, CD86 and MHC class II molecules through the NF-κB signaling pathway (163). In this way, immunization efficacy of various NP formulations such as erythrocyte membrane-enveloped poly(D,L-lactide-co-glycolide) (PLGA) NPs for antigenic peptide (hgp10025-33) and TLR-4 agonist, VLPs expressing RSV glycoproteins, chitosan-coated EphrinA1-PE38/GM-CSF, and several others have been improved (171–177). NPs can also control cell polarization and differentiation. Branched polyethylenimine-superparamagnetic iron oxide NPs (bPEI-SPIONs) promoted Th1 polarization of DCs (178). Another study by Sehgal et al. showed that NPs can also be used to target subsets of particular immune cells. They have shown that simultaneous targeting of DC subsets (i.e., DC-SIGN+ and BDCA3+DC) by NPs synergistically stimulated the activation of T cell-mediated immunity when compared with targeting of each DC subset separately (170).

Preclinical studies by different research groups have successfully demonstrated the efficacy of NP based vaccines in the induction of specific immune responses against tuberculosis (42, 179–182). Feng et al. developed a NP-based recombinant DNA vaccine that consists of Esat-6 and fms-like tyrosine kinase 3 ligand enveloped with chitosan NPs (42). Intramuscular prime vaccination followed by nasal boost of this recombinant DNA vaccine remarkably enhanced T cell responses in *Mycobacterium tuberculosis* challenged mice (42). Another study has shown that pulmonary administration of *M. tuberculosis* Ag85B antigen and CpG adjuvant conjugated polypropylene sulfide NPs (NP-Ag85B) induced *M. tuberculosis* specific polyfunctional Th1 responses and also reduced the lung bacterial burden (183).

TARGETED DELIVERY OF NANOPARTICLES CAN ACTIVATE INNATE AND ADAPTIVE IMMUNE RESPONSES

Innate Immunity

Macrophages and monocytes are highly heterologous cells that are distributed throughout the body. Macrophages process and present the antigens to elicit adaptive immune response. Due to their intrinsic phagocytic nature, macrophages can be easily targeted by surface engineered NPs, in which cognate ligands agonist to macrophage receptors can be conjugated on the NP surface (**Figure 1**). As discussed above several physico-chemical parameters of NPs such as size, surface charge, hydrophobicity, surface topography, and material composition can be optimized to facilitate the interactions between NPs and macrophage receptors (184–186). The rate of NP endocytosis also depends upon the type of cell surface receptors and the ligand conjugated to the NP surface. For example, NPs targeted via mannose and Fc receptors were rapidly internalized as compared to scavenger receptors (187). Endocytosis of IgG and anti-F4/80 antibody coated NPs showed more uptake rate and retention time inside the macrophages without affecting the cell viability (188, 189). Also, positively charged NPs interact more strongly with negatively charged phospholipid components of the cell membrane (190). Hyperactivation of some inflammatory cells can also be restricted through controlled release of stimulants using NPs. Upon activation, neutrophils can secrete variety of cytokines and hydrolytic enzymes in response to infection (191). Prolonged neutrophil activation often leads to acute inflammation and tissue damage at the localized site. Therefore, controlled release of molecules is

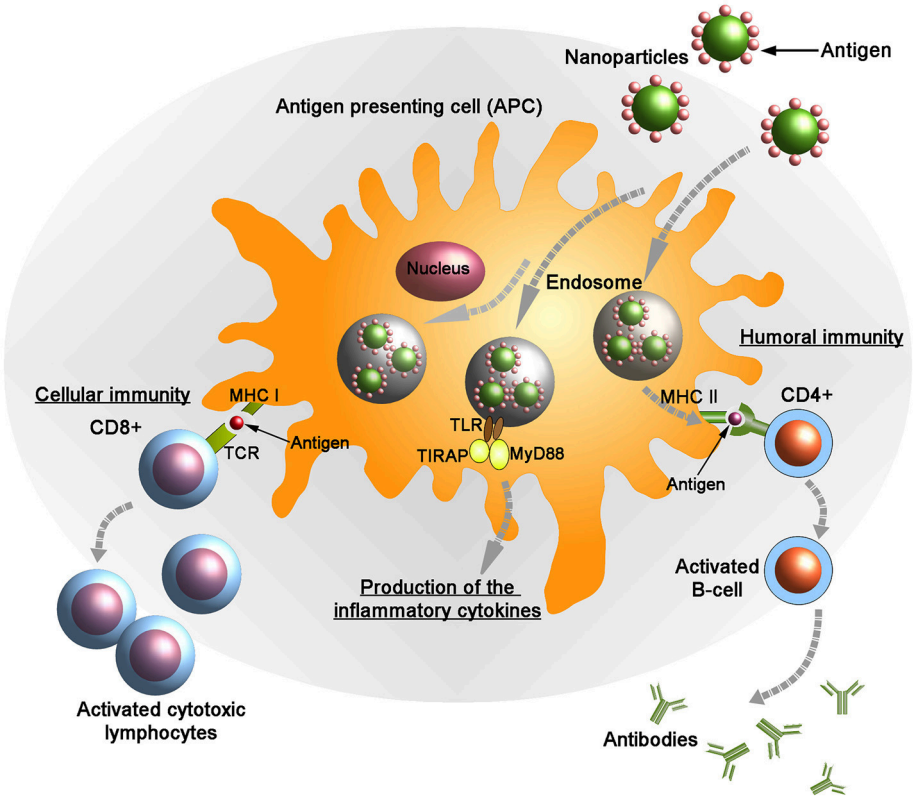

FIGURE 2 | Targeted delivery of antigenic molecules using surface engineered nanoparticles into the antigen presenting cells (APCs). Endogenously generated antigens are presented in complex with class I major histocompatibility complex (MHC I) on the membrane of APCs to CD8+ T lymphocytes. Following the interaction between MHC I and T-cell receptor (TCR) in presence of co-stimulatory molecules and cytokines the activated CD8+ cells kill the infected cells by inducing cytotoxicity. Also the antigens are presented on the APC surface by class II MHC molecules to the helper (CD4+) T cells. Subsequently, CD4+ cells activate B-cells that produce anti-microbial antibodies. Upon stimulation the adaptor proteins MyD88 (myeloid differentiation marker 88) and TIRAP (TIR domain containing adaptor protein) colocalize with TLR (toll-like receptor) allowing for activation of the NF-κB pathway and leading to the production of pro-inflammatory cytokines.

necessary to prevent the hyperactivation and massive recruitment of neutrophils. It has been reported that bovine serum albumin (BSA) NPs were able to modulate the functions of neutrophils following their internalization. Intravenous injection of anti-inflammatory peptide encapsulated polymeric NPs reduced neutrophil recruitment and subsequently hyperinflammation to prevent further tissue damage (192). The use of NPs to deliver vaccine/drugs in a controlled fashion is now considered as an attractive approach to develop therapeutic strategies against a range of acute and chronic inflammatory diseases (193).

Adpative Immunity

T and B-cells of the adaptive immune system express a repertoire of receptors to recognize a range of antigens. Activation or suppression of T-cell immunity can determine the fate of a disease. A number of NP based therapeutic strategies have been developed to regulate T-cell activity against viral, bacterial, or fungal infections. For example, antiviral siRNA or retroviral drug encapsulated lipid NPs or dendrimers were effectively delivered to $CD4^+$ T-cells to block HIV replication. This caused a significant reduction in HIV titer when compared with the use of non-encapsulated retroviral drugs (191, 194). T-cell activation also depends up on the type and size of NP used for the delivery of antigen. Liposome encapsulated antigens were better presented to $CD4^+$ T cells by APCs (195, 196) and delivery of 200 nm ova conjugated NPs increased MHC class I and II expression and also produced a higher percentage of antigen specific $CD4^+$T cells as compared to 30 nm ova conjugated particles (197).

B cells are able to recognize and respond to the microbial surface antigens through B-cell receptors (198). Activation and clonal expansion of antigen specific B-cells using engineered NPs have been exploited for the development of vaccines against different diseases (**Figure 2**). Encapsulation of antigen in virus like particles (VLPs) was able to induce strong and durable humoral responses when compared with the administration of exposed vaccine molecules (199). The potency of immune responses also depends upon the mode of antigen presentation to the target cells. Surface conjugated immunogenic proteins and peptides were able to activate B cells much stronger than encapsulated antigens (200). A single dose of PLGA NPs with surface displayed ovalbumin (OVA) elicited strong antibody responses *in vivo* as compared to free OVA (201, 202). NPs can also be used to activate specific immune responses. A study has shown that peptide conjugated carbon nanotubes

showed significant antigen specific IgG response in comparison to peptide or adjuvant alone (83).

NANOPARTICLES CAN BE USED TO INCREASE CROSS ANTIGEN PRESENTATION

In general, antigens captured by APCs from the extracellular environment are targeted to the endo-lysosomal compartments, where they are first processed into peptides and then loaded onto class II MHC molecules before presentation to $CD4^+$ helper T cells. However, cytosolic antigens are loaded on MHC class I molecules and presented to $CD8^+$ T-cells, which are crucial for the clearance of viral and intracellular infections (203). It is reported that some fraction of antigens delivered through NPs are trafficked to cytosolic vacuoles of APCs and presented by MHC class I molecules (203–205). The NP mediated cross antigen presentation was first demonstrated in antigens conjugated to iron oxide polymer NPs (206–209). In addition, inorganic and polymeric NPs have also been used for antigen delivery to cytosol (210–212). In this context, lipid NPs were shown to induce $CD8^+$ T cell expansion by efficient antigen cross presentation against viral infection in *in-vivo* models (102, 213). Similarly, invariant natural killer T cells (iNKT), which are a special subset of T-cells, recognize lipid antigens presented by CD1d cells. PLGA NPs conjugated with α-galactosylceramide glycolipid, an iNKT cell stimulant, increased cytokine release as well as expansion of antigen specific CD8+ T cells (214). The cross antigen presentation also depends upon the particle-antigen linkages. It has been shown that disulfide bonding between NP and antigens caused release of antigens into the endosomal compartment and also enhanced $CD8^+$ T cell formation as compared to non-degradable linkers (215, 216). Similarly, pulmonary administration of NPs efficiently enhanced cross antigen presentation, which resulted in at least 10-fold more effector $CD8^+$T cells in lungs (217).

NANOPARTICLES AS ADJUVANTS TO GENERATE IMMUNE RESPONSES IN LYMPHOID ORGANS

Adjuvants are known to enhance and prolong the immune responses against antigens. Delivery of adjuvants and antigens using NPs have been found useful to prolong their exposure in the lymphoid organs such as lymph nodes to generate robust immune responses. This is especially important for small adjuvant molecules, which are rapidly cleared from the bloodstream. NPs with a size ranging from 10–100 nm can penetrate the extracellular matrix and travel to the lymph nodes where they can be internalized by the resident macrophages to activate T-cell responses (218–220). The bio-distribution of NPs also depends upon the route of administration and size. It was observed that larger particles accumulated near the site of NPs and were subsequently endocytosed by the local APCs (160), whereas the smaller NPs drained to the blood capillaries (158, 218). PEG coated liposomes of 80–90 nm diameter showed higher accumulation in lymph nodes after subcutaneous administration as compared to intravenous and intraperitoneal administration (221).

CONCLUSIONS

The nano-immuno formulations can improve the antigen stability, targeted delivery and also enhance their immunogenicity properties. Most soluble antigens cannot be efficiently endocytosed by the APCs and hence are poorly effective in inducing protective immunity. The immunogenicity of such soluble vaccine antigens can be improved by conjugating them with nanocarriers that can facilitate the recognition and uptake by APCs. This strategy has already been proved effective for inducing/increasing the immunogenicity of poorly immunogenic antigens, such as polysaccharides of pneumococcal vaccines (222). In the last few years, the application of nanotechnology in the field of immune engineering is growing rapidly with a number of new carrier synthesis strategies. Furthermore, novel nano formulations also contain immunostimulatory molecules to enhance the adjuvant properties of the nanoparticles. Co-encapsulation of the TLR agonists [e.g., CpG, poly(I:C)] (77) or imiquimoid (78) into dextran or chitosan NPs, respectively enhanced receptor-based recognition of the nanovaccines with subsequent cell activation. The recent study by Margaroni et al. showed that vaccination with poly(D,L-lactide-co-glycolide; PLGA) nanoparticles with *Leishmania infantum* antigens (sLiAg) and surface-modified with a TNFα-mimicking eight-amino-acid peptide (p8) induced significant protection against parasite infection in BALB/c mice accompanied by activation of CD8+ T cells and increase in IFNγ production (223).

Additionally, NPs can be tailored for non-invasive administration and prolonged delivery of the vaccine antigens to a specific location, thus providing the possibility for formulation of the single dose vaccine. Several studies clearly demonstrated the efficacy of the non-invasively administered vaccines such as intranasal application of influenza nano vaccine (224), chitosan NPs with hemagglutinin protein of H1N1 influenza virus (225), *Streptococcus equi* proteins (226), hepatitis B surface antigen (pRc/CMV-HBs) (227) and plasmid encoding a multi-epitope protein against *M. tuberculosis* (pHSP65pep) (228) or antigen 85B (229) were used to provide protective immunity against infections. These considerations can improve the progress of ongoing strategies in the development of nanoparticle-based vaccines. In future, development of nanovaccines will address not only the possibility to induce the immune response but also the anti-infective therapeutic activity of NPs thus representing the feasibility to apply multifunctional particles for the treatment of diseases.

AUTHOR CONTRIBUTIONS

AS and RP wrote the manuscript. AS supervised the process. MS wrote the part on Use of nanocarriers in vaccine delivery to dendritic cells.

FUNDING

For financial support, we thank Department of Science and Technology (SR/NM/NS-1159/2016), Govt of India and Alexander von Humboldt Fellowship to AS. MS was supported by the Alexander von Humboldt Fellowship and by a grant of the Russian Science Foundation 14-50-00068 and by the Federal Agency of Scientific Organizations, Russia.

ACKNOWLEDGMENTS

The authors thank Nan-Jong Lee for figures preparation.

REFERENCES

1. Dye C. After 2015: infectious diseases in a new era of health and development. *Philos Trans R Soc Lond B Biol Sci.* (2014) 369:20130426. doi: 10.1098/rstb.2013.0426
2. WHO. *Global Tuberculosis Report*. World Health Organization (2016).
3. Kahn RE, Ma W, Richt JA. Swine and influenza: a challenge to one health research, in *Curr Top Microbiol Immunol.* (2014) 385:205–18. doi: 10.1007/82_2014_392
4. Braden CR, Dowell SF, Jernigan DB, Hughes JM. Progress in global surveillance and response capacity 10 years after severe acute respiratory syndrome. *Emerg Infect Dis.* (2013) 19:864–9. doi: 10.3201/eid1906.130192
5. Wejse C, Patsche CB, Kühle A, Bamba FJV, Mendes MS, Lemvik G, et al. Impact of HIV-1, HIV-2, and HIV-1+2 dual infection on the outcome of tuberculosis. *Int J Infect Dis.* (2015) 32:128–34. doi: 10.1016/j.ijid.2014.12.015
6. Greenwood B. The contribution of vaccination to global health: past, present and future. *Philos Trans R Soc B Biol Sci.* (2014) 369:20130433. doi: 10.1098/rstb.2013.0433
7. Ada GL. The ideal vaccine. *World J Microbiol Biotechnol.* (1991) 7:105–9. doi: 10.1007/BF00328978
8. Atkins HS, Morton M, Griffin KF, Stokes MGM, Nataro JP, Titball RW. Recombinant Salmonella vaccines for biodefence. *Vaccine* (2006) 24:2710–7. doi: 10.1016/j.vaccine.2005.12.046
9. Beverley PCL. Immunology of vaccination. *Br Med Bull.* (2002) 62:15–28. doi: 10.1093/bmb/62.1.15
10. Ulmer JB, Donnelly JJ, Parker SE, Rhodes GH, Felgner PL, Dwarki VJ, et al. Heterologous protection against influenza by injection of DNA encoding a viral protein. *Science* (1993) 259:1745–9. doi: 10.1126/science.8456302
11. Scallan CD, Tingley DW, Lindbloom JD, Toomey JS, Tucker SN. An adenovirus-based vaccine with a double-stranded RNA adjuvant protects mice and ferrets against H5N1 avian influenza in oral delivery models. *Clin Vaccine Immunol.* (2013) 20:85–94. doi: 10.1128/CVI.00552-12
12. Altenburg AF, Kreijtz JH, de Vries RD, Song F, Fux R, Rimmelzwaan GF, et al. Modified vaccinia virus ankara (MVA) as production platform forvaccines against influenza and other viral respiratory diseases. *Viruses* (2014) 6:2735–61. doi: 10.3390/v6072735
13. Nascimento IP, Leite LCC. Recombinant vaccines and the development of new vaccine strategies. *Braz J Med Biol Res.* (2012) 45:1102–11. doi: 10.1590/S0100-879X2012007500142
14. Donnelly JJ, Wahren B, Liu MA. DNA vaccines: progress and challenges. *J Immunol.* (2005) 175:633–9. doi: 10.4049/jimmunol.175.2.633
15. Skibinski DA, Baudner BC, Singh M, O'Hagan DT. Combination vaccines. *J Glob Infect Dis.* (2011) 3:63–72. doi: 10.4103/0974-777X.77298
16. Huber VC. Influenza vaccines: from whole virus preparations to recombinant protein technology. *Expert Rev Vaccines.* (2014) 13:31–42. doi: 10.1586/14760584.2014.852476
17. Means TK, Hayashi F, Smith KD, Aderem A, Luster AD. The Toll-like receptor 5 stimulus bacterial flagellin induces maturation and chemokine production in human dendritic cells. *J Immunol.* (2003) 170:5165–75. doi: 10.4049/jimmunol.170.10.5165
18. Mogensen TH. Pathogen recognition and inflammatory signaling in innate immune defenses. *Clin Microbiol Rev.* (2009) 22:240–73. doi: 10.1128/CMR.00046-08
19. Randolph GJ, Ochando J, Partida-Sánchez S. Migration of dendritic cell subsets and their precursors. *Annu Rev Immunol.* (2008) 26:293–316. doi: 10.1146/annurev.immunol.26.021607.090254
20. Smith DM, Simon JK, Baker JR. Applications of nanotechnology for immunology. *Nat Rev Immunol.* (2013) 13:592–605. doi: 10.1038/nri3488
21. Fifis T, Gamvrellis A, Crimeen-Irwin B, Pietersz GA, Li J, Mottram PL, et al. Size-dependent immunogenicity: therapeutic and protective properties of nano-vaccines against tumors. *J Immunol.* (2004) 173:3148–54. doi: 10.4049/jimmunol.173.5.3148
22. Mottram PL, Leong D, Crimeen-Irwin B, Gloster S, Xiang SD, Meanger J, et al. Type 1 and 2 immunity following vaccination is influenced by nanoparticle size: formulation of a model vaccine for respiratory syncytial virus. *Mol Pharm.* (2007) 4:73–84. doi: 10.1021/mp060096p
23. Schöler N, Hahn H, Müller RH, Liesenfeld O. Effect of lipid matrix and size of solid lipid nanoparticles (SLN) on the viability and cytokine production of macrophages. *Int J Pharm.* (2002) 231:167–76. doi: 10.1016/S0378-5173(01)00882-1
24. Schöler N, Olbrich C, Tabatt K, Müller RH, Hahn H, Liesenfeld O. Surfactant, but not the size of solid lipid nanoparticles (SLN) influences viability and cytokine production of macrophages. *Int J Pharm.* (2001) 221:57–67. doi: 10.1016/S0378-5173(01)00660-3
25. Vallhov H, Qin J, Johansson SM, Ahlborg N, Muhammed MA, Scheynius A, et al. The importance of an endotoxin-free environment during the production of nanoparticles used in medical applications. *Nano Lett.* (2006) 6:1682–6. doi: 10.1021/nl060860z
26. Shvedova AA, Kisin ER, Mercer R, Murray AR, Johnson VJ, Potapovich AI, et al. Unusual inflammatory and fibrogenic pulmonary responses to single-walled carbon nanotubes in mice. *Am J Physiol Cell Mol Physiol.* (2005) 289:L698–708. doi: 10.1152/ajplung.00084.2005
27. Wang X, Ishida T, Kiwada H. Anti-PEG IgM elicited by injection of liposomes is involved in the enhanced blood clearance of a subsequent dose of PEGylated liposomes. *J Control Release* (2007) 119:236–44. doi: 10.1016/j.jconrel.2007.02.010
28. Ishida T, Wang X, Shimizu T, Nawata K, Kiwada H. PEGylated liposomes elicit an anti-PEG IgM response in a T cell-independent manner. *J Control Release* (2007) 122:349–55. doi: 10.1016/j.jconrel.2007.05.015
29. Irvine DJ, Swartz MA, Szeto GL. Engineering synthetic vaccines using cues from natural immunity. *Nat Mater.* (2013) 12:978–90. doi: 10.1038/nmat3775
30. Pusic K, Aguilar Z, McLoughlin J, Kobuch S, Xu H, Tsang M, et al. Iron oxide nanoparticles as a clinically acceptable delivery platform for a recombinant blood-stage human malaria vaccine. *FASEB J.* (2013) 27:1153–66. doi: 10.1096/fj.12-218362
31. Lim JS, Lee K, Choi JN, Hwang YK, Yun MY, Kim HJ,et al. Intracellular protein delivery by hollow mesoporous silica capsules with a large surface hole. *Nanotechnology* (2012) 23:85101. doi: 10.1088/0957-4484/23/8/085101
32. Akagi T, Wang X, Uto T, Baba M, Akashi M. Protein direct delivery to dendritic cells using nanoparticles based on amphiphilic poly(amino acid) derivatives. *Biomaterials* (2007) 28:3427–36. doi: 10.1016/j.biomaterials.2007.04.023
33. Prego C, Paolicelli P, Díaz B, Vicente S, Sánchez A, González-Fernández Á, et al. Chitosan-based nanoparticles for improving immunization against hepatitis B infection. *Vaccine* (2010) 28:2607–14. doi: 10.1016/j.vaccine.2010.01.011
34. Shen H, Ackerman AL, Cody V, Giodini A, Hinson ER, Cresswell P, et al. Enhanced and prolonged cross-presentation following endosomal escape of exogenous antigens encapsulated in biodegradable nanoparticles. *Immunology* (2006) 117:78–88. doi: 10.1111/j.1365-2567.2005.02268.x
35. Diwan M, Tafaghodi M, Samuel J. Enhancement of immune responses by co-delivery of a CpG oligodeoxynucleotide and tetanus toxoid

in biodegradable nanospheres. *J Control Release* (2002) 85:247–62. doi: 10.1016/S0168-3659(02)00275-4
36. Mintern JD, Percival C, Kamphuis MMJ, Chin WJ, Caruso F, Johnston APR. Targeting dendritic cells: the role of specific receptors in the internalization of polymer capsules. *Adv Healthc Mater*. (2013) 2:940–4. doi: 10.1002/adhm.201200441
37. Wang X, Uto T, Akagi T, Akashi M, Baba M. Induction of potent CD8+ T-cell responses by novel biodegradable nanoparticles carrying human immunodeficiency virus type 1 gp120. *J Virol*. (2007) 81:10009–16. doi: 10.1128/JVI.00489-07
38. Richards RL, Rao M, Wassef NM, Glenn GM, Rothwell SW, Alving CR. Liposomes containing lipid A serve as an adjuvant for induction of antibody and cytotoxic T-cell responses against RTS,S malaria antigen. *Infect Immun*. (1998) 66:2859–65.
39. Tyler M, Tumban E, Peabody DS, Chackerian B. The use of hybrid virus-like particles to enhance the immunogenicity of a broadly protective HPV vaccine. *Biotechnol Bioeng*. (2014) 111:2398–406. doi: 10.1002/bit.25311
40. Slupetzky K, Gambhira R, Culp TD, Shafti-Keramat S, Schellenbacher C, Christensen ND, et al. A papillomavirus-like particle (VLP) vaccine displaying HPV16 L2 epitopes induces cross-neutralizing antibodies to HPV11. *Vaccine* (2007) 25:2001–10. doi: 10.1016/j.vaccine.2006.11.049
41. Manish M, Rahi A, Kaur M, Bhatnagar R, Singh S. A single-dose PLGA encapsulated protective antigen domain 4 nanoformulation protects mice against *Bacillus anthracis* spore challenge. *PLoS ONE* (2013) 8:e61885. doi: 10.1371/journal.pone.0061885
42. Feng G, Jiang Q, Xia M, Lu Y, Qiu W, Zhao D, et al. Enhanced immune response and protective effects of nano-chitosan-based DNA vaccine encoding T cell epitopes of Esat-6 and FL against *Mycobacterium Tuberculosis* infection. *PLoS ONE* (2013) 8:e61135. doi: 10.1371/journal.pone.0061135
43. Das I, Padhi A, Mukherjee S, Dash DP, Kar S, Sonawane A. Biocompatible chitosan nanoparticles as an efficient delivery vehicle for *Mycobacterium tuberculosis* lipids to induce potent cytokines and antibody response through activation of $\gamma\delta$ T cells in mice. *Nanotechnology* (2017) 28:165101. doi: 10.1088/1361-6528/aa60fd
44. Abraham E. Intranasal immunization with bacterial polysaccharide containing liposomes enhances antigen-specific pulmonary secretory antibody response. *Vaccine* (1992) 10:461–8. doi: 10.1016/0264-410X(92)90395-Z
45. Alving CR, Richards RL, Moss J, Alving LI, Clements JD, Shiba T, et al. Effectiveness of liposomes as potential carriers of vaccines: applications to cholera toxin and human malaria sporozoite antigen. *Vaccine* (1986) 4:166–72. doi: 10.1016/0264-410X(86)90005-8
46. Zhao W, Wu W, Xu X. Oral vaccination with liposome-encapsulated recombinant fusion peptide of urease B epitope and cholera toxin B subunit affords prophylactic and therapeutic effects against H. pylori infection in BALB/c mice. *Vaccine* (2007) 25:7664–73. doi: 10.1016/j.vaccine.2007.08.034
47. Makidon PE, Knowlton J, Groom J V., Blanco LP, LiPuma JJ, Bielinska AU, et al. Induction of immune response to the 17 kDa OMPA Burkholderia cenocepacia polypeptide and protection against pulmonary infection in mice after nasal vaccination with an OMP nanoemulsion-based vaccine. *Med Microbiol Immunol*. (2010) 199:81–92. doi: 10.1007/s00430-009-0137-2
48. Bielinska AU, Janczak KW, Landers JJ, Makidon P, Sower LE, Peterson JW, et al. Mucosal immunization with a novel nanoemulsion-based recombinant anthrax protective antigen vaccine protects against *Bacillus anthracis* spore challenge. *Infect Immun*. (2007) 75:4020–9. doi: 10.1128/IAI.00070-07
49. Kamath AT, Rochat AF, Christensen D, Agger EM, Andersen P, Lambert PH, et al. A liposome-based mycobacterial vaccine induces potent adult and neonatal multifunctional T cells through the exquisite targeting of dendritic cells. *PLoS ONE* (2009) 4:e5771. doi: 10.1371/journal.pone.0005771
50. Chen YS, Hung YC, Lin WH, Huang GS. Assessment of gold nanoparticles as a size-dependent vaccine carrier for enhancing the antibody response against synthetic foot-and-mouth disease virus peptide. *Nanotechnology* (2010) 21:195101. doi: 10.1088/0957-4484/21/19/195101
51. Tao W, Gill HS. M2e-immobilized gold nanoparticles as influenza A vaccine: role of soluble M2e and longevity of protection. *Vaccine* (2015) 33:2307–2315. doi: 10.1016/j.vaccine.2015.03.063
52. Xu L, Liu Y, Chen Z, Li W, Liu Y, Wang L, et al. Surface-engineered gold nanorods: promising DNA vaccine adjuvant for HIV-1 treatment. *Nano Lett*. (2012) 12:2003–12. doi: 10.1021/nl300027p
53. Raghuvanshi RS, Katare YK, Lalwani K, Ali MM, Singh O, Panda AK. Improved immune response from biodegradable polymer particles entrapping tetanus toxoid by use of different immunization protocol and adjuvants. *Int J Pharm*. (2002) 245:109–21. doi: 10.1016/S0378-5173(02)00342-3
54. Thomas C, Rawat A, Hope-Weeks L, Ahsan F. Aerosolized PLA and PLGA nanoparticles enhance humoral, mucosal and cytokine responses to hepatitis B vaccine. *Mol Pharm*. (2011) 8:405–15. doi: 10.1021/mp100255c
55. Borges O, Cordeiro-da-Silva A, Tavares J, Santarém N, de Sousa A, Borchard G, et al. Immune response by nasal delivery of hepatitis B surface antigen and codelivery of a CpG ODN in alginate coated chitosan nanoparticles. *Eur J Pharm Biopharm*. (2008) 69:405–16. doi: 10.1016/j.ejpb.2008.01.019
56. Zhao K, Chen G, Shi X, Gao T, Li W, Zhao Y, et al. Preparation and efficacy of a live newcastle disease virus vaccine encapsulated in chitosan nanoparticles. *PLoS ONE* (2012) 7:e53314. doi: 10.1371/journal.pone.0053314
57. Ball JM, Hardy ME, Atmar RL, Conner ME, Estes MK. Oral immunization with recombinant Norwalk virus-like particles induces a systemic and mucosal immune response in mice. *J Virol*. (1998) 72:1345–53.
58. Ball JM, Graham DY, Opekun AR, Gilger MA, Guerrero RA, Estes MK. Recombinant Norwalk virus-like particles given orally to volunteers: phase I study. *Gastroenterology* (1999) 117:40–8. doi: 10.1016/S0016-5085(99)70548-2
59. Bright RA, Carter DM, Daniluk S, Toapanta FR, Ahmad A, Gavrilov V, et al. Influenza virus-like particles elicit broader immune responses than whole virion inactivated influenza virus or recombinant hemagglutinin. *Vaccine* (2007) 25:3871–8. doi: 10.1016/j.vaccine.2007.01.106
60. Quan FS, Huang C, Compans RW, Kang SM. Virus-like particle vaccine induces protective immunity against homologous and heterologous strains of influenza virus. *J Virol*. (2007) 81:3514–24. doi: 10.1128/JVI.02052-06
61. Matassov D, Cupo A, Galarza JM. A novel intranasal virus-like particle (VLP) vaccine designed to protect against the pandemic 1918 influenza A virus (H1N1). *Viral Immunol*. (2007) 20:441–52. doi: 10.1089/vim.2007.0027
62. Bright RA, Carter DM, Crevar CJ, Toapanta FR, Steckbeck JD, Cole KS, et al. Cross-clade protective immune responses to influenza viruses with H5N1 HA and NA elicited by an influenza virus-like particle. *PLoS ONE* (2008) 3:e1501. doi: 10.1371/journal.pone.0001501
63. Mahmood K, Bright RA, Mytle N, Carter DM, Crevar CJ, Achenbach JE, et al. H5N1 VLP vaccine induced protection in ferrets against lethal challenge with highly pathogenic H5N1 influenza viruses. *Vaccine* (2008) 26:5393–9. doi: 10.1016/j.vaccine.2008.07.084
64. Guo L, Lu X, Kang SM, Chen C, Compans RW, Yao Q. Enhancement of mucosal immune responses by chimeric influenza HA/SHIV virus-like particles. *Virology* (2003) 313:502–13. doi: 10.1016/S0042-6822(03)00372-6
65. Geldmacher A, Skrastina D, Borisova G, Petrovskis I, Krüger DH, Pumpens P, e t al. A hantavirus nucleocapsid protein segment exposed on hepatitis B virus core particles is highly immunogenic in mice when applied without adjuvants or in the presence of pre-existing anti-core antibodies. *Vaccine* (2005) 23:3973–83. doi: 10.1016/j.vaccine.2005.02.025
66. Sadeyen JR, Tourne S, Shkreli M, Sizaret PY, Coursaget P. Insertion of a foreign sequence on capsid surface loops of human papillomavirus type 16 virus-like particles reduces their capacity to induce neutralizing antibodies and delineates a conformational neutralizing epitope. *Virology* (2003) 309:32–40. doi: 10.1016/S0042-6822(02)00134-4
67. Paz De la Rosa G, Monroy-García A, Mora-García M de L, Peña CGR, Hernández-Montes J, Weiss-Steider B, et al. An HPV 16 L1-based chimeric human papilloma virus-like particles containing a string of epitopes produced in plants is able to elicit humoral and cytotoxic T-cell activity in mice. *Virol J*. (2009) 6:2. doi: 10.1186/1743-422X-6-2
68. Oh YK, Sohn T, Park JS, Kang MJ, Choi HG, Kim JA, et al. Enhanced mucosal and systemic immunogenicity of human papillomavirus-like particles encapsidating interleukin-2 gene adjuvant. *Virology* (2004) 328:266–73. doi: 10.1016/j.virol.2004.06.047
69. O'Neal CM, Crawford SE, Estes MK, Conner ME. Rotavirus virus-like particles administered mucosally induce protective immunity. *J Virol*. (1997) 71:8707–17.

70. Parez N, Fourgeux C, Mohamed A, Dubuquoy C, Pillot M, Dehee A, et al. Rectal immunization with rotavirus virus-like particles induces systemic and mucosal humoral immune responses and protects mice against rotavirus infection. *J Virol*. (2006) 80:1752–61. doi: 10.1128/JVI.80.4.1752-1761.2006
71. Roy P, Bishop DH, LeBlois H, Erasmus BJ. Long-lasting protection of sheep against bluetongue challenge after vaccination with virus-like particles: evidence for homologous and partial heterologous protection. *Vaccine* (1994) 12:805–11. doi: 10.1016/0264-410X(94)90289-5
72. Deml L, Kratochwil G, Osterrieder N, Knüchel R, Wolf H, Wagner R. Increased incorporation of chimeric human immunodeficiency virus type 1 gp120 proteins into Pr55gag virus-like particles by an Epstein-Barr virus gp220/350-derived transmembrane domain. *Virology* (1997) 235:10–25. doi: 10.1006/viro.1997.8669
73. Crooks ET, Moore PL, Franti M, Cayanan CS, Zhu P, Jiang P, et al. A comparative immunogenicity study of HIV-1 virus-like particles bearing various forms of envelope proteins, particles bearing no envelope and soluble monomeric gp120. *Virology* (2007) 366:245–62. doi: 10.1016/j.virol.2007.04.033
74. Buonaguro L, Visciano ML, Tornesello ML, Tagliamonte M, Biryahwaho B, Buonaguro FM. Induction of systemic and mucosal cross-clade neutralizing antibodies in BALB/c mice immunized with human immunodeficiency virus type 1 clade A virus-like particles administered by different routes of inoculation. *J Virol*. (2005) 79:7059–67. doi: 10.1128/JVI.79.11.7059-7067.2005
75. Wang BZ, Liu W, Kang SM, Alam M, Huang C, Ye L, et al. Incorporation of high levels of chimeric human immunodeficiency virus envelope glycoproteins into virus-like particles. *J Virol*. (2007) 81:10869–78. doi: 10.1128/JVI.00542-07
76. Pimentel TAPF, Yan Z, Jeffers SA, Holmes K V., Hodges RS, Burkhard P. Peptide nanoparticles as novel immunogens: design and analysis of a prototypic severe acute respiratory syndrome vaccine. *Chem Biol Drug Des*. (2009) 73:53–61. doi: 10.1111/j.1747-0285.2008.00746.x
77. Kaba SA, Brando C, Guo Q, Mittelholzer C, Raman S, Tropel D, et al. A nonadjuvanted polypeptide nanoparticle vaccine confers long-lasting protection against rodent malaria. *J Immunol*. (2009) 183:7268–77. doi: 10.4049/jimmunol.0901957
78. Kazanji M, Laurent F, Péry P. Immune responses and protective effect in mice vaccinated orally with surface sporozoite protein of *Eimeria* falciformis in ISCOMs. *Vaccine* (1994) 12:798–804. doi: 10.1016/0264-410X(94)90288-7
79. Wang T, Zou M, Jiang H, Ji Z, Gao P, Cheng G. Synthesis of a novel kind of carbon nanoparticle with large mesopores and macropores and its application as an oral vaccine adjuvant. *Eur J Pharm Sci*. (2011) 44:653–9. doi: 10.1016/j.ejps.2011.10.012
80. Zhou X, Zhang X, Yu X, Zha X, Fu Q, Liu B, et al. The effect of conjugation to gold nanoparticles on the ability of low molecular weight chitosan to transfer DNA vaccine. *Biomaterials* (2008) 29:111–7. doi: 10.1016/j.biomaterials.2007.09.007
81. Turkevich J, Stevenson PC, Hillier J. A study of the nucleation and growth processes in the synthesis of colloidal gold. *Discuss Faraday Soc*. (1951) 11:55. doi: 10.1039/df9511100055
82. Silva CL, Bonato VLD, Coelho-Castelo AAM, De Souza AO, Santos SA, Lima KM,et al. Immunotherapy with plasmid DNA encoding mycobacterial hsp65 in association with chemotherapy is a more rapid and efficient form of treatment for tuberculosis in mice. *Gene Ther*. (2005) 12:281–7. doi: 10.1038/sj.gt.3302418
83. Villa CH, Dao T, Ahearn I, Fehrenbacher N, Casey E, Rey DA, et al. Single-walled carbon nanotubes deliver peptide antigen into dendritic cells and enhance IgG responses to tumor-associated antigens. *ACS Nano*. (2011) 5:5300–11. doi: 10.1021/nn200182x
84. Yu M, Jambhrunkar S, Thorn P, Chen J, Gu W, et al. Hyaluronic acid modified mesoporous silica nanoparticles for targeted drug delivery to CD44-overexpressing cancer cells. *Nanoscale* (2013) 5:178–83. doi: 10.1039/C2NR32145A
85. Xia T, Kovochich M, Liong M, Meng H, Kabehie S, George S, et al. Polyethyleneimine coating enhances the cellular uptake of mesoporous silica nanoparticles and allows safe delivery of siRNA and DNA constructs. *ACS Nano* (2009) 3:3273–86. doi: 10.1021/nn900918w
86. He X, Wang K, Tan W, Liu B, Lin X, et al. Bioconjugated nanoparticles for DNA protection from cleavage. *J Am Chem Soc*. (2003) 125:7168–9. doi: 10.1021/ja034450d
87. Li X, Deng X, Huang Z. *In vitro* protein release and degradation of poly-dl-lactide-poly(ethylene glycol) microspheres with entrapped human serum albumin: quantitative evaluation of the factors involved in protein release phases. *Pharm Res*. (2001) 18:117–24. doi: 10.1023/A:1011043230573
88. Demento SL, Cui W, Criscione JM, Stern E, Tulipan J, Kaech SM, et al. Role of sustained antigen release from nanoparticle vaccines in shaping the T cell memory phenotype. *Biomaterials* (2012) 33:4957–64. doi: 10.1016/j.biomaterials.2012.03.041
89. Lima VM, Bonato VL, Lima KM, Dos Santos SA, Dos Santos RR, Gonçalves ED, et al. Role of trehalose dimycolate in recruitment of cells and modulation of production of cytokines and NO in tuberculosis. *Infect Immun*. (2001) 69:5305–12. doi: 10.1128/IAI.69.9.5305-5312.2001
90. Hasegawa K, Noguchi Y, Koizumi F, Uenaka A, Tanaka M, Shimono M, et al. *In vitro* stimulation of CD8 and CD4 T cells by dendritic cells loaded with a complex of cholesterol-bearing hydrophobized pullulan and NY-ESO-1 protein: identification of a new HLA-DR15-binding CD4 T-cell epitope. *Clin Cancer Res*. (2006) 12:1921–7. doi: 10.1158/1078-0432.CCR-05-1900
91. Li P, Luo Z, Liu P, Gao N, Zhang Y, Pan H, et al. Bioreducible alginate-poly(ethylenimine) nanogels as an antigen-delivery system robustly enhance vaccine-elicited humoral and cellular immune responses. *J Control Release* (2013) 168:271–9. doi: 10.1016/j.jconrel.2013.03.025
92. Honda-Okubo Y, Saade F, Petrovsky N. Advax^{TM}, a polysaccharide adjuvant derived from delta inulin, provides improved influenza vaccine protection through broad-based enhancement of adaptive immune responses. *Vaccine* (2012) 30:5373–81. doi: 10.1016/j.vaccine.2012.06.021
93. Saade F, Honda-Okubo Y, Trec S, Petrovsky N. A novel hepatitis B vaccine containing Advax^{TM}, a polysaccharide adjuvant derived from delta inulin, induces robust humoral and cellular immunity with minimal reactogenicity in preclinical testing. *Vaccine* (2013) 31:1999–2007. doi: 10.1016/j.vaccine.2012.12.077
94. Götze O, Müller-Eberhard HJ. The C3-activator system: an alternate pathway of complement activation. *J Exp Med*. (1971) 134:90s−108s.
95. Pawar D, Mangal S, Goswami R, Jaganathan KS. Development and characterization of surface modified PLGA nanoparticles for nasal vaccine delivery: effect of mucoadhesive coating on antigen uptake and immune adjuvant activity. *Eur J Pharm Biopharm*. (2013) 85:550–9. doi: 10.1016/j.ejpb.2013.06.017
96. Sonaje K, Chuang EY, Lin KJ, Yen TC, Su FY, et al. Opening of epithelial tight junctions and enhancement of paracellular permeation by chitosan: microscopic, ultrastructural, and computed-tomographic observations. *Mol Pharm*. (2012) 9:1271–9. doi: 10.1021/mp200572t
97. de Titta A, Ballester M, Julier Z, Nembrini C, Jeanbart L, van der Vlies AJ, et al. Nanoparticle conjugation of CpG enhances adjuvancy for cellular immunity and memory recall at low dose. *Proc Natl Acad Sci USA*. (2013) 110:19902–7. doi: 10.1073/pnas.1313152110
98. Mohammed MA, Syeda JTM, Wasan KM, Wasan EK. An overview of chitosan nanoparticles and its application in non-parenteral drug delivery. *Pharmaceutics* (2017) 9:53. doi: 10.3390/pharmaceutics9040053
99. Sharma A. Liposomes in drug delivery: Progress and limitations. *Int J Pharm*. (1997) 154:123–40. doi: 10.1016/S0378-5173(97)00135-X
100. Storm G, Crommelin DJ. Liposomes: quo vadis? *Pharm Sci Technolo Today* (1998) 1:19–31. doi: 10.1016/S1461-5347(98)00007-8
101. Tyagi RK, Garg NK, Sahu T. Vaccination strategies against malaria: novel carrier(s) more than a tour de force. *J Control Release* (2012) 162:242–54. doi: 10.1016/j.jconrel.2012.04.037
102. Moon JJ, Suh H, Bershteyn A, Stephan MT, Liu H, Huang B, et al. Interbilayer-crosslinked multilamellar vesicles as synthetic vaccines for potent humoral and cellular immune responses. *Nat Mater*. (2011) 10:243–51. doi: 10.1038/nmat2960
103. Ichihashi T, Satoh T, Sugimoto C, Kajino K. Emulsified phosphatidylserine, simple and effective peptide carrier for induction of potent epitope-specific T cell responses. *PLoS ONE* (2013) 8:e60068. doi: 10.1371/journal.pone.0060068
104. Ribeiro AM, Souza ACO, Amaral AC, Vasconcelos NM, Jeronimo MS, Carneiro FP, et al. Nanobiotechnological approaches to delivery of DNA

vaccine against fungal infection. *J Biomed Nanotechnol*. (2013) 9:221–30. doi: 10.1166/jbn.2013.1491
105. Watson DS, Endsley AN, Huang L. Design considerations for liposomal vaccines: influence of formulation parameters on antibody and cell-mediated immune responses to liposome associated antigens. *Vaccine* (2012) 30:2256–72. doi: 10.1016/j.vaccine.2012.01.070
106. Vyas SP, Kannan ME, Jain S, Mishra V, Singh P. Design of liposomal aerosols for improved delivery of rifampicin to alveolar macrophages. *Int J Pharm*. (2004) 269:37–49. doi: 10.1016/j.ijpharm.2003.08.017
107. Vyas S, Quraishi S, Gupta S, Jaganathan K. Aerosolized liposome-based delivery of amphotericin B to alveolar macrophages. *Int J Pharm*. (2005) 296:12–25. doi: 10.1016/j.ijpharm.2005.02.003
108. Joseph A, Itskovitz-Cooper N, Samira S, Flasterstein O, Eliyahu H, Simberg D, et al. A new intranasal influenza vaccine based on a novel polycationic lipid–ceramide carbamoyl-spermine (CCS) I. Immunogenicity and efficacy studies in mice. *Vaccine* (2006) 24:3990–4006. doi: 10.1016/j.vaccine.2005.12.017
109. Postma NS, Hermsen CC, Zuidema J, Eling WM. Plasmodium vinckei: optimization of desferrioxamine B delivery in the treatment of murine malaria. *Exp Parasitol*. (1998) 89:323–30. doi: 10.1006/expr.1998.4282
110. Christensen D, Korsholm KS, Andersen P, Agger EM. Cationic liposomes as vaccine adjuvants. *Expert Rev Vaccines* (2011) 10:513–21. doi: 10.1586/erv.11.17
111. McNeil SE, Perrie Y. Gene delivery using cationic liposomes. *Expert Opin Ther Pat*. (2006) 16:1371–82. doi: 10.1517/13543776.16.10.1371
112. Alving CR, Beck Z, Matyas GR, Rao M. Liposomal adjuvants for human vaccines. *Expert Opin Drug Deliv*. (2016) 13:807–16. doi: 10.1517/17425247.2016.1151871
113. Kingsman SM, Kingsman AJ. Polyvalent recombinant antigens: a new vaccine strategy. *Vaccine* (1988) 6:304–6. doi: 10.1016/0264-410X(88)90174-0
114. Roldão A, Mellado MCM, Castilho LR, Carrondo MJ, Alves PM. Virus-like particles in vaccine development. *Expert Rev Vaccines* (2010) 9:1149–76. doi: 10.1586/erv.10.115
115. Zeltins A. Construction and characterization of virus-like particles: a review. *Mol Biotechnol*. (2013) 53:92–107. doi: 10.1007/s12033-012-9598-4
116. Grgacic EVL, Anderson DA. Virus-like particles: passport to immune recognition. *Methods* (2006) 40:60–5. doi: 10.1016/j.ymeth.2006.07.018
117. Strable E, Finn MG. Chemical modification of viruses and virus-like particles. *Curr Top Microbiol Immunol*. (2009) 327:1–21. doi: 10.1007/978-3-540-69379-6_1
118. Maurer P, Jennings GT, Willers J, Rohner F, Lindman Y, Roubicek K, et al. A therapeutic vaccine for nicotine dependence: preclinical efficacy, and Phase I safety and immunogenicity. *Eur J Immunol*. (2005) 35:2031–40. doi: 10.1002/eji.200526285
119. Patel KG, Swartz JR. Surface functionalization of virus-like particles by direct conjugation using azide–alkyne click chemistry. *Bioconjug Chem*. (2011) 22:376–87. doi: 10.1021/bc100367u
120. Kawano M, Matsui M, Handa H. SV40 virus-like particles as an effective delivery system and its application to a vaccine carrier. *Expert Rev Vaccines* (2013) 12:199–210. doi: 10.1586/erv.12.149
121. Tissot AC, Renhofa R, Schmitz N, Cielens I, Meijerink E, Ose V, et al. Versatile virus-like particle carrier for epitope based vaccines. *PLoS ONE* (2010) 5:e9809. doi: 10.1371/journal.pone.0009809
122. Gao Y, Wijewardhana C, Mann JFS. Virus-like particle, liposome, and polymeric particle-based vaccines against HIV-1. *Front Immunol*. (2018) 9:345. doi: 10.3389/fimmu.2018.00345
123. Chahal JS, Khan OF, Cooper CL, McPartlan JS, Tsosie JK, Tilley LD, et al. Dendrimer-RNA nanoparticles generate protective immunity against lethal Ebola, H1N1 influenza, and *Toxoplasma gondii* challenges with a single dose. *Proc Natl Acad Sci USA*. (2016) 113:E4133–42. doi: 10.1073/pnas.1600299113
124. Bahadoran A, Moeini H, Bejo MH, Hussein MZ, Omar AR. Development of Tat-conjugated dendrimer for transdermal DNA vaccine delivery. *J Pharm Pharm Sci*. (2016)19:325–38. doi: 10.18433/J3G31Q
125. Jaffer U, Wade RG, Gourlay T. Cytokines in the systemic inflammatory response syndrome: a review. *HSR Proc Intensive Care Cardiovasc Anesth*. (2010) 2:161–75.
126. Hora MS, Rana RK, Nunberg JH, Tice TR, Gilley RM, Hudson ME. Controlled release of interleukin-2 from biodegradable microspheres. *Biotechnology* (1990) 8:755–8.
127. Melissen PM, van Vianen W, Bidjai O, van Marion M, Bakker-Woudenberg IA. Free versus liposome-encapsulated muramyl tripeptide phosphatidylethanolamide (MTPPE) and interferon-y (IFN-y) in experimental infection with Listeria monocytogenes. *Biotherapy* (1993) 6:113–24. doi: 10.1007/BF01877424
128. Ali OA, Huebsch N, Cao L, Dranoff G, Mooney DJ. Infection-mimicking materials to program dendritic cells in situ. *Nat Mater*. (2009) 8:151–58. doi: 10.1038/nmat2357
129. Killion JJ, Fishbeck R, Bar-Eli M, Chernajovsky Y. Delivery of interferon to intracellular pathways by encapsulation of interferon into multilamellar liposomes is independent of the status of interferon receptors. *Cytokine* (1994) 6:443–9. doi: 10.1016/1043-4666(94)90069-8
130. Ha SJ, Park SH, Kim HJ, Kim SC, Kang HJ, Lee EG, et al. Enhanced immunogenicity and protective efficacy with the use of interleukin-12-encapsulated microspheres plus AS01B in tuberculosis subunit vaccination. *Infect Immun*. (2006) 74:4954–9. doi: 10.1128/IAI.01781-05
131. Kawai T, Akira S. Toll-like receptors and their crosstalk with other innate receptors in infection and immunity. *Immunity* (2011) 34:637–50. doi: 10.1016/j.immuni.2011.05.006
132. Schenten D, Medzhitov R. The control of adaptive immune responses by the innate immune system. *Adv Immunol*. (2011) 109:87–124. doi: 10.1016/B978-0-12-387664-5.00003-0
133. Lynn GM, Laga R, Darrah PA, Ishizuka AS, Balaci AJ, Dulcey AE, et al. *In vivo* characterization of the physicochemical properties of polymer-linked TLR agonists that enhance vaccine immunogenicity. *Nat Biotechnol*. (2015) 33:1201–10. doi: 10.1038/nbt.3371
134. Goldinger SM, Dummer R, Baumgaertner P, Mihic-Probst D, Schwarz K, Hammann-Haenni A, et al. Nano-particle vaccination combined with TLR-7 and−9 ligands triggers memory and effector $CD8^+$ T-cell responses in melanoma patients. *Eur J Immunol*. (2012) 42:3049–61. doi: 10.1002/eji.201142361
135. Dowling DJ, Scott EA, Scheid A, Bergelson I, Joshi S, Pietrasanta C, et al. Toll-like receptor 8 agonist nanoparticles mimic immunomodulating effects of the live BCG vaccine and enhance neonatal innate and adaptive immune responses. *J Allergy Clin Immunol*. (2017) 140:1339–50. doi: 10.1016/j.jaci.2016.12.985
136. Moradi B, Sankian M, Amini Y, Meshkat Z. Construction of a novel DNA vaccine candidate encoding an HspX-PPE44-EsxV fusion antigen of *Mycobacterium tuberculosis*. *Reports Biochem Mol Biol*. (2016) 4:89–97.
137. Xue T, Stavropoulos E, Yang M, Ragno S, Vordermeier M, Chambers M, et al. RNA encoding the MPT83 antigen induces protective immune responses against Mycobacterium tuberculosis infection. *Infect Immun*. (2004) 72:6324–9. doi: 10.1128/IAI.72.11.6324-6329.2004
138. Romalde JL, Luzardo-Alvárez A, Ravelo C, Toranzo AE, Blanco-Méndez J. Oral immunization using alginate microparticles as a useful strategy for booster vaccination against fish lactoccocosis. *Aquaculture* (2004) 236:119–29. doi: 10.1016/j.aquaculture.2004.02.028
139. Wendorf J, Singh M, Chesko J, Kazzaz J, Soewanan E, Ugozzoli M, et al. A practical approach to the use of nanoparticles for vaccine delivery. *J Pharm Sci*. (2006) 95:2738–50. doi: 10.1002/jps.20728
140. Stieneker F, Kreuter J, Löwer J. High antibody titres in mice with polymethylmethacrylate nanoparticles as adjuvant for HIV vaccines. *AIDS* (1991) 5:431–5.
141. He Q, Mitchell AR, Johnson SL, Wagner-Bartak C, Morcol T, Bell SJ. Calcium phosphate nanoparticle adjuvant. *Clin Diagn Lab Immunol*. (2000) 7:899–903. doi: 10.1128/CDLI.7.6.899-903.2000
142. Oyewumi MO, Kumar A, Cui Z. Nano-microparticles as immune adjuvants: correlating particle sizes and the resultant immune responses. *Expert Rev Vaccines* (2010) 9:1095–107. doi: 10.1586/erv.10.89
143. Biabanikhankahdani R, Alitheen NBM, Ho KL, Tan WS. pH-responsive virus-like nanoparticles with enhanced tumour-targeting ligands for cancer drug delivery. *Sci Rep*. (2016) 6:37891. doi: 10.1038/srep37891
144. Slütter B, Soema PC, Ding Z, Verheul R, Hennink W, Jiskoot W. Conjugation of ovalbumin to trimethyl chitosan improves immunogenicity of the antigen. *J Control Release* (2010) 143:207–14. doi: 10.1016/j.jconrel.2010.01.007

145. Giddam AK, Giddam AK, Zaman M, Skwarczynski M, Toth I. Liposome-based delivery system for vaccine candidates: constructing an effective formulation. *Nanomedicine* (2012) 7:1877–93. doi: 10.2217/nnm.12.157
146. Glück R, Moser C, Metcalfe IC. Influenza virosomes as an efficient system for adjuvanted vaccine delivery. *Expert Opin Biol Ther*. (2004) 4:1139–45. doi: 10.1517/14712598.4.7.1139
147. Morein B, Sundquist B, Höglund S, Dalsgaard K, Osterhaus A. Iscom, a novel structure for antigenic presentation of membrane proteins from enveloped viruses. *Nature* (1984) 308:457–60.
148. Homhuan A, Prakongpan S, Poomvises P, Maas RA, Crommelin DJA, Kersten GFA, et al. Virosome and ISCOM vaccines against Newcastle disease: preparation, characterization and immunogenicity. *Eur J Pharm Sci*. (2004) 22:459–68. doi: 10.1016/j.ejps.2004.05.005
149. Pedersen JS, Oliveira CLP, Hübschmann HB, Arleth L, Manniche S, Kirkby N, et al. Structure of immune stimulating complex matrices and immune stimulating complexes in suspension determined by small-angle X-ray scattering. *Biophys J*. (2012) 102:2372–80. doi: 10.1016/j.bpj.2012.03.071
150. Reid G. Soluble proteins incorporate into ISCOMs after covalent attachment of fatty acid. *Vaccine* (1992) 10:597–602. doi: 10.1016/0264-410X(92)90439-Q
151. Gregory AE, Williamson ED, Prior JL, Butcher WA, Thompson IJ, Shaw AM, et al. Conjugation of Y. pestis F1-antigen to gold nanoparticles improves immunogenicity. *Vaccine* (2012) 30:6777–82. doi: 10.1016/j.vaccine.2012.09.021
152. Reddy ST, Rehor A, Schmoekel HG, Hubbell JA, Swartz MA. *In vivo* targeting of dendritic cells in lymph nodes with poly (propylene sulfide) nanoparticles. *J Control Release* (2006) 112:26–34. doi: 10.1016/j.jconrel.2006.01.006
153. Sunshine JC, Perica K, Schneck JP, Green JJ. Particle shape dependence of CD8+ T cell activation by artificial antigen presenting cells. *Biomaterials* (2014) 35:269–77. doi: 10.1016/j.biomaterials.2013.09.050
154. Yameen B, Choi W Il, Vilos C, Swami A, Shi J, Farokhzad OC. Insight into nanoparticle cellular uptake and intracellular targeting. *J Control Release* (2014) 190:485–99. doi: 10.1016/j.jconrel.2014.06.038
155. Dobrovolskaia MA, Aggarwal P, Hall JB, McNeil SE. Preclinical studies to understand nanoparticle interaction with the immune system and its potential effects on nanoparticle biodistribution. *Mol Pharm*. (2008) 5:487–95. doi: 10.1021/mp800032f
156. Zolnik BS, González-Fernández Á, Sadrieh N, Dobrovolskaia MA. Minireview: nanoparticles and the immune system. *Endocrinology* (2010) 151:458–65. doi: 10.1210/en.2009-1082
157. Joshi VB, Geary SM, Salem AK. Biodegradable particles as vaccine delivery systems: size matters. *AAPS J*. (2013) 15:85–94. doi: 10.1208/s12248-012-9418-6
158. Manolova V, Flace A, Bauer M, Schwarz K, Saudan P, Bachmann MF. Nanoparticles target distinct dendritic cell populations according to their size. *Eur J Immunol*. (2008) 38:1404–13. doi: 10.1002/eji.200737984
159. Nishioka Y, Yoshino H. Lymphatic targeting with nanoparticulate system. *Adv Drug Deliv Rev*. (2001) 47:55–64. doi: 10.1016/S0169-409X(00)00121-6
160. Reddy ST, van der Vlies AJ, Simeoni E, Angeli V, Randolph GJ, O'Neil CP, et al. Exploiting lymphatic transport and complement activation in nanoparticle vaccines. *Nat Biotechnol*. (2007) 25:1159–64. doi: 10.1038/nbt1332
161. Kostarelos K, Lacerda L, Pastorin G, Wu W, Wieckowski S, Luangsivilay J, et al. Cellular uptake of functionalized carbon nanotubes is independent of functional group and cell type. *Nat Nanotechnol*. (2007) 2:108–13. doi: 10.1038/nnano.2006.209
162. Foged C, Brodin B, Frokjaer S, Sundblad A. Particle size and surface charge affect particle uptake by human dendritic cells in an *in vitro* model. *Int J Pharm*. (2005) 298:315–22. doi: 10.1016/j.ijpharm.2005.03.035
163. Thiele L, Merkle HP, Walter E. Phagocytosis and phagosomal fate of surface-modified microparticles in dendritic cells and macrophages. *Pharm Res*. (2003) 20:221–8. doi: 10.1023/A:1022271020390
164. Niikura K, Matsunaga T, Suzuki T, Kobayashi S, Yamaguchi H, Orba Y, et al. Gold nanoparticles as a vaccine platform: influence of size and shape on immunological responses *in vitro* and *in vivo*. *ACS Nano* (2013) 7:3926–38. doi: 10.1021/nn3057005
165. Kim ST, Saha K, Kim C, Rotello VM. The role of surface functionality in determining nanoparticle cytotoxicity. *Acc Chem Res*. (2013) 46:681–91. doi: 10.1021/ar3000647
166. Hillaireau H, Couvreur P. Nanocarriers' entry into the cell: relevance to drug delivery. *Cell Mol Life Sci*. (2009) 66:2873–96. doi: 10.1007/s00018-009-0053-z
167. Li A, Qin L, Zhu D, Zhu R, Sun J, Wang S. Signalling pathways involved in the activation of dendritic cells by layered double hydroxide nanoparticles. *Biomaterials* (2010) 31:748–56. doi: 10.1016/j.biomaterials.2009.09.095
168. Zhu R, Zhu Y, Zhang M, Xiao Y, Du X, Liu H, et al. The induction of maturation on dendritic cells by TiO2 and Fe3O4@TiO2 nanoparticles via NF-κB signaling pathway. *Mater Sci Eng C* (2014) 39:305–14. doi: 10.1016/j.msec.2014.03.005
169. Nawwab AL-Deen FM, Selomulya C, Kong YY, Xiang SD, Ma C, Coppel RL, et al. Design of magnetic polyplexes taken up efficiently by dendritic cell for enhanced DNA vaccine delivery. *Gene Ther*. (2014) 21:212–8. doi: 10.1038/gt.2013.77
170. Toki S, Omary RA, Wilson K, Gore JC, Peebles RS, Pham W. A comprehensive analysis of transfection-assisted delivery of iron oxide nanoparticles to dendritic cells. *Nanomedicine* (2013) 9:1235–44. doi: 10.1016/j.nano.2013.05.010
171. Lee YT, Ko EJ, Hwang HS, Lee JS, Kim KH, Kwon YM, et al. Respiratory syncytial virus-like nanoparticle vaccination induces long-term protection without pulmonary disease by modulating cytokines and T-cells partially through alveolar macrophages. *Int J Nanomed*. (2015) 10:4491–505. doi: 10.2147/IJN.S83493
172. Guo Y, Wang D, Song Q, Wu T, Zhuang X, Bao Y, et al. Erythrocyte membrane-enveloped polymeric nanoparticles as nanovaccine for induction of antitumor immunity against melanoma. *ACS Nano* (2015) 9:6918–33. doi: 10.1021/acsnano.5b01042
173. Li M, Wang B, Wu Z, Shi X, Zhang J, Han S. Treatment of Dutch rat models of glioma using EphrinA1-PE38/GM-CSF chitosan nanoparticles by in situ activation of dendritic cells. *Tumor Biol*. (2015) 36:7961–6. doi: 10.1007/s13277-015-3486-z
174. Campbell DF, Saenz R, Bharati IS, Seible D, Zhang L, Esener S, et al. Enhanced anti-tumor immune responses and delay of tumor development in human epidermal growth factor receptor 2 mice immunized with an immunostimulatory peptide in poly(D,L-lactic-co-glycolic) acid nanoparticles. *Breast Cancer Res*. (2015) 17:48. doi: 10.1186/s13058-015-0552-9
175. Hernández-Gil J, Cobaleda-Siles M, Zabaleta A, Salassa L, Calvo J, Mareque-Rivas JC. An iron oxide nanocarrier loaded with a Pt(IV) prodrug and immunostimulatory dsRNA for combining complementary cancer killing effects. *Adv Healthc Mater*. (2015) 4:1034–42. doi: 10.1002/adhm.201500080
176. Lu F, Mencia A, Bi L, Taylor A, Yao Y, HogenEsch H. Dendrimer-like alpha-d-glucan nanoparticles activate dendritic cells and are effective vaccine adjuvants. *J Control Release* (2015) 204:51–9. doi: 10.1016/j.jconrel.2015.03.002
177. Sehgal K, Ragheb R, Fahmy TM, Dhodapkar M V., Dhodapkar KM. Nanoparticle-mediated combinatorial targeting of multiple human Dendritic Cell (DC) subsets leads to enhanced T cell activation via IL-15–dependent DC crosstalk. *J Immunol*. (2014) 193:2297–305. doi: 10.4049/jimmunol.1400489
178. Hoang MD, Lee HJ, Lee HJ, Jung SH, Choi NR, Vo MC, etb al. Branched Polyethylenimine-Superparamagnetic Iron Oxide Nanoparticles (bPEI-SPIONs) improve the immunogenicity of tumor antigens and enhance Th1 polarization of dendritic cells. *J Immunol Res*. (2015) 2015:706379. doi: 10.1155/2015/706379
179. Mundayoor S, Kumar RA, Dhanasooraj S. Vaccine delivery system for tuberculosis based on nano-sized hepatitis B virus core protein particles. *Int J Nanomedicine* (2013) 8:835. doi: 10.2147/IJN.S40238
180. Amini Y, Moradi B, Tafaghodi M, Meshkat Z, Ghazvini K, Fasihi-Ramandi M. TB trifusion antigen adsorbed on calcium phosphate nanoparticles stimulates strong cellular immunity in mice. *Biotechnol Bioprocess Eng*. (2016) 21:653–8. doi: 10.1007/s12257-016-0326-y
181. Speth MT, Repnik U, Müller E, Spanier J, Kalinke U, Corthay A, et al. Poly(I:C)-encapsulating nanoparticles enhance innate immune responses to the tuberculosis vaccine Bacille Calmette–Guérin (BCG) via synergistic

activation of innate immune receptors. *Mol Pharm*. (2017) 14:4098–112. doi: 10.1021/acs.molpharmaceut.7b00795
182. Poecheim J, Barnier-Quer C, Collin N, Borchard G. Ag85A DNA vaccine delivery by nanoparticles: influence of the formulation characteristics on immune responses. *Vaccines* (2016) 4:32. doi: 10.3390/vaccines4030032
183. Ballester M, Nembrini C, Dhar N, de Titta A, de Piano C, et al. Nanoparticle conjugation and pulmonary delivery enhance the protective efficacy of Ag85B and CpG against tuberculosis. *Vaccine* (2011) 29:6959–66. doi: 10.1016/j.vaccine.2011.07.039
184. Nel AE, Mädler L, Velegol D, Xia T, Hoek EM V, Somasundaran P, et al. Understanding biophysicochemical interactions at the nano-bio interface. *Nat Mater*. (2009) 8:543–57. doi: 10.1038/nmat2442
185. Lynch I, Dawson KA. Protein-nanoparticle interactions. (2008) 3:40–7. doi: 10.1016/S1748-0132(08)70014-8
186. Vertegel AA, Siegel RW, Dordick JS. Silica nanoparticle size influences the structure and enzymatic activity of adsorbed lysozyme. *Langmuir* (2004) 20:6800–7. doi: 10.1021/la0497200
187. Taylor PR, Martinez-Pomares L, Stacey M, Lin HH, Brown GD, Gordon S. Macrophage receptors and immune recognition. *Annu Rev Immunol.* (2005) 23:901–44. doi: 10.1146/annurev.immunol.23.021704.115816
188. Beduneau A, Ma Z, Grotepas CB, Kabanov A, Rabinow BE, Gong N, et al. Facilitated monocyte-macrophage uptake and tissue distribution of superparmagnetic iron-oxide nanoparticles. *PLoS ONE* (2009) 4:e4343. doi: 10.1371/journal.pone.0004343
189. Laroui H, Viennois E, Xiao B, Canup BSB, Geem D, Denning TL, et al. Fab'-bearing siRNA TNFα-loaded nanoparticles targeted to colonic macrophages offer an effective therapy for experimental colitis. *J Control Release* (2014) 186:41–53. doi: 10.1016/j.jconrel.2014.04.046
190. Verma A, Stellacci F. Effect of surface properties on nanoparticle-cell interactions. *Small* (2010) 6:12–21. doi: 10.1002/smll.200901158
191. Kolaczkowska E, Kubes P. Neutrophil recruitment and function in health and inflammation. *Nat Rev Immunol*. (2013) 13:159–75. doi: 10.1038/nri3399
192. Kamaly N, Fredman G, Subramanian M, Gadde S, Pesic A, Cheung L, et al. Development and *in vivo* efficacy of targeted polymeric inflammation-resolving nanoparticles. *Proc Natl Acad Sci USA.,* (2013) 110:6506–11. doi: 10.1073/pnas.1303377110
193. Chu D, Gao J, Wang Z. Neutrophil-mediated delivery of therapeutic nanoparticles across blood vessel barrier for treatment of inflammation and infection. *ACS Nano* (2015) 9:11800–11. doi: 10.1021/acsnano.5b05583
194. Endsley AN, Ho RJY. Enhanced anti-HIV efficacy of indinavir after inclusion in CD4-targeted lipid nanoparticles. *JAIDS J Acquir Immune Defic Syndr*. (2012) 61:417–24. doi: 10.1097/QAI.0b013e3182653c1f
195. Perisé-Barrios AJ, Jiménez JL, Domínguez-Soto A, de la Mata FJ, Corbí AL, Gomez R, et al. Carbosilane dendrimers as gene delivery agents for the treatment of HIV infection. *J Control Release* (2014) 184:51–7. doi: 10.1016/j.jconrel.2014.03.048
196. Harding C V, Collins DS, Slot JW, Geuze HJ, Unanue ER. Liposome-encapsulated antigens are processed in lysosomes, recycled, and presented to T cells. *Cell* (1991) 64:393–401. doi: 10.1016/0092-8674(91)90647-H
197. Stano A, Nembrini C, Swartz MA, Hubbell JA, Simeoni E. Nanoparticle size influences the magnitude and quality of mucosal immune responses after intranasal immunization. *Vaccine* (2012) 30:7541–6. doi: 10.1016/j.vaccine.2012.10.050
198. Kim YM, Pan JYJ, Korbel GA, Peperzak V, Boes M, Ploegh HL. Monovalent ligation of the B cell receptor induces receptor activation but fails to promote antigen presentation. *Proc Natl Acad Sci USA*. (2006) 103:3327–32. doi: 10.1073/pnas.0511315103
199. Chackerian B, Lowy DR, Schiller JT. Conjugation of a self-antigen to papillomavirus-like particles allows for efficient induction of protective autoantibodies. *J Clin Invest*. (2001) 108:415–23. doi: 10.1172/JCI11849
200. Friede M, Muller S, Briand JP, Van Regenmortel MH, Schuber F. Induction of immune response against a short synthetic peptide antigen coupled to small neutral liposomes containing monophosphoryl lipid A. *Mol Immunol*. (1993) 30:539–47. doi: 10.1016/0161-5890(93)90028-A
201. Bershteyn A, Hanson MC, Crespo MP, Moon JJ, Li A V., Suh H, et al. Robust IgG responses to nanograms of antigen using a biomimetic lipid-coated particle vaccine. *J Control Release* (2012) 157:354–65. doi: 10.1016/j.jconrel.2011.07.029
202. Temchura VV, Kozlova D, Sokolova V, Uberla K, Epple M. Targeting and activation of antigen-specific B-cells by calcium phosphate nanoparticles loaded with protein antigen. *Biomaterials* (2014) 35:6098–105. doi: 10.1016/j.biomaterials.2014.04.010
203. Joffre OP, Segura E, Savina A, Amigorena S. Cross-presentation by dendritic cells. *Nat Rev Immunol*. (2012) 12:557–69. doi: 10.1038/nri3254
204. Brode S, Macary PA. Cross-presentation: dendritic cells and macrophages bite off more than they can chew! *Immunology* (2004) 112:345–51. doi: 10.1111/j.1365-2567.2004.01920.x
205. Amigorena S, Savina A. Intracellular mechanisms of antigen cross presentation in dendritic cells. *Curr Opin Immunol*. (2010) 22:109–17. doi: 10.1016/j.coi.2010.01.022
206. Kovacsovics-Bankowski M, Clark K, Benacerraf B, Rock KL. Efficient major histocompatibility complex class I presentation of exogenous antigen upon phagocytosis by macrophages. *Proc Natl Acad Sci USA*. (1993) 90:4942–6. doi: 10.1073/pnas.90.11.4942
207. Kovacsovics-Bankowski M, Rock KL. A phagosome-to-cytosol pathway for exogenous antigens presented on MHC class I molecules. *Science* (1995) 267:243–6. doi: 10.1126/science.7809629
208. Reis e Sousa C, Germain RN. Major histocompatibility complex class I presentation of peptides derived from soluble exogenous antigen by a subset of cells engaged in phagocytosis. *J Exp Med*. (1995) 182:841–51.
209. Harding C V, Song R. Phagocytic processing of exogenous particulate antigens by macrophages for presentation by class I MHC molecules. *J Immunol*. (1994) 153:4925–33.
210. Jain S, Yap WT, Irvine DJ. Synthesis of protein-loaded hydrogel particles in an aqueous two-phase system for coincident antigen and CpG oligonucleotide delivery to antigen-presenting cells. *Biomacromolecules* (2005) 6:2590–600. doi: 10.1021/bm0503221
211. Hamdy S, Elamanchili P, Alshamsan A, Molavi O, Satou T, Samuel J. Enhanced antigen-specific primary CD4+ and CD8+ responses by codelivery of ovalbumin and toll-like receptor ligand monophosphoryl lipid A in poly(D,L-lactic-co-glycolic acid) nanoparticles. *J Biomed Mater Res A* (2007) 81:652–62. doi: 10.1002/jbm.a.31019
212. Tanaka Y, Taneichi M, Kasai M, Kakiuchi T, Uchida T. Liposome-coupled antigens are internalized by antigen-presenting cells via pinocytosis and cross-presented to CD8 T cells. *PLoS ONE* (2010) 5:e15225. doi: 10.1371/journal.pone.0015225
213. Brandtzaeg P. Induction of secretory immunity and memory at mucosal surfaces. *Vaccine* (2007) 25:5467–84. doi: 10.1016/j.vaccine.2006.12.001
214. Macho Fernandez E, Chang J, Fontaine J, Bialecki E, Rodriguez F, Werkmeister E, et al. Activation of invariant Natural Killer T lymphocytes in response to the α-galactosylceramide analogue KRN7000 encapsulated in PLGA-based nanoparticles and microparticles. *Int J Pharm*. (2012) 423:45–54. doi: 10.1016/j.ijpharm.2011.04.068
215. van der Vlies AJ, O'Neil CP, Hasegawa U, Hammond N, Hubbell JA. Synthesis of pyridyl disulfide-functionalized nanoparticles for conjugating thiol-containing small molecules, peptides, and proteins. *Bioconjug Chem*. (2010) 21:653–62. doi: 10.1021/bc9004443
216. Hirosue S, Kourtis IC, van der Vlies AJ, Hubbell JA, Swartz MA. Antigen delivery to dendritic cells by poly(propylene sulfide) nanoparticles with disulfide conjugated peptides: cross-presentation and T cell activation. *Vaccine* (2010) 28:7897–906. doi: 10.1016/j.vaccine.2010.09.077
217. Nembrini C, Stano A, Dane KY, Ballester M, van der Vlies AJ, Marsland BJ, et al. Nanoparticle conjugation of antigen enhances cytotoxic T-cell responses in pulmonary vaccination. *Proc Natl Acad Sci USA*. (2011) 108:E989–97. doi: 10.1073/pnas.1104264108
218. Swartz MA. The physiology of the lymphatic system. *Adv Drug Deliv Rev*. (2001) 50:3–20. doi: 10.1016/S0169-409X(01)00150-8
219. Cubas R, Zhang S, Kwon S, Sevick-Muraca EM, Li M, Chen C, et al. Virus-like particle (VLP) lymphatic trafficking and immune response generation after immunization by different routes. *J Immunother*. (2009) 32:118–28. doi: 10.1097/CJI.0b013e31818f13c4
220. Dane KY, Nembrini C, Tomei AA, Eby JK, O'Neil CP, Velluto D, et al. Nano-sized drug-loaded micelles deliver payload to lymph node immune cells and prolong allograft survival. *J Control Release* (2011) 156:154–60. doi: 10.1016/j.jconrel.2011.08.009

221. Allen TM, Hansen CB, Guo LS. Subcutaneous administration of liposomes: a comparison with the intravenous and intraperitoneal routes of injection. *Biochim Biophys Acta* (1993) 1150:9–16. doi: 10.1016/0005-2736(93)90115-G
222. Vetro M, Safari D, Fallarini S, Salsabila K, Lahmann M, Penadés S, et al. Preparation and immunogenicity of gold glyco-nanoparticles as antipneumococcal vaccine model. *Nanomedicine (Lond)* (2017) 12:13–23. doi: 10.2217/nnm-2016-0306
223. Margaroni M, Agallou M, Athanasiou E, Kammona O, Kiparissides C, Gaitanaki C, et al. Vaccination with poly(D,L-lactide-co-glycolide) nanoparticles loaded with soluble Leishmania antigens and modified with a TNFα-mimicking peptide or monophosphoryl lipid A confers protection against experimental visceral leishmaniasis. *Int J Nanomedicine* (2017) 12:6169–84. doi: 10.2147/IJN.S141069
224. Qi M, Zhang XE, Sun X, Zhang X, Yao Y, Liu S, et al. Intranasal nanovaccine confers homo- and hetero-subtypic influenza protection. *Small* (2018) 14:e1703207. doi: 10.1002/smll.201703207
225. Sawaengsak C, Mori Y, Yamanishi K, Mitrevej A, Sinchaipanid N. Chitosan nanoparticle encapsulated hemagglutinin-split influenza virus mucosal vaccine. *AAPS PharmSciTech* (2014) 15:317–25. doi: 10.1208/s12249-013-0058-7
226. Figueiredo L, Cadete A, Gonçalves L, Corvo M, Almeida AJ. Intranasal immunisation of mice against Streptococcus equi using positively charged nanoparticulate carrier systems. *Vaccine* (2012) 30:6551–8. doi: 10.1016/j.vaccine.2012.08.050
227. Khatri K, Goyal AK, Gupta PN, Mishra N, Vyas SP. Plasmid DNA loaded chitosan nanoparticles for nasal mucosal immunization against hepatitis B. *Int J Pharm* (2008) 354:235–41. doi: 10.1016/j.ijpharm.2007.11.027
228. Ai W, Yue Y, Xiong S, Xu W. Enhanced protection against pulmonary mycobacterial challenge by chitosan-formulated polyepitope gene vaccine is associated with increased pulmonary secretory IgA and gamma-interferon(+) T cell responses. *Microbiol Immunol* (2013) 57:224–35. doi: 10.1111/1348-0421.12027
229. Meerak J, Wanichwecharungruang SP, Palaga T. Enhancement of immune response to a DNA vaccine against Mycobacterium tuberculosis Ag85B by incorporation of an autophagy inducing system. *Vaccine* (2013) 31:784–90. doi: 10.1016/j.vaccine.2012.11.075

Conflict of Interest Statement: The authors declare that the research was conducted in the absence of any commercial or financial relationships that could be construed as a potential conflict of interest.

Advantages of publishing in Frontiers

OPEN ACCESS
Articles are free to read for greatest visibility and readership

FAST PUBLICATION
Around 90 days from submission to decision

HIGH QUALITY PEER-REVIEW
Rigorous, collaborative, and constructive peer-review

TRANSPARENT PEER-REVIEW
Editors and reviewers acknowledged by name on published articles

Frontiers
Avenue du Tribunal-Fédéral 34
1005 Lausanne | Switzerland

Visit us: www.frontiersin.org
Contact us: info@frontiersin.org | +41 21 510 17 00

REPRODUCIBILITY OF RESEARCH
Support open data and methods to enhance research reproducibility

DIGITAL PUBLISHING
Articles designed for optimal readership across devices

FOLLOW US
@frontiersin

IMPACT METRICS
Advanced article metrics track visibility across digital media

EXTENSIVE PROMOTION
Marketing and promotion of impactful research

LOOP RESEARCH NETWORK
Our network increases your article's readership